

Inhibition Studies of Kynurenine 3-Monooxygenase



University of
St Andrews

600
YEARS

Gavin Milne

*Thesis submitted to the University of St. Andrews in application for the
degree of Doctor of Philosophy*

Supervisors: Dr Nigel Botting and Prof. David O'Hagan

May 2013

Declarations

1. Candidate's declarations:

I, Gavin Milne hereby certify that this thesis, which is approximately 60400 words in length, has been written by me, that it is the record of work carried out by me and that it has not been submitted in any previous application for a higher degree.

I was admitted as a research student in September 2009 and as a candidate for the degree of PhD in September 2010 the higher study for which this is a record was carried out in the University of St Andrews between 2009 and 2013.

Date signature of candidate

2. Supervisor's declaration:

I hereby certify that the candidate has fulfilled the conditions of the Resolution and Regulations appropriate for the degree of Doctor of Philosophy in the University of St Andrews and that the candidate is qualified to submit this thesis in application for that degree.

Date signature of supervisor

3. Permission for electronic publication:

In submitting this thesis to the University of St Andrews I understand that I am giving permission for it to be made available for use in accordance with the regulations of the University Library for the time being in force, subject to any copyright vested in the work not being affected thereby. I also understand that the title and the abstract will be published, and that a copy of the work may be made and supplied to any bona fide library or research worker, that my thesis will be electronically accessible for personal or research use unless exempt by award of an embargo as requested below, and that the library has the right to migrate my thesis into new electronic forms as required to ensure continued access to the thesis. I have obtained any third-party copyright permissions that may be required in order to allow such access and migration, or have requested the appropriate embargo below.

The following is an agreed request by candidate and supervisor regarding the electronic publication of this thesis:

Embargo on both all of printed copy and electronic copy for the same fixed period of 2 years on the following ground:

publication would preclude future publication;

Date signature of candidate

Signature of supervisor

Dedicated to Dr Nigel Botting

Acknowledgements

I would like to thank my second supervisor Prof. David O'Hagan for his guidance and support, in the most difficult of circumstances. Since I have joined the O'Hagan group I have learnt a lot about the subtle and not so subtle influences of fluorine. I would like to thank the University of St. Andrews for allowing me to undertake my PhD studies. I would also like to thank the EPSRC for the funding of this project.

I am grateful to Mrs Melanja Smith and Dr Tomas Lebl for the smooth running of the solution state NMR facility. I am also grateful to Dr Tomas Lebl for answering my NMR questions. I am indebted to Mrs Caroline Horsburgh for the mass spectrometry service she runs and the helpful advice she has from parenting to running. I would like to thank Mrs Sylvia Williamson for introducing me to the IR spectrophotometer and keeping its supplies topped up.

I would like to acknowledge the support and advice I have received from Dr Catherine Botting, Dr Sally Shirran, Prof. Alex Slawin and Prof. Derek Woollins. I would also like to thank Prof. Alex Slawin for the X-ray crystal structures that she solved.

I would like to thank Dr Chris Mowat, Martin Wilkinson, Helen Bell and Annemette Kjeldsen from Edinburgh University for the testing of my compounds against the bacterial enzyme and for all the co-crystal data, which was invaluable in the design of potent inhibitors.

I would like to thank Dr Damian Mole, Dr Scott Webster and Kris McGuire for testing my compounds against the human enzyme.

I would like to thank all the members of the NPB and DOH groups whom I have had the honour of working with. Special mentions go to Nikos Raheem and Su Cobb who helped me through some of the darkest days of my PhD. I would like to thank Stephen Thomson, for sharing the commute and scientific thoughts on the way to and from "Anster". I would like to thank Dr Neil Keddie for his support and proofreading of this thesis. I would also like to thank Dr Michael Corr for

proofreading my thesis. I am grateful to Dr Davide Bello for his help and advice in the lab. I am grateful to Dr Qingzhi Zhang for helping me run and understand the HPLC systems.

I would like to thank my parents for supporting and encouraging me through my PhD. I would also like to thank my wider family and friends for their support during my time in St. Andrews.

I would like to thank my wife Emma Milne for her support during my PhD, you are the ray of sunshine that brightens my life. I would also like to thank my son George Milne who keeps me on my toes when I am not at work.

Finally I would like to thank Dr Nigel Botting for his support and optimism with this project. I miss the open door and the time that you had for everyone no matter how silly the question was. I hope that your bravery and optimism lives on in the heart of all who got to know you.

Table of contents

Declarations	ii
Acknowledgements	v
Table of contents	vii
Abbreviations	ix
Abstract	xv

Chapter 1

Introduction	1
1.1 Kynurenine pathway.....	1
1.2 TDO and IDO	6
1.2.1 Biological and structural data for TDO	6
1.2.2 Biological and structural data for IDO.....	8
1.2.3 TDO and IDO mechanistic information.....	10
1.2.4 IDO inhibitors.....	13
1.3 Kynurenine aminotransferase	19
1.3.1 Kynurenine aminotransferase biology and structural data	19
1.3.2 Kynurenine aminotransferase mechanism	22
1.3.3 Kynurenine aminotransferase inhibitors	24
1.4 Kynurenine monooxygenase.....	28
1.4.1 Kynurenine monooxygenase biology and structural information.....	28
1.4.2 Kynurenine 3-monooxygenase mechanism	31
1.4.3 Kynurenine-3-monooxygenase inhibitors	34
1.5 3-Hydroxyanthranilate-3,4-dioxygenase.....	39
1.5.1 3-Hydroxyanthranilate-3,4-dioxygenase biology and structure	39
1.5.2 Mechanism of 3HAO	43
1.5.3 3HAO inhibitors	45
1.6 QPRTase.....	47
1.6.1 QPRTase biology and structural data	47
1.6.2 QPRTase mechanism	50
1.7 Acute pancreatitis and the role of kynurenines in secondary multiple organ failure	52
1.7.1 The pancreas	52
1.7.2 Acute pancreatitis.....	53
1.7.3 Multiple organ failure Induced by acute pancreatitis	54
1.8. Aims of research	56

Chapter 2

Exploring Chemical Space To Generate Inhibitors of K3MO.....	57
2.0 Introduction.....	57
2.1 Target validation.....	59
2.2 Initial amine and amino acid targets.....	61

2.3 Investigation into alternative motifs for inhibition of K3MO	67
2.4 Enzymatic assays of first generation compounds against K3MO	90
2.5 Conclusions	94

Chapter 3

The synthesis and development of 1,2,4-oxadiazole amides as inhibitors of K3MO..... 95

3.1 Synthesis and enzymatic assay of a first generation library of 1,2,4-oxadiazole amides	95
3.2 Protein X-ray crystallography of first generation amides with <i>P. fluorescens</i> K3MO .	101
3.3 Synthesis and K3MO enzyme assays of a second generation series of 1,2,4-oxadiazole amides.....	107
3.4 Protein X-ray crystallography of second generation amides with <i>P. fluorescens</i> K3MO	119
3.5 Synthesis and assay of a third generation series of 1,2,4-oxadiazole amides.....	129
3.6 Conclusions	138

Chapter 4

Unfinished business: Synthesis of kynurenine analogues 140

4.1 Introduction.....	140
4.2 Previous syntheses of kynurenine analogues	141
4.3 Aims and objectives in the synthesis of kynurenine analogues	145
4.4 Routes towards the synthesis of a pyridyl-kynurenine analogue	146
4.5 Attempted synthesis of 3-fluorokynurenine	151

Chapter 5

Experimental 157

5.1 General Considerations.....	157
5.2 Characterisation	160

References..... 283

Appendix..... 298

Single crystal X-ray diffraction data	298
---	-----

Abbreviations

3HAA	3-Hydroxyanthranilic acid
3HAO	3-Hydroxyanthranilate-3,4-dioxygenase
Å	Angstrom
ACMSA	Aminocarboxymuconate semialdehyde
ACMSD	Aminocarboxymuconate semialdehyde decarboxylase
AIDS	Acquired immunodeficiency syndrome
Anal.	Analytical
Arg	Arginine
Asp	Aspartate
Boc	<i>t</i> -Butoxycarbonyl
CHES	<i>N</i> -cyclohexyl-2-aminoethanesulfonic acid
CI	Chemical ionisation
CoA	Co-enzyme A
d	doublet
Db	Dibenzylideneacetone
DCC	<i>N,N'</i> -Dicyclohexylcarbodiimide
DCM	Dichloromethane
DEAM	Diethyl acetamidomalonate
DMAP	4-Dimethylaminopyridine
DMF	<i>N,N'</i> -Dimethylformamide

DMSO	Dimethyl sulfoxide
DTT	Dithiothreitol
EDCI	1-Ethyl-3-(3-dimethylaminopropyl)carbodiimide
eq.	Equivalents
ES	Electrospray ionisation
Et	Ethyl
FAD	Flavin adenine dinucleotide
Glu	Glutamate
Gly	Glycine
h	hour(s)
His	Histidine
HMBC	Heteronuclear multiple-bond correlation spectroscopy
HPLC	High performance liquid chromatography
HRMS	High resolution mass spectrometry
HSQC	Heteronuclear single-quantum correlation spectroscopy
Hz	Hertz
IC ₅₀	Half maximal inhibitory constant
IDO	Indoleamine 2,3-dioxygenase
Ile	Isoleucine
INF γ	Interferon-gamma
IR	Infra red
K3MO	Kynurenine-3-monooxygenase

KAT	Kynurenine aminotransferase
K_{cat}	Overall enzymatic catalytic rate
kDa	Kilo dalton
K_i	Enzyme-inhibitor constant
K_{inact}	Inactivation rate
K_m	Michaelis constant
LC-MS	Liquid chromatography-mass spectrometry
LC-MS/MS	Liquid chromatography-tandem mass spectroscopy
LDA	Lithium diisopropylamide
Leu	Leucine
Lit.	Literature value
LPS	Lipopolysaccharide
Lys	Lysine
m	multiplet
M	Molar
<i>m</i> CPBA	3-Chloroperoxybenzoic acid
Me	Methyl
MeOH	Methanol
Met	Methionine
MHz	Megahertz
min	Minute(s)
mL	Millilitre

MLN	Mesenteric lymph nodes
μM	Micromolar
mM	millimolar
MOF	Multiple organ failure
NADH	Nicotinamide adenine dinucleotide (reduced form)
NADPH	Nicotinamide adenine dinucleotide phosphate (reduced form)
NBS	<i>N</i> -Bromosuccinimide
nM	Nanomolar
NMDA	<i>N</i> -Methyl-D-aspartic acid
NMR	Nuclear Magnetic Resonance
NOE	Nuclear Overhauser effect spectroscopy
NOS	Nitric oxide synthase
NSAID	Nonsteroidal anti-inflammatory drugs
PBS	Phosphate buffered saline
pH	Hydrogen ion concentration
Phe	Phenylalanine
Piv	Pivaloyl
pKa	Acid dissociation constant
PLP	Pyridoxal-5'-phosphate
ppm	Parts per million
Pro	Proline
q	quartet

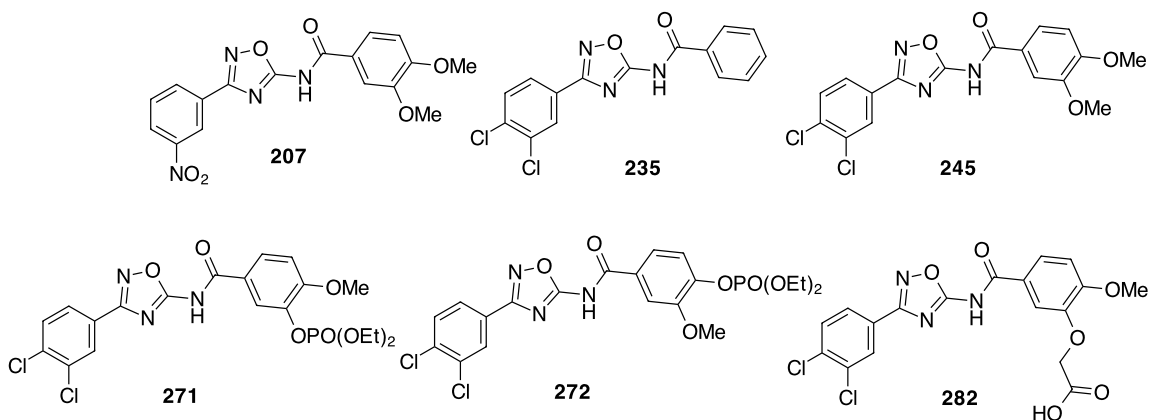
QPRTase	Quinolinate phosphoribosyl transferase
Quant	Quantitative
RP	Reverse phase
RT	Room temperature
s	singlet
Ser	Serine
S _N 1	Unimolecular nucleophilic substitution
S _N 2	Bimolecular nucleophilic substitution
t	triplet
TBAF	Tetra- <i>n</i> -butylammonium fluoride
TBS	<i>tert</i> -Butyldimethyl silyl
TDO	Tryptopan 2,3-dioxygenase
TFA	Trifluoroacetic acid
THF	Tetrahydrofuran
Thr	Threonine
TLC	Thin layer chromatography
TMS	Trimethylsilyl
TNF α	Tumor necrosis factor-alpha
Tyr	Tyrosine
v/v	Volume concentration
Val	Valine
v	Rate

v_{\max}	Maximal rate
w/v	Mass concentration

Abstract

Kynurenine 3-monooxygenase (K3MO) lies on the kynurenine pathway, the major pathway for the catabolism of L-tryptophan. It converts kynurenine to 3-hydroxy kynurenine. Inhibition of K3MO is important in several neurological diseases and there is evidence that inhibition of K3MO could also be targeted for the prevention of multiple organ failure, secondary to acute pancreatitis.

A structure activity relationship based upon the 1,2,4-oxadiazoles motif was carried out which revealed amide **207** as an inhibitor of *P. fluorescens* K3MO. Further structure activity relationships were developed based upon **207**. This revealed 3,4-dichloro substitution in **235** and **245** as optimum for inhibition. Co-crystallisation of these inhibitors with *P. fluorescens* K3MO revealed their interactions with the enzyme. It also highlighted new, potential interactions between the inhibitors and K3MO. This led to the synthesis of **271** and **272**, which were also potent inhibitors of K3MO. These amides were successfully co-crystallised with *P. fluorescens* K3MO. Further development of the amides followed, with amide **282** providing the most potent inhibitor of *P. fluorescens* K3MO to date ($K_i = 29.1$ nM).



Chapter 1

Introduction

1.1 Kynurenine pathway

The kynurenine pathway is the major route for the catabolism of tryptophan **1** ultimately leading to the *de novo* synthesis of NADH. The link between NADH synthesis and tryptophan catabolism was discovered in 1947.¹ Initial interest in the pathway waned when the important neurotransmitter 5-hydroxytryptamine **2** was revealed as an alternative catabolite of tryptophan.² It is estimated that in peripheral tissue 95% of tryptophan is metabolised to kynurenine **3** whilst less than 1% is metabolised to 5-hydroxytryptamine **2** (Figure 1.1).²

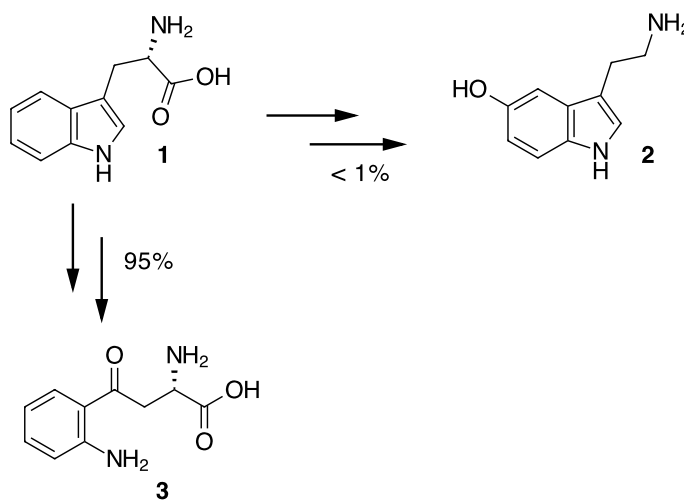
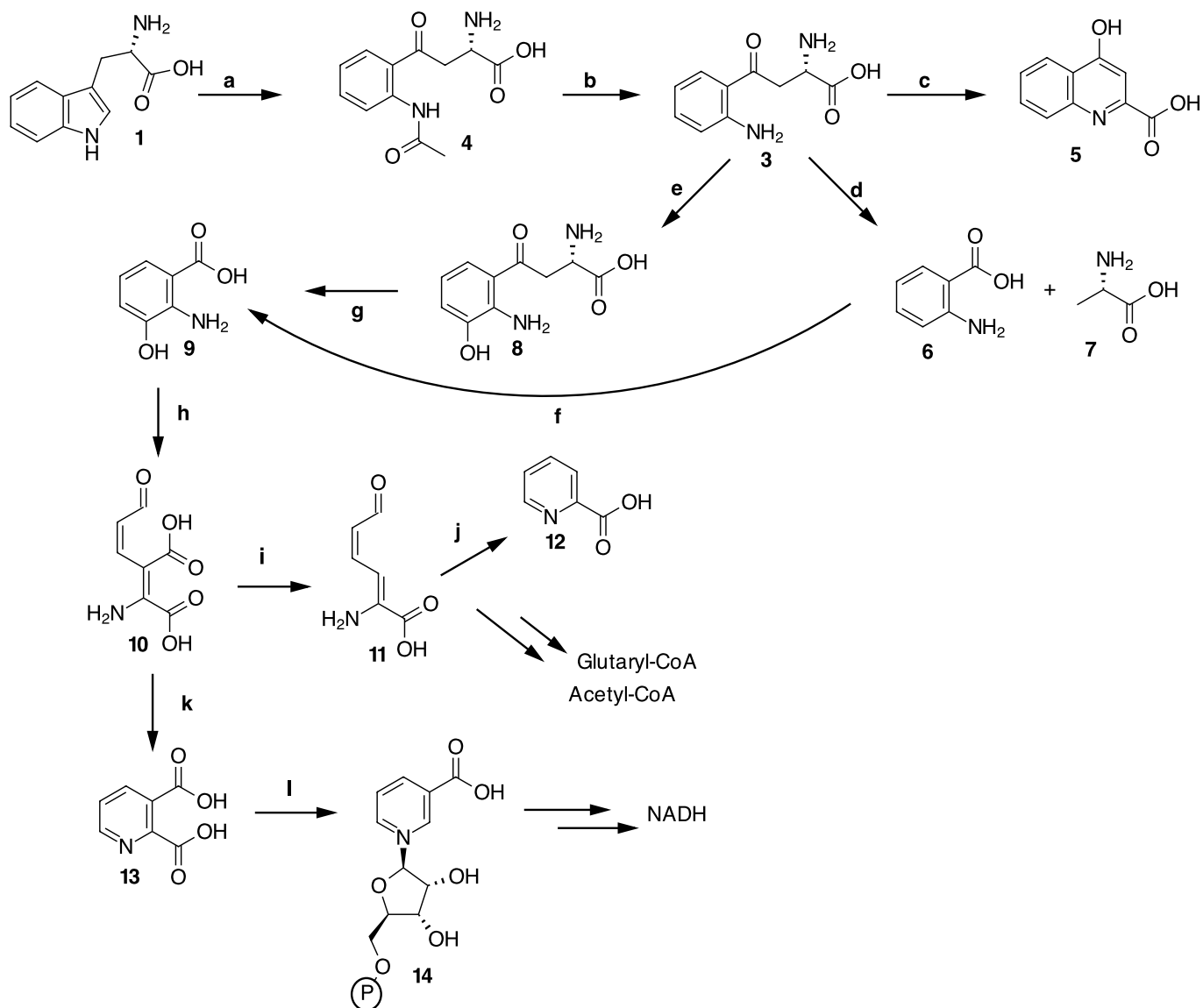


Figure 1.1. The majority (95%) of L-tryptophan is metabolised via the kynurenine pathway.

Interest in the kynurenine pathway increased when several of the catabolites were shown to be neurologically active. Quinolinic acid **13**, was shown to be an agonist of the NMDA receptor in 1981.³ The activation of the NMDA receptor by **13** leads to neurodegeneration.⁴ Shortly after this discovery in 1982, it was found that kynureninic acid **5** is an antagonist of the NMDA receptor.^{5, 6} A major research interest in the pathway involved altering the ratio of neurotoxic quinolinic acid **13** to neuroprotective kynureninic acid **5** through enzyme inhibition.⁴



Scheme 1.1. The kynurenine pathway: **a)** TDO or IDO, O_2 , haem; **b)** aryl formamidase, H_2O ; **c)** kynurenine aminotransferase, PLP; **d)** kynureninase, H_2O , PLP; **e)** kynurenine-3-monooxygenase (K3MO), FAD, NADH, O_2 ; **f)** non specific hydroxylation in the liver; **g)** kynureninase, H_2O , PLP; **h)** 3-hydroxyanthranilate 3,4-dioxygenase, O_2 , haem; **i)** aminocarboxymuconate-semialdehyde decarboxylase; **j)** non-enzymatic rearrangement; **k)** non-enzymatic rearrangement; **l)** quinolinate phosphoribosyltransferase.

The metabolism of tryptophan **1** *via* the kynurenine pathway, as illustrated in Scheme 1.1, commences with the oxidative cleavage of the indole C2-C3 carbon-carbon double bond by either tryptophan 2,3-dioxygenase (TDO) or indoleamine 2,3-dioxygenase (IDO). These haem-dependent enzymes use molecular oxygen

for this cleavage. The product of the reaction is formylkynurenine **4**, which is then hydrolysed by an aryl formamidase enzyme to give kynurenine **3**.^{2, 4}

At this point there is a branch in the pathway and kynurenine **3** has three distinct fates. The first is that kynurenine **3** is acted upon by kynurenine aminotransferase (KAT) to give kynurenic acid **5**. KAT catalyses a transamination reaction, using pyridoxal-5' phosphate (PLP) as a co-factor. Another PLP-dependent enzyme, kynureninase transforms kynurenine **3** into anthranilic acid **6** and alanine **7**. Anthranilic acid **6** is used in the biosynthesis of aromatic amino acids.² The third enzyme that catabolises kynurenine **3** is kynurenine-3-monooxygenase (K3MO). This FAD-dependent enzyme catalyses the selective oxidation of the phenyl ring of **3** to give 3-hydroxykynurenine **8**.^{2, 4}

Kynureninase also catalyses the cleavage of 3-hydroxykynurenine **8** to give 3-hydroxyanthranilic acid **9**. 3-Hydroxyanthranilic acid **9** can also be generated by the non-selective oxidation of anthranilic acid **6** by an, as yet, unknown enzyme.⁷ 3-Hydroxyanthranilic acid **9** is oxidatively cleaved by 3-hydroxyanthranilate 3,4-dioxygenase (3HAO), an iron dependent enzyme, to give 2-amino-3-carboxymuconate-semialdehyde **10**. 2-Amino-3-carboxymuconate-semialdehyde **10** has two fates. It is either decarboxylated by aminocarboxymuconate-semialdehyde decarboxylase (ACMSD) or it cyclises non-enzymatically, to quinolinic acid **13**.⁸ The decarboxylation by ACMSD gives amino-muconate-semialdehyde **11**, which can either undergo a non-enzymatic cyclisation to give picolinic acid **12** or it is further metabolised to glutaryl CoA and acetyl CoA. Quinolinate phosphoribosyl transferase (QPRTase) converts quinolinic acid **13** into nicotinic acid mononucleotide **14** and carbon dioxide.^{2, 4}

Under normal physiological conditions the majority of 2-amino-3-carboxymuconate-semialdehyde **10** formed is decarboxylated to **11**. Intermediate **10** had a half life of 33 mins in assays on bovine kidney 3HAO,⁹ which is long enough for decarboxylation by ACMSD. This means that under physiological conditions only a small amount of *de novo* NADH is made.¹⁰

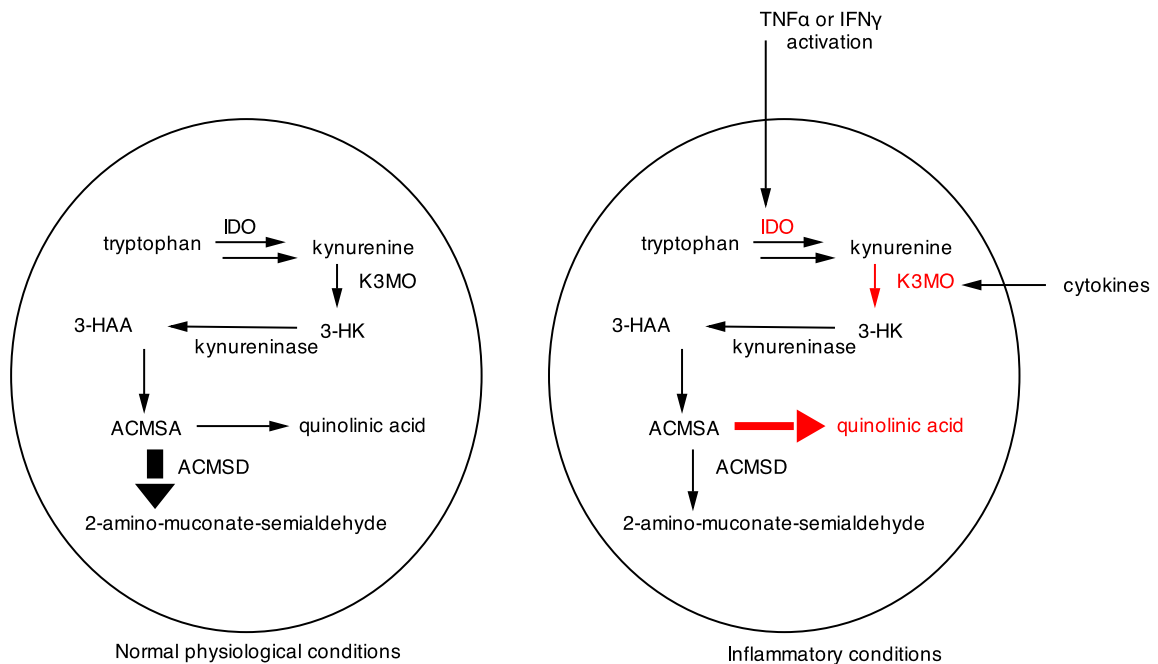


Figure 1.2. The effects that cytokines produce on the flux of the kynurenine pathway. (3-HK) = 3-hydroxykynurenine, (3-HAA) = 3-hydroxyanthranilic acid

However, under inflammatory conditions, pro-inflammatory cytokines interferon gamma ($\text{INF}\gamma$) and tumour necrosis factor alpha ($\text{TNF}\alpha$) activate IDO (Figure 1.2). This has the effect of increasing the metabolism of tryptophan *via* the kynurenine pathway. After lipopolysaccharide (LPS) injection into mice brains it was found that, 4 h after the injection, the expression of the K3MO gene was statistically reduced in the cortex but not in the hippocampus.¹¹ After 24 h the expression of the K3MO gene in both the cortex and hippocampus was increased. There was also an increase in pro-inflammatory cytokines 4 h post injection, in both the cortex and hippocampus and it has been proposed that these cytokines regulate the expression of K3MO.¹¹ The expression of K3MO in the brain appears to be tightly regulated.¹²

The kynurenine pathway has been linked to several neurodegenerative diseases including AIDS-related dementia, Huntingtons disease, Lyme disease and septicemia.² It is thought that quinolinic acid **13** has a role in all of these diseases.

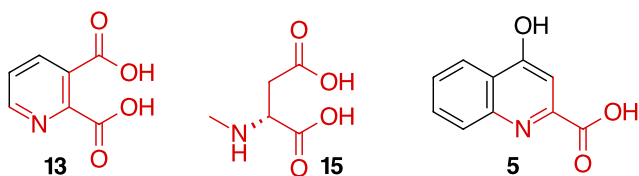


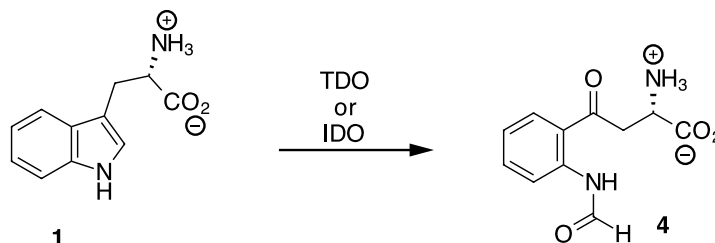
Figure 1.3. Comparison of quinolinic acid **13**, *N*-methyl-D-aspartic acid **15** and kynurenic acid **5**.

A comparison of the structures of quinolinic acid **13** and *N*-methyl-D-aspartic acid (NMDA) **15**, shows that quinolinic acid has a restricted conformation, and the dicarboxylic motif is similar to NMDA **15**. The binding mode of quinolinic acid **13** and NMDA **15** must be similar as both are agonists of the glutamate-NMDA receptor. Removal of the β -carboxylate appears to change the activity at the glutamate-NMDA receptor as kynurenic acid **5** is an antagonist of the NMDA receptor.

The following is a review of the enzymes that play a major role in certain human diseases such as AIDS related dementia, Huntingtons disease, schizophrenia and bipolar disorder. The enzyme mechanisms and known inhibitors will be discussed.

1.2 TDO and IDO

1.2.1 Biological and structural data for TDO



Scheme 1.2. The reaction catalysed by TDO or IDO.

Human TDO is a protein of 406 amino acids in length. It forms a tetramer¹³ with a molecular weight of ~190 KDa.¹⁴ The tetramer contains four haem units each capable of catalysing the oxidative cleavage of L-tryptophan **1**. TDO only catalyses the oxidative cleavage of L-tryptophan and derivatives e.g 6-fluoro-tryptophan, as illustrated in Scheme 1.2.¹⁵ TDO has less affinity for L-tryptophan than IDO with a K_m of 222 μ M, however, it has a similar K_{cat} .¹⁶ TDO is only found in the liver of humans.¹⁷

A protein crystal structure for TDO from the bacterium *Xanthomonas campestris* was obtained in 2007.¹⁵ Sequence alignment shows that human TDO and *X. campestris* enzymes have 34% sequence identity and it is thought that the key active site residues are conserved. Careful use of anaerobic conditions allowed the ferrous form of the enzyme to be crystallised with L-tryptophan bound at the active site. The oxidised ferric form of the enzyme has a much lower affinity for L-tryptophan. Interestingly the TDO monomer contains 12 α helices and no β -sheets.¹⁵

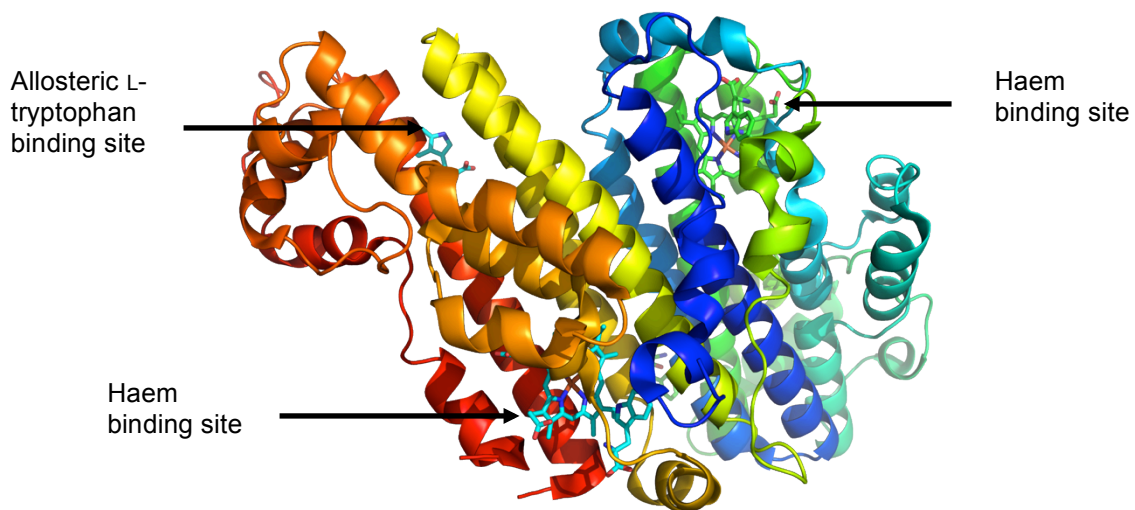


Figure 1.4. Crystal structure of dimeric *X. campestris* TDO, showing two haem-cofactors and L -tryptophan in the active site. L-Tryptophan can also be observed in an allosteric binding site.

The crystal structure revealed the binding site for L-tryptophan and its position relative to the haem units (Figure 1.4). The crystal structure shows the haem iron is five co-ordinate with His-240. This histidine that co-ordinates to the iron is conserved across all species.¹⁸ The indole ring has several hydrophobic interactions in the active site. The carboxylic acid of L-tryptophan has a hydrogen bonding interaction with Tyr-113 and an ion-pair interaction with Arg-117. It is thought that induced fit is important as changes in the orientation of the loops are visible when comparing the free and the substrate bound enzyme. Arg-117 has an alternative orientation in the free enzyme and it is proposed that substrate recognition by Arg-117 alters the shape of the active site allowing the substrate to bind.

There are four allosteric binding sites where four L-tryptophan molecules are located.¹⁵ The allosteric site is formed at the interfaces of the monomers. It is proposed that TDO is activated by allosteric binding of L-tryptophan.¹⁹

1.2.2 Biological and structural data for IDO

In humans there are two isoforms of IDO. IDO 1 is a monomeric protein with 403 amino acids and a molecular weight of ~45 kDa.²⁰ There is 21% sequence homology between human IDO 1 and human TDO. In 2007 a new gene with homology to IDO was found. Several groups have shown that the protein is able to metabolise tryptophan, and as such it has been named IDO 2.¹⁹ In humans IDO 1 is expressed in placenta, lung, small and large intestine, spleen, liver, kidney, stomach and the brain, whereas IDO 2 is mainly expressed in the kidneys but is also found in the testicles and liver. In humans IDO 1 and IDO 2 genes are found beside each other on chromosome 8. It has been suggested that these genes arose *via* gene duplication. IDO and IDO 2 have a more similar amino acid sequence with 44% sequence homology.

The K_m of IDO for L-tryptophan is ~20 μ M.²⁰ This high affinity allows the enzyme to deplete the local environment of L-tryptophan. It has been proposed that the rapid depletion of L-tryptophan is a mechanism for tumour evasion from the immune system. Several of the downstream metabolites of kynurenine were able to modulate the immune system by preventing T-cell proliferation.²¹ IDO oxidises several indoleamine substrates, e.g. 5-hydroxytryptamine, as well as D- and L-tryptophan.²

IDO is naturally regulated in the body by nitric oxide.²² IDO and nitric oxide synthase (NOS) are often induced at the same time. It is not clear what occurs when IDO and NOS are induced in the same cell.

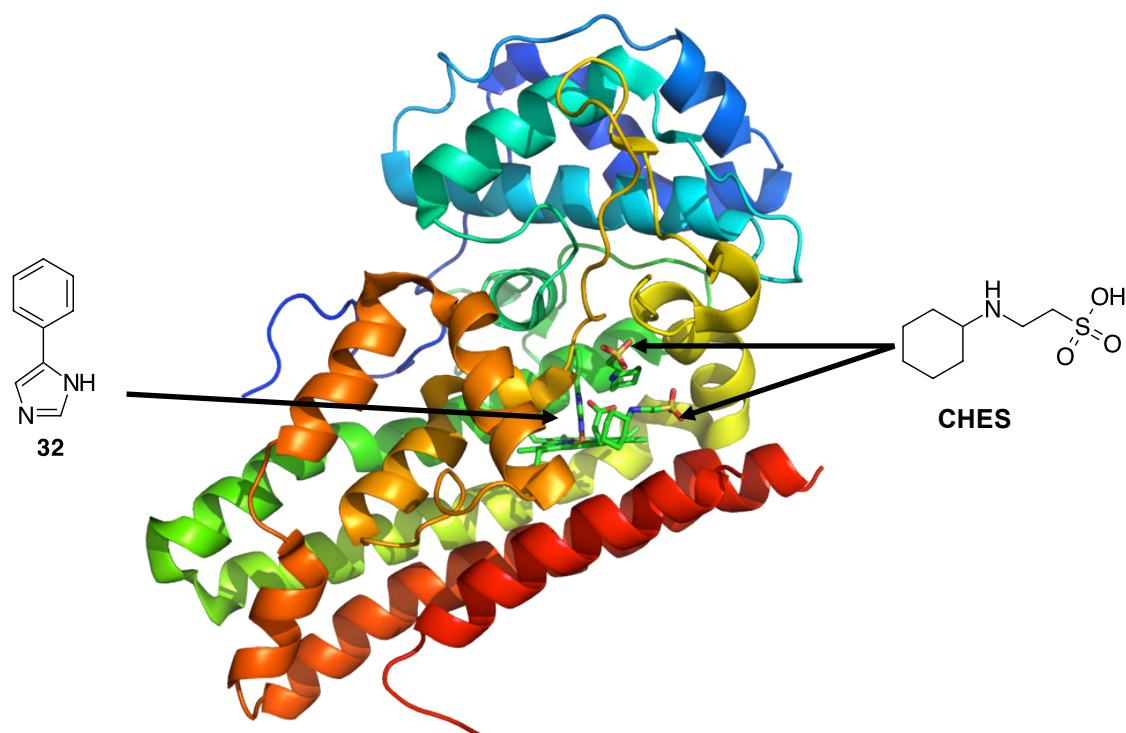


Figure 1.5. Crystal structure of monomeric IDO with phenylimidazole **32** and CHES bound in the active site.

A crystal structure for the human form of IDO was obtained in 2006²³. Crystals were obtained with phenylimidazole (an inhibitor of the enzyme) and cyanide bound at the active site at resolutions of 2.3 Å and 3.4 Å respectively. The crystal structure showed that IDO is a monomer, which folds into two distinct domains, a large and a small domain (Figure 1.5). The structure shows that His-346 is bound to the haem iron. Two molecules of *N*-cyclohexyl-2-aminoethanesulfonic acid (CHES) from the crystallisation buffer were observed in the active site entrance of both structures.

The active site has a large number of hydrophobic side chains with only one polar residue (Ser-167). It appears that Phe-163 makes π - π interactions with the bound phenylimidazole.

Mutants F226A and F227A showed much lower dioxygenase activity.²³ The crystal structure shows that both L-phenylalanine side chains are orientated into the active site. It is likely that they have key π - π interactions when L-tryptophan is bound.

Mutant R231A also had reduced dioxygenase activity, providing evidence for the role of Arg-231 for binding L-tryptophan.²³

1.2.3 TDO and IDO mechanistic information

The mechanisms of TDO and IDO are still not clear after 40 years of study. It is proposed that IDO and TDO use similar chemical mechanisms to carry out their oxidative cleavages. They may have a close evolutionary relationship.

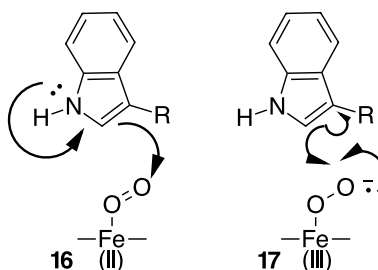
Both IDO and TDO require Fe in the ferrous (Fe^{II}) state to catalyse the oxidative cleavage of L-tryptophan. The ferrous-oxy complex for TDO has not been observed. It has been argued that the complex will be unstable and shortlived. It was not possible to determine whether substrate binding stabilises the complex, as this leads to turnover.¹⁶ This observation is consistent with TDO requiring L-tryptophan to bind before molecular oxygen binds. On the other hand, IDO can bind oxygen freely and as such the IDO haem is readily oxidised to the ferric (Fe^{III}) form. TDO shows more resistance to autoxidation than IDO.

IDO and TDO need to be kept in the reduced ferrous (Fe^{II}) form *in vivo* to be catalytically active. Numerous agents have been suggested as the *in vivo* reducing agents including superoxide, flavin mononucleotide and cytochrome b5.¹³ Interestingly activity of IDO is diminished in the presence of superoxide dismutase suggesting that IDO is reduced by superoxide.¹³

In the crystal structure of TDO from *X. campestris* there is a distal histidine residue (His-55) that forms hydrogen bonds to the indole proton on N-1. This has led to the suggestion that deprotonation of the indole nitrogen is relevant for the mechanism. However, several studies have argued against this for TDO and IDO. Whilst TDO has a distal base in the active site, human IDO has no such distal base. The position of (His-55) in TDO is replaced by a serine residue in IDO. Without an active site base it was proposed that proton abstraction of the indole proton by the bound oxygen was a relevant mechanism. Mutagenesis studies on *X. campestris* TDO have shown that the H55A mutant was still catalytically active, but

at a much lower level ($k_{\text{cat}} \sim 10\%$ of wild type).²⁴ This suggests that His-55 is not acting as a base but merely holds tryptophan in the correct orientation for the oxidative cleavage.

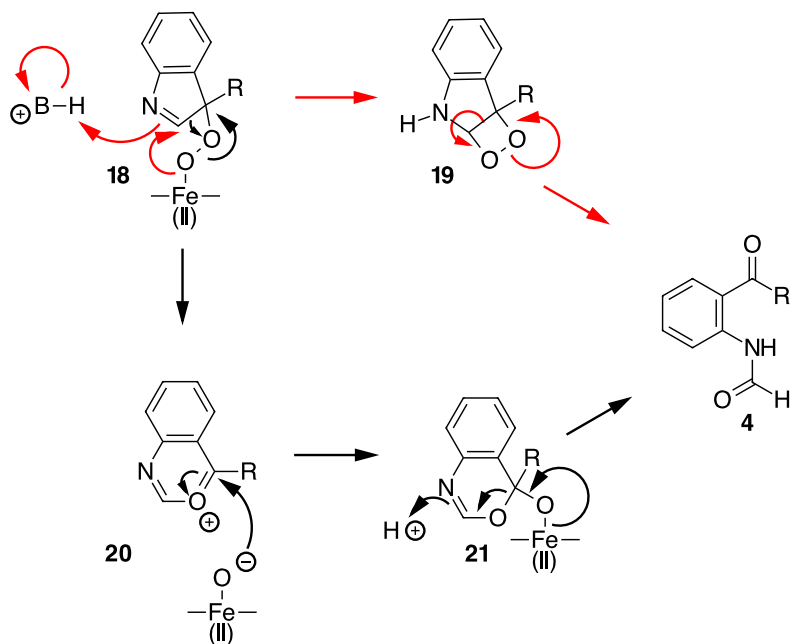
In 1991 it was shown that *N*-methyl tryptophan is an inhibitor of IDO.²⁵ It was proposed that inhibition of the enzyme was due to the inability to form an L-tryptophan anion. As there was no turnover with *N*-methyl tryptophan as a substrate a reaction mechanism involving singlet oxygen was ruled out.



Scheme 1.3. The proposed mechanisms for the initiation of oxidative cleavage of tryptophan: **16** Nucleophilic attack on the bound oxygen; **17** a radical process for catalysis.

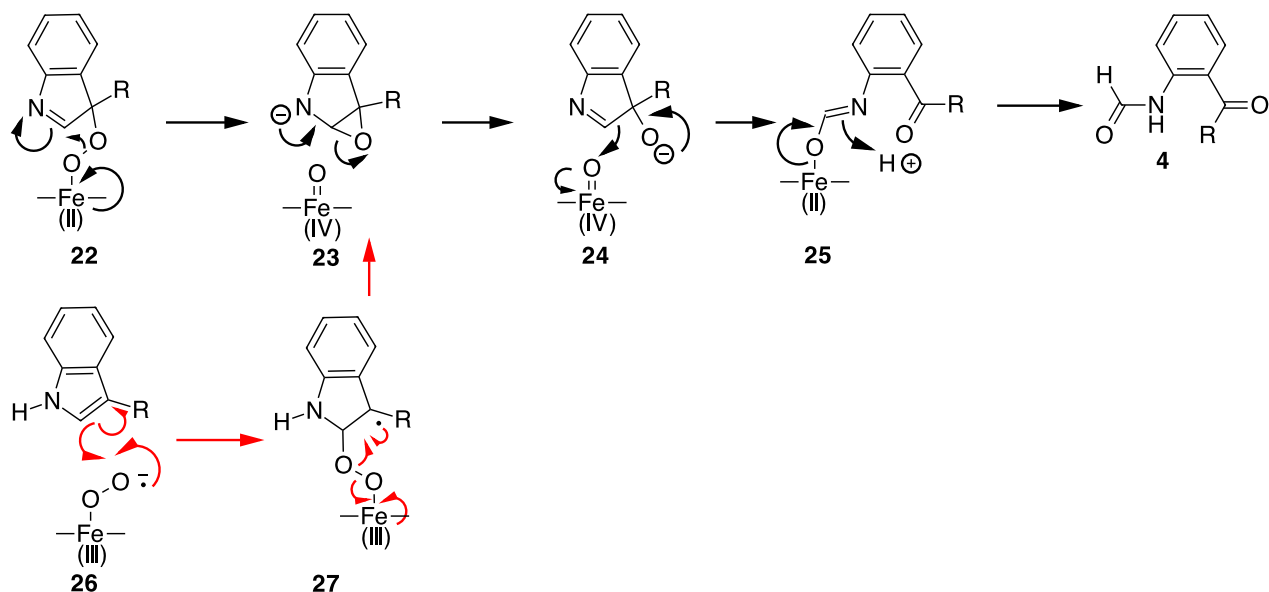
However, recent LC-MS work has shown that *N*-methyl tryptophan is a substrate for human IDO and histidine-mutants of human and *X. campestris* TDO. When His-55 is mutated there is room for *N*-methyl tryptophan to bind as a substrate. The fact that human IDO and the mutant TDO can turnover *N*-methyl tryptophan rules out the possibility of a base catalysed proton abstraction as a starting point in the mechanism.²⁶ As a result of this work two alternative mechanisms for initiation of catalysis by TDO and IDO have been proposed, as illustrated in Scheme 1.3.

The first mechanism, envisages the indole ring as a nucleophile in an electrophilic aromatic substitution at C-3 with the bound oxygen. An alternative mechanism has been investigated using computational chemistry, which proposes that the oxygen attacks C-2 in a radical process.



Scheme 1.4. Dioxetane (red) and Criegee (black) mechanism were initially proposed for TDO and IDO.

Criegee²⁷ and dioxetane mechanisms²⁸ have been proposed for the formation of the final product (Scheme 1.4). However, there is no experimental evidence for either mechanism. Criegee mechanisms are known to occur in enzymology.²⁹



Scheme 1.5. Alternative mechanisms for the production of tryptophan by IDO and TDO.

Computational studies do not support either of these mechanisms.³⁰ The dioxetane appears to be thermodynamically unfavourable. The breakdown of the

dioxetane would also be very exothermic and the expected emission of light has never been observed. Computational studies support epoxide formation,³⁰ as illustrated in Scheme 1.5. This could either be a radical or an ionic process. There is discussion on whether the protonated amine of the amino acid plays a role in the epoxide ring opening, although none of this has experimental evidence.^{30, 31}

1.2.4 IDO inhibitors

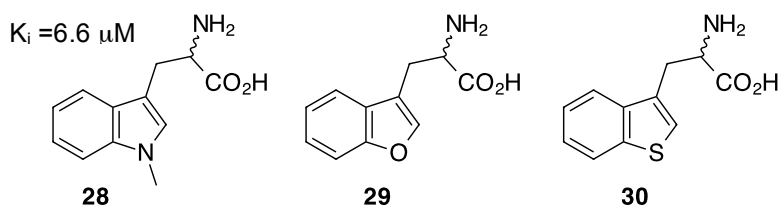


Figure 1.6. 1-Methyl-DL-tryptophan **28** and furan and thiophene analogues of tryptophan **29** and **30**.

IDO has been implicated as a key protein in the evasion of tumours from the immune system. Work by Munn *et al.* showed that IDO plays a central role in protecting foetuses from their mothers immune system during pregnancy.³² IDO expression has been found in patients with ovarian carcinoma, hepatocellular carcinoma, invasive cervical carcinoma, non-small lung carcinoma, colon carcinoma and endometrial carcinoma.³³ The discovery that the substrate analogues 1-methyl-DL-tryptophan **28** and the oxo-**29** and thio-**30** derivatives of tryptophan inhibit IDO (**28** with a K_i of $6.6 \mu\text{M}$) has led to **28** being used to study the role of IDO in immune escape (Figure 1.6).²⁵ Interestingly the D-isomer of 1-methyltryptophan **28** has entered clinical trials. IDO has a greater affinity for L-tryptophan and thus it is expected that the L-isomer of 1-methyltryptophan **28** would have the greatest chemotherapeutic effect. Whilst 1-methyl-D-tryptophan **28** showed inhibition of IDO in some cells, poor inhibition against the purified enzyme was puzzling. This was resolved with the identification of IDO 2 as the main target for 1-methyl-D-tryptophan **28**.³⁴ 1-Methyl-D-tryptophan **28** in conjunction with a chemotherapeutic agent showed a greater effect than the L-isomer, in *in vivo*

preclinical testing.³⁵ It has been proposed that IDO2 is more important in immune escape than IDO.

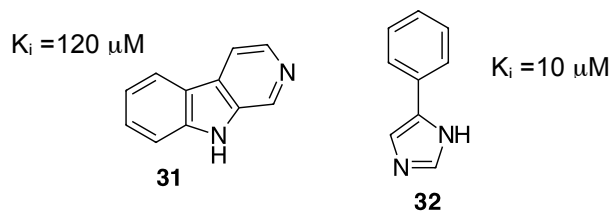


Figure 1.7. Norharman **31** and 4-phenylimidazole **32** are uncompetitive inhibitors of IDO.

Norharman **31** was the first organic inhibitor of IDO discovered (Figure 1.7). It was found to be an uncompetitive inhibitor with a K_i of 120 μM .³⁶ Further investigation of norharman **31** revealed that it competes with oxygen in binding to the haem in its ferrous form.³⁷ 4-Phenylimidazole **32** was also discovered as an uncompetitive inhibitor of IDO with a K_i of 10 μM .³⁷ Unlike norharman **31**, 4-phenylimidazole **32** preferentially binds to the inactive ferric form of the enzyme.

A number of IDO inhibitors are natural products, or their derivatives.

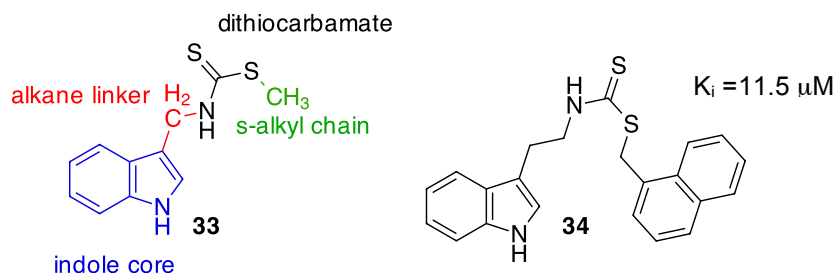


Figure 1.8. Brassinin **33** highlighted where alterations were made and its most potent analogue **34**.

Brassinin **33** is a natural product obtained from cruciferous plants. It is a phytoalexin, which is a modest inhibitor of IDO (K_i of 98 μM). A study into the structure-activity relationship of brassinin analogues was undertaken by Gaspari *et al.*³⁸ (Figure 1.8)

Altering the aromatic indole core was generally well accepted by the enzyme. Changing the indole to a single aromatic ring was also well accepted. The most surprising observation was that complete removal of the aromatic system was tolerated. The enzyme tolerated replacement of the aromatic ring with the bulky

adamantyl group, although the affinity for IDO was lower than brassinin (K_i of 179.6 μ M). Increasing the alkane chain length improved the inhibition, with the propyl linker being optimal. However, when the alkyl linker and S-alkyl chain were both modified, extension of the alkyl linker did not increase inhibition. Changes to the thiocarbamate reduced or totally destroyed inhibition of IDO. Alterations to the S-alkyl chain produced the most potent analogue of brassinin, **34** (Figure 1.8). Increasing the S-alkyl chain length did not improve inhibition, however, the introduction of aromatic rings did, indicating that the S-alkyl chain was binding into a large hydrophobic pocket.³⁸

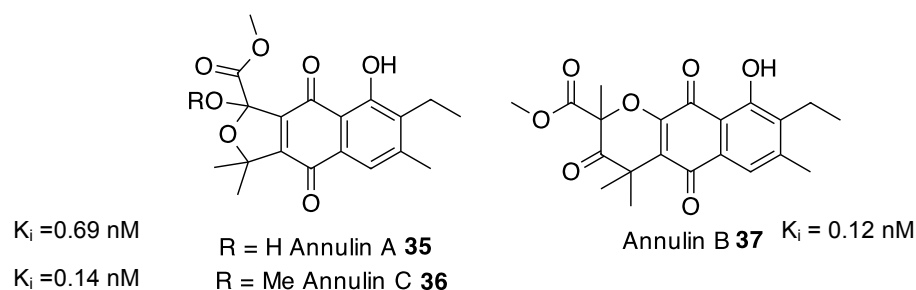


Figure 1.9. The annulin family are potent inhibitors of IDO.

Several polyketides isolated from the marine hydroid *Garveia annulata* are IDO inhibitors.³⁹ The most potent series of compounds against IDO were annulins **35-37**. Annulin B **37** and C **36** show strong inhibition with a K_i of 0.12 and 0.14 nM, respectively. Annulin A **35** is less potent with a K_i of 0.69 nM. However, in a yeast based study, the annulins did not inhibit IDO, suggesting that the annulin family are too polar to pass through the cell membrane.³⁹

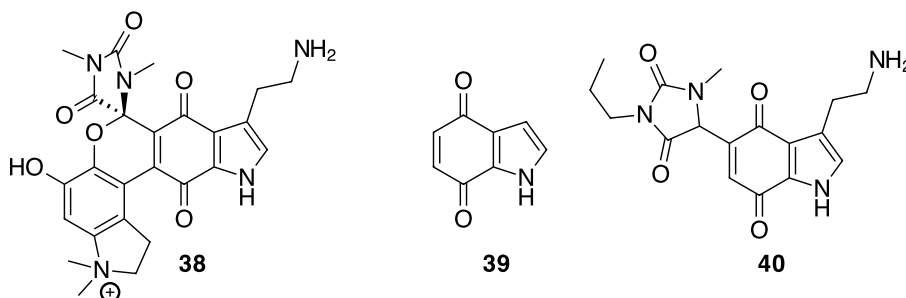


Figure 1.10. Exigauamine A **38** is a potent IDO inhibitor ($K_i = 41 \pm 3$ nM), analogue studies showed **39** and **40** ($K_i = 190 \pm 20$ nM and 200 ± 10 nM respectively) to be less potent than **38** but much more readily accessible.

Exiguamine A **38**, a marine natural product isolated from the sponge *Neopetrosia exiguais*, is a potent IDO inhibitor⁴⁰ (Figure 1.10). As the natural product is relatively complex, a structure activity relationship was explored. The hypothesis that the tryptamine quinone motif is key to IDO inhibition was tested. This was confirmed when unsubstituted indole quinone **39** was assayed against IDO showing a K_i of 190 nM. However, as **39** is likely to have off-target effects, the hydantoin moiety was reintroduced, with compound **40** showing good inhibition with a K_i of 200 nM. As analogue **40** is readily accessible and shows good inhibition of IDO it has emerged as an important tool for understanding the role IDO plays in immune escape and other diseases.⁴¹

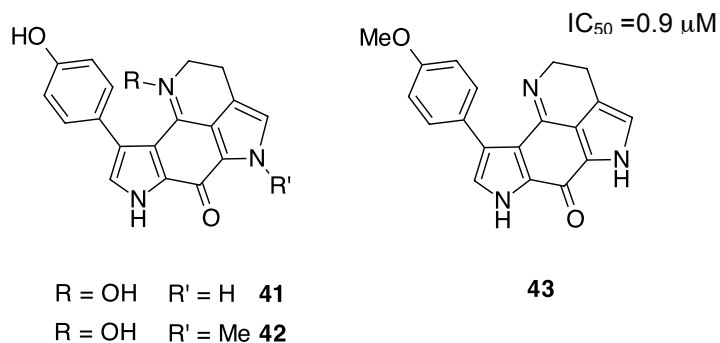


Figure 1.11. Tsitsikammamine family of natural products and the analogue **43** developed as an IDO inhibitor.

The tsitsikammamine family of alkaloids **41** and **42** have been isolated from South African sponges.⁴² Due to their activity against cancer cells⁴³ and their structural similarity to Exiguamine A **38**, a series of tsitsikammamine analogues were synthesised and tested against isolated and purified human IDO and in a whole cell assay. The assays proved that the compounds were inhibiting IDO and not interacting with the external reductant, methylene blue.⁴⁴ The whole cell assay also allowed an evaluation of how easily the compounds passed through the cell membrane. Analogue **43** (as shown in Figure 1.11) was a potent inhibitor of isolated IDO ($\text{IC}_{50} = 0.9 \mu\text{M}$), however, inhibition in the whole cell assay was poor in comparison with other analogues.⁴⁴

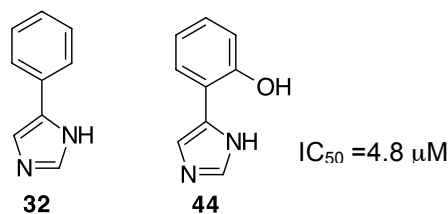


Figure 1.12. Structural relationship activity investigation into 4-phenylimidazole **32** gave analogue **44** as the most potent compound in the series.

Starting from the co-crystal structure obtained with 4-phenylimidazole **32** bound to IDO, analogues were prepared to improve inhibition of this motif.⁴⁵ The investigation focused upon improving binding at the active site entrance, the interior of the active site and the heme iron. Interactions with the entrance of the active site were probed by altering substitution on the imidazole ring. Binding in the active site was probed by varying substitution on the phenyl ring. Interactions of the imidazole ring with the heme iron were probed by changing the heterocycle and the effect of electronic changes caused by substitution of the phenyl ring was explored.⁴⁵

Substitution at *N*-1 and *C*-2 of the imidazole ring was ineffective, whereas substitution at *N*-3 was tolerated. *In silico* docking experiments predicted hydrogen bonding interactions at the 2- and 3- positions of the phenyl ring and possible disulfide linkages between thiol substituted phenyl rings and IDO. The most potent inhibitor was the 2-hydroxy substituted phenylimidazole **44** (Figure 1.12), which had an IC_{50} of 4.8 μM . The 3- and 4- thiols also showed good inhibition of IDO with IC_{50} 's of 7.6 μM and 7.7 μM respectively.⁴⁵

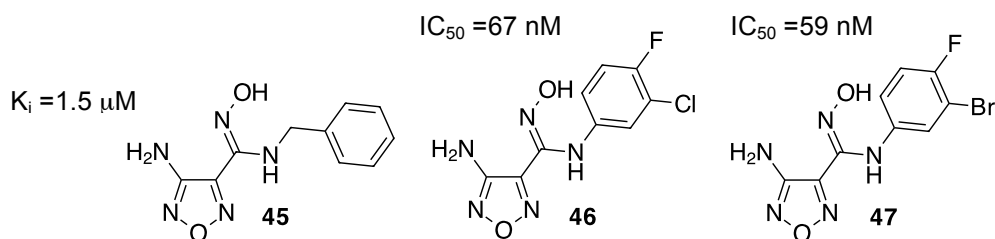


Figure 1.13. High throughput screening revealed **45** as a potent inhibitor of IDO. Investigations into the structural activity relationship yielded **46** and **47**, as very potent inhibitors of IDO.

Identification of 4-amino-1,2,5-oxadiazole-3-carboximidamide **45** as a low micromolar inhibitor of IDO in a high throughput screen led to the development of improved inhibitors after structure activity relationship studies.⁴⁶ Inhibitor **45** had good selectivity for IDO over TDO. Changes to the hydroxylamidine functional group led to complete loss of inhibition against IDO. It was proposed that this moiety was important as it forms a dative bond to the haem iron. Changing the benzyl for a phenyl group generated further potent compounds. There was a clear preference for *meta*-substitution with halogens and small alkyl groups. The addition of a fluorine atom at the *para*-position alongside a *meta*-chlorine or bromine substitution provided the most potent compounds of this series **46** and **47** with IC₅₀'s of 67 nM and 59 nM respectively. The addition of the fluorine atom at the *para* position lowers the clearance of these compounds *in vitro*, presumably by preventing metabolism at the *para* position.⁴⁶

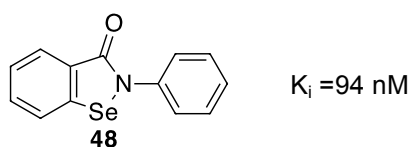


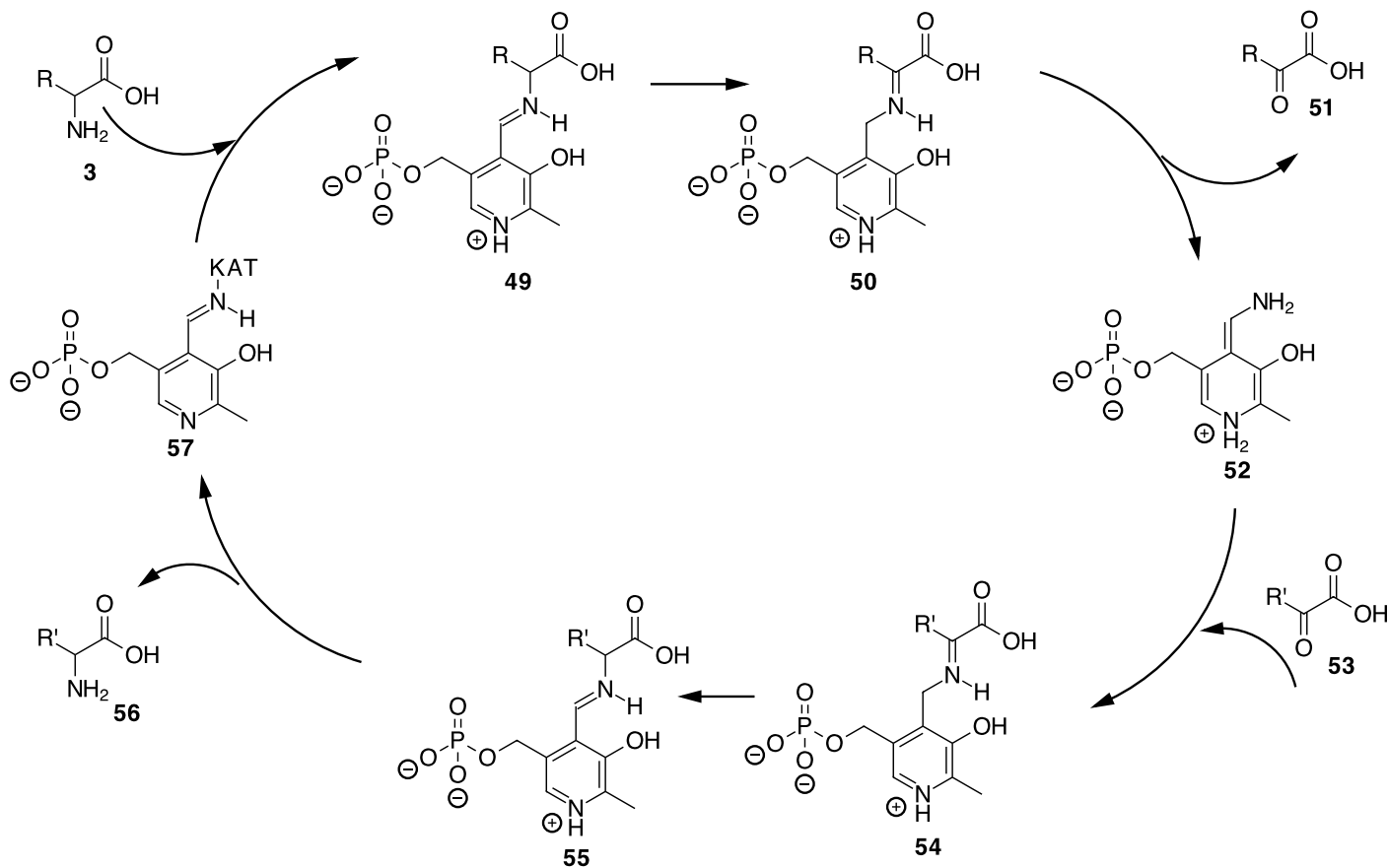
Figure 1.14. Ebselen **48**, a potent inhibitor of IDO.

The selenium based heterocycles ebselen (2-phenyl-1,2-benzioselenazol-3(2H)-one) **48** was a potent inhibitor of IDO with a K_i of 94 nM.⁴⁷ Through elegant mechanism studies it was shown that ebselen reacts with the cysteine residues in IDO and prevents IDO catalysis.⁴⁷ The number of cysteine residues that react was dependent upon the dose of ebselen delivered. It was thought that covalent modification with ebselen perturbs the three dimensional structure of IDO making the protein unstable.⁴⁷ As ebselen **48** is a strong electrophile, it will react with endogenous glutathione lowering its potential as an IDO drug, but it remains a powerful tool for understanding the role IDO plays in disease models.

1.3 Kynurenine aminotransferase

1.3.1 Kynurenine aminotransferase biology and structural data

Kynurenine aminotransferase (KAT) is a member of the PLP-dependent aminotransferase enzymes. It catalyses the reaction of kynurenine **3** to the α -keto acid **51** with concomitant formation of an amino acid from an alternative keto acid.



Scheme 1.6. A general scheme showing the catalytic cycle of KAT.

There are four different enzymes that all have kynurenine aminotransferase activity: KAT I, also known as glutamine transaminase k or cysteine conjugate beta-lyase⁴⁸; KAT II, also known as aminoadipate aminotransferase⁴⁸; KAT III, also known as cysteine conjugate beta-lyase II⁴⁸ and KAT IV, also known as glutamic-oxaloacetic transaminase or mitochondrial aspartate aminotransferase.⁴⁸ In humans KAT I and KAT III have the highest sequence identity of 52%. All of the

KAT enzymes can be found in the mitochondria, but only KAT I and II have been observed in the cytoplasm.⁴⁸

KAT I is an enzyme that has many functions. As well as converting kynurenine to kynurenic acid it also has cysteine conjugate beta lyase activity. The enzyme is most active against large, neutral or aromatic and sulfur containing amino acids. It can also employ a number of keto acids as amino group acceptors.⁴⁸ KAT I is mostly expressed in the liver and kidney in humans and rats.⁴⁹

KAT II, like KAT I has many functions, however, it is more selective than KAT I. It uses aminoadipate, kynurenine, L-methionine and L-glutamate. Unlike KAT I, it is not able to use a large range of keto acids as amino group acceptors.⁴⁸ It is thought that in mammalian brains KAT II is responsible for the majority of kynurenic acid production.⁵⁰ In KAT II knockout mice the levels of kynurenic acid in the brain is low in young mice but recovers as they mature. This suggests that one of the other enzymes is upregulated to increase kynurenic acid production.⁵¹

KAT III is present in rat, mouse and human brains as determined by studies on the mRNA levels and protein activity assays.^{48, 52} The enzyme is able to use aromatic and sulfur containing amino acids and a selection of 13 α -keto acids in the transamination reaction.⁴⁸

KAT IV was initially reported as a mitochondrial aspartate aminotransferase in *E. coli*⁵³ before being found in rat, mouse and human mitochondria.⁵⁰ As the enzyme had activity with kynurenine it was called KAT IV. As well as an involvement in kynurenic acid synthesis, KAT IV allows glutamate to enter the citric acid cycle. It is able to produce the neurotransmitter glutamate and it plays a role in the malate-aspartate shuttle, which is important for the ATP production in the brain.⁴⁸

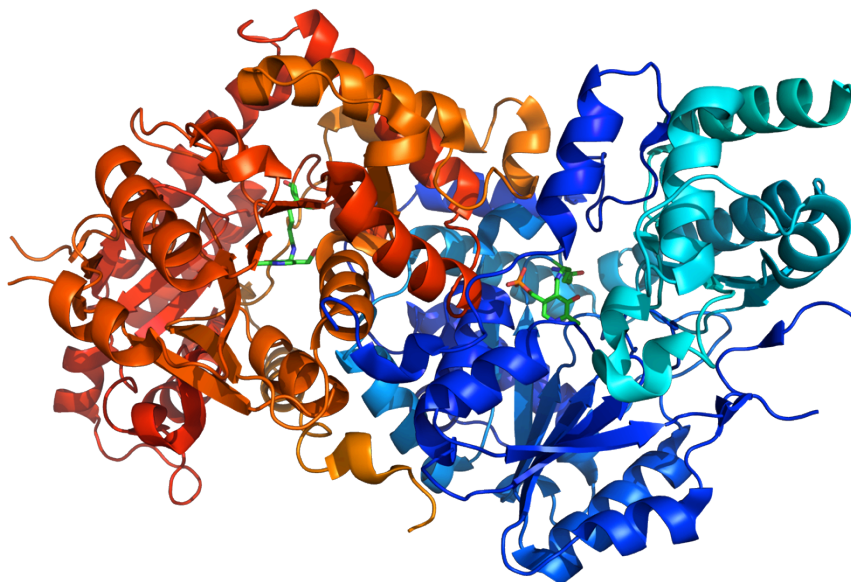


Figure 1.15. The crystal structure of KAT I with the PLP as the internal aldimine.

Crystal structures of KAT I⁵⁴ (Figure 1.15) and KAT II^{55, 56} (Figure 1.16), from humans, have been obtained. KAT III from mice⁵⁷ was successfully crystallised and a structure solved. There has been no human crystal structure of KAT IV reported, but structures from chicken and mice⁵⁸ have been obtained.

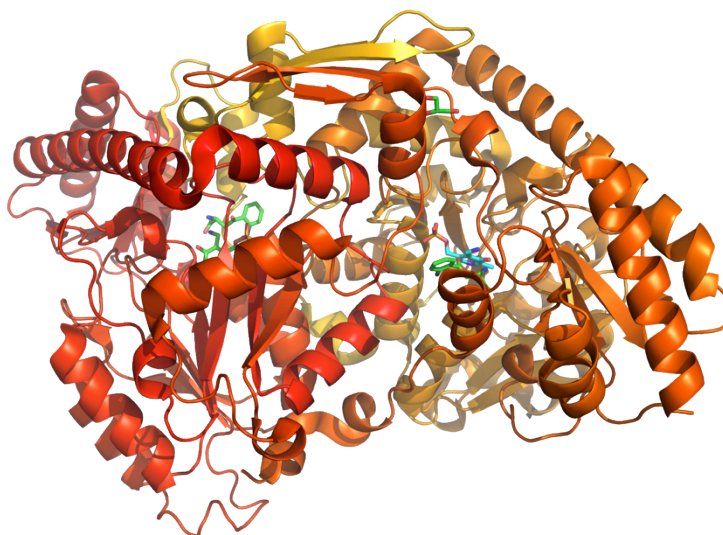


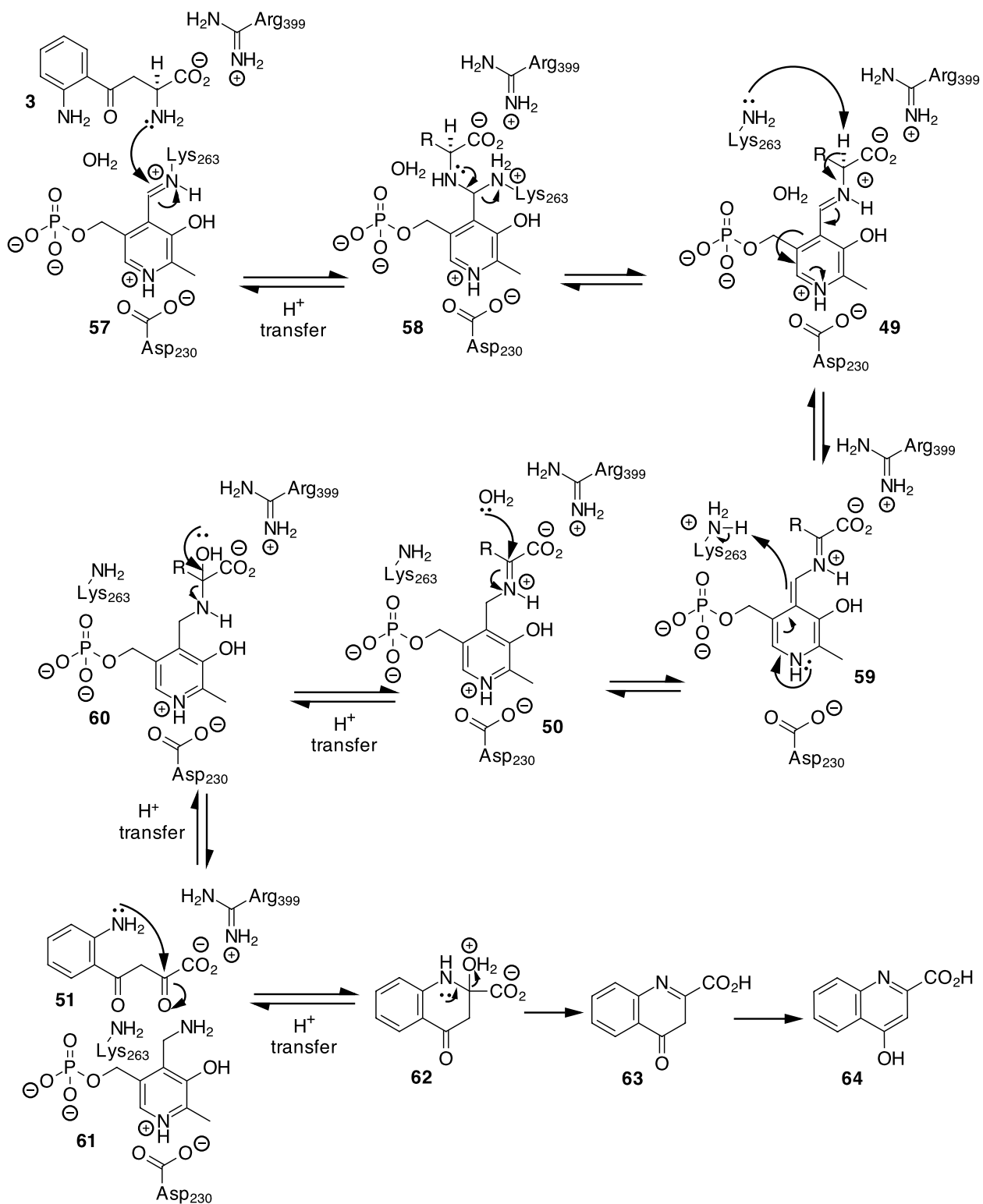
Figure 1.16. The crystal structure of KAT II was obtained with L-kynurenine bound at the active site.

The crystal structure of human KAT I was solved to 2.0 Å, with the enzyme in both PLP and PMP forms.⁵⁴ The crystal structure of human KAT II has also been solved. It was not possible to build a three dimensional model of KAT II, from KAT I as there is poor sequence alignment (11%) between the two enzymes. Work by two different groups generated three crystal structures of human KAT II, which were published concurrently in 2008.^{55, 56}

1.3.2 Kynurenine aminotransferase mechanism

The mechanism of kynurenine aminotransferases has not been well studied. A combined quantum mechanical and molecular mechanical modelling study was undertaken using the crystal structure of KAT II.⁵⁹ KAT II was used as the availability of both substrate bound and unbound structures meant that the substrate did not require modelling into the active site.⁵⁹

A proposed mechanism is illustrated in Scheme 1.7.



Scheme 1.7. A proposed mechanism of KAT.

1.3.3 Kynurenine aminotransferase inhibitors

Inhibition of KAT is important for investigation of the neuroprotective properties of kynurenic acid. It is also important as a number of diseases are associated with high levels of kynurenic acid. High concentrations of kynurenic acid have been found in the cerebral spinal fluid of schizophrenic patients and patients suffering from bipolar disorder.⁶⁰⁻⁶²

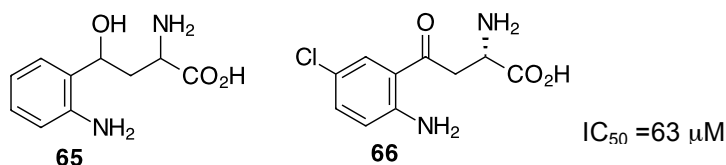


Figure 1.17. Kynurenine analogues were tested as KAT inhibitors, the L-isomer of **66** was the most potent inhibitor.

A series of kynurenine analogues were prepared by Varasi *et al.* to build a structure activity relationship for kynurenine aminotransferase (Figure 1.17).⁶³ Modification to the aniline group or to the acylalanine moiety, shown in **65**, was ineffective, suggesting that both structural features are required for substrate-like inhibition. A series of racemic kynurenines with alternative chlorine substitutions on the phenyl ring showed that KAT inhibition was most potent with the 5-chloro **66** and 6-chloro substituted kynurenines. Synthesis and subsequent assay of enantiopure 4-chloro kynurenine and 5-chloro kynurenine showed that the L-isomers were the most potent of the enantiomers. 5-Chloro-L-kynurenine **66** had an IC_{50} of 63 μ M against KAT. A series of alterations to the substitution at the 5-position provided inhibition of KAT in all cases. Both racemic 5-bromo-kynurenine and 5-*n*-propyl-kynurenine had similar inhibition to racemic 5-chloro-kynurenine. When 4-chloro-L-kynurenine and 5-chloro-L-kynurenine **66** were incubated with KAT, formation of 7-chloro-kynurenic acid and 6-chloro-kynurenic acid was observed. As 5-chloro-kynurenine **66** is a tighter binder to KAT, unsurprisingly, the production of 6-kynurenic acid was higher than 7-kynurenic acid.⁶³

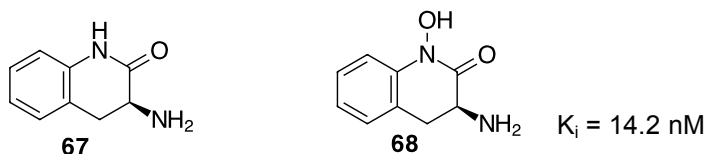


Figure 1.18. A high throughput screening revealed lactam **67** as a hit. Further testing showed it was the impurity **68** that actually inhibits KAT II.

A high throughput screen of compounds against KAT II revealed aminodihydroquinolone **67** as an interesting hit.⁶⁴ Further investigation showed that authentic **67** did not inhibit KAT II, but the inhibitor was an impurity (Figure 1.18). Through co-crystallisation with KAT II and elegant ¹³C NMR experiments it was shown that **68** is an irreversible inhibitor that forms an enamine adduct with the enzyme. Inhibitor **68** had good selectivity for KAT II over KAT I, KAT III and KAT IV. KAT II is hypothesised to play the major role in kynurenic acid biosynthesis in mammalian brains. Investigation into the stereochemistry of the 3-amino group showed that the *S*-enantiomer was approximately ten times more potent than the *R*-enantiomer.⁶⁴ Alterations to the hydroxamic acid moiety removed inhibition. Investigation into different substitutions on the aromatic ring revealed that small substituents at C-5 and C-8 (e.g. fluorine) are tolerated, however, none of the substituted analogues were as potent as the original hit. Substitution at C-6 and C-7 was accepted by the enzyme and gave an inhibition profile similar to **68**. Pharmacokinetic studies proved that **68** can pass through the blood brain barrier and reduced kynurenic acid levels in rats.⁶⁴

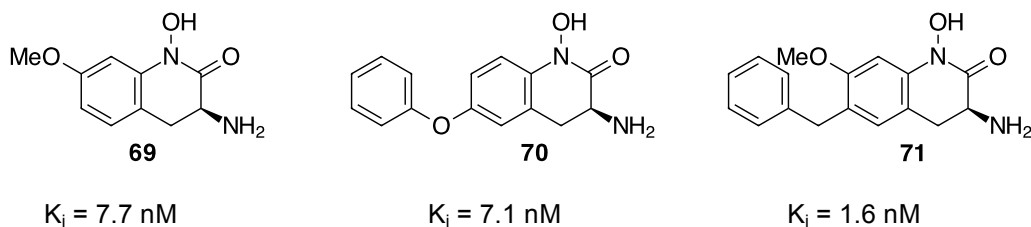


Figure 1.19. Further development of lactam **68** led to an increase in potency. Crystal structural data led to the development of **71**.

Further studies on the hydroxamate scaffold were undertaken with alterations at the C-6 and C-7 positions (Figure 1.19).⁶⁵ The introduction of the methoxy group at C-7 gave **71**, which had a similar IC_{50} to **68** but a higher K_{inact}/K_i . Co-crystal

structures with **69** and **70** bound revealed previously unseen lipophilic interactions. Compound **71** was prepared as a hybrid of both analogues. The phenoxy ether was changed to the benzyl moiety to prevent the formation of reactive catechol metabolites. Inhibitor **71** showed a 4-fold increase in potency as observed by K_{inact}/K_i . Administration of **71** to rats showed that there was a high degree of non-specific binding in the brain, however, **71** lowers the kynurenic acid levels over a longer time period than **68** at the same dose. The poor pharmacokinetics of **71** lowered its period of *in vivo* efficacy.⁶⁵

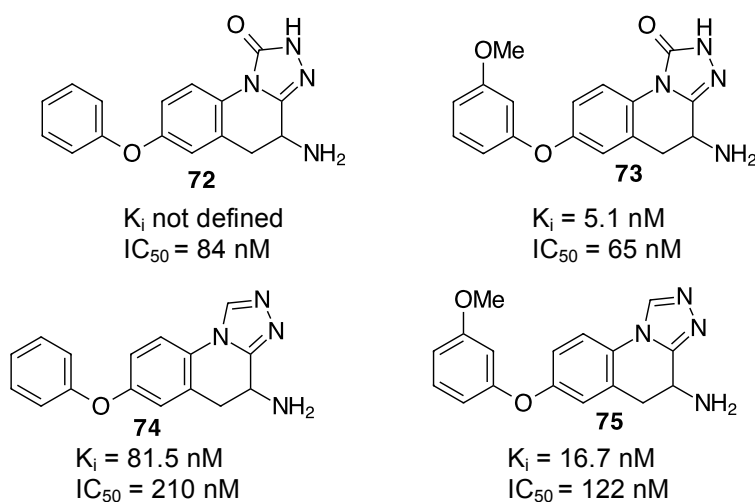


Figure 1.20. The development of triazolines **72** and **73** and triazoles **74** and **75**, to improve the pharmacokinetics of the hydroxamate scaffold.

As **68** was cleared quickly in human hepatocytes and liver microsomes as the O-glucoronide, further analogues **72-75** were synthesised with the aim of maintaining KAT inhibition whilst improving the pharmacokinetics of the compounds (Figure 1.20).⁶⁶ Analysis of the crystal structure of **68** bound to KAT II led to the identification of key interactions, including the amine-PLP interaction that leads to formation of an enamine and the hydrogen bond interactions of the hydroxamate moiety to Arg-399 and Asp-202. Modeling studies⁶⁶ suggested that a triazole or triazoline heterocycle could mimic the hydroxamate moiety. The triazoline analogues **72** and **73** had an increased IC_{50} (84 and 60 nM respectively), although **73** has a lower K_i than **68** showing that it binds more tightly in the active site. The triazoles **74** and **75** were less effective with IC_{50} s' of 201 nM and 122 nM

respectively. A co-crystal of **72** with KAT established that the triazoline was fulfilling hydrogen bonding interactions to Arg-399 and Asp-202 (Figure 1.21). Pharmacokinetic analysis showed that **73** and **74** were more stable and had a lower clearance than **68**. Furthermore both **73** and **74** were able to maintain penetration of the blood brain barrier.⁶⁶

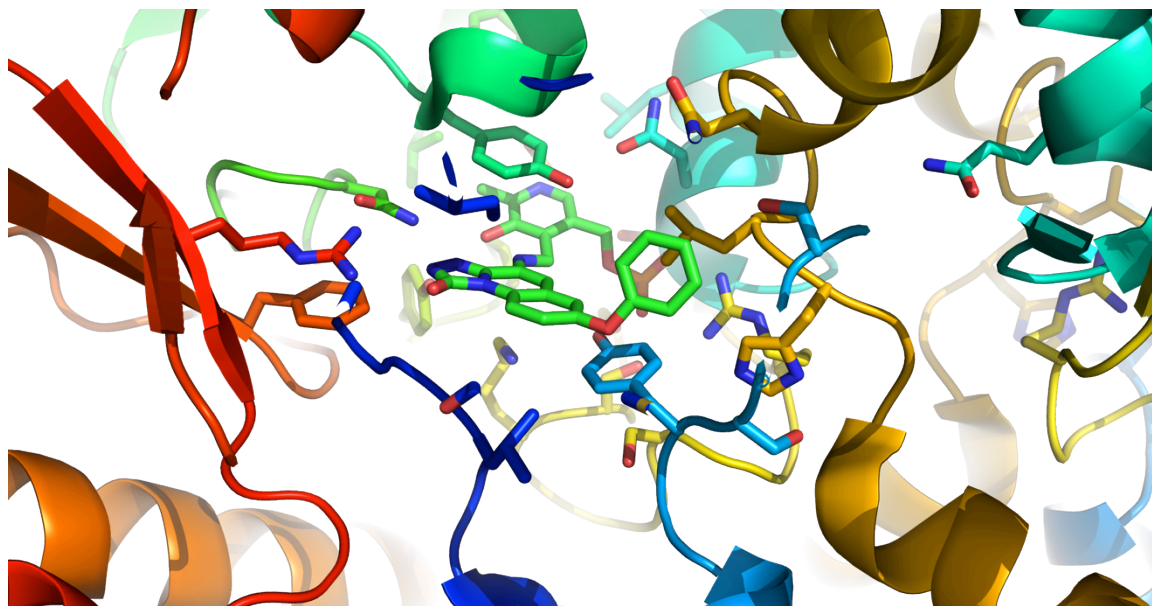


Figure 1.21. Crystal structure of KAT II with **72** bound to the PLP co-factor.⁶⁶

1.4 Kynurenine monooxygenase

1.4.1 Kynurenine monooxygenase biology and structural information

Kynurenine 3-monooxygenase (K3MO), also known as kynurenine 3-hydroxylase, is a flavin-dependent enzyme that selectively oxidises L-kynurenine to 3-hydroxy-L-kynurenine. The enzyme can use either NADH or NADPH as a reductant. When NADPH is the electron donor the V_{\max} of the enzyme increases and the K_m for L-kynurenine is slightly lower than with NADH, suggesting a preference for NADPH.² It has been shown that the oxygen required for turnover is derived from molecular oxygen.² The reaction of L-kynurenine with K3MO can either be monitored using [$3\text{-}^3\text{H}$]-kynurenine⁶⁷ or by following the decrease in absorption due to the NADPH. Recently a new fluorometric method has been developed for investigating the binding of inhibitors to flavin-dependent monooxygenases.⁶⁸

The mammalian enzyme is found on the outer membrane of the mitochondria.⁶⁹⁻⁷¹ Unfortunately, mammalian K3MOs are not stable and it is difficult to express the proteins in significant quantity.^{72, 73} Fortunately K3MO from the bacterial source *Pseudomonas fluorescens* is amenable to over-expression and purification.⁷⁴ *P. fluorescens* is one of a small number of bacteria that metabolise kynurenine by 3-hydroxykynurenine. K3MO from *P. fluorescens* has 36% sequence identity to the human K3MO. Biochemical studies indicate that there is only one FAD associated with each K3MO molecule, although it is not covalently bound in the active site.⁷² The use of stereospecifically deuterated NADH and NADPH has shown that the *pro-R* hydrogen of the nicotinamide is transferred to the FAD.²

The human enzyme is larger than the *P. fluorescens* enzyme with an amino acid length of 486 and 461 residues respectively.

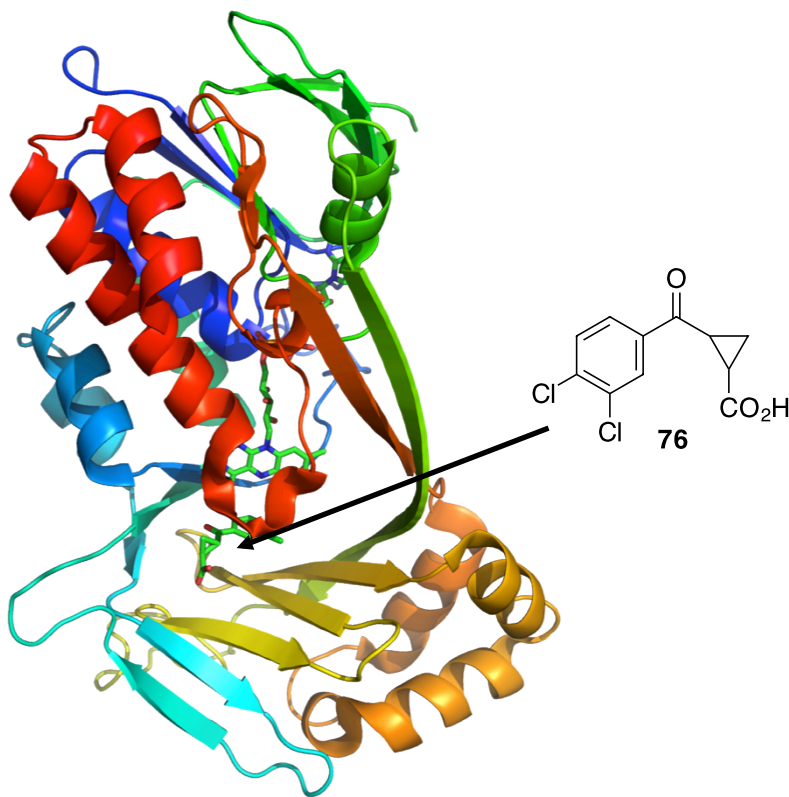


Figure 1.22. Crystal structure of *S. cerevisiae* K3MO with **76** bound at the active site.

A truncated form of K3MO from *Saccharomyces cerevisiae* has been expressed and crystallised in 2013.⁷⁵ The crystal structure was published during the writing of this thesis (Figure 1.22). The 396 amino acid truncate retained activity against kynurenine and was inhibited by **76**. The structure was solved at a resolution of 1.85 Å showing a dimer in the asymmetric unit cell.⁷⁵ The structure obtained had a similar fold to other flavin-dependent hydroxylases. There was disorder in residues 380-396 and residues 96-97 and 101-104. Comparison of the **76**-bound co-crystal with the unbound structure revealed key interactions in the binding of the inhibitor. As **76** is similar to kynurenine it appears that the key interactions are maintained for both inhibitor and substrate. There is a hydrophobic pocket in which the 3,4-dichloro-phenyl ring binds, with the hydrophobic Phe-322 moving away from the active site to accommodate the chlorine atoms. The carboxylate of **76** makes hydrogen bonding interactions to both Arg-83 and Tyr-97. Upon binding of **76** there is a reorientation of several residues that are hypothesised to occlude the binding

site for O₂ in the enzyme. This hypothesis is not entirely firm because when **76** binds to *S. cerevisiae* K3MO there is a 20-fold increase in the production of hydrogen peroxide.⁷⁵ The hydrogen peroxide is formed by destabilisation of the flavin-hydroperoxide intermediate, suggesting that O₂ can still bind at the active site. It was suggested that the truncated *S. cerevisiae* K3MO structure would be useful for the development of novel K3MO drugs that are able to pass through the blood brain barrier. Nevertheless it has been shown that the C-terminal domain, absent in the crystal structure of *S. cerevisiae* K3MO, plays a key role in the catalytic activity of mammalian K3MO.⁷¹

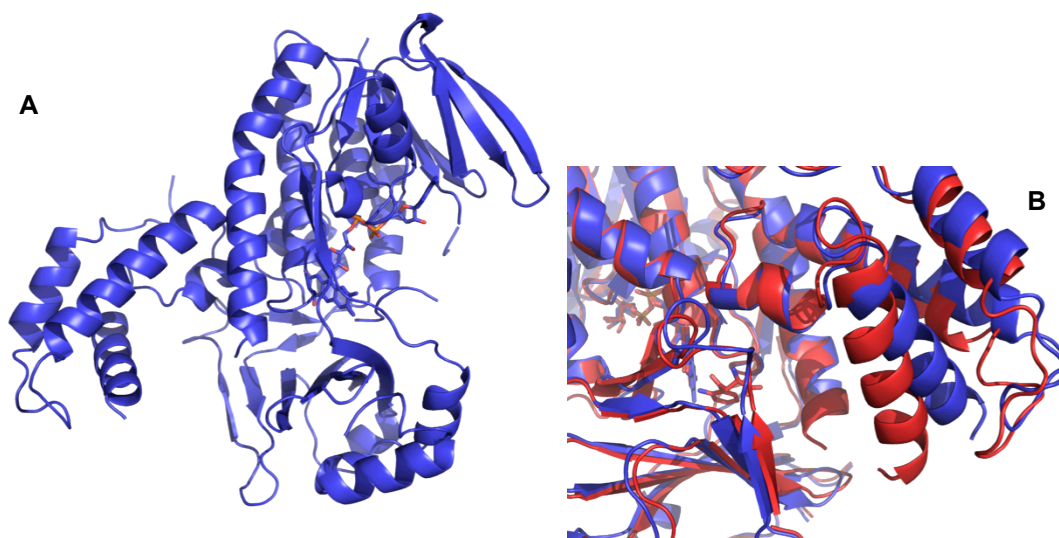


Figure 1.23. **A)** Crystal structure of *P. fluorescens* K3MO; **B)** Overlaying the L-kynurenine bound (red) and unbound (blue) structures reveals that the C-terminal domain shifts towards L-kynurenine.

Recently the crystal structure of the full length K3MO from *P. fluorescens* has been solved by our collaborators at Edinburgh University with both the substrate bound and unbound at resolutions of 3.4 Å and 2.25 Å respectively (Figure 1.23).⁷⁶ The structures show two domains, the C-terminal domain and a large second domain. The FAD co-factor is well placed in the middle of the large domain. Some of the loops are too disordered to be accurately assigned. The active site of the enzyme is found deep in the large domain. Upon binding of the kynurenine substrate the C-terminal domain shifts towards the active site to hold the substrate in place. It is

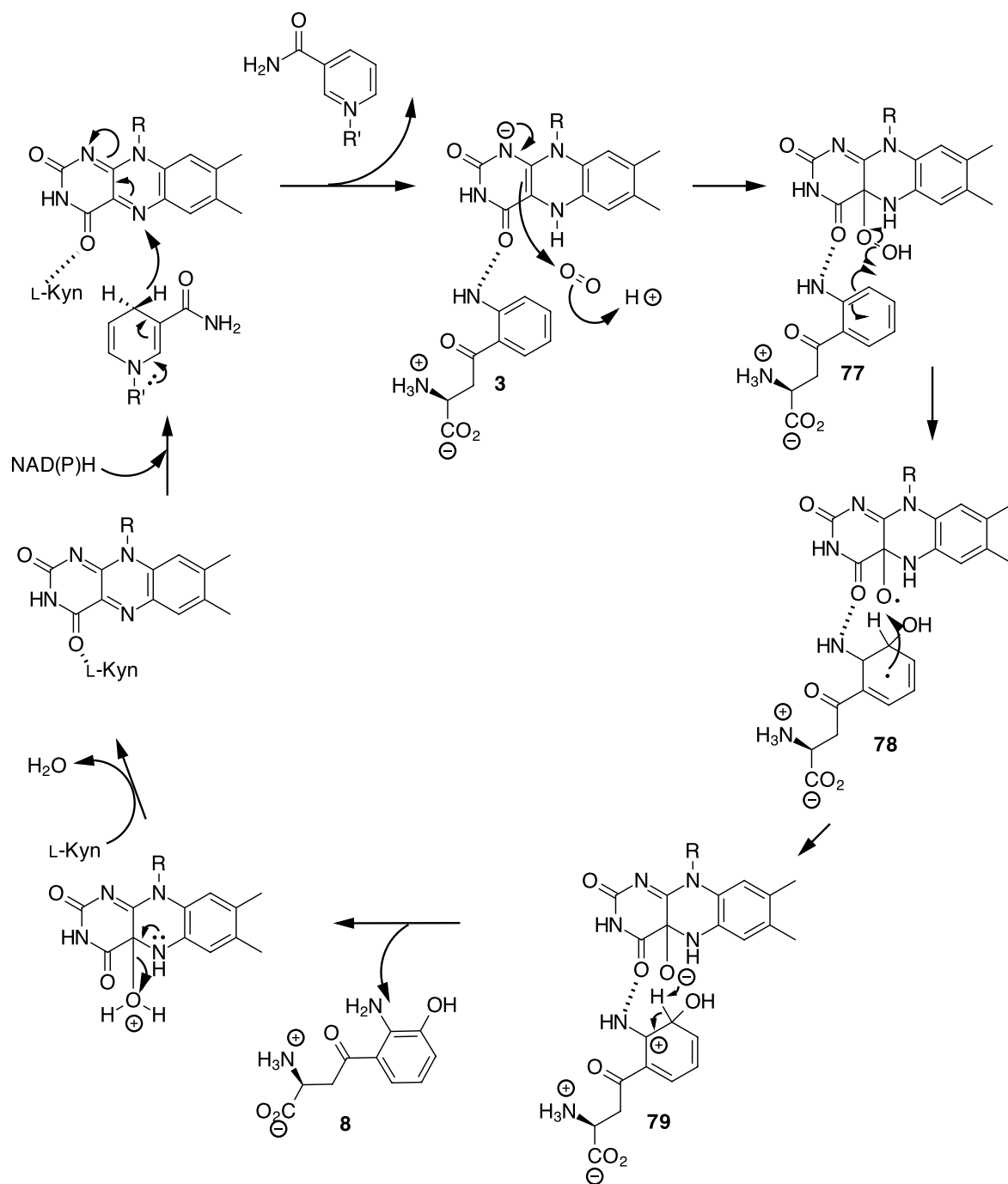
thought that the movement of the C-terminal domain is mediated by a hydrogen bonded network (Figure 1.23).

The phenyl ring of kynurenine is situated in a hydrophobic pocket and is flanked on one side by the FAD isoxazoline ring. Other important residues for the formation of the hydrophobic pocket are Pro-318, Phe-238, Tyr-193, Leu-213 and 226, Ile-224 and Met-222. The substrate amino group makes a strong hydrogen bond with the carbonyl of the FAD with a distance of 2.8 Å. This correlates well with observations that benzoylalanine inhibitors allow uncoupled reduction of the FAD by NADPH to give hydrogen peroxide. The turnover of NADPH occurs concomitant with binding of the inhibitor to the active site showing that the amino group is not required for substrate specificity. However, the rate of reaction is rapidly diminished without the amino group, suggesting that the amino-carbonyl interaction helps optimise turnover. The carboxylate forms a salt bridge with Arg-84, at a distance of 2.6 Å. Interestingly the ketone of the substrate does not appear to make any polar interactions with the protein. The amino group is orientated towards a hydrophilic pocket made up by Tyr-404 and Thr-408 and some of the main chain amides.

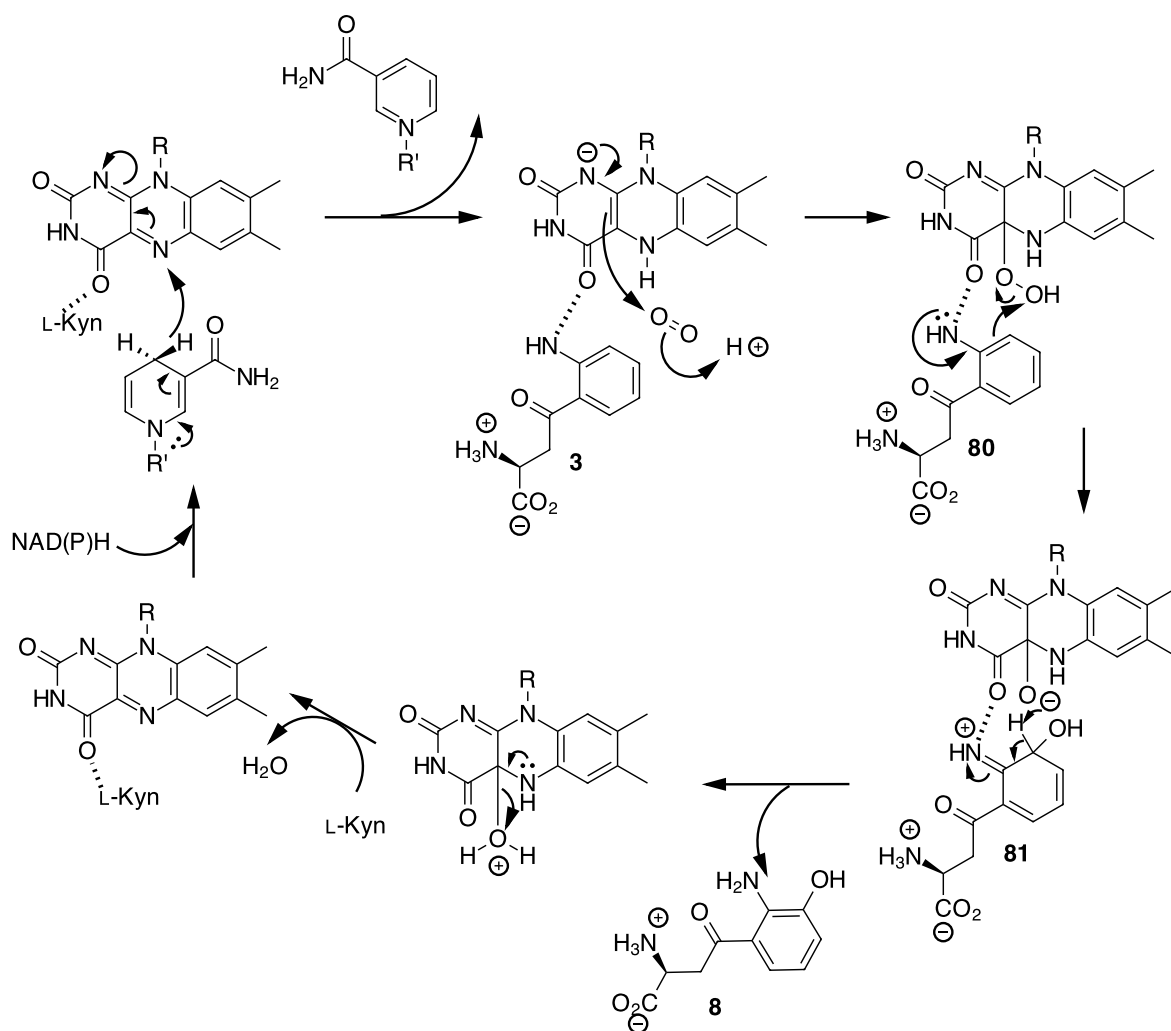
1.4.2 Kynurenine 3-monooxygenase mechanism

Two different mechanisms have been proposed for the selective oxidation of kynurenine **3** by K3MO.^{77, 78} The first was based on early kinetic and spectrophotometric data as well as available information on the mechanisms of other flavin hydroxylases. A single electron transfer from the substrate phenyl ring to the peroxy-flavin adduct is envisaged,⁷⁷ as is summarised in Scheme 1.8.

Stop-flow experiments with *P. fluorescens* K3MO suggest an alternative ionic mechanism⁷⁸ as shown in Scheme 1.9. The key step involves electrophilic aromatic substitution promoted by the lone pair of electrons on the substrate nitrogen. This mechanism is similar to that used by other flavin hydroxylases and is the preferred mechanism for the action of K3MO upon kynurenine.



Scheme 1.8. A proposed single electron transfer mechanism for the formation of 3-hydroxykynurenine **8**.⁷⁷



Scheme 1.9. An alternative ionic mechanism for the formation of 3-hydroxykynurenine **8**.⁷⁸

1.4.3 Kynurenine-3-monooxygenase inhibitors

The literature reports relatively few articles on inhibitors of kynurenine 3-monooxygenase, although there are approximately 16 patents⁷⁹⁻⁹⁴ on various inhibitor claims.

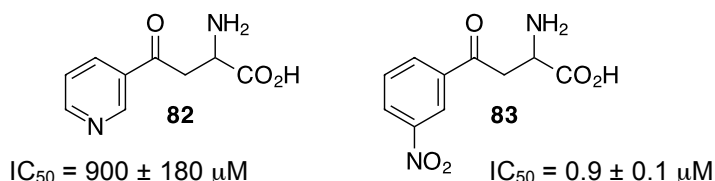


Figure 1.24. Benzoylalanine based inhibitors of K3MO **82** and **83**.

In 1994 Pellicciari *et al.*⁷⁷ developed some inhibitors based on the kynurenine motif. Four were tested, one replacing the phenyl ring with a pyridine **82** and the other three were isomers of nitrobenzoylalanine (*meta*, *ortho* and *para*) (Figure 1.24). The best inhibition was achieved with the *meta*-isomer **83**, which had good selectivity for K3MO over kynureninase. A molecular modelling study was undertaken using a “pseudo-active site”.⁷⁷ It was shown that one of the oxygens in the nitro group locates to the binding site of molecular oxygen and is hydrogen bonded to the FAD co-factor.⁷⁷

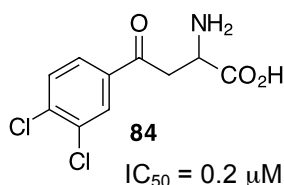


Figure 1.25. 3,4-Dichlorobenzoylalanine **84** developed as a K3MO inhibitor.

In 1996 Giordani *et al.*^{95, 96} synthesised the dichlorobenzoylalanine K3MO inhibitor **84** (Figure 1.25). It had low micromolar activity and *in vivo* testing in rats induced an increase in kynurenic acid **5**, associated with the inhibition of kynurenine 3-hydroxylase. Although benzoylalanine is a weak inhibitor of K3MO an investigation into the substitution pattern around the phenyl ring was undertaken.⁹⁶ Adding fluorine at C-3 resulted in a selective and potent inhibitor. Chlorine at C-3 created a more potent but less selective inhibitor and a C-3 bromine reduced the activity. None of the other substituents tested displayed activity.⁹⁶ Fluorine and chlorine at

C-4 also resulted in good inhibitors, but were less effective than the C-3 substituted analogues. This led to the 3,4-dichloro compound **84**, which had low micomolar activity ($IC_{50} = 0.2 \mu M$).⁹⁵ Further studies exploring **83** and **84** with *P. fluorescens* K3MO showed that although benzoylalanines inhibit the production of 3-hydroxykynurenine, they allowed uncoupled NADPH reduction of the flavin ring leading to hydrogen peroxide production.⁷⁸

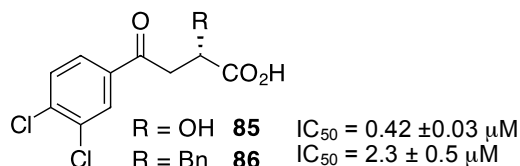


Figure 1.26. 3,4-Dichlorobenzoylalanine analogues **85** and **86** tested as K3MO inhibitors.

In 1998 Giordani *et al.*⁹⁷ developed compounds based upon their dichlorobenzoylalanine inhibitor **84** (Figure 1.26). They made modifications α to the carboxylic acid including methoxy, halogen or phenyl groups. However, they found the best inhibitors had a hydroxyl group **85** or a benzyl group **86**. In each case the S-enantiomer was the more active. Assays against kynureninase, kynurenine aminotransferase and other mono-oxidases showed that these compounds had good selectivity for KMO.⁹⁷

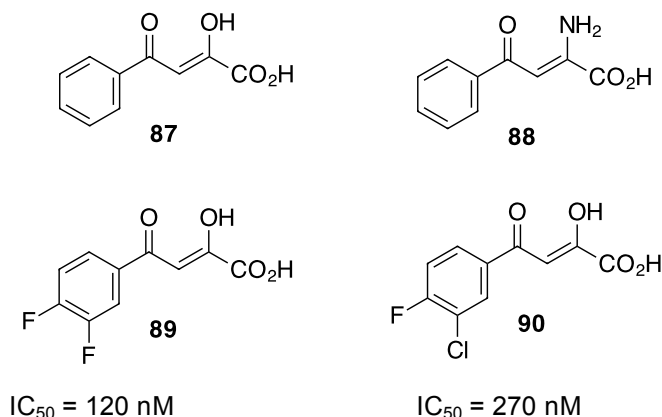


Figure 1.27. Enol analogues of **87** were tested against K3MO.

In 1999, Drysdale *et al.* investigated methyl esters and carboxylic acid derivatives of **87** and **88** (Figure 1.27).⁹⁸ In the synthesis of their targets they found that **87** existed entirely in the enol form.

The compounds were initially tested on K3MO isolated from a rat liver homogenate. The series based upon **88** were generally poor inhibitors of K3MO. Analogues of **87** gave much better inhibition. Carboxylic acids analogues were more potent than the methyl esters and substitution at the 3- and 4- positions also gave potent inhibition. The 3-chloro and 3-fluoro derivatives were very potent inhibitors with IC_{50} values of 320 nM and 580 nM respectively. 3,4-Dihalogenation further increased potency; the 3,4-difluoro and 3-chloro-4-fluoro compounds **89** and **90** were the most potent compounds tested, with IC_{50} values of 120 nM and 270 nM respectively. Interestingly the 3,4-dichloro derivative was less potent than either the 3,4-difluoro or 3-chloro-4-fluoro derivatives. When the potent compounds were tested in macrophages the trend of the acid being better than the ester was broken indicating problems with the carboxylic acid passing through the cell membrane.⁹⁸

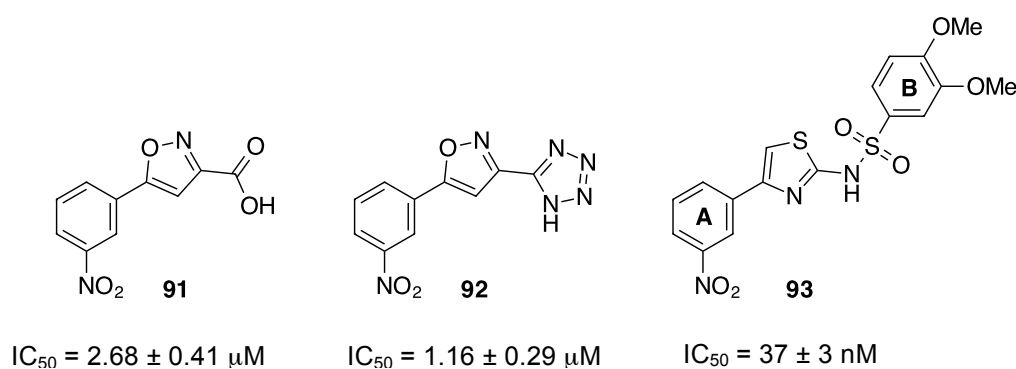


Figure 1.28. Isoxazoles **70** and **92** and thiazole sulfonamide **71** developed as K3MO inhibitors.

In 1997 Röver *et al.*⁶⁷ reported some of the most potent K3MO inhibitors in the literature to date. Starting from *m*-nitrobenzoylalanine **83** a series of modifications were made. The first modification was the removal of the amino group. This gave a less potent inhibitor by one order of magnitude, suggesting that the amino group is not bound to the enzyme *via* a salt bridge. Changing the ketone functionality to an isoxazole resulted in increased inhibition. However, due to the poor pharmacological properties of the free carboxylic acid, the tetrazole bioisostere was also prepared and the two isoxazoles **91** and **92** had very similar activity (Figure 1.28). This suggested that carboxylic acid bioisosterism was important for

binding. Screening a library of sulfonamides produced better inhibitors of K3MO and the thiazole sulfonamide **93** emerged as the most potent inhibitor. ($IC_{50} = 37$ nM)⁶⁷

3,4-Dichloro and 3-nitro substitution also improved inhibition suggesting that phenyl ring A binds in a similar orientation to **83** and **84**. Substitution of phenyl ring B with electron donating substituents gave much better inhibitors of K3MO. The best of these were the 3,4-dimethoxy and 4-amino derivatives. Whilst some of the compounds had similar activity *in vitro*, when tested in rats and gerbils it was found that the 3,4-dimethoxy derivative had a much greater activity *in vivo*. The nitro analogue was problematic as it is potentially mutagenic. 2-Fluoro-5-(trifluoromethyl) substitution on phenyl ring A gave good inhibition without the mutagenic effects.⁶⁷

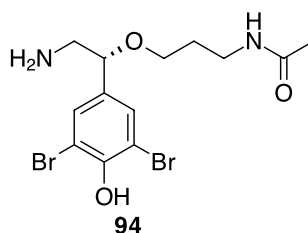


Figure 1.29. The proposed structure of lanthellamide A **94**.

In 2012, Feng and co-workers reported that the marine natural product lanthellamide A **94** (Figure 1.29),⁹⁹ isolated from the Australian sponge *Lanthella quadrangulata*, showed a reduction in 3-hydroxykynurenine production in an *in vitro* assay. Although there was good analytical evidence for the carbon skeleton of lanthellamide A **94** the stereochemistry was uncertain. A tentative assignment of the stereochemistry was based on a comparison with the optical rotation of *R*-octopamine.⁹⁹

Inhibitors described in the literature and patents can be classified into three distinct groups:

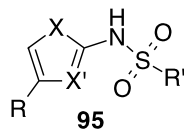


Figure 1.30. A general motif for the sulfonamide inhibitors in the patent literature.

The first are the heterocyclic sulfonamides **95**, similar to the compounds developed by Röver *et al.* (Figure 1.30).^{67, 79-81}

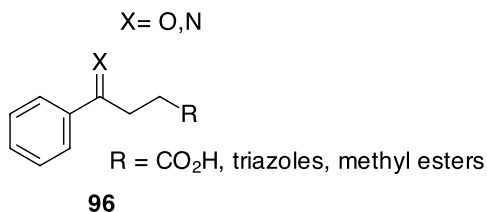


Figure 1.31. A general structure for substrate based inhibitors found in the patent literature.

The second class are substrate like inhibitors, which are compounds based on kynurenine with alterations that mimic the ketone or the addition of functionality, such as hydroxy groups (Figure 1.31).^{82-89, 93}

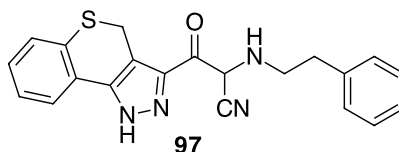


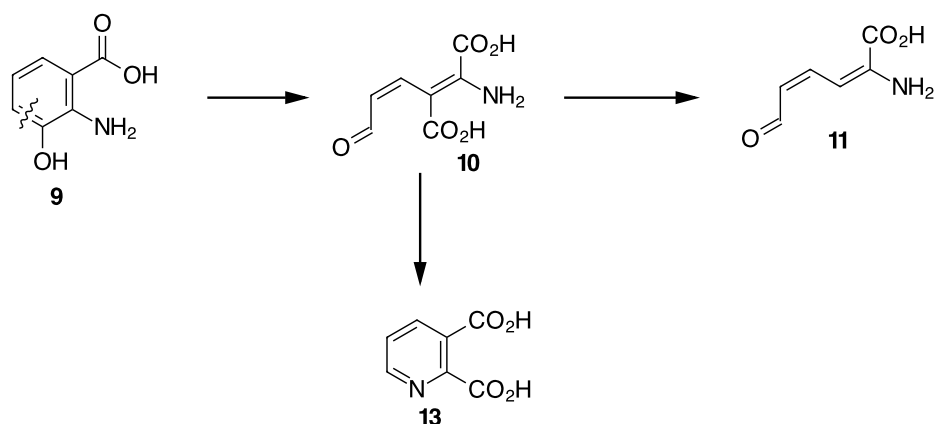
Figure 1.32. Tricyclic inhibitor **97** found in the patent literature.

The third group are a set of bicyclic and tricyclic compounds which have at least one heterocyclic component (Figure 1.32).⁹⁰⁻⁹⁴

1.5 3-Hydroxyanthranilate-3,4-dioxygenase

1.5.1 3-Hydroxyanthranilate-3,4-dioxygenase biology and structure

3-Hydroxyanthranilate-3,4-dioxygenase (3HAO) is a non-haem ferrous (Fe^{II}) dependent enzyme that cleaves the aromatic ring of 3-hydroxyanthranilic acid **9** between C-3 and C-4. This oxidative cleavage forms 2-amino-3-carboxymuconic acid semialdehyde (ACMSA) **10**. This metabolic intermediate can either cyclise to form quinolinic acid **13** or it can be decarboxylated by aminocarboxymuconate-semialdehyde decarboxylase to give **11**.



Scheme 1.10. The product of 3HAO catalysis ACMSA **10** has two fates, decarboxylation to give **11** or cyclisation to give quinolinic acid **13**.

3HAO is found widely in eukaryotes as well as some bacteria.¹⁰⁰ 3HAO from mammals has been difficult to isolate in significant amounts as a pure stable protein.^{9, 101, 102} Work on the bacterium *Ralstonia metallidurans* showed that the bacterial enzyme is more stable and amenable to over-expression than mammalian 3HAO.¹⁰³ 3HAO from *R. metallidurans* has 174 amino acids per monomer and a molecular weight of 22 kDa however, the enzyme functions as a dimer. After purification the enzyme was found to be inactive, but this was reversed by adding ferrous iron and DTT as a thiol reducing agent. The crystal structure of the enzyme has been solved (Figure 1.33).¹⁰³

In humans the enzyme is found in the cytosol as a functional monomer.¹⁰¹ It has been overexpressed in *E. coli* cells.¹⁰² The human enzyme is 286 amino acids long with a molecular weight of 32.6 kDa. In both purified human and bovine 3HAO the rate of the reaction decreases with time.^{9, 102} It has been proposed that this is due to inhibition of the enzyme by some unknown species, however, it could also be due to inactivation of the enzyme by oxidation of the ferrous to ferric iron or complete loss of the iron centre, which is known for this enzyme.¹⁰² A crystal structure of the human enzyme (PDB ID 2QNK, <http://www.rcsb.org>) has been deposited in the protein databank although it lacks an accompanying publication. The PDB shows that the iron has been displaced from the active site by a nickel atom, which is presumed to have occurred during the purification step. A crystal structure of the bovine form of the enzyme has also been solved.¹⁰⁴ The bovine form has 286 amino acids, like the human enzyme, but it has a slightly lower molecular mass of 32.5 kDa.

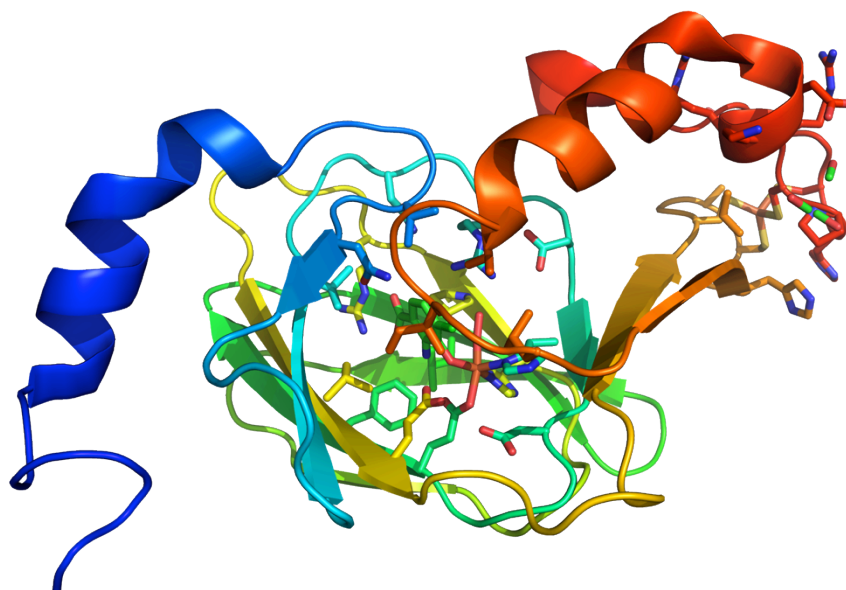


Figure 1.33. Crystal structure of *R. metallidurans* 3HAO monomer with **98** (Figure 1.34) bound in the active site.

The crystal structure of *R. metallidurans* 3HAO was solved in 2005 by Zhang *et al.*¹⁰³ and reveals a dimer with two iron binding sites in each monomer (Figure

1.33). The overall structure of the protein has been classified as a cupin barrel fold. There are two six stranded anti parallel β -sheets that form the cupin barrel.

The catalytic iron is found in the active site in a distorted octahedral geometry. The co-ordination ligands to the iron are two histidine residues, His-51 and His-95, and a bidentate glutamate residue, Glu-57. Water takes up the final co-ordination sites.¹⁰³ The second iron binding site is found 24 Å away from the catalytic ferrous iron and four cysteine residues are coordinated to the iron. This binding site has a structure similar to that found in the rubredoxin proteins, a class which participates in electron transfer reactions. It is not known why the bacterial form of the enzyme contains the additional rubredoxin motif.¹⁰³

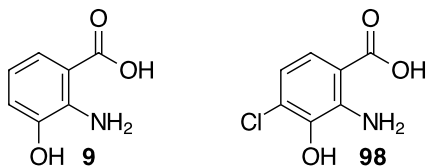


Figure 1.34. 3-Hydroxyanthranilic acid **9** and 4-chloro-3-hydroxyanthranilic acid **98** were co-crystallised with 3HAO.

Both 3-hydroxyanthranilic acid **9** and an inhibitor 4-chloro-3-hydroxyanthranilic acid **98** were successfully co-crystallised with the bacterial enzyme.¹⁰³ The inhibitor co-crystal was obtained with either oxygen or nitric oxide bound to the iron. With the inhibitor bound the iron is six coordinate with His-51 and His-95, Glu-57, the phenol of the inhibitor and O₂ or NO. In the substrate structure glutamate is no longer bidentate and both the amine and the phenol of the substrate coordinate to the iron. Important residues for binding are Glu-57 and Arg-99. Arg-99 forms two hydrogen bonds to the carboxylate of the substrate. There is a hydrophobic pocket made up of Val-25, Phe-121, Ile-142 and Leu-146. The hydrophobic pocket appears to interact with the non-polar area of the substrate and inhibitor.

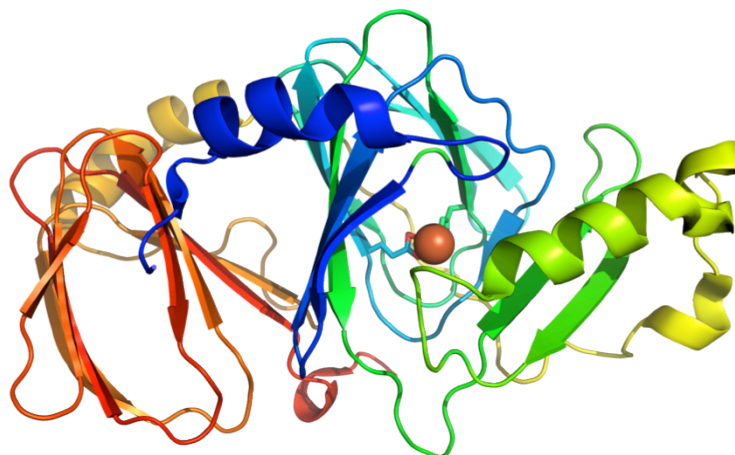


Figure 1.35. Crystal structure of bovine 3HAO. The ball represents Fe^{II} .

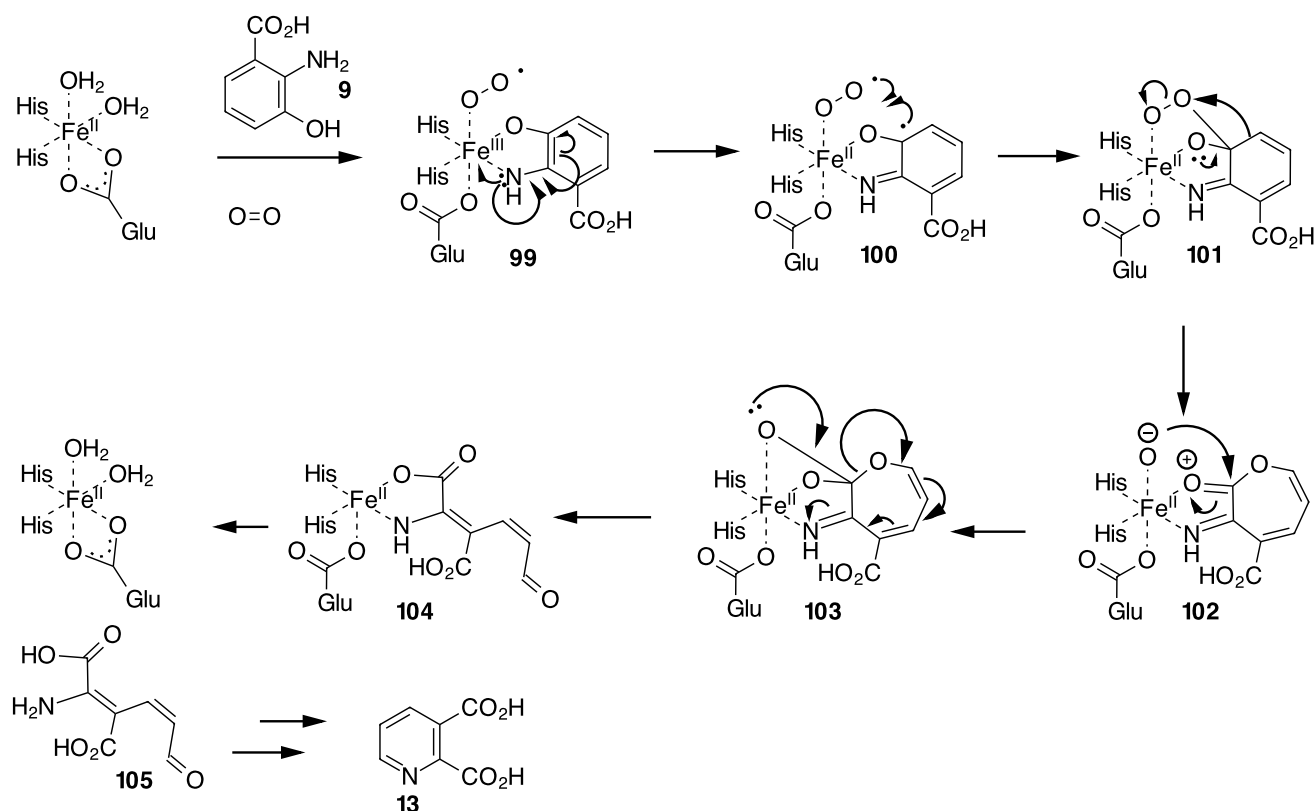
The bovine crystal structure was solved in 2009.¹⁰⁴ It shows that the enzyme exists as a monomer with two distinct domains (Figure 1.35). The larger domain correlates quite well to the monomer of the yeast 3HAO. This domain in the bovine structure has a cupin barrel fold. Two, six stranded anti-parallel β -sheets generate a characteristic shape. The smaller domain has a six and four stranded anti-parallel β -sheet. It is thought that the smaller domain in the bovine 3HAO correlates to the interface generated between the monomers in the bacterial and yeast enzymes. The main interactions between the domains are hydrophobic, however, some hydrogen bonding interaction between the domains occur. The bovine structure is similar to the human enzyme structure.

Comparison of the bovine and the bacterial structures shows that the three residues responsible for binding iron are conserved and in total 40 residues are conserved between the bovine, bacterial and yeast proteins.¹⁰⁴ The crystal structure shows the iron is bound deep into the active site and is 5-coordinate. His-47 and His-91 and a bidentate Glu-53, complex to the iron (Figure 35). The fifth coordination site has unusual electron density and it was not possible to determine the difference between a chloride ion or two water molecules due to the resolution of the crystal structure.¹⁰⁴

The entrance to the active site has both hydrophobic and hydrophilic characteristics. The hydrophilic character is generated by the side chains of Glu-

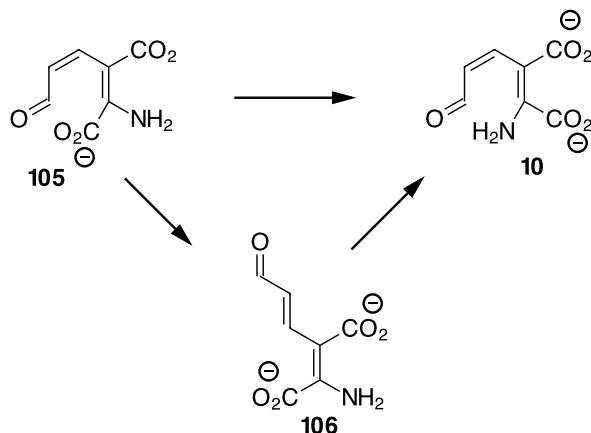
140, Asp-24 and Thr-139, the hydrophobic character is generated by the side chains of Gly-138, Val-22 and Leu-141. Gly-138 has an important role as a side chain at this position would block the active site. There are a large number of hydrophilic residues inside the active site which include Arg-43, 95 and 108, Asp-45 and 114 and Glu-105. There is also a hydrophobic pocket formed by Val-22 and Leu-116, 137 and 141. Overlaying the bovine structure with the structure from *R. metallidurans* shows that the conformations of the side chains in the two active sites are similar.¹⁰⁴

1.5.2 Mechanism of 3HAO



Scheme 1.11. A proposed mechanism for the oxidation of 3-hydroxyanthranilic acid **9** to ACMSA **10**.

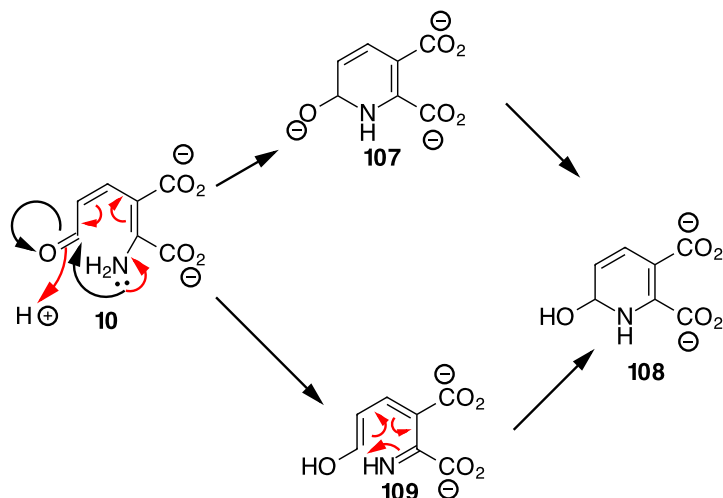
A mechanism for 3HAO has been proposed based upon the mechanism of the related reaction of catechol dioxygenase¹⁰⁵ (Scheme 1.11).



Scheme 1.12. Conformer **106** is the most stable form of ACMSA **10** in aqueous solutions.

The transformation of 3-hydroxyanthranilic acid to ACMSA **10** produces the initial product **105** with two *Z*-configured double bonds with the carboxylate groups *trans* to each other (Scheme 1.12).⁸ Cyclisation to quinolinic acid requires a configurational change to the double bond geometry placing the two carboxylates *cis*. Interestingly in solution it has been shown that the all *trans* isomer **106** is the most stable form.⁸ It is proposed that in solution the isomerisation of the double bonds is relatively facile through enol tautomerisation.⁸

There are two candidate mechanisms for the cyclisation of ACMSA **10** to quinolinic acid **13**.⁸ The first involves attack upon the aldehyde by amine, highlighted in black (Scheme 1.13), to form the six membered ring **107** followed by aromatisation. However, there are several problems with this mechanism. The amine of **10** is not a strong nucleophile, the overlap of the amine lone pair and the antibonding orbital of the aldehyde is poor and electron donation through the extended π -system reduces the electrophilicity of aldehyde **10**.⁸ When ACMSA **10** is treated with a strong nucleophile, for example hydroxylamine, there is no reaction. The low pK_a of the amine reduces its basicity.¹⁰⁶



Scheme 1.13. Two proposed mechanisms for the cyclisation of ACMSA to quinolinic acid. The cyclisation mechanism is shown in black, the tautomerisation and electrocyclic mechanism is shown in red.

An alternative mechanism, in red (scheme 1.13), involves tautomerisation of aldehyde **10** to enol **109**. Enol **109** can then undergo an electrocyclic reaction to form the six-membered ring **108**. A model study into the reverse reaction of a similar product showed such an electrocyclic reaction could occur.⁸

1.5.3 3HAO inhibitors

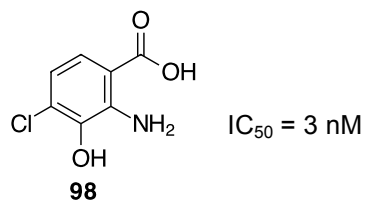


Figure 1.36. Metabolism of 6-chlorotryptophan yields **87**, an inhibitor of 3HAO.

4-Chloro-3-hydroxyanthranilic acid **98** (Figure 1.36) is a metabolite of 6-chlorotryptophan with an IC_{50} of 3 nM against rat brain 3HAO. Analysis of **98** with *R. metallidurans* 3HAO by mass spectrometry did not indicate covalent modification.¹⁰⁵ EPR spectroscopy revealed that the inhibited enzyme was in the ferric state,¹⁰⁵ whilst superoxide production by the inhibited enzyme was assessed using 2-methyl-6-(4-methoxyphenyl)-3,7-dihydroimidazo[1,2-a]pyrazin-3-one

(MCLA), which undergoes chemiluminescence in the presence of superoxide. This indicates that when **98** binds to 3HAO, oxidation of the iron centre and generation of superoxide occurs. This evidence suggests that **98** is a reversible inhibitor of 3HAO.¹⁰⁵

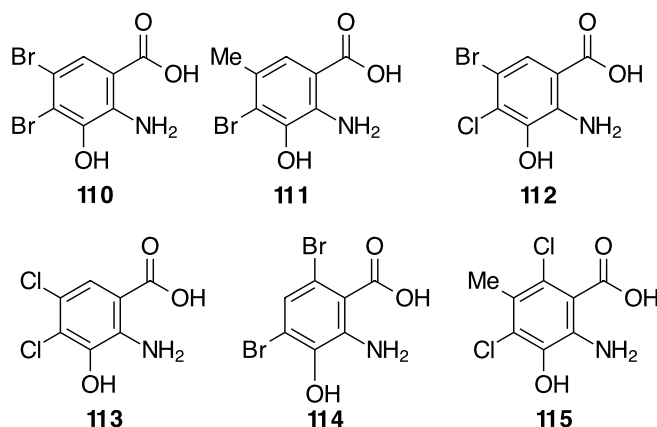
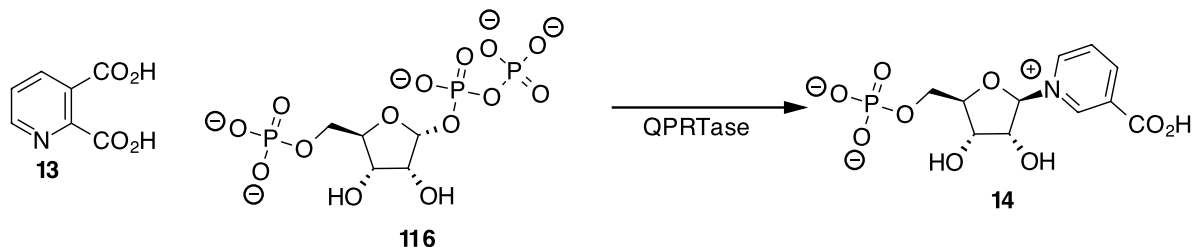


Figure 1.37. Analogues of 3-hydroxyanthranilic acid were tested as inhibitors of 3HAO.

A structure activity analysis of the 3-hydroxyanthranilic phenyl ring was undertaken (Figure 1.37).¹⁰⁷ The best *in vitro* inhibitors were **110-115**. However, not all of the compounds were stable in PBS buffer after 24 h. Although **110** has an IC_{50} of 0.3 nM, only 21% of **110** was left after 24 h in the stability assay. Key determinants for good inhibition of 3HAO are small electron withdrawing groups at C-6 and lipophilic, electron-withdrawing groups at C-5. Compounds **114** and **115** retained inhibition in an *in vivo* rat study, and although some of the compounds were highly potent in the *in vitro* study, the compounds show similar activity in the *in vivo* assay.

1.6 QPRTase

1.6.1 QPRTase biology and structural data



Scheme 1.14. The reaction catalysed by QPRTase to form nicotinic mononucleotide **14**.

Quinolinate phosphoribosyltransferase (QPRTase) is found widely in both eukaryotes and prokaryotes. QPRTase catalyses the reaction between quinolinic acid **13** and 5-phosphoribosyl-1-pyrophosphate **116** forming nicotinic acid mononucleotide **14** and carbon dioxide. This transformation is unique in the family of phosphoribosyltransfer reactions as the enzyme catalyses two discrete chemical reactions; coupling of the ribose ring to the pyridine forming quinolinic acid mononucleotide and the subsequent decarboxylation of quinolinic acid mononucleotide to give the product.²

QPRTase has been isolated from bacterial,^{108, 109} plant¹¹⁰ and mammalian sources, including rat, hog and human.¹¹¹ All forms of the enzyme utilise Mg^{2+} ions as co-factors. QPRTase forms monomers, dimers and hexamers depending upon the source of the enzyme. The human form of the enzyme is a hexamer, which correlates with other mammalian sources of QPRTase. Purification of QPRTase from human brain and liver revealed the hexamer had a molecular weight between 167-170 KDa. Investigations into Mg^{2+} concentrations revealed an optimum magnesium concentration at 1 mM. Incubating the purified human QPRTase with tritiated nicotinic acid mononucleotide showed there was no reverse reaction to quinolinic acid and 5-phosphoribosyl-1-pyrophosphate **116**. The human QPRTase has an optimum pH of 6.5-7.0.¹¹²

Kinetic analysis of human QPRTase expressed in *E. coli* revealed that its specific activity was similar to the reported values for bacterial QPRTases.¹¹² Kinetic

analysis has revealed that the affinity for quinolinic acid **13** is independent of the concentration of **116**.¹¹² This indicates that quinolinic acid binds at the active site before 5-phosphoribosyl-1-pyrophosphate **116**. Variation in the 5-phosphoribosyl-1-pyrophosphate **116** concentration revealed that above a concentration of 0.3 mM the enzyme becomes inhibited (quinolinic acid **13** fixed at 0.3 μ M).¹¹² Further investigation into the substrate inhibition of the enzyme by **116** revealed that it is a mixed inhibitor of human QPRTase, suggesting that **116** binds at both the active site and a second allosteric site that influences and inhibits reaction at the active site.¹¹² Initial reports on substrate binding in QPRTase isolated from *E. coli* suggested that **116** binds before quinolinic acid.¹¹³ However, analysis of QPRTase from *Salmonella typhimurium* and humans showed that the actual order of binding is quinolinic acid followed by **116**.^{112, 114}

Crystal structures have been obtained for QPRTase from *S. typhimurium*,¹¹⁵ *Mycobacterium tuberculosis*,¹¹⁶ *Thermotoga maritima*,¹¹⁷ *Helicobacter pylori*,¹¹⁸ Human^{112, 119} and *Saccharomyces cerevisiae*.¹²⁰ Prokaryote forms of QPRTase were crystallised as dimers, eukaryotic forms as hexamers. All of the structures have the same fold consisting of an *N*-terminal four stranded open-face β -sandwich domain and a *C*-terminal α/β -barrel domain.

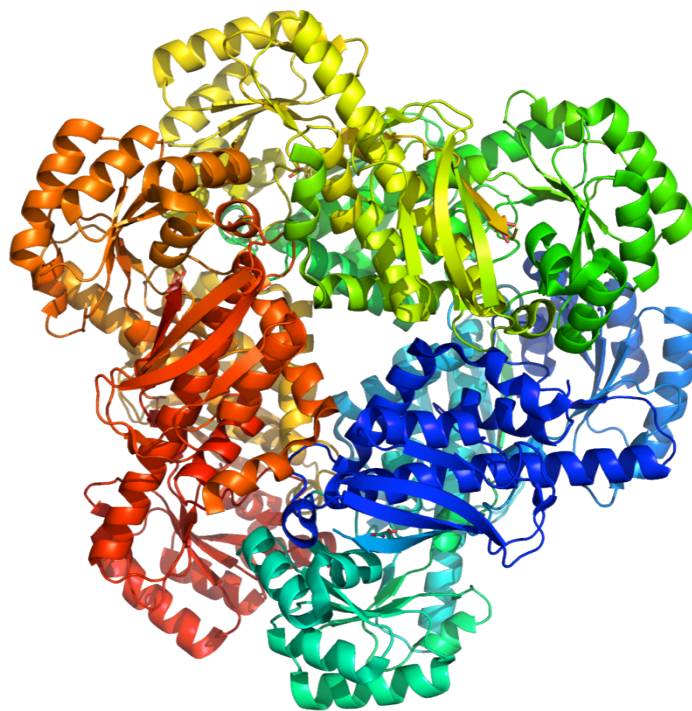


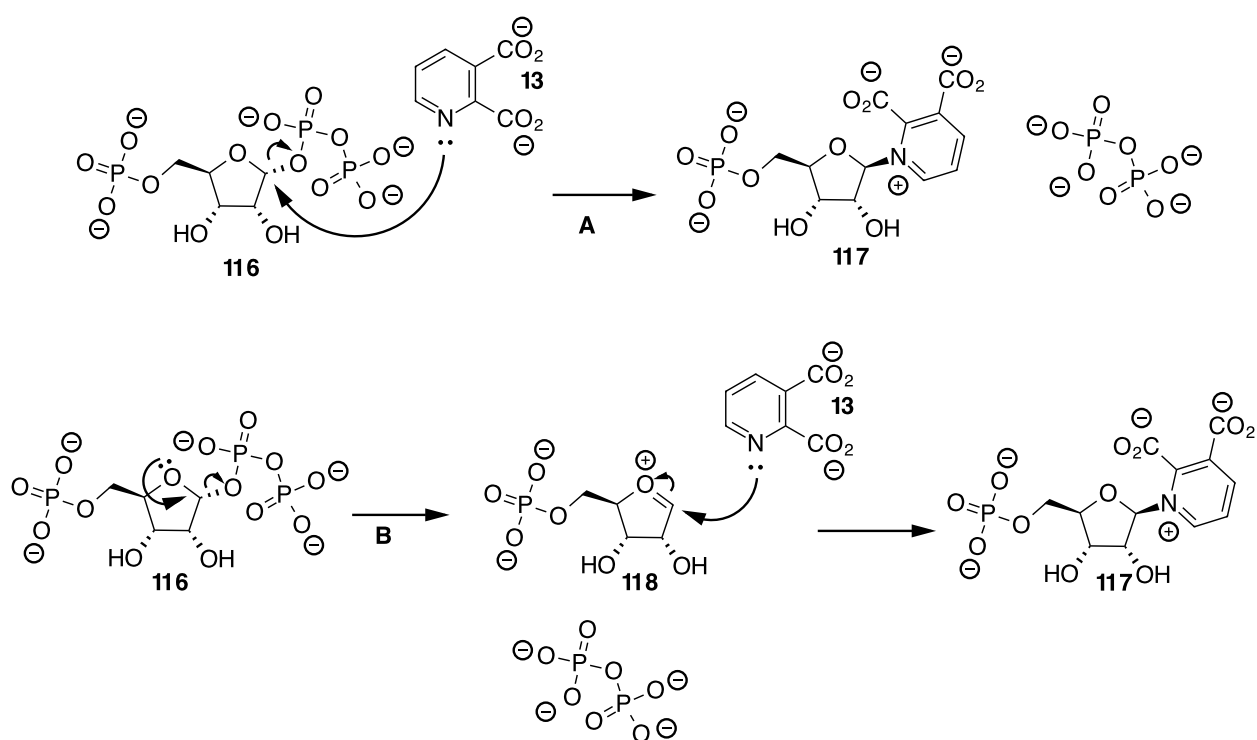
Figure 1.38. Crystal structure of hexameric human QPRTase.

It is useful to focus on the crystal structures obtained from human QPRTase as it is intricately involved in some disease states. The activity of 3HAO is approximately 100 times greater than the activity of QPRTase. This means that quinolinic acid **13** is formed faster than it is metabolised, leading to its accumulation.² The structure of human QPRTase is important in building a mechanistic model for QPRTase to understand the relative kinetics.

Human QPRTase enzyme crystallised as a hexamer with tartaric acid bound at the active site (Figure 1.38).¹¹² A structure was solved to 2.0 Å. The overall fold is similar to other QPRTases studied. A dimer is formed by the placement of the *N*-terminal domain of one subunit beside the *C*-terminal domain of the other. Three dimers arrange to form a hexamer with three fold symmetry. The active site is located between the interface of the α/β -barrel of one monomer and the β sandwich of the other monomer. The quinolinic acid binding site is composed of Arg-138, Arg-161, Arg-102, Lys-139 and Lys-171 and His-159. This generates a positively charged surface which can interact with the carboxylates of quinolinic

acid, as modelled in the structure by tartaric acid. Mutagenesis studies showed that Arg-138, Lys-139 and Lys-171 are essential for enzyme activity, Arg-102 and Arg-162 are important for substrate recognition but are not absolutely required for activity.

1.6.2 QPRTase mechanism

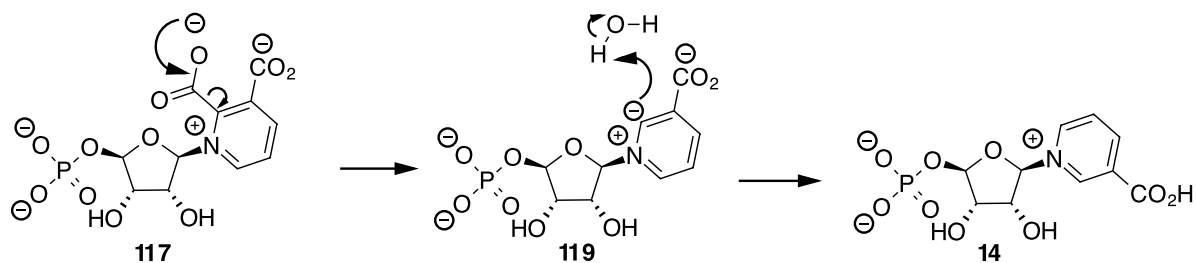


Scheme 1.15. There is debate whether QPRTase forms the nucleotide *via* an S_N2 mechanism as shown in **A** or an S_N1 mechanism as shown in **B**.

There are two distinct chemical steps in the reaction catalysed by QPRTase, these involve coupling of the substrates and decarboxylation. The full mechanism of the reaction has not been established, but details about the order of binding and a theory study on a model system of the reaction has allowed the development of a working hypothesis. A computational study into the reaction of quinolinic acid to 2-chlorotetrahydrofuran, as a model for **116**, showed that formation of the nucleotide

and subsequent decarboxylation is more energetically favourable than decarboxylation followed by nucleotide formation.¹²¹ Acid-promoted decarboxylation of quinolinic acid was not a mechanism studied computationally, however, as quinolinic acid **13** decarboxylates with a half life of approximately three days at a pH of 1 and at 95 °C this mechanism seems unlikely.²

The mechanism of nucleotide formation is still unclear. The reaction proceeds with an inversion of stereochemistry at C-1 of the ribose, as illustrated in Scheme 1.15. Kinetic isotope investigations into a related enzyme, orotate phosphoribosyl transferase, revealed that the transition state of the reaction resembled the classical oxocarbenium ion formed during an S_N1 mechanism.¹²² Clearly the required stereochemistry of the product is obtained by QPRTase holding the quinolinic acid substrate in the correct orientation for nucleophilic attack. In *M. tuberculosis* the crystal structure supports the S_N1 reaction mechanism as the residues Glu-201 and Asp-222 are orientated to aid stabilisation of the developing positive charge on the ribose ring.¹¹⁶ It has also been proposed that the magnesium ions required for catalysis aid stabilisation of the oxocarbenium intermediate.



Scheme 1.16. A proposed mechanism for the decarboxylation of quinolinate mononucleotide **117** to give nicotinic mononucleotide **14**.

There has been debate as to whether the intermediate quinolinate mononucleotide **117** decarboxylates free from the enzyme. The spontaneous decarboxylation of quinolinic acid requires very low pH and the current working hypothesis suggest the aid of QPRTase (Scheme 1.16).

1.7 Acute pancreatitis and the role of kynurenines in secondary multiple organ failure

1.7.1 The pancreas

The pancreas is a gland that sits below the stomach and above the first loop of the gut (Figure 1.39). The role of the pancreas as an endocrine and exocrine gland is important for digesting food and maintaining homeostasis of several systems in the body. Maintenance of glucose levels in the blood is the major homeostatic role performed by the pancreas.¹²³

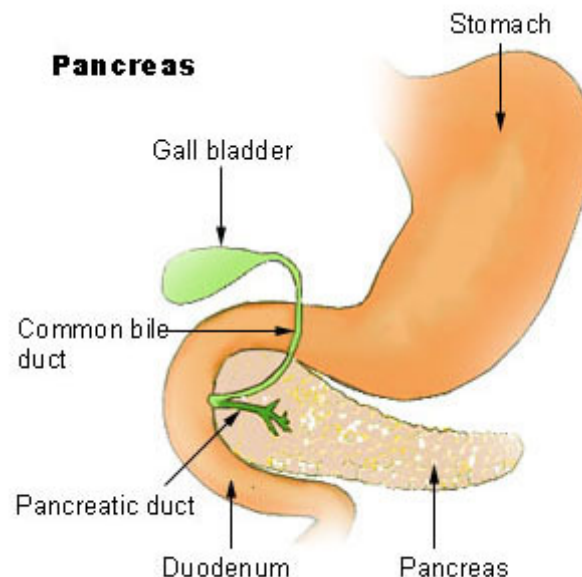


Figure 1.39. A diagram showing the location of the pancreas in relationship to other digestive organs. Courtesy of National Cancer Institute.

The pancreas produces pancreatic juice containing an alkaline solution of sodium hydrogen carbonate and powerful digestive enzymes. The enzymes and alkaline solution are created in clusters of secretory cells known as acini. These clusters are connected to ducts that ultimately flow into the gut. The pancreatic digestive enzymes work at their optimum in an environment that is neutral or slightly alkaline. The sodium hydrogen carbonate solution is important in neutralising the acidic

contents of the stomach to protect the gut wall and create an optimum environment for the pancreatic enzymes.¹²³

Pancreatic enzymes are classified into three separate groups, depending on the food type they break down. These are: proteolytic enzymes, which break down proteins; pancreatic amylase, which breaks down polysaccharides into disaccharides; pancreatic lipase, which break down fats and oils.¹²³

The endocrine system produces hormones that are released directly into the bloodstream. The four hormones produced by the pancreas are insulin, glucagons, somatostatin and pancreatic polypeptide. These hormones are produced in clusters of cells called the islets of Langerhans. Each hormone is produced by a specific cell and the ratio of cells in the islets of Langerhans varies along the length of the pancreas.¹²³

1.7.2 Acute pancreatitis

Acute pancreatitis is the inflammation of the pancreas, which can affect the pancreas as well as other organs.

Compared to chronic pancreatitis, acute pancreatitis is reversible, causes no significant structural changes in the organ and the endocrine and exocrine systems return to their normal function upon reversal of the condition. Although there are numerous causes, over 80% of cases are due to either gallstones or excessive alcohol consumption. It is important to identify the underlying cause to assess the chance of a recurrence of the disease. For example, if an NSAID was causing the acute pancreatitis it is important that the patient does not use the drug. In about 10% of cases no underlying cause (idiopathic pancreatitis) can be found, although two studies have found that in two thirds of cases diagnosed as idiopathic pancreatitis, small gallstones and biliary sludge were observed using endoscopic retrograde cholangiopancreatography.^{124, 125}

The average stay in intensive care for patients with acute pancreatitis is 7 days with a total time in hospital ranging from 40 days to 226 days. At a cost of £1500 per day, intensive care is a very expensive resource. It is the secondary injury to organs that means that patients need to enter intensive care. This makes the prevention of the secondary injury important, as it will help reduce costs to hospitals.¹²⁴

1.7.3 Multiple organ failure Induced by acute pancreatitis

In approximately 20% of acute pancreatitis patients the pancreatic injury is severe, furthermore, 15-25% of these patients will die. Up to 55% of acute pancreatitis cases result in secondary lung injury ranging from mild hypoxemia to acute respiratory distress syndrome.¹²⁶ Measurement of the partial pressure of oxygen in the blood has been used as an indicator for the severity of acute pancreatitis. It has been reported that in approximately 60% of cases the patients were suffering from hypoxia within 48 h after admission to hospital. The lower oxygen concentrations in hypoxia, can be correlated directly to damage to the lungs. Secondary lung injury is followed by renal failure.¹²⁶

A 1999 study into acute pancreatitis cases in Scotland (from 1984 to 1995) found that multiple organ failure within the first week of admission led to 54% of patients dying.¹²⁷ In patients who overcome the early multiple organ failure, the mortality drops rapidly and in a 2002 study there were no deaths in patients in which the multiple organ failure was resolved.

It has been shown that interleukin 1 β and TNF- α play an important role in the development of acute pancreatitis.¹²⁶ As the kynurenine pathway is upregulated by cytokines, it is possible that the increase in expression of cytokines produces an increase in the metabolism of tryptophan *via* the kynurenine pathway.

The mechanism of how acute pancreatitis affects organs, especially the lungs, is not yet entirely clear. It has been suggested that small molecule mediators have a role to play. For example, an increase in L-tryptophan metabolites from the

kynurenine pathway in the lymph were found in a rat model of acute pancreatitis.¹²⁸ In hospitalised patients with acute pancreatitis the concentration of L-tryptophan metabolites showed an increase in line with the occurrence of multiple organ failure.¹²⁸

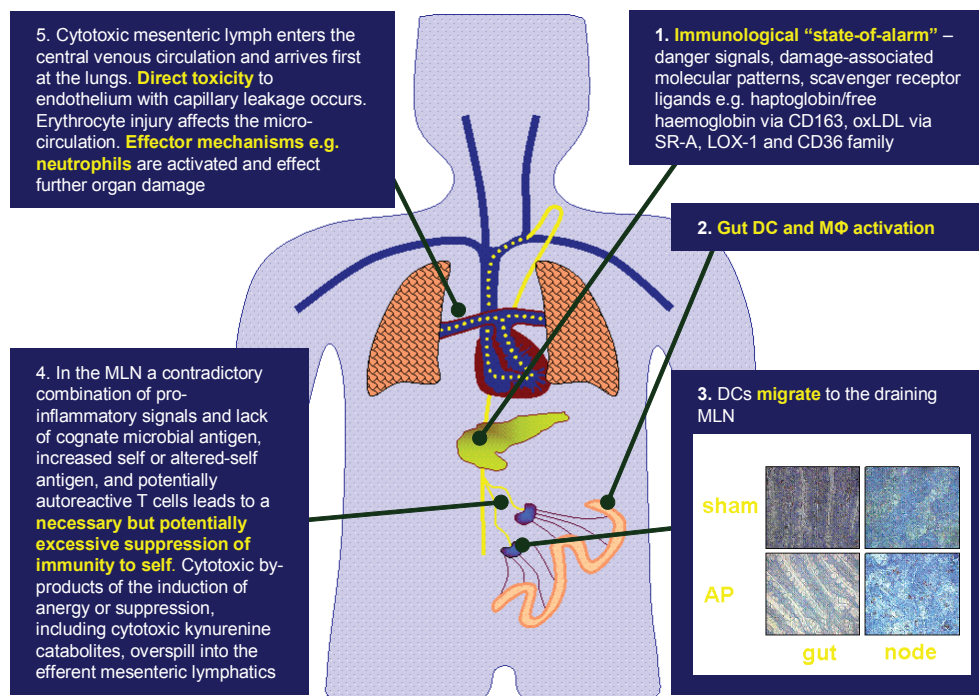


Figure 1.40. Proposed steps between acute pancreatitis and secondary MOF.¹²⁹

A hypothesis for how acute pancreatitis causes multiple organ failure has been proposed (Figure 1.40).¹²⁹ The initial events of acute pancreatitis sets off an immunological state of alert. This causes gut inflammation, which includes activation of dendritic cells and macrophages by numerous cytokines.¹³⁰ It has been shown that gut inflammation has a role in the way that acute pancreatitis causes multiple organ failure. Dendritic cells, a type of immune system cell, move to the mesenteric lymph nodes. Here the dendritic cells induce tolerance of the autoreactive T-cells through small molecule metabolites.

Kynurenines have been identified as relevant metabolites. Kynurenine 3-monooxygenase is a constitutively active enzyme, therefore any kynurenine **3** formed by the breakdown of L-tryptophan **1** would be converted to 3-hydroxykynurenine **8**. These kynurenines overflow into the mesenteric lymph. The

lymph travels through the body arriving at the lungs. Lung damage is attributed to the “toxicity” of the kynurenine metabolites. Further studies into the kynurenine metabolites showed that 3-hydrokynurenine **8** is cytotoxic to lung cells.

1.8. Aims of research

The aims of this project are to develop novel inhibitors of K3MO and the synthesis of kynurenine analogues for both mechanistic and inhibition studies. K3MO plays an important role in mediating multiple organ failure secondary to acute pancreatitis, as well as several neurologically important diseases for example, AIDS related dementia and Huntingtons disease. The development of novel inhibitors of K3MO is important as current generations of inhibitors trigger hydrogen peroxide through uncoupled NADPH oxidation. The production of hydrogen peroxide is undesirable as it is a strong oxidising agent, which can cause damage within cells.

Chapter 2

Exploring Chemical Space To Generate Inhibitors of K3MO

2.0 Introduction

The pivotal role that kynurenine-3-monooxygenase (K3MO) plays in the metabolism of L-tryptophan **1** makes it an attractive target for drug discovery. The main pathway for kynurenine metabolism in mammals is its conversion to 3-hydroxykynurenine **8** by K3MO. Inhibition of K3MO not only limits the production of the toxic metabolite 3-hydroxykynurenine **8**, but it also prevents the downstream formation of quinolinic acid **13**, a potent NMDA receptor agonist and neurotoxic agent, and it increases the concentration of kynurenic acid **5** in the brain.^{131, 132}

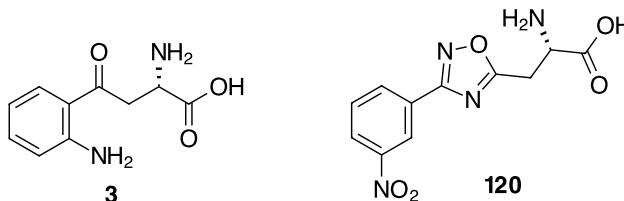


Figure 2.41. Kynurenine **3** and one of the target 1,2,4-oxadiazoles **120**.

A survey of the patent literature reveals a number of structural motifs that have been developed as K3MO inhibitors. The large number of sulfonamides in the patent literature for K3MO meant that alternative functionalities were explored. In addition the ketone functionality of kynurenine **3** is commonly replaced with a heterocycle. The 1,2,4-oxadiazole ring motif, illustrated in **120**, emerged as an attractive motif because 1,2,4-oxadiazoles were not covered in any of the previous patents. 1,2,4-Oxadiazoles have also been used as bioisosteres of both esters and amides.¹³³⁻¹³⁶ 1,2,4-Oxadiazoles are relatively accessible synthetic targets.

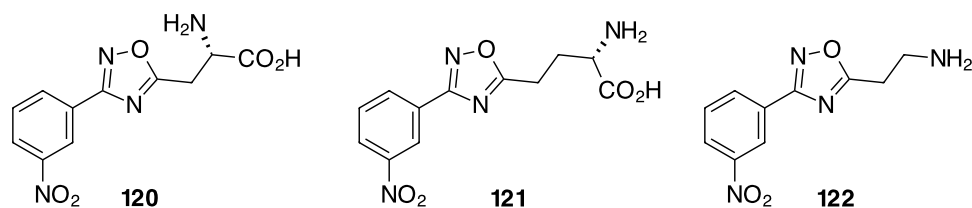
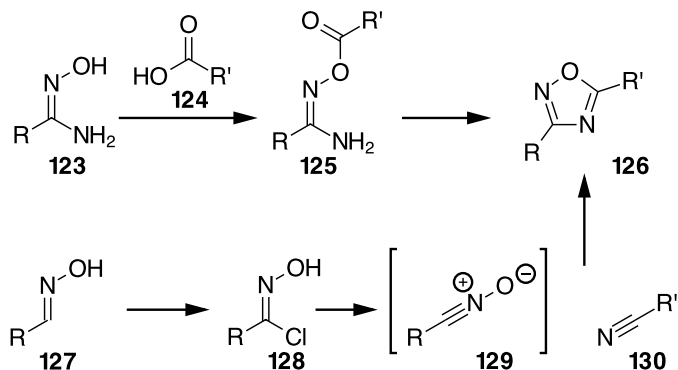


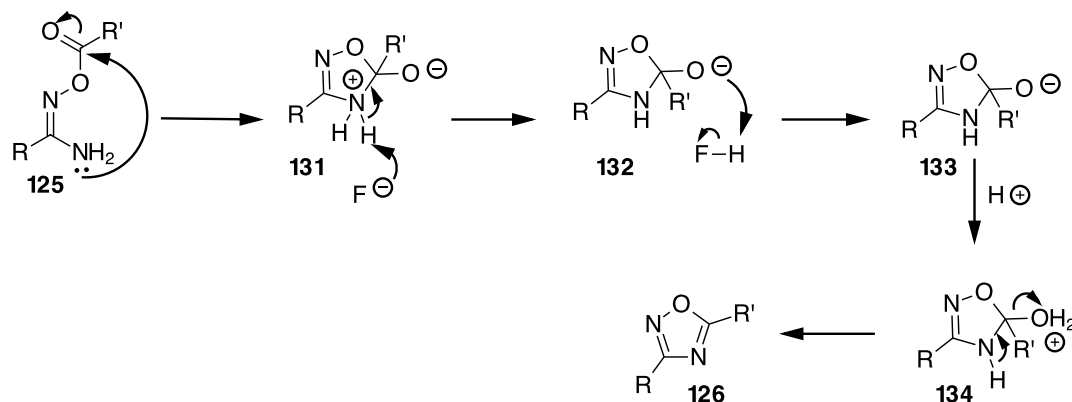
Figure 2.42. Initial targets for assay against K3MO.

The initial targets are shown in Figure 2.2. The *meta*-nitro phenyl group was retained as a structural motif, as it was already demonstrated to have high affinity for the enzyme. The amino acid and amine functionalities were retained in an attempt to replicate the amino acid functionality of kynurenine **3**.



Scheme 2.1. The most common methods for synthesis of the 1,2,4-oxadiazole ring.

The two most common methods for generating 1,2,4-oxadiazoles, are shown in Scheme 2.1. The first involves formation of an O-acyl amidoxime **125** from an amidoxime **123**. Cyclisation of the resultant O-acyl amidoxime **125** to the 1,2,4-oxadiazole **126** is achieved under thermal conditions. The cyclisation of **125** to the 1,2,4-oxadiazole **126** can also be achieved using catalytic TBAF at room temperature.¹³⁷ The alternative synthetic route to 1,2,4-oxadiazoles **126** involves a 1,3-dipolar cycloaddition of a nitrile oxide **129** with a nitrile **130**. Nitrile oxides are readily synthesised from oxime **127**, *via* an oximyl chloride **128**. Interestingly both synthetic routes involve the use of a nitrile, which allows the synthesis of isomeric compounds with R at either C-3 or C-5 in the 1,2,4-oxadiazole.¹³⁸

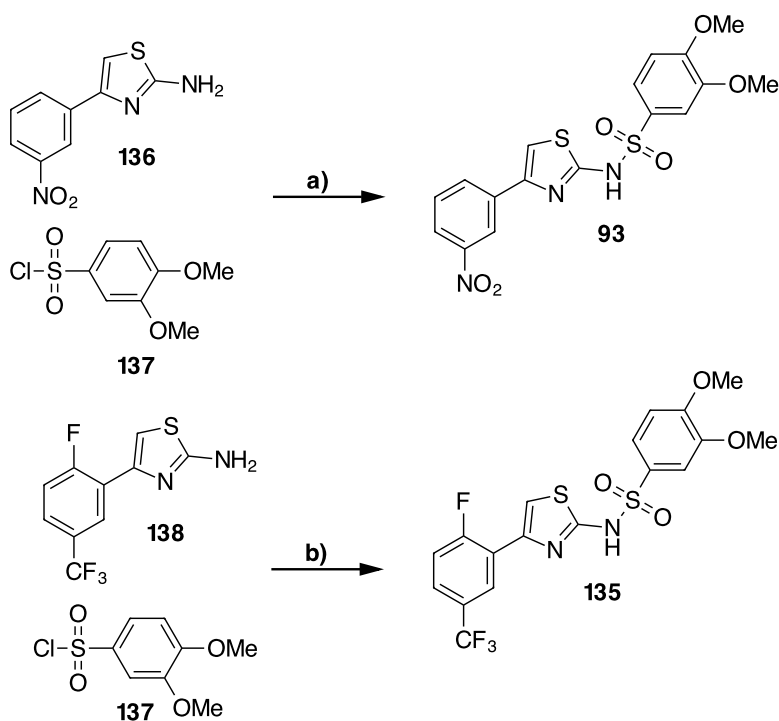


Scheme 2.2. The proposed mechanism of fluoride ion catalysis for formation of 1,2,4-oxadiazoles.

The proposed mechanism, as shown in Scheme 2.2, for the cyclisation of *O*-acyl amidoxime **125** to 1,2,4-oxadiazole **126**, with TBAF catalysis, involves intramolecular cyclisation of the amidoxime to form ionic intermediate **131**. Fluoride anion acts as a base and catalyses a proton transfer step. Investigations into the thermal cyclisation suggested that proton transfer is rate-limiting.¹³⁹

2.1 Target validation

The sulfonamides **93** and **135** were synthesised following literature protocols.⁶⁷ As **93** and **135** are known inhibitors of rat and gerbil K3MO, they were required to validate the working hypothesis that inhibition of K3MO prevents multiple organ failure following acute pancreatitis in a rat model.



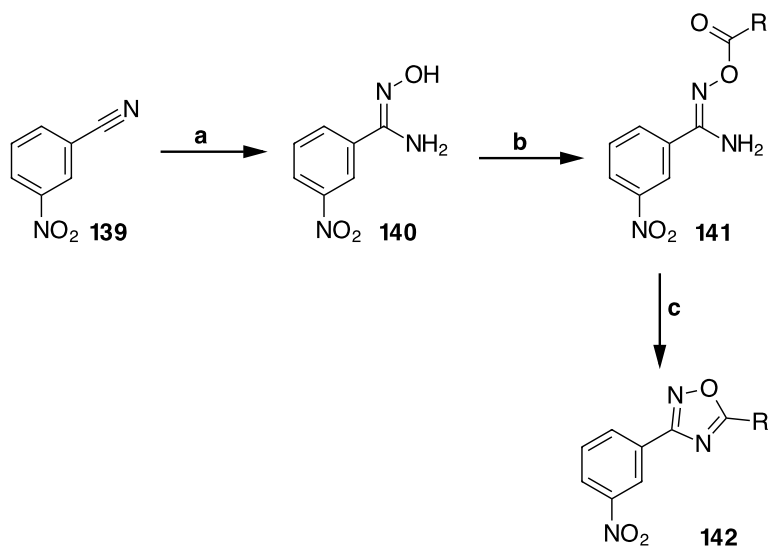
Scheme 2.3. Reagents and conditions: **a)** Pyridine, DCM, RT, 16 h, 24%; **b)** pyridine, DCM, RT, 16 h, 58%.

Initially, the synthesis of the sulfonamides using 2-aminothiazoles **136** and **138** and 3,4-dimethoxybenzenesulfonyl chloride **137** under basic conditions gave the desired products. However, the sulfonamides were not isolated due to difficulties with recrystallisation.⁶⁷ Purification of the sulfonamides by column chromatography was also complicated by the difficulty in separating the sulfonamide and sulfonic acid. This problem was overcome by carrying out the reaction in DCM with a stoichiometric volume of pyridine as shown in Scheme 2.3. The solvent was removed and the residue was run directly through a silica column. This gave both of the desired sulfonamides **93** and **135**, with yields comparable to those previously reported.⁶⁷

The sulfonamide inhibitors **93** and **135** were assayed against K3MO from *Homo sapiens* and *P. fluorescens*. The sulfonamides **93** and **135** have a K_i of 1 μM and 2 μM against the bacterial enzyme, respectively (Dr Chris Mowat and Martin Wilkinson, Edinburgh University), showing that **93** and **135** do not inhibit the bacterial enzyme to the same extent as rat K3MO. Against *H. sapiens* K3MO, sulfonamide **93** has an IC_{50} of 2.8 μM (Dr Scott Webster, Edinburgh University).

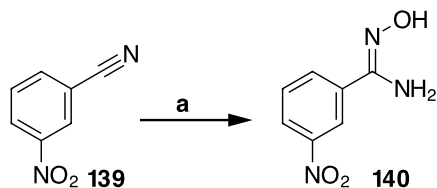
From the bacterial and human assays it is clear that sulfonamides **93** and **135** are not as potent. In a rat model of acute pancreatitis, secondary multiple organ failure (MOF) was reduced when sulfonamide **93** was given before and after the induction of acute pancreatitis (Dr Damian Mole, Edinburgh University).¹²⁹

2.2 Initial amine and amino acid targets



Scheme 2.4. Synthesis of 1,2,4-oxadiazoles via the amidoxime: **a**) Hydroxylamine; **b**) carboxylic acid, coupling reagent; **c**) Heat or TBAF.

A general procedure for the synthesis of the 1,2,4-oxadiazole ring **142** via the O-acyl amidoxime **141** is shown in Scheme 2.4. The O-acyl amidoxime **141** is prepared by reaction of an amidoxime **140** with a carboxylic acid using a suitable coupling reagent such as DCC. An alternative method for the preparation of the O-acyl amidoxime involves the reaction of amidoxime **140** with an acid chloride. The amidoxime **140** required as a substrate, was formed by the reaction of hydroxylamine upon benzonitrile **139** as shown in Scheme 2.4. In this study, the cyclisation of the O-acyl amidoximes **141** to the 1,2,4-oxadiazole ring **142** was achieved through the use of catalytic TBAF.¹³⁷



Scheme 2.5. Reagents and conditions: a) $\text{NH}_2\text{OH}\cdot\text{HCl}$, K_2CO_3 , MeOH, 80 °C for 2 h, then RT for 16 h, 84%.

Synthesis of *meta*-nitrobenzamidoxime **140** was accomplished using *meta*-nitrobenzonitrile **139**, hydroxylamine hydrochloride and potassium carbonate, as illustrated in Scheme 2.5. Heating the mixture under reflux was crucial to achieve a good yield. The product was recovered by recrystallisation from toluene. ^1H NMR spectroscopy confirmed the amidoxime **140** exists as the tautomer shown.

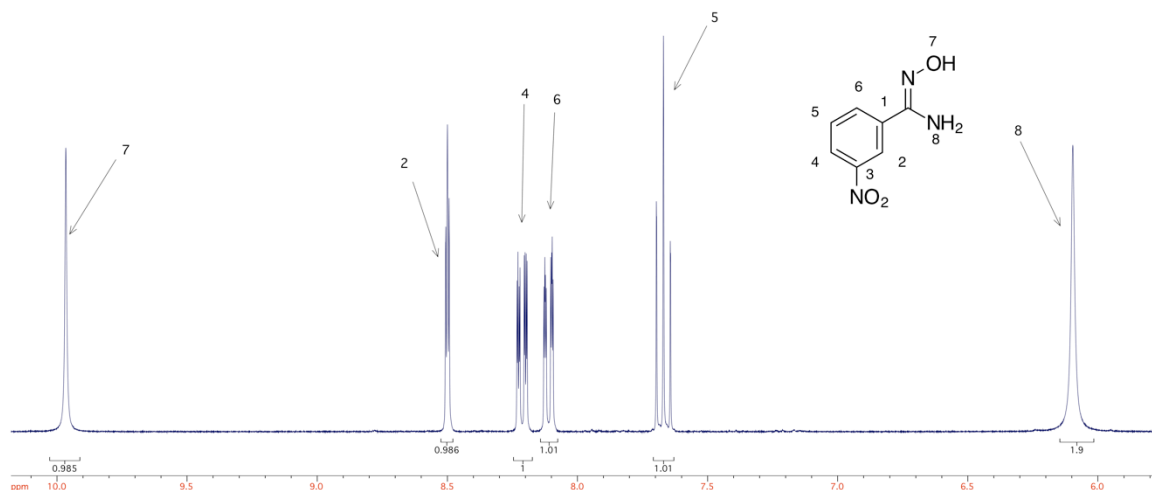
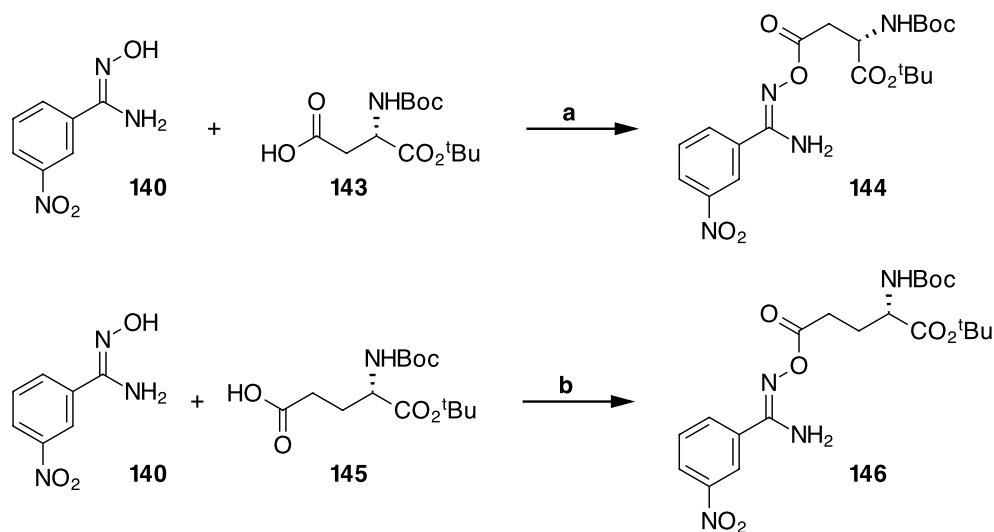


Figure 2.3. ^1H NMR spectrum of **140** in D_6 -DMSO confirming the tautomer shown.



Scheme 2.6. Reagents and conditions: **a**) DCC, DMAP, DCM, RT, 16 h, 88%; **b**) DCC, DMAP, DCM, RT, 16 h, 57%.

Protected aspartic acid **143** and glutamic acid **145** were then coupled to amidoxime **140** using DCC under Steiglich esterification conditions as illustrated in Scheme 2.6. The nature of the protecting groups allowed for a one step global deprotection using TFA in future steps. The synthesis of the O-acyl amidoximes **144** and **146** was also achieved through reaction of the respective amino acid-protected acid chlorides. However, usual routes to acid chlorides were not possible due to the acidic conditions used in their preparation. Cyanuric chloride allowed for the preparation of the protected acid chlorides under basic conditions.¹⁴⁰ Both the Steiglich esterification and acid chloride methods gave **144** and **146** in modest to good yields. Due to the ease of Steiglich esterification, this route was subsequently employed. Crystallisation of **146** allowed single crystal X-ray diffraction analysis of the product, confirming its identity, as illustrated in Figure 2.4.

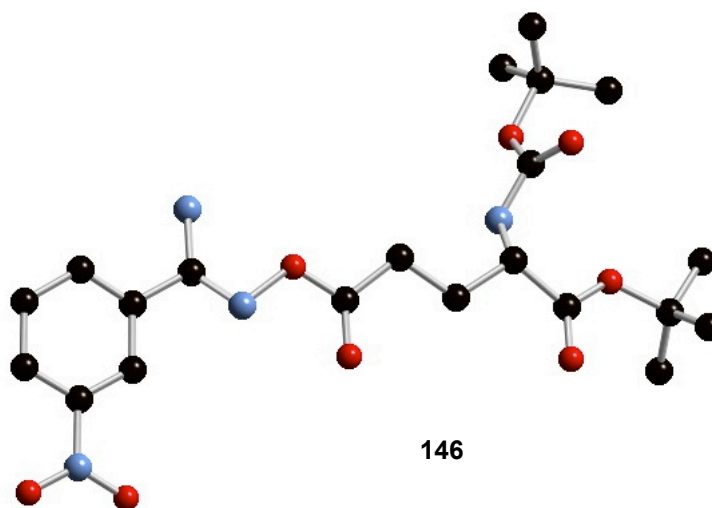
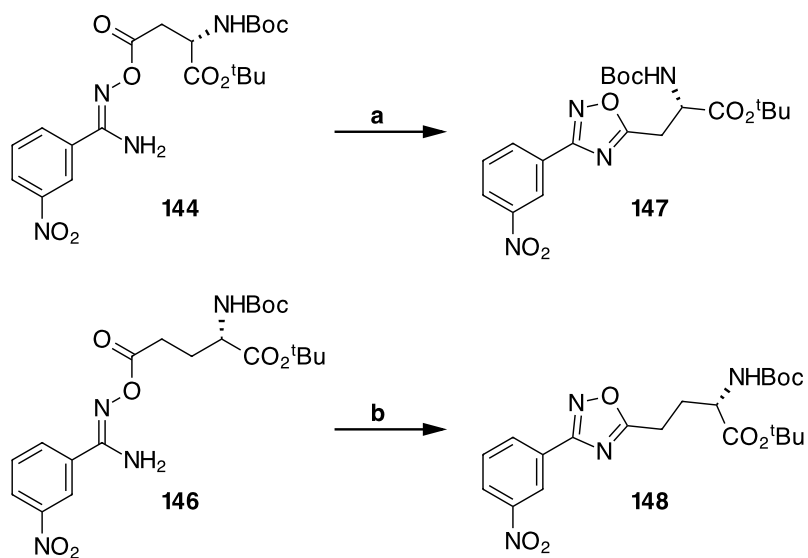
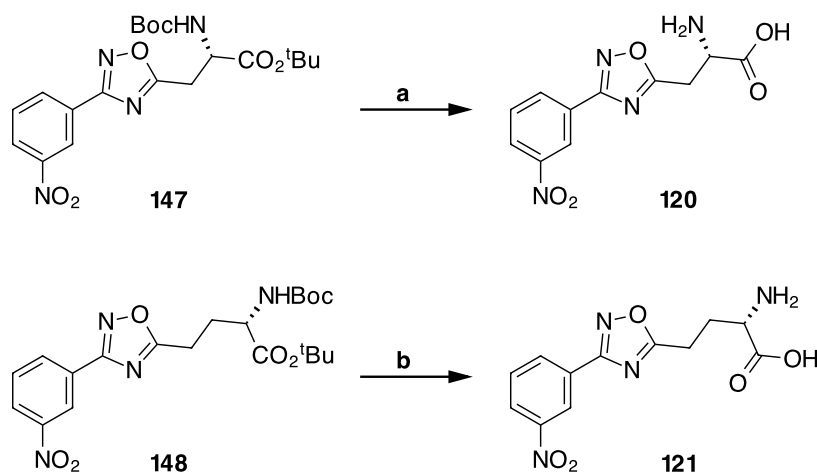


Figure 2.4. X-ray crystal structure of **146**.



Scheme 2.7. Reagents and conditions: **a)** TBAF, THF, RT, 16 h, 83%; **b)** TBAF, THF, RT, 16 h, 60%.

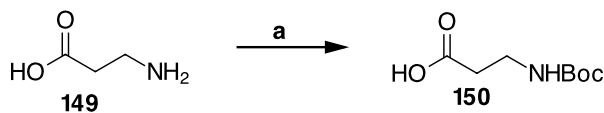
With the acyl amidoximes **144** and **146** in hand, cyclisation using TBAF was explored. This reaction went smoothly and the corresponding 1,2,4-oxadiazoles **147** and **148** were generated in good yields.



Scheme 2.8. Reagents and conditions: **a)** TFA, triethylsilane, RT, 16 h, followed by HCl, 50%; **b)** TFA, triethylsilane, RT, 16 h, followed by HCl, 18%.

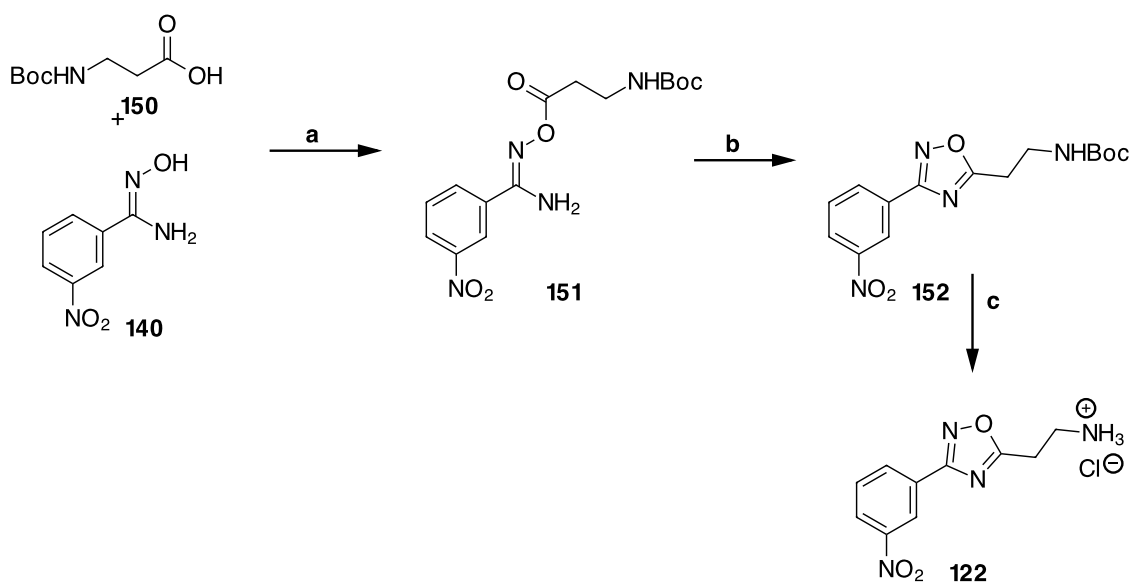
The final step in the synthesis of this class of compounds involved global deprotection of **147** and **148** with TFA to give amino acids **120** and **121**, as illustrated in Scheme 2.8. Triethylsilane was added as a scavenging reagent for the 2-methylprop-1-ene formed in the reaction. This method gave the products as their TFA salts, which had poor solubility in all solvents explored, making the products difficult to characterise. Accordingly, the TFA salts were redissolved in a large volume of 1 M HCl solution and the solvent was removed under reduced pressure. This gave the amino acids as their hydrochloride salts. However, the hydrochloride salts were still found to be relatively insoluble.

With the amino acids **120** and **121** successfully in hand, attention turned to the synthesis of the amine side chain. There was evidence that the sulfonamides in inhibitors **93** and **135** were acting as carboxylic acid bioisosteres.⁶⁷ The amine side chain allowed investigation into possible amine binding interactions in the active site of K3MO. 5-Ethylamine-1,2,4-oxadiazole **122** became a target compound and the planned synthesis commenced from β -alanine.



Scheme 2.9. Reagents and conditions: **a)** Boc₂O, dioxane:water 2:1, RT, 16 h, 82%.

The initial step, as illustrated in Scheme 2.9, was to protect the amine functionality of β -alanine **149**. Boc protection of the amine was chosen due to the ease with which the protecting group could be removed in the final step. The amine was protected in aqueous alkaline conditions, using a literature method,¹⁴¹ to give carboxylic acid **150** in good yield.



Scheme 2.10. Reagents and conditions: **a)** DCC, DMAP, DCM, RT, 16 h, 73%; **b)** TBAF, THF, RT, 16 h, 99%; **c)** HCl solution in dioxane, DCM, RT, 16 h, 78%.

Coupling of amidoxime **140** and carboxylic acid **150** was achieved using Steiglich esterification conditions to give O-acyl amidoxime **151**, as illustrated in Scheme 2.10. O-Acyl amidoxime **151** was then cyclised using TBAF to give 1,2,4-oxadiazole **152** in excellent yield. Single crystal X-ray crystallography confirmed the expected structure of **152**, as illustrated in Figure 2.5.

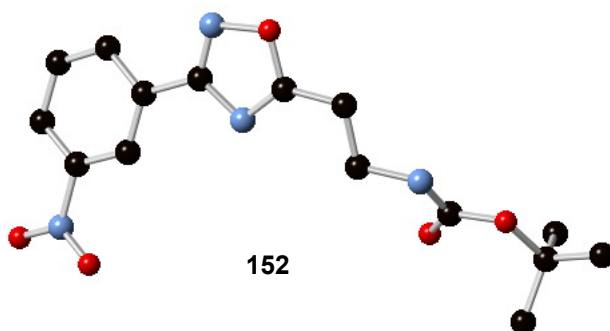


Figure 2.5. X-ray crystal structure of **152**.

Deprotection of **152**, as illustrated in Scheme 2.10 was accomplished in a straightforward manner through the use of HCl solution in 1,4-dioxane to give **122** as its hydrochloride salt.

2.3 Investigation into alternative motifs for inhibition of K3MO

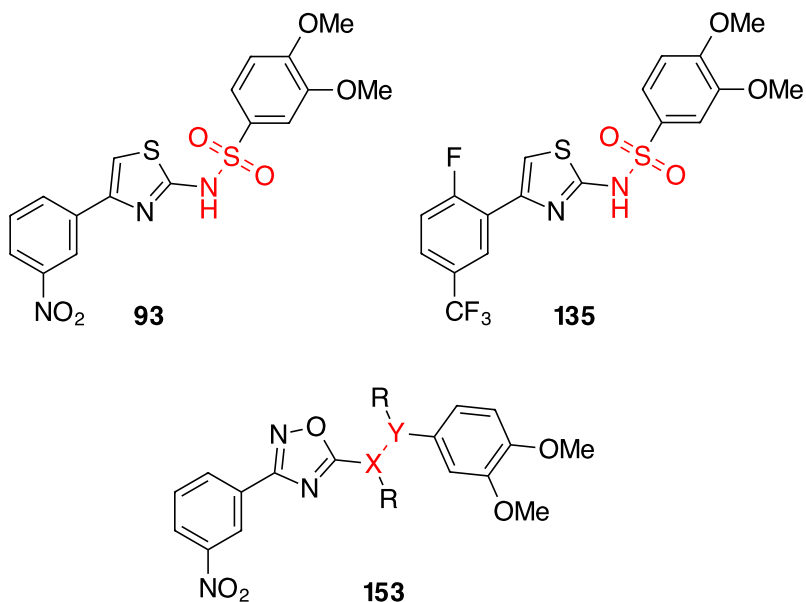
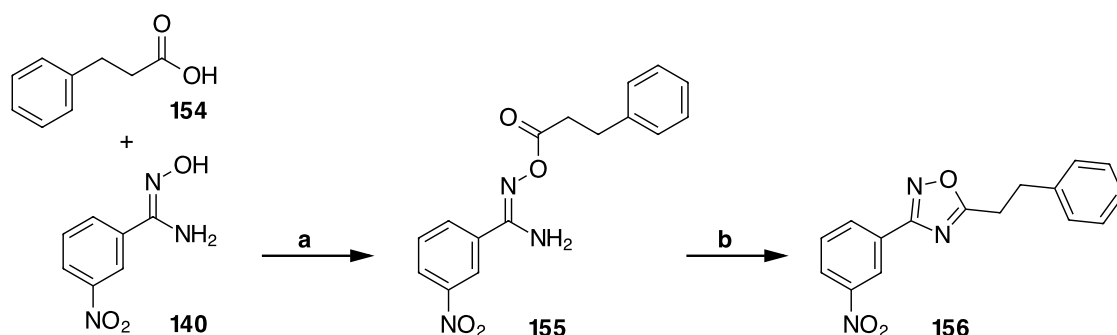


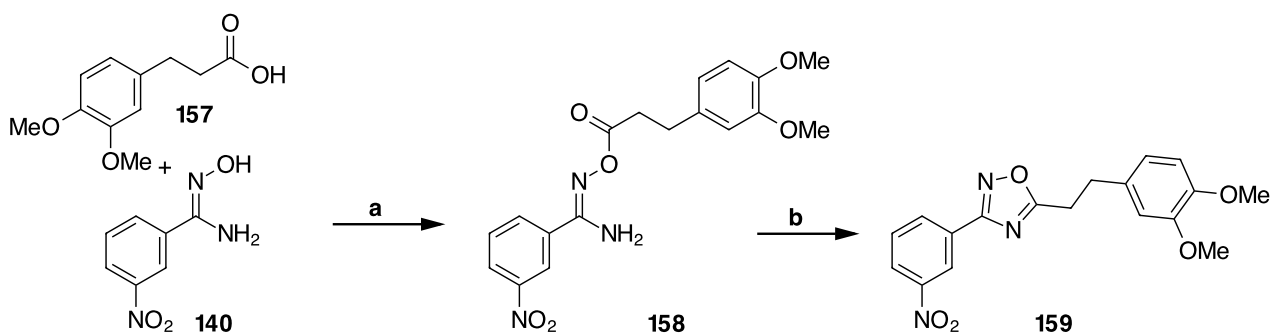
Figure 2.6. The sulfonamides **93** and **135** and the general structure for the SAR **153**. The two atoms targeted for structural change are highlighted in red.

The sulfonamides **93** and **135** originated as hits from a high throughput screen. There is no information on alteration of the sulfonamide functionality to alternative 2-atom linkers between the heterocycle and the 3,4-dimethoxy phenyl ring, such as in **153**. The relative ease of access to the 1,2,4-oxadiazole motif renders these compounds a good scaffold to replace the sulfonamide with carbon-carbon and carbon heteroatom bonds. To gain a greater understanding of the three-dimensional binding requirements the two-carbon linker was also varied with different functionalities.



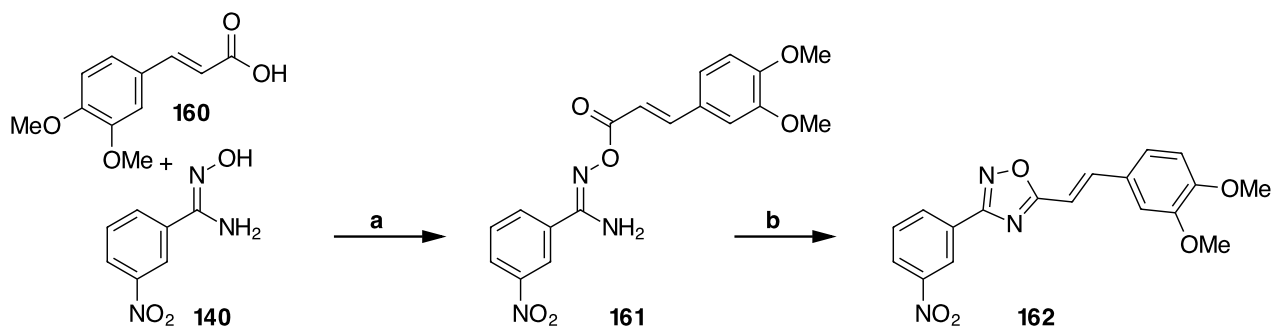
Scheme 2.11. Reagents and conditions: **a)** DCC, DMAP, DCM, RT, 16 h, 16%; **b)** TBAF, THF, RT, 16 h, 94%.

The 1,2,4-oxadiazole **156**, shown in Scheme 2.11, was prepared as a reference compound for this series. This compound does not have the 3,4-dimethoxy groups. Amidoxime **140** and 3-phenylpropionic acid **154** were coupled using Steiglich conditions to form O-acyl amidoxime **155**. The yield was poor, but enough material was obtained to carry out the TBAF cyclisation of O-acyl amidoxime **155**, to give 1,2,4-oxadiazole **156**. This second reaction was accomplished in an excellent yield, as illustrated in Scheme 2.11.



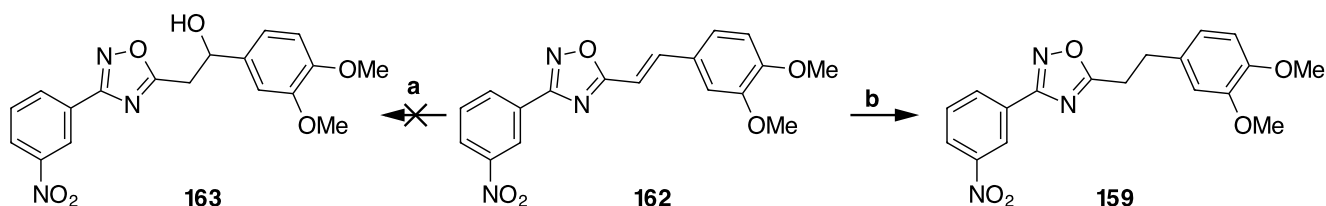
Scheme 2.12. Reagents and conditions: **a)** DCC, DMAP, DCM, RT, 16 h, 31%; **b)** TBAF, THF, RT, 16 h, 54%.

Oxadiazole **159** was targeted for investigation. In this compound the sulfonamide of **93** has been replaced with two methylene units. This enabled an exploration of the effect, if any, that the sulfonamide has on binding. O-Acyl amidoxime **158** was prepared using DCC and DMAP, as illustrated in Scheme 2.12. The product **158** was obtained in poor yield, however, enough material was obtained to complete the TBAF cyclisation to give 1,2,4-oxadiazole **159**.



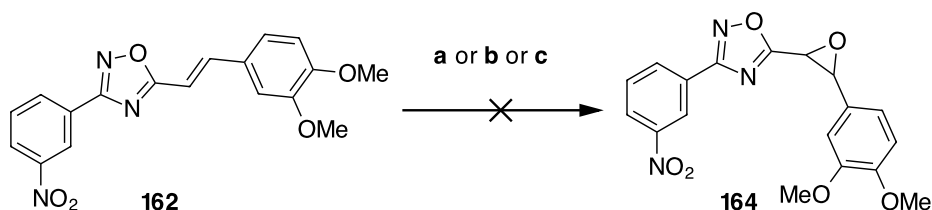
Scheme 2.13. Reagents and conditions: **a)** DCC, DMAP, DCM, RT, 16 h, 49%; **b)** TBAF, THF, RT, 16 h, 45%.

The introduction of a carbon-carbon double bond offered some versatility as it can be further elaborated. O-Acyl amidoxime **161** was synthesised using DCC, DMAP, carboxylic acid **160** and amidoxime **140**, as illustrated in Scheme 2.13. Initially, the product was purified by flash column chromatography, however, it proved easier to recrystallise **161** from ethanol and water. TBAF-mediated cyclisation of O-acyl amidoxime **161** gave the desired 1,2,4-oxadiazole **162** in a moderate yield. The product was difficult to purify and handle, as it had poor solubility in many solvents. This poor solubility made flash column chromatography difficult, as large volumes of solvent were required. This problem was overcome by recrystallisation of **162** from hot ethanol. The conjugated π system gave **162** an orange colour.



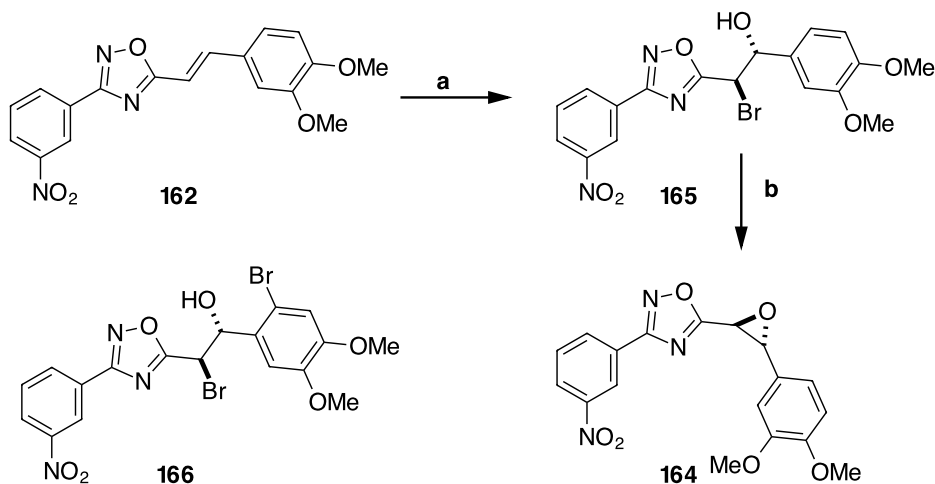
Scheme 2.14. Reagents and conditions: **a)** $\text{BH}_3\cdot\text{THF}$ (0.5 eq), THF, H_2O_2 , NaOH; **b)** $\text{BH}_3\cdot\text{THF}$ (2 eq), THF, H_2O_2 , NaOH, 45%.

With **162** in hand, elaboration of the double bond was explored. Hydroboration using 2 eq of the borane-THF complex was carried out, as illustrated in Scheme 2.14. This reduced the double bond to give a saturated ethane spacer **159** instead of the desired alcohol **163**.



Scheme 2.15. Reagents and conditions: **a)** *m*CPBA, DCM, RT, 16 h; **b)** H₂O₂, NaOH, MeOH; **c)** KHSO₅, K₂CO₃, acetone.

The synthesis of epoxide **164** directly from alkene **162** was unsuccessful (Scheme 2.15). Epoxidation using *m*CPBA, dimethyldioxirane¹⁴² and alkaline hydrogen peroxide was explored, however, these conditions did not show any conversion to the desired epoxide. Therefore, an alternative two-step route to epoxide **164** *via* a bromohydrin was explored, as illustrated in Scheme 2.16.



Scheme 2.16. Reagents and conditions: **a)** NBS (1.3 eq), THF, H₂O, exclusion of light, RT, 16 h, 75%; **b)** K₂CO₃, MeOH, 64%, RT, 16 h, 64%.

Alkene **162** was treated with NBS in aqueous THF to generate bromohydrin **165** (Scheme 2.16).¹⁴³ The reaction was optimal when alkene **162** was fully dissolved in the THF/water solution, however, an excess of water lead to alkene precipitation,

lowering the yield. The yield of the reaction was also reduced by the formation of side-product **166**, which arose from electrophilic aromatic substitution of the anisole ring. Optimal results were obtained with 1.3 eq of NBS; with less than 1.3 eq the reaction did not go to completion, which complicated purification. More than 1.3 eq led to increased formation of side-product **166**.

Bromohydrin **165** was recovered in good yield as a racemic single diastereoisomer. The regiochemistry of the bromohydrin was confirmed by 2D HMBC NMR analysis. Single crystal X-ray crystallography of the product also confirmed the regio- and relative stereo- chemistry of **165** as illustrated in Figure 2.7.

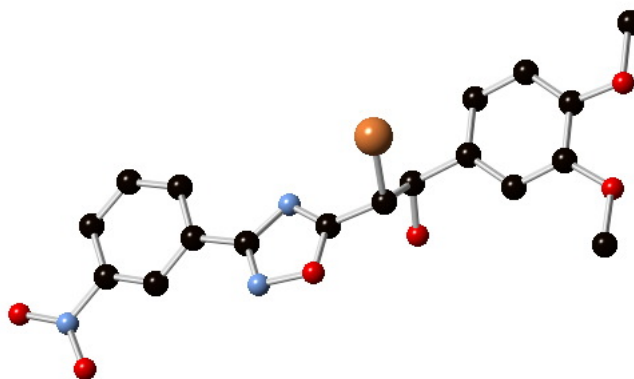
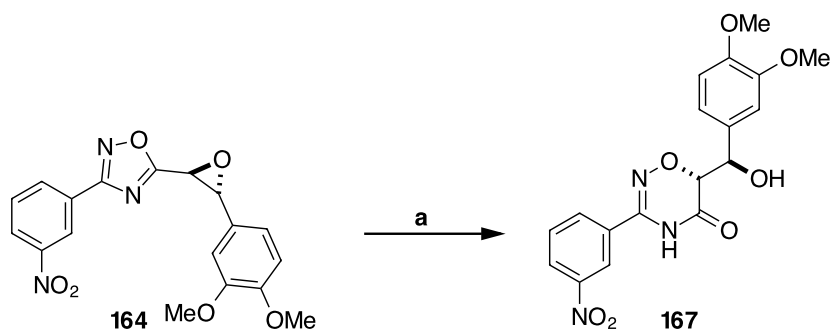


Figure 2.7. X-Ray crystal structure of **165**, proving the *anti* relationship of the bromohydrin.

Epoxide **164** was formed by intramolecular cyclisation of bromohydrin **165** using potassium carbonate, as illustrated in Scheme 2.16. Smaller scale reactions could be purified by careful column chromatography. On a larger scale (≥ 1 g), the product was found to precipitate on top of the column bed, causing the product to streak over a long elution. Attempts at recrystallisation were unsuccessful.

With epoxide **164** in hand, a series of reactions were explored to further functionalise the epoxide and generate more substrates for inhibition studies.



Scheme 2.17. Reagents and conditions: **a)** KOH, H₂O, MeOH, THF, 70 °C, 2 h, 50%.

Initial attempts to open the epoxide with hydroxide ion did not furnish the expected diol. Analysis of the product by single crystal X-ray crystallography (Figure 2.8) revealed the re-arranged heterocyclic product **167**, as illustrated in Scheme 2.17

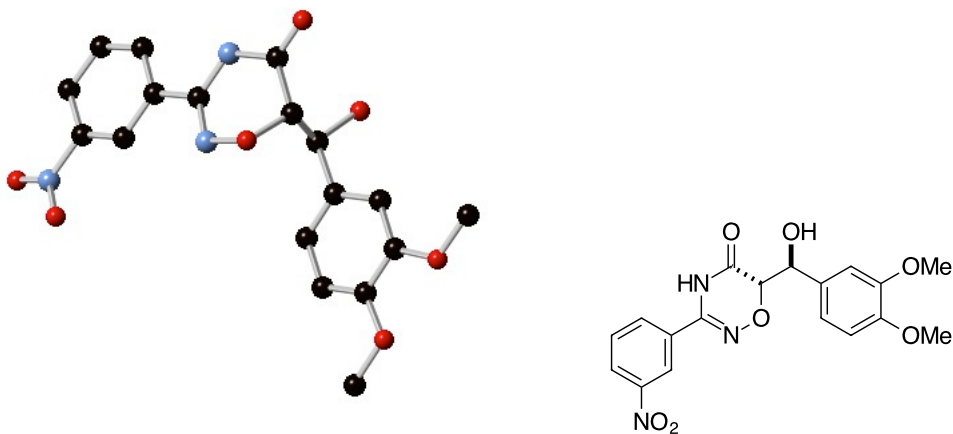
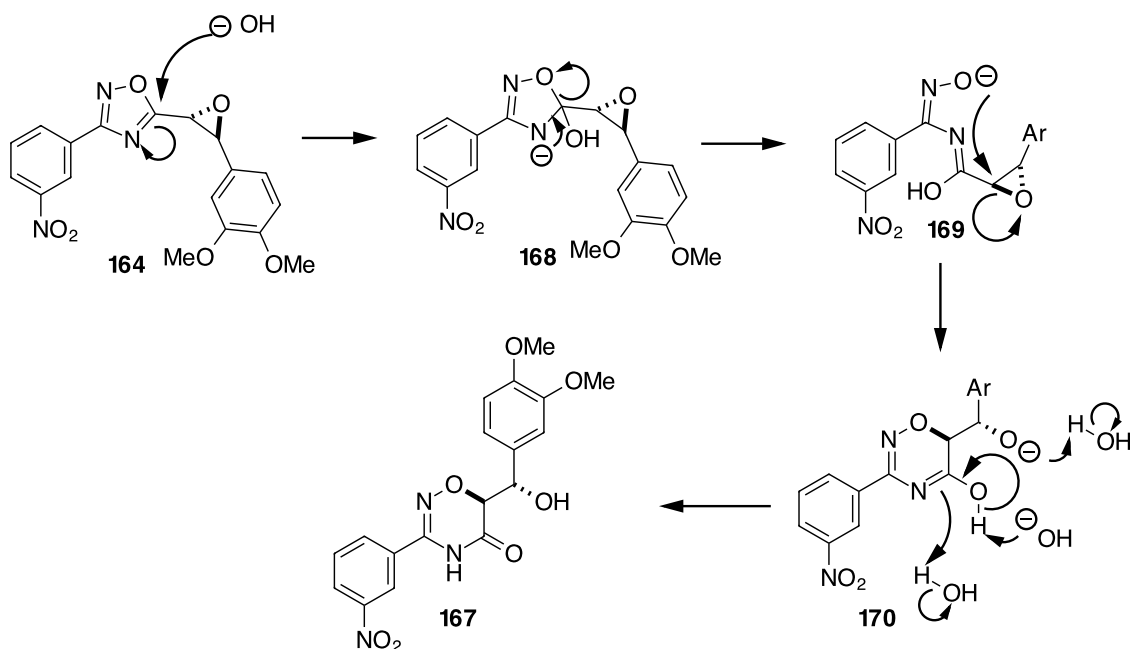


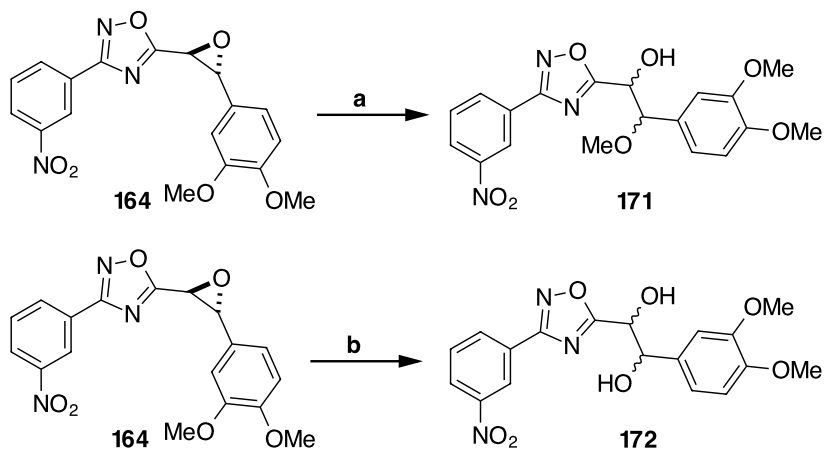
Figure 2.8. X-Ray crystal structure of **167**, confirming the rearrangement of the 1,2,4-oxadiazole (Scheme 2.17).



Scheme 2.18. A plausible mechanism for the rearrangement of the 1,2,4-oxadiazole heterocycle.

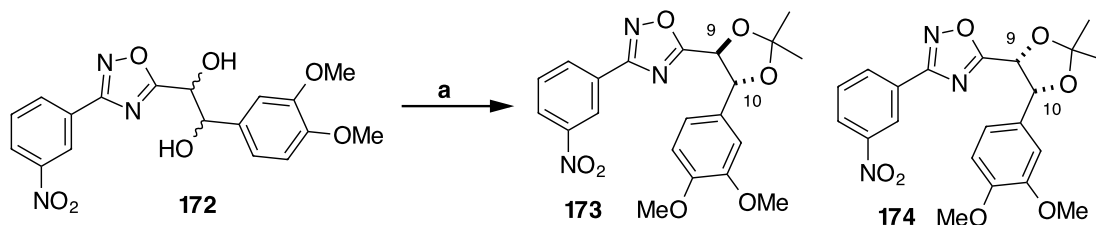
A plausible mechanism for this transformation is illustrated in Scheme 2.18. Product **167** exists as an amide as the carbonyl $\text{C}=\text{O}$ distance is 1.212 Å. A typical carbonyl $\text{C}=\text{O}$ bond length is 1.22 Å compared to a typical $\text{C}-\text{O}$ single bond length of 1.43 Å.

With basic conditions favouring attack at C-5 of the 1,2,4-oxadiazole heterocycle, hydrolytic ring opening of the epoxide under acidic conditions was explored.



Scheme 2.19. Reagents and conditions: **a**) HCl, MeOH, THF, H_2O , 70 °C, 3 h; **b**) HCl, THF, H_2O , 70 °C, 3 h, 98%.

When epoxide **164** was treated with acidic methanol solution, the major product isolated was an inseparable mixture of the methoxy diastereoisomers **171**. In the absence of methanol, an inseparable mixture of the diol diastereoisomers **172** was generated, as illustrated in Scheme 2.19. Separation of these diastereoisomers was not possible directly, however, a resolution of the diastereoisomers could be achieved after formation of acetonides **173** and **174**.



Scheme 2.20. Reagents and conditions: a) 2,2-Dimethoxypropane, *p*-TSA, DCM, RT, 16 h, 37% **173**, 57% **174**.

The acetonides **173** and **174** were formed in good yield using 2,2-dimethoxypropane under acid catalysis, as illustrated in Scheme 2.20. Stereoisomer **173**, obtained by column chromatography, had a ^1H NMR spectrum where H-9 and H-10 were sufficiently resolved to conduct an NOE experiment. In the ^1H NMR spectrum of stereoisomer **174**, the chemical shifts of H-9 and H-10 were too close for NOE resolution.

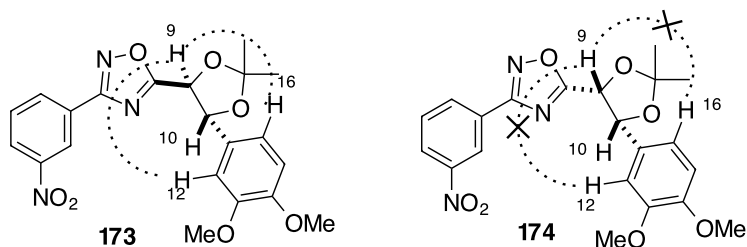


Figure 2.9. An NOE enhancement of H-12 and H-16 was observed for **173**. No such enhancement should exist for **174**.

For **173**, irradiation of H-9 led to a weak enhancement of the aromatic protons H-12 and H-16. This allowed a tentative assignment as the *anti* isomer. H-9 in the *anti* isomer is close enough in space to the aromatic protons to have an NOE enhancement, whereas a model of the *syn* stereoisomer indicates that H-9 is too

far from the aromatic protons for such an enhancement. Further confirmation of the relative configurations of **173** and **174** was obtained by X-ray crystallography. (Figure 2.10)

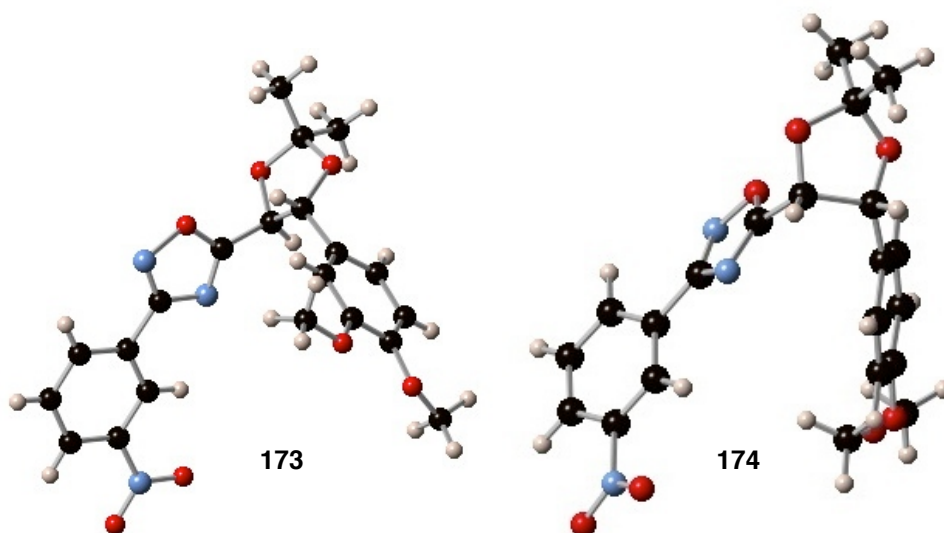
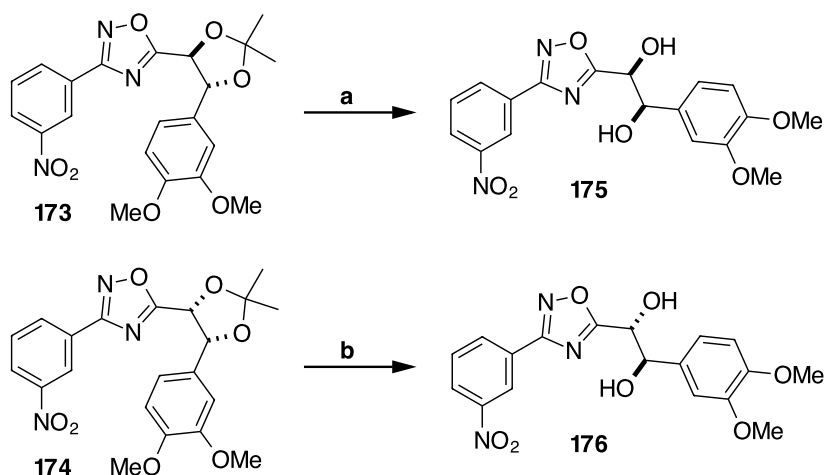


Figure 2.10. X-Ray crystallography confirmed the relative stereochemistry of acetonides **173** and **174** as *anti* and *syn*

With the diastereoisomers separated, removal of the acetonide groups gave the diols **175** and **176**.



Scheme 2.21. Reagents and conditions: **a**) Camphor sulfonic acid, HCl, MeOH, 90 °C, 2 h, 67%; **b**) camphor sulfonic acid, HCl, MeOH, 90 °C, 2 h, 64%.

The acetonide protecting groups of **173** and **174** were removed under acidic conditions to give diols **175** and **176** in good yield, as illustrated in Scheme 2.21. Confirmation of the relative stereochemistry of each diol was achieved by single crystal X-ray crystallography (Figure 2.11).

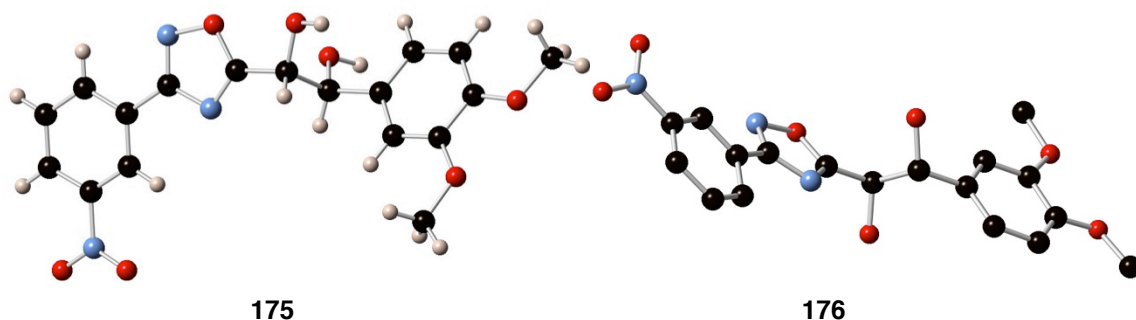
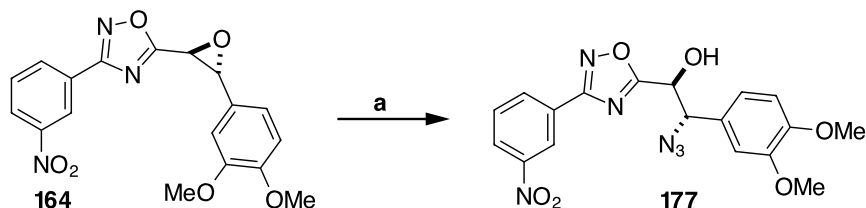


Figure 2.11. X-Ray crystallography confirmed the relative stereochemistry of diols **175** and **176**.

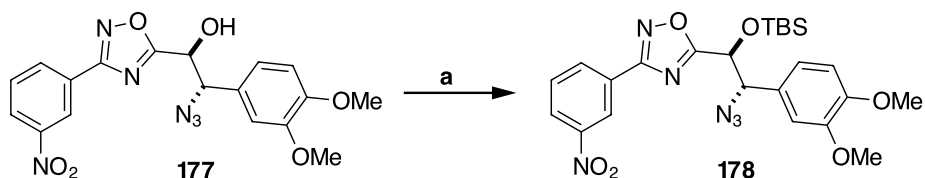


Scheme 2.22. Reagents and conditions: **a)** NaN_3 , NH_4Cl , MeOH , H_2O , 70°C , 2 h, 88%.

Ring opening of epoxide **164** was also explored using sodium azide under acidic conditions, as illustrated in Scheme 2.22. This reaction was successful and azido alcohol **177** was obtained in good yield as a single diastereoisomer. The product was obtained as a single regioisomer, presumably because the electron-rich aromatic ring promotes epoxide ring opening at C-10. The product could be purified by column chromatography and was stable for many months. The regioselectivity of the reaction was confirmed by 2D HSQC and HMBC NMR experiments, which showed that the azide was attached adjacent to the phenyl ring.

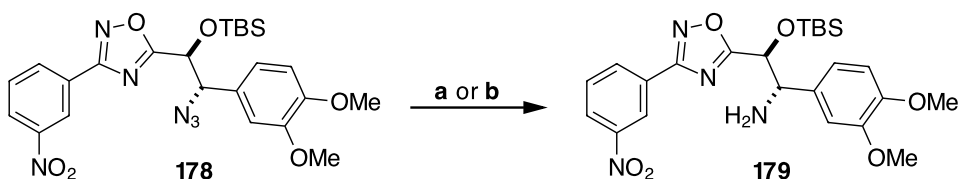
Initial attempts at reduction of the azide to the amine were unsuccessful. A Staudinger reduction using PPh_3 or a reduction using ferric chloride with sodium iodide¹⁴⁴ or zinc borohydride¹⁴⁵ did not furnish the desired amino alcohol. Reduction of the azide in the presence of the free alcohol was potentially

complicating the reaction, therefore, the alcohol was protected as a silyl ether, as illustrated in Scheme 2.23.



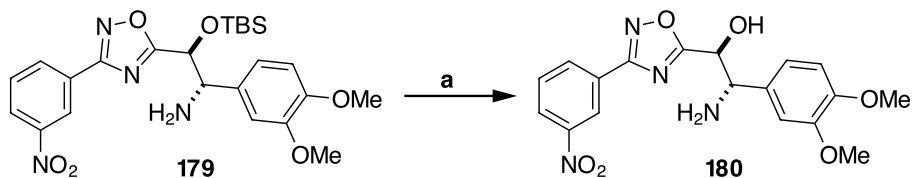
Scheme 2.23. Reagents and conditions: a) TBSCl, imidazole, DCM, RT, 16 h, 71%.

Protection of alcohol **177** was accomplished using TBSCl and imidazole to give TBS ether **178** in good yield. TBS protection provides some acid stability and removal of the protecting group could be easily achieved using a fluoride source, most commonly TBAF.



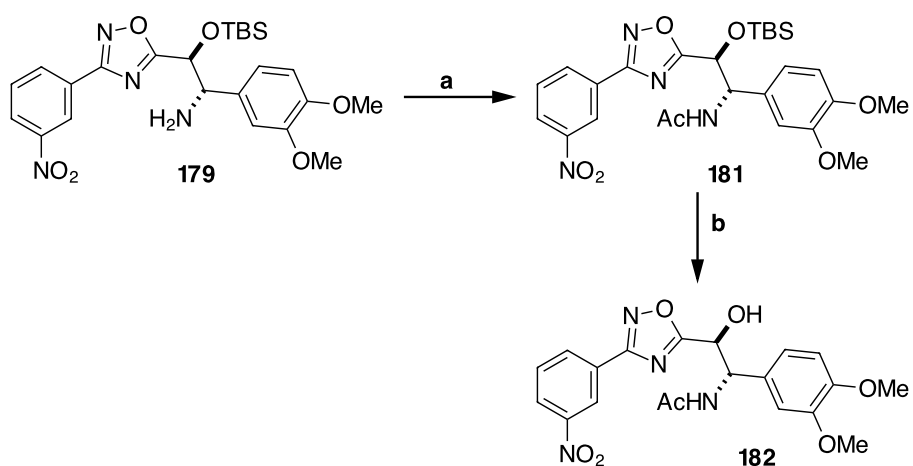
Scheme 2.24. Reagents and conditions: a) Resin bound triphenyl phosphine, THF, H₂O, 70 °C, 16 h, 62%; b) PMe₃, NaOH, THF, H₂O, RT, 16 h, 55%

Initial attempts at the Staudinger reduction using triphenylphosphine^{146, 147} worked well to give amine **179**, however, co-elution of the triphenylphosphine oxide byproduct complicated the purification. Using resin bound triphenylphosphine, as illustrated in Scheme 2.24, it was possible to separate the triphenylphosphine oxide by filtration of the solid support. This allowed amine **179** to be recovered by column chromatography in moderate yield. Resin bound triphenylphosphine is relatively expensive and so an alternative Staudinger reduction using trimethylphosphine^{148, 149} was explored. Trimethylphosphine oxide is water soluble and could be removed by careful washing during reaction work up. In the event trimethylphosphine gave a slightly lower yield of **179**, but it benefited from lower cost and milder reaction conditions.



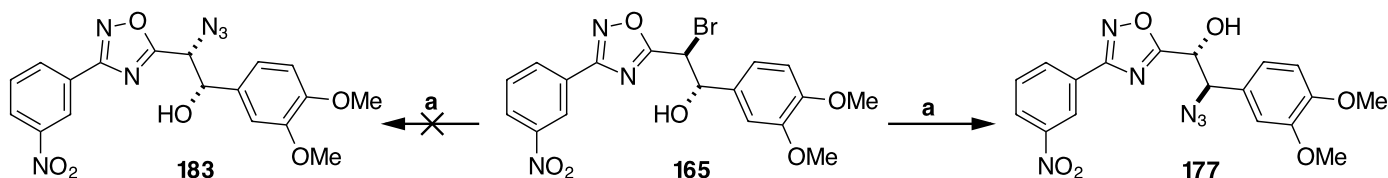
Scheme 2.25. Reagents and conditions: **a)** TBAF, THF, RT, 3 h, 68%.

With amine **179** in hand, the next step involved removal of the TBS protecting group. This was achieved using TBAF to give the desired amino alcohol **180** in a relatively straightforward manner,¹⁵⁰ as illustrated in Scheme 2.25.



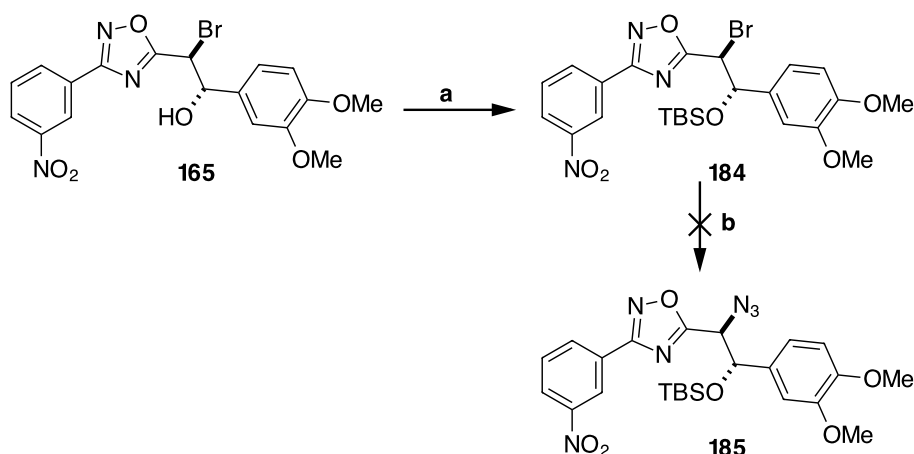
Scheme 2.26. Reagents and conditions: **a)** Ac₂O, DMAP, DCM, RT, 16 h, 51%; **b)** TBAF, THF, RT, 2 h, RT, 71%.

Acetamide **182** was prepared to explore differences between amine and amide functionality at the C-10 position. Thus, amine **179** was treated with acetic anhydride in the presence of DMAP to give acetamide **181** in a moderate yield, as illustrated in Scheme 2.26. With the protected acetamide **181** in hand, the TBS protecting group was successfully removed using TBAF to give alcohol **182**.



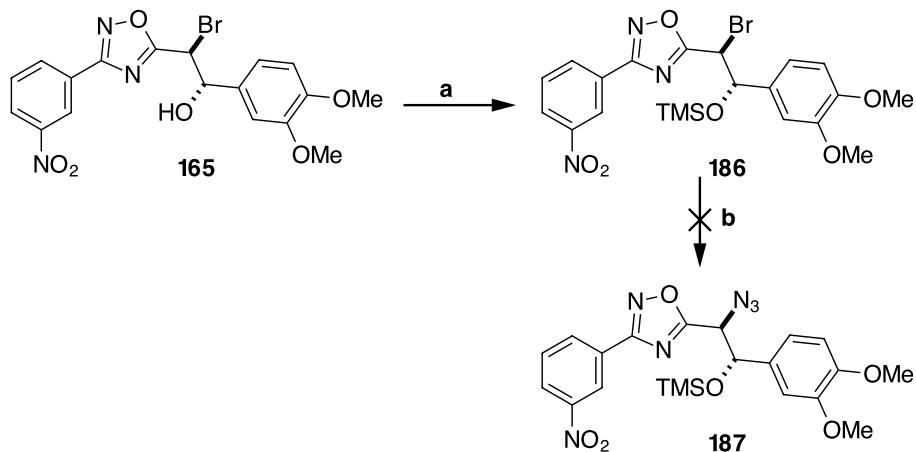
Scheme 2.27. Reagents and conditions: **a)** NaN₃ DMSO, 50 °C, 16 h.

Any attempt to directly substitute the bromide in bromohydrin **165** for azide, to give the alternative regioisomer of the azido alcohol **183**, was unsuccessful (Scheme 2.27). The product had identical ^1H and ^{13}C NMR spectra to the original isomer **177**. It is probable that under the $\text{S}_{\text{N}}2$ conditions the epoxide is generated and is then opened by the azide. Protection of the alcohol was then investigated to determine whether substitution of the bromide by azide could be favoured over epoxide formation.

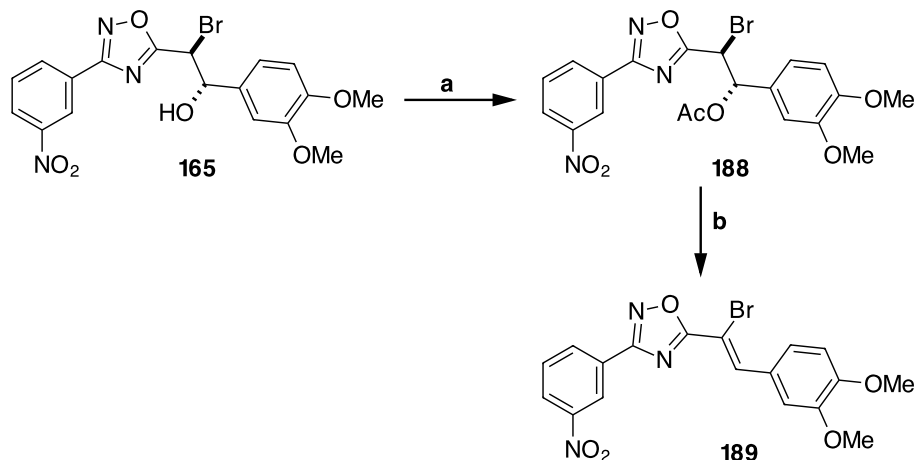


Scheme 2.28. Reagents and conditions: **a**) TBSCl, imidazole, DCM, RT, 8 h, 78%; **b**) NaN_3 , DMSO, 50 °C, 16 h.

Protection of bromohydrin **165** as the TBS silyl ether was accomplished in good yield, as illustrated in Scheme 2.28.^{151, 152} With the protected bromohydrin **184** in hand, azide substitution was explored under $\text{S}_{\text{N}}2$ conditions.¹⁵³ However, the reaction only returned starting material, even over extended reaction times. A similar reaction with the TMS silyl ether **186** was also unsuccessful, as illustrated in Scheme 2.29.



Scheme 2.29. Reagents and conditions: **a**) TMSCl, imidazole, DCM, RT, 8 h, 66%; **b**) NaN₃, DMSO, 50 °C, 16 h.



Scheme 2.30. Reagents and conditions: **a**) Ac₂O, pyridine, DCM, RT, 16 h, 87%; **b**) NaN₃, DMSO, 50 °C, 2h, 58%.

As the bulky silyl ethers did not show any reactivity, the free alcohol was protected as acetate **188**, as illustrated in Scheme 2.30. Azide substitution of the bromine was then explored. Analysis of the product by ¹H and ¹³C NMR spectroscopy revealed that an elimination reaction had occurred to produce **189**. Single crystal X-ray crystallography confirmed the structure of the elimination product illustrating that the Z-alkene had formed (Figure 2.12).

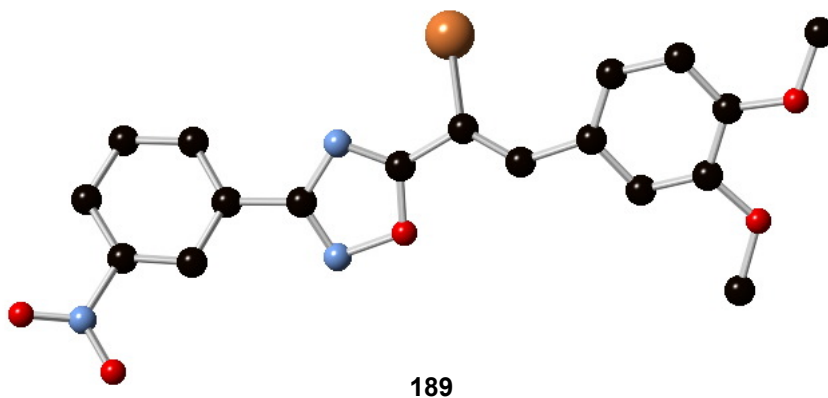
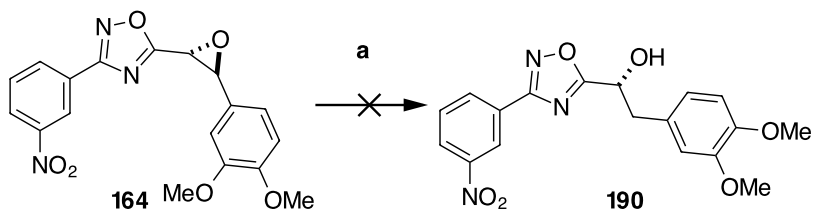
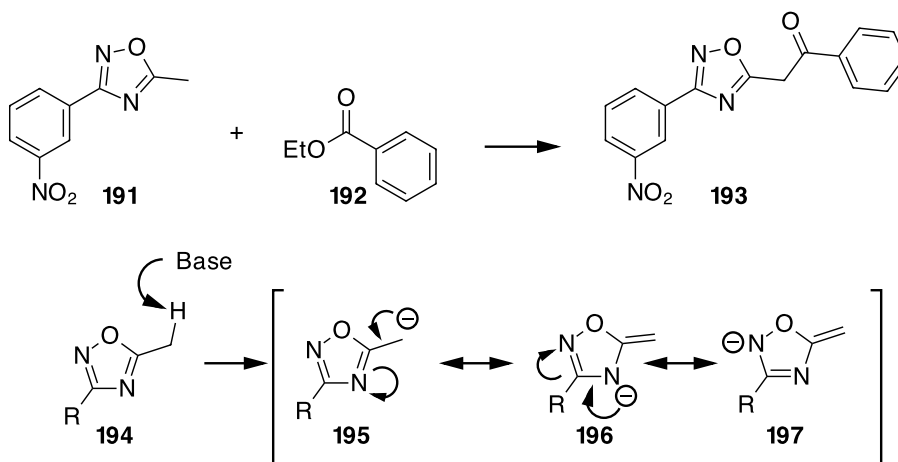


Figure 2.12. X-Ray crystal structure of elimination product **189**.



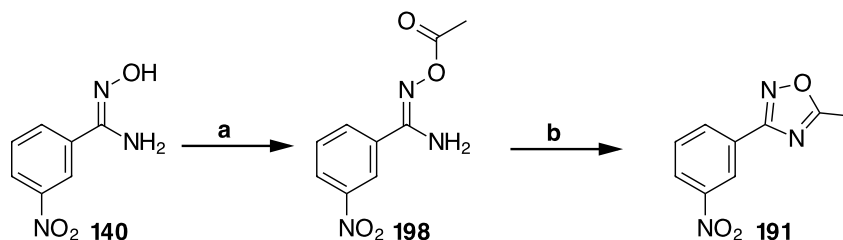
Scheme 2.31. Reagents and conditions: a) NaBH₄, MeOH, RT, 16 h.

Reduction of epoxide **164** to give the alcohol **190** was explored. Traditionally, the reduction of an epoxide is achieved using LiAlH₄, however, 1,2,4-oxadiazoles are not stable to LiAlH₄ as they are also susceptible to reduction. The less reactive sodium borohydride was explored, however, this was unreactive and only starting material was returned (Scheme 2.31).



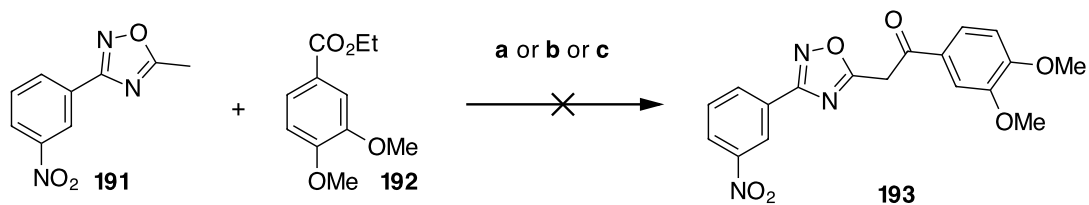
Scheme 2.32. Proposed synthesis of the ketone by Claisen condensation, via deprotonation of the 5-methyl-1,2,4-oxadiazole **191**.

The 5-methyl 1,2,4-oxadiazole **191** offered a potential synthetic route to ketone **193**. Strong bases^{154, 155} are able to deprotonate the methyl group of **191**. The resulting carbanion is relatively stable due to resonance stabilisation by the 1,2,4-oxadiazole (Scheme 2.32). There was an opportunity to use the resulting carbanion (**195-197**) in a Claisen or aldol-“like” reaction to give the desired products.



Scheme 2.33. Reagents and conditions: **a)** Ac_2O , Et_3N , DCM, RT, 16 h, 75%; **b)** TBAF, THF, RT, 16 h, 83%.

The synthesis of 5-methyl-1,2,4-oxadiazole **191** began with the reaction of amidoxime **140** and acetic anhydride to give O-acyl amidoxime **198**, as illustrated in Scheme 2.33. It was found that approximately 6% of the product had cyclised directly to 1,2,4-oxadiazole **191**. The purified O-acyl amidoxime **198** was readily cyclised to **191** using TBAF in good yield, as illustrated in Scheme 2.33.



Scheme 2.34. Reagents and conditions: **a)** *n*-BuLi, THF, -78 °C, 2 h; **b)** NaH, DMF, 0 °C, 3 h; **c)** NaOEt, THF, RT, 16 h.

With 5-methyl-1,2,4-oxadiazole **191** in hand the “Claisen”-like condensation was explored using ester **192**, as illustrated in Scheme 2.34. Deprotonation of **191** using LDA, *n*-BuLi, NaOEt and NaH were each attempted. Upon addition of any of these bases, a colour change occurred. However, the desired product **193** was not obtained in any of these cases. Attempts at an “aldol”-like reaction with trifluorobenzaldehyde also did not return the expected product and only starting material was recovered.

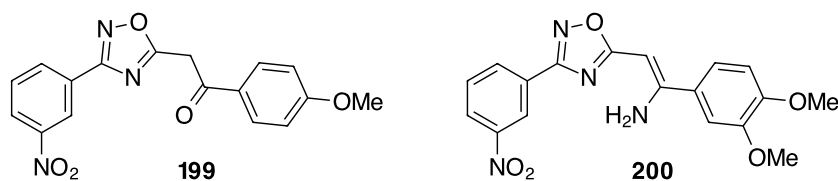
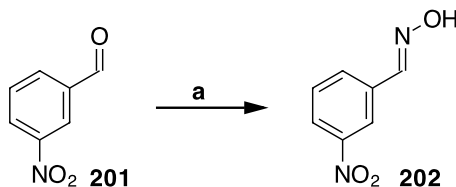


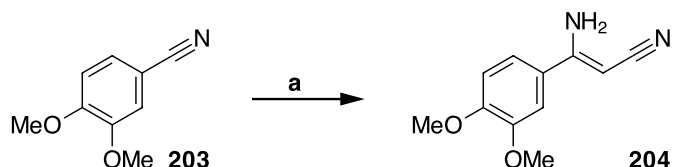
Figure 2.13. Ketone **199** has been previously reported. Enamine **200** offers an additional scaffold for enzyme assay.

A literature search revealed that ketone **199** had previously been synthesised¹⁵⁶ through the 1,3-dipolar cycloaddition of a nitrile oxide and an enaminonitrile, followed by hydrolysis (Figure 2.13). This was an attractive route to both ketone **193** but also gave an additional functionality for assay, namely enamine **200**.



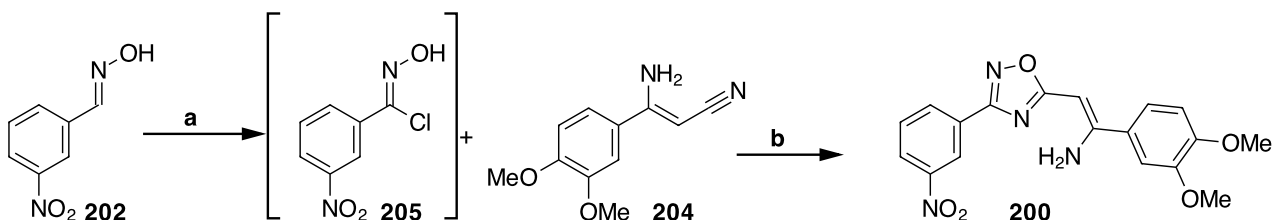
Scheme 2.35. Reagents and conditions: **a)** Hydroxylamine hydrochloride, NaOAc, acetonitrile:H₂O (2:1), RT, 16 h, 88%.

The nitrile oxide required for the 1,3-dipolar cycloaddition was generated *in situ* from oxime **202**. The oxime was synthesised by condensation of hydroxylamine with *meta*-nitrobenzaldehyde **201**, as illustrated in Scheme 2.35. Neutralisation of the acetic acid with sodium bicarbonate and the use of decolourising charcoal allowed the recovery of clean product in good yield.



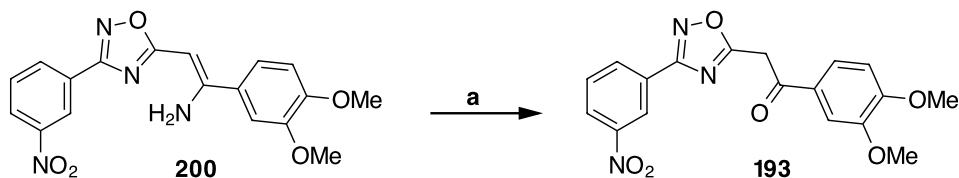
Scheme 2.36. Reagents and conditions: a) Acetonitrile, potassium *tert*-butoxide, toluene, RT, 16 h, 71%.

Enaminonitrile **204** was synthesised by the Thorpe reaction using acetonitrile, 3,4-dimethoxybenzonitrile **203** and potassium *tert*-butoxide as the base to give enaminonitrile **204** in good yield, as illustrated in Scheme 2.36.¹⁵⁷ ¹H NMR and ¹³C NMR spectroscopy showed the product existed as the enamine rather than the imine tautomer.



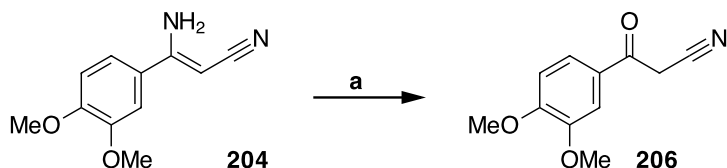
Scheme 2.37. Reagents and conditions: a) Sodium hypochlorite solution (1.6M), DCM, 3 min; b) Et₃N, 16 h, 1.7% (after recrystallisation).

With oxime **202** and enaminonitrile **204** in hand, attention turned to the 1,3-dipolar cycloaddition, as illustrated in Scheme 2.37. Oxime **202** was reacted with bleach as an electrophilic chlorine source and this generated oximyl chloride **205**. The oximyl chloride was used without any further purification and was added to a solution of enaminonitrile **204** in triethylamine. Triethylamine promotes the formation of the nitrile oxide. It is important that the dipolarophile is in the same solution as the triethylamine as nitrile oxides are known to dimerise, forming furoxans. In the event the yield from this reaction was very poor (10-15% before recrystallisation) and could not be improved.



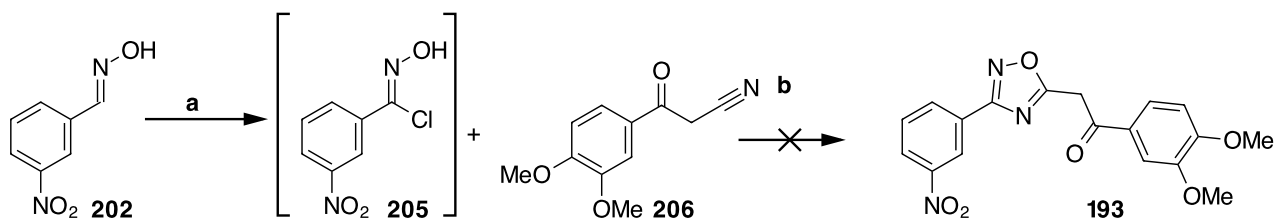
Scheme 2.38. Reagents and conditions: a) HCl, EtOH, 80 °C, 3 h, 13%.

Hydrolysis of enamine **200** to ketone **193** was undertaken, using concentrated hydrochloric acid in ethanol, as illustrated in Scheme 2.38. The hydrolysis was successful, however, purification of the product by column chromatography proved difficult. Purification of **193** by recrystallisation circumvented this problem. Despite the low yield, enough material was obtained to assay **193** against both the human and bacterial enzymes.



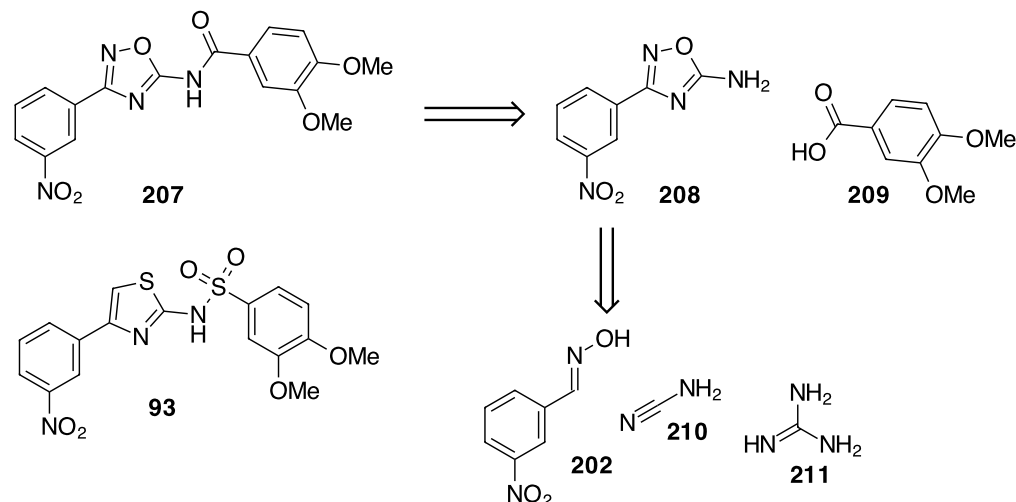
Scheme 2.39. Reagents and conditions: a) HCl (3 M solution), DCM, RT, 16 h, 60%.

Acid hydrolysis of enamine **204** was also investigated and this gave ketone **206** with retention of the nitrile functionality, as illustrated in Scheme 2.39.¹⁵⁸



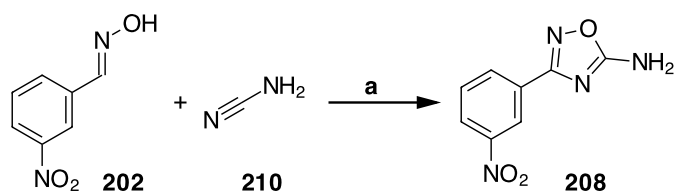
Scheme 2.40. Reagents and conditions: a) Sodium hypochlorite solution (1.6M), DCM, 3 min; b) Et₃N, 16 h.

Due to the poor reaction of enamine **204**, an investigation into the 1,3-dipolar cycloaddition reaction with ketone **206** was undertaken, however, this reaction proved unsuccessful returning none of the desired ketone **193** (Scheme 2.40).



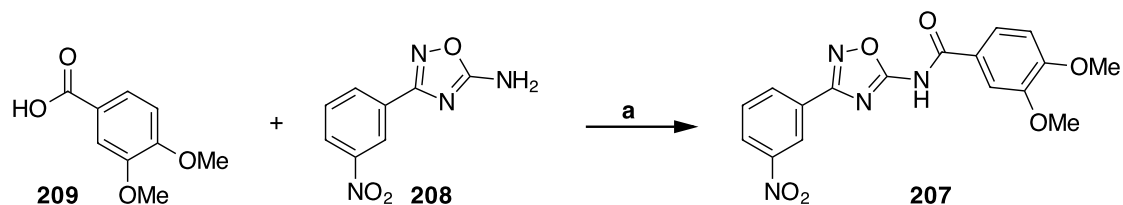
Scheme 2.41. Retrosynthetic analysis for the synthesis of amide **207**.

1,2,4-Oxadiazole **207** was synthesised for direct comparison with thiazole sulfonamide **93**. The connectivity of an amide and a sulfonamide are similar, however, their three-dimensional structures differ. This affects the interactions that each motif can make with the enzyme. The planned synthesis was to conduct the amide bond formation as the final step, as illustrated in Scheme 2.41. The required 5-amino-1,2,4-oxadiazole **208** would be synthesised through a 1,3-dipolar cycloaddition of the nitrile oxide intermediate, formed from oxime **202** and cyanamide **210**, or guanidine **211**, as illustrated in Scheme 2.41.^{159, 160}



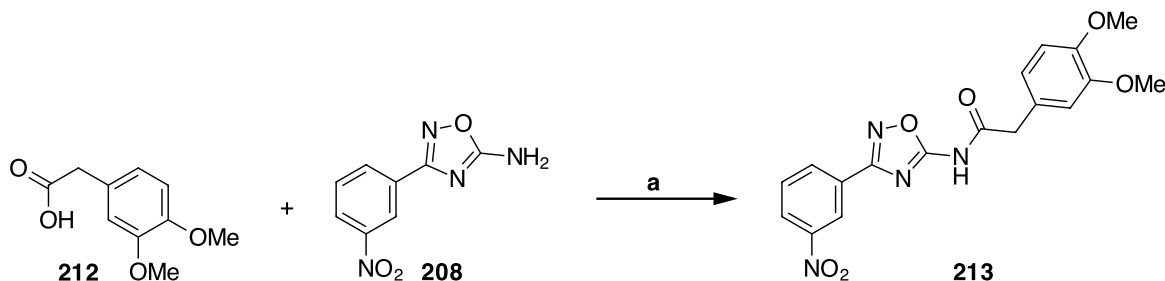
Scheme 2.42. Reagents and conditions: **a**) Sodium hypochlorite (1.6 M solution), DCM, 3 min then cyanamide, Et₃N, 68%.

The 1,3-dipolar cycloaddition was initially investigated using guanidine **211** as the dipolarophile, however, this gave low yields of 5-amino-1,2,4-oxadiazole **208**. The low reactivity was attributed to poor leaving group characteristics of the ammonia formed in the reaction. Changing the dipolarophile to cyanamide **210** increased the yield to 30%. Optimisation of the reaction, by altering the order of addition, further improved the yield to 68%, as illustrated in Scheme 2.42.



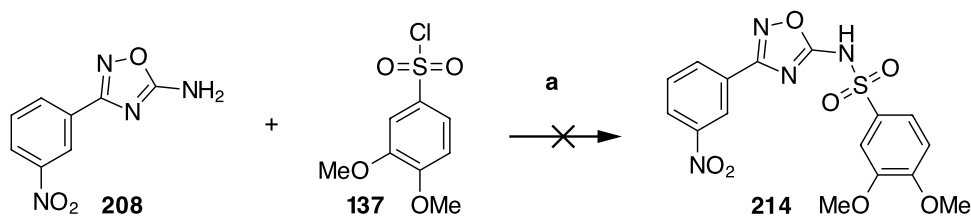
Scheme 2.43. Reagents and conditions: a) DCC, DCM, RT, 16 h, 21%.

With 5-amino-1,2,4-oxadiazole **208** in hand, amide **207** was prepared using DCC as a coupling agent, as illustrated in Scheme 2.43. The poor reactivity was attributed to the poor nucleophilicity of **208**. The nucleophilicity of **208** is reduced by the electron withdrawing effect of the 1,2,4-oxadiazole.



Scheme 2.44. Reagents and conditions: a) DCC, DMAP, DCM, RT, 16 h, 4%.

The synthesis of **213** was undertaken. It is an analogue of amide **207**, with an additional methylene group between the amide carbonyl and the 3,4-dimethoxyphenyl ring. The insertion of a carbon here introduces a new tetrahedral center adjacent to the amide. This allowed a comparison to be made with sulfonamide **93**. Amide **213** was synthesised with DCC as a coupling agent, as illustrated in Scheme 2.44. In the event, the reaction gave the amide **213** in poor yield, however, enough material was isolated for characterisation and enzyme assay.



Scheme 2.45. Reagents and conditions: a) Pyridine, DCM, RT, 16 h.

The synthesis of sulfonamide **214** from 5-amino-1,2,4-oxadiazole **208** and sulfonyl chloride **137** proved unsuccessful, even after several attempts, changing the solvent and the reaction temperature. It would appear that the low nucleophilicity of amine **208** impeded successful coupling.

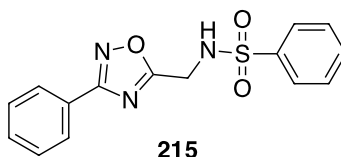
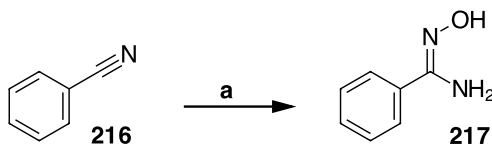


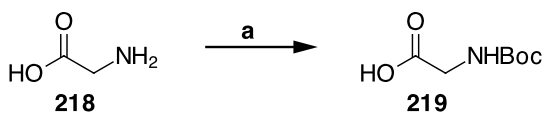
Figure 2.14. Alternative sulfonamide **215**.

Sulfonamide **215** was prepared for structure activity comparison with the thiazole sulfonamides **93** and **135**. As 5-amino-1,2,4-oxadiazole **208** did not react with sulfonyl chloride **137**, a methylene group was introduced between the oxadiazole and the amine in a bid to improve the reaction with sulfonyl chloride **137**. To ensure that any inhibition observed was due to the oxadiazole-sulfonamide motif all substituents from the aromatic rings were removed. If inhibition is observed, substitution could be reintroduced to increase inhibition.



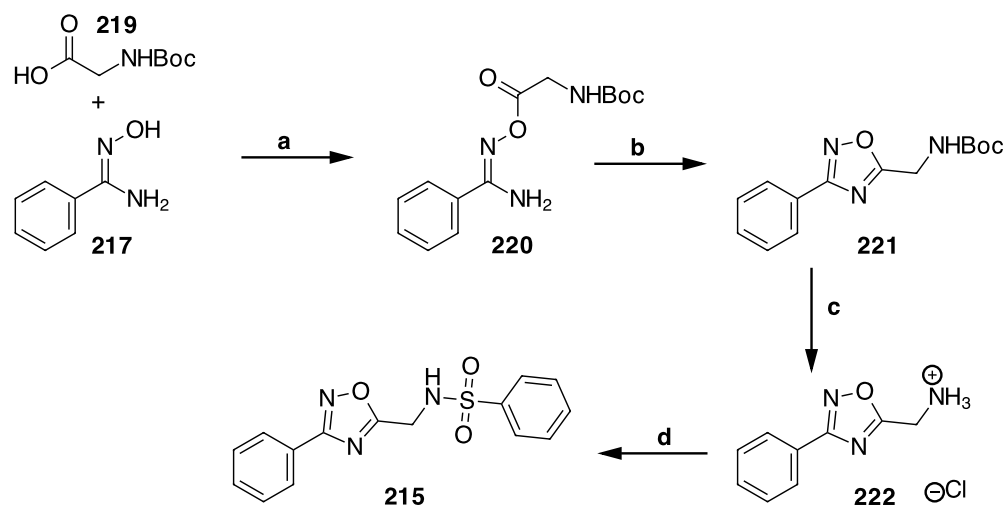
Scheme 2.46. *Reagents and conditions:* **a)** Hydroxylamine hydrochloride, K_2CO_3 , MeOH, 80 °C for 4 h, then RT for 16 h, 32%.

The synthesis of sulfonamide **215** began with the formation of phenyl amidoxime **217**, as illustrated in Scheme 2.46. Column chromatography gave enough material to proceed through the next steps.



Scheme 2.47. *Reagents and conditions:* **a)** Boc_2O , NaOH, 1,4-dioxane: H_2O 1:1, RT, 8 h, 87%.

The amino acid glycine **218** gave the required functionality for formation of the amino-1,2,4-oxadiazole. Protection of the amine with the Boc protecting group allowed for a relatively easy future deprotection step. In the event glycine **218** was protected as its Boc carbamate in good yield, as illustrated in Scheme 2.47.



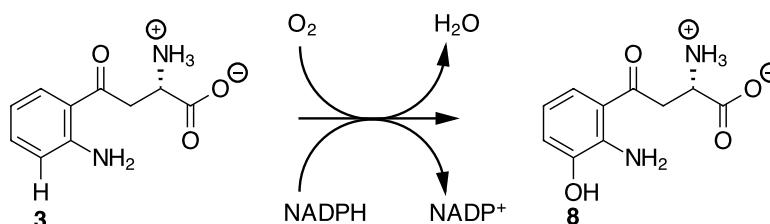
Scheme 2.48. Reagents and conditions: **a)** DCC, DMAP, DCM, RT, 8 h, 32%; **b)** TBAF, THF, RT, 2 h, 75%; **c)** HCl in dioxane, DCM, RT, 2 h, 63%; **d)** pyridine, RT, 8 h, quant.

Phenyl amidoxime **217** and Boc-protected glycine **219** were coupled to form O-acyl amidoxime **220**, as illustrated in Scheme 2.48. Cyclisation of the O-acyl amidoxime **220** with TBAF proceeded efficiently to give the desired 1,2,4-oxadiazole **221**.

Removal of the Boc group was accomplished under acidic conditions to give amine **22** as its hydrochloride salt. With **222** in hand, attention focused on the synthesis of sulfonamide **215**. This was successfully accomplished by dissolving the 1,2,4-oxadiazole amine salt **222** in pyridine, followed by the addition of benzenesulfonyl chloride. Sulfonamide **215** was obtained in an excellent yield.

2.4 Enzymatic assays of first generation compounds against K3MO

Compounds **120-122**, **156**, **159**, **162**, **164-165**, **167**, **173-176**, **180**, **193**, **200**, **207**, **213** and **215**, shown in Figure 2.16, were assayed against bacterial K3MO from *P. fluorescens* (Dr Chris Mowat and Martin Wilkinson). A cell lysate containing the human form of K3MO was also used to assay this set of compounds (Dr Scott Webster and Miss Kris McGuire). K3MO from *Pseudomonas fluorescens* is a relatively stable enzyme, allowing for its ready isolation and purification.



Scheme 2.49. Reaction catalysed by K3MO.

The compounds were initially screened as solutions in DMSO using a single cell cuvette assay. By following the rate of change in the absorption of NADH (340 nm) the rate of the reaction could be observed. L-Kynurenine **3**, NADPH and the inhibitor were all added to the assay buffer and left to equilibrate for approximately 1 min. The volume of the DMSO solution added was adjusted to give a final DMSO concentration of 2% (v/v). A higher concentration of DMSO inhibits the enzyme reaction. K3MO was then added and the cuvette inverted to mix the solution. The change in absorbance at 340 nm was recorded for the initial linear period. The reaction was also run with neat DMSO several times as a control reaction. Each of the rates were then converted into percentages by comparison to the neat DMSO rate. This gave the percentage activity of the enzyme with the inhibitor and is quoted as a percentage inhibition by subtracting the activity from 100%.

The best inhibitors were then subjected to further testing. Using the same setup for measuring the percentage inhibition, but varying the concentration of inhibitor and kynurenine, a K_i value was calculated. The rate of the reaction per molecule of

enzyme was then calculated. Dixon plots were used to calculate the K_i . Using this linear graphical method, the K_i is calculated by plotting $1/v$ at each inhibitor concentration. In the case of competitive inhibition, these lines converge above the x-axis. For non-competitive binding, the lines converge on the x-axis.^{161, 162} Non-linear regression was also used for the calculation of K_i .⁷⁶

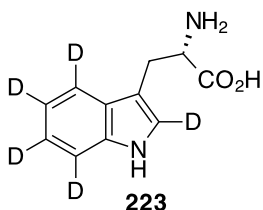


Figure 2.15. (S)-[2,4,5,6,7-²H₅]-Tryptophan **223** used as an internal standard in the human K3MO assay.

Testing of the compounds against the human K3MO was achieved using a cell lysate of HEK293 cells (Dr Scott Webster and Miss Kris McGuire). The cells were transfected with the human K3MO gene. L-kynurenine **3**, the inhibitors in DMSO and NADP were added to the lysate in 96-well plates. NADP is converted to NADPH in the assay by the addition of glucose-6-phosphate dehydrogenase. The volume of inhibitor solution added was kept constant to give a final DMSO concentration of 1% v/v. The solution was spiked with a known concentration of (2S)-[2,4,5,6,7-²H₅]-tryptophan **223**. Analysis of the lysate by LC-MS/MS and the area of the peak of 3-hydroxykynurenine **8** was compared to the D₅-tryptophan **223** peak to give a ratio. This was then compared to a standard curve of 3-hydroxykynurenine **8**/ D₅-tryptophan **223** ratios to calculate how much 3-hydroxykynurenine **8** was produced in each assay. Comparison with positive and negative controls allowed for the calculation of an IC₅₀.¹⁶³

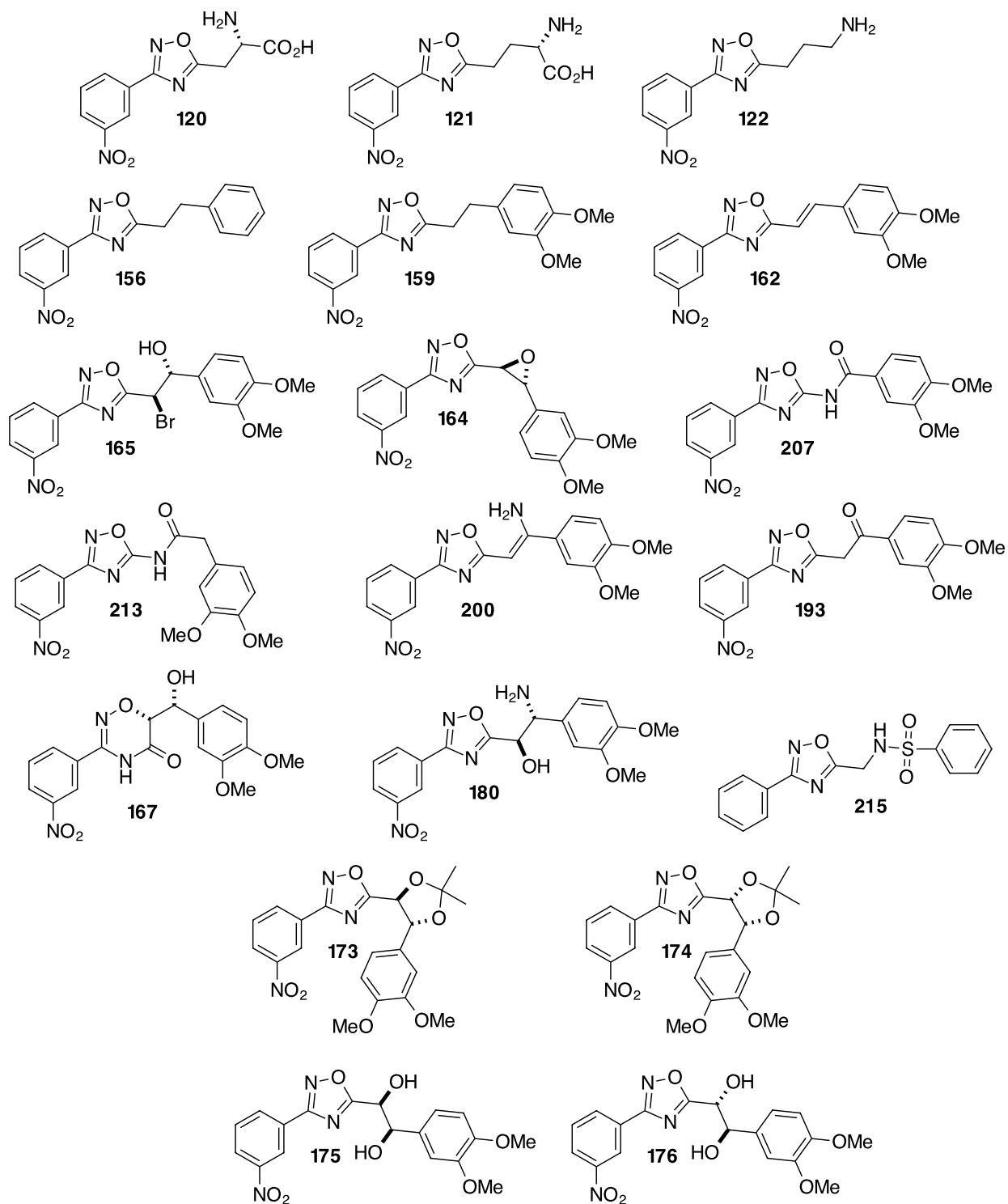


Figure 2.16. A summary of all the compounds from this series that were tested against human and *P. fluorescens* K3MO.

Compounds	K3MO activity % at 5 μ M	K3MO activity % at 10 μ M	K3MO inhibition % at 10 μ M	K _i (μ M)
120	99	-	-	-
121	95	-	-	-
122	100	-	-	-
156	86	-	-	-
159	99	-	-	-
162	86	-	-	-
164	95	-	-	-
165	91	84	16	-
167	-	100	-	-
173	-	104.7 \pm 5.8	-	-
174	-	96.9 \pm 2.2	3	-
175	-	101.1 \pm 2.5	-	-
176	-	97.6 \pm 4.0	2	-
180	-	106.0 \pm 6.3	-	-
193	-	85.1 \pm 20.6	15	-
200	-	85.6 \pm 22.8	14	-
207	82	68.0 \pm 11.7	32	1.30 \pm 0.21
213	-	68.0 \pm 11.7	32	1.82 \pm 0.38
215	-	97.9 \pm 3.2	2	-

Table 2.1. Enzymatic assay of selected compounds against *P. fluorescens* K3MO (Dr Chris Mowat, Martin Wilkinson, Helen Bell and Annemette Kjeldsen)

Only amides **207** and **213** showed interesting activity against K3MO from *P. fluorescens*. Determination of the K_i of **207** and **213** was undertaken giving values of 1.30 \pm 0.21 μ M and 1.82 \pm 0.38 μ M, respectively. The Dixon plot used to calculate the K_i of **207** is shown in Figure 2.17. When the compounds were assayed against the human K3MO they showed little or no inhibition.

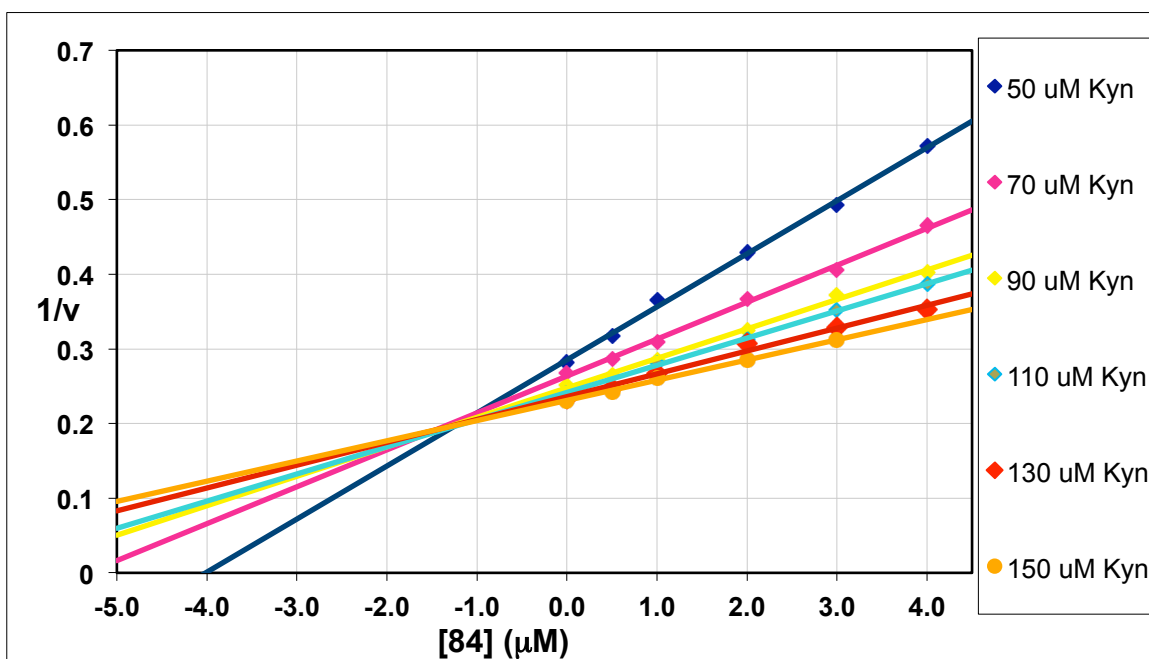


Figure 2.17. A Dixon plot obtained in the calculation of the K_i of **207**.

2.5 Conclusions

A wide range of potential inhibitors of K3MO were prepared based on a 1,2,4-oxadiazole motif. They were tested against bacterial and human K3MO. Amides **207** and **213** showed the most promise with K_i 's of 1.3 μM and 1.8 μM respectively. Amide **207** bears a resemblance to the sulfonamide inhibitor **93** and has a similar K_i . With the heterocycle-aryl linker optimised as the amide, the substitution on the phenyl rings was next to be explored. This is discussed in the subsequent chapter.

Chapter 3

The synthesis and development of 1,2,4-oxadiazole amides as inhibitors of K3MO

3.1 Synthesis and enzymatic assay of a first generation library of 1,2,4-oxadiazole amides

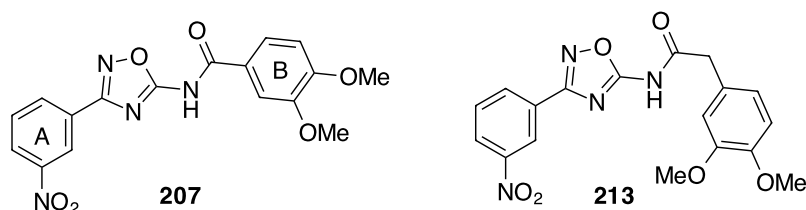


Figure 3.1. Lead compounds from structural activity relationship investigation (Chapter 1).

Amides **207** and **213** proved to be the best inhibitors of *P. fluorescens* K3MO synthesised thus far, and establishment of structure activity relationships around this motif was targeted to develop more potent inhibitors. Therefore, a small library of amides was envisaged, changing the substituents on both phenyl rings. It is known that nitro groups give toxic and mutagenic properties to compounds¹⁶⁴⁻¹⁶⁶ so the *meta* nitro group was removed in this phase of development. A first series involved changing the substituents on phenyl ring A of **207** and keeping phenyl ring B unsubstituted. A second series involved introducing the 3,4-dimethoxy substitution into ring B.

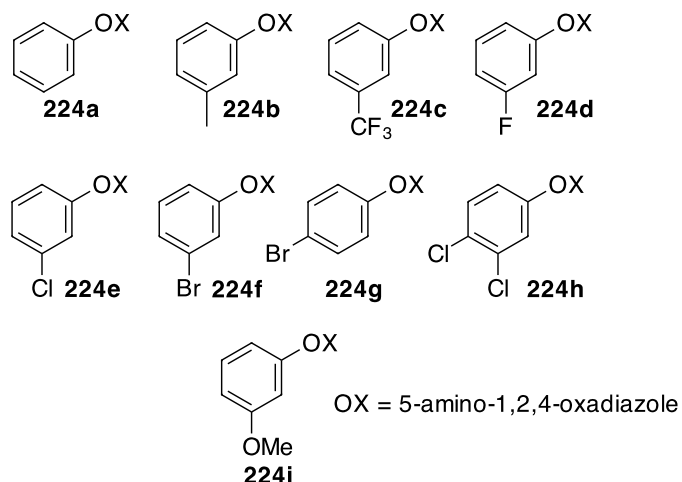
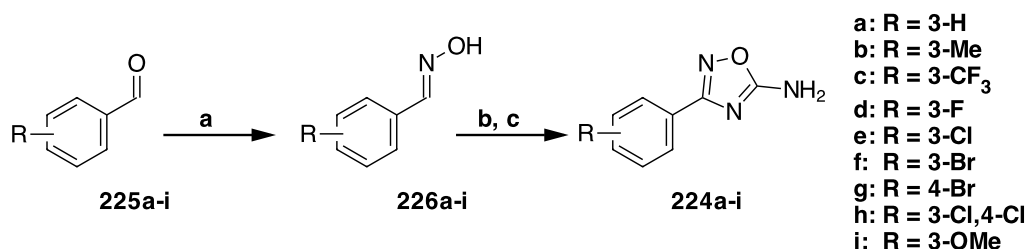


Figure 3.2. The selected substitution for phenyl ring A.

Substitutions were made predominately at the 3-position, as illustrated in Figure 3.2. Analogue **224g** was included in the library to explore the regiochemistry of substitution as an alternative to **224e** and **224f**. The 3,4-dichloro substitution was chosen, as it had already shown good inhibition e.g **84** (Chapter 1). The synthesis of the amides followed a similar route to that previously used in the synthesis of **207** and **213** (Chapter 2).

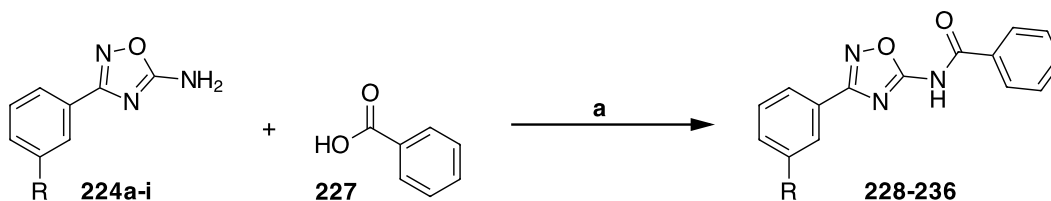


Scheme 3.1. Reagent and conditions: **a)** NH₂OH.HCl, NaOAc, acetonitrile:water, 2:1, 60-88%; **b)** sodium hypochlorite solution 1.6 M, DCM; **c)** cyanamide, Et₃N, 50-76%.

Formation of oxime intermediates **226a-i**, using hydroxylamine hydrochloride and sodium acetate, was accomplished in good yield for all the substitutions except for the 3-methoxy derivative **226i**, as illustrated in Scheme 3.1. The 3-methoxy derivative **226i** was a liquid and was, therefore, purified by distillation. The trifluoromethyl derivative **226c** was purified by removing excess 3-(trifluoromethyl)benzaldehyde **225c** through distillation under reduced pressure.

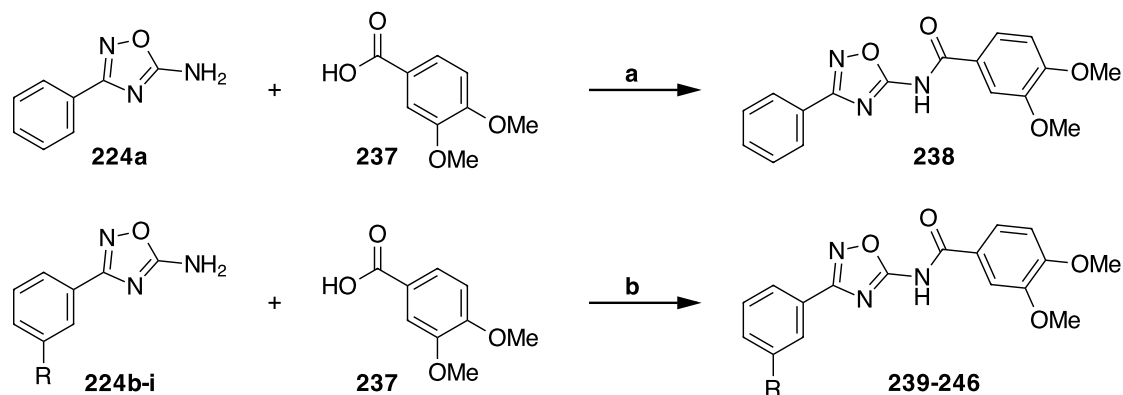
Upon cooling, the residue solidified and was characterised as a white solid. In order to obtain clean oximes it was important to neutralise all of the acetic acid that had formed in the reaction. This was accomplished using sodium bicarbonate. The addition of decolourising charcoal also helped remove any coloured contaminants from the products.

The oximes **226a-i** were transformed into the corresponding 5-amino-1,2,4-oxadiazoles **224a-i** by 1,3-dipolar cycloaddition of the corresponding nitrile oxides and cyanamide (Scheme 3.1). 5-Amino-1,2,4-oxadiazoles **224a-i**, were furnished in moderate to good yield using the protocol developed for 5-amino-1,2,4-oxadiazole **208** (Chapter 2). In an alteration to the purification of **208**, 5-amino-1,2,4-oxadiazoles **224a-i** were recrystallised from ethanol and water. This made their purification quicker and easier, as they had a tendency to precipitate on the column bed.



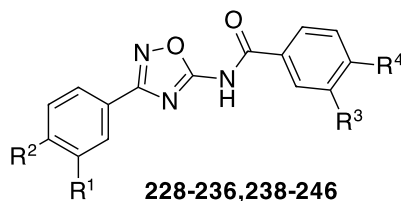
Scheme 3.2. Reagents and conditions: **a**) DCC, DMAP, DCM or acetonitrile, RT, 8 h, 12-63%.

The amides **228-236** were prepared in poor to moderate yields through a DCC coupling, as illustrated in Scheme 3.2. In all cases, sufficient material was prepared for assays against the human and *P. fluorescens* K3MO enzymes.



Scheme 3.3. Reagents and conditions: **a)** DCC, DMAP, DCM, RT, 8 h, 12-63%; **b)** EDCI, DMAP, DCM, RT, 8 h, 18-76%.

The 3,4-dimethoxy substitution targeted in series 2 was achieved by using 3,4-dimethoxy benzoic acid, as illustrated in Scheme 3.3. For 3-phenyl-5-amino-1,2,4-oxadiazole **238**, DCC and DMAP was used to prepare the amide in moderate yield. However, for the alternative substitutions on phenyl ring A **239-246**, the dicyclohexyl urea side product co-eluted with the product during flash column chromatography, complicating the purification. Although the majority of the urea was removed from the reaction by filtration, some still remained in solution. Accordingly, EDCI was employed as a coupling agent. EDCI generates a water-soluble urea, allowing for easy removal of the urea through dilute aqueous acid washes. The remaining amide couplings with EDCI gave poor to good yields of the amides. Again, enough material was obtained for assays against both the human and *P. fluorescens* K3MO enzymes.

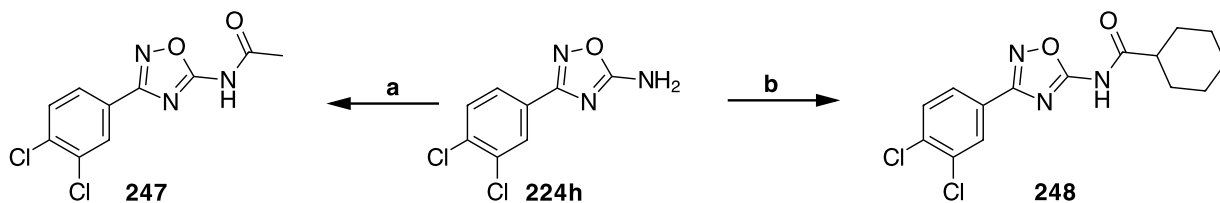


Compound	R ¹	R ²	R ³	R ⁴	Bacterial activity (as a % of uninhibited enzyme) at 10 μ M	Bacterial K _i (μ M)
228	H	H	H	H	89.7 \pm 9.5	19.99 \pm 3.59
229	Me	H	H	H	91.6 \pm 9.6	-
230	CF ₃	H	H	H	78.8 \pm 14.8	-
231	F	H	H	H	106.4 \pm 3.9	-
232	Cl	H	H	H	86.5 \pm 18.2	2.77 \pm 0.43
233	Br	H	H	H	88.2 \pm 8.4	1.58 \pm 0.20
234	H	Br	H	H	87.2 \pm 10.1	-
235	Cl	Cl	H	H	13.1 \pm 8.7	0.11 \pm 0.01
236	OMe	H	H	H	97.7 \pm 10.8	-
238	H	H	OMe	OMe	94.6 \pm 4.6	-
239	Me	H	OMe	OMe	98.3 \pm 10.8	-
240	CF ₃	H	OMe	OMe	63.5 \pm 18.2	-
241	F	H	OMe	OMe	97.3 \pm 12.2	1.06 \pm 0.30
242	Cl	H	OMe	OMe	47.1 \pm 16.9	0.78 \pm 0.05
243	Br	H	OMe	OMe	36.9 \pm 17.1	1.33 \pm 0.08
244	H	Br	OMe	OMe	52.4 \pm 16.7	-
245	Cl	Cl	OMe	OMe	6.5 \pm 2.7	0.14 \pm 0.02
246	OMe	H	OMe	OMe	83.7 \pm 14.0	-

Table 3.1. Table showing %inhibition and K_i against K3MO from *P. fluorescens* (Dr Chris Mowat, Martin Wilkinson, Helen Bell and Annemette Kjeldsen)

The data in Table 3.1 reports the bacterial K3MO assay using a plate reader and carried out in triplicate. There is a clear pattern; the 3,4-dichloro substitution **235** and **245** provided the best inhibition. The incorporation of the 3,4-dimethoxy substitution to phenyl ring B also increased the inhibition of K3MO. K_i values were determined through the use of a Dixon-plot or by non-linear regression. The Dixon plots showed that the amides were acting as competitive inhibitors of K3MO.

The compounds showed little or no inhibition against the human enzyme.



Scheme 3.4 Reagents and conditions: **a**) Acetic anhydride, DMAP, DCM, RT, 16 h, 81%; **b**) cyclohexylcarbonyl chloride, DMAP, DCM, RT, 16 h, 84%.

The 3,4-dichloro substitution on phenyl ring A gave the best assay results (see Table 3.1). Thus, two compounds were prepared; removing the benzoate amide ring B and replacing it with either an acetamide or a cyclohexyl carboxamide. The acetamide was generated by reacting 5-amino-1,2,4-oxadiazole **224h** with acetic anhydride and this gave acetamide **247** in good yield, as illustrated in Scheme 3.4. Cyclohexyl amide **248** was prepared using cyclohexylcarbonyl chloride, also in good yield.

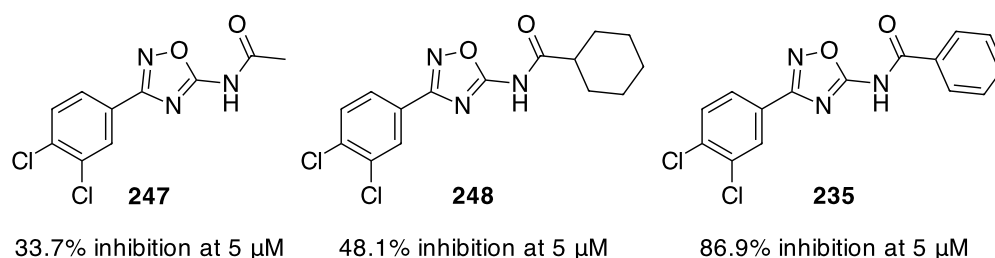


Figure 3.3. % Inhibition values against K3MO from *Pseudomonas fluorescens* for the **247** and **248** compared to **235**.

Enzymatic inhibition of the amides with *P. fluorescence* K3MO in a single cell cuvette assay gave percentage inhibition values, as illustrated in Figure 3.3. Acetamide **247** has a K_i of 1.99 μ M. The cyclohexyl amide **248** proved to be a better inhibitor than acetamide **247**. However, neither were as potent as **235**, the original compound with the phenyl group.

3.2 Protein X-ray crystallography of first generation amides with *P. fluorescens* K3MO



Figure 3.4. The crystal structure of *Pseudomonas fluorescens* K3MO with **235** bound in the active site

Co-crystallisation of the two most potent amides **235** and **245** with *P. fluorescens* K3MO was successfully achieved by our collaborators (Martin Wilkinson and Dr Chris Mowat, University of Edinburgh).⁷⁶ A crystal structure was obtained with **235** bound into the active site at a resolution of 2.18 Å. There are three non-equivalent protein molecules in the unit cell. Overlays of the three separate molecules showed there were small conformational changes in the side chains, however, the conformational changes were minor and presumably reflect the dynamic nature of the protein.

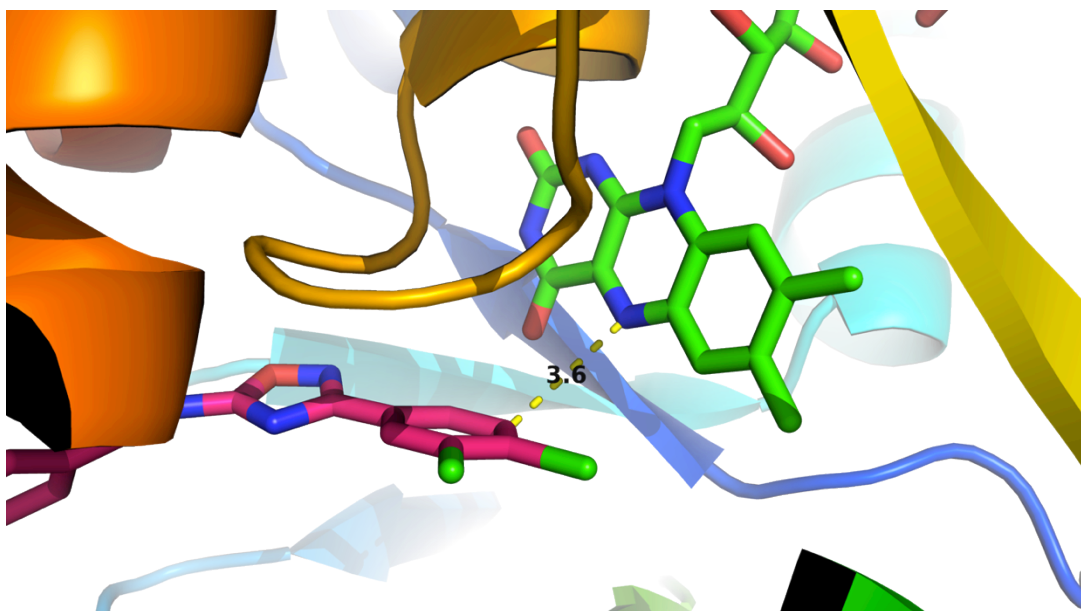


Figure 3.5. X-Ray studies of the active site and the orientation of the 3,4-dichlorophenyl ring and through space distance from the flavin co-factor. Distance is in (Å).

Examination of the crystal structure reveals that the 3,4-dichloro amides bind well into to the active site. The orientation of the 3,4-dichloro phenyl ring has the 3-chlorine atom orientated away from the FAD, into a hydrophobic pocket. Although the 5-H of the 3,4-dichloro ring appears to be in the correct orientation for oxidation, it is not oxidised by the FAD in the assays.

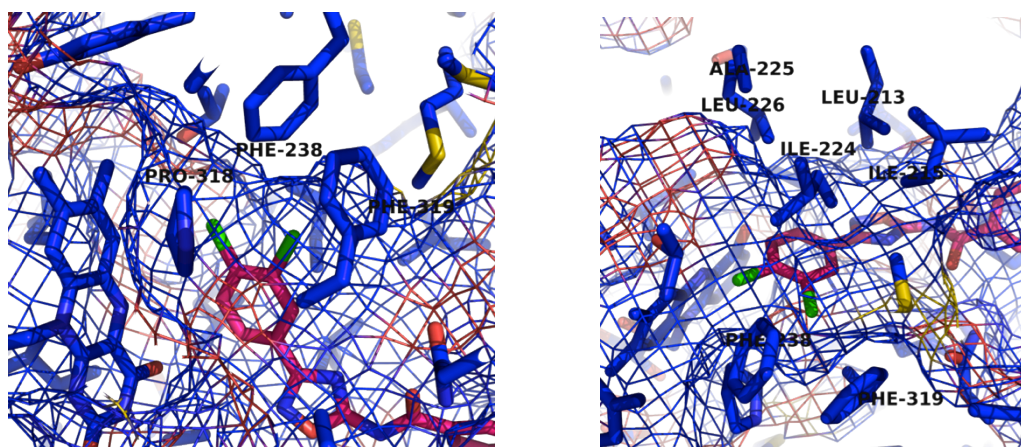


Figure 3.6. Representation of the Van der Waals surface as a wire mesh to show the hydrophobic pocket in the active site of K3MO.

The 3,4-dichloro phenyl ring sits in a hydrophobic pocket. This pocket is flanked by the flavin on one side. The side chains of Phe-238 and 319, Leu-213 and 226, Ile-

215 and 224 and Ala-225 modulate the shape of the hydrophobic pocket (Figure 3.6). The hydrophobic pocket is just large enough to accept both chlorine atoms.

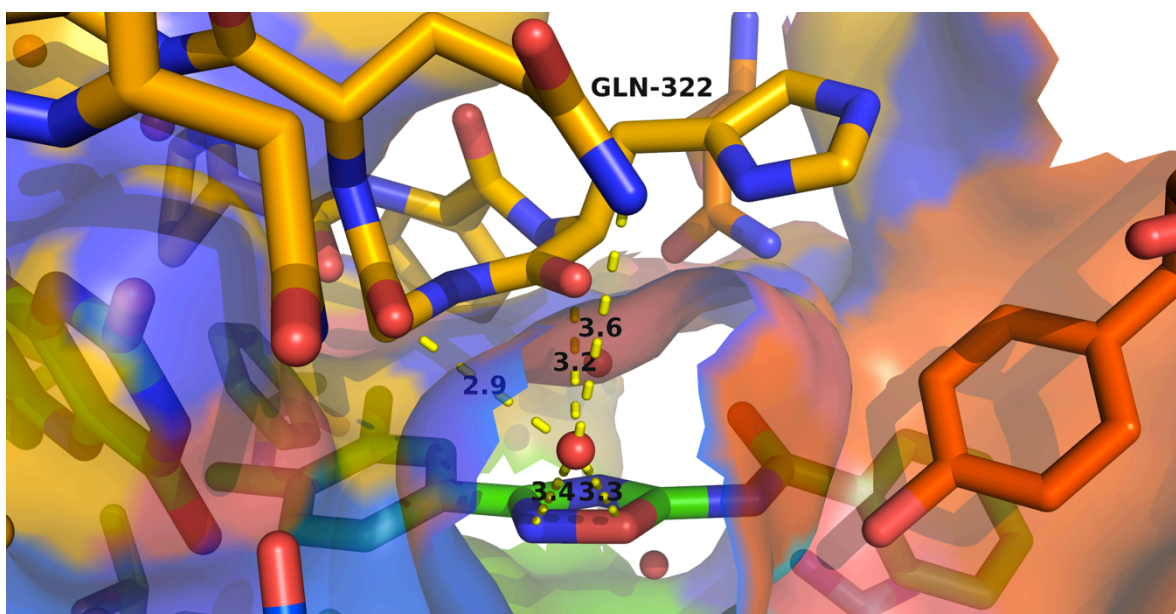


Figure 3.7. Interaction of the hydroxylamine portion of the 1,2,4-oxadiazole ring of **235** with the hydrophilic pocket. The surface shown is the Van der Waals surface. Distances are in (Å).

The 1,2,4-oxadiazole ring sits in a hydrophilic pocket of the active site (Figure 3.7). It makes potential hydrogen bonding contact with a water molecule, which is potentially stabilised by hydrogen bonding to the main chain amide of Gly-321. The second hydrogen atom of the water molecule prospectively sits almost equidistant between the nitrogen and oxygen of the 1,2,4-oxadiazole ring and appears to make a hydrogen bond to either the nitrogen or oxygen atoms of the ring (Figure 3.8).

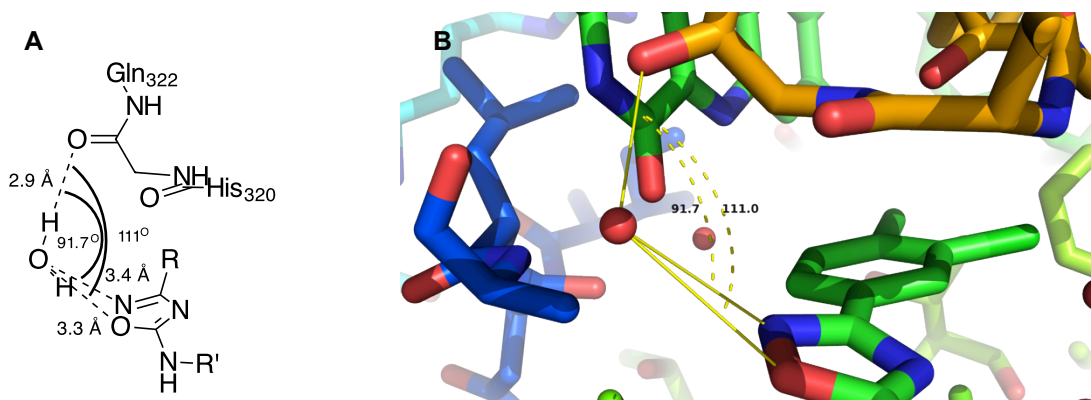


Figure 3.8. A) A graphical representation of the speculative hydrogen bonding between K3MO and **235** B) PyMol¹⁶⁷ representation of the interaction between the water molecule, the 1,2,4-oxadiazole of **235** and K3MO.

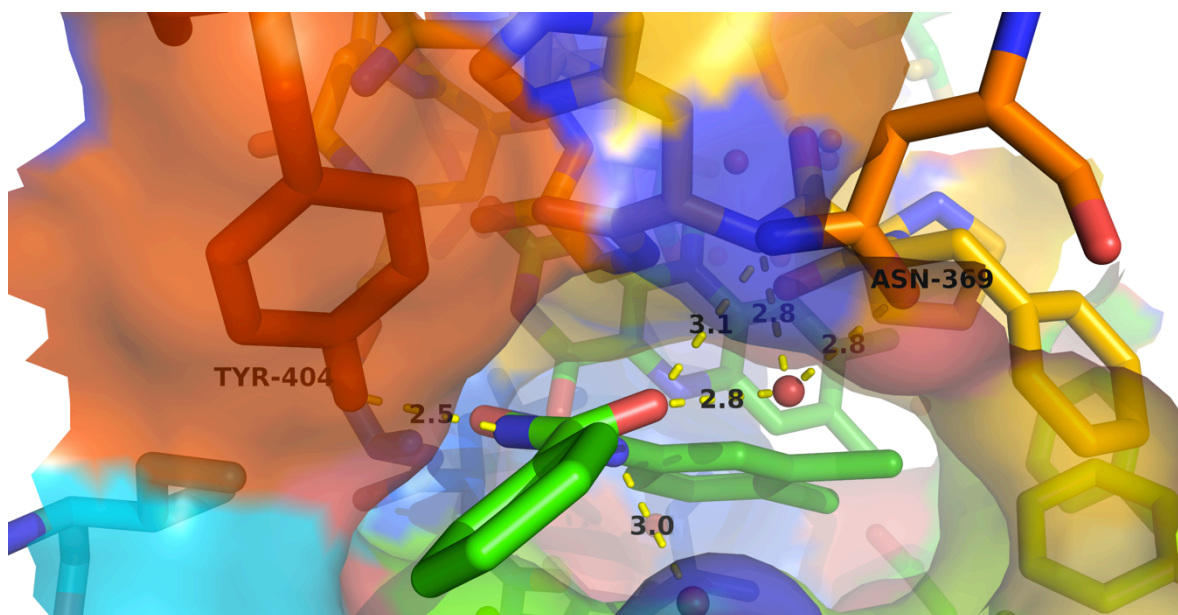


Figure 3.9. Co-crystallisation of amide **235** showing polar interactions in the active site.

The 1,2,4-oxadiazole amide carbonyl may make hydrogen bonding interactions with a bound water molecule, which is held in place by Asn-369 and the main chain amide of His-320 and Phe-319. This water molecule speculatively forms hydrogen bonds to the carbonyls of amide **235** and Asn-369. The water molecule could also act as a hydrogen bond acceptor, forming a hydrogen bond (2.8 Å), to the hydrogen of the main chain amide between His-320 and Phe-319. Asn-369 forms a

hydrogen bond (3.1 Å) to the carbonyl of **235**. The nitrogen on amide **235** makes a relatively short hydrogen bond (2.5 Å) to Tyr-404 (Figure 3.9).

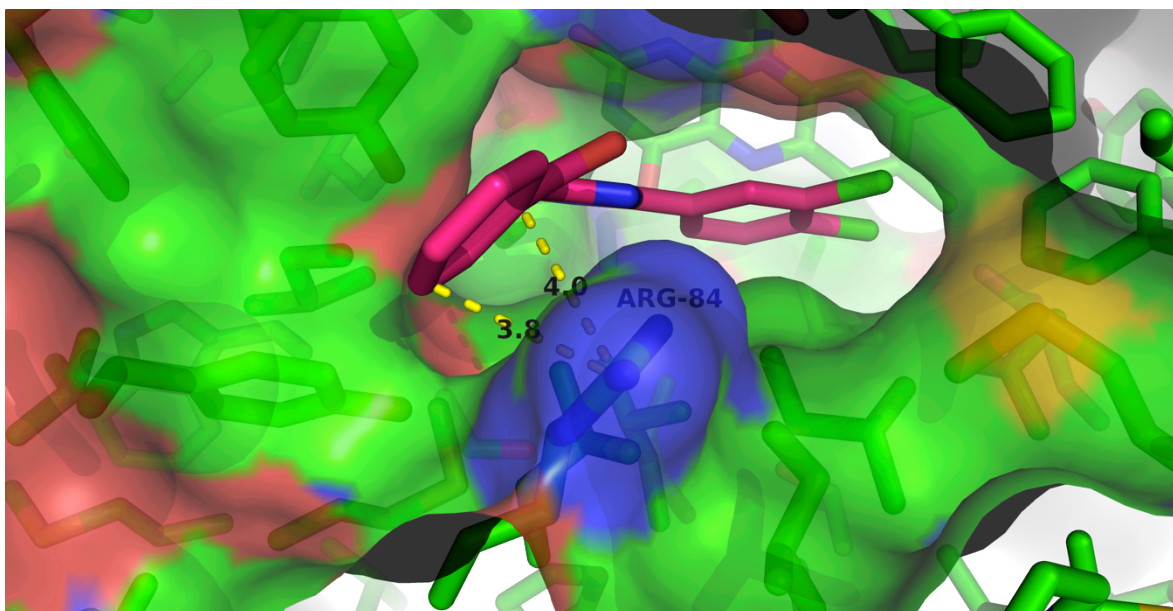


Figure 3.10. Short contacts suggest evidence for a π -cation interaction between **235** and Arg-84.

The co-crystal of **235** with the bacterial enzyme revealed that the nitrogens in the side chain of Arg-84 are all within 4 Å of the phenyl ring (Figure 3.10). The parallel orientation of the phenyl ring and Arg-84 suggests that there is a π -cation interaction between the phenyl ring and the guanadinium cation.¹⁶⁸ Such an interaction cannot occur to acetamide **247** or cyclohexylamide **248**.

It appears that the entire molecule contributes to the strong binding to the active site. The Van der Waals surface around the amide indicates that the active site prefers the flat motif of the amide compared to the tetrahedral sulfonamide, possibly explaining why the sulfonamides **93** and **135** (from Chapter 2) are not as potent against the bacterial enzyme.

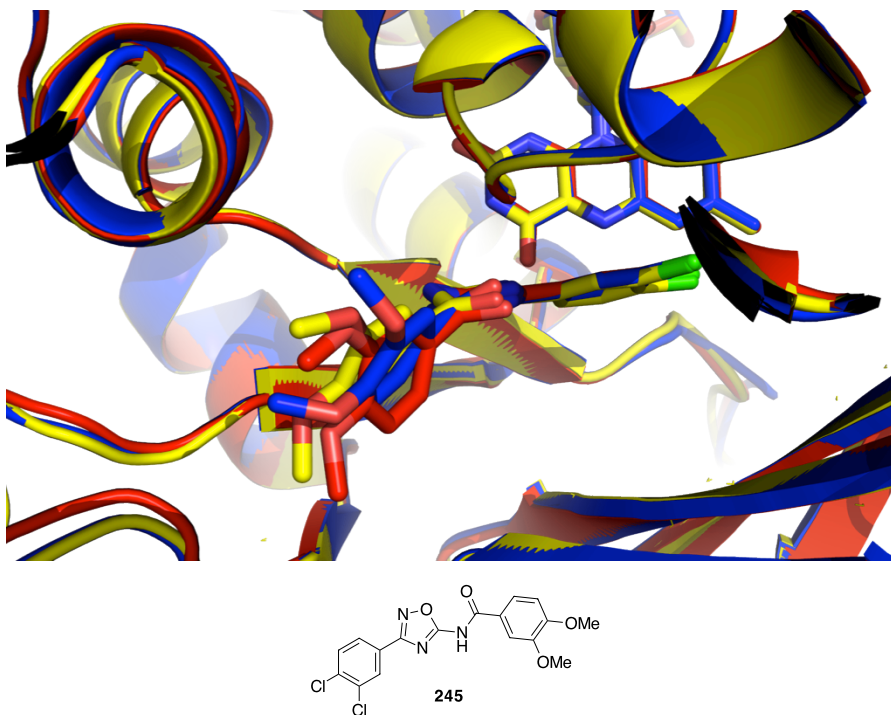


Figure 3.11. The disorder in the co-crystal of **245** and *P. fluorescens* K3MO arise due to the various different orientations of the 3,4-dimethoxy phenyl ring.

Co-crystals were also obtained with **245** bound in the active site of K3MO.⁷⁶ A structure at 2.25 Å resolution was achieved and is shown in Figure 3.11. There is again some disorder around the 3,4-dimethoxy phenyl ring, probably due to the active site opening up and allowing the phenyl ring to rotate.

3.3 Synthesis and K3MO enzyme assays of a second generation series of 1,2,4-oxadiazole amides

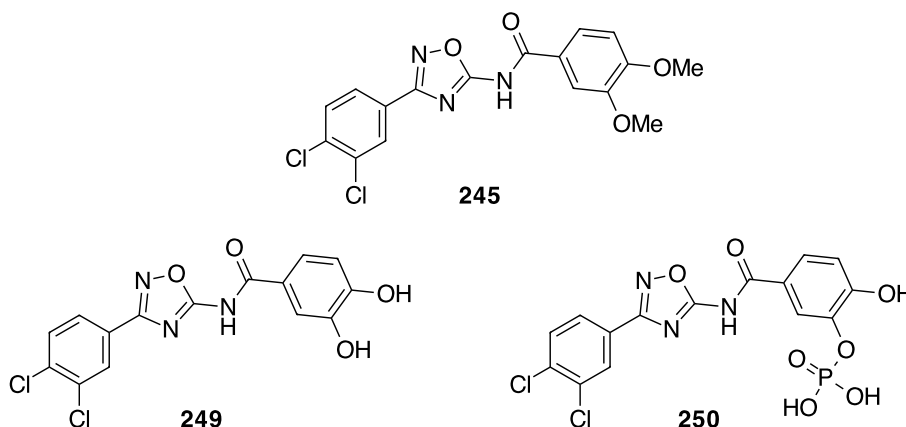
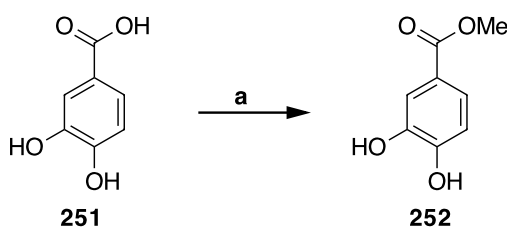


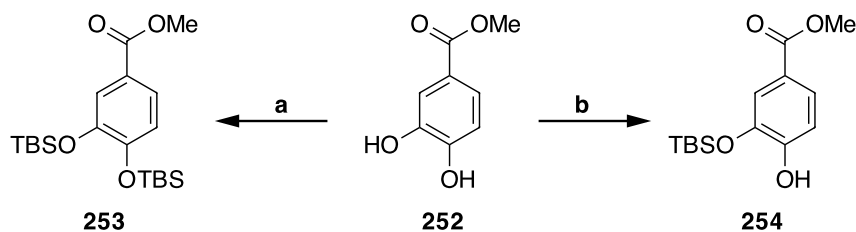
Figure 3.12. First generation lead compound **245** and the compounds **249** and **250**, targeted as second generation inhibitors.

A next generation of compounds was designed to address two objectives. The first was to increase water solubility, as the first generation compounds were highly lipophilic. The second was to exploit polar interactions with residues located near to the binding of the phenyl ring B. In this context, the introduction of a phosphate group at the 3- or 4- positions, such as **250**, may accommodate such polar interactions, particularly to Arg-84. Additionally, it was envisaged that the methoxyl ethers could be converted to the corresponding phenols, such as **249**, to possibly make polar interactions in the active site.



Scheme 3.5. Reagents and conditions: a) MeOH, concentrated H₂SO₄, 80 °C, 4 h, 89%.

3,4-Dihydroxybenzoic acid was converted to its methyl ester **252** in good yield, as illustrated in Scheme 3.5, using the method of Kita *et al.*¹⁶⁹



Scheme 3.6. Reagents and conditions: **a**) TBSCl, imidazole, 0 °C to RT, 16 h, 77%; **b**) TBSCl (1.1 eq), DIPEA, DMF, 0 °C, 20 min, 31%.

Reaction of 3,4-dihydroxybenzoate ester **252** with TBSCl (2.25 eq) and imidazole gave the di-protected benzoate ester **253** in good yield, as illustrated in Scheme 3.6. Selective protection at the 4-hydroxyl position of **252** was achieved using TBSCl and Hünig's base at 0 °C for 20 min. Careful control of the reaction time was critical in achieving selective protection at this site. Longer reaction times gave more of the di-protected product **253** and shorter reaction times resulted in low yields. The yield of product **254** was low, due to a low conversion within the short reaction time. The 2D HMBC spectrum (Figure 3.13) confirmed the regiochemistry and showed that the hydroxyl proton is coupled to carbons 3,4 and 5.

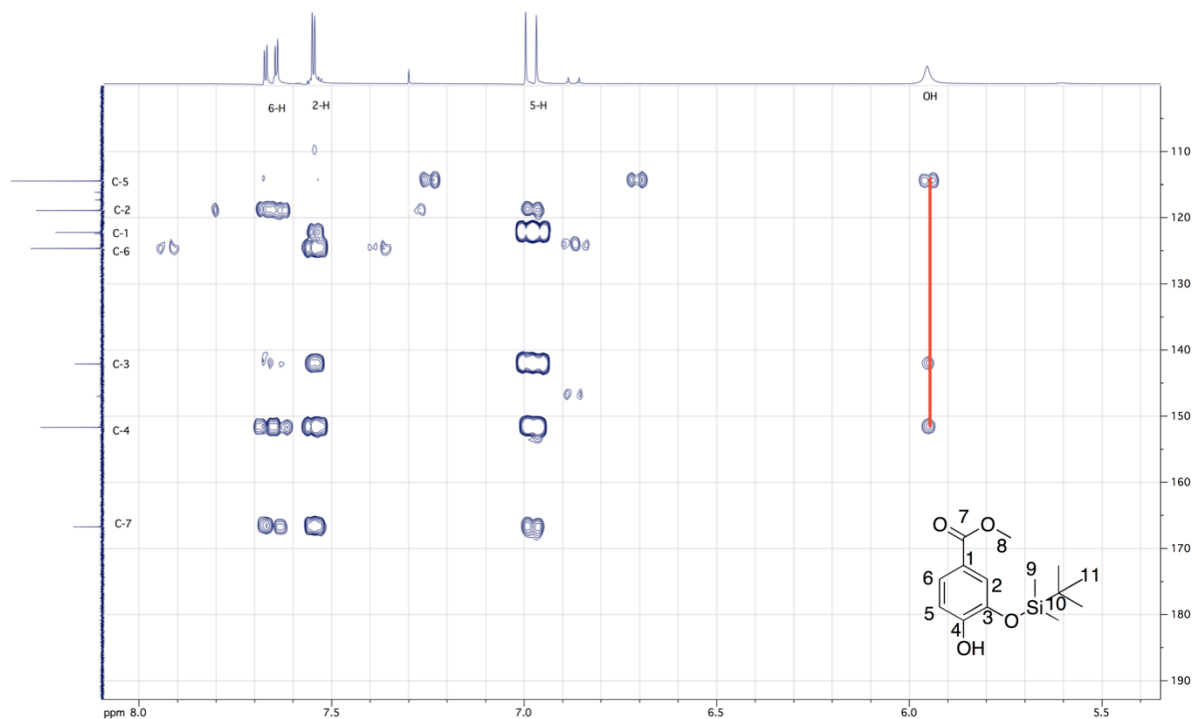
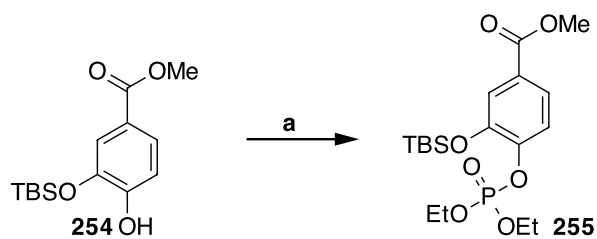
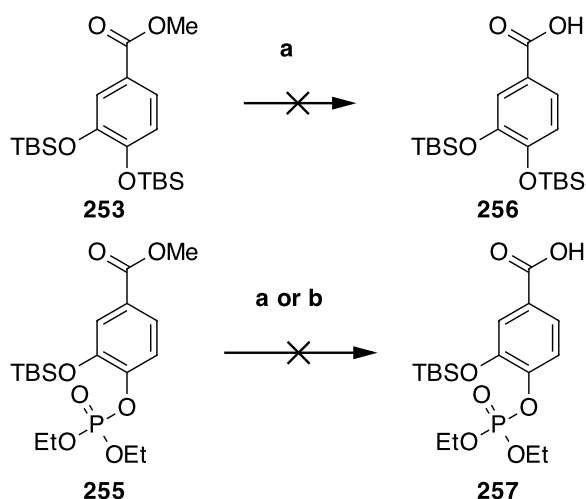


Figure 3.13. 2D ^1H - ^{13}C HMBC spectrum of **254** showing coupling of the phenol proton to carbons 3,4 and 5.



Scheme 3.7. Reagent and conditions: **a)** NaH, diethyl chlorophosphate, THF, 0 °C to 4 °C, 16 h, 71%.

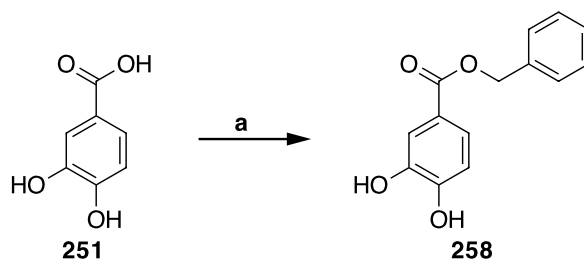
Formation of the phosphate ester **255** at the 4- position was achieved by reaction of phenol **254** with sodium hydride and diethyl chlorophosphate in good yield, as illustrated in Scheme 3.7.¹⁷⁰



Scheme 3.8. Reagents and conditions: **a)** NaOH, MeOH, RT, 16 h; **b)** porcine pancreatic lipase, H₂O, DMSO, 38 °C, 72 h.

Hydrolysis of the methyl ester moieties of **253** and **255** failed under basic conditions. In both cases, even with a careful acidic workup, the TBS protecting group was removed, but the methyl ester remained.

An alternative protecting group for the carboxylic acid was required. The benzyl ester was chosen as it can be removed under neutral conditions by hydrogenation to give the parent carboxylic acid.



Scheme 3.9. Reagents and conditions: **a)** Cs₂CO₃, BnBr, DMF, RT, 16 h, 44%.

The benzyl ester **258** was formed using caesium carbonate and benzyl bromide, as illustrated in Scheme 3.9. The yield for the reaction was poor in comparison to that previously reported.¹⁷¹ This was, in part, due to the difficulty of keeping the caesium salt in solution. Initially, deprotonation was carried out in an aqueous methanol solution. Removal of the aqueous solvent gave a solid, which was suspended in DMF. However, the solid did not dissolve as the reaction progressed

and thus, both steps were undertaken in DMF. This gave slightly better yields of benzyl ester **258**. The 2D HMBC confirmed the regiochemistry of **258**.

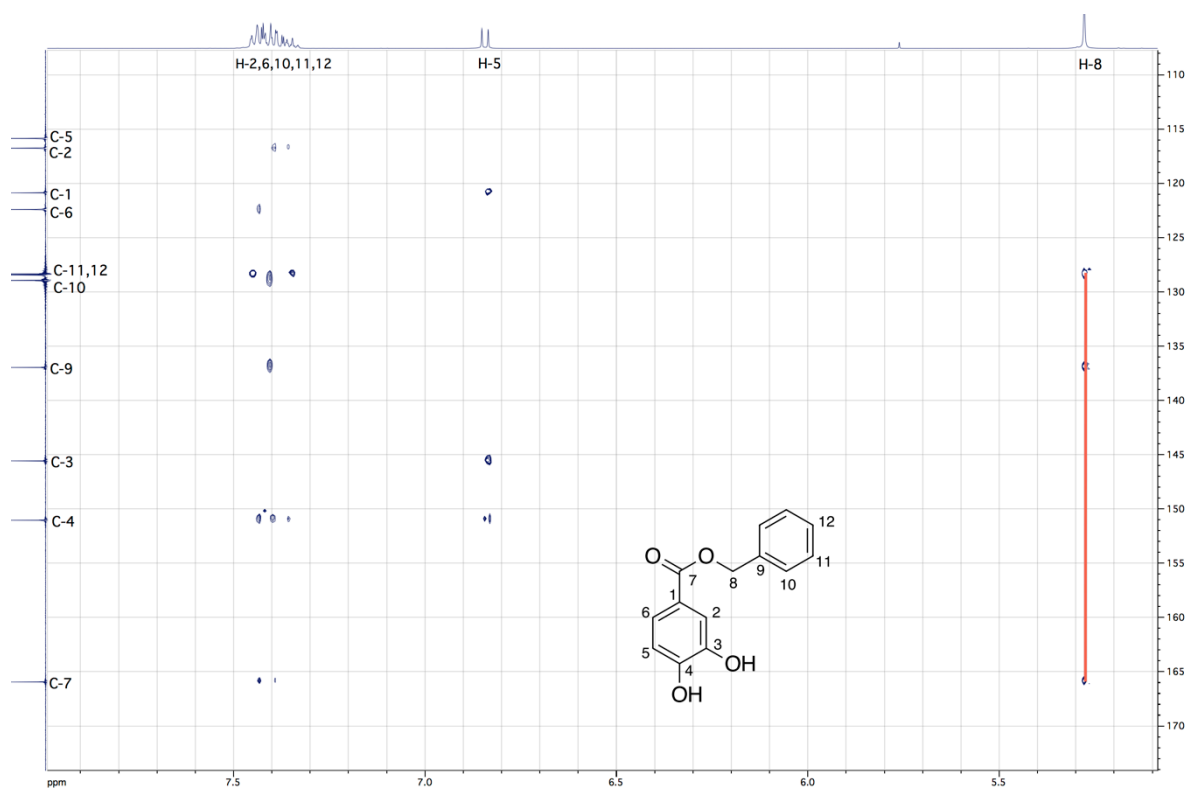
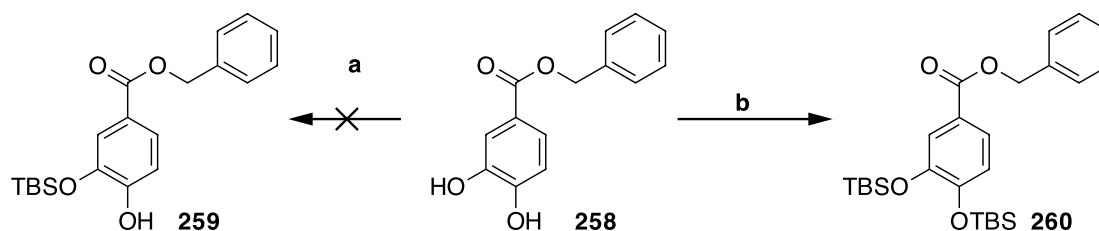
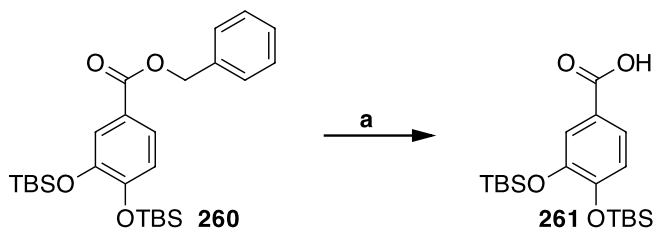


Figure 3.14. 2D ^1H - ^{13}C HMBC spectrum of **258** showing the coupling from C-8 to C-7, proving protection of the carboxylic acid as the benzyl ester.



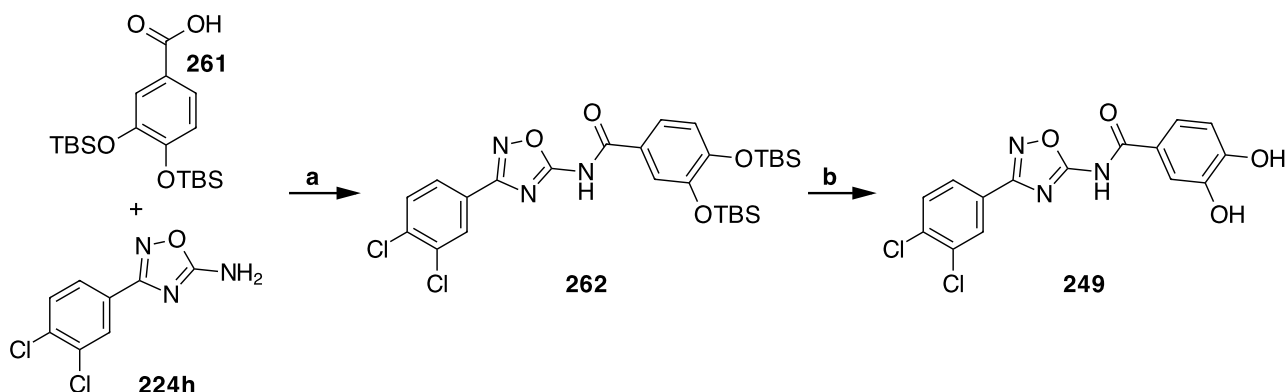
Scheme 3.10. Reagents and conditions: **a**) TBSCl (1.1 eq), DIPEA, DMF, 0 °C, 20 min; **b**) TBSCl, imidazole, DMF, 50 °C, 2 h, 90%.

Selective protection of phenol **258** was unsuccessful and the two regioisomers were inseparable by column chromatography. Full protection of benzyl ester **258** provided **260** through the use of TBSCl and imidazole at 50 °C, as illustrated in Scheme 3.10.



Scheme 3.11. Reagents and conditions: **a)** Pd black, H₂, MeOH, RT, 36 h, 45%.

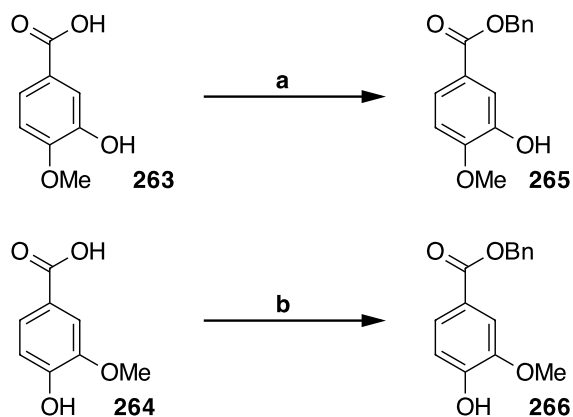
Under hydrogenation conditions Pd/C has been shown to cleave TBS protecting groups.¹⁷² It has been proposed that such unexpected deprotections are due to residual acid or PdCl₂ that are contaminants from the production of Pd/C. By using palladium black these potential problems were avoided. Cleavage of the benzyl ester **260**, as illustrated in Scheme 3.11, was accomplished in moderate yield and purification of the acid **261** by recrystallisation proved to be straightforward.



Scheme 3.12. Reagents and conditions: **a)** EDCI, DMAP, DCM, RT, 16 h, 30%; **b)** TBAF, THF, RT, 30 min, 85%.

With the di-protected carboxylic acid **251** in hand, amide **262** was synthesised using EDCI as the coupling agent, as illustrated in Scheme 3.12. Although the yield for the reaction was poor, enough material was obtained for characterisation and to achieve the final deprotection step.

Silyl deprotection of amide **262** with TBAF proceeded in good yield to give catechol **249**, however, purification of the product by column chromatography proved to be difficult due to the polar nature of the catechol.



Scheme 3.13. Reagents and conditions: **a**) Cs_2CO_3 , BnBr, DMF, RT, 16 h, 80%; **b**) Cs_2CO_3 , BnBr, DMF, RT, 16 h, 83%.

Benzyl esters **265** and **266** were prepared from the benzoic acids **263** and **264**, respectively, using caesium carbonate and benzyl bromide, as illustrated in Scheme 3.13. 2D HMBC analysis showed cross-peaks between the carbonyl of the ester and the CH_2 of the benzyl group in both **265** and **266**, confirming that the benzyl ester rather than the benzyl ether had formed (Figures 3.15 and 3.16).

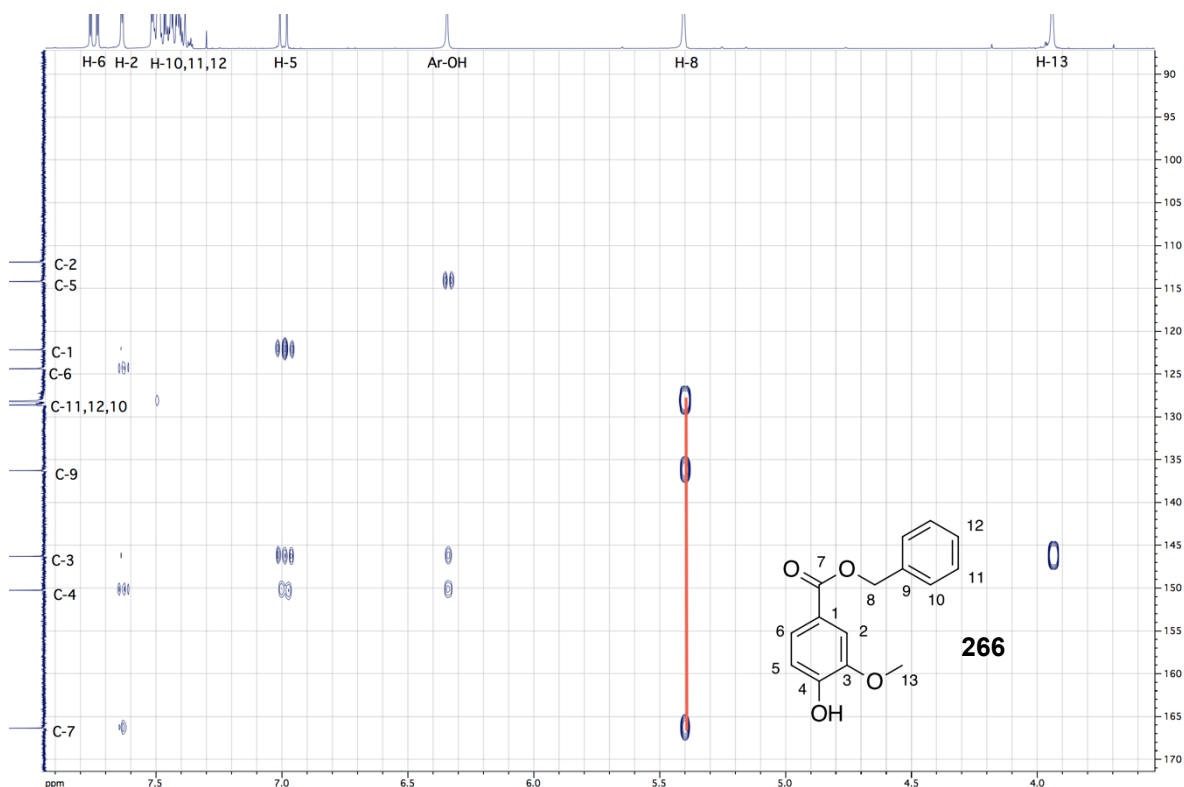


Figure 3.15. 2D ^1H - ^{13}C HMBC spectrum of **266** showing the coupling between H-8 and C-7.

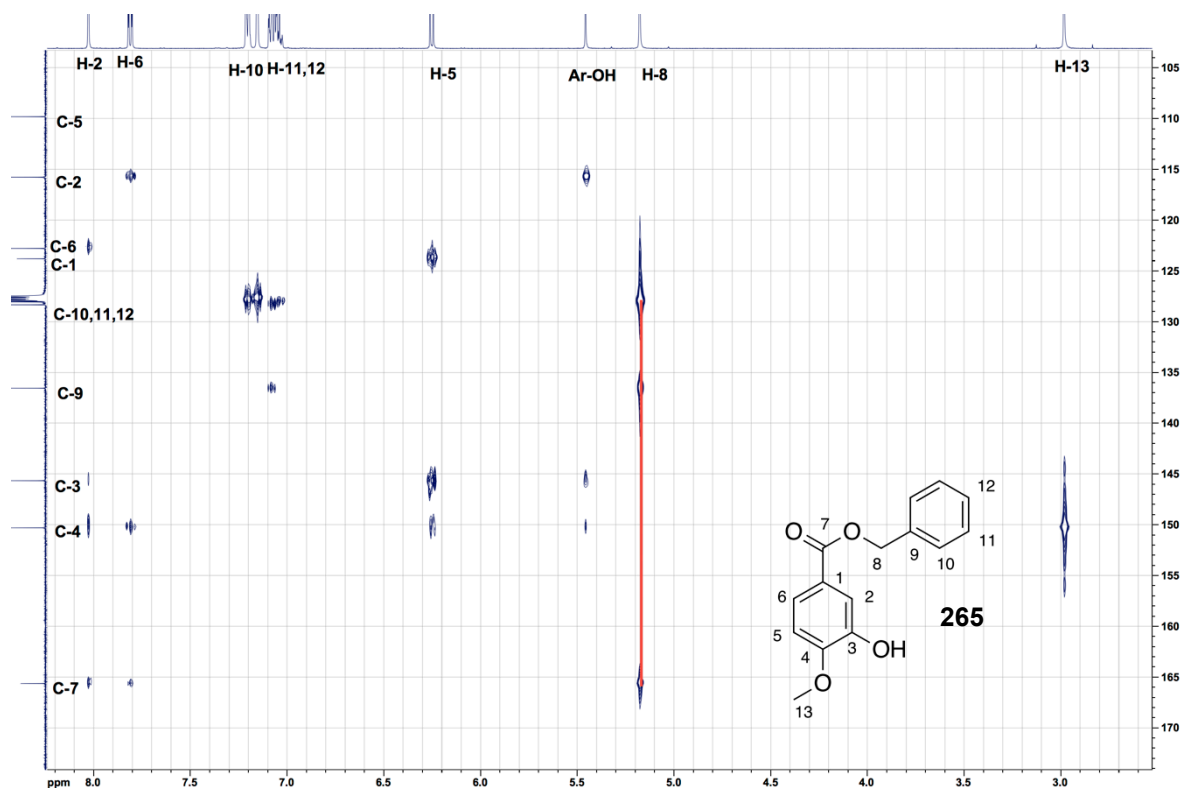
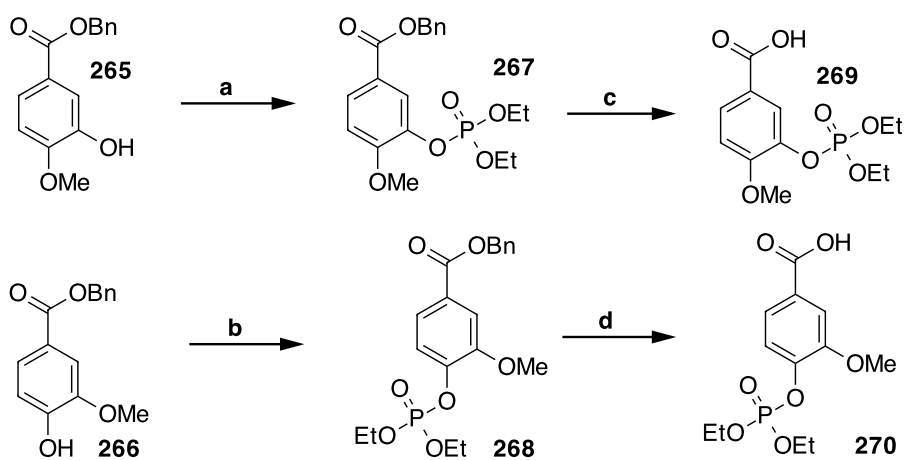


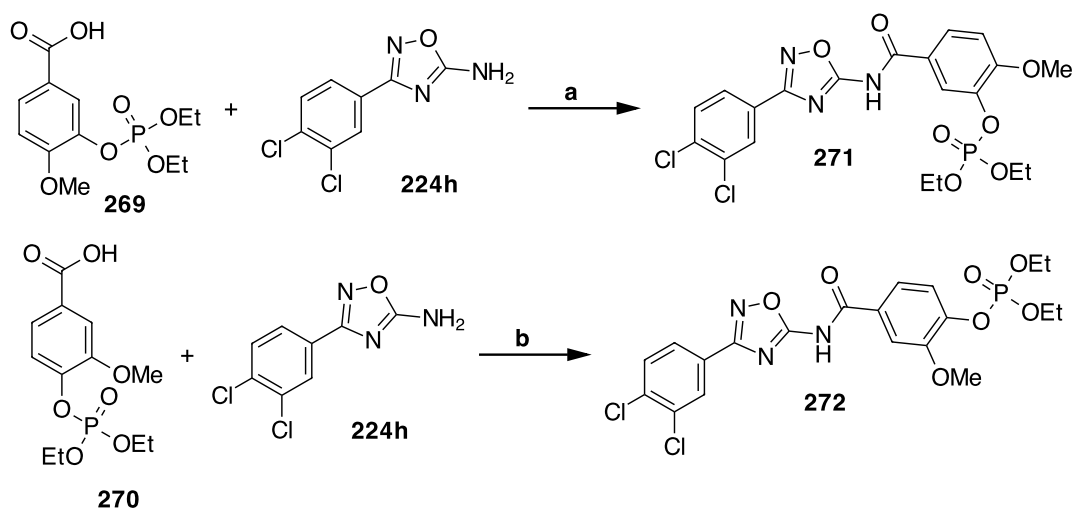
Figure 3.16. 2D ^1H - ^{13}C HMBC spectrum of **265** showing the coupling between H-8 and C-7.



Scheme 3.14. *Reagents and conditions:* **a)** Sodium hydride, diethyl chlorophosphate, THF, 0 °C to 4 °C, 16 h, 92%; **b)** sodium hydride, diethyl chlorophosphate, THF, 0 °C to 4 °C, 16 h, 80%; **c)** Pd/C, H_2 , EtOAc, RT, 48 h, 68%; **d)** Pd black, H_2 , EtOAc, RT, 48 h, 56%.

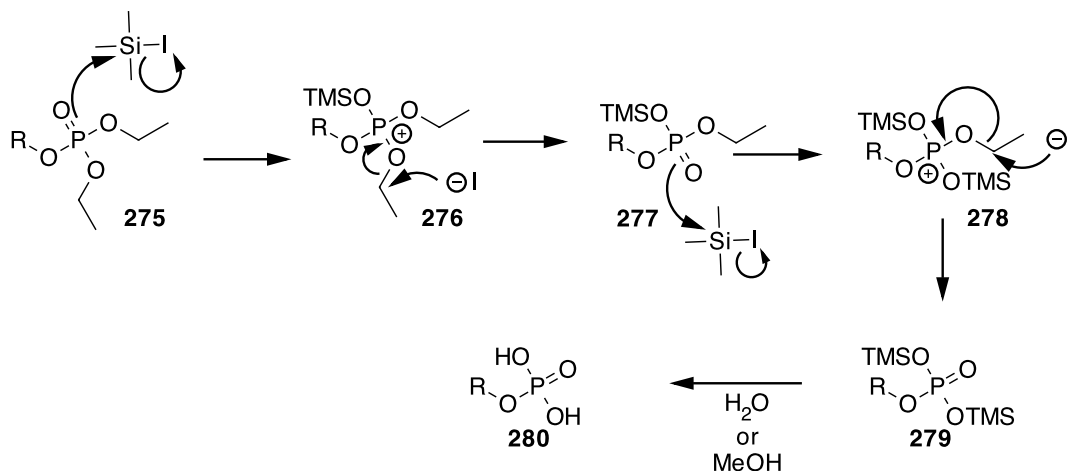
Diethyl chlorophosphate were reacted with **265** and **266** in the presence of sodium hydride to generate the diethyl phosphates **267** and **268** in good yield, as illustrated in Scheme 3.14.

Deprotection of benzyl ester **267** using Pd/C, under a positive pressure of hydrogen, gave the benzoic acid **269** in good yield, as illustrated in Scheme 3.14. This product could easily be purified by recrystallisation from ethanol and water. Deprotection of benzyl ester **268** to give **270** was achieved using palladium black. The more reactive palladium black was no better than Pd/C for this deprotection. Recrystallisation of product **270** was unsuccessful, therefore, the product was purified by flash column chromatography, although the yield was compromised.



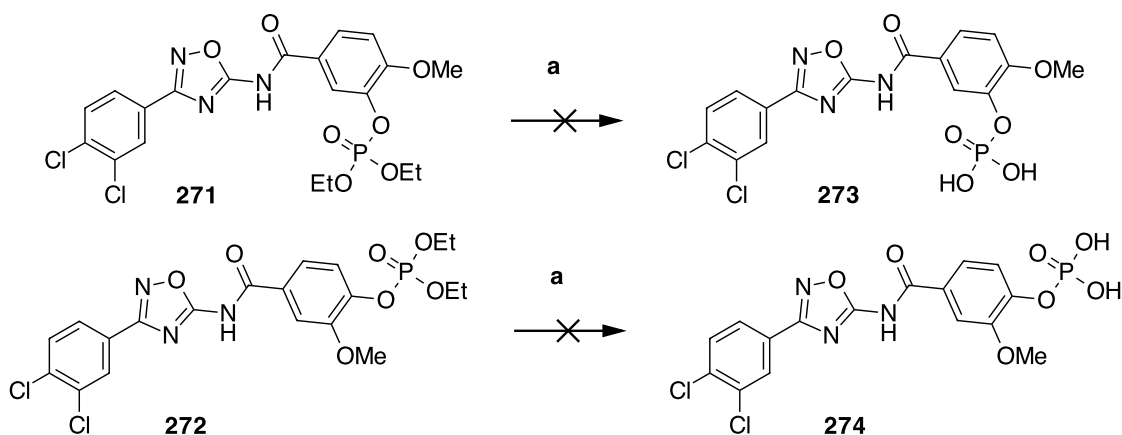
Scheme 3.15. Reagents and conditions: **a**) EDCI, DMAP, DCM, RT, 22 h, 49%; **b**) EDCI, DMAP, DCM, RT, 22 h, 85%.

With the benzoic acids **269** and **270** in hand, attention turned to forming amides **271** and **272**, as illustrated in Scheme 3.15. These amides were formed in moderate to good yield through EDCI coupling reactions with amine **224h**.



Scheme 3.16. The proposed mechanism for ethyl deprotection.

Deprotection of diethyl phosphates has been achieved using TMSBr ^{173, 174} and TMSI ,¹⁷⁵ a reaction which gives the disilylphosphate **279** as an intermediate. This intermediate is then hydrolysed in the work up to give the free phosphate, as illustrated in Scheme 3.16.

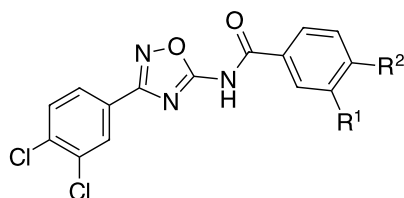


Scheme 3.17. Reagents and conditions: **a)** TMSI , CDCl_3 , RT, 1 h, then H_2O and MeOH .

TMSI rather than TMSBr was used for the deprotection of **271** and **272** as it had been reported as a milder method (Scheme 3.17). The deprotection was carried out in deuterated chloroform, which aided monitoring of the reaction directly by ^1H and ^{31}P NMR.

The ^1H NMR spectrum of the reaction showed the presence of ethyl iodide. The ^{31}P NMR spectra showed that the diethyl phosphate peak disappeared and two

new peaks appeared at -13.5 and -24.2 ppm, which reasonably correspond to the monosilyl and disilyl phosphates respectively. After hydrolysis with water/MeOH attempts were made to purify the product. However, the products **273** and **274** could not be obtained after either recrystallisation or flash column chromatography.



Compound	R ¹	R ²	Bacterial K _i (nM)
245	OMe	OMe	136.4 ± 16.7
249	OH	OH	66.7 ± 17.8
271	OPO(OEt) ₂	OMe	46.8 ± 7.6
272	OMe	OPO(OEt) ₂	65.5 ± 7.5

Table 3.2. Inhibition data for **245**, **249**, **271** and **272** (Dr Chris Mowat, Martin Wilkinson, Helen Bell and Annemette Kjeldsen)

Although the free phosphates **273** and **274** proved elusive, **249**, **271** and **272** were subject to assay against both bacterial and human K3MO enzymes. The change from the dimethoxy ether **245** to the phenol **249** provided better inhibition against the bacterial enzyme. Both diethyl phosphate compounds **271** and **272** are even better inhibitors than **245**. Calculation of the K_i was achieved using non-linear regression, from the single cell cuvette assay. This gave K_i values of 46.8 nM and 65.5 nM for **271** and **272**, respectively. The Dixon plot for **272** is shown in Figure 3.17. **271** binds to bacterial K3MO approximately three times better than **245** which has a K_i of 136 nM. The Dixon plots show that **249**, **272** and **273** are competitive inhibitors of K3MO. The compounds showed little or no inhibition at 10 μM against human K3MO.

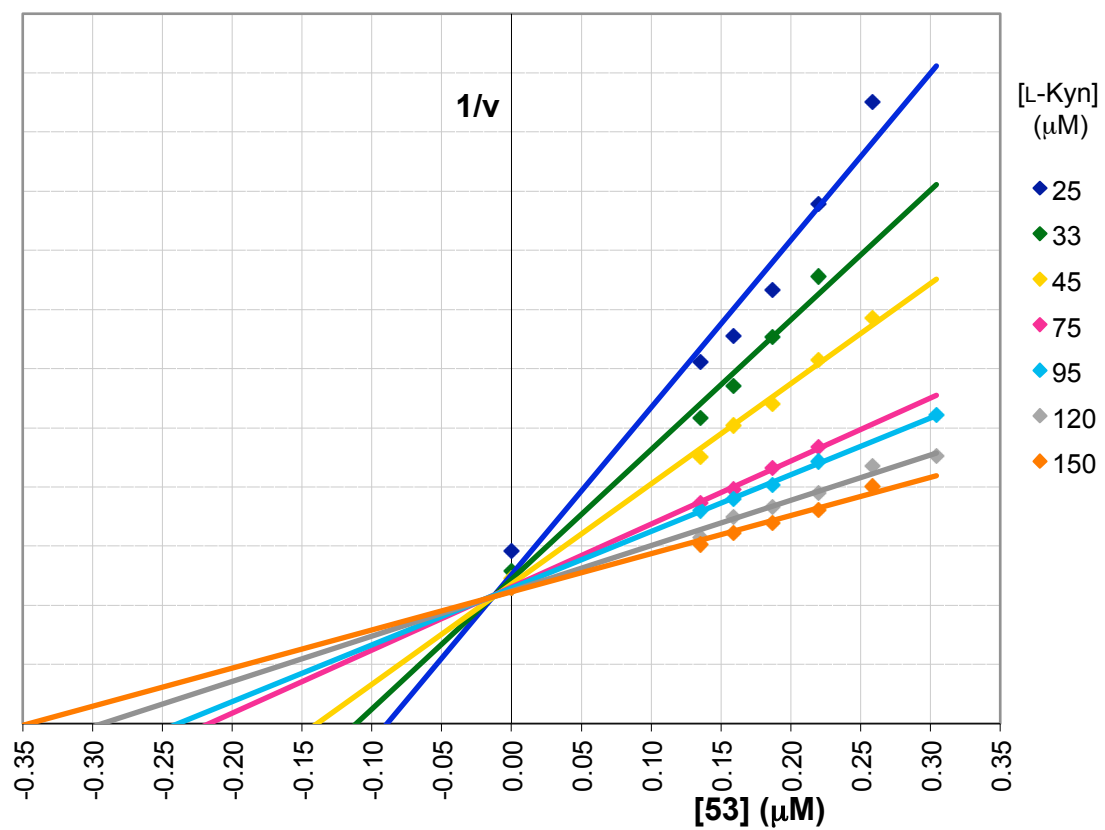


Figure 3.17. A Dixon plot obtained for competitive inhibitor 272 against *P. fluorescens* K3MO.

3.4 Protein X-ray crystallography of second generation amides with *P. fluorescens* K3MO



Figure 3.18. The crystal structure of *P. fluorescens* K3MO with **271** bound in the active site.

A co-crystal structure, at a resolution of 2.40 Å, was obtained with **271** bound into the active site of K3MO from *P. fluorescens*, as illustrated in Figure 3.18 (Dr Chris Mowat and Martin Wilkinson, Edinburgh University).⁷⁶ There are three non-equivalent protein molecules in the unit cell. This is due to changes in the orientation of the amino acid side chains. The large void at the entrance to the active site allows the diethyl phosphate substituted phenyl ring to change its orientation, creating three “snapshots” of how the inhibitor is bound. Changes between the three structures are minor and the key interactions are homologous.

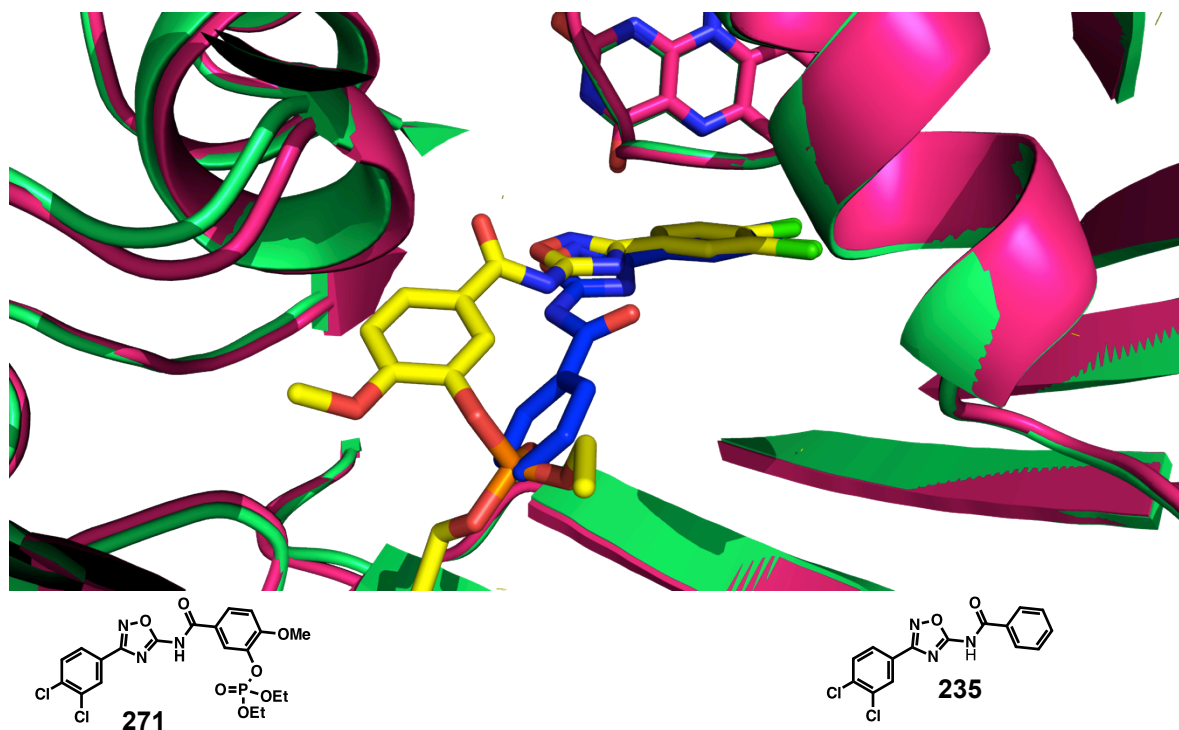


Figure 3.19. Comparison of the crystal structures with **235** and **271** bound in the active site. Inhibitor **271** (yellow) has a different binding mode to **235** (blue)

Alignment of the co-crystal structure of *P. fluorescens* K3MO with **235** (blue) and **271** (yellow) allows comparisons of the two binding modes. The 3,4-dichloro phenyl ring orients similarly for both **235** and **271**. However, the orientation of the amide changes by almost 180 degrees (Figure 3.19). Such a change allows the diethyl phosphate to orientate into free space. It also allows the phosphate to interact with Arg-84. The change in orientation of the amide means that the inhibitor is closer to the left-hand side of the active site moving the 1,2,4-oxadiazole ring further into the hydrophilic pocket.

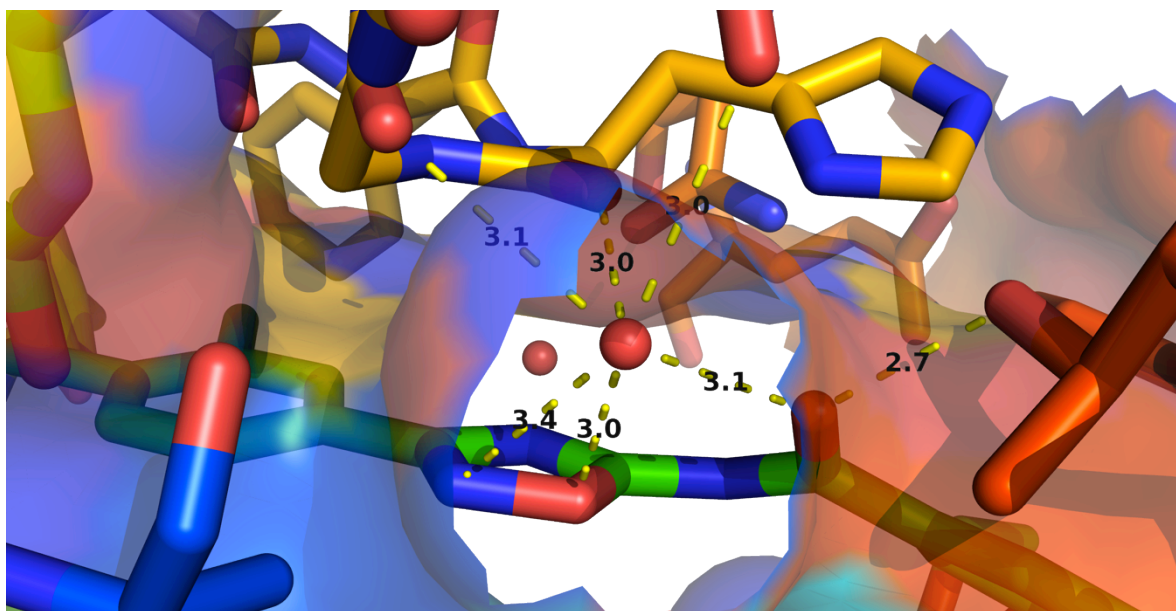


Figure 3.20. A view of the hydrophilic pocket with **271** bound in the active site and the interactions of the 1,2,4-oxadiazole and the amide carbonyl with the hydrophilic pocket. Distances are in (Å).

One of the benefits of the alternative binding mode of **271** is that it allows the amide carbonyl to interact with the hydrophilic pocket. The amide carbonyl is 3.1 Å from a water molecule, which is in the correct range for a hydrogen bonding interaction, as illustrated in Figure 3.20. The amide carbonyl is further stabilised in this orientation by a hydrogen bond (2.8 Å) to Thr-408, as illustrated in Fig. 3.21.

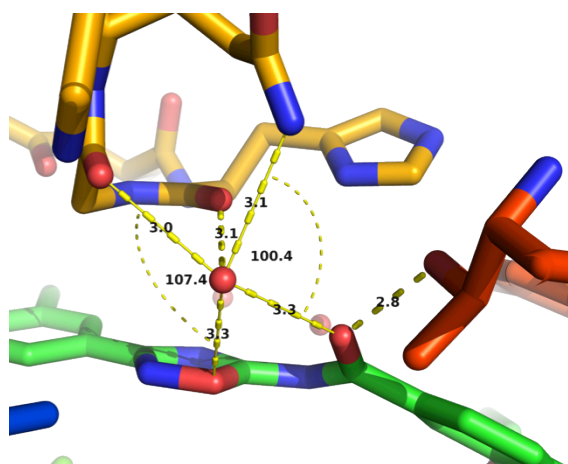


Figure 3.21. Angles and distances between the oxygen atom of the 1,2,4-oxadiazole ring, the inhibitor carbonyl and the main chain amides of *P. fluorescens* K3MO. Distances are in (Å).

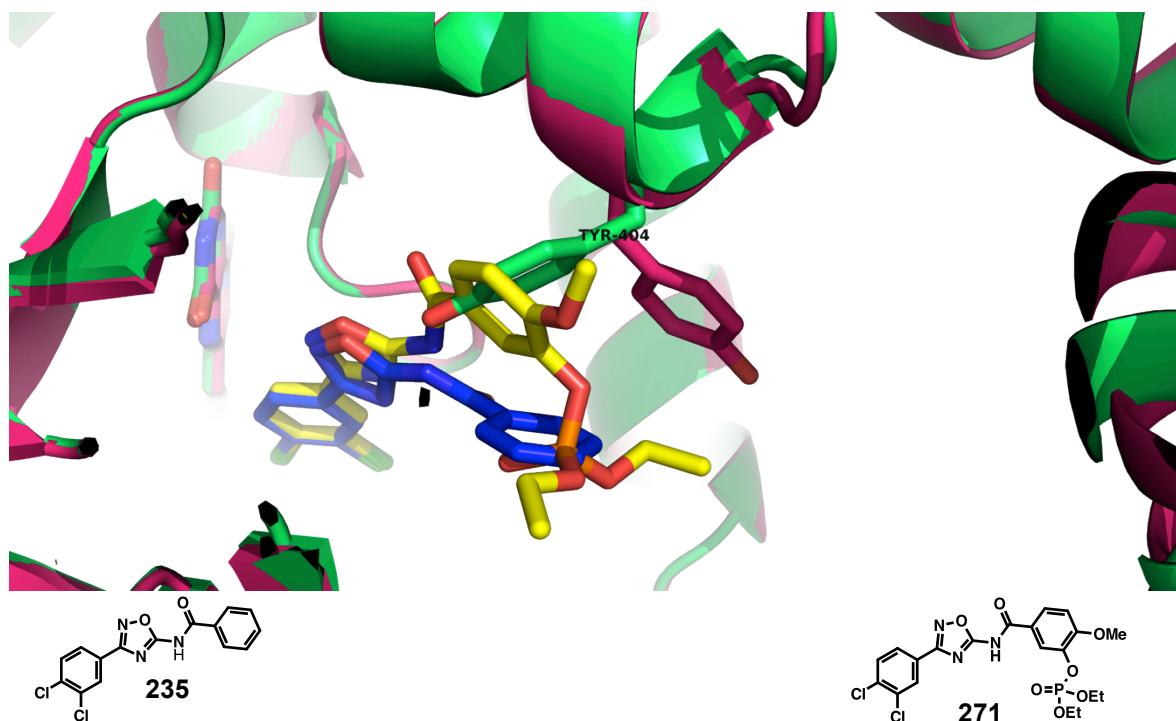


Figure 3.22. An overlay of K3MO (green) with **235** (blue) bound and K3MO (pink) when **271** (yellow) bound and the movement of Tyr-404 that is caused by the different binding mode of **271**.

The alternative orientation of the amide affects the orientation of the Tyr-404 side chain in the active site. With both substrate and **235** co-crystals, Tyr-404 adopts the orientation shown in green. In the co-crystal with **235** there is a hydrogen bond between the amide NH and the tyrosine OH, which stabilises this orientation. However, with **271**, the change in amide orientation forces the phosphate phenyl ring to sit in the space that is occupied by Tyr-404 in the co-crystal with **235**. This produces a change in orientation of the tyrosine side chain away from the diethylphosphate phenyl ring. The orientation of Tyr-404 in the co-crystal of **271** is stabilised by a hydrogen bond (3.1 Å) to Glu-372.

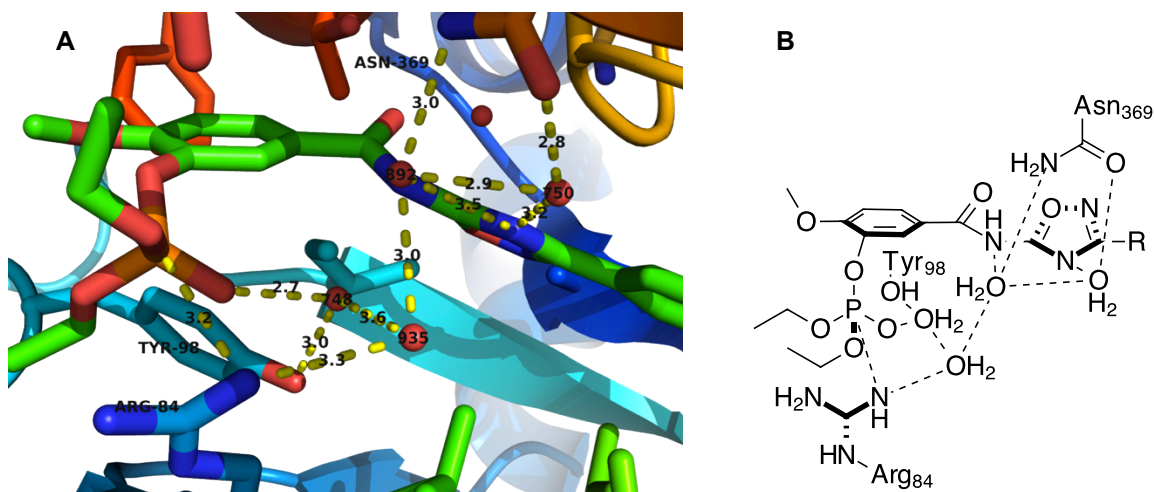


Figure 3.23. A) Interactions of **271** with some of the polar residues and water in the active site visualised with PyMol.¹⁶⁷ Distances are in (Å); **B)** A simplified representation of the interactions of the diethyl phosphate, amide NH and the 4-N of the 1,2,4-oxadiazole and bound water molecules.

The phosphate **271** interacts with the side chain of Arg-84 and potentially forms a hydrogen bond (2.7 Å) to water molecule 748. A speculative hydrogen bonding network is formed by water molecules-748, 935, 392 and 750, the side chains of Arg-84, Tyr-98 and Asp-369, the amide nitrogen of **271** and a nitrogen atom in the 1,2,4-oxadiazole of **271**. The amide NH of **271** possibly makes a relatively short hydrogen bond (2.7 Å) to water 392. This speculative hydrogen-bonding network appears to stabilise **271** in the active site. (Figure 3.23)

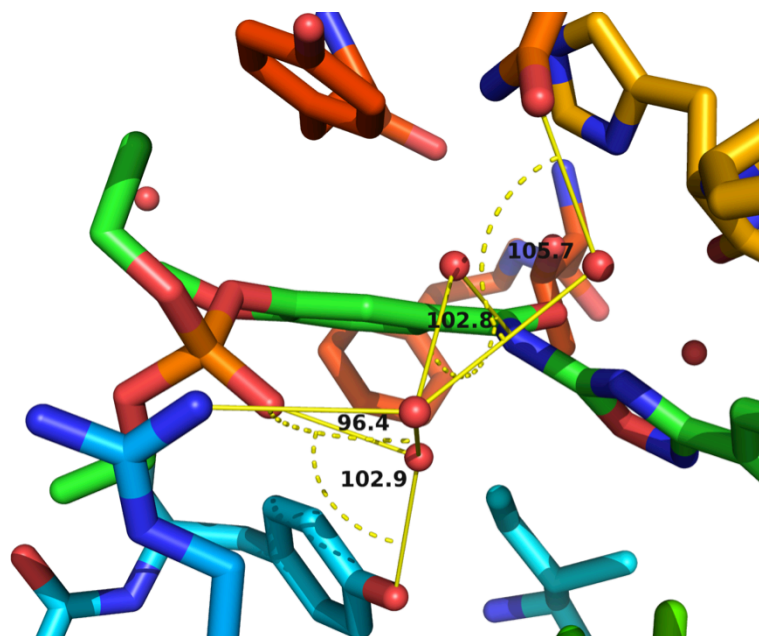


Figure 3.24. Bond angles in the speculative hydrogen bonding network suggests the locations of the water hydrogen atoms are found on the angle lines.



Figure 3.25. The crystal structure of *Pseudomonas fluorescens* K3MO with **272** bound in the active site.

A co-crystal structure, at a resolution of 2.30 Å, was obtained with **272** bound into the active site of K3MO from *P. fluorescens*, as illustrated in Figure 3.25 (Dr Chris

Mowat and Martin Wilkinson Edinburgh University).⁷⁶ Again, there are three non-equivalent protein molecules in the unit cell.

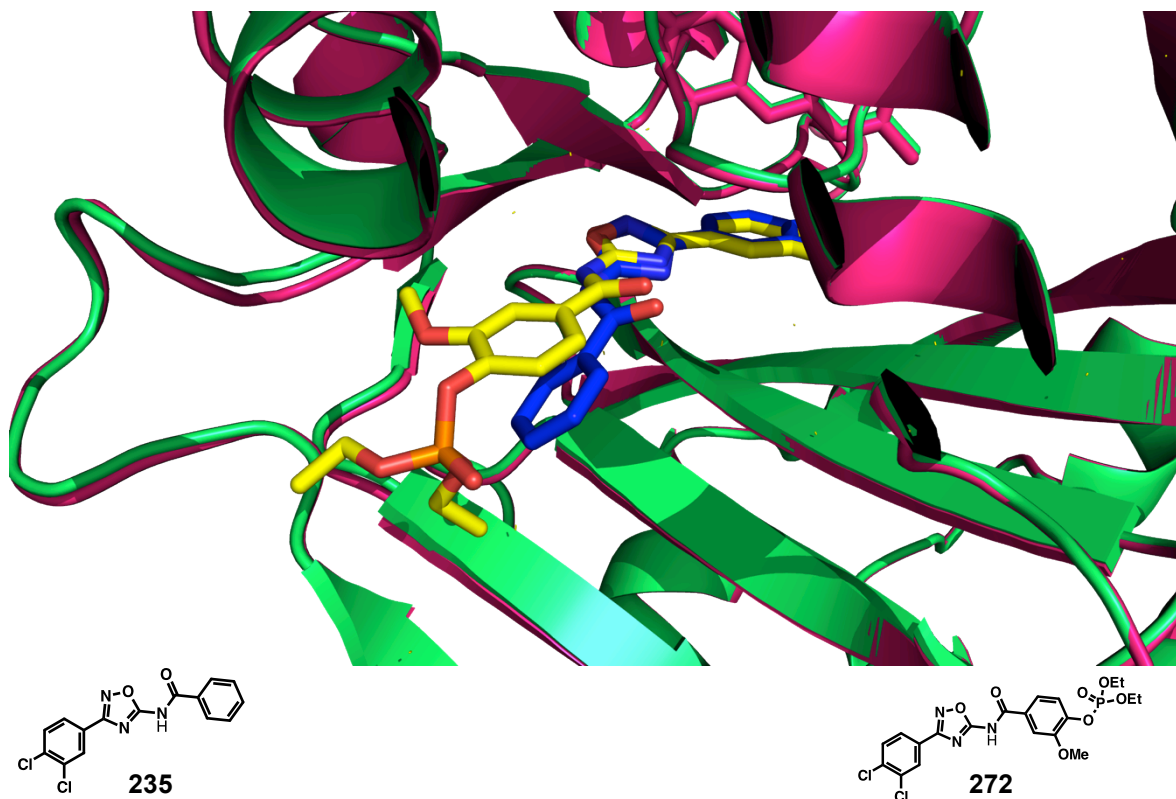


Figure 3.26. Comparison of the crystal structures with **235** and **272** bound in the active site. **272** (yellow) has a similar binding mode for the amide as **235** (blue).

Alignment of the co-crystal structures with **235** (blue) and **272** (yellow) allows comparisons of the different binding modes (Figure 3.26). The 3,4-dichloro substituted phenyl ring binds in the same orientation in both cases. In contrast to the crystal structure with **271** bound at the active site, the amide of **272** has a similar orientation to the amide of **235**.

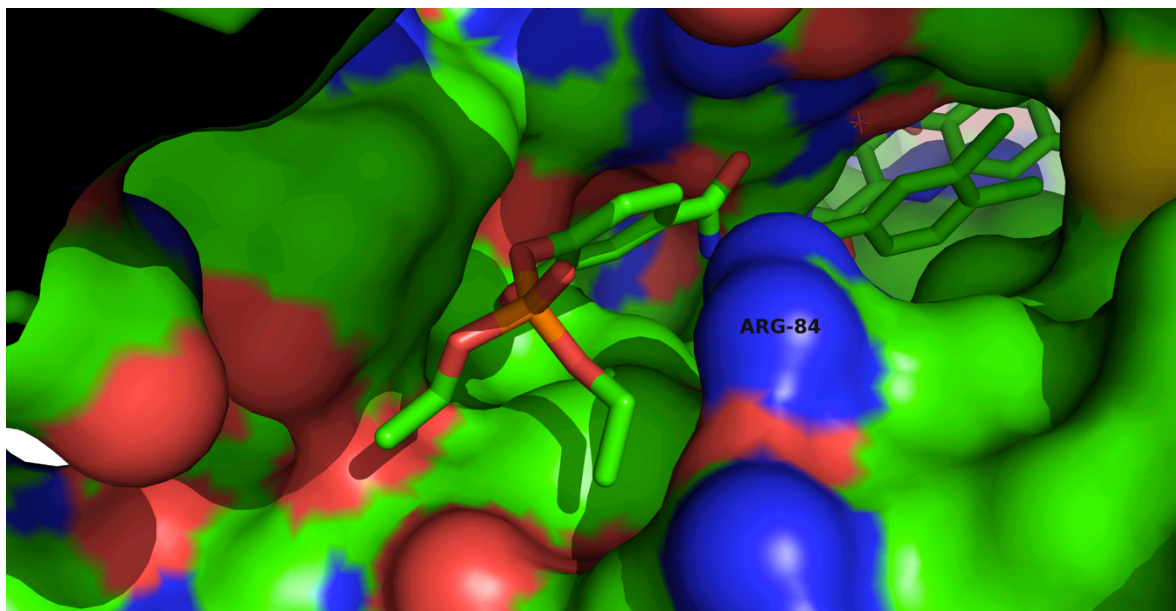


Figure 3.27. The Van der Waals surface of the active site and **272** showing the phosphate group orientating itself into space.

Addition of the Van der Waals surface to the protein structure helps rationalise why an alternative orientation of the phenyl ring is adopted (Figure 3.27). The phenyl ring is not able to form a π -cation interaction with Arg-84 as found with **235**. This alternative orientation allows the diethyl phosphate to sit in space because the phenyl ring has moved towards the left hand side of the active site. The interaction of the 1,2,4-oxadiazole with the hydrophilic pocket is nearly identical to that observed for **235**. The amide also makes similar interactions to that found for **235**.

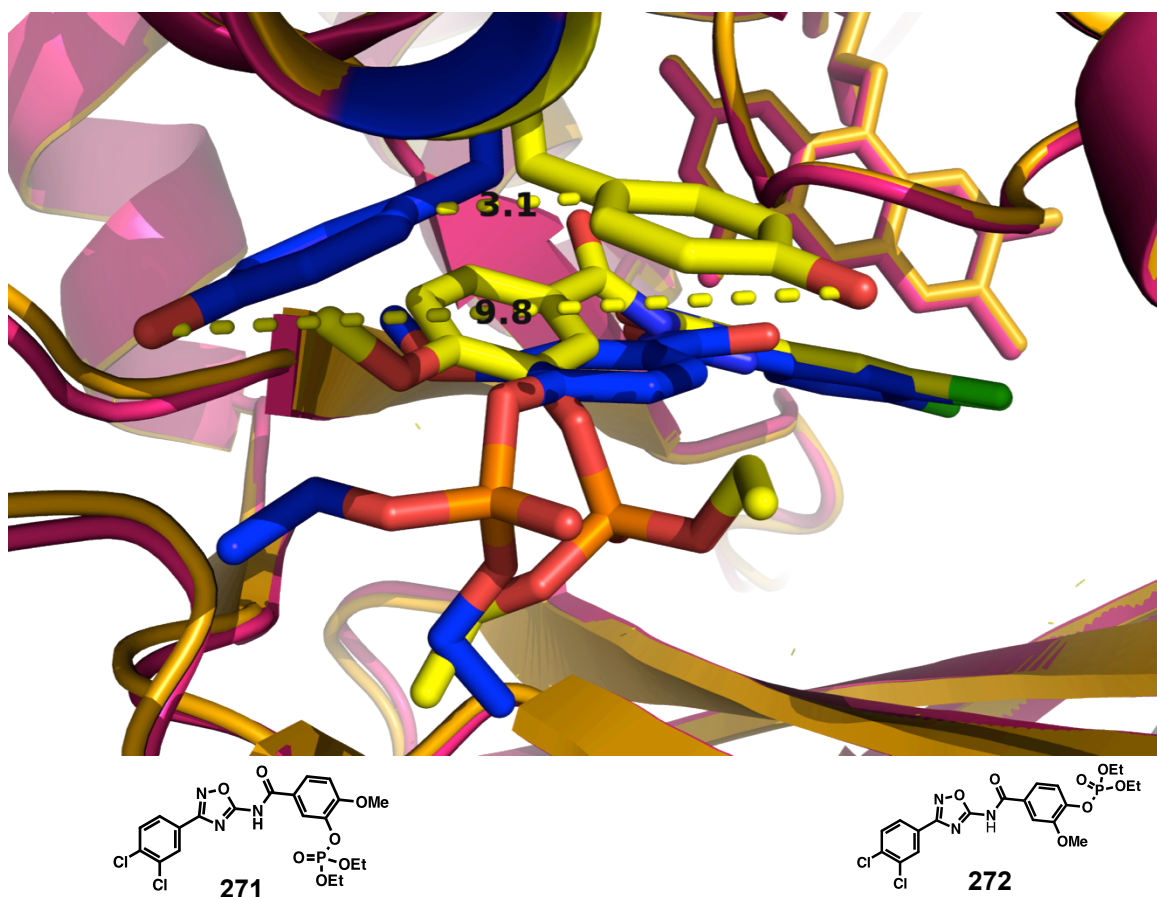


Figure 3.28. An overlay of K3MO with **272** (blue) bound and K3MO when **271** (yellow) bound and the movement of Tyr-404 to an orientation that has not previously been observed. Distances are in (Å).

Interestingly, when **272** (in blue) was bound into the active site, the side chain of Tyr-404 rotates by approximately 180 degrees. It is not clear why Tyr-404 adopts this orientation relative to that found for **271**. It is possible that the two phenyl rings come too close together and the relative orientations make π - π stacking difficult. Without any stabilising interactions the tyrosine simply moves into free space (Figure 3.28 and Figure 3.29).

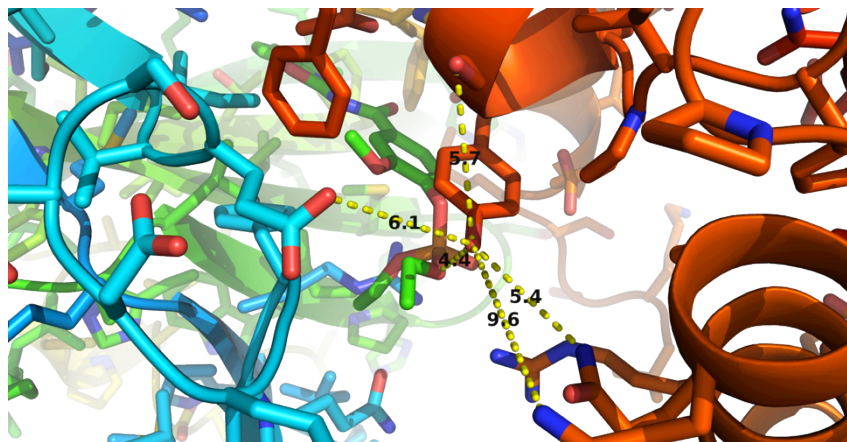


Figure 3.29. Tyr-404 moves into free space to avoid any clashes with **272**, in the active site of K3MO.

The co-crystals of **271** and **272** provide important information for the development of next generation inhibitors. Both **271** and **272** are accepted into the active site, although they employ different binding modes. It is clear from the inhibition data that **271** is a stronger binder than **272**. This is presumably due the fact that the binding orientation allows the phosphate to come in close contact with Arg-84 and allow additional electrostatic interaction in the hydrophilic pocket.

3.5 Synthesis and assay of a third generation series of 1,2,4-oxadiazole amides

With the diethyl phosphates **271** and **272** showing excellent inhibition of the bacterial enzyme, the synthesis of some derivatives was undertaken to progress a third generation of compounds.

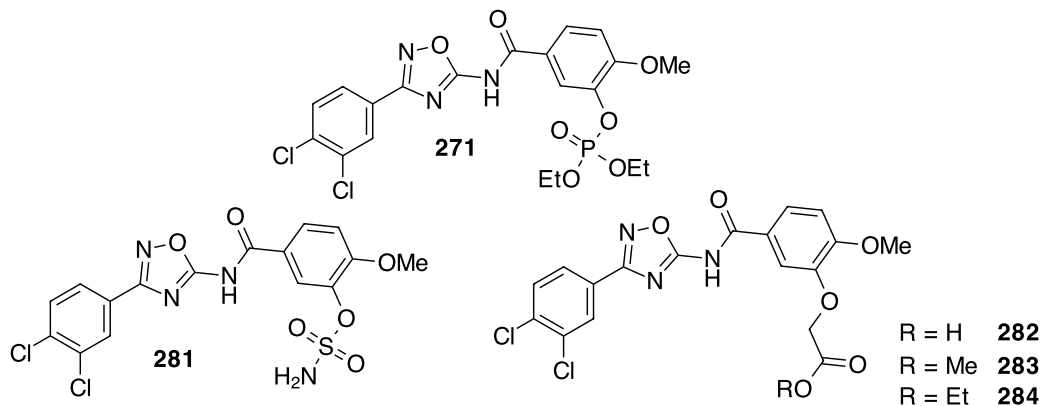
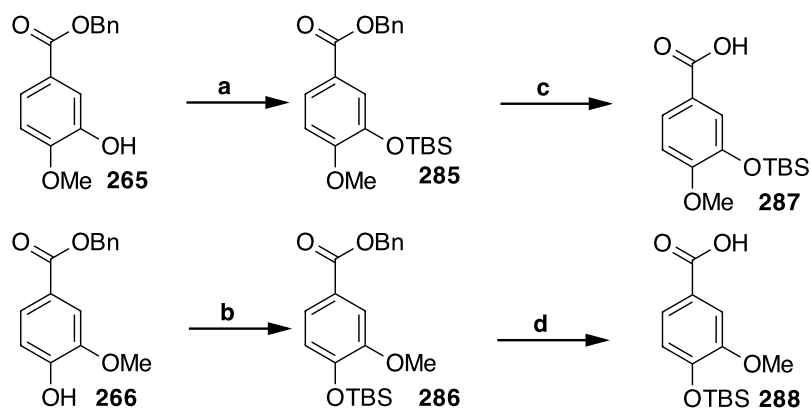


Figure 3.30. Comparison between the second generation compound **271** and the third generation compounds containing phosphate bioisosteres.

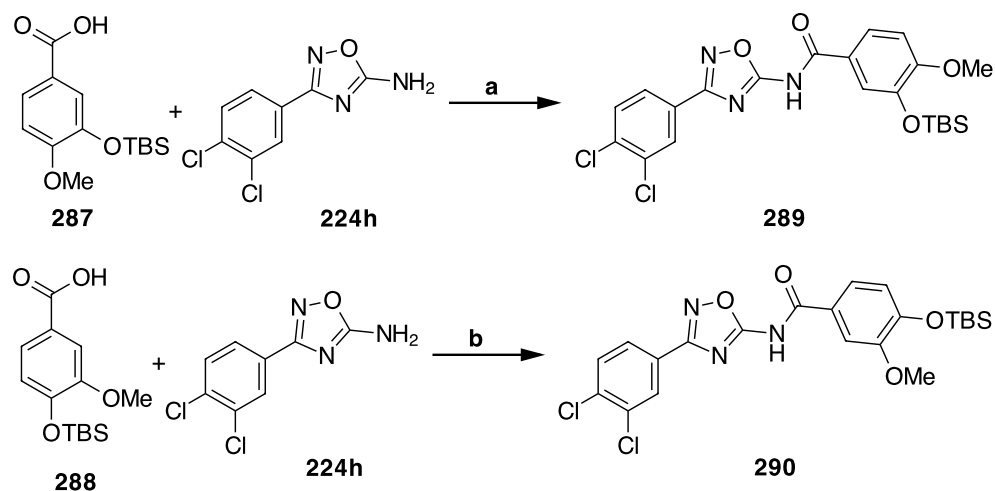
Replacement of the diethylphosphate group of **271** with phosphate bioisosteres, namely a sulfamate **281** and a carboxylic acid **282**, was explored.¹⁷⁶ The methyl and ethyl esters **283** and **284** were included in the series as the parent carboxylic acids are ionised at physiological pH, preventing the molecule from passing through cell membranes. The esters are potentially prodrugs for the carboxylic acid.¹⁷⁷ However, sulfamates, unlike carboxylic acids, are able to cross cell membranes. With a pKa of 15.6 methyl sulfamate is not ionised under physiological conditions.¹⁷⁶



Scheme 3.18. Reagents and conditions: **a**) TBSCl, imidazole, DCM, RT, 16 h, 97%; **b**) TBSCl, imidazole, DCM, RT, 16 h, 84%; **c**) Pd black, H₂, MeOH, RT, 72 h, 34%; **d**) Pd black, H₂, MeOH, RT, 72 h, 82%.

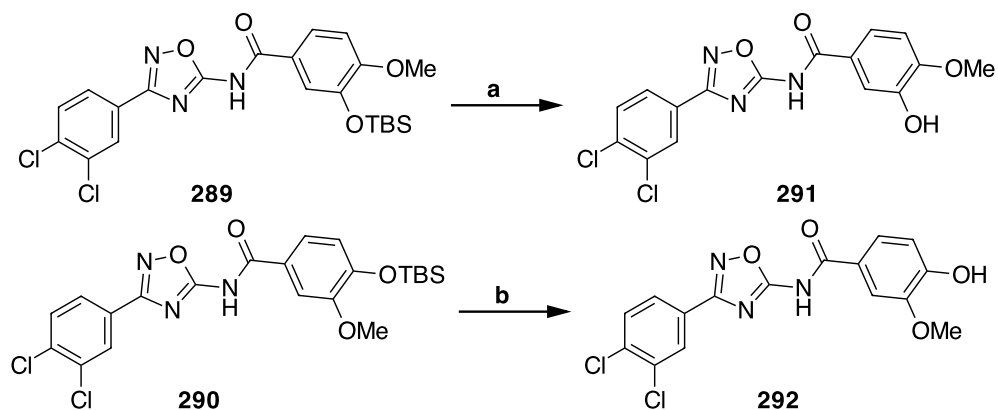
The planned route for introduction of the sulfamate was to incorporate the functionality in the final step. The phenol required for sulfamate incorporation requires protection during the amide formation step. Protection of the phenol as a TBS ether, allowed for a facile deprotection post amide formation. Protection of the phenols **265** and **266** was accomplished using TBSCl and imidazole, to give **285** and **286** in good yield, as illustrated in Scheme 3.18.

Hydrogenation of the benzyl esters **285** and **286** gave benzoic acids **287** and **288** in moderate to good yields, as illustrated in Scheme 3.19. Carboxylic acids **287** and **288** were not amenable to recrystallisation, thus column chromatography was used to purify them.



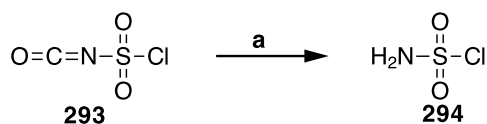
Scheme 3.19: Reagents and conditions: **a)** EDCI, DMAP, DCM, RT, 16 h, 52%; **b)** EDCI, DMAP, DCM, RT, 16 h, 51%.

The carboxylic acids **287** and **288** were reacted with **224h** using EDCI as the coupling agent to give amides **289** and **290**, as illustrated in Scheme 3.19. Both amides **289** and **290** required two sequential purifications by flash column chromatography to obtain clean products.



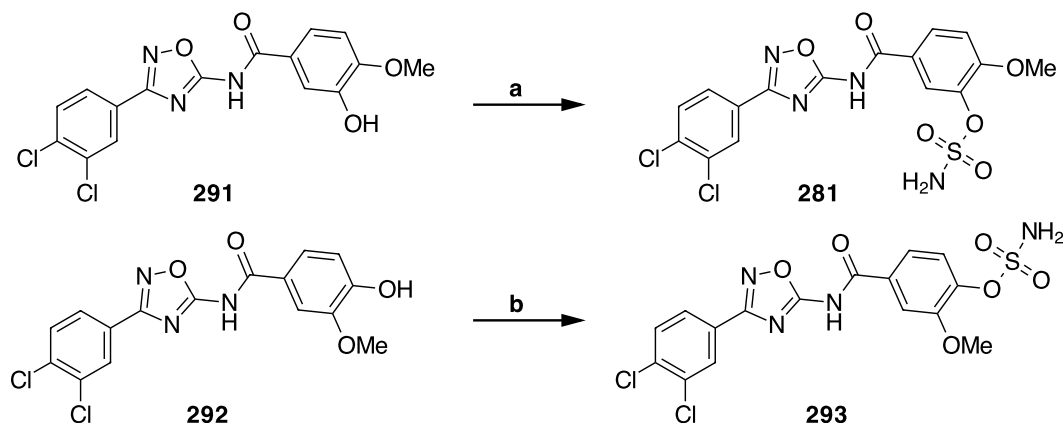
Scheme 3.20. Reagents and conditions: **a)** TBAF, THF, RT, 30 min, 58%; **b)** TBAF, THF, RT, 30 min, 68%.

Deprotection of amides **289** and **290** using TBAF gave the phenols **291** and **292**, respectively, in moderate yields (Scheme 3.20). However, enough material was obtained for characterisation, preparation of the sulfamates and for enzymatic assay.



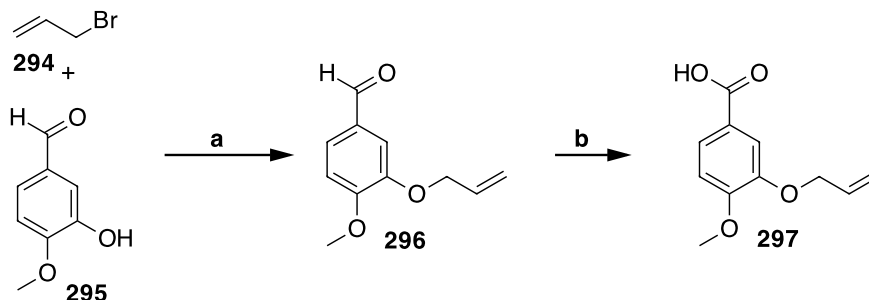
Scheme 3.21. Reagents and conditions: **a**) HCO_2H , DCM.

The incorporation of the sulfamate group is generally undertaken through the reaction of an alcohol with sulfamoyl chloride. The sulfamoyl chloride can be produced by the acid mediated decomposition of isocyanate **293** to give a solution of **294** in DCM (Scheme 3.21).¹⁷⁸ This was stored and used without any further purification as a 1 M solution of **294** in DCM.



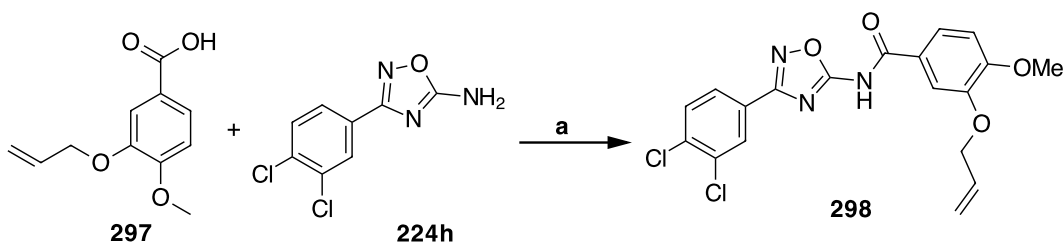
Scheme 3.22: Reagents and conditions: **a**) Sulfamoyl chloride (1 M in DCM), DMA, 0 °C to RT, 16 h, 87%; **b**) sulfamoyl chloride (1 M in DCM), DMA, 0 °C to RT, 16 h, 61%.

Sulfamoylation of the phenols **291** and **292** following the procedure developed by Okada *et al.*¹⁷⁹ was undertaken. In that protocol, DMA was used as the solvent. The reaction proceeded well to give the sulfamates **281** and **293** in good yield, as illustrated in Scheme 3.22.



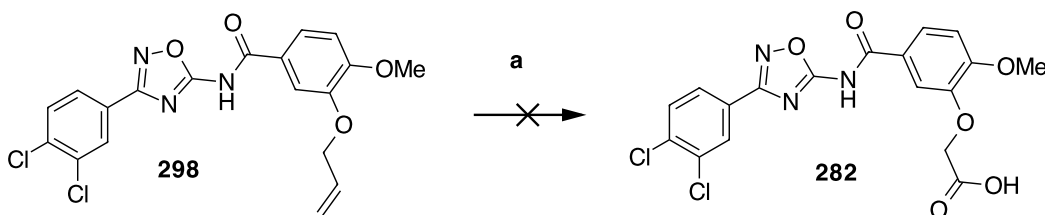
Scheme 3.23. Reagents and conditions: **a)** Allyl bromide **294**, K₂CO₃, DMF, 50 °C, 3 h, quant.; **b)** CrO₃, H₂SO₄, acetone, H₂O, 0 °C to RT, 3 h, 44%.

The planned synthesis for the carboxylic acid **282** involved a late stage RuO₄ oxidative cleavage of a double bond. However, the presence of the double bond at this stage ruled out hydrogenation of a benzyl ester, so oxidation of the aldehyde to the carboxylic acid was investigated. Synthesis of benzaldehyde **296** was achieved using allyl bromide **294** in the presence of potassium carbonate, as illustrated in Scheme 3.23.¹⁸⁰ Chromate oxidation of aldehyde **296** to benzoic acid **297** worked in moderate yield, as illustrated in Scheme 3.23, following a modified procedure of that used by Koning *et al.*¹⁸⁰



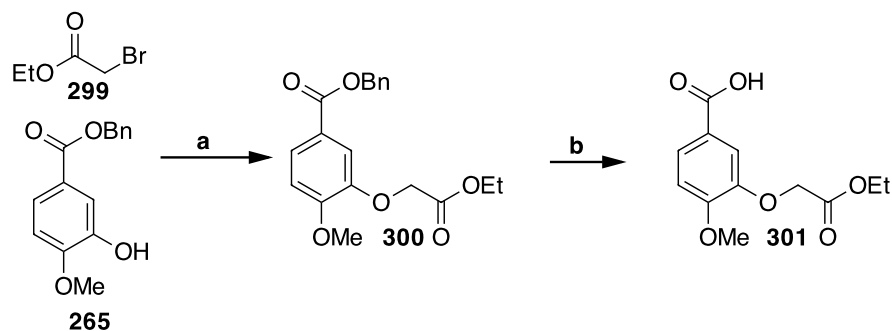
Scheme 3.24. Reagents and conditions: **a)** EDCI, DMAP, DCM, RT, 16 h, 80%.

Amide **298** was then prepared using EDCI as a coupling agent in good yield, as illustrated in Scheme 3.24.



Scheme 3.25. Reagents and conditions: **a)** RuCl₃, NaIO₄, CCl₄, MeCN, H₂O, RT, 16 h.

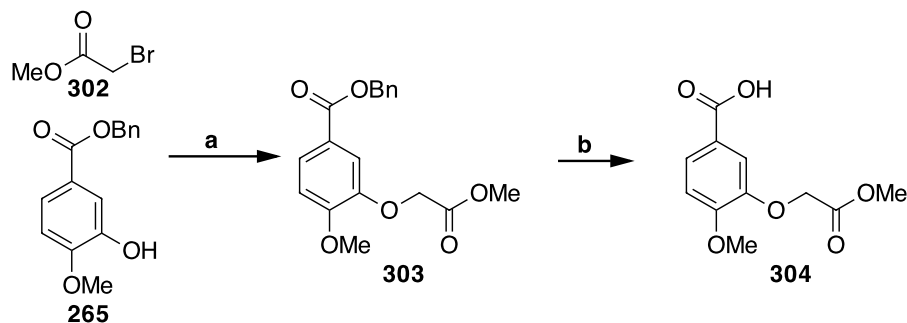
Oxidation of the allyl group of **298** to give the carboxylic acid **282** was attempted using the RuO_4 method developed by Sharpless *et al.*¹⁸¹ However, the published procedure did not afford any carboxylic acid. The major product, isolated after flash column chromatography, still had the allyl group intact.



Scheme 3.26. Reagents and conditions: **a)** K_2CO_3 , ethyl bromoacetate **299**, DMF, 60 °C, 3 h, 96%; **b)** Pd/C , H_2 , MeOH, RT, 48 h, 60%.

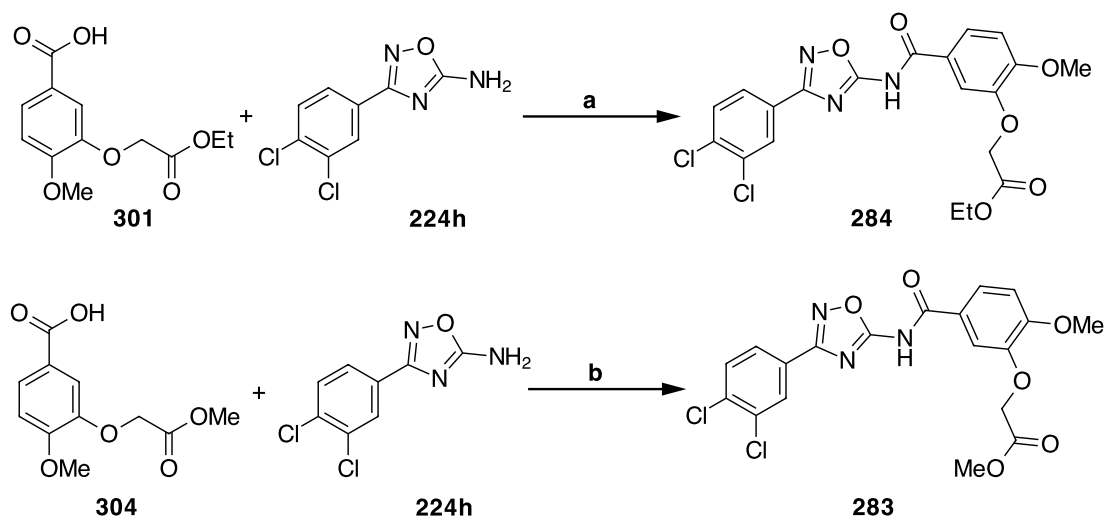
With the failure of the ruthenium oxidation, focus switched to the synthesis of the ethyl and methyl esters. The esters could clearly be hydrolysed to give the desired carboxylic acid. Ester **300** was prepared using ethyl bromoacetate **299** and benzyl ester **265** following a modified procedure used by Shah *et al.*¹⁸² Heating the mixture at 60 °C for 3 h gave **300** in an excellent yield, as illustrated in Scheme 3.26.

The benzyl ester moiety of **300** was then deprotected using hydrogenation to give the benzoic acid **301** in good yield, as illustrated in Scheme 3.26. The product could be purified by recrystallisation or by flash column chromatography. Recrystallisation proved to be the preferred method of purification.



Scheme 3.27. Reagents and conditions: **a)** K_2CO_3 , methyl bromoacetate **302**, DMF, 60 °C, 3 h, 88%; **b)** Pd/C, H_2 , MeOH, RT, 48 h, 71%

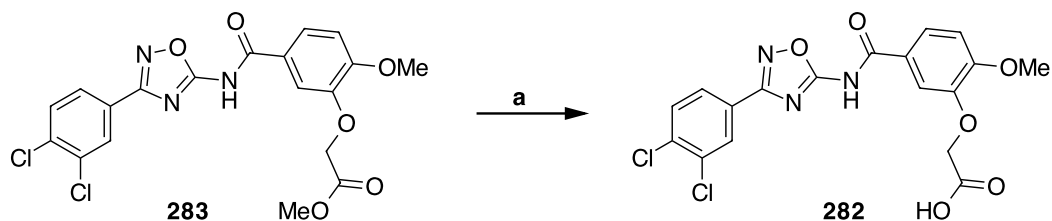
In a similar manner to that used to produce **300**, methyl bromoacetate **302** and benzyl ester **265** were reacted at 60 °C for 3 h, as illustrated in Scheme 3.29. Product **303** was recovered in good yield. Palladium-catalysed hydrogenation of benzyl ester **303** generated benzoic acid **304** in good yield, as illustrated in Scheme 3.27. The product was not amenable to recrystallisation and so purification of the carboxylic acid was carried out by flash chromatography. Due to the polar nature of the compound 5% MeOH in DCM was required to elute the compound on silica.



Scheme 3.28. Reagents and conditions: **a)** EDCI, DMAP, DCM, RT, 16 h, 75%; **b)** EDCI, DMAP, DCM, RT, 16h, 74%.

With benzoic acids **301** and **304** in hand, focus turned to forming amides **283** and **284**. The amides were formed in good yield using EDCI as the coupling agent, as

illustrated in Scheme 3.28. Purification of methyl ester **283** by flash chromatography proved difficult, due to its poor solubility. Ethyl ester **284** was purified by recrystallisation from ethanol.



Scheme 3.29. Reagents and conditions: **a)** NaOH, H₂O, THF, RT, 1 h, then HCl solution, 61%.

Hydrolysis of methyl ester **283** to the corresponding carboxylic acid **282** was carried out under basic conditions in a sodium hydroxide solution (Scheme 3.29). THF was added to aid the dissolution of the ester and the product was isolated after neutralisation.

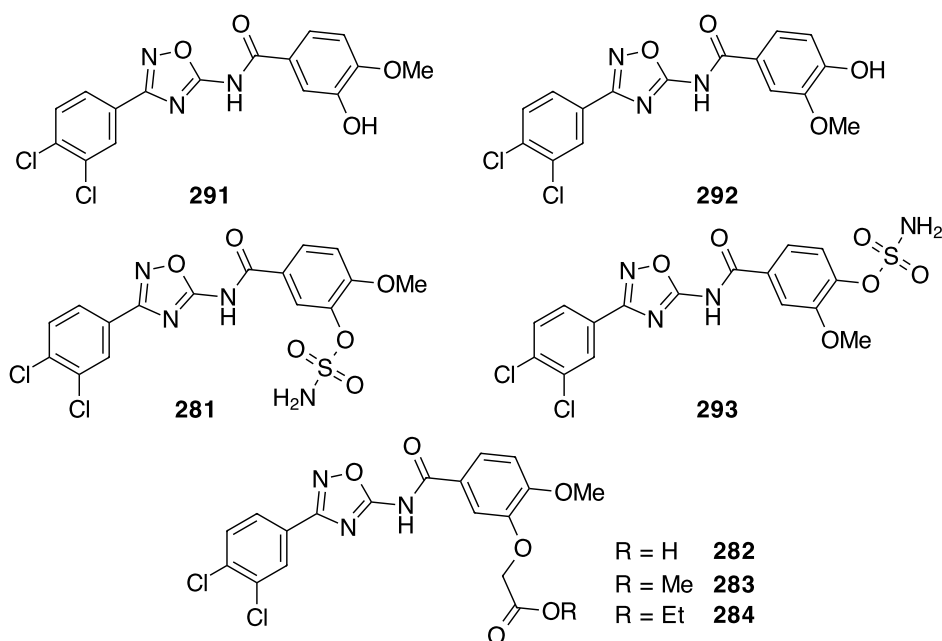
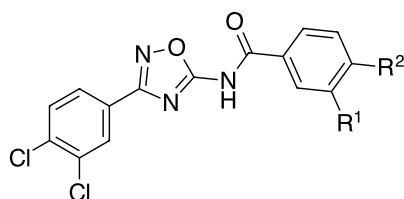


Figure 3.31. Third generation compounds tested against both human and bacterial K3MO.

Assays were then conducted with **281-284** and **291-293** (Figure 3.31) against *P. fluorescens* and human K3MO (Table 3.3). Initial indications suggest sulfamates **281** and **293** are not as good inhibitors as the diethyl phosphates **271** and **272**

based upon their percentage inhibition at 10 μ M. There does appear to be some preference for having the sulfamate at the 3- position over the 4- position, however, this cannot be assumed until K_i data becomes available. Both of the phenols **291** and **292** gave very similar values for inhibition. A trend can be observed with the carboxylic acid and its esters. The carboxylic acid **282** gave the best inhibition of the third generation compounds and of the whole series with a K_i of 29.1 ± 11.8 nM. It is possible that the carboxylic acid is forming a salt bridge with Arg-84. The increase in inhibition from the ethyl ester **284** to methyl ester **283** presumably reflects the importance of the interaction of Arg-84 with the ester, as **284** cannot approach Arg-84 as closely as **283**. Co-crystals of these potent inhibitors will be important for determining the key interactions and the development of further inhibitors. Although **282** shows good inhibition against the isolated K3MO, it is unlikely to cross through membranes.



	R ¹	R ²	Bacterial inhibition % at 10 μ M	Bacterial K_i (nM)
291	OH	OMe	95	68.1 ± 36.5
292	OMe	OH	95	120.1 ± 29.1
281	O-SO ₂ NH ₂	OMe	90	150.4 ± 96.0
293	OMe	O-SO ₂ NH ₂	85	
284	O-CH ₂ CO ₂ Et	OMe	93	39.0 ± 23.1
283	O-CH ₂ CO ₂ Me	OMe	96	
282	O-CH ₂ CO ₂ H	OMe	99	29.1 ± 11.8
271	O-PO(OEt) ₂	OMe	97.6 ± 0.1	65.5 ± 7.5

Table 3.3. Inhibition data for phosphate bioisosteres. (Dr Chris Mowat and Martin Wilkinson, Helen Bell and Annemette Kjeldsen)

3.6 Conclusions

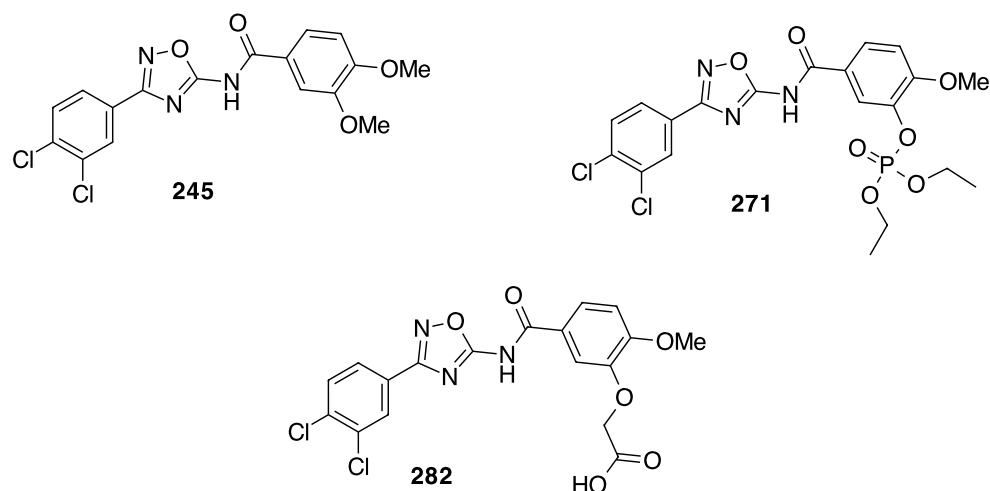


Figure 3.32. A summary of the best inhibitors of K3MO from each generation.

A small library of amides were synthesised and it was shown that the best inhibition against *P. fluorescens* K3MO was achieved when 3,4-dichloro substitution was introduced (for example with compounds **235** and **245**). Co-crystallisation of **235** and **245** with *P. fluorescens* K3MO revealed the interactions within the active site. It also revealed potential interactions that could be developed by changing substituents on the aromatic ring. All of the co-crystals show the role that the 1,2,4-oxadiazole plays in binding. The 1,2,4-oxadiazole locates in a hydrophilic pocket in the active site and does not act as a bioisostere of the kynurenine ketone. The introduction of the diethyl phosphate group in **271** and **272** generated compounds with a higher affinity for *P. fluorescens* K3MO. Co-crystallisation of **271** and **272** showed that the phosphate-substituted aromatic ring could bind in two different orientations. The orientation of **271** allows the interaction of the diethyl phosphate with Arg-84. The orientation of **272** does not allow the same interaction to be made. Both of the co-crystal structures revealed that the active site becomes more accommodating around the phosphate-bound aromatic ring. The co-crystal structures of **271** and **272** led to the replacement of the diethyl

phosphate with phosphate bioisosteres. Sulfonamides **281** and **293** were less potent than was expected. Carboxylic acid **282** has the highest binding affinity in this study against isolated *P. fluorescens* K3MO, however, it may not pass through membranes.

Unfinished business: Synthesis of kynurenine analogues

4.1 Introduction

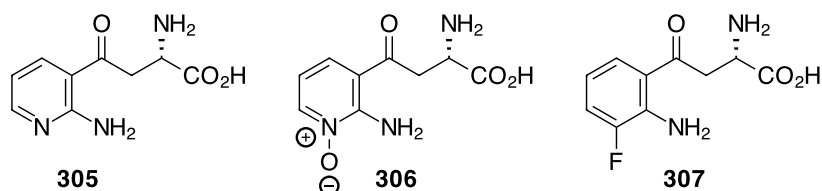


Figure 4.1. Synthetic targets: analogues of kynurenine.

The synthesis of kynurenine analogues **305** and **307** was considered, each a rationally designed (potential) inhibitor of K3MO. Kynurenine analogues have not been reported as inhibitors of K3MO. Unlike previously reported benzoylalanine inhibitors, kynurenine analogue **305** may mitigate the formation of hydrogen peroxide by uncoupled NADPH oxidation through interactions of the pyridine nitrogen with the FAD co-factor. The pyridine nitrogen should orientate towards the flavin-hydroperoxide and may generate *N*-oxide **306** *in situ*. This *N*-oxide **306** was also identified as a synthetic target as an authentic sample could be used to verify the biotransformation of **305** to **306** by K3MO. These compounds have not been previously reported.

3-Fluoro-kynurenine **307** had the potential to offer both a substrate-like inhibitor and an NMR probe for substrate-enzyme interactions of K3MO. If the enzyme accepts 3-fluoro-kynurenine **307** as a substrate this would allow the reaction to be monitored by ^{19}F NMR spectroscopy. Shifts in the ^{19}F NMR spectrum may provide insight into substrate binding and add detail to understanding K3MO binding.

4.2 Previous syntheses of kynurenine analogues

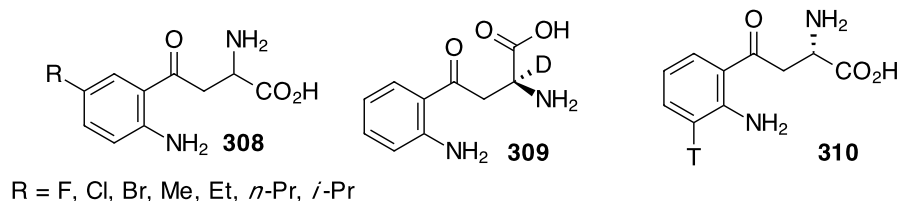
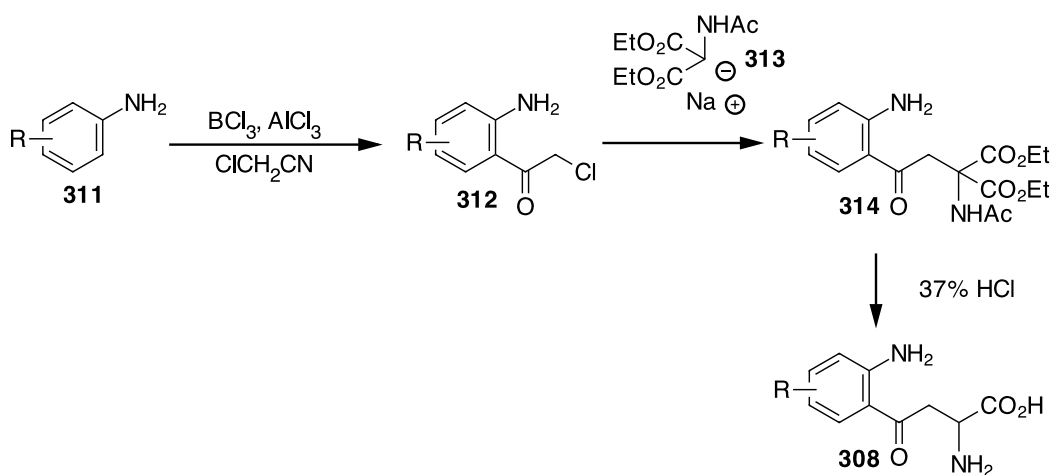


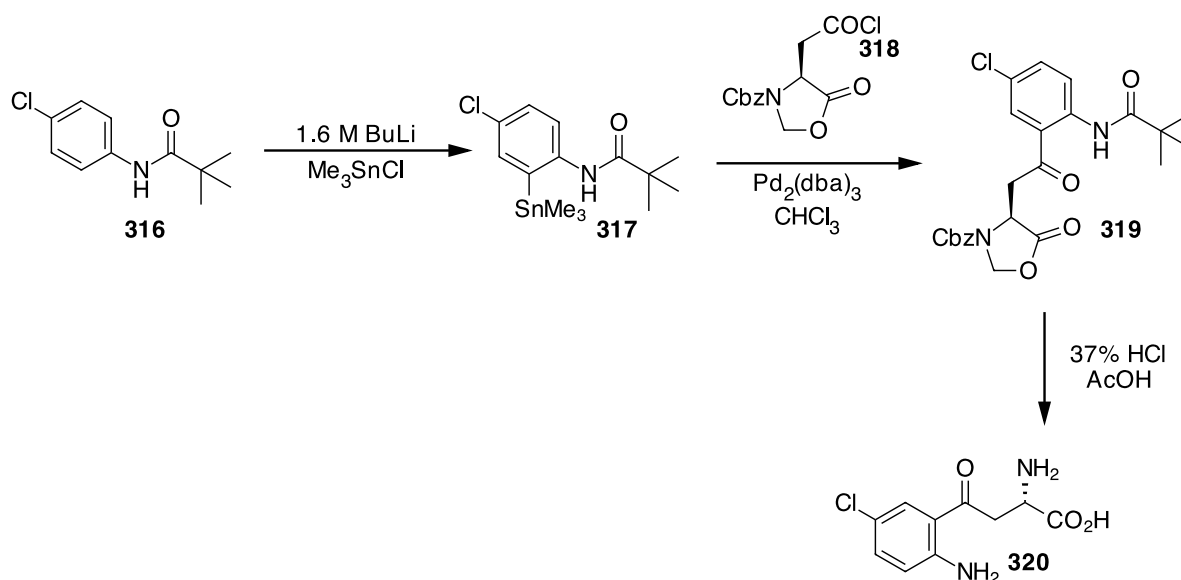
Figure 4.2. Previously synthesised kynurenine derivatives.

The synthesis of some related kynurenine analogues have previously been carried out. The kynurenines **308** were studied as KAT inhibitors (Chapter 1).⁶³ [2-²H]-Kynurenine **309** has been used in a study on the kinetic isotope effect of kynureninase¹⁸³ and [3-³H]-kynurenine **310** has been used in assays to monitor inhibition of K3MO.⁶⁷



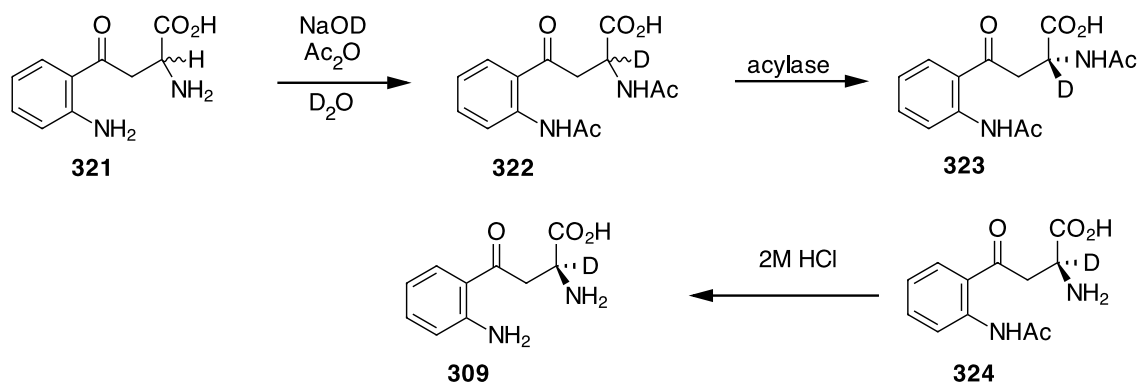
Scheme 4.1. The general route employed to generate racemic kynurenine analogues **308**.⁶³

Analogues **308** were all synthesised by Varasi *et al.*⁶³ as racemates, as illustrated in Scheme 4.1. 5-Chlorokynurenine was also synthesised in an enantiospecific manner in a separate synthesis. The first step in the formation of racemic kynurenine analogues was a Hoesch reaction using chloroacetonitrile with Lewis acid catalysis to form the α -chloroacetophenone **312**. Reaction of **312** with diethyl acetamidomalonate **313**, generated acetamidomalonate **314**. Finally acid mediated decarboxylation and deprotection yielded the desired racemic kynurenines **308**.⁶³



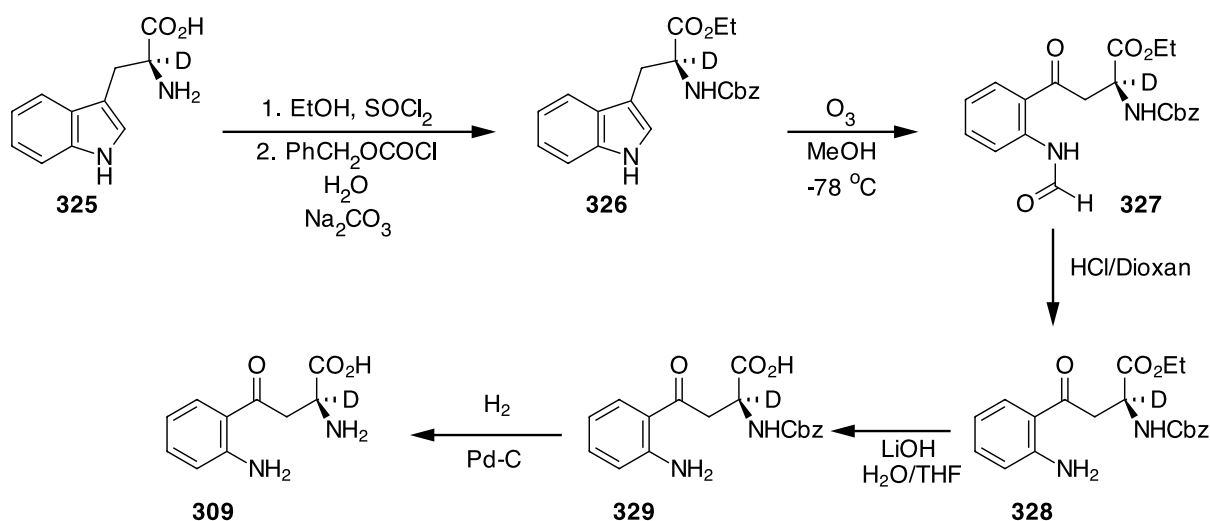
Scheme 4.2. An enantiospecific synthesis of L-5-chloro-kynurenine **320**.⁶³ (dba) = dibenzylideneacetone.

The reported enantiospecific synthesis of L-5-chloro-kynurenine **320** is illustrated in Scheme 4.2. The key step involved a Stille coupling between **317** and **318**.⁶³ This route lends itself to the synthesis of alternative L-kynurenine analogues, although the use of toxic trimethylstannyl chloride is not so attractive, especially when the final analogues are destined for biological testing.



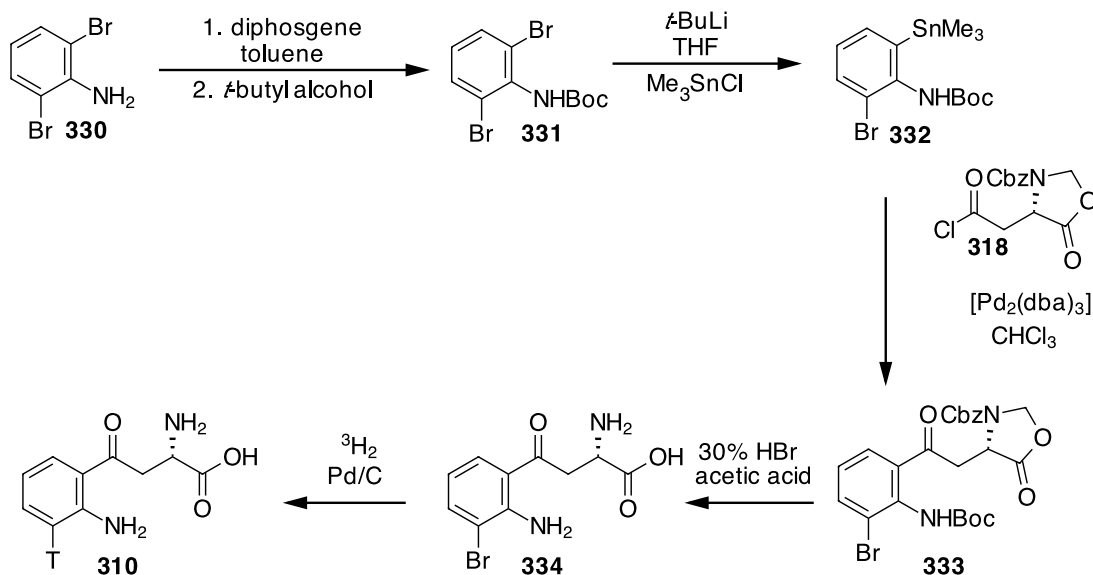
Scheme 4.3. The initial route to L-[2-²H]kynurenine **309** starting from DL-kynurenine **321**.¹⁸³

Two routes were developed towards the synthesis of L-[2-²H]kynurenine **309** by Ross *et al.*¹⁸³ The first started from racemic kynurenine, as illustrated in Scheme 4.3. The deuterium was incorporated at the C-2 position during the acylation reaction. A key step in this route involved the enzymatic hydrolytic resolution of **322**¹⁸³ although clearly only a maximum of 50% can be recovered.



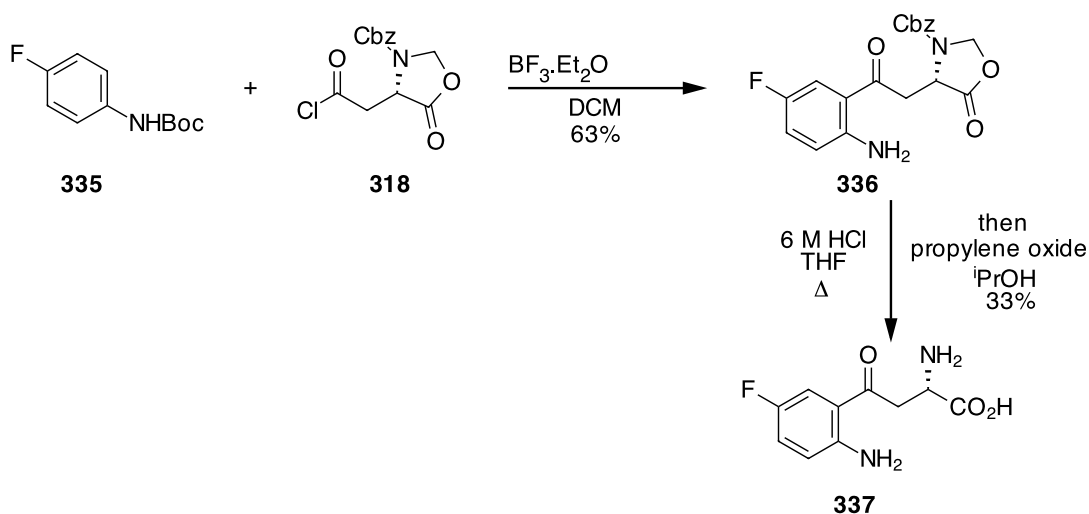
Scheme 4.4. Synthesis of L-[2-²H]kynurenine **309** starting from L-[2-²H]tryptophan **325**.¹⁸³

Racemisation of L-tryptophan followed by an acylase resolution, similar to that used in Scheme 4.3, generated L-[²H]-tryptophan **325** with an enantiomeric excess of 99%. Sequential protection of the carboxylic acid and amine moieties generated **326**. The indole ring was then oxidatively cleaved at the C-2,C-3 double bond to provide deuterated formylkynurenine **327**. Finally sequential removal of the three protecting groups gave L-[2-²H]kynurenine **309**.¹⁸³



Scheme 4.5. Synthesis of L-[3-³H]-kynurenine **310** via a Stille coupling.⁶⁷ (dba) = dibenzylideneacetone.

Isotopically labelled L-[3-³H]-kynurenine **310** was prepared by Röver *et al.*⁶⁷ from the 3-bromokynurenine analogue **334**. L-3-Bromokynurenine was synthesised *via* a Stille coupling with **318**, giving **333**, as illustrated in Scheme 4.5. Reaction of 3-bromokynurenine **334** under a tritium atmosphere using Pd/C catalysis gave the desired L-[3-³H]-kynurenine **310**.⁶⁷



Scheme 4.6. Route to L-5-fluorokynurenine **337** taken from K.Muirhead and N.Botting (2002).¹⁸⁴

Previously within the group a route was developed to 5-fluorokynurenine **337**.¹⁸⁴ This route is shown in Scheme 4.6, where the key step was a Friedel-Crafts acylation. It was possible to acylate a protected 4-fluoroaniline **335** using $\text{BF}_3 \cdot \text{Et}_2\text{O}$ as a Lewis acid catalyst with the protected aspartic acid chloride **318** in good yield. Deprotection of the amino acid under acidic conditions gave the fluorinated analogue **337**.¹⁸⁴ However, the synthesis was not so efficient and the product was recovered in a relatively low yield.

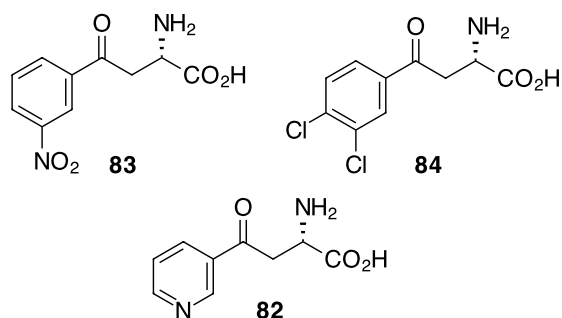
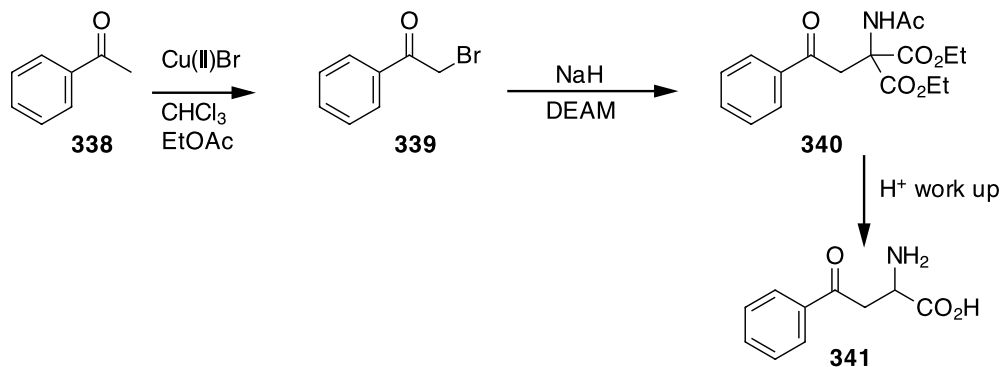


Figure 4.3. Previous benzoylalanine inhibitors of K3MO.

Benzoylalanines are known substrate-like inhibitors of K3MO.^{77, 96, 185} Investigation into benzoylalanines as inhibitors of kynureninase^{186, 187} and kynurenine aminotransferase¹⁸⁸ have also been carried out.



Scheme 4.7. The most common route to benzoylalanines is through α -bromoacetophenone.

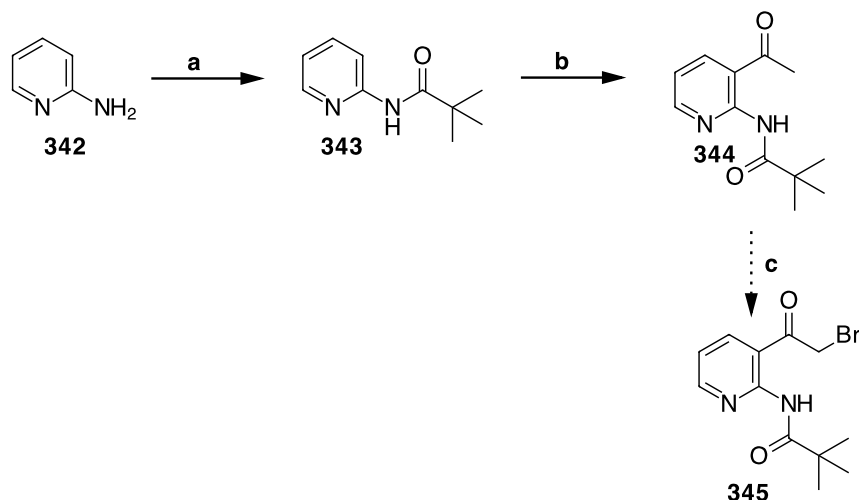
Key steps in the general method for the preparation of benzoylalanines^{186, 187} are illustrated in Scheme 4.7. If the α -bromoacetophenone is not commercially available it can generally be prepared by the reaction of the required acetophenone **338** with Cu(II)Br₂. Nucleophilic substitution of **339**, by diethyl acetamidomalonate (DEAM) gave **340**, which is an immediate precursor to the required amino acid. Acid mediated decarboxylation/deprotection then allowed preparation of the benzoylalanine **341** as a racemate. Single enantiomers can be prepared by a modification of this route using the Schollkopf method in place of diethyl acetamidomalonate.

4.3 Aims and objectives in the synthesis of kynurenine analogues

The aim for this work was to synthesise the kynurenine analogues **305**, **306** and **307**. The compounds were initially targeted as their racemates to simplify their preparation and to carry out an initial assay to determine whether they are substrates for K3MO. The use of trimethylstannyl chloride was avoided to prevent any toxic tin by-products from potentially affecting the bioassays. An analogous

route to that used in the synthesis of benzoylalanines, using Cu(II)Br₂ was initially envisaged to generate the amino acid.

4.4 Routes towards the synthesis of a pyridyl-kynurenine analogue



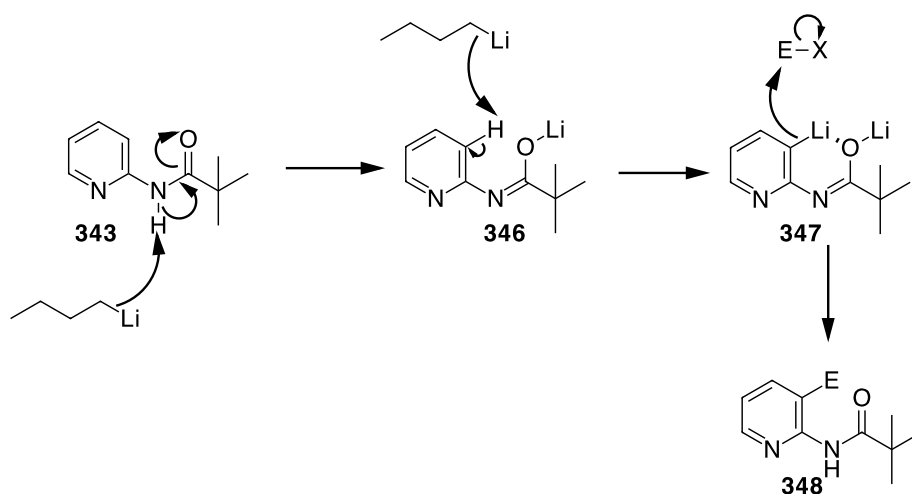
Scheme 4.8. Reagents and conditions: **a)** Trimethylacetyl chloride, DMAP, DCM, 0 °C to RT, 16 h, 91%; **b)** *n*-BuLi, acetylmorpholine, THF, -50 °C to 0 °C, 1.5 h, then -40 °C, 1 h, 63%; **c)** Cu(II)Br, CHCl₃, EtOAc, 80 °C, 16 h.

Ketone **344** had already been reported by Murray *et al.* and it was envisaged that the bromide **345** could be directly prepared from pyridine **344** through the use of Cu(II)Br₂, following a similar procedure to that used to form benzoylalanines.

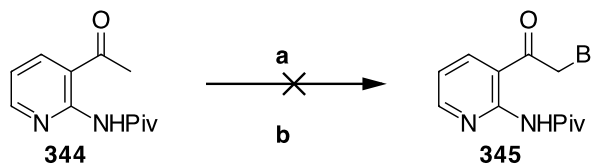
2-Aminopyridine **342** was initially protected as its pivaloyl amide **343** using trimethylacetyl chloride and DMAP in an excellent yield (Scheme 4.8).^{189, 190} *Ortho*-lithiation of **343** was then accomplished using *n*-butyllithium (2.5 eq).

It is proposed (Scheme 4.9) that the first equivalent of *n*-butyllithium deprotonates the amide of **343**, and then the second equivalent selectively deprotonates at C-3 of the pyridine.¹⁹⁰ A colourless precipitate formed after complete addition of *n*-butyllithium, which is assumed to be the dilithio species **347**. Upon addition of the electrophile, in this case *N*-acetyl morpholine, the precipitate starts to dissolve. Purification using the literature conditions gave an impure product. However,

optimisation of the solvent system during column chromatography provided ketone **344** in good yield.¹⁹¹



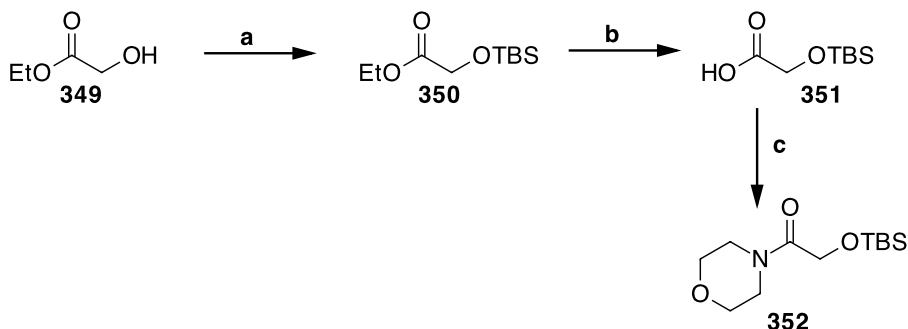
Scheme 4.9. Proposed mechanism for *ortho*-lithiation of amino pyridines.



Scheme 4.10. Reagents and conditions: **a**) Cu(II)Br, CHCl₃, EtOAc, 80 °C, 16 h; **b**) HBr, Br₂, AcOH, 0 °C to 75 °C, 8 h.

Bromination of ketone **344** was attempted using Cu(II)Br₂ in chloroform/ethyl acetate, as illustrated in Scheme 4.10.¹⁹² However, the reaction was unsuccessful under the reported conditions and only starting material was returned. Attempts at brominating **344** using HBr and elemental Br₂ only returned the hydrobromide salt of **344**.

Due to the failure of the bromination step a modified approach was taken involving acylation with an α -hydroxy ether. This required synthesis of the functionalised *N*-acetyl morpholine **352**. By deploying a silyl ether the alcohol could undergo readily accessible protecting group manipulations. Conversion of the alcohol could then be explored to give bromide, chloride or tosyl leaving groups.

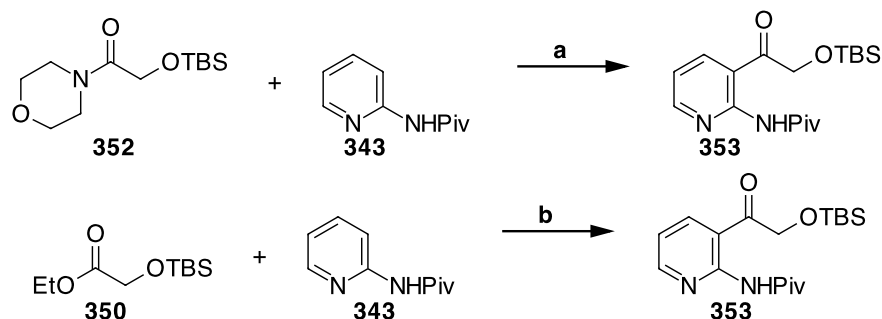


Scheme 4.11. *Reagents and conditions:* **a)** TBSCl, imidazole, DCM, RT, 16 h, 89%; **b)** KOH, EtOH, RT, 16 h, 67%; **c)** DCC, DMAP, morpholine, DCM, RT, 16 h, 38%.

The alcohol moiety of ethyl glycolate **349** was protected as its TBS ether **350** in very good yield, as illustrated is Scheme 4.11. However, the product proved difficult to purify. Flash column chromatography gave **350** with traces of the TBS silol, although this was volatile and was removed under high vacuum, affording pure **350**.¹⁹³

Hydrolysis of the silyl protected ester **350** to carboxylic acid **351** was achieved using potassium hydroxide in ethanol. Instead of acidifying the product with concentrated HCl,¹⁹⁴ saturated ammonium chloride and DCM were added, affording the carboxylic acid **351** in higher yield than had previously been reported.¹⁹³

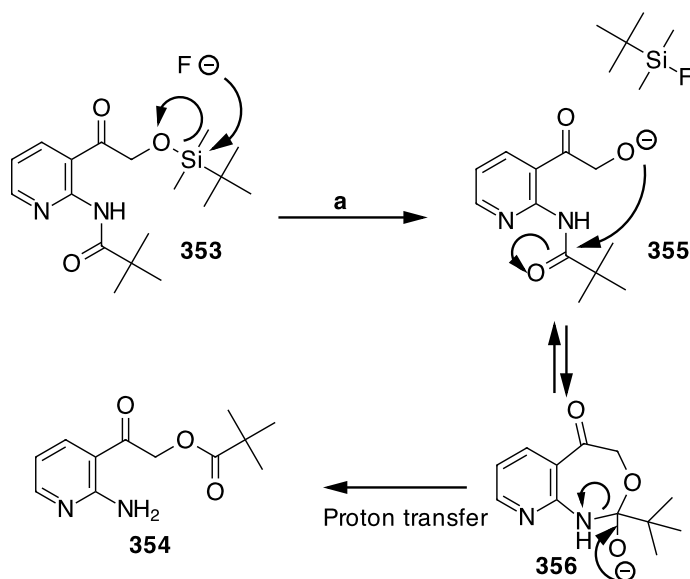
With carboxylic acid **351** in hand attention turned to the formation of morpholine amide **352**. This could be achieved, but in poor yield (38%), using DCC and DMAP. Nonetheless, sufficient material was prepared to progress.



Scheme 4.12. *Reagents and conditions: a) n -BuLi, THF, $-50\text{ }^{\circ}\text{C}$ to $0\text{ }^{\circ}\text{C}$, 1.5 h, then addition of morpholino-amide **352**, $-40\text{ }^{\circ}\text{C}$ for 1 h, 38%; b) n -BuLi, THF, $-50\text{ }^{\circ}\text{C}$ to $0\text{ }^{\circ}\text{C}$, 1.5 h, then addition of ethyl ester **350**, $-40\text{ }^{\circ}\text{C}$ for 1 h, 61%.*

With the morpholine amide **352** in hand a direct acylation between pyridine **343** and amide **352** was attempted, following the procedure used in Scheme 4.8. In the event the reaction worked to give the acylated product **353** in 38% yield.

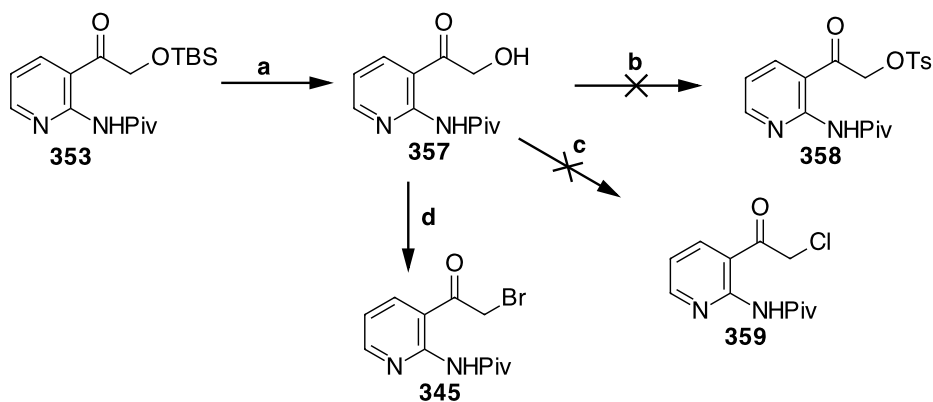
Due to the low yields for the ester hydrolysis and amide formation steps (Scheme 4.11) acylation of pyridine **343** was carried out directly with ethyl ester **350** (Scheme 4.12). This gave a superior yield compared to that with morpholine amide **352**.



Scheme 4.13. The reaction of TBAF with **353** leads to acyl migration. *Reagents and conditions: a) TBAF, THF, RT, 2 h, 32%.*

With ketone **353** in hand, removal of the TBS protecting group was explored using a fluoride anion source. TBAF in THF did not give the expected product although depletion of the starting material was almost instantaneous as monitored by TLC analysis. The TBAF solution turned the reaction solution black when added. Purification by flash column chromatography on silica gave **354** as the major product. The 2D HMBC spectrum showed that the pivaloyl group had migrated to the alcohol. A crosspeak between the CH₂ adjacent to the ketone and the carbonyl of the pivaloyl group proved the migration.

A proposed mechanism for the acyl migration involves intermediate alkoxide **355** as is illustrated in Scheme 4.13.

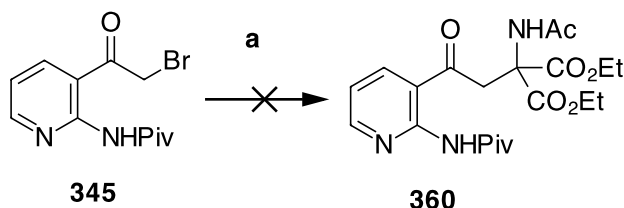


Scheme 4.14. Reagents and conditions: **a)** Acetyl chloride, MeOH, RT, 3 h, 57%; **b)** tosyl chloride, Et₃N, DCM, RT, 16 h; **c)** SOCl₂, DCM, RT, 8 h; **d)** PPh₃, CBr₄, DCM, exclusion of light, RT, 8 h, 32%.

Silyl ether deprotection of **353** was eventually achieved using a non-basic approach. A solution of acetyl chloride in dry methanol was used to selectively cleave the TBS ether, giving alcohol **357** in a moderate yield, as illustrated in Scheme 4.14.

It was now required to convert alcohol **357** into a good leaving group. Tosylation of **357** proved unsuccessful. The starting material was consumed, however, none of the desired product **358** could be recovered. Chlorination to generate **359** was also unsuccessful. However, the synthesis of alkyl bromide **345** was accomplished by an Appel reaction of **357** with CBr₄/PPh₃. The product **345** was isolated in a relatively low yield. In reactions of less than 250 mg of alcohol **357**, separation of

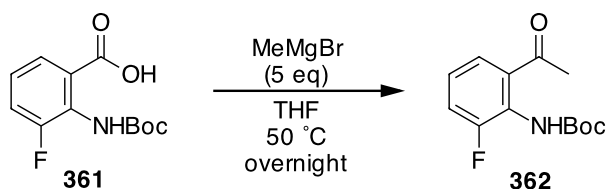
the alkyl bromide **345** and triphenyl phosphine oxide was achievable by column chromatography. However, on larger scales this proved difficult and the product was always contaminated with triphenylphosphine oxide. Attempts at improving the conversion using resin bound triphenylphosphine proved unsuccessful.



Scheme 4.15. Reagents and conditions: a) NaH, DEAM, DMF, 0 °C, 16 h.

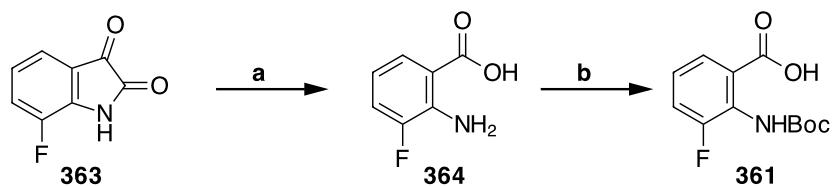
A substitution reaction of α -bromo-ketone **345** with the sodium salt of diethyl acetamidomalonate was unsuccessful and none of the desired product was obtained. At this point it was clear that the functionalised pyridine motif was interfering with the desired reactivity. This synthesis was not progressed further.

4.5 Attempted synthesis of 3-fluorokynurenine



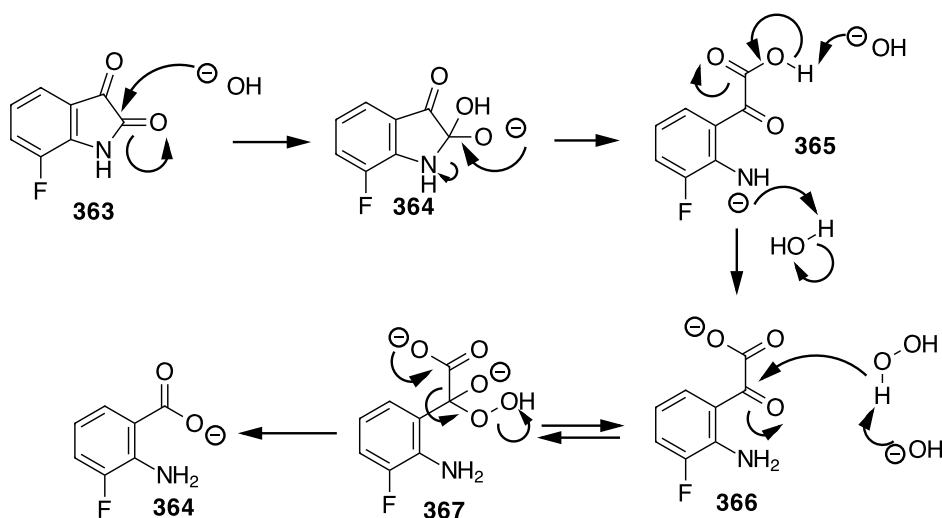
Scheme 4.16. Published route to the fluoro-ketone **370**.¹⁹⁵

The reaction of anthranilic acid **361** with methylmagnesium bromide in THF to give the ketone **362** was reported in 2001.¹⁹⁵ Normally the reaction of a carboxylic acid with a Grignard reagent would provide the tertiary alcohol and perhaps low yields of the ketone. However, the high yield (80%) of ketone **362** made this an attractive reaction. It was envisaged that the methyl ketone **362** could then be converted to the corresponding α -bromo-ketone, an attractive intermediate for progressing to 3-fluoro-kynurenine **308**.



Scheme 4.17. Reagents and conditions: **a)** NaOH, H₂O₂, H₂O, 50 °C, 30 min, 55%; **b)** Boc₂O, NaOH, THF:H₂O 1:1, RT, 16 h, 65%.

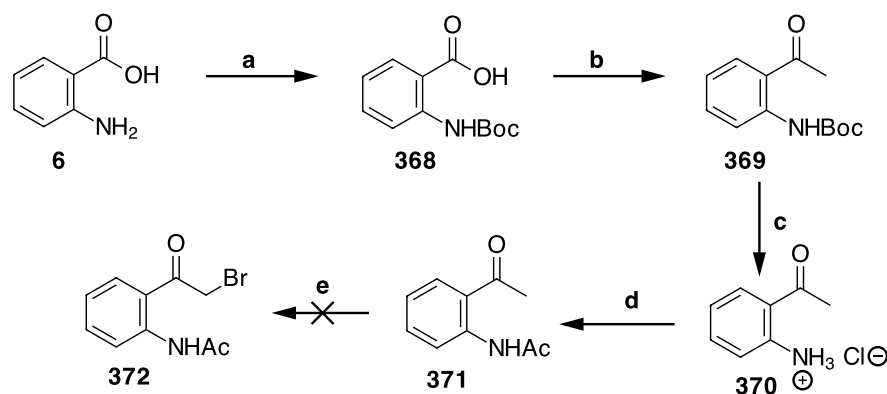
As a starting point for this synthesis an oxidative cleavage of 7-fluoroisatin **363** using hydrogen peroxide under basic conditions was used to give 3-fluoro-anthranilic acid **364** (Scheme 4.17).¹⁹⁶



Scheme 4.18. Proposed mechanism for the formation of 3-fluoro-anthranilic acid **372** from 7-fluoroisatin **371**.

A proposed mechanism for the reaction of hydrogen peroxide with 7-fluoroisatin **363** is illustrated in Scheme 4.18.

Boc protection of anthranilic acid **364** was not always reproducible, therefore the unsubstituted anthranilic acid **6** was explored in a model study for direct preparation of the desired brominated ketone **372**.



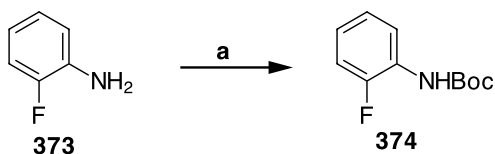
Scheme 4.19. Reagents and conditions: **a)** Boc_2O , NaOH , H_2O :1,4-dioxane 1:1, RT, 16 h, 51%; **b)** MeMgBr (5 eq), THF, 0 °C to RT, 16 h, 49%; **c)** HCl (4 M in 1,4-dioxan), Et_2O , RT, 1 h, 53%; **d)** Ac_2O , pyridine, RT, 16 h, 73%; **e)** Cu(II)Br , CHCl_3 , EtOAc , 80 °C, 16 h.

Boc protection of anthranilic acid **6** gave **368** in moderate yield.^{197, 198} With **368** in hand attention turned to the preparation of ketone **369** using the original conditions. These conditions worked well giving ketone **369** in 49% yield, higher than the previously reported.¹⁹⁵

The Boc protecting group was removed under acidic conditions to generate amine hydrochloride **370** as illustrated in Scheme 4.19.¹⁹⁹ The amine was then protected as its acetamide **371**. This exchange of protecting groups was carried out because the acetamide is more stable than the Boc protecting group under the acidic conditions required for the bromination reaction.^{200, 201}

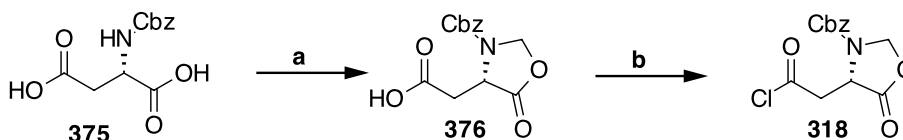
Bromination of **371** was explored using Cu(II)Br_2 in chloroform and ethyl acetate. This reaction did not work and TLC analysis indicated that very little reaction had occurred and only starting material was returned.

As bromination of **371** proved difficult, it is unlikely that 3-fluorokynurenine could be synthesised *via* this route. At this point, modification of the route used in the preparation of 5-fluorokynurenine **337** (Scheme 4.6) looked attractive for the synthesis of 3-fluorokynurenine **308**.



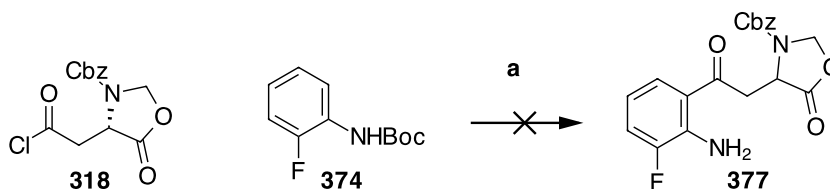
Scheme 4.20. Reagents and conditions: **a**) Boc_2O , 80°C , 2 h, 56%.

Protection of aniline **373** was achieved using the method developed by Thomas *et al.*²⁰¹ to give the Boc protected aniline **374** in moderate yield, as illustrated in Scheme 4.20.



Scheme 4.21. Reagents and conditions: **a**) Paraformaldehyde, *p*-TSA, toluene, 120°C , 5 h; **b**) oxalyl chloride, toluene, DMF, 120°C , 3 h, 71%.

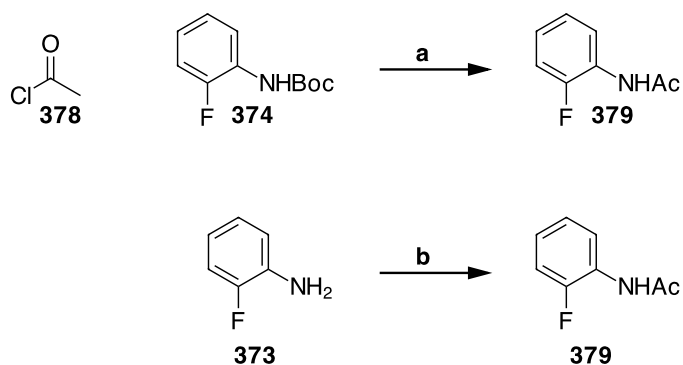
Cbz-protected aspartic acid **375** was converted to oxazolidine **376** to prevent racemisation of the amino acid, as illustrated in Scheme 4.21.²⁰² After purification the product was obtained as a colourless oil and then scratching of the oil initiated crystallisation to give a white solid. Carboxylic acid **376** was converted into the acid chloride **318** by oxalyl chloride in a similar yield to that previously reported.^{184, 203, 204} The acid chloride was then used without any further purification in the Friedel-Crafts acylation.



Scheme 4.22. Reagents and conditions: **a**) $\text{BF}_3 \cdot \text{Et}_2\text{O}$, DCM, RT, 16 h.

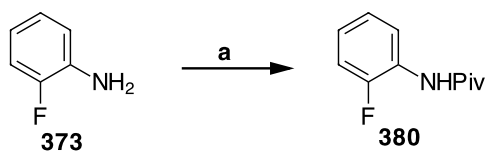
A Friedel-Crafts acylation was carried out, as illustrated in Scheme 4.22.¹⁸⁴ However, this reaction provided little of the desired product **377**. ^1H NMR spectroscopy showed multiple products and although mass spectrometry gave a peak, which corresponded to the expected molecular mass, m/z 373, however, it was not clear whether acylation had occurred on the amine or the aromatic ring. In

the reported synthesis of 5-fluorokynurenine the Boc protecting group was removed in the Friedel-Crafts acylation step and it was expected that the Boc group would also be removed under the reaction conditions. A model investigation using acetyl chloride was undertaken to explore whether electrophilic aromatic substitution could occur. Under the reported Friedel-Crafts acylation conditions the only product obtained was acetamide **379**, indicating that the Boc protecting group is readily cleaved under the conditions and formation of the acetamide **379** can then occur.



Scheme 4.23. Reagents and conditions: **a**) $\text{BF}_3 \cdot \text{Et}_2\text{O}$, DCM, RT, 16 h; **b**) Ac_2O , Et_3N , DCM, RT, 16 h, 54%.

To confirm that acetamide **379** had formed in the Friedel-Crafts acylation an authentic sample of acetamide **379** was synthesised from 2-fluoroaniline **373**, as illustrated in Scheme 4.23. The ^1H and ^{13}C NMR spectra were identical to that obtained from the Friedel-Crafts acylation with acetyl chloride.



Scheme 4.24. Reagents and conditions: **a**) Et_3N , trimethylacetyl chloride, DCM, 0°C to RT, 16 h, quant.

An alternative amine protecting group that is stable to BF_3 was desired. This led to the use of the pivaloyl protecting group. Aniline **373** was protected using trimethylacetyl chloride under basic conditions, to give amide **380** in very good yield, as illustrated in Scheme 4.24.



156

Chapter 5

Experimental

5.1 General Considerations

All chemicals and solvents were purchased from Sigma Aldrich UK, Acros Organics UK, Alfa Aesar UK, Fisher Scientific UK, Fluorochem UK and VWR UK. These were used without further purification unless otherwise specified.

All air and moisture sensitive reactions were performed under an inert argon atmosphere in flame-dried apparatus. Anhydrous reagents were handled under argon using standard techniques.

Dry DCM, toluene, diethyl ether and THF were obtained from an mBraun MB SPS-800 solvent purification system by passage of the solvent through a drying column and dispensing under an argon atmosphere. Methanol was distilled from calcium hydride in a recycling still under argon. Anhydrous DMF was purchased from Merck UK

Hydrogenations were carried out using an autoclave with a hydrogen pressure of 30 bar.

Thin layer chromatography (TLC) analyses was run on glass plated 0.2 mm thick silica gel 60 F₂₅₄ plates (Merck). They were visualised under a 254 nm ultraviolet lamp and/ or by treatment with alkaline potassium permanganate dip or an ethanolic anisaldehyde dip, followed by thermal development with a heat gun. Column chromatography was conducted using Merck Geduran Si-60 silica-gel (40-63 µm particle size) under a positive pressure of compressed air. Petroleum ether refers to the fraction with boiling point 40-60 °C.

Melting points were determined using Griffin Melting Point Apparatus. Values are reported to the nearest 1 °C and are uncorrected.

Infrared spectra were recorded using a Perkin-Elmer Spectrum GX FT-IR spectrometer. Samples were analysed as nujol mulls or thin films on NaCl plates. Absorption maxima are reported in wavenumbers (cm^{-1})

Nuclear magnetic resonance (NMR) spectra were recorded on Bruker Avance 300, Bruker Avance II 400, Bruker Avance 500 and Bruker Avance III 500 instruments. ^1H NMR spectra were recorded at 300, 400 and 500 MHz. ^{13}C NMR spectra were recorded at 75, 100 and 125 MHz. ^{19}F NMR spectrum were recorded at 282, 376 and 470 MHz. ^{31}P NMR spectrum were recorded at 121, 162 and 202 MHz. Chemical shifts were recorded as δ values in parts per million (ppm). The spectra were internally referenced to the residual solvent peaks in the ^1H and ^{13}C NMR spectra. Spectra were obtained using CDCl_3 , D_6 -DMSO, CD_3OD as solvents. ^1H NMR data are reported as following: chemical shift (δ), relative integral, multiplicity (defined as: s = singlet, d = doublet, dd = doublet of doublets, ddd = doublet of doublet of doublet, dddd = doublet of doublet of doublet of doublet, dt = doublet of triplets, ddt = doublet of doublet of triplets, t = triplets, q = quartet, quin = quintet), coupling constant(s) J (Hz), assignment. Identical coupling constants were averaged and are reported to the nearest 0.1 Hz. The assignment of signals observed in NMR spectra was assisted by conducting homonuclear (^1H - ^1H) correlation spectroscopy (COSY), heteronuclear (^1H - ^{13}C) single quantum correlation spectroscopy (HSQC), heteronuclear (^1H - ^{13}C) multiple bond correlation spectroscopy (HMBC) and Nuclear Overhauser effect spectroscopy (NOESY).

Electrospray mass spectrometry was performed on a Thermo Fisher exactive orbitrap mass spectrometer or on a Waters micromass, LCT to Time of Flight mass spectrometer, coupled to a Waters 2975 HPLC using methanol, acetonitrile and water as solvents. Chemical ionisation was performed on a Waters micromass GCT Time of Flight mass spectrometer. m/z values are reported in Daltons and followed by their percentage abundance in parenthesis.

Optical rotations were measured using a Perkin-Elmer model 341 polarimeter, referenced to the sodium D line (589 nm) at 20 °C. Measurements were made in spectroscopic grade solvents specified at the concentration (*c*, g/100 mL) indicated. The measurements were made using a cell with a path length of 1 dm. Specific rotations are reported in the implied units of 10⁻¹ deg cm² g⁻¹.

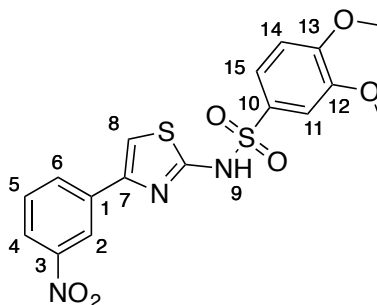
Freeze drying was carried out using a Christ Alpha 1-2LD Plus freeze dryer equipped with an Edwards RV3 rotary-vane oil pump.

Room temperature varied between 19-25 °C. "Removed under reduced pressure" refers to the use of a rotary evaporator attached to a diaphragm pump, with a water bath temperature of 40 °C.

HPLC analysis was performed on a Varian Prostar system consisting of a Varian Prostar Auto Sampler 400, Varian Prostar 240 solvent delivery system and a Varian Prostar UV-Vis 325 module. Compound elution was monitored at 254 nm. A Phenomenex kingsorb 3μ C18 (150 mm × 4.6 mm, 3 μM) column was used for analysis. Solvents used were 1% formic acid in water and 1% formic acid in methanol. A linear gradient from 50:50 water:methanol to 0:100 water:methanol over 35 min was used. After each run the column was equilibrated for 15 min. The flow rate was set at 1 mL/min.

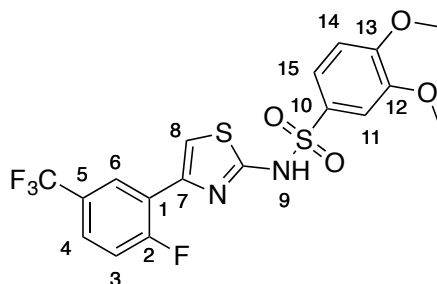
5.2 Characterisation

3,4-Dimethoxy-*N*-(4-(3-nitrophenyl)thiazol-2-yl)benzenesulfonamide **93** ⁶⁷



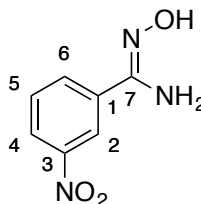
4-(3-Nitrophenyl)thiazol-2-amine (275 mg, 1.2 mmol), 3,4-dimethoxybenzene sulfonyl chloride (353 mg, 1.49 mmol) and pyridine (485 μ l, 6 mmol) were added to a flask containing 4 Å molecular sieves. DCM (2 mL) was added and the mixture was stirred for 16 h. The mixture was filtered and the filtrate was concentrated under reduced pressure. The residue was purified by column chromatography (20% ethyl acetate/petroleum ether to 40% ethyl acetate/petroleum ether) to give the product **93** as a yellow solid (120 mg, 24%): m.p. 95-100 °C (Lit.⁶⁷ 185 °C); δ_{H} (300 MHz, CDCl_3), 8.21-8.18 (1H, m, 2-H), 8.01 (1H, ddd, J = 8.2, 2.2, 1.0 Hz, 4-H), 7.75 (1H, ddd, J = 7.8, 1.8, 1.0 Hz, 6-H), 7.57 (1H, d, J = 8.6, 2.2 Hz, 15-H), 7.47 (1H, d, J = 2.2 Hz, 11-H), 7.45-7.39 (1H, m, 5-H), 6.84 (1H, s, 8-H), 6.81 (1H, d, J = 8.6 Hz, 14-H), 3.82 (3H, s, OMe), 3.81 (3H, s, OMe), 1.98 (1H, s, NH).

N-(4-(2-fluoro-5-(trifluoromethyl)phenyl)thiazol-2-yl)-3,4-dimethoxybenzenesulfonamide **135**⁶⁷



4-(2-Fluoro-5-(trifluoromethyl)phenyl)thiazol-2-amine (77 mg, 0.29 mmol), 3,4-dimethoxybenzene-1-sulfonyl chloride (104 mg, 0.44 mmol) and pyridine (111 μ l, 1.47 mmol) were added to a flask containing 4 Å molecular sieves. DCM (2 mL) was added. After 16 h the mixture was filtered and the filtrate was concentrated under reduce pressure. The residue was purified by column chromatography on silica (20% ethyl acetate/ petroleum ether to 30% ethyl acetate/ petroleum ether) to give the product **135** as a white solid (78 mg, 58%): m.p. 78-80 °C (Lit.⁶⁷ 126-128 °C); δ_{H} (300 MHz, CDCl_3) 7.71 (1H, dd, J = 6.7, 1.7 Hz, 4-H), 7.58 (1H, dd, J = 8.5, 2.1 Hz, 15-H), 7.47 (1H, d, J = 2.1 Hz, 11-H), 7.46-7.39 (1H, m, 6-H), 7.13-7.05 (1H, m, 3-H), 6.96 (1H, d, J = 1.1 Hz, 8-H), 6.82 (1H, d, J = 8.5 Hz, 14-H), 3.86 (6H, s, OMe); m/z (ES^+) 460.73 ($[\text{M}+\text{Na}]^+$, 100%).

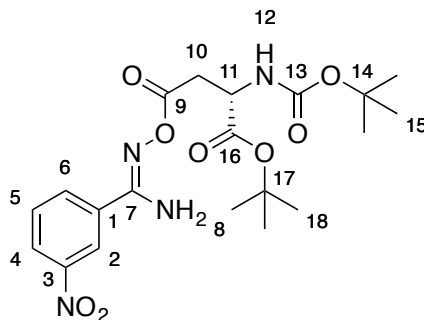
N-Hydroxy-3-nitrobenzimidamide **140**²⁰⁵



Hydroxylamine hydrochloride (5.87 g, 91.1 mmol) and anhydrous potassium carbonate (12.8 g, 91.1 mmol) were added to a solution of 3-nitrobenzonitrile (10 g, 67.5 mmol) in methanol (200 mL). The mixture was heated under reflux for 2 h then left to stir at room temperature for 16 h. The mixture was filtered and the

filtrate was concentrated under reduced pressure to yield a yellow solid, which was recrystallised from toluene to give the product **140** as yellow crystals (10.31 g, 84%): m.p. 178-182 °C (Lit.²⁰⁵ 180-182 °C); $\nu_{\text{max}}/\text{cm}^{-1}$ (nujol) 3498, 3400, 1666, 1598, 1535, 1147, 1089, 949; δ_{H} (300 MHz, D₆-DMSO) 9.96 (1H, br s, OH), 8.50 (1H, ddd, J = 2.3, 1.7, 0.4 Hz, 2-H), 8.21 (1H, ddd, J = 8.2, 2.3, 1.0 Hz, 4-H), 8.11 (1H, ddd, J = 7.9, 1.7, 1.0 Hz, 6-H), 7.67 (1H, ddd, J = 8.2, 7.9, 0.4 Hz, 5-H), 6.09 (2H, br s, NH₂); δ_{C} (75 MHz, D₆-DMSO) 149.9 (C-3), 148.6 (C-7), 135.76 (C-1), 132.4 (C-6), 130.6 (C-5), 124.3 (C-4), 120.8 (C-2); HRMS m/z (ES⁺) 182.0560 ([M+H]⁺, 100%) C₇H₈O₃N₃ requires 182.0560.

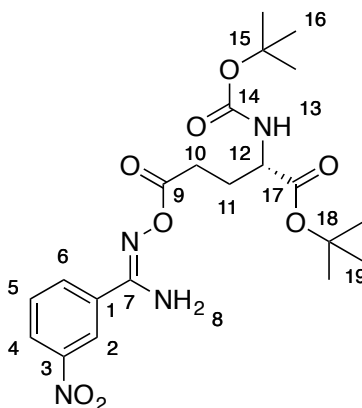
(*S*)-*tert*-Butyl-4-(((amino(3-nitrophenyl)methylene)amino)oxy)-2-((*tert*-butoxycarbonyl)amino)-4-oxobutanoate **144**



(*S*)-4-(*tert*-Butoxy)-3-((*tert*-butoxycarbonyl)amino)-4-oxobutanoic acid (267 mg, 0.92 mmol), DCC (190 mg, 0.92 mmol) and DMAP (51 mg, 0.41 mmol) were added to a solution of amidoxime **140** (150 mg, 0.84 mmol) in DCM (20 mL). After stirring for 16 h the solid was filtered off. The filtrate was concentrated under reduced pressure to give a yellow oil. The product was purified by column chromatography on silica (20% ethyl acetate/petroleum ether to 35% ethyl acetate/petroleum ether) to give the product **144** as a white solid (334 mg, 88%): m.p. 136-140 °C; $\nu_{\text{max}}/\text{cm}^{-1}$ (nujol) 3502 (NH), 3394 (NH), 3350 (NH), 1737 (C=O), 1725 (C=O), 1695 (C=N); δ_{H} (300 MHz, CDCl₃) 8.48-8.44 (1H, m, 2-H), 8.36 (1H, ddd, J = 8.0, 2.0, 1.1 Hz, 4-H), 8.13 (1H, ddd, J = 8.0, 2.0, 1.1 Hz, 6-H), 7.68-7.62 (1H, m, 5-H), 5.57-5.43 (3H, m, 8,12-H), 4.67-4.60 (1H, m, 11-H), 3.11 (2H, d, J = 5.1 Hz, 10-H), 1.51 (9H, s,

(CH₃)₃), 1.47 (9H, s, (CH₃)₃); δ_C (75 MHz, CDCl₃) 207 (C-16), 171 (C-9), 155 (C-13), 149 (C-3), 133 (C-5), 130 (C-6), 127 (C-1), 126 (C-4), 122 (C-2), 83.3 (C(CH₃)₃), 80.4 (C(CH₃)₃), 51 (C-11), 37 (C-10), 28 (2 \times ^tBu); HRMS m/z (ES⁺) 475.1814 ([M+Na]⁺, 100%) C₂₀H₂₈N₄O₈Na requires 475.1805.

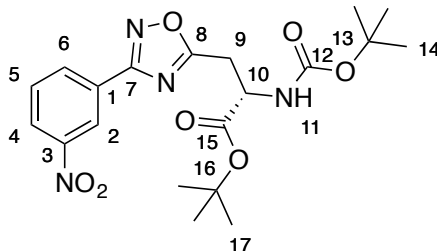
(S)-*tert*-Butyl-5-(((amino(3-nitrophenyl)methylene)amino)oxy)-2-((*tert*-butoxycarbonyl)amino)-5-oxopentanoate **146**



5-(*tert*-Butoxy)-4-((*tert*-butoxycarbonyl)amino)-5-oxopentanoic acid (919 mg, 3.03 mmol), DCC (625 mg, 3.03 mmol) and DMAP (169 mg, 1.38 mmol) were added to a solution of amidoxime **140** (500 mg, 2.76 mmol) in DCM (20 mL). After stirring for 16 h the mixture was filtered and the filtrate was concentrated under reduced pressure. The product was purified by column chromatography on silica (30% ethyl acetate/petroleum ether to 50 % ethyl acetate/petroleum ether) to give the product **146** as a yellow solid (739 mg, 57%): m.p. 112-114 °C; $\nu_{\max}/\text{cm}^{-1}$ (nujol) 3461 (NH), 3397 (NH), 3359 (NH), 1757 (C=O), 1731 (C=O), 1713 (C=N), 1699 (C=O); δ_H (300 MHz, CDCl₃) 8.49-8.46 (1H, m, 2-H), 8.27 (1H, ddd, J = 8.2, 2, 1.1 Hz, 4-H), 8.07-8.05 (1H, m, 6-H), 7.58-7.53 (1H, m, 5-H), 5.56 (2H, br s, 8-NH₂), 5.12 (1H, d, J = 8.4 Hz, 13-H), 4.28-4.18 (1H, m, 12-H), 2.58-2.48 (2H, m, 12-H), 2.26-2.14 (1H, m, 11-H), 1.95-1.82 (1H, m, 11-H), 1.41 (9H, s, (CH₃)₃), 1.39 (9H, s, (CH₃)₃); δ_C (75 MHz, CDCl₃) 171.3 (C-17), 170.5 (C-9), 155.7 (C-14), 148.1 (C-3), 133.1 (C-1), 133.0 (C-6), 129.7 (C-5), 125.4 (C-4), 121.9 (C-2), 82.8 (C(CH₃)₃), 80.1 (C(CH₃)₃), 53.4 (C-12), 29.3 (C-10), 28.5 (C-11), 28.3 (^tBu), 28.0 (^tBu); m/z 489.1948

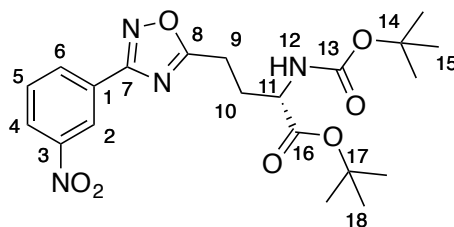
($[M+Na]^+$, 37%), 423.2230 ($[M+H]^+$, 100), 367.1605 (38), 311.0980 (93); HRMS m/z (ES^+) 489.1948 ($M+Na^+$, 37%) $C_{21}H_{30}O_8N_4Na$ requires 489.1961

(*S*)-*tert*-Butyl-2-(*tert*-butoxycarbonylamino)-3-(3-(3-nitrophenyl)-1,2,4-oxadiazol-5-yl)propanoate **147**



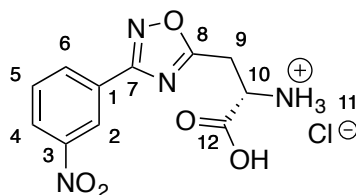
TBAF (47 μ l, 1 M in THF, 0.04 mmol) was added to a solution of *O*-acyl amidoxime **144** (215 mg, 0.48 mol) in THF (5 mL) and the solution was stirred for 16 h. When TLC analysis indicated the consumption of all the starting material, ethyl acetate (25 mL) was added. The solvent was removed under reduced pressure and the product was purified by column chromatography on silica (10% ethyl acetate/petroleum ether) to give the product as a white solid (170 mg, 83%): m.p. 86-90 $^{\circ}C$; ν_{max}/cm^{-1} (nujol) 3390 (NH), 1728, 1691; δ_H (300 MHz, $CDCl_3$) 8.99-8.97 (1H, m, 2-H), 8.45 (1H, ddd, J = 8.0, 1.9, 1.1 Hz, 4-H), 8.40 (1H, ddd, J = 8.0, 1.9, 1.1 Hz, 6-H), 7.75-7.70 (1H, m, 5-H), 5.25 (1H, d, J = 5.8 Hz, 11-NH), 4.4 (1H, q, J = 5.8 Hz, 10-H), 3.20-3.00 (2H, m, 9-H), 1.54 (9H, s, $(CH_3)_3$), 1.48 (9H, s, $(CH_3)_3$); δ_C (75 MHz, $CDCl_3$) 177.3 (C-15), 168.9 (C-8), 166.7 (C-7), 155.1 (C-12), 148.6 (C-3), 133.0 (C-6), 130.1 (C-5), 128.5 (C-1), 125.8 (C-4), 122.5 (C-2), 83.3 ($C(CH_3)_3$), 80.4 ($C(CH_3)_3$), 51.7 (C-10), 30.0 (C-9), 28.3 (tBu), 27.9(tBu); HRMS m/z (ES^+) 457.1695 ($[M+Na]^+$, 100%) $C_{20}H_{26}N_4O_7Na$ requires 457.1699.

(S)-*tert*-Butyl 2-((*tert*-butoxycarbonyl)amino)-4-(3-(3-nitrophenyl)-1,2,4-oxadiazol-5-yl)butanoate **148**



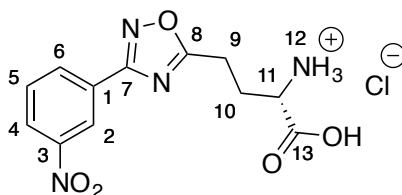
TBAF (45 μ L, 1M in THF, 0.045 mmol) was added to a solution of *O*-acyl amidoxime **146** (208 mg, 0.45 mmol) in dry THF (5 mL). The mixture was allowed to stir for 16 h. When TLC analysis indicated the consumption of the starting material, ethyl acetate (25 mL) was added. The solvent was removed under reduced pressure. The product was purified by column chromatography on silica (20% ethyl acetate/petroleum ether to 30% ethyl acetate/petroleum ether) to give the product **148** as a yellow solid (120 mg, 60%): m.p. 126-130 $^{\circ}$ C; $\nu_{\text{max}}/\text{cm}^{-1}$ (nujol) 3404 (NH), 3383 (NH), 1735 (C=O), 1729 (C=O), 1697 (C=N); δ_{H} (300 MHz, CDCl_3) 8.88-8.85 (1H, m, 2-H), 8.34 (1H, ddd, J = 8.0, 1.9, 1.1 Hz, 4-H), 8.29 (1H, ddd, J = 8.0, 1.9, 1.1 Hz, 6-H), 7.65-7.58 (1H, m, 5-H), 5.15 (1H, d, J = 7.2 Hz, 12-NH), 4.29 (1H, q, J = 6.2 Hz, 11-H), 3.09-2.89 (2H, m, 9-H), 2.45-2.32 (1H, m, 10-H), 2.19-2.05 (1H, m, 10-H), 1.41 (9H, s, $(\text{CH}_3)_3$), 1.37 (9H, s, $(\text{CH}_3)_3$); δ_{C} (75 MHz, CDCl_3) 179.8 (C-16), 170.8 (C-8), 166.7 (C-7), 155.4 (C-13), 148.7 (C-3), 133.0 (C-6), 130 (C-5), 128.7 (C-1), 125.6 (C-4), 122.5 (C-2), 82.8 ($\text{C}(\text{CH}_3)_3$), 80.1 ($\text{C}(\text{CH}_3)_3$), 53.3 (C-11), 29.8 (C-9), 28.3 (^tBu), 28.1 (^tBu), 23.0 (C-10); HRMS m/z (ES^+) 471.1837 ($[\text{M}+\text{Na}]^+$, 100%) $\text{C}_{21}\text{H}_{28}\text{O}_7\text{N}_4\text{Na}$ requires 471.1851.

(S)-2-Amino-3-(3-(3-nitrophenyl)-1,2,4-oxadiazol-5-yl)propanoic acid **120**



Triethylsilane (270 μ l, 1.7 mmol) was added to a solution of 1,2,4-oxadiazole-**147** (291 mg, 0.66 mmol) in trifluoroacetic acid (10 mL). The solution was stirred for 16 h. The solvent was removed under reduced pressure and the solid was redissolved in HCl solution (1M, 25 mL). The solvent was removed under reduced pressure to yield an off-white solid, which was recrystallised from water and ethanol to give the product as an off-white solid as the hydrochloride salt **120** (104 mg, 50%): m.p. 210-212 $^{\circ}$ C; $\nu_{\text{max}}/\text{cm}^{-1}$ (nujol) 3359 (NH), 3182 (OH), 1698 (C=N); δ_{H} (400 MHz, D_6 -DMSO) 8.72-8.71 (1H, m, 2-H), 8.45-8.44 (1H, m, 4-H), 8.43-8.42 (1H, m, 6-H), 7.90-7.86 (1H, m, 5-H), 3.77 (1H, dd, J = 7.9, 5.9, 10-H), 3.54 (1H, dd, J = 16.1, 5.9, 9-H), 3.29 (1H, dd, J = 16.1, 7.9, 9'-H); δ_{C} (75 MHz, D_6 -DMSO), 178.6 (C-12), 167.5 (C-8), 165.9 (C-7), 148.3 (C-3), 133.0 (C-6), 131.2 (C-5), 127.8 (C-1), 126.1 (C-4), 121.5 (C-2), 51.6 (C-9), 29.3 (C-10); m/z (ES^+) 301 ($[\text{M}+\text{Na}]^+$, 100%), (ES^-) 277 ($[\text{M}-\text{H}]^-$, 53%), 260 (100).

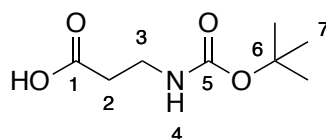
(S)-2-Amino-4-(3-(3-nitrophenyl)-1,2,4-oxadiazol-5-yl)butanoic acid **121**



Triethylsilane (515 μ l, 3.22 mmol) was added to a solution of 1,2,4-oxadiazole **148** (579 mg, 1.3 mmol) in trifluoroacetic acid (5 mL) and was stirred for 16 h. The solvent was removed under reduced pressure and the solid was redissolved in 1M HCl (25 mL) and the solvent was removed under reduced pressure. The product was purified by recrystallisation from water and ethanol to give the product **121** as

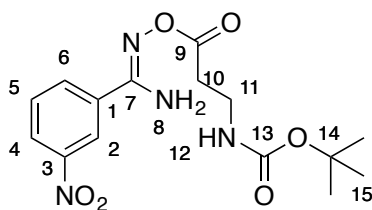
an off-white solid (78 mg, 18%): m.p. 207-209 °C (decomp.); $\nu_{\max}/\text{cm}^{-1}$ (nujol) 3399 (NH), 1719 (C=N); δ_{H} (400 MHz, D₆-DMSO) 8.70-8.69 (1H, m, 2-H), 8.46-8.42 (2H, m, 4,6-H), 7.89 (1H, dd, J = 8.2, 7.9 Hz, 5-H), 3.22-3.10 (2H, m, 9-H), 2.24-2.22 (2H, m, 10-H), 1.98-1.97 (1H, m, 11-H); δ_{C} (125 MHz, D₆-DMSO) 180.5 (C-13), 168.9 (C-8), 166.0 (C-7), 148.2 (C-3), 133.0 (C-6), 131.2 (C-5), 127.7 (C-1), 126.0 (C-4), 121.4 (C-3), 52.8 (C-11), 27.6 (CH₂), 22.8 (CH₂); m/z (ES⁺) 315 ([M+Na]⁺, 100%), 292.95 ([M+H]⁺, 65%), (ES⁻) 291 ([M-H]⁻, 100%).

3-((*tert*-butoxycarbonyl)amino)propanoic acid **150** ^{141, 206}



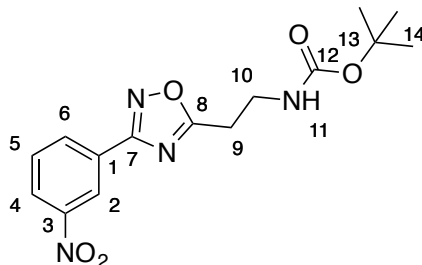
β -Alanine (2.0 g, 22.6 mmol) was added to a solution of sodium hydroxide (992 mg, 24.8 mmol) in water and 1,4-dioxane (1:1 50 mL). The mixture was cooled to 0 °C for 10 min. Di-*tert*-butyl dicarbonate (5.5 g, 24.8 mmol) was added in small portions. The temperature was kept at 0 °C for 20 min with stirring and allowed to warm to room temperature overnight. The solvent was removed under reduced pressure and water (50 mL) was added. The reaction mixture was washed with diethyl ether (3 \times 30 mL). The pH was adjusted to pH4 using citric acid. The product was extracted with ethyl acetate (3 \times 50 mL). The organic layer was dried with magnesium sulfate and the solvent was removed under reduced pressure to yield the product **150** as a white solid (3.54 g, 82%): m.p. 70-72 °C (Lit. ¹⁴¹ 71-72 °C); $\nu_{\max}/\text{cm}^{-1}$ (nujol) 3441, 1714, 1513, 1249, 1238, 1167, 979; δ_{H} (300 MHz, D₆-DMSO) 12.16 (1H, s, 4-H), 3.10 (2H, td, J = 7.1, 5.8 Hz, 3-H), 2.33 (2H, t, J = 7.1 Hz, 2-H), 1.35 (9H, s, 7-H); δ_{C} (75 MHz, D₆-DMSO) 173.7 (C-1), 156.3 (C-5), 78.5 (C-6), 37.0 (C-3), 35.1 (C-2), 29.1 (C-7); HRMS m/z (ES⁺) 212.0890 ([M+Na]⁺, 100%) C₈H₁₅O₄NNa requires 212.0899

tert-Butyl(3-(((amino(3-nitrophenyl)methylene)amino)oxy)-3-oxopropyl)carbamate
151



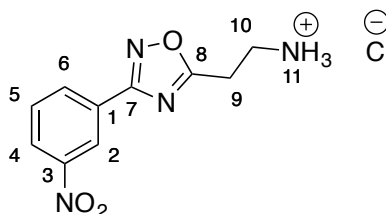
Carboxylic acid **150** (573 mg, 3.03 mmol), DCC (625 mg, 3.03 mmol) and DMAP (169 mg, 1.38 mmol) were added to a solution of amidoxime **140** (500 mg, 2.76 mmol) in DCM (20 mL). The mixture was stirred overnight. The mixture was filtered and the filtrate was concentrated under reduced pressure. The product was purified by column chromatography on silica (30% ethyl acetate/petroleum ether to 70% ethyl acetate/petroleum ether) to give the product **151** as a white solid (715 mg, 73%): m.p. 128-136 °C; $\nu_{\text{max}}/\text{cm}^{-1}$ (nujol) 3437 (NH), 3331 (NH), 1752, 1740; δ_{H} (300 MHz, CDCl_3) 8.47-8.45 (1H, m, 2-H), 8.28 (1H, ddd, $J = 8.0, 2.0, 1.1$ Hz, 6-H), 8.04 (1H, ddd, $J = 8.0, 2.0, 1.1$ Hz, 4-H), 7.59-7.54 (1H, m, 5-H), 5.31 (2H, br s, 8-NH₂), 4.97 (1H, s, 12-NH), 3.47 (2H, q, $J = 5.9$ Hz, 11-H), 2.68 (2H, t, $J = 5.9$ Hz, 10-H), 1.37 (9H, s, (CH₃)₃); δ_{C} (100 MHz, CDCl_3) 169.8 (C-9), 156.1 (C-13), 154.6 (C-7), 148.2 (C-3), 133.0 (C-1), 132.9 (C-6), 129.9 (C-5), 125.6 (C-4), 121.8 (C-2), 36.0 (C-11), 33.9 (C-10), 28.4 (C-15); HRMS m/z (ES⁺) 375.1276 ([M+Na]⁺, 100%) C₁₅H₂₀N₄O₆Na requires 375.1281.

tert-Butyl(2-(3-(3-nitrophenyl)-1,2,4-oxadiazol-5-yl)ethyl)carbamate **152**



TBAF (163 μ l, 1 M in THF, 0.16 mmol) was added to a solution of *O*-acyl amidoxime **151** (576 mg, 1.63 mmol) in dry THF (5 mL) and the reaction was stirred for 16 h. The mixture was poured into ethyl acetate (30 mL) and the solvent was removed under reduced pressure. The product was purified by column chromatography on silica (25% ethyl acetate/petroleum ether) to give the product **152** as a white solid (538 mg, 99%): m.p. 102-104 $^{\circ}$ C; $\nu_{\text{max}}/\text{cm}^{-1}$ (nujol) 3362, 1824, 1752, 1678, 1622, 1593, 1574, 1519, 1162, 1072, 978, 914, 870; δ_{H} (300 MHz, CDCl_3) 8.91-8.90 (1H, m, 2-H), 8.39 (1H, ddd, J = 8.0, 1.9, 1.1 Hz, 4-H), 8.34 (1H, ddd, J = 8.0, 1.9, 1.1 Hz, 6-H), 7.66-7.59 (1H, m, 5-H), 5.05-4.95 (1H, m, 11-NH), 3.66 (2H, q, J = 6.1 Hz, 10-H), 3.16 (2H, t, J = 6.1 Hz, 9-H), 2.14 (9H, s, $(\text{CH}_3)_3$); δ_{C} (75 MHz, CDCl_3) 167.1 (C-7), 165.6 (C-8), 156 (C-12), 149.0 (C-3), 133.4 (C-6), 130.5 (C-5), 129.0 (C-1), 126.2 (C-4), 123.0 (C-2), 77.6 (C-13) 37.7 (C-10), 28.8 (C-14), 28.1 (C-9); HRMS m/z (ES^+) 357.1171 ($[\text{M}+\text{Na}]^+$, 100) $\text{C}_{15}\text{H}_{18}\text{N}_4\text{O}_5\text{Na}$ requires 357.1175.

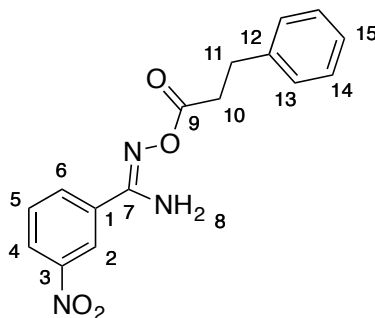
2-(3-(3-nitrophenyl)-1,2,4-oxadiazol-5-yl)ethanamine hydrochloride **122**



HCl in 1,4 dioxan (4M, 1.2 mL, 4.8 mmol) was added to a solution **152** (537 mg, 1.6 mmol) in DCM (5 mL) and the mixture was stirred for 16 h. The

solvent was removed under reduced pressure and the oil was titrated with diethyl ether to yield the product **122** as a white solid (338 mg, 78%): m.p. 184-190 °C; $\nu_{\text{max}}/\text{cm}^{-1}$ (nujol) 3423 (NH), 1715 (C=N); δ_{H} (300 MHz, CD₃OD) 8.92-8.90 (1H, m, 2-H), 8.49 (1H, ddd, J = 8.1, 2.0, 1.0 Hz, 4-H), 8.44 (1H, ddd, J = 8.1, 2.0, 1.0, 6-H), 7.86-7.79 (1H, m, 5-H), 3.60-3.53 (2H, m, 10-H), 3.49-3.43 (2H, m, 9-H); δ_{C} (75 MHz, CD₃OD) 179.1 (C-8), 168.6 (C-7), 150.5 (C-3), 134.5 (C-4), 132.2 (C-6), 130.0 (C-1), 127.4 (C-5), 123.6 (C-2), 37.8 (C-10), 26 (C-9); HRMS m/z (CI⁺) 235.0827 ([M+H]⁺, 37%) C₁₀H₁₁N₄O₃ requires 235.0831

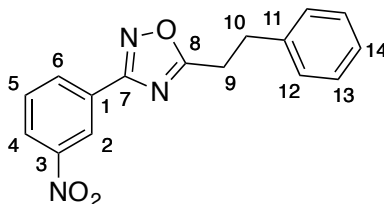
3-Nitro-*N'*-((3-phenylpropanoyl)oxy)benzimidamide **155**



3-Phenylpropanoic acid (455 mg, 3.03 mmol), DCC (625 mg, 3.03 mmol) and DMAP (169 mg, 1.38 mmol) were added to a solution of amidoxime **140** (500 mg, 2.76 mmol) in dry DCM (20 mL) and the mixture was stirred overnight. The mixture was filtered and the filtrate was concentrated under reduced pressure. The product was purified by column chromatography on silica (20% ethyl acetate/petroleum ether to 35% ethyl acetate/petroleum ether) to give the product **155** as a white solid (136 mg, 16%): m.p. 82-85 °C; $\nu_{\text{max}}/\text{cm}^{-1}$ (nujol) 3432, 3174, 1746, 1574, 1543, 1155; δ_{H} (300 MHz, CDCl₃) 8.43-8.40 (1H, m, 2-H), 8.26 (1H, J = 8.0, 2.0, 1.1 Hz, 6-H), 8.01 (1H, ddd, J = 8.0, 2.0, 1.1 Hz, 4-H), 7.58-7.51 (1H, m, 5-H), 7.29-7.20 (4H, m, 13,14-H), 7.18-7.13 (1H, m, 15-H), 4.89 (2H, br s, 8-NH₂), 3.01 (2H, t, J = 7.5 Hz, 11-H), 2.82-2.76 (2H, m, 10-H); δ_{C} (75 MHz, CDCl₃) 170.1 (C-9), 154.2 (C-8), 148.1 (C-3), 140.3 (C-12), 132.9 (C-6), 132.9 (C-1), 130.0 (C-5), 128.7 (C-14),

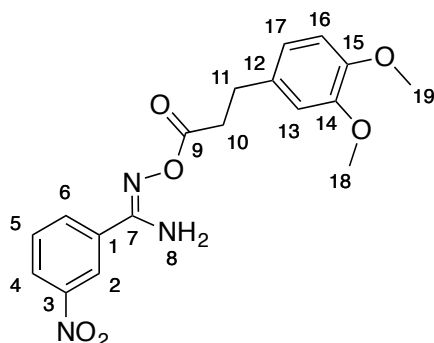
128.4 (C-13), 126.5 (C-15), 125.7 (C-4), 121.6 (C-2), 34.8 (C-10), 31.1 (C-11); HRMS m/z (ES⁻) 312.0985 ([M-H]⁻, 100%) C₁₆H₁₄N₃O₄ requires 312.0990.

3-(3-Nitrophenyl)-5-phenethyl-1,2,4-oxadiazole **156**



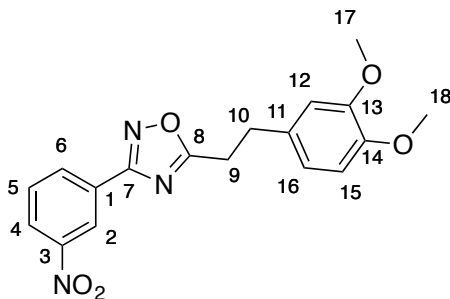
TBAF (61 μ l, 1M in THF, 0.06 mmol) was added to a solution of *O*-acyl amidoxime **155** (190 mg, 0.61 mmol) in THF (5 mL). The mixture was stirred for 16 h at room temperature. The mixture was then poured into ethyl acetate (25 mL) and the solvent was removed under reduced pressure. The product was purified by column chromatography on silica (10% ethyl acetate/petroleum ether) to give the product **156** as a yellow solid (169 mg, 94%): m.p. 51-53 °C; $\nu_{\max}/\text{cm}^{-1}$ (nujol) 1717 (C=N); δ_{H} (300 MHz, CDCl₃) 8.94 (1H, ddd, J = 2.3, 1.6, 0.5 Hz, 2-H), 8.41 (1H, ddd, J = 7.8, 1.6, 1.1 Hz, 4-H), 8.36 (1H, ddd, J = 8.3, 2.3, 1.1 Hz, 6-H), 7.69 (1H, ddd, J =8.3, 7.8, 0.5 Hz, 5-H), 7.33-7.29 (2H, m, 12-H), 7.28-7.26 (2H, m, 13-H), 7.26-7.23 (1H, m, 14-H), 3.34-3.27 (2H, m, 9-H), 3.26-3.17 (2H, m, 10-H); δ_{C} (75 MHz, CDCl₃) 179.9 (C-8), 166.7 (C-7), 148.7 (C-3), 139.2 (C-11), 133.0 (C-6), 130.0 (C-5), 128.8 (C-1), 128.7 (C-12), 128.3 (C-13), 126.9 (C-14), 125.7 (C-4), 122.6 (C-2), 32.6 (C-10), 28.5 (C-9); HRMS m/z (ES⁺) 318.0856 ([M+Na]⁺) C₁₆H₁₃N₃O₅Na requires 318.0855.

N'-((3-(3,4-Dimethoxyphenyl)propanoyl)oxy)-3-nitrobenzimidamide **158**



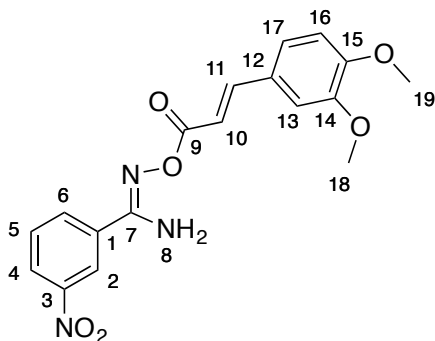
3-(3,4-dimethoxyphenyl)propanoic acid (636 mg, 3.03 mmol), DCC (625 mg, 3.03 mmol) and DMAP (340 mg, 2.76 mmol) were added to a solution of amidoxime **140** (500 mg, 2.76 mmol in DCM (20 mL). The mixture was stirred for 16 h. The mixture was filtered and the filtrate was concentrated under reduced pressure. The product was purified by column chromatography on silica (30% ethyl acetate/petroleum ether to 50% ethyl acetate/petroleum ether) to give the product **158** a yellow solid (322 mg, 31%): m.p. 102-106 °C; $\nu_{\text{max}}/\text{cm}^{-1}$ (nujol) 3486, 3326, 1739, 1619, 1575, 1546, 1258, 1137, 897; δ_{H} (300 MHz, CDCl_3) 8.50 (1H, ddd, J = 2.3, 1.4, 0.4 Hz, 2-H), 8.33 (1H, ddd, J = 8.2, 2.3, 1.7 Hz, 4-H), 8.08 (1H, ddd, J = 7.8, 1.7, 1.4 Hz, 6-H), 7.62 (1H, ddd, J = 8.2, 7.8, 0.4 Hz, 5-H), 6.82-6.79 (3H, m, 13,16,17-H), 5.01 (2H, br s, 8-NH₂), 3.88 (3H, s, OMe), 3.86 (3H, s, OMe), 3.02 (2H, t, J = 7.5 Hz, 10-H), 2.85-2.81 (2H, m, 11-H); δ_{C} (75 MHz, CDCl_3) 170.6 (C-9), 154.6 (C-7), 148.9 (C-OMe), 148.0 (C-OMe), 147.5 (C-3), 133.0 (C-12), 132.8 (C-6), 129.8 (C-5), 125.5 (C-4), 121.8 (C-2), 120.2 (C-17), 111.8 (C-16), 111.5 (C-13), 55.9 (OMe), 55.8 (OMe), 35.0 (C-11), 30.6 (C-10); HRMS m/z (ES^+) 396.1170 ($[\text{M}+\text{Na}]^+$, 100%) $\text{C}_{18}\text{H}_{19}\text{N}_3\text{O}_6\text{Na}$ requires 396.1172.

5-(3,4-Dimethoxyphenethyl)-3-(3-nitrophenyl)-1,2,4-oxadiazole **159**



TBAF (210 μ l, 1M in THF, 0.21 mmol) was added to a solution O-acyl amidoxime **158** (156 mg, 0.42 mmol) in THF (5 mL). The mixture was stirred for 16 h at room temperature. The mixture was poured into ethyl acetate (30 mL) and the solvent was removed under reduced pressure. The product was purified by column chromatography on silica (10% ethyl acetate/ petroleum ether) to give the product **159** as a yellow solid (81 mg, 54%): m.p. 74-76 $^{\circ}$ C; $\nu_{\text{max}}/\text{cm}^{-1}$ (nujol) 1715 (C=N); δ_{H} (300 MHz, CDCl_3) 8.88 (1H, ddd, J = 2.3, 1.6, 0.5 Hz, 2-H), 8.34 (1H, ddd, J = 7.8, 1.6, 1.1 Hz, 4-H), 8.29 (1H, ddd, J = 8.3, 2.3, 1.1 Hz, 6-H), 7.62 (1H, ddd, J = 8.3, 7.8, 0.5 Hz, 5-H), 6.75-6.72 (2H, m, 15,16-H), 6.70 (1H, s, 12-H), 3.80 (3H, s, OMe), 3.79 (3H, s, OMe), 3.25-3.18 (2H, m, 9-H), 3.07 (2H, ddd, J = 8.5, 6.8, 1.7 Hz, 10-H); δ_{C} (75 MHz, CDCl_3) 180.0 (C-8), 166.7 (C-7), 149.1 (C-OMe \times 2), 147.9 (C-3), 133.0 (C-6), 131.7 (C-11), 130.1 (C-5), 128.7 (C-1), 125.7 (C-4), 122.6 (C-2), 120.2 (C-16), 111.6 (C-12), 111.5 (C-15), 56.0 (OMe), 55.9 (OMe), 32.2 (C-10), 28.8 (C-9); HRMS m/z (ES^+) 378.1066 ($[\text{M}+\text{Na}]^+$, 100%) $\text{C}_{18}\text{H}_{17}\text{N}_3\text{O}_5\text{Na}$ requires 378.1066.

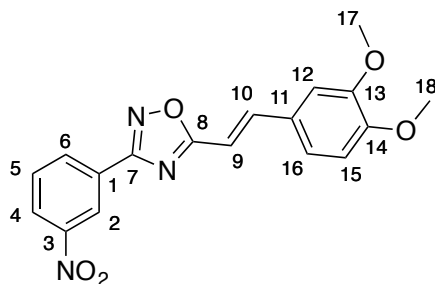
N'-(((*E*)-3-(3,4-dimethoxyphenyl)acryloyl)oxy)-3-nitrobenzimidamide **161**



3,4-Dimethoxycinnamic acid (630 mg, 3.03 mmol), DCC (625 mg, 3.03 mmol) and DMAP (340 mg, 2.76 mmol) were added to a solution of amidoxime **140** (500 mg, 2.76 mmol in dry DCM (20 mL). The mixture was stirred for 16 h. The mixture was then filtered and the filtrate was concentrated under reduced pressure. The product was purified by column chromatography on silica (30% ethyl acetate/petroleum ether to 60% ethyl acetate/petroleum ether) to give the product **161** as a yellow solid (503 mg, 49%): m.p. 146-148 °C; $\nu_{\text{max}}/\text{cm}^{-1}$ (nujol) cm^{-1} 3321 (NH), 1717 (C=N), 1634 (C=O); δ_{H} (300 MHz, CDCl_3) 8.58-8.54 (1H, m, 2-H), 8.30-8.26 (1H, m, 4-H), 8.17-8.11 (1H, m, 6-H), 7.76 (1H, d, J = 15.9 Hz, 11-H), 7.61-7.55 (1H, m, 5-H), 7.12 (1H, dd, J = 8.3, 1.9 Hz, 17-H), 7.07 (1H, d, J = 1.9 Hz, 13-H), 6.86 (1H, d, J = 8.3 Hz, 16-H), 6.45 (1H, d, J = 15.9 Hz, 10-H), 5.59 (2H, br s, 8-NH₂), 3.9 (3H, s, OCH₃), 3.89 (3H, s, OCH₃); δ_{C} (75 MHz, CDCl_3) 165.2 (C-8), 154.9 (C-7), 151.8 (C-OMe), 149.6 (C-OMe), 148.6 (C-3), 146.5 (C-10), 133.5 (C-1), 133.4 (C-6), 130.2 (C-5), 127.6 (C-12), 125.9 (C-4), 123.3 (C-17), 122.2 (C-2), 113.4 (C-9), 111.5 (C-16), 110.1 (C-13), 56.4 (OMe), 56.3 (OMe); HRMS m/z (ES⁺) 394.1008 ([M+Na]⁺, 42%) C₁₈H₁₇O₆N₃Na requires 394.1010.

N.B. On larger scales (1 g- 5 g) recrystallisation from ethanol/ water was used

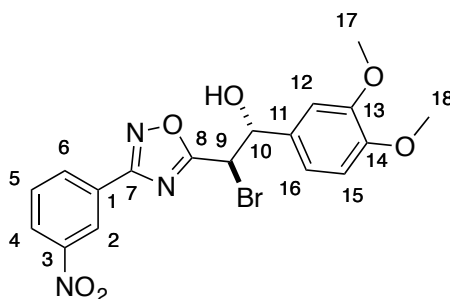
(*E*)-5-(3,4-Dimethoxystyryl)-3-(3-nitrophenyl)-1,2,4-oxadiazole **162**



TBAF (171 μ l, 1M in THF, 0.17 mmol) was added to a solution of *O*-acyl amidoxime **161** (635 mg, 1.71 mmol) in THF (10 mL). The mixture was stirred for 16 h at room temperature and then poured into ethyl acetate (25 mL). The solvent was removed under reduced pressure. The product was purified by column chromatography on silica (30% ethyl acetate/petroleum ether) to give the product **162** as an orange solid (270 mg, 45%): m.p. 148-151 $^{\circ}$ C; $\nu_{\text{max}}/\text{cm}^{-1}$ (nujol) 1717 (C=N), 974 (C=C); δ_{H} (300 MHz, CDCl_3) 8.80 (1H, dd, J = 2.3, 1.6 Hz, 2-H), 8.29 (1H, ddd, J = 7.7, 1.6, 1.1 Hz, 4-H), 8.23 (1H, ddd, J = 8.3, 2.3, 1.1 Hz, 6-H), 7.73 (1H, d, J = 16.2 Hz, 10-H), 7.62-7.54 (1H, m, 5-H), 7.09 (1H, dd, J = 8.5, 2.0 Hz, 16-H), 7.03 (1H, d, J = 2.0 Hz, 12-H), 6.81 (1H, d, J = 16.2 Hz, 9-H), 6.79 (1H, d, J = 8.5 Hz, 15-H), 3.81 (3H, s, OCH₃), 3.76 (3H, s, OCH₃); δ_{C} (100 MHz, D_6 -DMSO), 176.5 (C-8), 166.4 (C-7), 151.3 (OMe), 149.0 (OMe), 148.2 (C-3), 143.7 (C-10), 133.0 (C-6), 131.1 (C-5), 127.9 (C-1), 127.0 (C-11), 126.0 (C-4), 123.4 (C-9), 121.5 (C-2), 111.5 (C-15), 110.3 (C-12), 107.3 (C-16), 55.7 (OMe), 55.6 (OMe); HRMS m/z (ES^+) 376.0907 ($[\text{M}+\text{Na}]^+$, 100%) $\text{C}_{18}\text{H}_{15}\text{N}_3\text{O}_5\text{Na}$ requires 376.0909

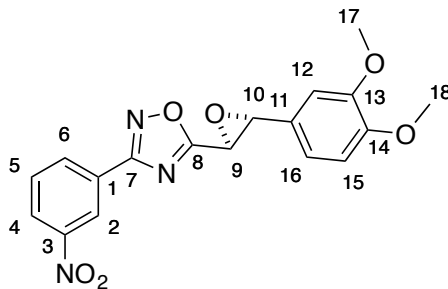
N.B On larger scales (1 g- 5 g) the product was purified by recrystallisation from ethanol.

2-Bromo-1-(3,4-dimethoxyphenyl)-2-(3-(3-nitrophenyl)-1,2,4-oxadiazol-5-yl)ethanol
165



N-Bromosuccinimide (1.62 g, 9.1 mmol) was added to a solution of 1,2,4-oxadiazole **162** (2.92 g, 8.3 mmol) in THF (300 mL) and water (20 mL) and the mixture was stirred for 16 h. DCM was added and the layers were separated. The aqueous layer was re-extracted with DCM (3 × 30 mL). The combined organic layers were washed with brine solution. The organic layer was separated and then dried with magnesium sulfate. The solvent was removed under reduced pressure. The product was purified by column chromatography on silica (20% ethyl acetate/petroleum ether to 30% ethyl acetate/petroleum ether) to give the product **165** as a yellow solid (2.82 g, 75%): m.p. 157-160 °C; $\nu_{\text{max}}/\text{cm}^{-1}$ (nujol) 3465, 1773, 1699, 1593, 1571, 1516, 1142, 1024; δ_{H} (300 MHz, CDCl_3) 8.90 (1H, ddd, J = 2.2, 1.6, 0.5 Hz, 2-H), 8.37 (1H, ddd, J = 7.8, 1.6, 1.1 Hz, 4-H), 8.33 (1H, ddd, J = 8.1, 2.2, 1.1 Hz, 6-H), 7.65 (1H, ddd, J = 8.1, 7.8, 0.5 Hz, 5-H), 6.95 (1H, dd, J = 8.3, 1.9 Hz, 16-H), 6.90 (1H, d, J = 1.9 Hz, 12-H), 6.82 (1H, d, J = 8.3 Hz, 15-H), 5.32 (1H, dd, J = 8.0, 4.4 Hz, 10-H), 5.16 (1H, d, J = 8.0 Hz, 9-H), 3.81 (6H, s, OMe), 2.97 (1H, d, J = 4.4 Hz, OH); δ_{C} (75 MHz, CDCl_3) 177.7 (C-8), 167.5 (C-7), 149.9 (COMe), 149.5 (COMe), 148.94 (C-3), 133.5 (C-6), 131.6 (C-11), 130.6 (C-5), 128.3 (C-1), 126.5 (C-4), 123.0 (C-2), 120.1 (C-16), 111.3 (C-15), 109.9 (C-12), 76.3 (C-10), 56.3 (OMe), 56.2 (OMe), 41.7 (C-9); HRMS m/z (ES^+) 472.0114 ($[\text{M}+\text{Na}]^+$, 100%) $\text{C}_{18}\text{H}_{16}\text{O}_6\text{N}_3^{79}\text{BrNa}$ requires 472.0115.

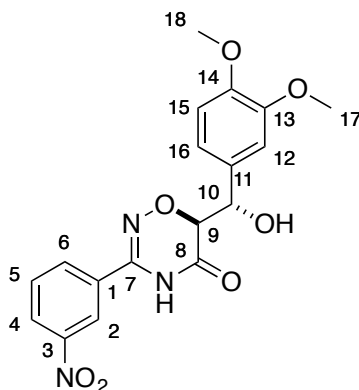
5-(3-(3,4-Dimethoxyphenyl)oxiran-2-yl)-3-(3-nitrophenyl)-1,2,4-oxadiazole **164**



Potassium carbonate (270 mg, 1.95 mmol) was added to a solution of bromohydrin **165** (800 mg, 1.78 mmol) in methanol (20 mL) and the mixture was stirred for 16 h. The mixture was then filtered and the filtrate was concentrated under reduced pressure. On a small scale the product was purified by column chromatography (20% ethyl acetate/petroleum ether) to give the product **164** as an off-white solid (419 mg, 64%): m.p. 136-138 °C; $\nu_{\text{max}}/\text{cm}^{-1}$ (nujol) 3079, 1721, 1597, 1573, 1520, 1269, 1240, 1156, 1143, 1025, 916; δ_{H} (300 MHz, CDCl_3) 9.00 (1H, ddd, J = 2.2, 1.6, 0.5 Hz, 2-H), 8.47 (1H, ddd, J = 7.8, 1.6, 1.1 Hz, 4-H), 8.42 (1H, ddd, J = 8.3, 2.2, 1.1 Hz, 6-H), 7.74 (1H, ddd, J = 8.3, 7.8, 0.5 Hz, 5-H), 7.03 (1H, dd, J = 8.4, 2 Hz, 16-H), 6.94 (1H, d, J = 8.4 Hz, 15-H), 6.87 (1H, d, J = 2, 12-H), 4.53 (1H, d, J = 1.8 Hz, 10-H), 4.27 (1H, d, J = 1.8 Hz, 9-H), 3.95 (3H, s, OMe), 3.94 (3H, s, OMe); δ_{C} (75 MHz, CDCl_3) 176.2 (C-8), 167.6 (C-7), 158.4 (C-11), 150.5 (COMe), 150.0 (COMe), 149.1 (C-3), 133.5 (C-6), 130.6 (C-5), 128.5 (C-1), 126.5 (C-4), 123.1 (C-2), 119.4 (C-16), 111.7 (C-15), 108.4 (C-12), 61.2 (C-10), 56.5 (OMe), 56.4 (OMe), 53.3 (C-9); HRMS m/z (ES^+) 392.0867 ($[\text{M}+\text{Na}]^+$, 100) $\text{C}_{18}\text{H}_{15}\text{N}_3\text{O}_6\text{Na}$ requires 392.0859.

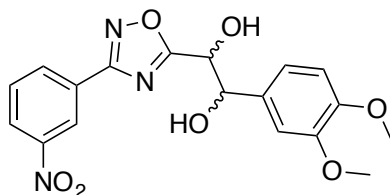
N.B On larger scales the product was taken on to the next step in its crude form.

(3,4-dimethoxyphenyl)(hydroxy)methyl)-3-(3-nitrophenyl)-4*H*-1,2,4-oxadiazin-5(6*H*)-one **167**



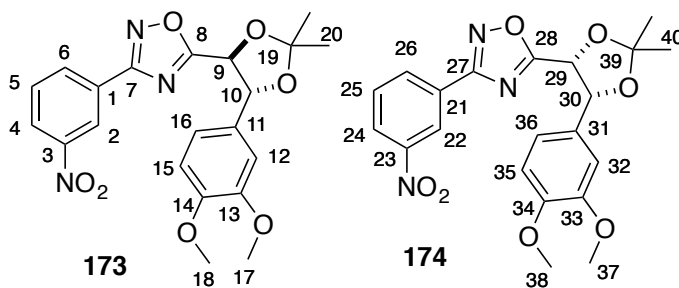
Potassium hydroxide (33 mg, 0.6 mmol) was added to a solution of epoxide **164** (200 mg, 0.54 mmol) in methanol (10 mL). THF (10 mL) and water (5 mL) were added. The mixture was heated under reflux for 2 h. The solvent was removed under reduced pressure. The mixture was then acidified with 2M HCl. The aqueous layer was extracted with ethyl acetate (3 × 50 mL) and the organic layers were dried with magnesium sulfate. The solvent was removed under reduced pressure and the crude product was purified by column chromatography on silica (30% ethyl acetate/petroleum ether to 50% ethyl acetate/petroleum ether) to give the product **167** as a white solid (105 mg, 50%): m.p. 188-190 °C; $\nu_{\max}/\text{cm}^{-1}$ (nujol) 3474 (OH), 1718; δ_{H} (400 MHz, D₆-DMSO) 11.59 (1H, s, OH), 8.47-8.46 (1H, m, 2-H), 8.36 (1H, ddd, J = 8.3, 2.3, 1.0 Hz, 4-H), 8.11 (1H, ddd, J = 7.9, 1.7, 1.0 Hz, 6-H), 7.78-7.74 (1H, m, 5-H), 7.01 (1H, d, J = 1.8 Hz, 12-H), 6.88 (1H, dd, J = 8.4, 1.8 Hz, 16-H), 6.85 (1H, d, J = 8.4 Hz, 15-H), 5.83 (1H, d, J = 5.3 Hz, OH), 4.94 (1H, dd, J = 5.3, 5.1 Hz, 10-H), 4.58 (1H, d, J = 5.1 Hz, 9-H), 3.70 (3H, s, OMe), 3.68 (3H, s, OMe); δ_{C} (100 MHz, D₆-DMSO) 164.7 (C-8), 163.4 (C-7), 148.9 (C-OMe), 148.2 (C-3), 147.7 (C-OMe), 133.1 (C-11), 132.8 (C-6), 130.6 (C-5), 130.3 (C-1), 125.5 (C-4), 121.3 (C-2), 119.3 (C-15), 111.0 (C-16), 110.7 (C-12), 79.8 (C-9), 70.4 (C-10), 55.4 (OMe), 55.4 (OMe); m/z (ES⁺) 410.0952 ([M+Na]⁺, 100%) C₁₈H₁₇N₃O₇Na requires 410.0964.

1-(3,4-Dimethoxyphenyl)-2-(3-phenyl-1,2,4-oxadiazol-5-yl)ethane-1,2-diol **172**



HCl (2N, 560 μ l, 1.2 mmol) was added to a solution of epoxide **164** (2.2 g, 5.96 mmol) in THF/ water (100/20 mL) and the solution was heated under reflux for 3 h. The solution was allowed to cool and water (20 mL) was added. The mixture was extracted with DCM (3 \times 100 mL) and the organic layer was dried with magnesium sulfate. The solvent was removed under reduced pressure. The diastereoisomers were inseparable and were purified together using column chromatography on silica (30% ethyl acetate/ petroleum ether to 50% ethyl acetate/ petroleum ether) to give the diastereoisomers **172** as a solid (2.26 g, 98%)

threo-5-(3,4-Dimethoxyphenyl)-2,2-dimethyl-1,3-dioxolan-4-yl)-3-(3-nitrophenyl)-1,2,4-oxadiazole **173** and *erythro*-5-(3,4-dimethoxyphenyl)-2,2-dimethyl-1,3-dioxolan-4-yl)-3-(3-nitrophenyl)-1,2,4-oxadiazole **174**



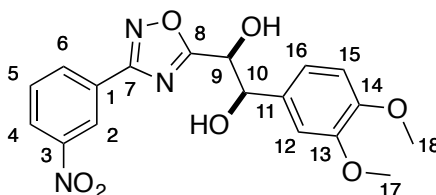
Diol **172**, as an inseparable mixture of diastereoisomers, (422 mg, 1.09 mmol) was dissolved in DCM (20 mL). *p*-Toluenesulfonic acid (21 mg, 0.1 mmol) and 2,2-dimethoxypropane (147 μ l, 1.2 mmol) was added and the mixture was stirred for 16 h. Water (20 mL) and DCM (20 mL) were added and the layers were separated. The aqueous layer was re-extracted with DCM (2 \times 20 mL). The combined organic layers were washed with brine solution (30 mL). The organic layer was dried with

magnesium sulfate and the solvent was removed under reduced pressure. The product was purified by column chromatography on silica (20% ethyl acetate/petroleum ether) to give

threo-5-(3,4-dimethoxyphenyl)-2,2-dimethyl-1,3-dioxolan-4-yl)-3-(3-nitrophenyl)-1,2,4-oxadiazole **173** as a yellow solid (172 mg, 37%): m.p 78-80 °C; $\nu_{\max}/\text{cm}^{-1}$ (nujol) 1734, 1686, 1598, 1520; δ_{H} (300 MHz, CDCl_3) 8.94 (1H, ddd, J = 2.3, 1.6, 0.4 Hz, 2-H), 8.44 (1H, ddd, J = 7.8, 1.6, 1.1 Hz, 4-H), 8.37 (1H, ddd, J = 8.3, 2.3, 1.1 Hz, 6-H), 7.70 (1H, ddd, J = 8.3, 7.8, 0.4 Hz, 5-H), 7.03 (1H, d, J = 2.0 Hz, 12-H), 6.99 (1H, ddd, J = 8.2, 2.0, 0.4 Hz, 16-H), 6.88 (1H, dd, J = 8.2 Hz, 15-H), 5.47 (1H, d, J = 8.0 Hz, 10-H), 5.07 (1H, d, J = 8.0 Hz, 9-H), 3.90 (3H, s, OMe), 3.88 (3H, s, OMe), 1.71 (3H, s, Me), 1.67 (3H, s, Me); δ_{C} (75 MHz, CDCl_3) 177.1 (C-8), 167.0 (C-7), 149.7 (C-OMe), 149.4 (C-OMe), 148.6 (C-3), 133.1 (C-4), 130.1 (C-5), 128.2 (C-1), 128.1 (C-11), 125.9 (C-6), 122.6 (C-2), 119.2 (C-16), 112.2 (C-17), 111.3 (C-15), 109.4 (C-12), 81.7 (C-10), 76.4 (C-9), 55.9 (OMe \times 2), 27.0 (Me), 26.1 (Me); HRMS m/z (ES^+) 450.1285 ($[\text{M}+\text{Na}]^+$, 100%) $\text{C}_{21}\text{H}_{21}\text{N}_3\text{O}_7\text{Na}$ requires 450.1277.

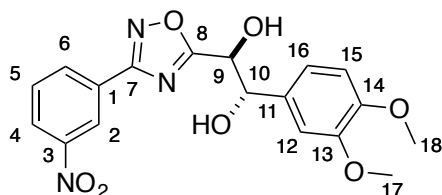
and *erythro*-5-(3,4-dimethoxyphenyl)-2,2-dimethyl-1,3-dioxolan-4-yl)-3-(3-nitrophenyl)-1,2,4-oxadiazole **174** as a yellow solid (266 mg, 57%): m.p 121-125 °C; $\nu_{\max}/\text{cm}^{-1}$ (nujol) 1746, 1724, 1570, 1544, 1521; δ_{H} (300 MHz, CDCl_3) 8.75 (1H, ddd, J = 2.3, 1.6, 0.5 Hz, 22-H), 8.32 (1H, ddd, J = 8.2, 2.3, 1.1 Hz, 26-H), 8.24 (1H, ddd, J = 7.8, 1.6, 1.1 Hz, 24-H), 7.63 (1H, ddd, J = 8.2, 7.8, 0.5 Hz, 25-H), 6.85 (1H, ddd, J = 8.3, 2.0, 0.4 Hz, 36-H), 6.73 (1H, d, J = 2.0 Hz, 32-H), 6.72 (1H, d, J = 8.3 Hz, 35-H), 5.63 (1H, d, J = 6.7 Hz, 29-H), 5.60 (1H, d, J = 6.7 Hz, 30-H), 3.76 (3H, s, OMe), 3.72 (3H, s, OMe), 1.94 (3H, s, Me), 1.63 (3H, s, Me); δ_{C} (75 MHz, CDCl_3) 177.5 (C-28), 166.4 (C-27), 149.2 (C-OMe), 149.0 (C-OMe), 148.6 (C-23), 132.9 (C-24), 130.0 (C-25), 128.3 (C-21), 126.0 (C-31), 125.8 (C-26), 122.5 (C-22), 119.2 (C-36), 112.0 (C-37), 110.8 (C-35), 108.6 (C-32), 80.4 (C-30), 75.3 (C-29), 55.8 (OMe), 55.8 (OMe), 26.8 (Me), 25.5 (Me); HRMS m/z (ES^+) 450.1266 ($[\text{M}+\text{Na}]^+$, 100%) $\text{C}_{21}\text{H}_{21}\text{N}_3\text{O}_7\text{Na}$ requires 450.1277.

threo 1-(3,4-Dimethoxyphenyl)-2-(3-(3-nitrophenyl)-1,2,4-oxadiazol-5-yl)ethane-1,2-diol **175**



Camphor-sulfonic acid (35 mg, 0.15 mmol) was added to a solution of acetone **173** (666 mg, 1.5 mmol) in methanol (20 mL). The mixture was stirred for 2 h. HCl (2N, 2 mL) was added and the solution was heated to 90 °C for 2 h. When TLC analysis indicated consumption of the starting material a saturated solution of sodium bicarbonate (20 mL) and ethyl acetate (30 mL) was added. The layers were separated and the aqueous layer was re-extracted with ethyl acetate (3 × 30 mL). The combined organic layers were dried with magnesium sulfate and the solvent was removed under reduced pressure. The product was purified by column chromatography on silica (30% ethyl acetate/petroleum ether to 50% ethyl acetate/petroleum ether) to give the product **175** as a yellow solid (389 mg, 67%); m.p 124-126 °C; $\nu_{\text{max}}/\text{cm}^{-1}$ (nujol mull) 3504, 3330, 1730, 1593; δ_{H} (300 MHz, CDCl_3) 8.86 (1H, ddd, $J = 2.2, 1.7, 0.4$ Hz, 2-H), 8.35-8.28 (2H, m, 4,6-H), 7.62 (1H, ddd, $J = 8.2, 7.8, 0.4$ Hz, 5-H), 6.87-6.84 (2H, m, 12,16-H), 6.77 (1H, d, $J = 8.2$ Hz, 15-H), 5.11 (1H, d, $J = 5.0$ Hz, 10-H), 5.06 (1H, d, $J = 5.0$ Hz, 9-H), 3.79 (6H, s, OMe); δ_{C} (75 MHz, CDCl_3) 178.7 (C-8), 166.6 (C-7), 149.4 (C-OMe), 149.3 (C-OMe), 148.7 (C-3), 133.1 (C-4), 130.7 (C-11), 130.2 (C-5), 128.1 (C-1), 126.0 (C-6), 122.7 (C-2), 119.0 (C-16), 111.2 (C-15), 109.5 (C-12), 75.3 (C-10), 71.5 (C-9), 56.0 (OMe), 56.0 (OMe); HRMS m/z (ES^+) 410.0964 ($[\text{M}+\text{Na}]^+$, 100%) $\text{C}_{18}\text{H}_{17}\text{N}_3\text{O}_7\text{Na}$ requires 410.0964.

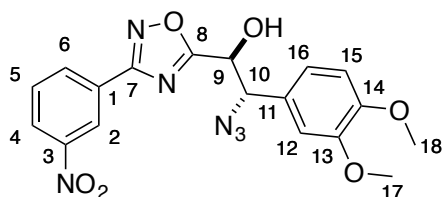
erythro 1-(3,4-Dimethoxyphenyl)-2-(3-(3-nitrophenyl)-1,2,4-oxadiazol-5-yl)ethane-1,2-diol **176**



Camphor-sulfonic acid (30 mg, 0.13 mmol) was added to a solution of acetonide **174** (561 mg, 1.3 mmol) in methanol (20 mL). The mixture was stirred for 2 h. HCl (2N, 2 mL) was added and the solution was heated to 90 °C for 2 h. When TLC analysis indicated consumption of the starting material a saturated solution of sodium bicarbonate (20 mL) and ethyl acetate (30 mL) was added. The layers were separated and the aqueous layer was re-extracted with ethyl acetate (3 × 30 mL). The combined organic layers were dried with magnesium sulfate and the solvent was removed under reduced pressure. The product was purified by column chromatography on silica (30% ethyl acetate/petroleum ether to 50% ethyl acetate/petroleum ether) to give the product **176** as a yellow solid (320 mg, 64%): m.p 164-168 °C; $\nu_{\max}/\text{cm}^{-1}$ (nujol) 3457, 3469, 1675, 1594, 1515, 1138, 1025; δ_{H} (300 MHz, D₆DMSO) 8.75 (1H, ddd, J = 2.2, 1.8, 0.4 Hz, 2-H), 8.49-8.44 (2H, m, 4,6-H), 7.91 (1H, ddd, J = 8.3, 7.8, 0.4 Hz, 5-H), 7.07 (1H, d, J = 1.7 Hz, 12-H) 6.97 (1H, dd, J = 8.3, 1.7 Hz, 16-H), 6.93 (1H, d, J = 8.3 Hz, 15-H), 6.33 (1H, d, J = 6.1 Hz, 9-OH), 5.77 (1H, d, J = 4.6 Hz, 10-OH), 4.88 (1H, dd, J = 8.3, 6.1 Hz, 9H), 4.82 (1H, dd, J = 8.3, 4.6 Hz, 10-H), 3.76 (3H, s, OMe), 3.75 (3H, s, OMe); δ_{C} (75 MHz, D₆DMSO) 181.6 (C-8), 162.0 (C-7), 148.4 (C-OMe), 148.3 (C-OMe), 148.3 (C-1), 134.5 (C-11), 133.0 (C-4), 131.3 (C-5), 127.7 (C-3), 126.1 (C-6), 121.6 (C-2), 119.6 (C-16), 111.3 (C-15), 110.8 (C-12), 74.5 (C-10), 70.3 (C-9), 55.6 (OMe), 55.4 (OMe); HRMS m/z (ES⁺) 410.0957 ([M+Na]⁺, 100%) C₁₈H₁₇N₃O₇Na requires 410.0964.

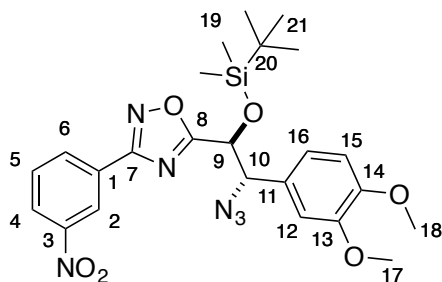
2-Azido-2-(3,4-dimethoxyphenyl)-1-(3-(3-nitrophenyl)-1,2,4-oxadiazol-5-yl)ethanol

177



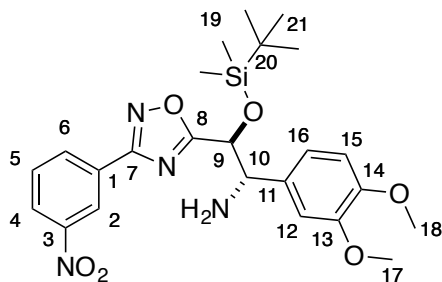
Epoxide **164** (739 mg, 2 mmol) was added to a solution of ammonium chloride (160 mg, 3 mmol) in water (1 mL) and methanol (3 mL). Sodium azide (260 mg, 4 mmol) was added to the mixture, which was then heated under reflux for 2 h. The solvent was removed under reduced pressure. DCM (50 mL) and water (10 mL) were added and the organic layer was separated. The organic layer was dried with magnesium sulfate and the solvent was removed under reduced pressure to give the crude product as a yellow solid. The product was purified by column chromatography on silica (30% ethyl acetate/petroleum ether to 50% ethyl acetate/petroleum ether) to give the product **177** as a yellow solid (729 mg, 88%): m.p. 141-144 °C; $\nu_{\text{max}}/\text{cm}^{-1}$ (nujol) 3430 (OH), 2118 (N_3); δ_{H} (300 MHz, D_6 -DMSO) 8.72-8.71 (1H, m, 2-H), 8.48-8.42 (1H, m, 4,6-H), 7.92-7.87 (1H, m, 5-H), 7.10 (1H, d, J = 1.9 Hz, 12-H), 7.03 (1H, dd, J = 8.4, 1.9 Hz, 16-H), 6.97 (1H, d, J = 8.4 Hz, 15-H), 6.83 (1H, d, J = 6.0 Hz, OH), 5.33 (1H, dd, J = 8.0, 6.0 Hz, 9-H), 5.16 (1H, d, J = 8.0 Hz, 10-H), 3.75 (3H, s, OMe), 3.74 (3H, s, OMe); δ_{C} (75 MHz, D_6 -DMSO) 180.4 (C-7), 166.6 (C-8), 149.4 (C-OMe), 149.0 (C-OMe), 148.7 (C-3), 133.4 (C-6), 131.7 (C-5), 127.9, 127.7, 126.7 (C-4), 122.0 (C-2), 121.3 (C-16), 111.9 (C-12), 111.8 (C-15), 68.5 (C-9), 67.2 (C-10), 55.9 (OMe), 55.8 (OMe); m/z (ES^+) 435 ($[\text{M}+\text{Na}]^+$, 100%).

5-(2-Azido-1-((tert-butyldimethylsilyl)oxy)-2-(3,4-dimethoxyphenyl)ethyl)-3-(3-nitrophenyl)-1,2,4-oxadiazole **178**



Imidazole (345 mg, 5 mmol) and TBSCl (300 mg, 2 mmol) were added to a solution of azido alcohol **177** (578 mg, 1.4 mmol) in DCM (40 mL). The solution was stirred for 16 h. The solution was diluted with DCM (100 mL) and washed with a saturated solution of sodium bicarbonate. The organic layer was dried with magnesium sulfate and the solvent was removed under reduced pressure. The product was purified by column chromatography on silica (ethyl acetate/petroleum ether) to give the product **178** a yellow oil (520mg, 71%): $\nu_{\text{max}}/\text{cm}^{-1}$ (thin film) 3556, 3437, 3341, 3086, 2927, 2856, 2113, 1717, 1593, 1514, 1466, 1267, 1142, 1028, 841; δ_{H} (300 MHz, CDCl_3) 8.99 (1H, ddd, J = 2.3, 1.5, 0.3 Hz, 2-H), 8.46 (1H, ddd, J = 7.8, 1.5, 1.1 Hz, 4-H), 8.39 (1H, ddd, J = 8.2, 2.3, 1.1 Hz, 6-H), 7.71 (1H, ddd, J = 8.2, 7.8, 0.3 Hz, 5-H), 6.99 (1H, dd, J = 8.1, 1.9 Hz, 16-H), 6.96 (1H, d, J = 1.9 Hz, 12-H), 6.90 (1H, d, J = 8.1 Hz, 15-H), 5.03 (1H, d, J = 8.1 Hz, 9-H), 4.97 (1H, d, J = 8.1 Hz, 10-H), 3.91 (3H, s, OMe), 3.90 (3H, s, OMe), 0.75 (9H, s, $(\text{CH}_3)_3$), -0.11 (3H, s, Me), -0.18 (3H, s, Me); δ_{C} (75 MHz, CDCl_3) 178.9 (C-8), 166.8 (C-7), 149.8 (C-OMe), 149.3 (C-OMe), 148.7 (C-3), 133.1 (C-6), 130.1 (C-5), 128.4 (C-1), 127.7 (C-11), 125.9 (C-4), 122.8 (C-2), 121.1 (C-16), 111.1 (C-15), 111.0 (C-12), 70.9 (C-9), 68.5 (C-10), 56.0 (OMe \times 2), 25.4 (C-21), 18.0 (C-20), -5.5 (C-19) -5.6(C-19); HRMS m/z (ES^+) 549.1894 ($[\text{M}+\text{Na}]^+$, 100%) $\text{C}_{24}\text{H}_{30}\text{N}_6\text{O}_6\text{NaSi}$ requires 549.1894.

2-((*tert*-Butyldimethylsilyl)oxy)-1-(3,4-dimethoxyphenyl)-2-(3-(3-nitrophenyl)-1,2,4-oxadiazol-5-yl)ethanamine **179**



method 1: using polymer supported triphenyl phosphine

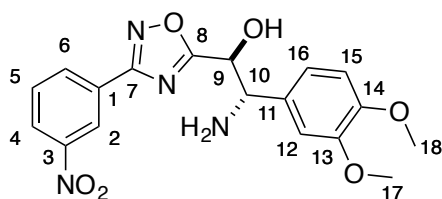
Silyl protected azido alcohol **178** (1.28 g, 2.4 mmol) was added to a solution of THF/H₂O (100/20 mL). Polymer supported triphenyl phosphine (2.6 g, 3.6 mmol) was added to the solution and the mixture was heated under reflux overnight. The mixture was left cool to room temperature. The mixture was filtered and water (100 mL) was added to the filtrate. The suspension was extracted with ethyl acetate (3 × 100 mL). The organic layer was dried with magnesium sulfate and the solvent was removed under reduced pressure. The product was purified by column chromatography on silica (30% ethyl acetate/ petroleum ether to 40% ethyl acetate/petroleum ether) to give the product **179** as a yellow oil (746 mg, 62%).

method 2: using trimethylphosphine

Silyl protected azido alcohol **178** (1.15 g, 2.2 mmol) was added to a solution of THF/H₂O (50/10 mL). A solution of trimethylphosphine in THF (1N, 2.6 mL, 2.6 mmol) was added dropwise to the azide solution. The mixture was stirred for 45 min before sodium hydroxide (235 mg, 5.9 mmol) was added and the solution was stirred overnight. Water (50 mL) was added and the product was extracted with ethyl acetate (3 × 50 mL). The organic layer was dried with magnesium sulfate and the solvent was removed under reduce pressure. The product was purified by column chromatography on silica (30% ethyl acetate/petroleum ether to 40% ethyl acetate/petroleum ether) to give the product **179** as a yellow oil (606 mg, 55%): δ_{H} (300 MHz, CDCl₃) 9.06- 9.05 (1H, m, 2-H), 8.53 (1H, ddd, J = 7.8, 1.5, 1.1 Hz, 4-H), 8.47 (1H, ddd, J = 8.3, 2.3, 1.1 Hz, 6-H), 7.82-7.76 (1H, m, 5-H) 7.04- 6.99 (2H, m,

12,16-H), 6.94 (1H, d, $J=8.8$ Hz, 15-H), 5.11 (1H, d, $J=7.3$ Hz, 9-H), 4.48 (1H, d, $J=7.3$ Hz, 10-H), 3.97 (3H, s, OMe), 3.96 (3H, s, OMe), 1.80 (2H, s, NH_2), 0.88 (9H, s, $(\text{CH}_3)_3$), 0.00 (3H, s, Me), -0.06 (3H, s, Me); δ_{C} (75 MHz, CDCl_3) 180.0 (C-8), 166.6 (C-7), 149.0 (C-OMe), 148.8 (C-OMe), 148.7 (C-3), 133.8 (C-11), 133.1 (C-4), 130.1 (C-5), 128.6 (C-1), 125.8 (C-6), 122.7 (C-2), 119.8 (C-16), 111.1 (C-15), 110.5 (C-12), 73.1 (C-9), 59.9 (C-10), 56.0 (OMe), 55.9 (OMe), 25.5 ($(\text{CH}_3)_3$), 18.1 ($\text{C}(\text{CH}_3)_3$), -5.3 (Me), -5.5 (Me); m/z (ES^+) 523.1984 ($\text{M}+\text{Na}^+$, 20%), $\text{C}_{24}\text{H}_{32}\text{N}_4\text{O}_6\text{SiNa}$ requires 523.1989.

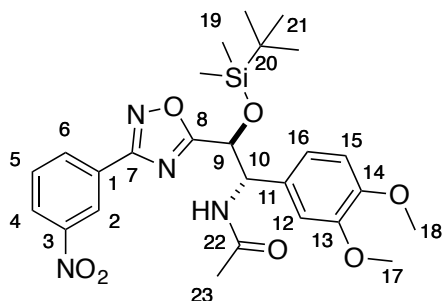
(2-Amino-2-(3,4-dimethoxyphenyl)-1-(3-(3-nitrophenyl)-1,2,4-oxadiazol-5-yl)ethanol
180



TBAF (1.1 mL, 1 M in THF 1.1 mmol) was added dropwise to a solution of silyl protected amino alcohol **179** (278 mg, 0.55 mmol) in THF (20 mL) and the mixture was stirred for 3 h. The solvent was removed under reduced pressure and the product was purified by column chromatography on silica (10% methanol/DCM) to give a yellow oil. The oil was dissolved in DCM and HCl (1M, 30 mL) was added and the aqueous layer was retained. The aqueous layer was basified with sodium hydroxide and the product was extracted with DCM (3 \times 30 mL). The organic layer was dried with magnesium sulfate and most of the solvent was removed under reduced pressure. The product was triturated by the addition of petroleum ether to give **180** as a yellow solid (145 mg, 68%): m.p 142-148 $^{\circ}\text{C}$; $\nu_{\text{max}}/\text{cm}^{-1}$ (nujol) 3464, 3391, 3329, 3072, 1686, 1593, 1539, 1517; δ_{H} (300 MHz, $\text{D}_6\text{-DMSO}$) 8.73 (1H, dd, $J=1.9, 1.9$ Hz, 2-H), 8.46 (1H, dd, $J=8.1, 1.0$ Hz, 6-H), 8.45 (1H, d, $J=8.2$ Hz, 4-H), 7.90 (1H, dd, $J=8.2, 8.1$ Hz, 5-H), 7.06 (1H, d, $J=1.5$ Hz, 12-H), 6.92 (1H, dd, $J=8.3, 1.5$ Hz, 16-H), 6.87 (1H, d, $J=8.3$ Hz, 15-H), 6.26 (1H, s, OH), 4.94 (1H, d,

$J = 8.0$ Hz, 9-H), 4.17 (1H, d, $J = 8.0$ Hz, 10-H), 3.74 (6H, s, OMe), 2.09 (2H, s, NH_2); δ_{C} (75 MHz, D_6 -DMSO) 181.7 (C-8), 165.9 (C-7), 148.4 (C-1), 148.3 (C-OMe), 147.8 (C-OMe), 135.8 (C-11), 133.0 (C-4), 131.2 (C-5), 127.8 (C-3), 126.1 (C-6), 121.6 (C-2), 119.6 (C-16), 111.3 (C-15), 111.1 (C-12), 70.8 (C-9), 59.2 (C-10), 55.5 (OMe), 55.4 (OMe); m/z (ES^+) 409.1113 ($[\text{M}+\text{Na}]^+$, 100%) $\text{C}_{18}\text{H}_{18}\text{N}_4\text{O}_6\text{Na}$ requires 409.1124.

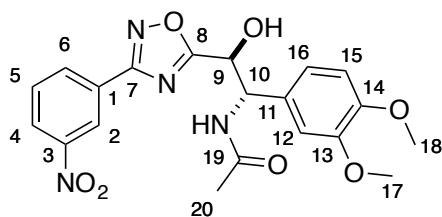
N-((2-((*tert*-Butyldimethylsilyl)oxy)-1-(3,4-dimethoxyphenyl)-2-(3-(3-nitrophenyl)-1,2,4-oxadiazol-5-yl)ethyl))acetamide **181**



DMAP (120 mg, 1.0 mmol) was added to a solution of silyl protected amino alcohol **179** (514 mg, 1.02 mmol) in DCM (20 mL). Acetic anhydride (116 μL , 1.2 mmol) was added to the solution. The mixture was stirred overnight. A solution of saturated sodium bicarbonate was added until the effervescence was finished. The product was extracted using DCM (3 \times 50 mL). The organic layer was dried using magnesium sulfate and the solvent was removed under reduced pressure. The product was purified by column chromatography on silica (40% ethyl acetate/petroleum ether) to give the product **181** as a yellow oil (283 mg, 51%): $\nu_{\text{max}}/\text{cm}^{-1}$ (thin film) 3296, 3083, 2929, 2856, 1654, 1593, 1567, 1518, 1464, 1349, 1263, 1143, 1028; δ_{H} (300 MHz, CDCl_3) 8.82 (1H, ddd, $J = 2.0, 1.9, 0.4$ Hz, 2-H), 8.31 (1H, d, $J = 2.0$ Hz, 4-H), 8.29-8.28 (1H, m, 6-H), 7.65-7.58 (1H, m, 5-H), 6.85 (1H, d, $J = 2.0$ Hz, 12-H), 6.82 (1H, dd, $J = 8.2, 2.0$ Hz, 16-H), 6.69 (1H, d, $J = 8.2$ Hz, 15-H), 6.13 (1H, d, $J = 7.0$ Hz, NH), 5.45-5.38 (2H, m, 9,10-H), 3.76 (3H, s, OMe), 3.75

(3H, s, OMe), 1.98 (3H, s, 23-H), 0.89 (9H, s, 21-H), 0.02 (3H, s, Me), 0.00 (3H, s, Me); δ_{C} (125 MHz, CDCl_3) 178.8 (C-22), 169.4 (C-8), 166.5 (C-7), 149.0 (C-OMe), 148.9 (C-OMe), 148.6 (C-3), 133.0 (C-4), 130.1 (C-5), 129.1 (C-11), 128.3 (C-1), 125.8 (C-6), 122.6 (C-2), 120.2 (C-16), 111.1 (C-12, C-15), 70.3 (C-10), 56.8 (C-9), 55.9 (OMe), 55.8 (OMe), 25.6 (C-21), 23.4 (C-23), 18.2 (C-20), -5.2 (C-19), -5.3 (C-19); HRMS m/z (ES^+) 565.2090 ($[\text{M}+\text{Na}]^+$, 100%) $\text{C}_{26}\text{H}_{34}\text{N}_4\text{O}_7\text{SiNa}$ requires 565.2094.

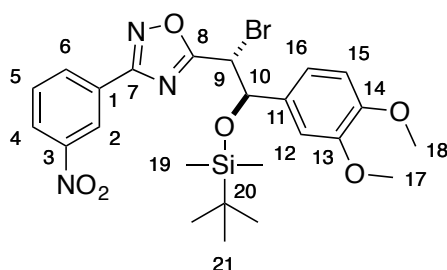
N-(1-(3,4-Dimethoxyphenyl)-2-hydroxy-2-(3-(3-nitrophenyl)-1,2,4-oxadiazol-5-yl)ethyl)acetamide **182**



TBAF (1.44 mL, 1 M in THF 1.44 mmol) was added dropwise to a solution of acetamide **181** (523 mg, 0.9 mmol) in THF (20 mL). The solution was stirred for 2 h. Ethyl acetate (30 mL) and water (30 mL) were added and the layers were separated. The aqueous layer was re-extracted with ethyl acetate (2 × 30 mL). The combined organic layers were washed with brine solution (30 mL). The organic layer was dried with magnesium sulfate and the solvent was removed under reduced pressure. The product was purified by column chromatography on silica (80% ethyl acetate/petroleum ether to 100% ethyl acetate) to give the product **182** as a yellow solid (275 mg, 71%): m.p 63-66 °C; $\nu_{\text{max}}/\text{cm}^{-1}$ (nujol) 3344, 1743, 1717, 1656, 1594, 1540, 1517, 1262, 1145, 1025; δ_{H} (300 MHz, CDCl_3) 8.88 (1H, dd, J = 1.9, 1.7 Hz, 2-H), 8.40-8.39 (1H, m, 6-H), 8.37-8.36 (1H, m, 4-H), 7.70 (1H, dd, J = 8.0, 8.0, Hz, 5-H), 6.88-6.80 (2H, m, 15,16-H), 6.79 (1H, d, J = 1.7 Hz, 12-H), 6.62 (1H, d, J = 7.3 Hz, OH), 5.58 (1H, dd, J = 7.3, 3.7 Hz, 9-H), 5.46 (1H, d, J = 3.7 Hz, 10-H), 3.84 (3H, s, OMe), 3.80 (3H, s, OMe), 2.16 (3H, s, 20-H); δ_{C} (75 MHz,

CDCl₃) 179.0 (C-8), 171.6 (C-19), 166.8 (C-7), 149.7 (C-OMe), 149.6 (C-OMe), 149.0 (C-3), 133.4 (C-6), 130.6 (C-5), 128.4 (C-10), 128.3 (C-11), 126.4 (C-4), 123.0 (C-1), 119.9 (C-16), 111.7 (C-15), 111.0 (C-12), 70.8 (C-10), 58.0 (C-9), 56.3 (OMe), 56.3 (OMe), 23.7 (C-18); HRMS *m/z* (ES⁺) 451.1223 ([M+Na]⁺, 100%) C₂₀H₂₀O₇N₄Na requires 451.1230.

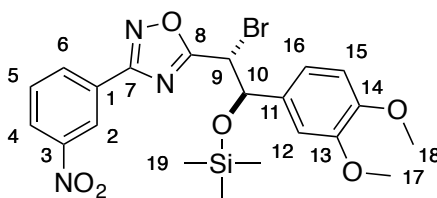
5-(1-Bromo-2-((tert-butyldimethylsilyl)oxy)-2-(3,4-dimethoxyphenyl)ethyl)-3-(3-nitrophenyl)-1,2,4-oxadiazole **185**



Imidazole (793 mg, mmol) and TBSCl (1.17 g, 7.8 mmol) were added to a solution of bromohydrin **165** (1.75 g, 3.9 mmol) in DCM (40 mL). The mixture was stirred for 8 h. The solution was diluted with DCM (100 mL) and then washed with saturated sodium bicarbonate solution. The organic layer was dried with magnesium sulfate. The solvent was removed under reduced pressure. The product was purified by column chromatography on silica (10% ethyl acetate/petroleum ether to 15 % ethyl acetate/petroleum ether) to give the product **185** a colourless solid (1.72 g, 78%): m.p 98-100 °C; $\nu_{\text{max}}/\text{cm}^{-1}$ (nujol) 1684, 1594, 1546, 1519; δ_{H} (300 MHz, CDCl₃) 8.88 (1H, ddd, *J*= 2.3, 1.6, 0.5 Hz, 2-H), 8.35 (1H, ddd, *J*= 7.8, 1.6, 1.1 Hz, 4-H), 8.30 (1H, ddd, *J*= 8.3, 2.3, 1.1 Hz, 6-H), 7.62 (1H, ddd, *J*= 8.3, 7.8, 0.5 Hz, 5-H), 6.92 (1H, dd, *J*= 8.2, 1.9 Hz, 16-H), 6.88 (1H, d, *J*= 1.9 Hz, 12-H), 6.79 (1H, d, *J*= 8.2 Hz, 15-H), 5.16 (1H, d, *J*= 9.3 Hz, 10-H), 4.97 (1H, d, *J*= 9.3 Hz, 9-H), 3.82 (6H, s, OMe), 0.56 (9H, s, (CH₃)₃), -0.19 (3H, s, Me), -0.34 (3H, s, Me); δ_{C} (75 MHz, CDCl₃) 178.4 (C-8), 167.5 (C-7), 149.9 (C-OMe), 149.5 (C-OMe), 149.1 (C-1), 133.4 (C-4), 132.5 (C-11), 130.6 (C-5), 128.7 (C-3), 126.4 (C-6), 123.0 (C-2), 120.9 (C-16), 110.9 (C-15), 109.9 (C-12), 77.8 (C-10), 56.3 (OMe), 56.3 (OMe), 42.8 (C-

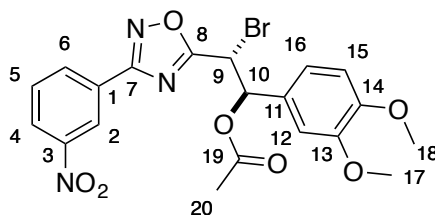
9), 25.7 (C-21), 18.2 (C-20), -4.3 (Me), -5.1 (Me); HRMS m/z (ES^+) 586.0981 ($[M+Na]^+$, 100%), $C_{24}H_{30}N_3O_6Si^{79}BrNa$ requires 586.0985.

5-(1-Bromo-2-(3,4-dimethoxyphenyl)-2-((trimethylsilyl)oxy)ethyl)-3-(3-nitrophenyl)-1,2,4-oxadiazole **186**



Imidazole (228 mg, 3.3 mmol) and TMSCl (281 μ l, 2.2 mmol) were added to a solution bromohydrin **165** (500 mg, 1.1 mmol) in DCM (40 mL). The solution was stirred for 8 h. The solution was diluted with DCM (100 mL) and then washed with saturated sodium bicarbonate solution. The organic layer was dried with magnesium sulfate. The solvent was removed under reduced pressure. The product was purified by column chromatography on silica (15% ethyl acetate/petroleum ether) to give the product **186** as a white solid (377 mg, 66%): m.p 104-108 $^{\circ}C$; ν_{max}/cm^{-1} (nujol) 1738, 1621, 1592, 1567, 1540, 1517, 1254, 1162, 1134, 1076, 1025, 916, 869, 845, 709; δ_H (300 MHz, $CDCl_3$) 9.09 (1H, ddd, J = 2.3, 1.6, 0.4 Hz, 2-H), 8.56 (1H, ddd, J = 7.8, 1.6, 1.1 Hz, 4-H), 8.49 (1H, ddd, J = 8.2, 2.3, 1.1 Hz, 6-H), 7.82 (1H, ddd, J = 8.2, 7.8, 0.4 Hz, 5-H), 7.12 (1H, dd, J = 8.2, 2.0 Hz, 16-H), 7.09 (1H, d, J = 2.0 Hz, 12-H), 6.98 (1H, d, J = 8.2 Hz, 15-H), 5.36 (1H, d, J = 9.4 Hz, 10-H), 5.15 (1H, d, J = 9.4 Hz, 9-H), 4.02 (3H, s, OMe), 4.01 (3H, s, OMe), 0.00 (9H, s, 3 \times CH_3); δ_C (75 MHz, $CDCl_3$) 178.2 (C-8), 167.2 (C-7), 149.7 (C-OMe), 149.3 (C-OMe), 148.9 (C-1), 133.2 (C-4), 132.2 (C-11), 130.4 (C-5), 128.5 (C-3), 126.1 (C-6), 122.9 (C-2), 120.6 (C-16), 110.8 (C-15), 109.8 (C-12), 77.4 (C-10), 56.2 (OMe), 56.1 (OMe), 42.6 (C-9), 0.0 (3 \times CH_3); HRMS m/z (ES^+) 544.0516 ($[M+Na]^+$, 100%) $C_{21}H_{24}N_3O_6SiBrNa$ requires 544.0515.

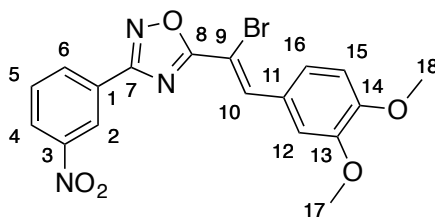
2-Bromo-1-(3,4-dimethoxyphenyl)-2-(3-(3-nitrophenyl)-1,2,4-oxadiazol-5-yl)ethyl acetate **188**



Acetic anhydride (99 μ L, 1.05 mmol) and pyridine (85 μ L, 1.05 mmol) were added to a solution of bromohydrin **165** (190 mg, 0.42 mmol) in DCM (20 mL). The mixture was left to stir for 16 h. The solution was diluted with DCM (100 mL) and washed with saturated sodium bicarbonate solution. The organic layer was dried with magnesium sulfate and the solvent was removed under reduced pressure. The product was purified by column chromatography on silica (10% ethyl acetate/petroleum ether to 20% ethyl acetate/petroleum ether) to give the product **188** as a yellow oil (181 mg, 87%): δ_{H} (300 MHz, CDCl_3) 8.98 (1H, ddd, $J = 2.2, 1.7, 0.5$ Hz, 2-H), 8.46 (1H, ddd, $J = 7.8, 1.7, 1.1$ Hz, 4-H), 8.42 (1H, ddd, $J = 8.2, 2.2, 1.1$ Hz, 6-H), 7.74 (1H, ddd, $J = 8.2, 7.8, 0.5$ Hz, 5-H), 7.07 (1H, dd, $J = 8.4, 2.1$ Hz, 16-H), 6.97 (1H, d, $J = 2.1$ Hz, 12-H), 6.91 (1H, d, $J = 8.4$ Hz, 15-H), 6.42 (1H, d, $J = 9.1$ Hz, 10-H), 5.40 (1H, d, $J = 9.1$ Hz, 9-H), 3.93 (3H, s, OMe), 3.92 (3H, s, OMe), 2.02 (3H, s, Me); δ_{C} (125 MHz, CDCl_3) 176.4 (C-8), 168.7 (C-19), 167.2 (C-7), 149.9 (C-OMe), 149.10 (C-OMe), 148.7 (C-3), 133.1 (C-6), 130.2 (C-5), 127.9 (C-1), 127.8 (C-11), 126.1 (C-4), 122.7 (C-2), 120.4 (C-16), 111.0 (C-15), 110.4 (C-12), 75.7 (C-10), 56.0 (OMe), 55.9 (OMe), 39.1 (C-9), 20.8 (C-20); HRMS m/z (ES^+) 514.0219 ($[\text{M}+\text{Na}]^+$, 100%) $\text{C}_{20}\text{H}_{18}\text{N}_3\text{O}_7^{79}\text{BrNa}$ requires 514.0226, 516.0187 ($[\text{M}+\text{Na}]^+$, 78.55) $\text{C}_{20}\text{H}_{18}\text{N}_3\text{O}_7^{81}\text{BrNa}$ requires 516.0205.

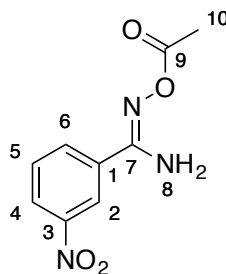
(*Z*)-5-(1-Bromo-2-(3,4-dimethoxyphenyl)vinyl)-3-(3-nitrophenyl)-1,2,4-oxadiazole

189



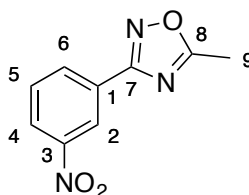
Sodium azide (63 mg, 0.9 mmol) was added to a solution of bromo-acetate **188** (160 mg, 0.3 mmol) in DMSO (5 mL). The solution was heated at 50 °C for 2 h and a precipitate formed. The mixture was allowed to cool before water (10 mL) and DCM (10 mL) were added. The layers were separated and the aqueous layer was extracted with DCM (3 × 20 mL) the combined organic layers were washed with brine solution (50 mL). The organic layer was dried with magnesium sulfate and the solvent was removed under reduced pressure. The product was purified by column chromatography on silica (20% ethyl acetate/ petroleum ether) to give the product **189** as a yellow solid (82 mg, 58%): m.p 158-160 °C; $\nu_{\text{max}}/\text{cm}^{-1}$ (nujol) 1615, 1589, 1574, 1540, 1516, 1245, 1144, 1023; δ_{H} (300 MHz, CDCl_3) 9.04 (1H, ddd, J = 2.3, 1.6, 0.5 Hz, 2-H), 8.51 (1H, ddd, J = 7.8, 1.6, 1.1 Hz, 6-H), 8.42 (1H, ddd, J = 8.3, 2.3, 1.1 Hz, 4-H), 8.40 (1H, s, 10-H), 7.77- 7.71 (2H, m, 5,12-H), 7.61 (1H, ddd, J = 8.5, 2.1, 0.5 Hz, 16-H), 7.00 (1H, d, J = 8.5 Hz, 15-H), 4.01 (3H, s, OMe), 4.00 (3H, s, OMe); δ_{C} (75 MHz, $\text{D}_6\text{-DMSO}$) 175.8 (C-8), 167.6 (C-7), 152.2 (C-OMe), 149.1 (C-OMe), 149.0 (C-3), 141.2 (C-10), 133.9 (C-6), 132.0 (C-5), 128.3 (C-1), 127.1 (C-4), 126.4 (C-11), 125.9 (C-16), 122.4 (C-2), 114.4 (C-12), 112.3 (C-15), 99.7 (C-9), 56.5 (OMe), 56.4 (OMe); m/z (ES^+) 454.0020 ($[\text{M}+\text{Na}]^+$, 26%), 376.0913 ($[\text{M}+\text{Na}-\text{Br}]^+$, 21), 136.0760 (100), 118.0654 (62); HRMS m/z (ES^+) 454.0020 ($[\text{M}+\text{Na}]^+$, 26%) $\text{C}_{18}\text{H}_{14}\text{O}_5\text{N}_3\text{BrNa}$ requires 454.0015.

N'-Acetoxy-3-nitrobenzimidamide **198**



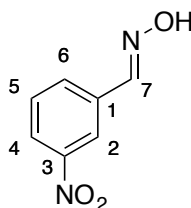
Triethylamine (2.05 mL, 14.6 mmol) was added to a solution of amidoxime **140** (1.33 g, 7.3 mmol) in DCM (20 mL). Acetic anhydride (900 μ l, 9.5 mmol) was added dropwise. After 16 h a saturated solution of sodium bicarbonate (20 mL) was added and the layers were separated. The aqueous phase was re-extracted with DCM (3 \times 20 mL). The combined organic layers were washed with a saturated solution of brine (20 mL). The organic layer was dried with magnesium sulfate and the solvent was removed under reduced pressure. The product was purified by column chromatography on silica (20% ethyl acetate/ petroleum ether to 50% ethyl acetate/ petroleum ether) to give the product **198** as a white solid (1.22 g, 75%): m.p. 118-120 $^{\circ}$ C; $\nu_{\text{max}}/\text{cm}^{-1}$ (nujol) 3473 (NH), 3359 (NH), 3309 (NH), 1751 (C=O); δ_{H} (400 MHz, CDCl_3) 8.46-8.42 (1H, m, 2-H), 8.26 (1H, ddd, J = 8.2, 2.3, 1.1 Hz, 4-H), 8.04-8.00 (1H, m, 6-H), 7.57-7.52 (1H, m, 5-H), 5.21 (2H, br s, 8-H), 2.19 (3H, s, 10-H); δ_{C} (125 MHz, CDCl_3) 168.5 (C-9), 154.0 (C-7), 148.2 (C-3), 132.9 (C-1), 132.9 (C-6), 129.9 (C-5), 125.6 (C-4), 121.7 (C-2), 19.8 (C-10); m/z (ES^+) 246 ($[\text{M}+\text{Na}]^+$, 100%).

5-Methyl-3-(3-nitrophenyl)-1,2,4-oxadiazole **191** ²⁰⁷



TBAF (1.7 mL, 1 M in THF, 1.7 mmol) was added to a solution of *O*-acyl amidoxime **198** (763 mg, 3.4 mmol) in THF (20 mL). The mixture was stirred for 16 h. Water (10 mL) was added and the product was extracted with DCM (3 × 50 mL). The organic phase was dried with magnesium sulfate and the solvent was removed under reduced pressure. The product was purified by column chromatography on silica (20% ethyl acetate/petroleum ether to 30% ethyl acetate/petroleum ether) to give the product **191** as a white solid (585 mg, 83%): m.p. 102-104 °C (Lit. ²⁰⁷ 109-100 °C); $\nu_{\text{max}}/\text{cm}^{-1}$ (nujol) 1600, 1579; δ_{H} (400 MHz, CDCl_3) 8.87 (1H, ddd, J = 2.3, 1.6, 0.5 Hz, 2-H), 8.33 (1H, ddd, J = 7.8, 1.6, 1.1 Hz, 4-H), 8.29 (1H, ddd, J = 8.2, 2.3, 1.1 Hz, 6-H), 7.62 (1H, ddd, J = 8.2, 7.8, 0.5 Hz, 5-H), 2.63 (3H, s, 9-H); δ_{C} (125 MHz, CDCl_3) 177.4 (C-8), 166.8 (C-7), 148.6 (C-3), 132.0 (C-4), 130.0 (C-5), 128.6 (C-1), 125.6 (C-6), 122.4 (C-2), 12.4 (C-9); m/z (ES^+) 228 ($[\text{M}+\text{Na}]^+$, 100%).

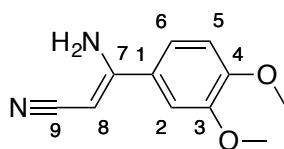
(*E*)-3-Nitrobenzaldehyde oxime **202** ^{208, 209}



Hydroxylamine hydrochloride (5.11 g, 79.4 mmol) and sodium acetate (8.74 g, 99.3 mmol) were added to a solution of 3-nitrobenzaldehyde (10.0 g, 66 mmol) in acetonitrile and water (2:1, 120 mL). DCM (100 mL) was added and the organic layer was separated. The organic layer was neutralised with NaHCO_3 solid then decolourising charcoal was added. The solution was filtered and the filtrate was dried with magnesium sulfate. The solvent was removed under reduced pressure

to give the product **202** as an off-white solid (9.63 g, 88%): m.p. 112-114 °C (Lit.²⁰⁹ 125 °C); $\nu_{\max}/\text{cm}^{-1}$ (nujol) 3290, 1618, 1537, 1308, 1218, 1104, 980, 939; δ_{H} (300 MHz, CDCl_3) 8.47 (1H, dd, $J = 2.2, 1.1$ Hz, 2-H), 8.27 (1H, ddd, $J = 8.0, 2.2, 1.1$ Hz, 4-H), 8.24 (1H, s, OH), 7.97-7.91 (1H, m, 6-H), 7.70 (1H, s, 7-H), 7.64-7.58 (1H, m, 5-H); δ_{C} (75 MHz, CDCl_3) 148.6 (C-3), 148.2 (C-7), 133.9 (C-1), 132.5 (C-6), 129.8 (C-5), 124.4 (C-4), 121.8 (C-2); m/z (ES^-) 165 ($[\text{M}-\text{H}]^-$, 100%).

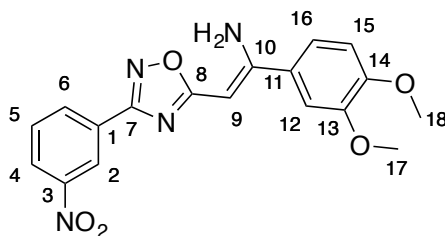
(Z)-3-Amino-3-(3,4-dimethoxyphenyl)acrylonitrile **204**²¹⁰



Potassium *tert*-butoxide (16.8 g, 150 mmol) was slowly added to a solution of 3,4-dimethoxybenzonitrile (8.16 g, 50 mmol) and acetonitrile (5.2 mL, 100 mmol) in toluene (200 mL) and the mixture was left to stir overnight. If the starting material was still present more acetonitrile was added. A solution of saturated sodium bicarbonate was added (100 mL). DCM (100 mL) was added and the organic layer was separated. The aqueous layer was washed with DCM (3 × 100 mL). The organic layer was dried with magnesium sulfate and the solvent was removed under reduced pressure to give a yellow solid. This solid was recrystallised from 50% ethyl acetate/ petroleum ether to give the product **204** as a colourless solid (7.23 g, 71%): m.p. 116-118 °C (Lit.²¹⁰ 122-124 °C); $\nu_{\max}/\text{cm}^{-1}$ (nujol) 3410 (NH), 3332 (NH), 3244 (NH), 2186 ($\text{C}\equiv\text{N}$), 1648 ($\text{C}=\text{C}$); δ_{H} (300 MHz, CDCl_3) 7.14 (1H, dd, $J = 8.4, 2.2$ Hz, 6-H), 7.02 (1H, d, $J = 2.2$ Hz, 2-H), 6.93 (1H, d, $J = 8.4$ Hz, 5-H), 4.92 (2H, br s, NH_2), 4.25 (1H, s, 8-H), 3.97 (6H, s, OMe); δ_{C} (75 MHz, CDCl_3) 161.3 (C-1), 151.4 (C-4), 149.2 (C-3), 128.0 (C-7), 119.7 (C-9), 119.0 (C-6), 111.1 (C-5), 109.1 (C-2), 63.1 (C-8), 56.1 (2 × OMe); m/z (ES^+) 227.0793 ($[\text{M}+\text{Na}]^+$, 100) $\text{C}_{11}\text{H}_{12}\text{N}_2\text{O}_2\text{Na}$ requires 227.0796.

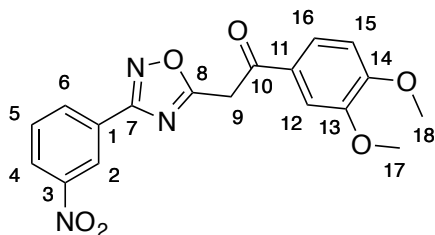
(Z)-1-(3,4-Dimethoxyphenyl)-2-(3-(3-nitrophenyl)-1,2,4-oxadiazol-5-yl)ethenamine

200



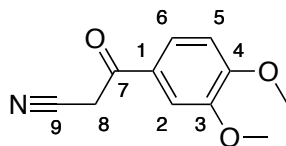
Oxime **202** (598 mg, 3.6 mmol), was dissolved in DCM (300 mL). The solution was shaken with bleach (9 mL, 1.6M) for 3 min. The organic layer was separated and added to a solution of enaminonitrile **204** (750 mg, 3.6 mmol) in triethylamine (1 mL). The mixture was left to stir for 24 h. Triethylamine hydrochloride was filtered off and the solvent was removed under reduced pressure. The product was purified by column chromatography on silica (20% ethyl acetate/ petroleum ether to 30% ethyl acetate petroleum ether), to give a yellow solid. This solid was recrystallised from ethanol to give the product **200** as a yellow solid (23 mg, 1.7%): m.p. 212-216 °C; $\nu_{\text{max}}/\text{cm}^{-1}$ (nujol) 3396 (NH), 3311 (NH), 3204 (NH), 1634 (C=C); δ_{H} (400 MHz, CDCl₃) 8.99-8.97 (1H, m, 2-H), 8.49 (1H, ddd, $J = 7.8, 1.5, 1.1$ Hz, 4-H), 8.38 (1H, ddd, $J = 8.3, 2.3, 1.1$ Hz, 6-H), 7.74-7.69 (1H, m, 5-H), 7.28 (1H, dd, $J = 8.4, 2.1$ Hz, 16-H), 7.17 (1H, d, $J = 2.1$ Hz, 12-H), 6.98 (1H, d, $J = 8.4$ Hz, 15-H), 5.58 (1H, s, 9-H), 3.99 (3H, s, OMe), 3.97 (3H, s, OMe), 1.63 (2H, s, NH₂); δ_{C} (100 MHz, CDCl₃) 177.2 (C-8), 165.5 (C-7), 151.2 (COMe), 151.1 (COMe), 149.3 (C-3), 148.6 (C-10), 133.0 (C-6), 129.9 (C-5), 129.6 (C-11), 129.6 (C-1), 125.3 (C-4), 122.5 (C-2), 119.1 (C-16), 111.2 (C-15), 109.3 (C-12), 72.3 (C-9), 56.1 (OMe), 56.1 (OMe); m/z (ES⁺) 391.12 ([M+Na]⁺, 19%), 259.91 ([M+Na-C₇H₄NO₂]⁺, 100), HRMS m/z (ES⁺) 391.1212 ([M+Na]⁺, 19%) C₁₈H₁₆N₄O₅Na requires 391.1018.

1-(3,4-Dimethoxyphenyl)-2-(3-(3-nitrophenyl)-1,2,4-oxadiazol-5-yl)ethanone **193**



Concentrated HCl (0.5 mL) was added to a solution of enamine **200** (56 mg, 0.15 mmol) in ethanol (2 mL). The mixture was heated under reflux for 3 h. A saturated solution of sodium bicarbonate was added until the solution was neutral. The product was extracted with DCM (3 × 50 mL) and the organic layer was dried with magnesium sulfate. The solvent was removed under reduced pressure and the product was purified by column chromatography on silica (20% ethyl acetate/petroleum ether) followed by recrystallisation from ethanol to give the product **193** as a white solid (7 mg, 12.5%): m.p 140-142 °C; $\nu_{\text{max}}/\text{cm}^{-1}$ (nujol) 1693 (C=O); δ_{H} (400 MHz, CDCl_3) 8.98 (1H, ddd, J = 2.3, 1.6, 0.5 Hz, 2-H), 8.46 (1H, ddd, J = 7.8, 1.6, 1.1 Hz, 4-H), 8.40 (1H, ddd, J = 8.3, 2.3, 1.1 Hz, 6-H), 7.72 (1H, ddd, J = 8.3, 7.8, 0.5 Hz, 5-H), 7.68 (1H, dd, J = 8.5, 2.1 Hz, 16-H), 7.60 (1H, d, J = 2.1 Hz, 12-H), 6.98 (1H, d, J = 8.5 Hz, 15-H), 4.71 (2H, s, 9-H), 4.01 (3H, s, OMe), 3.98 (3H, s, OMe); δ_{C} (100 MHz, CDCl_3) 189.3 (C-10), 174.7 (C-8), 167.1 (C-7), 154.4 (COMe), 149.5 (COMe), 148.6 (C-3), 133.1 (C-6), 130.1 (C-5), 128.5 (C-11), 128.4 (C-1), 125.8 (C-4), 123.6 (C-16), 122.7 (C-2), 110.4 (C-15), 110.3 (C-12), 56.3 (OMe), 56.1 (OMe), 37.0 (C-9).

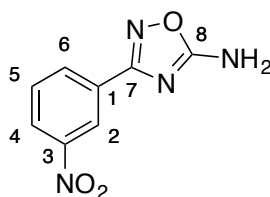
3-(3,4-Dimethoxyphenyl)-3-oxopropanenitrile **206**²¹¹



HCl (5 mL, 3 N, 15 mmol) was added to a solution of enamionitrile **206** (1g, 4.9 mmol) in DCM (10 mL) and the biphasic system was stirred for 16 h. The organic

layer was then separated and washed with a saturated solution of sodium bicarbonate (50 mL). The organic layer was dried with magnesium sulfate and the solvent was removed under reduced pressure. The product was purified by recrystallisation from 50% ethyl acetate/petroleum ether to give the product as a colourless solid (609 mg, 60%): m.p. 137-138 °C (Lit. ²¹¹ 138-139 °C); $\nu_{\text{max}}/\text{cm}^{-1}$ (nujol) 2251 (C≡N), 1674 (C=O); δ_{H} (400 MHz, CDCl₃) 7.45-7.41 (2H, m, 2,6-H), 6.85 (1H, d, J = 8.6 Hz, 5-H), 3.97 (2H, s, 8-H), 3.91 (3H, s, OMe), 3.88 (3H, s, OMe); δ_{C} (100 MHz, CDCl₃) 185.5 (C-7), 154.7 (COMe), 149.6 (COMe), 127.5 (C-1), 123.5 (C-6), 114.1 (C-9), 110.3 (C-5), 110.2 (C-2), 56.3 (OMe), 56.2 (OMe), 29.0 (C-8); HRMS m/z (ES⁺) 228.0638 ([M+Na]⁺, 100%) C₁₁H₁₁NO₃ requires 228.0637.

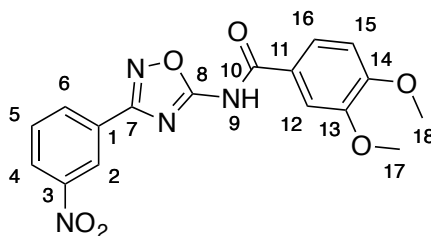
3-(3-Nitrophenyl)-1,2,4-oxadiazol-5-amine **208**²¹²



Oxime **202** (5 g, 30 mmol), was dissolved in DCM (300 mL). The solution was shaken with bleach (75 mL, 1.6M) for 3 min. The organic layer was separated and added to a solution of cyanamide (5.05 g, 120 mmol) in triethylamine (4.2 mL, 30 mmol) and the mixture was stirred for 16 h. Saturated sodium bicarbonate (25 mL) was then added. The mixture was extracted with ethyl acetate (3 × 50 mL). The organic layer was dried with magnesium sulfate. The solvent was removed under reduced pressure. The product was purified by column chromatography on silica (20% ethyl acetate/petroleum ether to 30% ethyl acetate/petroleum ether) to give the product **208** as a white solid (334 mg, 68%): m.p. 214-218 °C (Lit. ²¹² 228 °C); $\nu_{\text{max}}/\text{cm}^{-1}$ (nujol) cm^{-1} 3200 (NH₂), 3100(NH₂), 1688 (C=N); δ_{H} (300 MHz, D₆-DMSO) 8.57 (1H, ddd, J = 2.3, 1.6, 0.4 Hz, 2-H), 8.35 (1H, ddd, J = 8.3, 2.4, 1.1 Hz, 4-H), 8.27 (1H, ddd, J = 7.8, 1.6 1.1 Hz, 6-H), 8.11 (2H, s, NH₂), 7.82-7.78 (1H, m, 5-H); δ_{C} (100 MHz, D₆-DMSO) 172.4 (C-8), 166.0 (C-7), 148.0 (C-3), 132.5 (C-6),

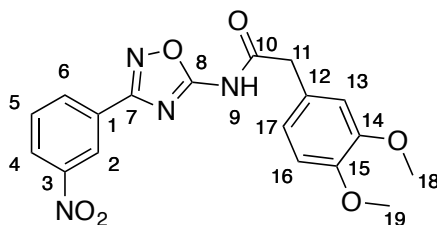
130.7 (C-5), 129.0 (C-1), 125.3 (C-4), 121.0 (C-2); HRMS m/z (Cl^+) 207.0520 ($[\text{M}+\text{H}]^+$, 100%); $\text{C}_8\text{H}_7\text{N}_4\text{O}_3$ requires 207.0518.

3,4-Dimethoxy-*N*-(3-(3-nitrophenyl)-1,2,4-oxadiazol-5-yl)benzamide **207**



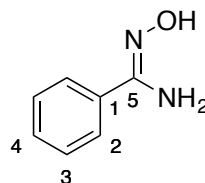
3,4-Dimethoxybenzoic acid (102 mg, 0.56 mmol) was added to a solution of 5-amino-1,2,4-oxadiazole **208** (106 mg, 0.51 mmol) in DCM (5 mL). DCC (115 mg, 0.56 mmol) was added and the mixture was stirred for 16 h. The mixture was filtered and the filtrate was washed with a solution of saturated sodium bicarbonate. The product was extracted with DCM (3 × 50 mL). The organic phase was dried with magnesium sulfate and the solvent was removed under reduced pressure. The product was purified by column chromatography on silica (30% ethyl acetate/ petroleum ether to 40% ethyl acetate/petroleum ether). The product was then purified further by recrystallisation from ethanol/water to give the product **207** as a white solid (39 mg, 21%): m.p. 182-184 °C; $\nu_{\text{max}}/\text{cm}^{-1}$ (nujol) 3290 (NH), 1687 (C=O); δ_{H} (400 MHz, CDCl_3) 9.01 (1H, s, NH), 8.84 (1H, ddd, J = 2.3, 1.6, 0.4 Hz, 2-H), 8.34 (1H, ddd, J = 7.8, 1.6, 1.1 Hz, 4-H), 8.31 (1H, ddd, J = 8.2, 2.3, 1.1 Hz, 6-H), 7.62 (1H, ddd, J = 8.2, 7.8, 0.4 Hz, 5-H), 7.49 (1H, d, J = 2.2 Hz, 12-H), 7.45 (1H, dd, J = 8.4, 2.2 Hz, 16-H), 6.90 (1H, d, J = 8.4 Hz, 15-H), 3.91 (6H, s, OMe); δ_{C} (75 MHz, $\text{D}_6\text{-DMSO}$) 168.6 (C-8), 166.3 (C-7), 163.9 (C-10), 153.4 (C-14), 148.8 (C-15), 148.7 (C-3), 133.2 (C-6), 131.6 (C-5), 128.4 (C-1), 126.5 (C-4), 124.3 (C-11), 123.1 (C-16), 121.9 (C-2), 111.8 (C-12), 111.6 (C-13), 56.2 (OMe), 56.1 (OMe); m/z (ES^+) 393.00 ($[\text{M}+\text{Na}]^+$, 55%), 247.01 ($[\text{M}+\text{Na}-\text{C}_7\text{H}_4\text{N}_2\text{O}_2]^+$, 100); HRMS (ES^-) 369.0832 ($[\text{M}-\text{H}]^-$, 100%) $\text{C}_{17}\text{H}_{13}\text{N}_4\text{O}_6$ requires 369.0835.

2-(3,4-Dimethoxyphenyl)-*N*-(3-(3-nitrophenyl)-1,2,4-oxadiazol-5-yl)acetamide **213**



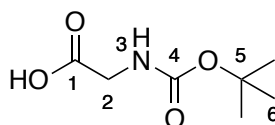
2-(3,4-dimethoxyphenyl)acetic acid (314 mg, 1.6 mmol) and DMAP (196 mg, 1.60 mmol) were added to a solution of 5-amino-1,2,4-oxadiazole **208** (300 mg, 1.46 mmol) in DCM (10 mL). DCC (330 mg, 1.6 mmol) was added to the solution. After 16 h the mixture was filtered and the filtrate was washed with a saturated solution of sodium bicarbonate. The product was extracted with DCM (3 × 30 mL) and the organic phase was dried with magnesium sulfate. The solvent was removed under reduced pressure. The product was then purified by column chromatography (20% ethyl acetate/petroleum ether to 40 % ethyl acetate/petroleum ether). The product was then recrystallised from ethanol to give the product **213** as a white solid (23 mg, 4%): m.p. 176-178 °C; $\nu_{\text{max}}/\text{cm}^{-1}$ (nujol) 3250 (NH), 1739 (NC=O); δ_{H} (300 MHz, CDCl_3) 8.86 (1H, s, NH), 8.80-8.79 (1H, m, 2-H), 8.32-8.28 (2H, m, 6,4-H), 7.63-7.58 (1H, m, 5-H), 6.86-6.83 (2H, m, 16,17-H), 6.79 (1H, s, 13-H), 3.86 (2H, s, 11-H), 3.84 (3H, s, OMe), 3.83 (3H, s, OMe); δ_{C} (75 MHz, $\text{D}_6\text{-DMSO}$) 169.2 (C-10), 167.7 (C-8), 166.3 (C-7), 149.0 (C-OMe), 148.6 (C-3), 148.3 (C-OMe), 133.3 (C-6), 131.6 (C-5), 128.3 (C-1), 126.9 (C-11), 126.5 (C-4), 121.9 (C-17), 121.8 (C-2), 113.7 (C-13), 112.3 (C-16), 56.0 (OMe), 55.9 (OMe), 42.6 (C-11); HRMS m/z (ES^+) 407.0963 ($[\text{M}+\text{Na}]^+$, 100%) $\text{C}_{18}\text{H}_{16}\text{N}_4\text{O}_6\text{Na}$ requires 407.0968.

N'-hydroxybenzimidamide **217**²⁰⁵



Hydroxylamine hydrochloride (8.45 g, 131 mmol), and potassium carbonate (18.1 g, 131 mmol) were added to a solution of benzonitrile (10 g, 97 mmol) in methanol. The mixture was heated under reflux for 4 h. The mixture was cooled and stirred for 16 h. The mixture was filtered and the solvent was removed under reduced pressure to give a colourless oil. The product was purified by column chromatography on silica (30% ethyl acetate/ petroleum ether) to give the product **217** as a white solid (3.56 g, 32%); m.p 72-74 °C (Lit.²⁰⁵ 67-68 °C); $\nu_{\text{max}}/\text{cm}^{-1}$ (nujol) 3453, 3360, 3212, 1649, 1050; δ_{H} (300 MHz, D₆-DMSO) 9.62 (1H, s, OH), 7.69-7.66 (2H, m, 2-H), 7.39-7.35 (3H, m, 3,4-H), 5.79 (2H, s, NH₂); δ_{C} (75 MHz, D₆-DMSO) 150.8 (C-5), 133.3 (C-1), 128.8 (C-4), 128.1 (C-3), 125.4 (C-2); HRMS m/z (ES⁺) 159.0530 ([M+Na]⁺, 100%) C₇H₈N₂ONa requires 159.0534.

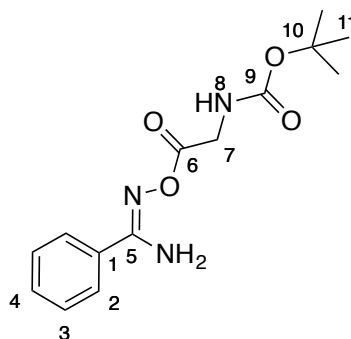
2-((*tert*-Butoxycarbonyl)amino)acetic acid **219**²¹³



Sodium hydroxide (2.66 g, 66 mmol) was added to a solution of glycine (5 g, 66 mmol) in a mixture of water and 1,4-dioxan (1:1, 200 mL). The mixture was cooled to 0 °C. Di-*tert*-butyl dicarbonate (14.5 g, 66 mmol) was added in small batches. After stirring at 0 °C for 15 min the reaction was warmed up to room temperature and stirring was continued for 8 h. Once the reaction was complete the solvent was removed under reduced pressure. The product was redissolved in water (200 mL) and washed with diethyl ether (3 × 100 mL). The aqueous layer was then acidified

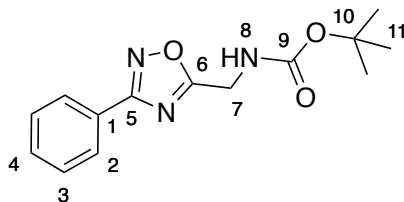
to pH 4 using citric acid solution (10% w/v) and the product was extracted with ethyl acetate (3 × 200 mL). The organic layer was dried with magnesium sulfate and the solvent was removed under reduced pressure to furnish the product **219** as a white solid (10.19 g, 87%): m.p 81-85 °C (Lit. ²¹³ 84-86 °C); $\nu_{\text{max}}/\text{cm}^{-1}$ (nujol) 3406, 3341, 1748, 1669; δ_{H} (500 MHz, CDCl₃) 9.43 (1H, s, NH), 3.98 (1H, d, J = 5.5 Hz, 2-H), 3.92 (1H, d, J = 3.7 Hz, 2-H), 1.47 (9H, s, H); δ_{C} (125 MHz, CDCl₃) 174.8 (C-1), 157.2 (C-4), 80.5 (C-2), 42.2 (C-5), 28.3 (C-6); HRMS m/z (ES⁺) 198.0737 ([M+Na]⁺, 100%) C₇H₁₃NO₄Na requires 198.0742.

tert-Butyl (2-(((amino(phenyl)methylene)amino)oxy)-2-oxoethyl)carbamate **220**



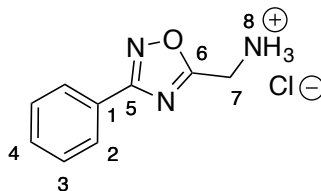
Carboxylic acid **219** (965 mg, 5.5 mmol) and DMAP (448 mg, 3.6 mmol) were added to a solution of amidoxime **217** (500 mg, 3.6 mmol) in DCM (20 mL). DCC (1.14 g, 5.5 mmol) was added and the solution was stirred for 8 h. The mixture was filtered and the filtrate was concentrated under reduce pressure. The product was purified by column chromatography on silica (30% ethyl acetate/petroleum ether) to give **220** as a white solid (333 mg, 32%): m.p 140-143 °C; (nujol) 3373, 3325, 1754, 1719, 1622, 1520, 1163, 946; δ_{H} (300 MHz, CDCl₃) 7.71-7.67 (2H, m, 3-H), 7.53-7.47 (1H, m, 4-H), 7.47-7.39 (2H, m, 2-H), 5.19 (2H, s, NH₂), 4.17 (2H, d, J = 5.6 Hz, 7-H), 1.47 (9H, s, (CH₃)₃); δ_{C} (75 MHz, CDCl₃) 169.5 (C-6), 157.1 (C-5) 156.2 (C-9), 131.7 (C-4), 131.2 (C-1), 129.2 (C-2), 127.1 (C-3), 80.0 (C(CH₃)₃), 42.7 (C-7), 28.8 (CH₃)₃; HRMS m/z (ES⁻) 292.1302 ([M-H]⁻, 100%) C₁₄H₁₈N₃O₄ requires 292.1303.

tert-Butyl ((3-phenyl-1,2,4-oxadiazol-5-yl)methyl)carbamate **221**



TBAF (1 M in THF, 2.1 mL, 2.1 mmol) was added to a solution of *O*-acyl amidoxime **220** (1.26 g, 4.3 mmol) in THF (20 mL). The solution was stirred for 2 h. The solution was diluted with ethyl acetate. The solvent was removed under reduced pressure. The product was purified by column chromatography on silica (10% ethyl acetate/ petroleum ether to 20% ethyl acetate petroleum ether) to give the product **221** as a white solid (1.18 g, 75%): m.p 59-61 °C; $\nu_{\max}/\text{cm}^{-1}$ (nujol) 3365, 1680, 1595, 1575, 1524, 1169, 1160; δ_{H} (500 MHz, CDCl_3) 8.08 (2H, dd, J = 8.1, 1.4 Hz, 3-H), 7.53-7.48 (3H, m, 2,4-H), 5.29 (1H, s, NH), 4.66 (2H, d, J = 5.7 Hz, 7-H), 1.5 (9H, s, 11-H); δ_{C} (125 MHz, CDCl_3) 176.5 (C-6), 168.4 (C-5), 155.4 (C-9), 131.3 (C-4), 128.9 (C-2), 127.5 (C-3), 126.4 (C-1), 80.7 (C-10), 37.2 (C-7), 28.3 (C-11); HRMS m/z (ES^+) 298.1173 ($[\text{M}+\text{Na}]^+$, 100%) $\text{C}_{14}\text{H}_{17}\text{N}_3\text{O}_3\text{Na}$ requires 298.1168

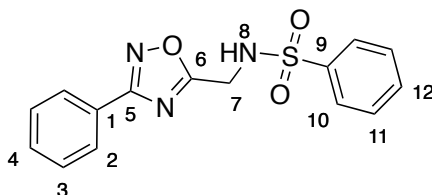
(3-Phenyl-1,2,4-oxadiazol-5-yl)methanaminium chloride **222**



HCl in 1,4-dioxan (4N, 2.3 mL, 9.3 mmol) was added to a solution of 1,2,4-oxadiazole **221** (852 mg, 3 mmol) in DCM (5 mL) and the mixture was stirred for 2 h. The precipitate was filtered and dissolved in water and ethanol. The solution was lyophilised to give the product **222** a white solid (400 mg, 63%): m.p. 176-180 °C

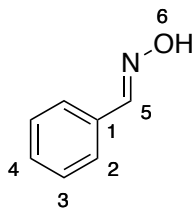
(decomp.); $\nu_{\max}/\text{cm}^{-1}$ (nujol) 3394, 1605, 1462, 1377; δ_{H} (300 MHz, D_6 -DMSO) 9.13 (3H, s, 8-NH), 8.04-7.99 (2H, m, 2-H), 7.64-7.60 (2H, m, 3-H), 7.59-7.55 (1H, m, 4-H), 4.54 (2H, s, 7-H); δ_{C} (75 MHz, D_6 -DMSO) 174.7 (C-6), 168.0 (C-5), 132.3 (C-4), 129.8 (C-3), 127.4 (C-2), 125.9 (C-1), 35.0 (C-7); m/z (ES^+) 176.0818 ($[\text{M}+\text{H}]^+$, 100%) $\text{C}_9\text{H}_{10}\text{N}_3\text{O}$ requires 176.0824.

N-((3-Phenyl-1,2,4-oxadiazol-5-yl)methyl)benzenesulfonamide **215**



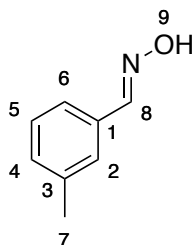
Benzenesulfonyl chloride (217 μL , 1.7 mmol) was added to a solution of amine **222** (300 mg, 1.4 mmol) in pyridine (10 mL). The solution was stirred for 8 h. HCl (2N, 100mL) was added to the solution and the product was extracted with ethyl acetate (3 \times 100 mL). The organic layer was dried with magnesium sulfate and the solvent was removed under reduced pressure. The product was purified by column chromatography on silica (10% ethyl acetate/petroleum ether to 20% ethyl acetate/petroleum ether) to give a white solid (447 mg, quant.): m.p 122-126 $^{\circ}\text{C}$; $\nu_{\max}/\text{cm}^{-1}$ (nujol) 3259 (NH), 1680 (C=N), 1457, 1378; δ_{H} (300 MHz, CDCl_3) 7.94-7.91 (2H, m, 2-H), 7.89-7.86 (2H, m, 10-H), 7.54-7.47 (3H, m, Ar-H), 7.47-7.43 (3H, m, Ar-H), 5.39 (1H, t, J = 6.2 Hz, NH), 4.56 (2H, d, J = 6.2 Hz, 7-H); δ_{C} (75 MHz, CDCl_3) 174.9 (C-6), 168.6 (C-5), 139.5 (C-9), 133.6 (C-12), 131.9 (C-4), 129.6 (C-Ar), 129.3 (C-Ar), 127.8 (C-2), 127.6 (C-10), 126.4 (C-Ar), 39.4 (C-7); HRMS m/z (ES^+) 338.0587 ($[\text{M}+\text{Na}]^+$, 100%) $\text{C}_{15}\text{H}_{13}\text{N}_3\text{O}_3\text{SNa}$ requires 338.0575.

(*E*)-Benzaldehyde oxime **226a**²¹⁴



Benzaldehyde (10 mL, 10.45 g, 98 mmol), hydroxylamine hydrochloride (7.62 g, 118 mmol) and sodium acetate (12.11 g, 147 mmol) were added to a solution of acetonitrile and water (2:1, 120 mL). The mixture was stirred for 8 h. DCM (100 mL) was added and the organic layer was separated. The organic layer was neutralised with sodium bicarbonate, then decolourising charcoal was added. The solution was filtered and the filtrate was dried with magnesium sulfate and the solvent was removed under reduced pressure to give the product **226a** as an off-white solid (9.6 g, 81%): m.p. 28-30 °C (Lit.²¹⁴ 30-33 °C); $\nu_{\text{max}}/\text{cm}^{-1}$ (nujol) 3330, 1634, 1074; δ_{H} (300 MHz, CDCl_3) 8.97 (1H, s, OH), 8.17 (1H, s, 5-H), 7.60-7.56 (2H, m, 2-H), 7.41-7.37 (3H, m, 3,4-H); δ_{C} (75 MHz, C_6D_6) 150.6 (C-5), 132.7 (C-1), 130.2 (C-4), 129.1 (C-3), 127.5 (C-2); m/z (ES^+) 122.06 ($[\text{M}+\text{H}]^+$, 100%).

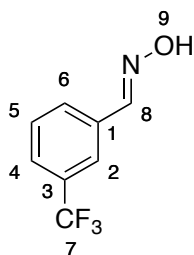
(*E*)-3-Methylbenzaldehyde oxime **226b**²¹⁵



3-Methylbenzaldehyde (4.00 g, 3.9 mL, 33.3 mmol), hydroxylamine hydrochloride (2.58 g, 39.9 mmol) and sodium acetate (4.10 g, 49.9 mmol) were added to a solution of acetonitrile and water (3:1, 120 mL). The mixture was stirred for 8 h. DCM (100 mL) was added and the organic layer was separated. The organic layer was neutralised with sodium bicarbonate then decolourising charcoal was added. The solution was filtered and the filtrate was dried with magnesium sulfate and the

solvent was removed under reduced pressure to give the product **226b** as a brown solid (3.33 g, 74%): m.p. 55-57 °C (Lit.²¹⁵ 51-53 °C); $\nu_{\text{max}}/\text{cm}^{-1}$ (nujol) 3178, 3085, 1636, 1605; δ_{H} (300 MHz, CDCl_3) 8.17 (1H, s, 8-H), 7.88 (1H, br s, OH), 7.46-7.40 (2H, m, 2,6-H), 7.31 (1H, d, J = 7.0 Hz, 5-H), 7.27-7.23 (1H, m, 4-H), 2.42 (3H, s, Me); δ_{C} (75 MHz, CDCl_3) 150.6 (C-8), 138.55 (C-3), 131.8 (C-1), 131.0 (C-4), 128.7 (C-5), 127.6 (C-2), 124.4 (C-6), 21.4 (C-7); m/z (Cl^+) 136.08 ($[\text{M}+\text{H}]^+$, 100%), 118.07 ($[\text{M}-\text{OH}]^+$, 60); HRMS m/z (Cl^+) 136.0764 ($[\text{M}+\text{H}]^+$, 100) $\text{C}_8\text{H}_{10}\text{NO}$ requires 136.0762.

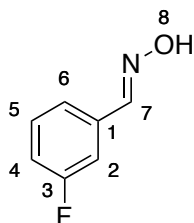
(*E*)-3-(Trifluoromethyl)benzaldehyde oxime **226c**²¹⁶



3-(Trifluoromethyl)benzaldehyde (16.75 g, 96.2 mmol), hydroxylamine hydrochloride (7.43 g, 115 mmol) and sodium acetate (11.83 g, 144 mmol) were added to a solution of acetonitrile and water (3:1, 200 mL). The mixture was stirred for 8 h. DCM (100 mL) was added and the organic layer was separated. The organic layer was neutralised with sodium bicarbonate then decolourising charcoal was added. The solution was filtered and the filtrate was dried with magnesium sulfate and the solvent was removed under reduced pressure to give an oil. The excess 3-(trifluoromethyl)benzaldehyde was removed by distillation under reduced pressure to give the product **226c** as a white solid (14.56 g, 80%): m.p. 37-39 °C (Lit.²¹⁶ 46-47 °C); δ_{H} (300 MHz, CDCl_3) 8.19 (1H, s, 8-H), 7.86-7.83 (1H, m, 2-H), 7.78-7.73 (1H, m, 6-H), 7.65 (1H, dddd, J = 7.8, 1.8, 1.2, 0.6, 4-H), 7.56-7.48 (1H, m, 5-H); δ_{C} (75 MHz, CDCl_3) 149.5 (C-8) 133.3 (C-1), 131.7 (d, J = 32.6 Hz, C-3), 130.5 (q, J = 1.2 Hz, C-6), 129.7 (C-5), 126.9 (q, J = 3.7 Hz, C-4), 124.2 (q, J = 3.9 Hz, C-2); $\delta_{\text{F}}\{^1\text{H}\}$ (282 MHz, CDCl_3) -63.4 (s); m/z (Cl^+) 190.05 ($[\text{M}+\text{H}]^+$, 95%), 172.04

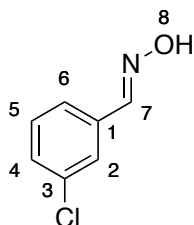
([M-OH]⁺, 50), 170.04 ([M-F]⁺, 100); HRMS *m/z* (Cl⁺) 190.0478 ([M+H]⁺, 95) C₈H₇NOF₃ requires 190.0480.

(*E*)-3-Fluorobenzaldehyde oxime **226d**²¹⁷



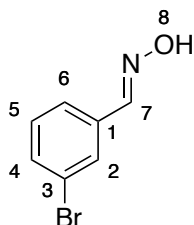
3-Fluorobenzaldehyde (9.00 g, 7.7 mL, 72.5 mmol), hydroxylamine hydrochloride (5.61 g, 87 mmol) and sodium acetate (8.92 g, 108 mmol) were added to a solution of acetonitrile and water (3:1, 320 mL). The mixture was stirred for 8 h. DCM (100 mL) was added and the organic layer was separated. The organic layer was neutralised with solid sodium bicarbonate then decolourising charcoal was added. The solution was filtered and the filtrate was dried with magnesium sulfate and the solvent was removed under reduced pressure to give the product **226d** as a white solid (8.64 g, 86%): m.p. 57-60 °C (Lit.²¹⁷ 63 °C); $\nu_{\text{max}}/\text{cm}^{-1}$ (nujol) 3334, 1675, 1611, δ_{H} (300 MHz, CDCl₃) 8.93 (1H, br s, OH), 8.15 (1H, s, 7-H), 7.38-7.31 (3H, m, 2,5,6-H), 7.13-7.06 (1H, m, 4-H); δ_{C} (75 MHz, CDCl₃) 163.4 (d, *J*= 246.6 Hz, C-3), 149.9 (d, *J*= 2.9 Hz, C-7), 134.5 (d, *J*= 7.8 Hz, C-1), 130.8 (d, *J*= 8.3 Hz, C-5), 123.6 (d, *J*= 3.1 Hz, C-6), 117.5 (d, *J*= 21.5 Hz, C-4), 113.8 (d, *J*= 22.7 Hz, C-2); δ_{F} (376 MHz, CDCl₃) -112.30 (td, *J*= 8.9, 5.5 Hz); *m/z* (Cl⁺) 140.05 ([M+H]⁺, 100), 122.04 ([M-OH]⁺, 56); HRMS *m/z* (Cl⁺) 140.0510 ([M+H]⁺, 100) C₇H₇NOF requires 140.0512.

(*E*)-3-Chlorobenzaldehyde oxime **226e**²¹⁸



3-Chlorobenzaldehyde (10.0 g, 8 mL, 71.1 mmol), hydroxylamine hydrochloride (5.5 g, 85.3 mmol) and sodium acetate (8.75 g, 107 mmol) were added to a solution of acetonitrile and water (2:1, 120 mL). The mixture was stirred for 8 h. DCM (100 mL) was added and the organic layer was separated. The organic layer was neutralised with sodium bicarbonate then decolourising charcoal was added. The solution was filtered and the filtrate was dried with magnesium sulfate and the solvent was removed under reduced pressure to give the product **226e** as a white solid (8.45 g, 76%): m.p. 60-63 °C (Lit.²¹⁸ 69-69.5 °C); $\nu_{\text{max}}/\text{cm}^{-1}$ (nujol) 3183, 1685, 1629, 1594, 1560, 1209; δ_{H} (300 MHz, CDCl_3) 8.13 (1H, s, 7-H), 7.99 (1H, br s, OH), 7.64-7.62 (1H, m, 2-H), 7.50-7.47 (1H, m, 6-H), 7.41-7.38 (1H, m, 4-H), 7.37 (1H, dd, J = 7.9, 0.7 Hz, 5-H); δ_{C} (75 MHz, CDCl_3) 149.6 (C-7), 135.3 (C-3), 134.1 (C-1), 130.5 (Ar-H), 130.5 (Ar-H), 127.5 (C-2), 125.7 (C-6); m/z (Cl^+) 186.05 ($[\text{M}^{37}\text{Cl}+\text{C}_2\text{H}_5]^+$, 8%), 184.06 ($[\text{M}^{35}\text{Cl}+\text{C}_2\text{H}_5]^+$, 21), 158.02 ($[\text{M}^{37}\text{Cl}+\text{H}]^+$, 31), 156.02 ($[\text{M}^{35}\text{Cl}+\text{H}]^+$, 100), 140.02 ($[\text{M}^{37}\text{Cl}-\text{OH}]^+$, 32), 138.01 ($[\text{M}^{35}\text{Cl}-\text{OH}]^+$, 66); HRMS m/z (Cl^+) 156.0214 ($[\text{M}^{35}\text{Cl}+\text{H}]^+$, 100%), $\text{C}_7\text{H}_7\text{NO}^{35}\text{Cl}$ requires 156.0216.

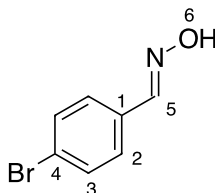
(*E*)-3-Bromobenzaldehyde oxime **226f**²¹⁹



3-Bromobenzaldehyde (10 mL, 15.77 g, 85.2 mmol), hydroxylamine hydrochloride (6.59 g, 102 mmol) and sodium acetate (10.48 g, 127 mmol) were added to a

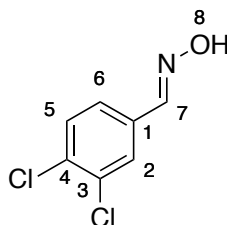
solution of acetonitrile and water (2:1, 120 mL). The mixture was stirred for 8 h. DCM (100 mL) was added and the organic layer was separated. The organic layer was neutralised with sodium bicarbonate then decolourising charcoal was added. The solution was filtered and the filtrate was dried with magnesium sulfate and the solvent was removed under reduced pressure to give the product **226f** as a white solid (13.29 g, 78%): m.p. 65-69 °C (Lit.²¹⁹ 73 °C); $\nu_{\text{max}}/\text{cm}^{-1}$ (nujol) 3173, 3103, 1684 (C=N) δ_{H} (300 MHz, CDCl_3) 8.55 (1H, s, OH), 8.10 (1H, s, 7-H), 7.74 (1H, dd, J = 2.0, 1.6 Hz, 2-H), 7.53-7.47 (2H, m, 4,6-H), 7.29-7.22 (1H, m, 5-H); δ_{C} (75 MHz, CDCl_3) 149.5 (C-7), 134.3 (C-1), 133.4 (C-4), 130.7 (C-5), 130.2 (C-2), 126.1 (C-6), 123.4 (C-3); m/z (ES^-) 197.96 ($[\text{M}^{79}\text{Br-H}]^-$, 100%), 199.96 ($[\text{M}^{81}\text{Br-H}]^-$, 85).

(*E*)-4-Bromobenzaldehyde oxime **226g**²²⁰



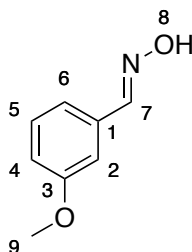
4-Bromobenzaldehyde (2.77 g, 14.9 mmol), hydroxylamine hydrochloride (1.16 g, 17.9 mmol) and sodium acetate (1.84 g, 22.4 mmol) were added to a solution of acetonitrile and water (2:1, 75 mL). The mixture was stirred for 8 h. DCM (100 mL) was added and the organic layer was separated. The organic layer was neutralised with sodium bicarbonate then decolourising charcoal was added. The solution was filtered and the filtrate was dried with magnesium sulfate and the solvent was removed under reduced pressure to give the product **226g** as a white solid (2.14 g, 72%): m.p. 108-110 °C (Lit.²²⁰ 112 °C); $\nu_{\text{max}}/\text{cm}^{-1}$ (nujol) 3298, 1641, 1609, 1586; δ_{H} (300 MHz, CDCl_3) 8.55 (1H, s, OH), 7.52 (2H, d, J = 8.5 Hz, 2-H), 7.44 (2H, d, J = 8.5 Hz, 3-H); δ_{C} (75 MHz, CDCl_3) 149.9 (C-5), 131.5 (C-3), 131.2 (C-1), 128.9 (C-2), 124.8 (C-4); HRMS m/z (ES^-) 199.9531 ($[\text{M}^{81}\text{Br-H}]^-$, 97%) $\text{C}_7\text{H}_5\text{NO}^{81}\text{Br}$ requires 199.9534; 197.9550 ($[\text{M}^{79}\text{Br-H}]^-$, 100) $\text{C}_7\text{H}_5\text{NO}^{79}\text{Br}$ requires 197.9554.

(*E*)-3,4-Dichlorobenzaldehyde oxime **226h**²²¹



3,4-Dichlorobenzaldehyde (10 g, 57.1 mmol), hydroxylamine hydrochloride (4.42 g, 68.5 mmol) and sodium acetate (7.03g, 85.7 mmol) were added to a solution of acetonitrile and water (2:1, 120 mL). The mixture was stirred for 8 h. DCM (100 mL) was added and the organic layer was separated. The organic layer was neutralised with sodium bicarbonate then decolourising charcoal was added. The solution was filtered and the filtrate was dried with magnesium sulfate and the solvent was removed under reduced pressure to give the product **226h** as a white solid (9.64 g, 88%): m.p. 118-120 °C (Lit.²²¹ 120-122 °C); $\nu_{\max}/\text{cm}^{-1}$ (nujol) 3309, 1632, 1554; δ_{H} (300 MHz, CDCl_3) 8.06 (1H, s, 7-H), 7.80 (1H, OH), 7.68 (1H, d, $J=1.9$ Hz, 2-H), 7.46 (1H, d, $J=8.3$ Hz, 5-H), 7.40 (1H, dd, $J=8.3, 1.9$ Hz, 6-H); δ_{C} (75 MHz, CDCl_3) 148.3 (C-7), 134.0 (C-3), 133.2 (C-4), 132.1 (C-1), 130.8 (C-5), 128.6 (C-2), 126.1 (C-6); m/z (Cl^+) 191.98 ($[\text{M}^{37}\text{Cl}_2+\text{H}]^+$, 53% 189.98 ($[\text{M}^{35}\text{Cl}_2+\text{H}]^+$, 100), 173.97 ($[\text{M}^{37}\text{Cl}_2-\text{OH}]^+$, 35), 171.97 ($[\text{M}^{35}\text{Cl}_2-\text{OH}]^+$, 48); HRMS m/z (Cl^+) 189.9825 ($[\text{M}+\text{H}]^+$, 100) $\text{C}_7\text{H}_6\text{NO}^{35}\text{Cl}_2$ requires 189.9826.

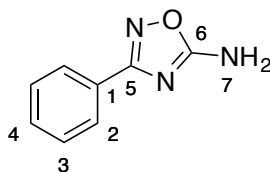
(*E*)-3-Methoxybenzaldehyde oxime **226i**²²²



3-Methoxybenzaldehyde (10.0 g, 8.9 mL, 73.5 mmol), hydroxylamine hydrochloride (5.68 g, 88.1 mmol) and sodium acetate (9.04 g, 110 mmol) were added to a

solution of acetonitrile and water (2:1, 120 mL). The mixture was stirred for 8 h. DCM (100 mL) was added and the organic layer was separated. The organic layer was neutralised with sodium bicarbonate then decolourising charcoal was added. The solution was filtered and the filtrate was dried with magnesium sulfate and the solvent was removed under reduced pressure. The product was purified by distillation under reduced pressure to give the product **226i** as a yellow oil (6.62 g, 60%): b.p 175 °C at 10 mbar; $\nu_{\text{max}}/\text{cm}^{-1}$ (thin film) 3331, 1934, 1628, 1601, 1579, 1492, 1456, 1321, 1289, 1169, 1158; δ_{H} 8.05 (1H, s, 7-H), 7.83 (1H, br s, OH), 7.23 (1H, m, 5-H), 7.10 (1H, dd, J = 2.6, 1.5 Hz, 2-H), 7.05 (1H, dddd, J = 7.6, 1.5, 1.1, 0.4 Hz, 6-H), 6.88 (1H, ddd, J =8.3, 2.6, 1.1 Hz, 4-H), 3.76 (3H, s, 9-H); δ_{C} (75 MHz, CDCl_3) 159.8 (C-3), 150.4 (C-7), 133.2 (C-1), 129.9 (C-5), 120.2 (C-6), 116.5 (C-4), 111.3 (C-2), 55.4 (C-9); HRMS m/z (ES^+) 152.0701 ($[\text{M}+\text{H}]^+$, 100%) $\text{C}_8\text{H}_{10}\text{O}_2\text{N}$ requires 152.0707.

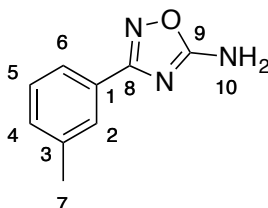
3-Phenyl-1,2,4-oxadiazol-5-amine **224a**²²³



Oxime **226a** (1 g, 8.25 mmol), was dissolved in DCM (100 mL). The solution was shaken with bleach (21 mL, 1.6 M, 33.6 mmol) for 3 min. The organic layer was separated and added to a solution of cyanamide (1.39 g, 33 mmol) in triethylamine (4.6 mL, 30 mmol) and the mixture was stirred for 8 h. The solvent was removed under reduce pressure to give a yellow solid. The product was purified by recrystallisation using ethanol and water, to give the product **224a** as a white solid (956 mg, 72%): m.p 142-145 °C (Lit. ²²³ 147-148 °C); $\nu_{\text{max}}/\text{cm}^{-1}$ (nujol) 3286, 3113, 1675, 1599; δ_{H} (300 MHz, D_6 -DMSO) 7.93 (2H, s, NH_2), 7.90-7.85 (2H, m, 2-H), 7.53-7.46 (3H, m, 3,4-H); δ_{C} (75 MHz, D_6 -DMSO) 172.1 (C-6), 167.5 (C-5), 130.8 (C-4), 128.9 (C-3), 127.6 (C-1), 126.5 (C-2); m/z (CI^+) 162.07 ($[\text{M}+\text{H}]^+$, 100%),

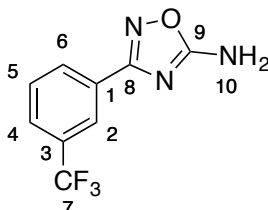
161.06 ($[M]^+$, 37), 119.06 ($[M-CN_2H_2]^+$, 48); HRMS m/z (Cl^+) 162.0668 ($[M+H]^+$, 100) $C_8H_8N_3O$ requires 162.0667.

3-(*m*-Tolyl)-1,2,4-oxadiazol-5-amine **224b**



Oxime (1 g, 7.4 mmol), was dissolved in DCM (300 mL). The solution was shaken with bleach (18.5 mL, 1.6 M, 29.5 mmol) for 3 min. The organic layer was separated and added to a solution of cyanamide (1.24 g, 29.5 mmol) in triethylamine (4.1 mL, 29.5 mmol) and the mixture was stirred for 8 h. The solvent was removed under reduce pressure to give a yellow solid. The product was purified by recrystallisation using ethanol and water, to give the product as a white solid (958 mg, 74%): m.p 198-201 °C; ν_{max}/cm^{-1} (nujol) 3240, 3201, 3098, 1682, 1605; δ_H (300 MHz, D_6 -DMSO) 7.90 (2H, s, NH_2), 7.70-7.65 (2H, m, 2,6-H), 7.41-7.36 (1H, m, 5-H), 7.31-7.34 (1H, m, 4-H), 2.36 (3H, s Me); δ_C (75 MHz, D_6 -DMSO), 172.0 (C-9), 167.5 (C-8), 138.1 (C-3), 131.4 (C-4), 128.7 (C-5), 127.5 (C-1), 127.0 (C-2), 123.7 (C-6), 20.9 (C-7); HRMS m/z (ES^+) 198.0640 ($[M+Na]^+$) $C_9H_9N_3ONa$ requires 198.0643.

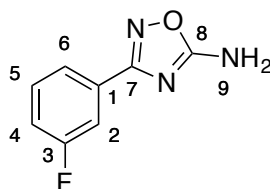
3-(3-(Trifluoromethyl)phenyl)-1,2,4-oxadiazol-5-amine **224c**



Oxime **226c** (1 g, 5.3 mmol), was dissolved in DCM (65 mL). The solution was shaken with bleach (13 mL, 1.6 M, 20.8 mmol) for 3 min. The organic layer was separated and added to a solution of cyanamide (869 mg, 21.1 mmol) in

triethylamine (2.9 mL, 21.1 mmol) and the mixture was stirred for 8 h. The solvent was removed under reduce pressure to give a yellow solid. The product was purified by recrystallisation using ethanol and water, to give the product **224c** as a colourless solid (847 mg, 70%): m.p 208-210 °C; $\nu_{\max}\text{cm}^{-1}$ (nujol) 3294 (NH), 3126 (NH), 1684 (C=N); δ_{H} (300 MHz, D₆-DMSO) 8.15 (1H, dd, J = 7.5, 0.7 Hz, 6-H), 8.10 (1H, m, 2-H), 8.07 (2H, s, 10-NH₂), 7.88-7.91 (1H, m, 4-H), 7.78-7.72 (1H, m, 5-H); δ_{C} (300 MHz, D₆-DMSO) 172.7 (C-9), 166.8 (C-8), 130.8 (d, J = 1.2 Hz, C-6), 130.7 (C-5), 130.0 (d, J = 32.1 Hz, C-3), 129.0 (C-1), 127.8 (q, J = 3.7 Hz, C-4), 124.2 (q, J = 272.3 Hz, C-7), 123.2 (q, J = 4.0 Hz, C-2); δ_{F} (282 MHz, D₆-DMSO) - 62.1 (s); HRMS m/z (ES⁻) 228.0392 ([M-H]⁻, 100%) C₉H₅N₃OF₃ requires 228.0390.

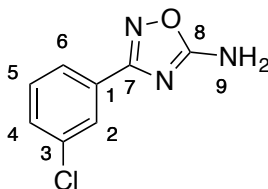
3-(3-Fluorophenyl)-1,2,4-oxadiazol-5-amine **224d**



Oxime **226d** (1 g, 7.2 mmol), was dissolved in DCM (90 mL). The solution was shaken with bleach (18 mL, 1.6 M, 28.8 mmol) for 3 min. The organic layer was separated and added to a solution of cyanamide (1.2 g, 28.8 mmol) in triethylamine (4 mL, 28.8 mmol) and the mixture was stirred for 8 h. The solvent was removed under reduce pressure to give a yellow solid. The product was purified by recrystallisation using ethanol and water, to give the product **224d** as a white solid (928 mg, 72 %): m.p 177-181 °C; $\nu_{\max}/\text{cm}^{-1}$ (nujol) 3342, 3268, 3128, 1685; δ_{H} (300 MHz, D₆-DMSO) 8.01 (2H, s, 9-NH₂), 7.71 (1H, ddd, J = 7.8, 1.2, 1.2 Hz, 6-H), 7.60-7.51 (2H, m, 2,5-H), 7.37 (1H, dddd, J = 9.2, 8.2, 2.5, 0.9 Hz, 4-H); δ_{C} (75 MHz, D₆-DMSO) 172.6 (C-8) 167.0 (d, J = 2.9 Hz, C-7)), 162.5 (d, J = 247.2 Hz, C-3), 131.6 (d, J = 8.3 Hz, C-5), 130.2 (d, J = 8.4 Hz, C-1), 123.1 (d, J = 2.9 Hz, C-6), 118.1 (d, J = 21Hz, C-4), 113.5 (d, J =23.3 Hz, C-2); δ_{F} (282 MHz, D₆-DMSO) -112.7 (1F, dt,

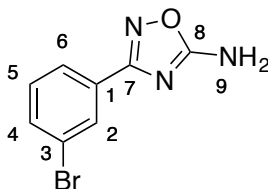
$J = 9.2, 6.0$ Hz); m/z (Cl^+) 180.06 ($[\text{M}+\text{H}]^+$, 100%), 179.05 ($[\text{M}]^+$, 45), 137.05 ($[\text{M}-\text{CN}_2\text{H}_2]^+$, 40); HRMS m/z (Cl^+) 180.0569 ($[\text{M}+\text{H}]^+$, 100%), $\text{C}_8\text{H}_7\text{N}_3\text{OF}$ requires 180.0573.

3-(3-Chlorophenyl)-1,2,4-oxadiazol-5-amine **224e**



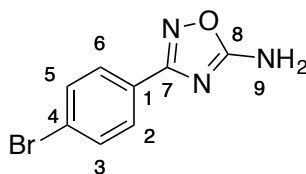
Oxime **226e** (1 g, 6.42 mmol), was dissolved in DCM (65 mL). The solution was shaken with bleach (16 mL, 1.6 M, 25.7 mmol) for 3 min. The organic layer was separated and added to a solution of cyanamide (1.08 g, 25.7 mmol) in triethylamine (3.58 mL, 25.7 mmol) and the mixture was stirred for 8 h. The solvent was removed under reduce pressure to give a yellow solid. The product was purified by recrystallisation using ethanol and water, to give the product **224e** as a white solid (955 mg, 76%): m.p 218-222 °C; $\nu_{\text{max}}/\text{cm}^{-1}$ (nujol) 3254, 3115, 3068, 1685, 1609, 1531; δ_{H} (300 MHz, D_6 -DMSO) 8.03 (2H, s, 9- NH_2), 7.85-7.81 (2H, m, 2,6-H), 7.61 (1H, ddd, $J = 8.1, 2.1, 1.4$ Hz, 4-H), 7.57-7.52 (1H, m, 5-H); δ_{C} (75 MHz, D_6 -DMSO) 172.2 (C-8), 166.4 (C-7), 133.6 (C-3), 131.0 (C-5), 130.7 (C-4), 129.6 (C-1), 126.1 (C-2), 125.2 (C-6); HRMS m/z (ES^-) 194.0125 ($[\text{M}-\text{H}]^-$, 100%) $\text{C}_8\text{H}_5\text{N}_3\text{OCl}$ requires 194.0121.

3-(3-Bromophenyl)-1,2,4-oxadiazol-5-amine **224f**



Oxime **226f** (1 g, 5 mmol), was dissolved in DCM (65 mL). The solution was shaken with bleach (12.5 mL, 1.6 M, 20 mmol) for 3 min. The organic layer was separated and added to a solution of cyanamide (840 mg, 20 mmol) in triethylamine (2.7 mL, 20 mmol) and the mixture was stirred for 8 h. The solvent was removed under reduce pressure to give a yellow solid. The product was purified by recrystallisation using ethanol and water, to give the product **224f** as a white solid (910 mg, 76 %): m.p 222-225 °C; $\nu_{\text{max}}/\text{cm}^{-1}$ (nujol) 3248, 3112, 1683, 1608; δ_{H} (300 MHz, D₆-DMSO) 8.00 (2H, s, 9-NH₂), 7.97-7.95 (1H, m, 2-H), 7.88-7.83 (1H, m, 6-H), 7.72 (1H, ddd, J = 8.0, 2.0, 1.0 Hz, 4-H), 7.46 (1H, m, 5-H); δ_{C} (75 MHz, CDCl₃) 172.2 (C-8), 166.3 (C-7), 133.5 (C-4), 131.2 (C-5), 129.78 (C-3), 129.0 (C-2), 125.5 (C-6), 122.0 (C-1); m/z (Cl⁺) 241.98 ([M⁸¹Br+H]⁺, 90%), 239.98 ([M⁷⁹Br], 100), 198.97 ([M⁸¹Br-CH₂N₂]⁺, 58), 196.97 ([M⁷⁹Br-CH₂N₂]⁺, 55); HRMS m/z (Cl⁺) 239.9768 ([M⁷⁹Br+H]⁺, 100) C₈H₇N₃O⁷⁹Br requires 239.9772.

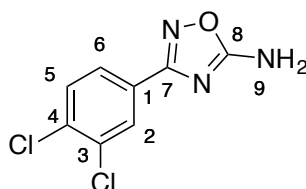
3-(4-Bromophenyl)-1,2,4-oxadiazol-5-amine **224g**



Oxime **226g** (5 g, 30 mmol), was dissolved in DCM (300 mL). The solution was shaken with bleach (75 mL, 1.6 M, 120 mmol) for 3 min. The organic layer was separated and added to a solution of cyanamide (5.05 g, 120 mmol) in triethylamine (4.2 mL, 30 mmol) and the mixture was stirred for 8 h. The solvent was removed under reduce pressure to give a yellow solid. The product was purified by recrystallisation using ethanol and water, to give the product **224g** as a white solid (841 mg, 70%): m.p 250-254 °C; $\nu_{\text{max}}/\text{cm}^{-1}$ (nujol) 3315, 3114, 1672, 1592, 1576; δ_{H} (300 MHz, D₆-DMSO) 7.90 (2H, s, NH₂), 7.80 (2H, d, J = 8.5 Hz, 2-H), 7.71 (2H, d, J = 8.5 Hz, 3-H); δ_{C} (75 MHz, D₆-DMSO) 172.2 (C-6), 166.8 (C-5), 132.0 (C-3), 128.5 (C-2), 126.8 (C-4), 124.2 (C-1); HRMS m/z (ES⁻) 237.9613

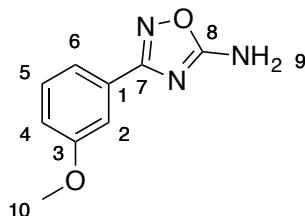
([M⁷⁹Br-H]⁺, 100%) C₈H₅N₃O⁷⁹Br requires 237.9616; 239.9599 ([M⁸¹Br-H]⁺, 81) C₈H₅N₃O⁸¹Br requires 239.9596.

3-(3,4-Dichlorophenyl)-1,2,4-oxadiazol-5-amine **224h**



Oxime **226h** (5 g, 26.3 mmol), was dissolved in DCM (330 mL). The solution was shaken with bleach (66 mL, 1.6 M, 105 mmol) for 3 min. The organic layer was separated and added to a solution of cyanamide (4.42 g, 105 mmol) in triethylamine (14.6 mL, 105 mmol) and the mixture was stirred for 8 h. The solvent was removed under reduce pressure to give a yellow solid. The product was purified by recrystallisation using ethanol and water, to give the product **224h** as a colourless solid (3.01 g, 50 %): m.p 103-107 °C; δ_H (300 MHz, D₆-DMSO) 8.07 (2H, s, 9-NH₂), 7.99 (1H, d, *J*= 1.8 Hz, 2-H), 7.83 (1H, dd, *J*= 8.4, 1.8 Hz, 6-H), 7.78 (1H, d, *J*= 8.4 Hz, 5-H); δ_C (75 MHz, D₆-DMSO) 172.3 (C-8), 165.8 (C-7), 133.4 (C-4), 131.7 (C-3), 131.4 (C-5), 128.1 (C-2), 128.1 (C-1), 126.6 (C-6); HRMS *m/z* (ES⁻) 227.9740 ([M-H]⁻, 100%) C₈H₄N₃OCl₂ requires 227.9731.

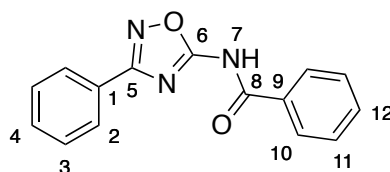
3-(3-Methoxyphenyl)-1,2,4-oxadiazol-5-amine **224i**



Oxime **226i** (1 g, 6.6 mmol), was dissolved in DCM (80 mL). The solution was shaken with bleach (16.5 mL, 1.6 M, 26.5 mmol) for 3 min. The organic layer was separated and added to a solution of cyanamide (1.11 g, 26.5 mmol) in triethylamine (3.7 mL, 26.5 mmol) and the mixture was stirred for 8 h. The solvent

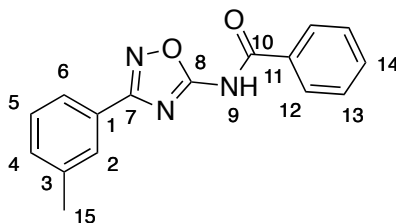
was removed under reduce pressure to give a yellow solid. The product was purified by recrystallisation using ethanol and water, to give the product **224i** as a colourless solid (776 mg, 61%): m.p 187-189 °C; $\nu_{\text{max}}/\text{cm}^{-1}$ (nujol) 3285, 3121, 1678, 1608, 1535; δ_{H} (300 MHz, D₆-DMSO) 7.94 (2H, s, 9-NH₂), 7.46 (1H, ddd, J = 7.6, 1.4, 1.4 Hz, 6-H), 7.42 (1H, d, J = 7.9 Hz, 5-H), 7.39-7.37 (1H, m, 2-H), 7.09 (1H, ddd, J = 7.9, 2.7, 1.4 Hz, 4-H), 3.78 (3H, s, 10-H); δ_{C} (75 MHz, D₆-DMSO) 172.1 (C-8), 167.4 (C-7), 159.4 (C-3), 130.1 (C-5), 128.9 (C-1), 118.8 (C-6), 116.6 (C-4), 111.5 (C-2), 55.1 (C-10); m/z (CI⁺) 192.08 ([M+H]⁺, 100%), 192.07 ([M]⁺, 45), 149.07 ([M-CN₂H₂]⁺, 48); HRMS m/z (CI⁺) 192.0771 ([M+H]⁺, 100%) C₉H₁₀N₃O₂ requires 192.0773.

N-(3-Phenyl-1,2,4-oxadiazol-5-yl)benzamide **228**



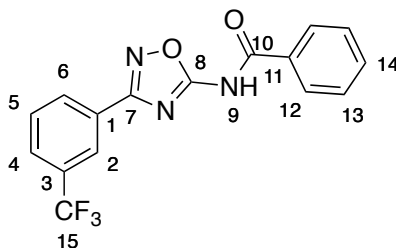
Benzoic acid (208 mg, 1.7 mmol) and DMAP (189 mg, 1.55 mmol) were added to a solution of 5-amino-1,2,4-oxadiazole **224a** (250 mg, 1.55 mmol) in acetonitrile (20 mL). DCC (352 mg, 1.7 mmol) was added and the mixture was stirred for 8 h. The mixture was filtered to remove the urea byproduct. The filtrate was concentrated under reduced pressure to give a yellow oil. The product was purified by column chromatography on silica (10% ethyl acetate/ petroleum ether). The oil was triturated with diethyl ether to give the product **228** as a white solid (198 mg, 48%): m.p 98-100 °C; Anal. RP HPLC: t_{R} 13.18 min (purity 99.97%); $\nu_{\text{max}}/\text{cm}^{-1}$ (nujol) 3499, 1708, 1694, 1557; δ_{H} (300 MHz, D₆-DMSO) 9.79 (1H, br s, NH), 8.00-7.97 (2H, m, Ar-H), 7.96 (2H, dd, J = 2.8, 1.5 Hz, Ar-H), 7.63-7.57 (1H, m), 7.51-7.47 (2H, m, Ar-H), 7.47-7.45 (1H, m, Ar-H), 7.44-7.39 (2H, m, Ar-H); δ_{C} (75 MHz, D₆-DMSO) 162.8 (C-8), 161.2 (C-6), 158.2 (C-5), 128.3 (Ar-H), 126.5 (Ar), 126.1 (Ar-H), 123.8 (Ar-H), 123.5 (Ar-H), 122.7 (Ar-H), 122.2 (Ar-H), 121.1 (Ar); HRMS m/z (ES⁺) 288.0746 C₁₅H₁₁N₃O₂Na requires 288.0749.

N-(3-(*m*-Tolyl)-1,2,4-oxadiazol-5-yl)benzamide **229**



Benzoic acid (191 mg, 1.6 mmol) and DMAP (17 mg, 0.14 mmol) were added to a solution of 5-amino-1,2,4-oxadiazole **224b** (250 mg, 1.4 mmol) in acetonitrile (20 mL). DCC (323 mg, 1.6 mmol) was added and the mixture was stirred for 8 h. The mixture was filtered to remove the urea byproduct. The filtrate was concentrated under reduced pressure to give a yellow oil. The product was purified by column chromatography on silica (15% ethyl acetate/ petroleum ether) to give the product **229** as a white solid (252 mg, 63%): m.p 108-111 °C; Anal. RP HPLC: t_R 16.53 min (purity 99.72%); ν_{max}/cm^{-1} (nujol) 3178, 1695, 1568, 1487; δ_H (300 MHz, D_6 -DMSO) 12.65 (1H, s, NH), 8.02-8.05 (2H, m, 12-H), 7.81-7.77 (2H, m, 2,6-H), 7.69- 7.64 (1H, m, 14-H), 7.58-7.53 (2H, m, 13-H), 7.48-7.41 (1H, m, 4-H), 7.41-7.36 (1H, m, 5-H), 2.39 (3H, s, 15-H); δ_C (75 MHz, D_6 -DMSO) 167.8 (C-7), 167.8 (C-8), 164.8 (C-10), 138.9 (C-3), 133.5 (C-14), 132.6 (C-5), 132.5 (C-11), 129.5 (C-4), 129.0 (C-12), 128.9 (C-13), 127.6 (C-2), 126. 7 (C-1), 124.4 (C-6), 21.3 (C-15); HRMS m/z (ES^+) 302.0897 ($[M+Na]^+$, 100%) $C_{16}H_{13}N_3O_2Na$ requires 302.0905.

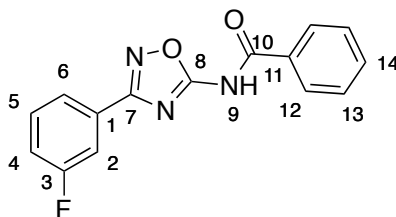
N-(3-(3-(Trifluoromethyl)phenyl)-1,2,4-oxadiazol-5-yl)benzamide **230**



Benzoic acid (147 mg, 1.2 mmol) and DMAP (133 mg, 1.09 mmol) were added to a solution of 5-amino-1,2,4-oxadiazole **224c** (250 mg, 1.09 mmol) in acetonitrile (20

mL). DCC (247 mg, 1.2 mmol) was added and the mixture was stirred for 8 h. The mixture was filtered to remove the urea byproduct. The filtrate was concentrated under reduced pressure to give a yellow oil. The product was purified by column chromatography on silica (15% ethyl acetate/ petroleum ether) to give the product **230** as a white solid (125 mg, 34%): m.p 130-132 °C; $\nu_{\text{max}}/\text{cm}^{-1}$ (nujol) 3246, 3170, 1708, 1629, 1616; δ_{H} (300 MHz, D₆-DMSO) 12.76 (1H, s, NH), 8.31 (1H, d, J = 7.8 Hz, 6-H), 8.25-8.23 (1H, m, 2-H), 8.07-8.03 (2H, m, 12-H), 8.02-8.00 (1H, m, 4-H) 7.89-7.82 (1H, m, 5-H), 7.72-7.67 (1H, m, 14-H), 7.61-7.55 (2H, m, 13-H); δ_{C} (75 MHz, D₆-DMSO) 167.9 (C-8), 166.3 (C-7), 164.3 (C-10), 133.2 (C-14), 132.1 (C-11), 130.7 (C-6,5), 129.9 (d, J = 32.2 Hz, C-3), 128.7 (C-13), 128.5 (C-12), 128.2-128.1 (m, C-4), 127.5 (C-1), 123.2-123.0 (m, C-2), 123.7 (d, J = 271 Hz, C-15); δ_{F} (376 MHz, D₆-DMSO) -61.52 (s); HRMS m/z (ES⁺) 356.0611 ([M+Na]⁺, 100%) C₁₆H₁₀N₃O₂F₃Na requires 356.0618.

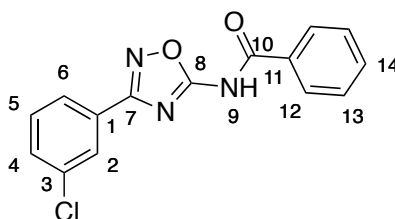
N-(3-(3-Fluorophenyl)-1,2,4-oxadiazol-5-yl)benzamide **231**



Benzoic acid (188 mg, 1.5 mmol) and DMAP (17 mg, 0.14 mmol) were added to a solution of 5-amino-1,2,4-oxadiazole **224d** (250 mg, 1.4 mmol), in acetonitrile (20 mL). DCC (317 mg, 1.5 mmol) was added and the mixture was stirred for 8 h. The mixture was filtered to remove the urea byproduct. The filtrate was concentrated under reduced pressure to give a yellow oil. The product was purified by column chromatography on silica (15% ethyl acetate/petroleum ether to 20% ethyl acetate/petroleum ether) to give the product **231** as a white solid (211 mg, 53 %): m.p 108-110 °C; Anal. RP HPLC: t_{R} 15.19 min, (purity 98.25%); $\nu_{\text{max}}/\text{cm}^{-1}$ (nujol) 3515, 3456, 1700; δ_{H} (300 MHz, D₆-DMSO) 12.73 (1H, s, NH), 8.05-8.02 (2H, m, 12-H), 7.85 (1H, dd, J = 7.7, 1.3, 1.2 Hz, 6-H), 7.71 (1H, ddd, J = 9.6, 2.7, 1.3 Hz, 2-

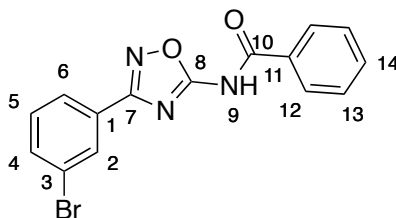
H), 7.68 (1H, t, J = 2.2 Hz, 14-H), 7.64 (1H, dd, J = 8.2, 1.8 Hz, 5-H) 7.60-7.54 (2H, m, 13-H), 7.5-7.43 (1H, m, 4-H); δ_{C} (75 MHz, DMSO- d_6) 168.1 (C-8), 166.9 (d, J = 2.9 Hz, C-7), 164.8 (C-10), 162.6 (d, J = 245.2 Hz, C-3), 133.6 (C-14), 132.5 (C-11), 132.0 (d, J = 8.4 Hz, C-5), 129.0 (C-13), 128.9 (C-12), 123.5 (d, J = 2.9 Hz, C-6), 118.9 (d, J = 21.0 Hz, C-4), 113.8 (d, J = 23.4 Hz, C-2); δ_{F} (282 MHz, D_6 -DMSO) -112.2 (1F, td, J = 9.2, 6.0 Hz); HRMS m/z (ES^+) 306.0659 ($[\text{M}+\text{Na}]^+$, 100%) $\text{C}_{15}\text{H}_{10}\text{N}_3\text{O}_2\text{FNa}$ requires 306.0655.

N-(3-(3-Chlorophenyl)-1,2,4-oxadiazol-5-yl)benzamide **232**



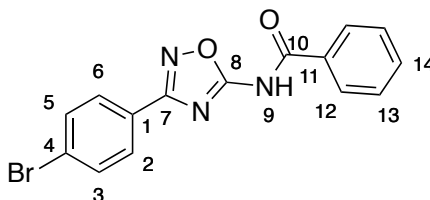
Benzoic acid (171 mg, 1.4 mmol) and DMAP (16 mg, 0.14 mmol) were added to a solution of 5-amino-1,2,4-oxadiazole **234e** (250 mg, 1.3 mmol) in acetonitrile (20 mL). DCC (290 mg, 1.4 mmol) was added and the mixture was stirred for 8 h. The mixture was filtered to remove the urea byproduct. The filtrate was concentrated under reduced pressure to give a yellow oil. The product was purified by column chromatography on silica (15% ethyl acetate/petroleum ether) to give the product **232** as a colourless solid (136 mg, 35%): m.p 94-99 °C; $\nu_{\text{max}}/\text{cm}^{-1}$ (nujol) 3301, 3233, 3158, 1706, 1624, 1536, 1250; δ_{H} (300 MHz, D_6 -DMSO) 12.72 (1H, s, NH), 8.05- 8.02 (2H, m, 12-H), 7.96 (1H, dd, J = 3.3, 1.7 Hz, 2-H), 7.94 (1H, dd, J = 2.7, 1.3 Hz, 6-H), 7.65-7.70 (2H, m, 4,11-H), 7.64-7.61 (1H, m, 5-H), 7.57 (2H, dd, J = 6.6, 1.2 Hz, 13-H); δ_{C} (75 MHz, D_6 -DMSO) 168.1 (C-8), 166.7 (C-7), 164.8 (C-10), 134.2 (C-3), 133.6 (C-11), 132.5 (C-1), 131.8 (C-4), 131.7 (C-5), 129.0 (C-13), 128.9 (C-12), 128.8 (C-14), 126.8 (C-2), 125.9 (C-6); HRMS m/z (ES^+) 322.0359 ($[\text{M}+\text{Na}]^+$, 100%), $\text{C}_{15}\text{H}_{10}\text{N}_3\text{O}_2\text{ClNa}$ requires 322.0359.

N-(3-(3-Bromophenyl)-1,2,4-oxadiazol-5-yl)benzamide **233**



Benzoic acid (128 mg, 1.14 mmol) and DMAP (127 mg, 1.04 mmol) were added to a solution of 5-amino-1,2,4-oxadiazole **224f** (250 mg, 1.04 mmol) in acetonitrile (50 mL). DCC (236 mg, 1.14 mmol) was added and the mixture was stirred for 8 h. The mixture was filtered to remove the urea byproduct. The filtrate was concentrated under reduced pressure to give a yellow oil. The product was purified by column chromatography on silica (15% ethyl acetate/petroleum ether) to give the product **233** as a colourless solid (51 mg, 14.2%): m.p 140-144 °C; Anal. RP HPLC: t_R 19.41 min (purity 99.41%); $\nu_{\max}/\text{cm}^{-1}$ (nujol) 3281, 1700, 1598, 1539; δ_H (300 MHz, D_6 -DMSO) 12.72 (1H, s, 9-NH), 8.09 (1H, ddd, J = 2.0, 1.6, 0.4 Hz, 2-H), 8.05-8.01 (2H, m, 12-H), 7.99 (1H, ddd, J = 7.8, 1.6, 1.1 Hz, 4-H), 7.82 (1H, ddd, J = 8.1, 2.0, 1.1 Hz, 6-H), 7.71-7.65 (1H, m, 14-H), 7.60-7.52 (3H, m, 5,13-H); δ_C (75 MHz, D_6 -DMSO) 168.1 (C-7), 166.6 (C-10), 164.7 (C-8), 134.7 (C-4), 133.5 (C-14), 132.5 (C-11), 131.9 (C-5), 129.6 (C-2), 129.0 (C-13), 129.0 (C-3), 128.9 (C-12), 126.2 (C-6), 122.6 (C-1); HRMS m/z (ES⁻) 341.9885 ($[M^{79}\text{Br-H}]^+$, 100%) $C_{15}H_9N_3O_2^{79}\text{Br}$ requires 341.9878; 343.9858 ($[M^{81}\text{Br-H}]^+$, 95) $C_{15}H_9N_3O_2^{81}\text{Br}$ requires 343.9853.

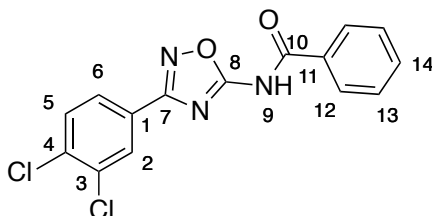
N-(3-(4-Bromophenyl)-1,2,4-oxadiazol-5-yl)benzamide **234**



Benzoic acid (128 mg, 1.14 mmol) and DMAP (127 mg, 1.04 mmol) were added to a solution of 5-amino-1,2,4-oxadiazole **224g** (250 mg, 1.04 mmol) in acetonitrile (20

mL). DCC (236 mg, 1.14 mmol) was added and the mixture was stirred for 8 h. The mixture was filtered to remove the urea byproduct. The filtrate was concentrated under reduced pressure to give a yellow oil. The product was purified by column chromatography on silica (12.5% ethyl acetate/ petroleum ether) to give the product **234** as a white solid (45 mg, 12.6%): m.p 118-120 °C; Anal. RP HPLC: t_R 20.05 min (purity 98.27%); $\nu_{\max}/\text{cm}^{-1}$ (nujol) 3508, 3466, 1700, 1573; δ_H (300 MHz, D_6 -DMSO) 12.71 (1H, s, NH), 8.06-8.02 (2H, m, 9-H), 7.94 (2H, d, J = 8.8 Hz, 2-H), 7.80 (2H, d, J = 8.8 Hz, 3-H), 7.72-7.66 (1H, m, 11-H), 7.60-7.55 (2H, m, 10-H); δ_C (75 MHz, D_6 -DMSO) 168.1 (C-6), 167.1 (C-5), 164.8 (C-8), 133.5 (C-11), 132.7 (C-3), 132.5 (C-12), 129.2 (C-10), 129.0 (C-2), 128.9 (C-9), 126.0 (C-4), 125.5 (C-1); m/z (ES^-) 341.9879 ($[M-H]^-$, 100%) $C_{15}H_9N_3O_2Br$ requires 341.9884.

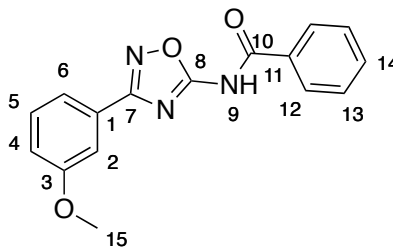
N-(3-(3,4-Dichlorophenyl)-1,2,4-oxadiazol-5-yl)benzamide **235**



Benzoic acid (145 mg, 1.2 mmol) and DMAP (132 mg, 1.09 mmol) were added to a solution of 5-amino-1,2,4-oxadiazole **224h** (250 mg, 1.09 mmol) in acetonitrile (20 mL). DCC (g, mmol) was added and the mixture was stirred for 8 h. The mixture was filtered to remove the urea byproduct. The filtrate was concentrated under reduced pressure to give a yellow oil. The product was purified by column chromatography on silica (15% ethyl acetate/petroleum ether) to give the product **235** as a colourless solid (57 mg, 16%): m.p 134-136 °C; $\nu_{\max}/\text{cm}^{-1}$ (nujol) 3182, 1707, 1651, 1586; δ_H (300 MHz, D_6 -DMSO) 12.74 (1H, s, NH), 8.13 (1H, d, J = 1.9 Hz, 2-H), 8.04 (2H, dt, J = 8.3, 1.6 Hz, 13-H), 7.96 (1H, dd, J = 8.4, 1.9 Hz, 6-H), 7.87 (1H, d, J = 8.4 Hz, 5-H), 7.72-7.66 (1H, m, 14-H), 7.58 (2H, td, J = 7.4, 1.2 Hz, 12-H); δ_C (75 MHz, D_6 -DMSO) 167.9 (C-9), 165.7 (C-7), 164.4 (C-8), 134.3 (C-1), 133.2 (C-13), 132.1 (C-10), 132.1 (C-4), 131.7 (C-5), 128.6 (C-12), 128.5 (C-11),

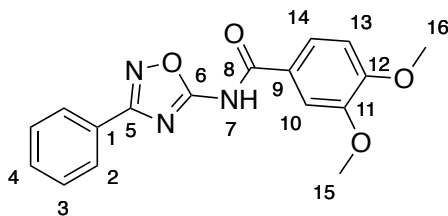
128.4 (C-2), 127.0 (C-6), 126.9 (C-3); HRMS m/z (ES^+) 355.9968 ($[M+Na]^+$, 100%) $C_{15}H_9Cl_2N_3O_2Na$ requires 355.9970.

N-(3-(3-Methoxyphenyl)-1,2,4-oxadiazol-5-yl)benzamide **236**



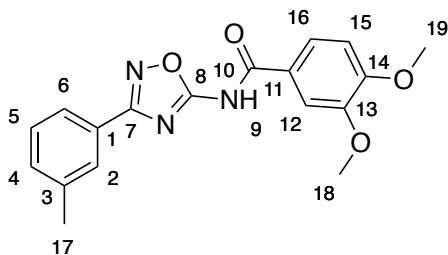
Benzoic acid (175 mg, 1.4 mmol) and DMAP (16 mg, 0.13 mmol) were added to a solution of 5-amino-1,2,4-oxadiazole **224i** (250 mg, 1.3 mmol) in acetonitrile (20 mL). DCC (297 mg, 1.4 mmol) was added and the mixture was stirred for 8 h. The mixture was filtered to remove the urea byproduct. The filtrate was concentrated under reduced pressure to give a yellow oil. The product was purified by column chromatography on silica (15% ethyl acetate/petroleum ether) to give the product **236** as a colourless solid (90 mg, 23 %): m.p 110-114 °C; Anal. RP HPLC: t_R 14.68 min (purity 99.02%); ν_{max}/cm^{-1} (nujol) 3505, 3438, 1695, 1562; δ_H (300 MHz, D_6 -DMSO) 8.06-8.03 (2H, m, 12-H), 7.71-7.65 (1H, m, 14-H), 7.61-7.54 (3H, m, 6,13-H), 7.52-7.47 (2H, m, 2,5-H), 7.17 (1H, ddd, J = 8.2, 2.7, 1.0 Hz, 4-H), 3.84 (3H, s, 15-H); δ_C (75 MHz, D_6 -DMSO) 167.6 (C-8), 167.2 (C-7), 164.5 (C-10), 159.6 (C-3), 133.1 (C-14), 132.2 (C-11), 130.5 (C-5), 128.6 (C-13), 128.5 (C-12), 127.7 (C-1), 119.1 (C-6), 117.4 (C-4), 111.7 (C-2), 55.3 (C-15); HRMS m/z (ES^+) 318.0857 ($[M+Na]^+$, 100%) $C_{16}H_{13}N_3O_3Na$ requires 318.0855.

3,4-Dimethoxy-*N*-(3-phenyl-1,2,4-oxadiazol-5-yl)benzamide **238**



3,4-Dimethoxybenzoic acid (310 mg, 1.7 mmol) and DMAP (182 mg, 1.55 mmol) were added to a solution of 5-amino-1,2,4-oxadiazole **224a** (250 mg, 1.55 mmol) in acetonitrile (20 mL). DCC (352 mg, 1.7 mmol) was added and the mixture was stirred for 8 h. The mixture was filtered to remove the urea byproduct. The filtrate was concentrated under reduced pressure to give a yellow oil. The product was purified by column chromatography on silica (25% ethyl acetate/ petroleum ether to 30% ethyl acetate/petroleum ether) to give the product **238** as a colourless solid (216 mg, 43%): m.p 110-115 °C; Anal. RP HPLC: t_R 12.56 min (purity 96.00%); ν_{max}/cm^{-1} (nujol) 3562, 3410, 1709, 1627, 1550; δ_H (300 MHz, D_6 -DMSO) 12.51 (1H, s, NH), 8.02-7.99 (2H, m, 2-H), 7.74 (1H, dd, $J=8.5, 2.2$ Hz, 14-H), 7.67 (1H, d, $J= 2.2$ Hz, 10-H), 7.62-7.56 (3H, m, 3,4-H), 7.13 (1H, d, $J= 8.5$ Hz, 13-H), 3.86 (6H, OMe); δ_C (75 MHz, D_6 -DMSO) 167.7 (C-6), 167.2 (C-5), 163.5 (C-8), 152.9 (C-OMe), 148.3 (C-OMe), 131.5 (C-4), 129.2 (C-3), 126.8 (C-2), 126.5 (C-1), 123.9 (C-9), 122.6 (C-14), 111.3 (C-10), 111.1 (C-13), 55.8 (OMe), 55.7 (OMe); HRMS m/z (ES⁺) 348.0949 ($[M+Na]^+$, 100%) $C_{17}H_{15}O_4N_3Na$ requires 348.0955.

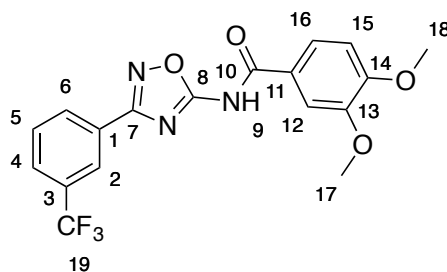
3,4-Dimethoxy-*N*-(3-(*m*-tolyl)-1,2,4-oxadiazol-5-yl)benzamide **239**



3,4-Dimethoxybenzoic acid (285 mg, 1.6 mmol) and DMAP (174 mg, 1.4 mmol) were added to a solution of 5-amino-1,2,4-oxadiazole **224b** (250 mg, 1.4 mmol) in

DCM (20 mL). EDCI (410 mg, 2.1 mmol) was added and the mixture was stirred for 8 h. The mixture was washed with hydrochloric acid (2 M, 40 mL). The aqueous layer was washed with DCM (3 × 20 mL) and the organic fractions were combined and dried with magnesium sulfate. The solvent was removed under reduced pressure to give a yellow oil. The product was purified by column chromatography on silica (20% ethyl acetate/petroleum ether to 25% ethyl acetate/petroleum ether) to give the product **239** as a colourless solid (365 mg, 76%): m.p 167-170 °C; $\nu_{\text{max}}/\text{cm}^{-1}$ (nujol) 3200, 1772, 1685, 1514; δ_{H} (300 MHz, D₆-DMSO) 12.49 (1H, s, NH), 7.81-7.77 (2H, m, 2,6-H), 7.72 (1H, dd, J = 8.5, 1.8 Hz, 16-H), 7.65 (1H, d, J = 1.8 Hz, 12-H), 7.48-7.37 (2H, m, 4,5-H), 7.11 (1H, d, J = 8.5 Hz, 15-H) 3.84 (6H, s, OMe), 2.40 (3H, s, Me); δ_{C} (75 MHz, D₆-DMSO) 168.0 (C-8), 167.7 (C-7), 163.9 (C-10), 153.2 (C-OMe), 148.7 (C-OMe), 138.9 (C-3), 132.5 (C-4), 129.5 (C-5), 127.6 (C-2), 126.8 (C-1), 124.4 (C-6), 124.3 (C-11), 123.0 (C-16), 111.7 (C-12), 111.5 (C-15), 56.1 (OMe), 56.0 (OMe), 21.3 (C-17); HRMS m/z (ES⁺) 362.1120 ([M+Na]⁺, 100%) C₁₈H₁₇N₃O₄Na requires 362.1117.

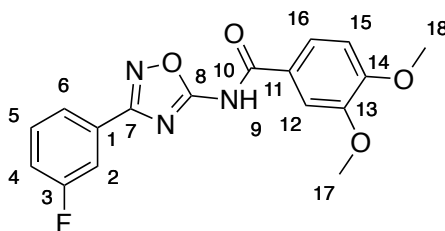
3,4-Dimethoxy-*N*-(3-(3-(trifluoromethyl)phenyl)-1,2,4-oxadiazol-5-yl)benzamide **240**



3,4-Dimethoxybenzoic acid (262 mg, 1.4 mmol) and DMAP (80 mg, 0.65 mmol) were added to a solution of 5-amino-1,2,4-oxadiazole **244c** (300 mg, 1.3 mmol) in DCM (20 mL). EDCI (376 mg, 1.96 mmol) was added and the mixture was stirred for 8 h. The mixture was washed with hydrochloric acid (2 M, 40 mL). The aqueous layer was washed with DCM (3 × 20 mL) and the organic layers were combined and dried with magnesium sulfate. The solvent was removed under reduced pressure to give a yellow oil. This oil was purified by column chromatography on silica (20% ethyl acetate/ petroleum ether to 30% ethyl acetate/ petroleum ether) to

give the product **240** as a white solid (338 mg, 66%): m.p 166-170 °C; $\nu_{\text{max}}/\text{cm}^{-1}$ (nujol) 3269, 1695, 1559; δ_{H} (300 MHz, D₆-DMSO) 12.56 (1H, s, 9-NH), 8.30-8.27 (1H, m, 6-H), 8.24-8.21 (1H, m, 2-H), 8.01-7.98 (1H, m, 4-H), 7.87-7.80 (1H, m, 5-H), 7.72 (1H, dd, J = 8.6, 2.1 Hz, 16-H), 7.65 (1H, d, J = 2.1 Hz, 12-H), 7.12 (1H, d, J = 8.6 Hz, 15-H), 3.85 (6H, s, OMe); δ_{C} (75 MHz, D₆-DMSO) 168.4 (C-8), 166.6 (C-7), 163.8 (C-10), 153.3 (C-OMe), 148.7 (C-OMe), 131.1-131.0 (m, C-5,6), 130.5 (C-1), 130.4 (d, J = 32.3 MHz, C-3), 127.9 (C-4), 124.2 (C-11), 123.6- 123.4 (m, C-2), 123.0 (C-16), 111.7 (C-12), 111.5 (C-15), 56.2 (OMe), 56.0 (OMe); δ_{F} (282 MHz, D₆-DMSO) -61.56 (s); HRMS m/z (ES⁺) 416.0838 ([M+Na]⁺, 100%) C₁₈H₁₄N₃O₄F₃Na requires 416.0834.

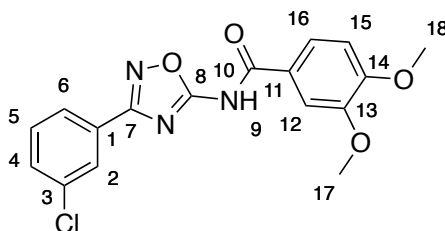
N-(3-(3-Fluorophenyl)-1,2,4-oxadiazol-5-yl)-3,4-dimethoxybenzamide **241**



3,4-Dimethoxybenzoic acid (336 mg, 1.8 mmol) and DMAP (20 mg, 0.16 mmol) were added to a solution of 5-amino-1,2,4-oxadiazole **224d** (300 mg, 1.7 mmol) in DCM (20 mL). EDCI (353 mg, 1.8 mmol) was added and the mixture was stirred for 8 h. The mixture was washed with hydrochloric acid (2 M, 40 mL). The aqueous layer was washed with DCM (3 × 20 mL) and the organic fractions were combined and dried with magnesium sulfate. The solvent was removed under reduced pressure to give a yellow oil. This oil was purified by column chromatography on silica (25% ethyl acetate/petroleum ether to 30% ethyl acetate/petroleum ether) to give the product **241** as a colourless solid (133 mg, 23%): m.p 114-118 °C; $\nu_{\text{max}}/\text{cm}^{-1}$ (nujol) 3494, 3204, 1703, 1461; δ_{H} (300 MHz, D₆-DMSO) 12.55 (1H, s, NH), 7.84 (1H, ddd, J = 7.7, 1.4, 1.0 Hz, 6-H), 7.74-7.66 (2H, m, 2,16-H) 7.66-7.60 (2H, m, 5,12-H), 7.50-7.43 (1H, m, 4-H) 7.12 (1H, d, J = 8.6 Hz, 15-H), 3.85 (6H, s, OMe); δ_{C} (75 MHz, D₆-DMSO) 168.3 (C-8), 164.2 (C-7), 163.9 (C-10) 153.3 (C-

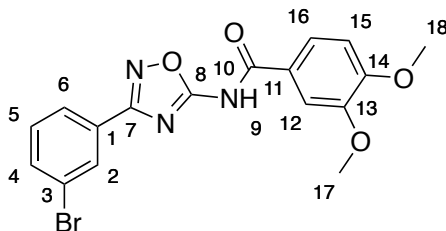
OMe), 148.7 (C-OMe), 132.0 (d, $J = 8.5$ Hz, C-5), 129.1 (1), 129.0 (11), 123.4 (d, $J = 3.1$ Hz, C-6), 123.0 (C-16), 119.0 (C-4), 113.8 (d, $J = 23.2$ Hz, C-2), 111.7 (C-15), 111.5 (C-12), 56.2 (OMe), 56.0 (OMe); δ_F (282 MHz, D_6 -DMSO) -111.67 (1F, td, $J = 9.1, 5.8$ Hz); HRMS m/z (Cl^+) 344.1042 ($[M+H]^+$, 20%), $C_{17}H_{15}N_3O_4F$ requires 344.1047.

N-(3-(3-Chlorophenyl)-1,2,4-oxadiazol-5-yl)-3,4-dimethoxybenzamide **242**



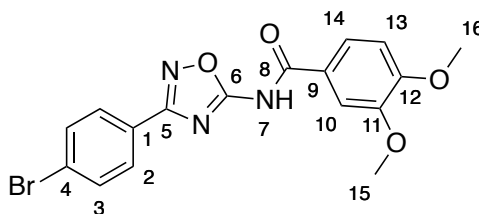
3,4-Dimethoxybenzoic acid (307 mg, 1.7 mmol) and DMAP (93 mg, 0.75 mmol) were added to a solution of 5-amino-1,2,4-oxadiazole **224e** (300 mg, 1.5 mmol) in DCM (20 mL). EDCI (441 mg, 2.3 mmol) was added and the mixture was stirred for 8 h. The mixture was washed with hydrochloric acid (2 M, 40 mL). The aqueous layer was washed with DCM (3 \times 20 mL) and the organic layers were combined and dried with magnesium sulfate. The solvent was removed under reduced pressure to give a yellow oil. This oil was purified by column chromatography on silica (20% ethyl acetate/ petroleum ether to 30% ethyl acetate/ petroleum ether) to give the product **242** as a white solid (348 mg, 63%): m.p 119-122 $^{\circ}C$; ν_{max}/cm^{-1} (nujol) 3279, 1691, 1599, 1539, 1506; δ_H (300 MHz, D_6 -DMSO) 12.55 (1H, s, 9-NH), 7.98-7.95 (2H, m, 2,6-H), 7.75-7.68 (2H, m, 4,16-H), 7.66-7.60 (2H, m, 5,12-H), 7.13 (1H, d, $J = 8.6$ Hz, 15-H), 3.85 (6H, s, OMe); δ_C (75 MHz, D_6 -DMSO) 168.0 (C-8), 166.2 (C-7), 163.5 (C-10), 152.9 (C-OMe), 148.3 (C-OMe), 133.8 (C-3), 131.4 (C-4), 131.3 (C-5), 128.5 (C-1), 126.4 (C-6), 125.5 (C-2), 123.9 (C-11), 122.7 (C-16), 111.4 (C-12), 111.1 (C-15), 55.8 (OMe), 55.7 (OMe); HRMS m/z (ES^+) 382.0567 ($[M+Na]^+$, 100%) $C_{17}H_{14}N_3O_4ClNa$ requires 382.0571.

N-(3-(3-Bromophenyl)-1,2,4-oxadiazol-5-yl)-3,4-dimethoxybenzamide **243**



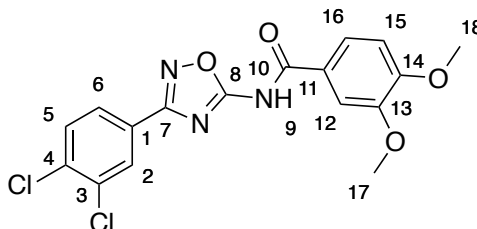
3,4-Dimethoxybenzoic acid (250 mg, 1.4 mmol) and DMAP (76 mg, 0.6 mmol) were added to a solution of 5-amino-1,2,4-oxadiazole **224f** (300 mg, 1.2 mmol) in DCM (20 mL). EDCI (264 g, 1.4 mmol) was added and the mixture was stirred for 8 h. The mixture was washed with hydrochloric acid (2 M, 40 mL). The aqueous layer was washed with DCM (3 × 20 mL) and the organic fractions were combined and dried with magnesium sulfate. The solvent was removed under reduced pressure to give a yellow oil. This oil was purified by column chromatography on silica (25% ethyl acetate/petroleum ether to 30% ethyl acetate/petroleum ether) to give the product **243** as a white solid (198 mg, 41%): m.p 138-142 °C; $\nu_{\text{max}}/\text{cm}^{-1}$ (nujol) 3231, 3176, 1770, 1684; δ_{H} (300 MHz, D_6 -DMSO) 12.54 (1H, s, NH), 8.13-8.10 (1H, m, 2-H), 8.00 (1H, ddd, J = 7.8, 1.5, 1.1 Hz, 4-H), 7.83 (1H, ddd, J = 8.1, 2.1, 1.1 Hz, 6-H), 7.73 (1H, dd, J = 8.6, 2.1 Hz, 16-H), 7.66 (1H, d, J = 2.1 Hz, 12-H), 7.60-7.53 (1H, m, 5-H), 7.14 (1H, d, J = 8.6 Hz, 15-H), 3.86 (6H, s, OMe); δ_{C} (75 MHz, D_6 -DMSO) 167.9 (C-8), 166.1 (C-7), 163.4 (C-10), 152.9 (C-OMe), 148.3 (C-OMe), 134.6 (C-6), 131.8 (C-5), 131.5 (C-1), 129.2 (C-2), 125.8 (C-4), 123.9 (C-11), 122.6 (C-16), 122.2 (C-3), 111.4 (C-12), 111.1 (C-15), 55.8 (OMe), 55.7 (OMe); HRMS m/z (ES^+) 426.0067 ($[\text{M}+\text{Na}]^+$, 100%) $\text{C}_{17}\text{H}_{14}\text{N}_3\text{O}_4\text{Na}^{79}\text{Br}$ requires 426.0065.

N-(3-(4-Bromophenyl)-1,2,4-oxadiazol-5-yl)-3,4-dimethoxybenzamide **244**



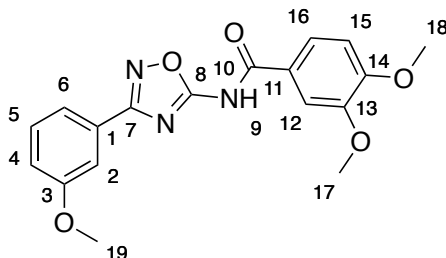
3,4-dimethoxybenzoic acid (209 mg, 1.14 mmol) and DMAP (127 mg, 1.04 mmol) were added to a solution of 5-amino-1,2,4-oxadiazole **224g** (250 mg, 1.04 mmol) in DCM (20 mL). EDCI (300 mg, 1.56 mmol) was added and the mixture was stirred for 8 h. The mixture was washed with hydrochloric acid (2 M, 40 mL). The aqueous layer was washed with DCM (3 × 20 mL) and the organic layers were combined and dried with magnesium sulfate. The solvent was removed under reduced pressure to give a yellow oil. This oil was purified by column chromatography on silica (20% ethyl acetate/petroleum ether to 30% ethyl acetate/petroleum ether) to give the product **244** a white solid (298 mg, 71%); m.p 140-144 °C; Anal. RP HPLC: t_R 19.43 min (99.52%); $\nu_{\max}/\text{cm}^{-1}$ (nujol) 3545, 3434, 1713, 1629, 1600, 1552; δ_H (300 MHz, D_6 -DMSO) 12.49 (1H, br s, 9-NH), 7.92 (2H, d, J = 8.6 Hz, 2-H), 7.78 (2H, d, J = 8.6 Hz, 3-H), 7.71 (1H, dd, J = 8.6, 2.1 Hz, 14-H), 7.64 (1H, d, J = 2.1 Hz, 10-H), 7.11 (1H, d, J = 8.6 Hz, 13-H), 3.83 (6H, s, OMe); δ_C (75 MHz, D_6 -DMSO) 167.9 (C-5), 166.6 (C-6), 163.5 (C-8), 152.9 (C-OMe), 148.3 (C-OMe), 132.3 (C-3), 128.8 (C-2), 125.7 (C-4), 125.0 (C-1), 123.9 (C-9), 122.6 (C-14), 111.4 (C-10), 111.1 (C-13), 55.8 (OMe), 55.7 (OMe); m/z (ES^+) 427.77 ($[M^{81}Br+Na]^+$, 90%), 425.77 ($[M^{79}Br+Na]^+$, 100); HRMS m/z (ES^+) 426.0059 ($[M+Na]^+$, 100), $C_{17}H_{14}N_3O_4BrNa$ requires 426.0065.

N-(3-(3,4-Dichlorophenyl)-1,2,4-oxadiazol-5-yl)-3,4-dimethoxybenzamide **245**



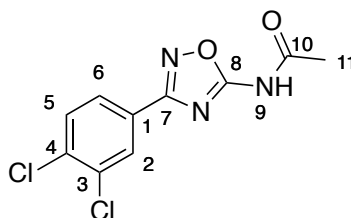
3,4-Dimethoxybenzoic acid (261 mg, 1.4 mmol) and DMAP (16 mg, 0.13 mmol) were added to a solution of 5-amino-1,2,4-oxadiazole **224h** (300 mg, 1.3 mmol) in DCM (20 mL). EDCI (275 mg, 1.4 mmol) was added and the mixture was stirred for 8 h. The mixture was washed with hydrochloric acid (2 M, 40 mL). The aqueous layer was washed with DCM (3 × 20 mL) and the organic layer was dried with magnesium sulfate. The solvent was removed under reduced pressure to give a yellow oil. This oil was purified by column chromatography on silica (25% ethyl acetate/petroleum ether) to give the product **245** as a colourless solid (90 mg, 18%): m.p 178-180 °C; Anal. RP HPLC: t_R 24.15 min (purity 96.68%); $\nu_{\max}/\text{cm}^{-1}$ (nujol) 3412 (NH), 1692, 1661, 1625; δ_H (300 MHz, D_6 -DMSO) 12.55 (1H, s, 9-NH), 8.10 (1H, d, J = 1.9 Hz, 2-H), 7.93 (1H, dd, J = 8.4, 1.9 Hz, 6-H), 7.85 (1H, d, J = 8.4 Hz, 5-H), 7.71 (1H, dd, J = 8.5, 2.1 Hz, 12-H), 7.63 (1H, d, J = 2.1 Hz, 16-H), 7.11 (1H, d, J = 8.5 Hz, 13-H), 3.84 (6H, s, OMe); δ_C (75 MHz, D_6 -DMSO) 168.1 (C-8), 165.6 (C-7), 163.5 (C-10), 152.9 (C-15), 148.3 (C-14), 134.2 (C-4), 132.1 (C-3), 131.7 (C-5), 128.4 (C-2), 127.1 (C-1), 126.9 (C-6), 122.6 (C-12), 111.4 (C-16), 111.1 (C-13), 55.8 (OMe), 55.6 (OMe); HRMS m/z (ES^-) 392.0199 ($[M-H]^-$, 100%) $C_{17}H_{12}N_3O_4Cl_2$ requires 392.0205.

3,4-Dimethoxy-*N*-(3-(3-methoxyphenyl)-1,2,4-oxadiazol-5-yl)benzamide **246**



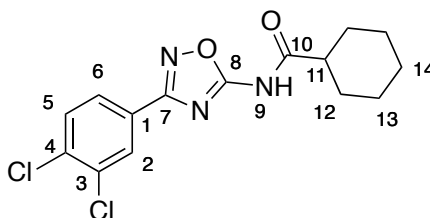
3,4-Dimethoxybenzoic acid (314 mg, 1.7 mmol) and DMAP (95 mg, 0.78 mmol) were added to a solution of 5-amino-1,2,4-oxadiazole **224i** (300 mg, 1.6 mmol) in DCM (20 mL). EDCI (451 mg, 2.3 mmol) was added and the mixture was stirred for 8 h. The mixture was washed with hydrochloric acid (2 M, 40 mL). The aqueous layer was washed with DCM (3 × 20 mL) and the organic layers were combined and dried with magnesium sulfate. The solvent was removed under reduced pressure to give a yellow oil. This oil was purified by column chromatography on silica (20% ethyl acetate/petroleum ether to 30% ethyl acetate/petroleum ether) to give the product **246** as a white solid (130 mg, 23%): m.p 100-104 °C; $\nu_{\text{max}}/\text{cm}^{-1}$ (nujol mull) 3500, 3428, 1693, 1568; δ_{H} (300 MHz, D_6 -DMSO) 12.50 (1H, s, 9-NH), 7.74 (1H, dd, J = 8.5, 2.1 Hz, 16-H), 7.67 (1H, d, J = 2.1 Hz, 12-H), 7.59 (1H, ddd, J = 7.7, 1.1, 1.1 Hz, 6-H), 7.52-7.47 (2H, m, 2,5-H), 7.18 (1H, ddd, J = 8.2, 2.7, 1.1 Hz, 4-H), 7.13 (1H, d, J = 8.5, Hz, 15-H), 3.86 (6H, s, OMe), 3.84 (3H, s, OMe); δ_{C} (75 MHz, D_6 -DMSO) 167.7 (C-7), 167.1 (C-8), 163.5 (C-10), 159.6 (C-3), 152.9 (C-14), 148.3 (C-13), 130.5 (C-5), 127.7 (C-1), 123.9 (C-11), 122.6 (C-16), 119.1 (C-6), 117.4 (C-4), 111.6 (C-2), 111.4 (C-12), 111.1 (C-15), 55.8 (OMe), 55.7 (OMe), 55.3 (OMe); HRMS m/z (ES^+) 378.1072 ($[\text{M}+\text{Na}]^+$, 100%) $\text{C}_{18}\text{H}_{17}\text{N}_3\text{O}_5\text{Na}$ requires 378.1066.

N-(3-(3,4-Dichlorophenyl)-1,2,4-oxadiazol-5-yl)acetamide **247**



DMAP (238 mg, 1.9 mmol) and acetic anhydride (183 μ l, 1.9 mmol) were added to a solution of 5-amino-1,2,4-oxadiazole **224h** (300 mg, 1.3 mmol) in toluene. The mixture was heated under reflux for 16 h. DCM (100 mL) was added to the solution. The solution was washed with saturated sodium bicarbonate solution and the organic layer was dried with magnesium sulfate. The solvent was removed under reduced pressure. The product was purified by column chromatography on silica (20% ethyl acetate/petroleum ether) to give the product **247** as a colourless solid (287 mg, 81%): m.p 174-178 $^{\circ}$ C; Anal. RP HPLC: t_R 16.90 min (purity 99.22%); ν_{max}/cm^{-1} (nujol) 3091, 1692, 1605, 1569; δ_H (300 MHz, $CDCl_3$) 8.50 (1H, s, 9-NH), 8.06 (1H, d, J = 2.0 Hz, 2-H), 7.81 (1H, dd, J = 8.4, 2.0 Hz, 6-H), 7.49 (1H, d, J = 8.4 Hz, 5-H), 2.48 (3H, s, Me); δ_C (75 MHz, $CDCl_3$) 168.2 (C-10), 167.4 (C-8), 165.8 (C-7), 134.6 (C-4), 132.4 (C-3), 132.0 (C-5), 128.7 (C-2), 127.2 (C-6), 127.2 (C-1), 24.1 (C-11); HRMS m/z (ES^+) 293.9824 ($[M+Na]^+$, 100) $C_{10}H_7N_3O_2^{35}Cl_2Na$ requires 293.9813.

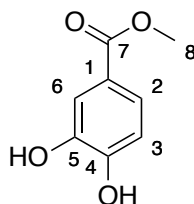
N-(3-(3,4-Dichlorophenyl)-1,2,4-oxadiazol-5-yl)cyclohexanecarboxamide **248**



DMAP (476 mg, 3.9 mmol) and cyclohexanecarbonyl chloride (208 μ l, 1.55 mmol) were added to a solution of 5-amino-1,2,4-oxadiazole **244h** (265 mg, 1.15 mmol) in DCM (20 mL). The solution was stirred for 16 h. The solvent was removed under

reduce pressure. The product was purified by column chromatography on silica (10% ethyl acetate/petroleum ether) to give the product **248** as a colourless solid (329 mg, 84%): m.p 193-198 °C; $\nu_{\text{max}}/\text{cm}^{-1}$ (nujol) 3218, 3085, 1709, 1598, 1566; δ_{H} (300 MHz, D₆-DMSO) 12.21 (1H, s, 9-H), 8.03 (1H, d, J = 1.9 Hz, 2-H), 7.87 (1H, dd, J = 8.4, 1.9 Hz, 6-H), 7.81 (1H, d, J = 8.4 Hz, 5-H), 2.51-2.49 (1H, m, 11-H), 1.84 (2H, d, J = 12.8 Hz, 12-H), 1.74 (2H, d, J = 10.6 Hz, 13-H), 1.63 (1H, d, J = 8.4 Hz, 14-H), 1.45-1.16 (5H, m, 12-H, 13-H, 14-H); δ_{C} (75 MHz, D₆-DMSO) 173.7 (C-10), 167.7 (C-8), 165.9 (C-7), 134.6 (C-4), 132.5 (C-3), 132.0 (C-5), 128.8 (C-2), 127.4 (C-1), 127.3 (C-6), 44.5 (C-11), 29.0 (C-12), 25.7 (C-14), 25.4 (C-13); HRMS m/z (ES⁺) 362.0439 ([M+Na]⁺, 100%) C₁₅H₁₅N₃O₂³⁵Cl₂Na requires 362.0439/

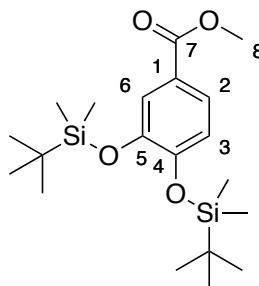
Methyl 3,4-dihydroxybenzoate **252**^{169, 224}



Concentrated sulfuric acid (3 mL) was added to a solution of 3,4-dihydroxy benzoic acid (4.62 g, 30 mmol) in methanol (60 mL). The solution was heated under reflux for 4 h. When TLC analysis indicated consumption of the starting material the solution was cooled and the solvent was removed under reduced pressure. Water (60 mL) and ethyl acetate (60 mL) were added and the layers were separated. The aqueous layer was re-extracted with ethyl acetate (3 × 60 mL). The combined organic layers were washed with brine solution (60 mL). The organic layer was dried with magnesium sulfate and the solvent was removed under reduced pressure. The product was purified by column chromatography on silica (50% ethyl acetate/petroleum ether) to give the product **252** as a white solid (4.49 g, 89%): m.p 120-122 °C (Lit.²²⁴ 126-128 °C); $\nu_{\text{max}}/\text{cm}^{-1}$ (nujol) 3467, 3259, 1687, 1610, 1295, 984; δ_{H} (300 MHz, CDCl₃) 7.63 (1H, d, J = 2 Hz, 2-H), 7.58 (1H, dd, J = 8.3, 2 Hz, 6-H), 6.91 (1H, d, J = 8.3 Hz, 5-H), 5.80 (2H, s, OH), 3.89 (3H, s, Me); δ_{C} (75 MHz, CDCl₃) 167.6 (C-7), 149.2 (C-3), 143.0 (C-4), 124.2 (C-6), 123.1 (C-1), 117.0

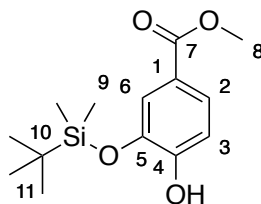
(C-2), 115.1 (C-5), 52.5 (C-8); m/z (ES^-) 167.01 ($[M-H]^-$, 100%), (ES^+) 190.99 ($[M+Na]^+$, 100), 169.03 ($[M+H]^+$, 63), HRMS m/z (ES^+) 191.0325 ($[M+Na]^+$, 100%) $C_8H_8O_4Na$ requires 191.0320.

Methyl 3,4-*bis*((*tert*-butyldimethylsilyl)oxy)benzoate **253**³⁴



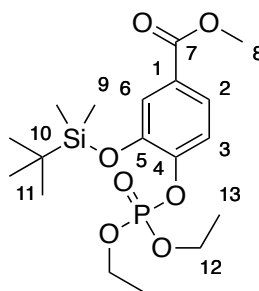
Imidazole (3.56 g, 52.3 mmol) and TBSCl (3.94 g, 26.9 mmol) was added to a solution of methyl ester **252** (2 g, 11.9 mmol) in DCM (20 mL) at 0 °C. The mixture was warmed to room temperature and stirred for 16 h. Water (40 mL) and DCM (40 mL) were added and the layers were separated. The aqueous layer was re-extracted with DCM (3 × 30 mL). The combined organic layers were washed with brine solution. The organic layer was dried with magnesium sulfate and the solvent was removed under reduced pressure. The product was purified by column chromatography on silica (5% ethyl acetate/petroleum ether) to give the product **253** as a colourless solid (3.61 g, 77%): m.p 44-46 °C (Lit.³⁴ 46-47 °C); ν_{max}/cm^{-1} (thin film) 3434, 2955, 2856, 1726, 1598, 1577, 1509; δ_H (500 MHz, $CDCl_3$) 7.54 (1H, dd, J = 8.3, 2.1 Hz, 6-H), 7.51 (1H, d, J = 2.1 Hz, 2-H), 6.84 (1H, d, J = 8.3 Hz, 5-H), 3.86 (3H, s, 8-H), 0.99 (9H, s, $(CH_3)_3$), 0.98 (9H, s, $(CH_3)_3$), 0.22 (6H, s, CH_3), 0.21 (6H, s, CH_3); δ_C (125 MHz, $CDCl_3$) 167.0 (C-7), 151.8 (C-4), 146.8 (C-3), 123.7 (C-6), 123.5 (C-1), 122.4 (C-2), 120.6 (C-5), 52.1 (C-8), 26.0 ($(CH_3)_3$), 26.0 ($(CH_3)_3$), 18.7 (C(CH_3)₃), 18.6 (C(CH_3)₃), -3.9 (Si- CH_3), -4.0 (Si- CH_3); HRMS m/z (ES^+) 419.2050 ($[M+Na]^+$, 100%) $C_{20}H_{36}O_4Si_2Na$ requires 419.2050.

Methyl 3-((*tert*-butyldimethylsilyl)oxy)-4-hydroxybenzoate **254**



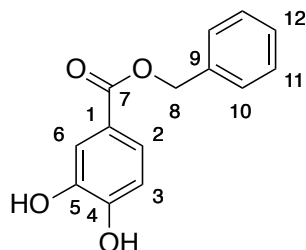
Hunigs base (9.6 mL, 53.5 mmol) was added to a solution of methyl ester **252** (6 g, 35.7 mmol) in DMF (30 mL) at 0 °C. TBSCl (5.92 g, 39.3 mmol) was added portionwise. The solution was stirred at 0 °C for 20 min. Water (50 mL) and ethyl acetate (50 mL) were added and the layers were separated. The aqueous layer was washed with ethyl acetate (2 × 20 mL). The combined organic layers were washed with water (3 × 30 mL). The organic layer was dried with magnesium sulfate and the solvent was removed under reduced pressure. The product was purified by column chromatography on silica (5% ethyl acetate/ petroleum ether to give the product **254** as a white solid (3.13 g, 31%): m.p 64-68 °C; $\nu_{\text{max}}/\text{cm}^{-1}$ (nujol) 3321, 1726, 1688; δ_{H} (300 MHz, CDCl_3) 7.66 (1H, dd, J = 8.4, 2.0 Hz, 6-H), 7.55 (1H, d, J = 2.0 Hz, 2-H), 6.98 (1H, d, J = 8.4 Hz, 5-H), 5.95 (1H, s, OH), 3.91 (3H, s, 8-H), 1.06 (9H, s, 11-H), 0.34 (6H, s, 9-H); δ_{C} (75 MHz, CDCl_3) 166.7 (C-7), 151.7 (C-4), 142.1 (C-3), 124.7 (C-6), 122.2 (C-1), 118.9 (C-2), 114.5 (C-5), 51.9 (C-8), 25.7 (C-11), 18.2 (C-10), -4.3 (C-9); HRMS m/z (ES^-) 281.1203 ($[\text{M}-\text{H}]^-$, 100%), $\text{C}_{14}\text{H}_{21}\text{O}_4\text{Si}$ requires 281.1209.

Methyl 3-((*tert*-butyldimethylsilyl)oxy)-4-((diethoxyphosphoryl)oxy)benzoate **255**



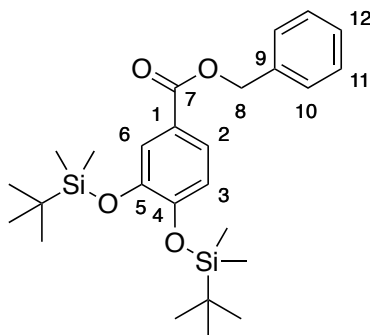
Sodium hydride (60% in mineral oil, 310 mg, 7.8 mmol) was added to a solution of silyl ether **254** (2 g, 7 mmol) in THF (25 mL) and the solution was cooled to 0 °C. Once the evolution of hydrogen was complete diethyl chlorophosphate (1.2 mL, 7 mmol) was added dropwise. The mixture was warmed to 4 °C and stirred for 16 h. Saturated ammonium chloride solution (20 mL) and DCM (30 mL) were added and the layers were separated. The aqueous layer was washed with DCM (3 × 30 mL). The combined organic layers were washed with brine solution (30 mL). The organic layer was dried with magnesium sulfate and the solvent was removed under reduced pressure. The product was purified by column chromatography (10% ethyl acetate/petroleum ether) to give the product **255** as a colourless oil (2.11 g, 71%): $\nu_{\text{max}}/\text{cm}^{-1}$ (thin film) 3430, 3181, 2932, 1724, 1588; δ_{H} (300 MHz, CDCl_3) 7.64 (1H, dd, $J = 8.5, 2.1$ Hz, 6-H), 7.6-7.57 (1H, m, 2-H), 7.49- 7.46 (1H, m, 5-H), 4.3-4.19 (4H, m, 12-H), 3.91 (3H, s, 8-H), 1.38-1.33 (6H, m, 13-H), 1.04 (9H, s, 11-H), 0.25 (3H, s, 9-H), 0.25 (3H, s, 9-H); δ_{C} (75 MHz, CDCl_3) 166.3 (C-7), 146.2 (d, $J = 7.4$ Hz, C-4), 146.0 (d, $J = 6.5$ Hz, C-3), 127.2 (d, $J = 0.9$ Hz, C-1), 123.4 (d, $J = 0.9$ Hz, C-6), 122.5 (C-2), 120.5 (d, $J = 2.5$ Hz, C-5), 64.7 (d, $J = 6.1$ Hz, C-12), 52.2 (8), 25.6 (C-11), 18.3 (C-10), 16.1 (d, $J = 6.9$ Hz, C-13), -4.5 (C-9); m/z (Cl^+) 419.16 ($[\text{M}+\text{H}]^+$, 100%), 361.09 ($[\text{M}-\text{C}_4\text{H}_9]^+$, 52) HRMS m/z (Cl^+) 419.1660 ($[\text{M}+\text{H}]^+$, 100%) $\text{C}_{18}\text{H}_{32}\text{O}_7\text{SiP}$ requires 419.1655.

Benzyl 3,4-dihydroxybenzoate **258** ¹⁷¹



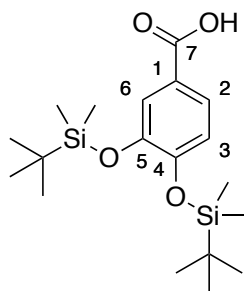
Cesium carbonate (5.29 g 16.2 mmol) was added to a solution of 3,4-dihydroxybenzoic acid (5 g, 32.4 mmol) in DMF (100 mL). The mixture was stirred for 10 min. Benzyl bromide (4.2 mL, 35.6 mmol) was added and the mixture was stirred for 16 h. Water (100 mL) and diethyl ether (100 mL) was added and the layers were separated. The aqueous layer was washed with diethyl ether (2 × 50 mL). The combined organic layers were washed with water (2 × 50 mL) and brine solution (50 mL). The organic layer was dried with magnesium sulfate and the solvent was removed under reduced pressure. The product was purified by recrystallisation (water/ethanol) to give the product **258** as a colourless solid (3.49 g, 44%): m.p 139-142 °C (Lit.¹⁷¹ 120-122 °C); $\nu_{\text{max}}/\text{cm}^{-1}$ (nujol mull) 3497, 3335, 1687, 1609; δ_{H} (500 MHz, D₆-DMSO) 9.82 (1H, s, Ar-OH), 9.45 (1H, s, Ar-OH), 7.46-7.44 (2H, m, 11-H), 7.42 (1H, d, J = 2.0 Hz, 2-H), 7.42-7.40 (2H, m, 10-H), 7.38 (1H, dd, J = 8.3, 2.0 Hz, 6-H), 7.36-7.33 (1H, m, 12-H), 6.84 (1H, d, J = 8.3 Hz, 5-H), 5.28 (2H, s, 8-H); δ_{C} (125 MHz, D₆-DMSO) 166.0 (C-7), 151.0 (C-4), 145.6 (C-3), 137.0 (C-9), 129.0 (C-11), 128.5 (C-12), 128.4 (C-10), 122.4 (C-6), 120.8 (C-1), 116.7 (C-2), 115.8 (C-5), 66.0 (C-8); m/z (CI⁺) 245.08 ([M+H]⁺, 8%), 244.07 (M⁺, 29), 137.02 ([M-C₇H₇O]⁺, 33), 91.05 ([M-C₇H₅O₄]⁺, 100), HRMS m/z (CI⁺) 245.0819 ([M+H]⁺, 20%) C₁₄H₁₃O₄ requires 245.0814; 244.0742 (M⁺, 100) C₁₄H₁₂O₄ requires 244.0736

Benzyl 3,4-*bis*((*tert*-butyldimethylsilyl)oxy)benzoate **260**



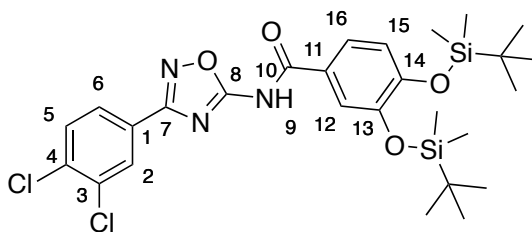
TBSCl (2.28 g, 15.1 mmol), and imidazole (2.32 g, 34.5 mmol) were added to a solution of benzyl ester **258** (1.68 g, 6.9 mmol) was dissolved in DMF (30 mL). The mixture was heated to 50 °C for 2 h. Once TLC analysis confirmed consumption of the starting material the mixture was cooled and water (30 mL) and DCM (30 mL) were added. The layers were separated and the aqueous layer was washed with DCM (2 × 30 mL). The combined organic layers were washed with water (3 × 30 mL). The organic layer was dried with magnesium sulfate and the solvent was removed under reduced pressure. The product was purified by column chromatography on silica (5% ethyl acetate/petroleum ether) to give the product **260** as a colourless oil (2.93 g, 90%): $\nu_{\text{max}}/\text{cm}^{-1}$ (thin film) 2956, 2931, 2886, 2859, 1720, 1599, 1576, 1509, 1421; δ_{H} (300 MHz, CDCl_3) 7.63 (1H, dd, J = 8.9, 2.0 Hz, 6-H), 7.62 (1H, d, J = 2.0 Hz, 2-H), 7.49-7.39 (5H, m, 10,11,12-H), 6.89 (1H, d, J = 8.9 Hz, 5-H), 5.37 (2H, s, 8-H), 1.04 (9H, s, $((\text{CH}_3)_3)$), 1.03 (9H, s, $((\text{CH}_3)_3)$), 0.27 (6H, s, CH_3), 0.26 (6, s, CH_3); δ_{C} (75 MHz, CDCl_3) 166.1 (C-7), 151.8 (C-OTBS), 146.8 (C-OTBS), 136.4 (C-9), 128.5 (C-11), 128.1 (C-12), 127.9 (C-10), 123.7 (C-6), 123.3 (C-1), 122.4 (C-2), 120.5 (C-5), 66.3 (C-8), 25.9 $((\text{CH}_3)_3)$, 25.9 $((\text{CH}_3)_3)$, 18.5 (C(CH₃)₃), 18.5 (C(CH₃)₃), -4.1 (Me), -4.1 (Me).

3,4-*bis*((*tert*-butyldimethylsilyl)oxy)benzoic acid **261**



Palladium black (200 mg, 1.88 mmol) was added to a solution of benzyl ester **260** (2.51 g, 5.3 mmol) in methanol (30 mL). The mixture was stirred over a hydrogen atmosphere for 36 h. The mixture was filtered through a plug of celite. The celite was washed with methanol (3 × 50 mL) and the solvent was removed under reduced pressure from the combined filtrate and washings. The product was purified by recrystallisation from water ethanol to give the product as a colourless solid (923 mg, 45%): m.p 140-144 °C; δ_{H} (400 MHz, CDCl_3) 7.62 (1H, dd, J = 8.3, 2.2 Hz, 6-H), 7.58 (1H, d, J = 2.2 Hz, 2-H), 6.88 (1H, d, J = 8.3 Hz, 5-H), 1.01 (9H, s, $(\text{CH}_3)_3$), 1.01 (9H, s, $(\text{CH}_3)_3$), 0.25 (6H, s, CH_3), 0.24 (6H, s, CH_3); δ_{C} (125 MHz, CDCl_3) 165.7 (C-7), 160.2 (C-4), 157.4 (C-2), 136.5 (C-1), 133.1 (C-6), 128.5 (C-10), 128.3 (C-11), 128.0 (C-12), 115.7 (C-1), 113.3 (C-5), 112.6 (C-3), 66.1 (C-8), 25.7 ($(\text{CH}_3)_3$), 25.6 ($(\text{CH}_3)_3$), 18.4 ($\text{C}(\text{CH}_3)_3$), 18.3 ($\text{C}(\text{CH}_3)_3$), -4.3 (CH_3), -4.3 (CH_3).

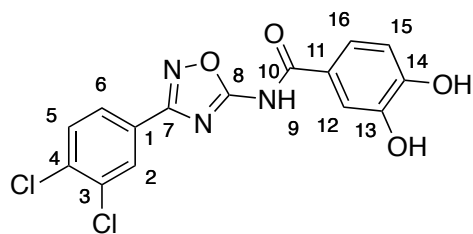
3,4-*bis*((*tert*-Butyldimethylsilyl)oxy)-*N*-(3-(3,4-dichlorophenyl)-1,2,4-oxadiazol-5-yl)benzamide **262**



DMAP (160 mg, 1.3 mmol) and silylprotected carboxylic acid **261** (550 mg, 1.4 mmol) were added to a solution of 5-amino-1,2,4-oxadiazole **224h** (300 mg, 1.3

mmol) in DCM (20 mL). EDCI (325 mg, 1.7 mmol) was added and the mixture was stirred for 16 h. Water (30 mL) and DCM (30 mL) were added and the layers separated. The aqueous layer was washed with DCM (3 × 30 mL). The combined organic layers were washed with 2N HCl (20 mL) and brine solution (20 mL). The organic layer was dried with magnesium sulfate and the solvent was removed under reduced pressure. The product was purified by column chromatography (10 % ethyl acetate/petroleum ether) to give the product **262** as an oil (230 mg, 30%): $\nu_{\text{max}}/\text{cm}^{-1}$ (nujol) 3243, 1694, 1611, 1599, 900, 840; δ_{H} (300 MHz, CDCl_3) 8.92 (1H, s, 9-NH), 8.23 (1H, d, J = 1.9 Hz, 2-H), 7.96 (1H, dd, J = 8.4, 1.9 Hz, 6-H), 7.60 (1H, d, J = 8.4 Hz, 5-H), 7.55 (1H, d, J = 2.3 Hz, 12-H), 7.39 (1H, dd, J = 8.4, 2.3 Hz, 16-H), 6.97 (1H, d, J = 8.4 Hz, 15-H), 1.05 (9H, s, $(\text{CH}_3)_3$), 1.04 (9H, s, $(\text{CH}_3)_3$), 0.30 (6H, s, CH_3), 0.28 (6H, s, CH_3); δ_{C} (75 MHz, CDCl_3) 166.6 (C-8), 166.5 (C-7), 162.1 (C-6), 152.6 (C-13), 147.9 (C-14), 135.7 (C-4), 133.4 (C-3), 130.9 (C-5), 129.3 (C-2), 126.5 (C-6), 124.5 (C-11), 122.7 (C-1), 121.3 (C-12), 120.9 (C-15), 120.8 (C-16), 25.9 ($(\text{CH}_3)_3$), 25.8 ($(\text{CH}_3)_3$), 18.6 ($\text{C}(\text{CH}_3)_3$), 18.5 ($\text{C}(\text{CH}_3)_3$), -4.0 (CH_3), -4.1 (CH_3); m/z (ES^-) 591.75 ($[\text{M}-\text{H}]^-$, 100%), 593.78 ($[\text{M}-\text{H}]^-$, 80), (ES^+) 615.73 ($[\text{M}+\text{Na}]^+$, 100), 617.77 ($[\text{M}+\text{Na}]^+$, 80), HRMS m/z (ES^-) 592.1628 ($[\text{M}-\text{H}]^-$, 100%) $\text{C}_{27}\text{H}_{36}\text{N}_3\text{O}_4\text{Si}_2\text{Cl}_2$ requires 592.1621.

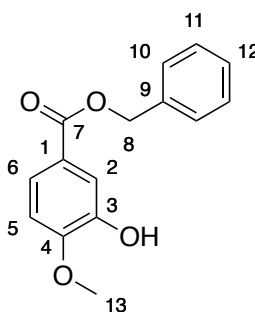
N-(3-(3,4-Dichlorophenyl)-1,2,4-oxadiazol-5-yl)-3,4-dihydroxybenzamide **249**



TBAF (1N solution in THF, 0.68 mL, 0.68 mmol) was added dropwise to a solution of silyl-protected amide **262** (188 mg, 0.31 mmol) in THF (10 mL). The solution was left to stir for 30 min. A saturated solution of sodium bicarbonate (20 mL) was added. The product was extracted with DCM (3 × 50 mL). The organic layer was

dried with magnesium sulfate. The product was purified by column chromatography on silica (5% methanol/DCM) to give the product **249** as a white solid (99 mg, 85%): m.p 228-230 °C (decomp.); $\nu_{\text{max}}/\text{cm}^{-1}$ (nujol) 3335, 1703, 1626, 1600, 1564, 1538, 1200; δ_{H} (500 MHz, D_6 -DMSO) 12.37 (1H, s, 9-H), 9.96 (1H, s, 14-OH), 9.44 (1H, s, 13-OH), 8.13 (1H, dd, J = 1.0, 0.8 Hz, 2-H), 7.96 (1H, ddd, J = 8.3, 0.9, 0.9 Hz, 6-H), 7.88 (1H, d, J = 8.3 Hz, 5-H), 7.49- 7.46 (2H, m, 12,16-H), 6.86 (1H, d, J = 8.2 Hz, 15-H); δ_{C} (125 MHz, D_6 -DMSO) 168.6 (C-8), 166.1 (C-7), 164.2 (C-10), 151.1 (C-13), 145.7 (C-14), 134.7 (C-4), 132.5 (C-3), 132.2 (C-5), 128.9 (C-2), 127.6 (C-1), 127.4 (C-6), 123.3 (C-11), 121.6 (C-16), 116.5 (C-12), 115.5 (C-15); HRMS m/z (ES^-) 363.9892 ($[\text{M}-\text{H}]^-$, 100%) $\text{C}_{15}\text{H}_8\text{O}_4\text{N}_3\text{Cl}_2$ requires 363.9897.

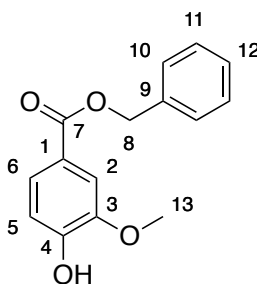
Benzyl 3-hydroxy-4-methoxybenzoate **265** ¹⁷¹



Cesium carbonate (4.84g 14.9 mmol) was added to a solution of 3-hydroxy-4-methoxybenzoic acid (5 g, 29.7 mmol) in DMF (60 mL). The mixture was stirred for 10 min. Benzyl bromide (3.9 mL, 32.7 mmol) was added and the mixture was stirred for 16 h. Water (100 mL) and diethyl ether (100 mL) was added and the layers were separated. The aqueous layer was washed with diethyl ether (2 × 50 mL). The combined organic layers were washed with water (2 × 50 mL) and brine solution (50 mL). The organic layer was dried with magnesium sulfate and the solvent was removed under reduced pressure. The product was purified by column chromatography on silica (10% ethyl acetate/petroleum ether to 20% ethyl acetate/petroleum ether to 25% ethyl acetate/petroleum ether) to give the product **265** as a colourless solid (6.122 g, 80%): m.p 69-72 °C (Lit.¹⁷¹ 72-74 °C); $\nu_{\text{max}}/\text{cm}^{-1}$

¹ (nujol) 3404, 1709, 1616; δ_{H} (500 MHz, C₆D₆) 8.03 (1H, d, $J=2.1$ Hz, 2-H), 7.81 (1H, dd, $J= 8.4, 2.1$ Hz, 6-H), 7.21-7.20 (2H, m, H), 7.10-7.04 (3H, m, H), 6.25 (1H, d, $J= 8.5$ Hz, 5-H), 5.46 (1H, s, OH), 5.18 (2H, s, 8-H), 2.98 (3H, s, 13-H); δ_{C} (125 MHz, C₆D₆) 165.6 (C-7), 150.3 (C-4), 145.7 (C-3), 136.6 (C-9), 128.4 (C-12), 128.1 (C-10), 127.8 (C-11), 123.8 (C-1), 122.8 (C-6), 115.8 (C-2), 109.8 (C-5), 66.2 (C-8), 54.9 (C-13); m/z (ES⁻) 256.86 ([M-H]⁻, 100%), HRMS m/z (ES⁻) 257.0813 ([M-H]⁻, 100%), C₁₅H₁₃O₄ requires 257.0814.

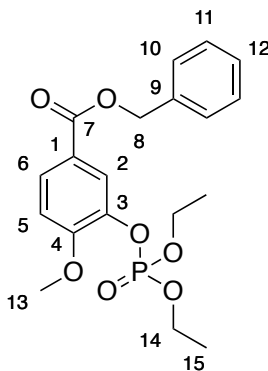
Benzyl 4-hydroxy-3-methoxybenzoate **266** ¹⁷¹



Ceasium carbonate (4.84g 14.9 mmol) was added to a solution of 4-hydroxy-3-methoxybenzoic acid (5 g, 29.7 mmol) in DMF (60 mL). The mixture was stirred for 10 min. Benzyl bromide (3.9 mL, 32.7 mmol) was added and the mixture was stirred for 16 h. Water (100 mL) and diethyl ether (100 mL) was added and the layers were separated. The aqueous layer was washed with diethyl ether (2 × 50 mL). The combined organic layers were washed with water (2 × 50 mL) and brine solution (50 mL). The organic layer was dried with magnesium sulfate and the solvent was removed under reduced pressure. The product was purified by column chromatography on silica (10% ethyl acetate/petroleum ether to 20% ethyl acetate/petroleum ether) to give the product **266** as a colourless oil (6.41 g, 83%): $\nu_{\text{max}}/\text{cm}^{-1}$ (thin film) 3401, 2940, 1709, 1596; δ_{H} (300 MHz, CDCl₃) 7.72 (1H, dd, $J= 8.3, 1.9$ Hz, 6-H), 7.62 (1H, d, $J= 1.9$ Hz, 2-H), 7.50- 7.46 (2H, m, H), 7.45-7.34 (3H, m, 12-H), 6.97 (1H, d, $J= 8.3$ Hz, 5-H), 5.38 (2H, s, 8-H), 3.95 (3H, s, 13-H); δ_{C} (75 MHz, CDCl₃) 166.4 (C-7), 150.3 (C-4), 146.3 (C-3), 136.3 (C-9), 128.6 (C-1), 128.2 (C-12), 128.2 (C-10), 124.39 (C-6), 122.2 (C-1), 114.2 (C-5), 111.9 (C-2),

66.6 (C-8), 56.1 (C-13); m/z (ES^+) 280.85 ($[M+Na]^+$, 100%), (ES^-) 256.86 ($[M-H]^-$, 100), HRMS m/z (ES^-) 257.0816 ($[M-H]^-$, 100%) $C_{15}H_{13}O_4$ requires 257.0814.

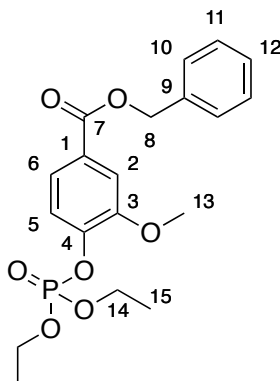
Benzyl 3-((diethoxyphosphoryl)oxy)-4-methoxybenzoate **267**



Sodium hydride (60% dispersion in mineral oil, 851 mg, 21.2 mmol) was added portionwise to a solution of benzyl ester **265** (5 g, 19.4 mmol) in THF (30 mL) at 0 °C. The mixture was stirred at 0 °C for 30 min. Diethyl chlorophosphate (3.1 mL, 21.2 mmol) was added dropwise. The mixture was warmed to R.T over 3 h. Water (30 mL) and DCM (30 mL) was added and the layers were separated. The aqueous layer was washed with DCM (3 × 30 mL). The combined organic layers were washed with brine solution (30 mL). The organic layer was dried with magnesium sulfate and the solvent was removed under reduced pressure. The product was purified by column chromatography on silica (30% ethyl acetate/ petroleum ether to 40% ethyl acetate/ petroleum ether) to give the product **267** as a colourless oil (6.994 g, 92%): ν_{max}/cm^{-1} (thin film) 3489, 2984, 2939, 1717, 1609, 1516; δ_H (500 MHz, $CDCl_3$) 7.96- 7.94 (1H, m, 2-H), 7.91 (1H, ddd, J = 8.6, 2.1, 1.0 Hz, 6-H), 7.44- 7.42 (2H, m, 10-H), 7.39- 7.33 (3H, m, 11,12-H), 6.97 (1H, d, J = 8.6 Hz, 5-H), 5.33 (2H, s, 8-H), 4.31- 4.21 (4H, m, 14-H), 1.36 (6H, dt, J = 7.1, 1.1 Hz, 15-H); δ_C (125 MHz, $CDCl_3$) 165.4 (C-7), 154.8 (d, J = 5.3 Hz, C-4), 139.5 (d, J = 7.3 Hz, C-3), 136.1 (C-9), 128.6 (C-11), 128.2 (C-12), 128.2 (C-6), 128.1 (C-10), 122.7 (d, J = 3.0 Hz, C-2), 122.7 (d, J = 2.0 Hz, C-1), 111.8 (C-5), 66.6 (C-8), 64.7 (d, J = 6.3 Hz, C-14), 56.1 (C-13), 16.1 (d, J = 7.1 Hz, C-15); δ_P (121 MHz, $CDCl_3$) -

5.97 (quintet, $J = 7.9$ Hz); HRMS m/z (ES^+) 417.1073 ($[M+Na]^+$, 100%) $C_{19}H_{23}O_7Na$ requires 417.1079.

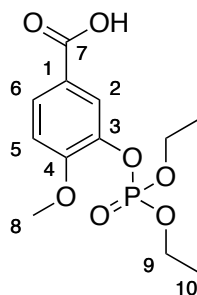
Benzyl 4-((diethoxyphosphoryl)oxy)-3-methoxybenzoate **268**



Sodium hydride (60% dispersion in mineral oil, 851 mg, 21.2 mmol) was added portionwise to a solution of benzyl ester **266** (5 g, 19.4 mmol) in THF (30 mL) at 0 °C. The mixture was stirred at 0 °C for 30 min. Diethyl chlorophosphate (3.1 mL, 21.2 mmol) was added dropwise. The mixture was warmed to R.T over 3 h. Water (30 mL) and DCM (30 mL) was added and the layers were separated. The aqueous layer was washed with DCM (3 × 30 mL). The combined organic layers were washed with brine solution (30 mL). The organic layer was dried with magnesium sulfate and the solvent was removed under reduced pressure. The product was purified by column chromatography on silica (30% ethyl acetate/ petroleum ether to 40% ethyl acetate/ petroleum ether) to give the product **268** as a colourless oil (6.08 g, 80%): ν_{max}/cm^{-1} (thin film) 3489 (C-O), 2984 (C-H), 2912 (C-H), 1719 (C=O), 1600, 1509, 1415, 1287; δ_H (500 MHz, $CDCl_3$) 7.70 (1H, dd, $J = 8.3, 1.7$ Hz, 6-H), 7.68-7.66 (1H, m, 2-H), 7.56 (1H, dd, $J = 8.3, 1.2$ Hz, 5-H), 7.25-7.23 (2H, m, 11-H), 7.14-7.10 (2H, m, 10-H), 7.09- 7.05 (1H, m, 12-H), 5.19 (2H, s, 8-H), 4.07-3.95 (4H, m, 14-H), 3.19 (3H, s, 13-H), 0.99 (6H, dt, $J = 7.1, 1.0$ Hz, 15-H); δ_C (125 MHz, $CDCl_3$) 165.3 (C-7), 150.8 (C-3), 144.3 (d, $J = 6.6$ Hz, C-4), 136.3 (C-9) 128.4 (C-10), 128.2 (C-11), 128.0 (C-12), 127.6 (C-1), 122.7 (d, $J = 1.3$ Hz, C-6), 121.1 (d, $J = 3$ Hz, C-5), 113.8 (C-2), 66.5 (C-8), 64.1 (d, $J = 6.2$ Hz, C-14), 55.0

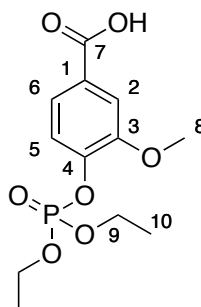
(C-13), 15.7 (d, $J = 6.6$ Hz, C-15); δ_P (121 MHz, $CDCl_3$) -6.51 (quintet, $J = 8.1$ Hz); HRMS m/z (ES^+) 417.1082 ($[M+Na]^+$, 100%) $C_{19}H_{23}O_7NaP$ requires 417.1079.

3-((Diethoxyphosphoryl)oxy)-4-methoxybenzoic acid **269**



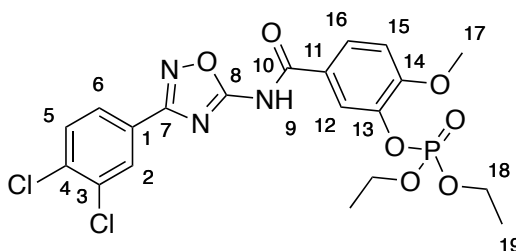
Pd/C (10%, 150 mg, 1.9 mmol) was added to a solution of benzyl ester **267** (1.53 g, 3.9 mmol) in ethyl acetate (30 mL). The mixture was stirred under a hydrogen atmosphere for 48 h. The mixture was filtered through a pad of celite and the celite was washed with methanol (3×30 mL). The filtrate and washings were combined and the solvent was removed under reduced pressure. The product was purified by recrystallisation ethanol/ water to give the product **269** as a colourless solid. (790 mg, 68%): m.p 86-90 °C; ν_{max}/cm^{-1} (nujol) 3409, 1713, 1610; δ_H (500 MHz, $CDCl_3$) 8.00 (1H, dd, $J = 1.9, 1.5$ Hz, 2-H), 7.94 (1H, ddd, $J = 8.6, 1.9, 0.6$ Hz, 6-H), 7.01 (1H, d, $J = 8.6$ Hz, 5-H), 4.36-4.28 (4H, m, 9-H), 3.96 (3H, s, 8-H) 1.41 (6H, dt, $J = 7.1, 1.0$ Hz, 10-H); δ_C (125 MHz, $CDCl_3$) 169.6 (C-7), 155.2 (d, $J = 4.6$ Hz, C-4), 139.4 (d, $J = 7.0$ Hz, C-3), 128.8 (C-6) 123.3 (d, $J = 3.1$ Hz, C-2), 122.2 (d, $J = 1.3$ Hz, C-1), 111.8 (C-5), 64.9 (d, $J = 5.8$ Hz, C-9), 56.1 (C-8), 16.1 (d, $J = 7.0$ Hz, C-10); $\delta_{P\{H\}}$ (202 MHz, $CDCl_3$) -5.95 (s); m/z (ES^+) 326.82 ($[M+Na]^+$, 100%), (ES^-) 302.83 ($[M-H]^-$, 100); HRMS m/z (ES^+) 327.0607 $C_{12}H_{17}O_7PNa$ requires 327.0610

4-((Diethoxyphosphoryl)oxy)-3-methoxybenzoic acid **270**



Palladium black (200 mg, 1.9 mmol) was added to a solution of benzyl ester **268** (1.88 g, 4.8 mmol) in ethyl acetate (30 mL). The mixture was stirred under a hydrogen atmosphere for 48 h. The mixture was filtered through a pad of celite and the celite was washed with methanol (3 × 30 mL). The filtrate and washings were combined and the solvent was removed under reduced pressure. The product was purified by column chromatography (5% methanol/DCM) to give the product **270** as a colourless solid (817 mg, 56%): m.p 76-78 °C; $\nu_{\text{max}}/\text{cm}^{-1}$ (nujol) 1715, 1605; δ_{H} (300 MHz, CDCl_3) 7.68 (1H, ddd, J = 8.3, 2.0, 0.4 Hz, H⁶), 7.65-7.63 (1H, m, 2-H), 7.37 (1H, dd, J = 8.3, 1.3 Hz, 5-H), 4.32 (4H, ddq, J = 8.3, 7.1, 1.2, 9-H), 3.95 (3H, s, 8-H), 1.41 (6H, td, J = 7.1, 1.1 Hz, 10-H); δ_{C} (125 MHz, CDCl_3) 169.6 (C-7), 150.5 (d, J = 5.5 Hz, C-3), 143.8 (d, J = 7.1 Hz, C-4), 127.3 (C-1), 123.3 (C-6), 121.1 (d, J = 2.7 Hz, C-5), 113.9 (C-2), 65.1 (d, J = 6.2 Hz, C-9), 56.1 (C-8), 16.1 (d, J = 6.9 Hz, C-10); δ_{P} (282 MHz, CDCl_3) -6.48 (t, J = 7.7 Hz); m/z (ES^+) 326.85 ($[\text{M}+\text{Na}]^+$, 100%), (ES^-) 302.75 ($[\text{M}-\text{H}]^-$, 100); HRMS m/z (ES^+) 327.0602 ($[\text{M}+\text{Na}]^+$, 100%) $\text{C}_{12}\text{H}_{17}\text{O}_7\text{PNa}$ requires 327.0610.

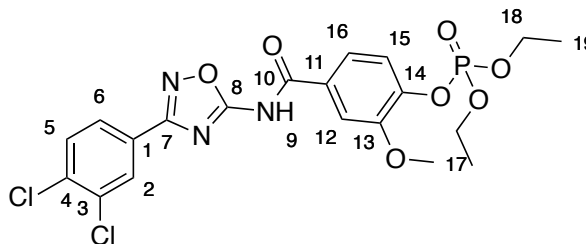
5-((3-(3,4-Dichlorophenyl)-1,2,4-oxadiazol-5-yl)carbamoyl)-2-methoxyphenyl diethyl phosphate **271**



Benzoic acid **269** (436 mg, 1.43 mmol) and DMAP (160 mg, 1.3 mmol) were dissolved in a solution of 5-amino-1,2,4-oxadiazole **224h** (300 mg, 1.3 mmol) in DCM (30 mL) and THF (20 mL). EDCI (375 mg, 1.95 mmol) was added and the mixture was stirred for 16 h after which an additional portion of benzoic acid **269** (250 mg, 0.82 mmol) and EDCI (400 mg, 2 mmol) were added and the mixture was stirred for an additional 6 h. DCM (20 mL) and water (20 mL) were added and the product was extracted using DCM (3 × 50 mL). The organic layer was washed with 1N HCl (25 mL). The organic layers were dried with magnesium sulfate and the solvent was removed under reduced pressure. The white solid was dissolved in methanol and magnesium sulfate (10 g) was added. The methanol was removed under reduced pressure. The magnesium sulfate/ product mixture was dry loaded on to a silica column. The product was purified by column chromatography on silica (30% ethyl acetate/petroleum ether to 50% ethyl acetate/ petroleum ether to 2% methanol/DCM) to give the product **271** as a white solid (331 mg, 49%): m.p 194-197 °C; $\nu_{\max}/\text{cm}^{-1}$ (nujol) 3396, 3218, 3125, 1705, 1611; δ_{H} (500 MHz, D_6 -DMSO) 12.72 (1H, s, 9-NH), 8.13 (1H, d, J = 1.9 Hz, 2-H), 8.00 (1H, dd, J = 8.8, 1.9 Hz, 16-H), 7.96 (1H, dd, J = 8.4, 1.9 Hz, 6-H), 7.91-7.90 (1H, m, 12-H), 7.87 (1H, d, J = 8.4 Hz, 5-H), 7.32 (1H, d, J = 8.8 Hz, 15-H), 4.23-4.15 (4H, m, 18-H), 3.93 (3H, s, 17-H), 1.29 (6H, t, J = 7.0 Hz, 19-H); δ_{C} (125 MHz, D_6 -DMSO) 168.4 (C-8), 166.1 (C-7), 163.3 (C-10), 155.0 (d, J = 5.0 Hz, C-14), 139.5 (d, J = 6.0 Hz, C-13), 134.7 (C-4), 132.6 (C-3), 132.2 (C-5), 128.9 (C-2), 127.6 (C-16), 127.5 (C-6), 127.4 (C-1), 124.5 (C-11), 121.9 (d, J = 2.5 Hz, C-12), 113.2 (C-15), 64.9 (d, J = 5.5 Hz, C-18), 56.8 (C-18), 16.4 (d, J = 7.0 Hz, C-19); δ_{P} (162 MHz, D_6 -DMSO) -6.60 (1P, quin, J = 8.8 Hz);

m/z (ES^-) 515.99 ($[M-H]^-$, 91%), 513.98 ($[M-H]^-$, 100); HRMS m/z (ES^+) 538.0308 ($[M+Na]^+$, 100%) $C_{20}H_{20}N_3O_7PCl_2Na$ requires 538.0314.

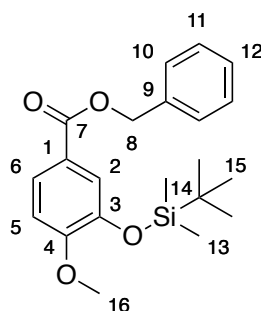
4-((3-(3,4-Dichlorophenyl)-1,2,4-oxadiazol-5-yl)carbamoyl)-2-methoxyphenyl diethyl phosphate **272**



Benzoic acid **270** (365 mg, 1.2 mmol) and DMAP (122 mg, 1 mmol) were added to a solution of 5-amino-1,2,4-oxadiazole (230 mg, 1mmol) in THF (10 mL). EDCI (287 mg, 1.5 mmol) was added to the solution. The mixture was stirred for 16 h when an additional portion of benzoic acid **270** (200 mg, 0.66 mmol) and EDCI (200 mg, 1.0 mmol) were added and the mixture was stirred for an additional 6 h. DCM (20 mL) and water (20 mL) were added and the product was extracted using DCM (3 × 50 mL). The organic layer was washed with 1N HCl (25 mL). The organic layers were dried with magnesium sulfate and the solvent was removed under reduced pressure. The white solid was dissolved in methanol and magnesium sulfate (10 g) was added. The methanol was removed under reduced pressure. The magnesium sulfate/ product mixture was dry loaded on to a silica column. The product was purified by column chromatography on silica (30% ethyl acetate/petroleum ether to 50% ethyl acetate/petroleum ether to 2% methanol/DCM where the product was collected) to give the product **272** as a white solid (437 mg, 85%): m.p. 216-218 °C; Anal. RP HPLC: t_R 27.36 min (purity 96.60%); ν_{max}/cm^{-1} (nujol) 3431, 1708, 1618; δ_H (500 MHz, D_6 -DMSO) 12.78 (1H, s, 9-NH), 8.13 (1H, d, J = 1.9 Hz, 2-H), 7.96 (1H, dd, J = 8.5, 1.9 Hz, 6-H), 7.87 (1H, d, J = 8.5 Hz, 5-H), 7.79 (1H, d, J = 1.8Hz, 12-H), 7.66 (1H, dd, J = 8.5, 1.8 Hz, 16-H), 7.39 (1H, d, J = 8.5 Hz, 15-H), 4.22-4.16 (4H, m, 18-H), 3.93 (3H, s, 17-H), 1.29

(6H, t, J = 7.0 Hz, 19-H); δ_C (125 MHz, D_6 -DMSO) 168.3 (C-8), 166.1 (C-7), 163.7 (C-10), 150.6 (d, J = 5.2 Hz, C-13), 143.4 (d, J = 7.1 Hz, C-14), 134.8 (C-1), 132.6 (C-2, C-3), 132.2 (C-5), 129.8 (C-11), 128.9 (C-2), 127.4 (C-6), 122.2 (C-16), 121.4 (d, J = 2.6 Hz, C-15), 113.5 (C-12), 65.0 (d, J = 6.7 Hz, C-18), 56.7 (C-17), 16.3 (d, J = 5.8 Hz, C-19); δ_P (162 MHz, D_6 -DMSO) -6.49 (1P, quin, J = 8.4 Hz); HRMS m/z (ES^+) 538.0305 ($[M+Na]^+$, 100) $C_{20}H_{20}N_3O_7NaCl_2P$ requires 538.0314.

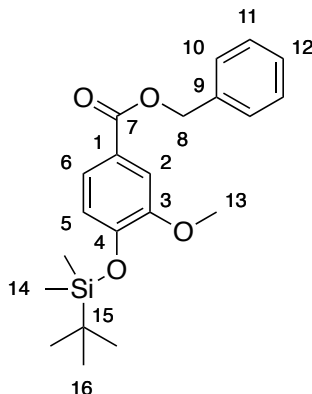
Benzyl 3-((*tert*-butyldimethylsilyl)oxy)-4-methoxybenzoate **285**



TBSCl (3.2 g, 21.2 mmol) and imidazole (2.63 g, 38 mmol) were added to a solution of benzyl ester **265** (5 g, 19.4 mmol) in DCM (60 mL). The mixture was stirred for 16 h. Water (60 mL) was added and the layers were separated. The aqueous layer was washed with DCM (3 × 30 mL). The combined organic layers were washed with brine solution (50 mL). The organic layer was dried with magnesium sulfate and the solvent was removed under reduced pressure. The product was purified by column chromatography on silica (5% ethyl acetate/petroleum ether) to give the product **285** as a colourless oil (7.0 g, 97%): ν_{max}/cm^{-1} (thin film) 2955, 2895, 2858, 1716, 1602, 1583, 1512, 1375, 1131; δ_H (500 MHz, $CDCl_3$) 7.74 (1H, dd, J = 8.5, 2.1 Hz, 6-H), 7.61 (1H, d, J = 2.1 Hz, 2-H), 7.48 (2H, d, J = 7.3 Hz, 10-H), 7.45-7.40 (2H, m, 11-H), 7.38-7.35 (1H, m, 12-H), 6.89 (1H, d, J = 8.5 Hz, 5-H), 5.37 (2H, s, 8-H), 3.89 (3H, s, 16-H), 1.04 (9H, s, 15-H), 0.20 (6H, s, 13-H); δ_C (125 MHz, $CDCl_3$) 166.2 (C-7), 155.2 (C-4), 144.6 (C-3), 136.4 (C-9), 128.6 (C-11), 128.1 (C-12), 128.0 (C-10), 124.41 (C-6), 122.7 (C-1)

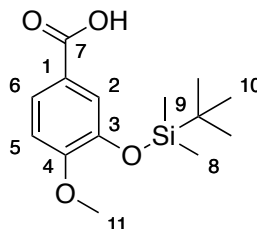
122.0 (C-2), 110.9 (C-5), 66.4 (C-8), 55.5 (C-16), 25.7 (C-15), 18.5 (C-14), -4.6 (C-13); HRMS m/z (ES^+) 395.1658 ($[M+Na]^+$, 100%) $C_{21}H_{28}O_4SiNa$ requires 395.1655.

Benzyl 4-((*tert*-butyldimethylsilyl)oxy)-3-methoxybenzoate **286**



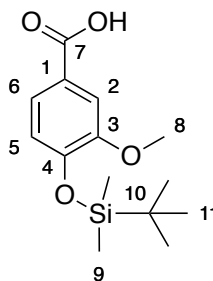
TBSCl (3.2 g, 21.2 mmol) and imidazole (2.63 g, 38 mmol) were added to a solution of benzyl ester **266** (5 g, 19.4 mmol) in DCM (60 mL). The mixture was stirred for 16 h. Water (60 mL) was added and the layers were separated. The aqueous layer was washed with DCM (3 × 30 mL). The combined organic layers were washed with brine solution (50 mL). The organic layer was dried with magnesium sulfate and the solvent was removed under reduced pressure. The product was purified by column chromatography on silica (5% ethyl acetate/petroleum ether) to give the product **286** as a colourless oil (6.07 g, 84%): ν_{max}/cm^{-1} (thin film) 3412, 3034, 2956, 2885, 2858, 1718, 1599, 1511, 1464, 1376, 1362, 1290, 1179, 1125, 1036, 969, 912, 804, 784, 765; δ_H (300 MHz, $CDCl_3$) 7.69 (1H, dd, J = 8.2, 2.0 Hz, 6-H), 7.64 (1H, d, J = 2.0 Hz, 2-H), 7.52-7.48 (2H, m, 10-H), 7.47-7.38 (3H, m, 11-H, 12-H), 6.93 (1H, d, J = 8.2 Hz, 5-H), 5.40 (2H, s, 8-H), 3.90 (3H, s, 13-H), 1.06 (9H, s, 16-H), 0.24 (6H, s, 14-H); δ_C (75 MHz, $CDCl_3$) 166.3 (C-7), 150.8 (C-3), 149.8 (C-4), 136.3 (C-9), 128.6 (C-11), 128.2 (C-10), 123.6 (C-1), 123.5 (C-6), 120.5 (C-5), 113.1 (C-2), 66.5 (C-8), 55.5 (C-13), 25.7 (C-16), 18.6 (C-15), -4.6 (C-14); m/z (ES^+) 395.16 ($[M+Na]^+$, 100%), 373.18 ($[M+H]^+$, 36), HRMS m/z (ES^+) 395.1640 ($[M+Na]^+$, 100%), $C_{21}H_{28}O_4SiNa$ requires 395.1655.

3-((*tert*-Butyldimethylsilyl)oxy)-4-methoxybenzoic acid **287**²²⁵



Palladium black (300 mg, 2.8 mmol) was added to a solution of benzyl ester **285** (7.0 g, 18.8 mmol) in methanol (30 mL) and the mixture was stirred under a hydrogen atmosphere for 72 h. The mixture was filtered through a pad of celite and the celite was washed with methanol (2 × 30 mL). The filtrate and washings were combined and the solvent was removed under reduced pressure to give a solid. The product was purified by column chromatography on silica (30 % ethyl acetate/petroleum ether) to give the product **287** as a colourless solid (1.8 g, 34%): m.p 148-152 °C (Lit.²²⁵ 163.5-164.5 °C); $\nu_{\text{max}}/\text{cm}^{-1}$ (nujol) 3454, 1775, 1682, 1602; δ_{H} (300 MHz, D₆-DMSO) 12.64 (1H, s, 7-OH), 7.56 (1H, dd, J = 8.5, 2.1 Hz, 6-H), 7.33 (1H, d, J = 2.1 Hz, 2-H), 7.05 (1H, d, J = 8.5 Hz, 5-H), 3.81 (3H, s, 11-H), 0.94 (9H, s, 10-H), 0.11 (6H, s, 8-H); δ_{C} (75 MHz, D₆-DMSO) 167.7 (C-7), 155.3 (C-4), 144.6 (C-3), 125.0 (C-1), 124.0 (C-6), 121.8 (C-2), 112.6 (C-5), 56.4 (C-11), 26.4 (C-10), 19.0 (C-9), -3.9 (C-8); HRMS m/z (ES⁻) 281.1215 ([M-H]⁻, 100%) C₁₄H₂₁O₄Si requires 281.1209.

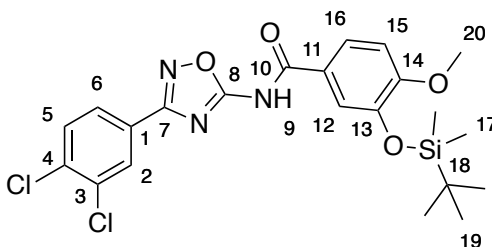
4-((*tert*-Butyldimethylsilyl)oxy)-3-methoxybenzoic acid **288**



Palladium black (250 mg, 2.3 mmol) was added to a solution of benzyl ester **286** (5.0 g, 13.4 mmol) in methanol (30 mL) and the mixture was stirred under a

hydrogen atmosphere for 72 h. The mixture was filtered through a pad of celite and the celite was washed with methanol (2 × 30 mL). The filtrate and washings were combined and the solvent was removed under reduced pressure to give a solid. The product was purified by column chromatography on silica (20% ethyl acetate/petroleum ether to 30 % ethyl acetate/petroleum ether) to give the product **288** as a white solid (3.09 g, 82%): m.p 125-128 °C; $\nu_{\text{max}}/\text{cm}^{-1}$ (nujol) 3443, 1677, 1599, 1580, 1290, 1230; δ_{H} (300 MHz, CDCl_3) 7.72 (1H, dd, J = 8.3, 2.0 Hz, 6-H), 7.64 (1H, d, J = 2.0 Hz, 2-H), 6.94 (1H, d, J = 8.3 Hz, 5-H), 3.91 (3H, s, 8-H), 1.05 (9H, s, 11-H), 0.23 (6H, s, 9-H); δ_{C} (75 MHz, CDCl_3) 172.2 (C-7), 150.8 (C-3), 150.5 (C-4), 124.3 (C-6), 122.6 (C-1), 120.6 (C-5), 113.4 (C-2), 55.5 (C-8), 25.6 (C-11), 18.5 (C-10), -4.6 (C-9); m/z (ES^-) 281.12 ($[\text{M}-\text{H}]^-$, 100%), (ES^+) 305.12 ($[\text{M}+\text{Na}]^+$, 86), 265.13 ($[\text{M}-\text{OH}]^+$, 100), HRMS m/z (ES^-) 281.1215 ($[\text{M}-\text{H}]^-$, 100%) $\text{C}_{14}\text{H}_{21}\text{O}_4\text{Si}$ requires 281.1209.

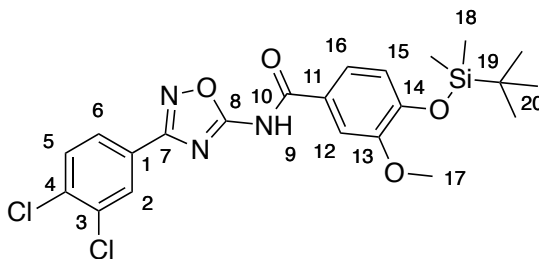
3-((*tert*-Butyldimethylsilyl)oxy)-*N*-(3-(3,4-dichlorophenyl)-1,2,4-oxadiazol-5-yl)-4-methoxybenzamide **289**



Benzoic acid **287** (736 mg, 2.6 mmol) and DMAP (797 mg, 6.5 mmol) were added to a solution of 5-amino-1,2,4-oxadiazole (500 mg, 2.2 mmol) in THF (20 mL). EDCI (625 mg, 3.3 mmol) was added to the solution which was stirred for 16 h. Water was added and the layers were separated. The aqueous layer was washed with DCM (3 × 30 mL). The combined organic layers were washed with 2N HCl (30 mL) and brine solution (30 mL). The organic layer was dried with magnesium sulfate and the solvent was removed under reduced pressure. The product was dry loaded onto magnesium sulfate. The product was purified by sequential column chromatography on silica (50% diethyl ether/petroleum ether) followed by (20%

ethyl acetate/petroleum ether) to give the product **289** as a colourless solid (479 mg, 52%): m.p 98-102 °C; $\nu_{\text{max}}/\text{cm}^{-1}$ (nujol) 3210, 1687, 1607, 1552; δ_{H} (300 MHz, CDCl_3) 9.52 (1H, s, 9-NH), 8.20 (1H, d, J = 1.8 Hz, 2-H), 7.93 (1H, dd, J = 8.4, 1.8 Hz, 6-H), 7.63 (1H, dd, J = 8.3, 2.2 Hz, 16-H), 7.60 (1H, d, J = 8.4 Hz, 5-H), 7.54 (1H, d, J = 2.2 Hz, 12-H), 6.98 (1H, d, J = 8.3 Hz, 15-H), 3.94 (3H, s, 20-H), 1.05 (9H, s, 19-H), 0.22 (6H, s, 17-H); δ_{C} (75 MHz, CDCl_3) 166.9 (C-8), 166.4 (C-7), 162.6 (C-10), 155.8 (C-14), 145.5 (C-13), 135.7 (C-1), 133.3 (C-3), 130.9 (C-5), 129.3 (C-2), 126.4 (C-4), 126.4 (C-6), 123.9 (C-11), 122.3 (C-16), 120.6 (C-12), 111.4 (C-15), 55.6 (C-20), 25.7 (C-19), 18.5 (C-18), -4.6 (C-17); HRMS m/z (ES^+) 516.0872 ($[\text{M}+\text{Na}]^+$, 100%) $\text{C}_{22}\text{H}_{25}\text{Cl}_2\text{N}_3\text{O}_4\text{SiNa}$ requires 516.0889.

4-((*tert*-Butyldimethylsilyl)oxy)-*N*-(3-(3,4-dichlorophenyl)-1,2,4-oxadiazol-5-yl)-3-methoxybenzamide **290**

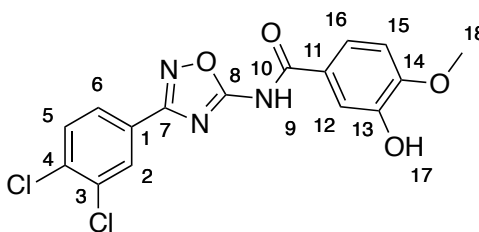


Benzoic acid **288** (736 mg, 2.6 mmol) and DMAP (797 mg, 6.5 mmol) were added to a solution of 5-amino-1,2,4-oxadiazole **224h** (500 mg, 2.1 mmol) in DCM (40 mL). EDCI (625 mg, 3.25 mmol) was added to the mixture, which was stirred for 16 h. Water (30 mL) and DCM (30 mL) were added and the layers were separated. The aqueous layer was washed with DCM (30 mL). The combined organic layers were washed with 2N HCl (30 mL) and brine solution (30 mL). The organic layer was dried with magnesium sulfate. The product was purified by sequential column chromatography on silica (50% diethyl ether/DCM followed by 10% ethyl acetate/petroleum ether) to give the product **290** as a colourless solid (550 mg, 51%): m.p 117-120 °C; $\nu_{\text{max}}/\text{cm}^{-1}$ (nujol) 3463, 1701, 1635, 1592, 1122, 1035, 903, 837, 810, 786, 758; δ_{H} (300 MHz, CDCl_3) 10.08 (1H, 9-NH), 8.02 (1H, d J = 1.9 Hz,

2-H), 7.76 (1H, dd, J = 8.4, 1.9 Hz, 6-H), 7.62 (1H, d, J = 2.2 Hz, 12-H), 7.55 (1H, dd, J = 8.3, 2.2 Hz, 16-H), 7.46 (1H, d, J = 8.4 Hz, 5-H), 6.91 (1H, d, J = 8.3 Hz, 15-H), 3.87 (3H, s, 17-H), 1.01 (9H, s, 20-H), 0.19 (6H, s, 18-H); δ_{C} (75 MHz, CDCl_3) 167.0 (C-8), 166.5 (C-7), 163.3 (C-10), 151.4 (C-13), 150.5 (C-14), 135.6 (C-1), 133.2 (C-3), 130.8 (C-5), 129.1 (C-2), 126.3 (C-6), 126.3 (C-4), 124.8 (C-11), 121.2 (C-16), 120.7 (C-15), 112.2 (C-12), 55.6 (C-17), 25.6 (C-20), 18.5 (C-19), -4.6 (C-18); m/z (ES^+) 516.09 ($[\text{M}+\text{Na}]^+$, 100%), (ES^-) 492.09 ($[\text{M}-\text{H}]^-$, 100), HRMS m/z (ES^+) 516.0875 ($[\text{M}+\text{Na}]^+$, 100%) $\text{C}_{22}\text{H}_{25}\text{Cl}_2\text{N}_3\text{O}_4\text{SiNa}$ requires 516.0889.

N-(3-(3,4-dichlorophenyl)-1,2,4-oxadiazol-5-yl)-3-hydroxy-4-methoxybenzamide

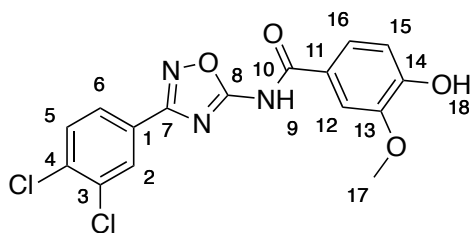
291



TBAF (1N solution in THF, 530 μL , 0.53 mmol) was added dropwise to a solution of silyl-protected amide **289** (175 mg, 0.35 mmol) in THF (10 mL). The solution was stirred for 30 min after which TLC analysis indicated that all of the starting material was consumed. Water (20 mL) and ethyl acetate (20 mL) was added and the layers were separated. The aqueous layer was re-extracted with ethyl acetate (2 \times 20 mL). The combined organic layers were washed with brine solution (30 mL). The organic layer was dried with magnesium sulfate and the solvent was removed under reduced pressure. The product was purified by column chromatography on silica (2% methanol/ DCM) to give the product **291** as a colourless solid (78 mg, 58%): m.p 237-240 $^{\circ}\text{C}$; $\nu_{\text{max}}/\text{cm}^{-1}$ (nujol) 3386, 3337, 1705, 1687; δ_{H} (300 MHz, D_6 -DMSO) 12.47 (1H, s, 9-NH), 9.48 (1H, s, 17-H), 8.13 (1H, d, J = 1.8 Hz, 2-H), 7.96 (1H, dd, J = 8.4, 1.8 Hz, 6-H), 7.87 (1H, d, J = 8.4 Hz, 5-H), 7.60 (1H, dd, J = 8.5, 2.3 Hz, 16-H), 7.47 (1H, d, J = 2.3 Hz, 12-H), 7.08 (1H, d, J = 8.5 Hz, 15-H), 3.87 (3H, s, 18-H); δ_{C} (75 MHz, D_6 -DMSO) 168.4 (C-8), 166.1 (C-7), 164.0 (C-10), 152.5 (C-

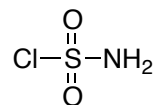
14), 146.8 (C-13), 134.6 (C-1), 132.5 (C-3), 132.1 (C-5), 128.8 (C-2), 127.5 (C-4), 127.3 (C-6), 124.6 (C-11), 121.3 (C-16), 116.0 (C-12), 111.7 (C-15), 56.2 (C-18); HRMS m/z (ES^-) 378.0050 ($[M-H]^-$, 100%) $C_{16}H_{10}O_4N_3Cl_2$ requires 378.0054.

N-(3-(3,4-Dichlorophenyl)-1,2,4-oxadiazol-5-yl)-4-hydroxy-3-methoxybenzamide
292



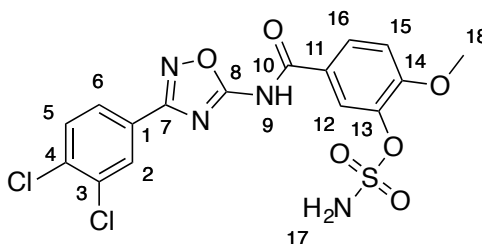
TBAF (1N solution in THF, 1.4 ml, 1.4 mmol) was added dropwise to a solution of silyl-protected amide **290** (451 mg, 0.91 mmol) in THF (10 mL). The mixture was stirred for 30 min after which TLC analysis indicated that all of the starting material was consumed. Water (20 mL) and ethyl acetate (20 mL) was added and the layers were separated. The aqueous layer was re-extracted with ethyl acetate (2 × 20 mL). The combined organic layers were washed with brine solution (30 mL). The organic layer was dried with magnesium sulfate and the solvent was removed under reduced pressure. The product was purified by column chromatography on silica (50% ethyl acetate/ petroleum ether) to give the product **290** as a white solid (235 mg, 68%): m.p 190-193 °C; ν_{max}/cm^{-1} (nujol mull) 3362, 1722, 1620, 1598, 1256, 1193; δ_H (300 MHz, D_6 -DMSO) 12.47 (1H, s, 9-NH), 10.06 (1H, s, 18-H), 8.12 (1H, d, J = 1.9 Hz, 2-H), 7.95 (1H, dd, J = 8.4, 1.9 Hz, 6-H), 7.87 (1H, d, J = 8.4 Hz, 5-H), 7.65 (1H, d, J = 2.1 Hz, 12-H), 7.60 (1H, dd, J = 8.3, 2.1 Hz, 16-H), 6.91 (1H, d, J = 8.3 Hz, 15-H), 3.87 (3H, s, 17-H); δ_C (75 MHz, D_6 -DMSO) 168.6 (C-8), 166.1 (C-7), 164.0 (C-10), 152.0 (C-14), 147.8 (C-13), 134.7 (C-1), 132.5 (C-3), 132.2 (C-5), 128.9 (C-2), 127.5 (C-4), 127.4 (C-6), 123.5 (C-11), 123.0 (C-16), 115.6 (C-15), 112.6 (C-12), 56.2 (C-17); HRMS m/z (ES^-) 378.0049 ($[M-H]^-$, 100%) $C_{16}H_{10}O_4N_3Cl_2$ requires 378.0054.

Sulfamoyl chloride **294**¹⁷⁸



Chlorosulfonyl isocyanate (4.95 g, 3.1 mL, 35 mmol) was dissolved in DCM (35 mL) and the solution was cooled to 0 °C. Formic acid (1.7 g, 1.4 mL, 36.8 mmol) was added dropwise to the solution. The solution was stirred for 1 h at 0 °C then warmed to room temperature for 16 h. A gas was evolved and a precipitate formed which redissolved after 16 h. The product was used without any further purification as a 1N solution.

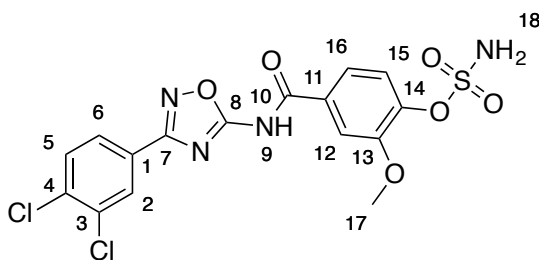
5-((3-(3,4-Dichlorophenyl)-1,2,4-oxadiazol-5-yl)carbamoyl)-2-methoxyphenyl sulfamate **281**



Amide **291** (105 mg, 0.28 mmol) was dissolved in dimethylacetamide (1 mL) and the solution was cooled to 0 °C. Sulfamoyl chloride (1N solution in DCM, 550 μ l, 0.55 mmol) was added to the solution. The solution was warmed to room temperature and the solution was stirred for 16 h. Water (15 mL) and ethyl acetate (15 mL) were added and the layers were separated. The aqueous layer was reextracted with ethyl acetate (2 \times 15 mL). The combined organic layers were washed with brine solution (30 mL). The organic layer was dried with magnesium sulfate and the solvent was removed under reduced pressure. The product was purified by column chromatography on silica (50% ethyl acetate/ petroleum ether) to give the product **281** as a colourless solid (110 mg, 87%): m.p. 210-214 °C; ν_{max} /cm⁻¹ (nujol) 3318, 3220, 1708, 1606, 1597, 1560, 1508, 116; δ_{H} (500 MHz,

D₆-DMSO) 12.69 (1H, s, 9-NH), 8.14 (1H, d, *J* = 2.0 Hz, 2-H), 8.08 (2H, s, 17-H), 8.06 (1H, dd, *J* = 8.7, 2.3 Hz, 16-H), 8.02 (1H, d, *J* = 2.3 Hz, 12-H), 7.96 (1H, dd, *J* = 8.4, 2.0 Hz, 6-H), 7.88 (1H, d, *J* = 8.4 Hz, 5-H), 7.35 (1H, d, *J* = 8.7 Hz, 15-H), 3.92 (3H, s, 18-H); δ_C (125 MHz, D₆-DMSO) 168.3 (C-8), 166.1 (C-7), 163.3 (C-10), 156.4 (C-14), 139.0 (C-13), 134.7 (C-1), 132.6 (C-3), 132.2 (C-5), 129.0 (C-16), 128.9 (C-2), 127.4 (C-6), 124.4 (C-11), 124.3 (C-12), 113.5 (C-15), 56.8 (C-18); HRMS *m/z* (ES⁻) 456.97779 ([M-H]⁻, 100%) C₁₆H₁₁O₆N₄Cl₂S requires 456.9782.

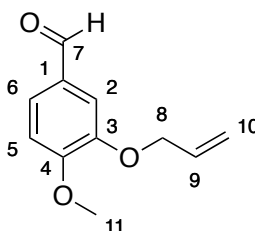
4-((3-(3,4-Dichlorophenyl)-1,2,4-oxadiazol-5-yl)carbamoyl)-2-methoxyphenyl sulfamate **293**



Amide **292** (105 mg, 0.28 mmol) was dissolved in dimethylacetamide (1 mL) and the solution was cooled to 0 °C. Sulfamoyl chloride (1N solution in DCM, 550 μ l, 0.55 mmol) was added to the solution. The solution was warmed to room temperature and the solution was stirred for 16 h. Water (15 mL) and ethyl acetate (15 mL) were added and the layers were separated. The aqueous layer was re-extracted with ethyl acetate (2 \times 15 mL). The combined organic layers were washed with brine solution (30 mL). The organic layer was dried with magnesium sulfate and the solvent was removed under reduced pressure. The product was purified by column chromatography on silica (50% ethyl acetate/ petroleum ether) to give the product **293** as a colourless solid (78 mg, 61%): m.p 199-204 °C; $\nu_{\max}/\text{cm}^{-1}$ (nujol) 3432, 3340, 3188, 1712, 1600, 1168, 1129; δ_H (500 MHz, D₆-DMSO) 12.83 (1H, s, 9-NH), 8.17 (2H, s, 18-H), 8.14 (1H, d, *J* = 1.8 Hz, 2-H), 7.97 (1H, dd, *J* = 8.3, 1.8 Hz, 6-H), 7.88 (1H, d, *J* = 8.3 Hz, 5-H), 7.82 (1H, d, *J* = 1.8 Hz, 12-H), 7.69 (1H, dd, *J* = 8.4, 1.8 Hz, 16-H), 7.49 (1H, d, *J* = 8.4 Hz, 15-H), 3.92 (3H, s, 17-H); δ_C (125 MHz, D₆-DMSO) 168.3 (C-8), 168.2 (C-7), 163.8 (C-10), 152.0 (C-13), 142.9 (C-14), 134.8 (C-4), 132.6 (C-3), 132.2 (C-5), 131.1 (C-11),

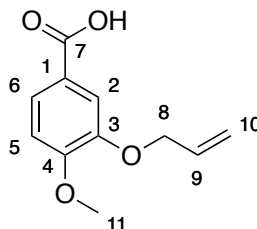
128.9 (C-2), 127.4 (C-6), 127.4 (C-1), 123.5 (C-15), 121.8 (C-16), 113.7 (C-12), 56.6 (C-17); HRMS m/z (ES^-) 456.9781 ($[M-H]^-$, 100%) $C_{16}H_{11}O_6N_4Cl_2S$ requires 456.9782.

3-(Allyloxy)-4-methoxybenzaldehyde **296** ^{180, 226}



Allyl bromide (4.25 mL, 49.2 mmol) and potassium carbonate (6.8 g, 49.2 mmol) were added to a solution of 3-hydroxy-4-methoxybenzaldehyde (3 g, 19.7 mmol) in DMF (30 mL). The mixture was heated to 50 °C for 3 h. Water (30 mL) was added. Ethyl acetate (60 mL) was added and the layers were separated. The aqueous layer was washed with ethyl acetate (2 × 50 mL). The combined organic layers were washed with water (3 × 30 mL) and brine solution (30 mL). The organic layer was dried with magnesium sulfate and the solvent was removed under reduced pressure. The product was purified by column chromatography on silica (10% ethyl acetate/petroleum ether to 20% ethyl acetate/ petroleum ether to 25% ethyl acetate/petroleum ether) to give the product **296** as a pale yellow oil (3.82 g, quant.): ν_{max}/cm^{-1} (thin film) 3081, 2935, 1683, 1595, 1508; δ_H (500 MHz, $CDCl_3$) 9.83 (1H, s, 7-H), 7.46 (1H, dd, J = 8.2, 1.8 Hz, 6-H), 7.40 (1H, d, J = 1.8 Hz, 2-H), 6.99 (1H, d, J = 8.2 Hz, 5-H), 6.09 (1H, ddt, J = 17.1, 10.7, 5.5 Hz, 9-H), 5.44 (1H, dd, J = 17.1, 1.2 Hz, 10 cis-H), 5.32 (1H, dd, J = 10.7, 1.2 Hz, 10 trans-H), 4.67 (2H, d, J = 5.5 Hz, 8-H), 3.96 (3H, s, 11-H); δ_C (125 MHz, $CDCl_3$) 190.9 (C-7), 154.8 (C-4), 148.5 (C-3), 132.5 (C-9), 130.0 (C-1), 126.8 (C-6), 118.6 (C-10), 110.7 (C-2), 110.6 (C-5), 69.7 (C-8), 56.2 (C-11); HRMS m/z (ES^+) 215.0682 ($[M+Na]^+$, 100%) $C_{11}H_{12}O_3Na$ requires 215.0684.

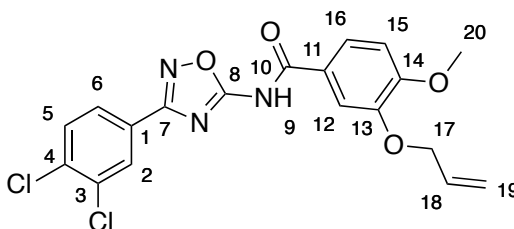
3-(Allyloxy)-4-methoxybenzoic acid **297**¹⁸⁰



Aldehyde **296** (3g, 15.6 mmol) was dissolved in acetone (50 mL) and cooled to 0 °C. Chromium trioxide (3.28 g, 32.7 mmol) and concentrated sulfuric acid (2.79 mL, 52.2 mmol) were dissolved in 5.3 mL of water. The chromium mixture was added dropwise to the acetone solution. The mixture was stirred for 30 min at 0 °C and then warmed to room temperature for 3 h. Excess chromium trioxide was destroyed by the addition of 2-propanol. The solvent was mostly removed under reduced pressure. Diethyl ether (50 mL) was added and the organic layer was removed. The aqueous layer was washed with diethyl ether (2 × 50 mL). The organic layers were combined and dried with magnesium sulfate. The solvent was removed under reduced pressure to give a yellow solid. The product was purified by column chromatography on silica (50% ethyl acetate/petroleum ether) to give the product **297** as a white solid (1.42 g, 44%): m.p 126-130 °C (Lit.¹⁸⁰ 146-147 °C); $\nu_{\text{max}}/\text{cm}^{-1}$ (nujol) 3450, 3197, 1679, 1599, 1586, 1518, 1266 δ_{H} (300 MHz, D₆-DMSO) 12.66 (1H, s, 7-OH), 7.55 (1H, dd, J = 8.5, 2.0 Hz, 6-H), 7.43 (1H, d, J = 2.0 Hz, 2-H), 7.05 (1H, d, J = 8.5 Hz, 5-H), 6.03 (1H, ddt, J = 17.3, 10.5, 5.2 Hz, 9-H), 5.38 (1H, dq, J = 17.3, 1.7 Hz, 10 trans-H), 5.25 (1H, dq, J = 10.5, 1.7 Hz, 10 cis-H), 4.58 (2H, dt, J = 5.2, 1.7 Hz, 8-H), 3.82 (3H, s, 11-H); δ_{C} (75 MHz, D₆-DMSO) 167.9 (C-7), 153.7 (C-3), 147.9 (C-4), 134.4 (C-9), 124.2 (C-6), 123.7 (C-1), 118.5 (C-10), 114.4 (C-2), 112.1 (C-5), 69.7 (C-8), 56.5 (C-11); HRMS m/z (ES⁻) 207.0660 ([M-H]⁻, 100%) C₁₁H₁₁O₄ requires 207.0657.

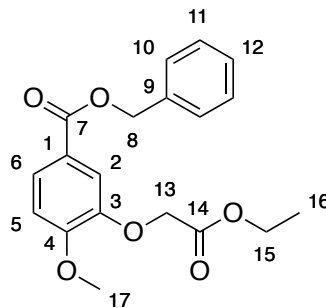
3-(Allyloxy)-*N*-(3-(3,4-dichlorophenyl)-1,2,4-oxadiazol-5-yl)-4-methoxybenzamide

298



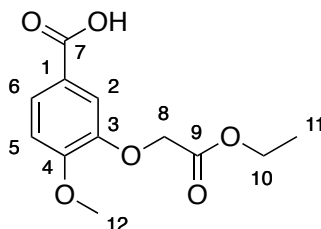
Benzoic acid **297** (260 mg, 1.25 mmol) and DMAP (478 mg, 3.9 mmol) were added to a solution of 5-amino-1,2,4-oxadiazole **224h** (230 mg, 1mmol) in DCM (20 mL). EDCI (300 mg, 1.6 mmol) was added to the solution. The mixture was stirred for 16 h. Water was added and the mixture was separated. The aqueous layer was washed with DCM (2 × 30 mL). The combined organic layers were washed with 2N HCl solution (30 mL) and a saturated solution of brine (30 mL). The organic layer was dried with magnesium sulfate and the solvent was removed under reduced pressure. The product was dry loaded on magnesium sulfate and purified by column chromatography (2% diethyl ether/DCM to 5% diethyl ether/DCM) to give the product **298** as a colourless solid (335 mg, 80%): m.p 134-138 °C; $\nu_{\text{max}}/\text{cm}^{-1}$ (nujol mull) 3320, 1687, 1599, 1561, 1265; δ_{H} (300 MHz, CDCl_3) 9.21 (1H, s, 9-NH), 8.18 (1H, d, J = 1.9 Hz, 2-H), 7.92 (1H, dd, J = 8.4, 1.9 Hz, 6-H), 7.60-7.57 (2H, m, 5,12-H), 7.54 (1H, dd, J = 8.4, 2.2 Hz, 16-H), 6.99 (1H, d, J = 8.4 Hz, 15-H), 6.13 (ddt, J = 17.3, 10.5, 5.5 Hz, 18-H), 5.49 (1H, dq, J = 17.3, 1.5 Hz, 19 trans-H), 5.38 (1H, dq, J = 10.5, 1.3 Hz, 19 cis-H), 4.73 (2H, dt, J = 5.5, 1.5 Hz, 17-H), 4.00 (3H, s, 20-H); δ_{C} (100 MHz, D_6 -DMSO) 168.5 (C-8), 166.1 (C-7), 163.8 (C-10), 153.7 (C-14), 147.6 (C-13), 134.7 (C-1), 133.9 (C-18), 132.6 (C-3), 132.2 (C-5), 128.9 (C-2), 127.5 (C-4), 127.4 (C-6), 124.2 (C-11), 123.4 (C-16), 118.3 (C-19), 113.3 (C-12), 111.8 (C-15), 69.6 (C-17), 56.3 (C-20); m/z (ES^+) 442.03 ($[\text{M}+\text{Na}]^+$, 100%), (ES^-) 418.04 ($[\text{M}-\text{H}]^-$, 100), HRMS m/z (ES^+) 442.0323 ($[\text{M}+\text{Na}]^+$, 100%) $\text{C}_{19}\text{H}_{15}\text{O}_4\text{N}_3\text{Cl}_2\text{Na}$ requires 442.0337.

Benzyl 3-(2-ethoxy-2-oxoethoxy)-4-methoxybenzoate **300**



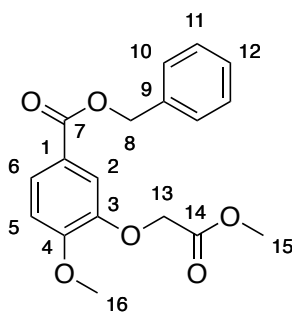
Ethyl bromoacetate (1.03 mL, 9.2 mmol) and potassium carbonate (1.34 g, 9.6 mmol) were added to a solution of benzyl ester **265** (2g, 7.7 mmol) in DMF (50 mL). The mixture was stirred at 60 °C for 3 h. Water (50 mL) was added and the product was extracted with ethyl acetate. The aqueous layer was washed with ethyl acetate (3 × 50 mL). The combined organic layers were washed with water (3 × 30 mL) and brine solution (30 mL). The organic layer was dried with magnesium sulfate and the solvent was removed under reduced pressure. The product was purified by column chromatography on silica (20% ethyl acetate/petroleum ether to 25% ethyl acetate/petroleum ether) to give the product **300** as a colourless oil (2.56 g, 96%): $\nu_{\text{max}}/\text{cm}^{-1}$ (thin film) 3204, 2980, 2937, 1758, 1712, 1603, 1515; δ_{H} (500 MHz, CDCl_3) 7.80 (1H, dd, J = 8.5, 2.0 Hz, 6-H), 7.54 (1H, d, J = 2.0 Hz, 2-H), 7.46 (2H, dd, J = 7.8, 1.0 Hz, 10-H), 7.43-7.36 (3H, m, 11,12-H), 6.94 (1H, d, J = 8.5 Hz, 5-H), 5.36 (2H, s, 8-H), 4.75 (2H, s, 13-H), 4.28 (2H, q, J = 7.1 Hz, 15-H), 3.96 (3H, s, 17-H), 1.30 (3H, t, J = 7.1 Hz, 16-H); δ_{C} (125 MHz, CDCl_3) 168.5 (C-14), 165.9 (C-7), 153.6 (C-4), 146.8 (C-3), 136.2 (C-9), 128.6 (C-11), 128.2 (C-12), 128.1 (C-10), 125.1 (C-6), 122.5 (C-1), 114.6 (C-2), 111.0 (C-5), 66.6 (C-8), 66.2 (C-13), 61.4 (C-15), 56.1 (C-17), 14.2 (C-16); HRMS m/z (ES^+) 367.1143 ($[\text{M}+\text{Na}]^+$, 100%) $\text{C}_{19}\text{H}_{20}\text{O}_6\text{Na}$ requires 367.1158.

3-(2-Ethoxy-2-oxoethoxy)-4-methoxybenzoic acid **301**



10% Pd/C (200 mg, 0.19 mmol) was added to a solution of benzyl ester **300** (2g, 5.81 mmol) in methanol (30 mL). The mixture was stirred under a hydrogen atmosphere for 48 h. The mixture was filtered through a pad of celite and the celite was washed with methanol (2 × 30 mL). The filtrate and washings were combined and the solvent was removed under reduced pressure to give a solid. The product was purified by column chromatography on silica (50 % ethyl acetate/petroleum ether) or by recrystallisation (ethyl acetate/ hexane) to give the product **301** as a white solid (882 mg, 60%): m.p. 118-122 °C; $\nu_{\text{max}}/\text{cm}^{-1}$ (nujol) 3474, 3197, 1749, 1686, 1601, 1269; δ_{H} (500 MHz, D_6 -DMSO) 7.59 (1H, dd, J = 8.4, 1.2 Hz, 6-H), 7.37 (1H, d, J = 1.2 HZ, 2-H), 7.07 (1H, d, J = 8.4 Hz, 5-H), 4.82 (2H, s, 8-H), 4.12 (2H, q, J = 7.1 Hz, 10-H), 3.85 (3H, s, 12-H), 1.22 (3H, t, J = 7.1 Hz, 11-H); δ_{C} (75 MHz, D_6 -DMSO) 169.1 (C-9), 167.6 (C-7), 152.8 (C-4), 146.9 (C-3), 124.6 (C-1), 124.4 (C-6), 114.4 (C-2), 111.9 (C-5), 65.8 (C-8), 61.1 (C-10), 56.2 (C-12), 14.5 (C-11); HRMS m/z (ES^+) 277.0676 ($[\text{M}+\text{Na}]^+$, 100%) $\text{C}_{12}\text{H}_{14}\text{O}_6\text{Na}$ requires 277.0688.

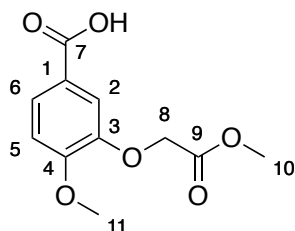
Benzyl 4-methoxy-3-(2-methoxy-2-oxoethoxy)benzoate **303**



Potassium carbonate (2 g, 14.5 mmol) and methyl bromoacetate (1.32 mL, 13.9 mmol) were added to a solution of benzyl ester **265** (3 g, 11.6 mmol) in DMF (50

mL). The mixture was heated to 60 °C for 3 h. Water (30 mL) and DCM (30 mL) were added and the layers were separated. The aqueous layer was washed with DCM (3 × 30 mL). The combined organic layers were washed with water (2 × 30 mL) and brine solution (30 mL). The organic layer was dried with magnesium sulfate and the solvent was removed under reduced pressure. The product was purified by column chromatography on silica (30% ethyl acetate/petroleum ether) to give the product **303** as a colourless oil (3.41 g, 88%): $\nu_{\text{max}}/\text{cm}^{-1}$ (thin film) 3405, 3088, 3007, 2954, 2842, 2614, 2038, 1880, 1760, 1716, 1603, 1588, 1515, 1427, 1294; δ_{H} (400 MHz, CDCl_3) 7.80 (1H, dd, J = 8.5, 2.0 Hz, 6-H), 7.54 (1H, d, J = 2.0 Hz, 2-H), 7.47- 7.36 (5H, m, 10,11,12-H), 6.94 (1H, d, J = 8.5 Hz, 5-H), 5.35 (2H, s, 8-H), 4.76 (2H, s, 13-H), 3.96 (3H, s, 16-H), 3.81 (3H, s, 15-H); δ_{C} (100 MHz, CDCl_3) 168.9 (C-14), 165.9 (C-7), 153.6 (C-4), 146.7 (C-3), 136.2 (C-9), 128.6 (C-10), 128.2 (C-12), 128.1 (C-11), 125.1 (C-6), 122.5 (C-1), 114.5 (C-2), 111.0 (C-5), 66.6 (C-8), 66.1 (C-13), 56.1 (C-16), 52.3 (C-15); HRMS m/z (ES^+) 353.0986 ($[\text{M}+\text{Na}]^+$, 100%) $\text{C}_{18}\text{H}_{18}\text{O}_6\text{Na}$ requires 353.1001.

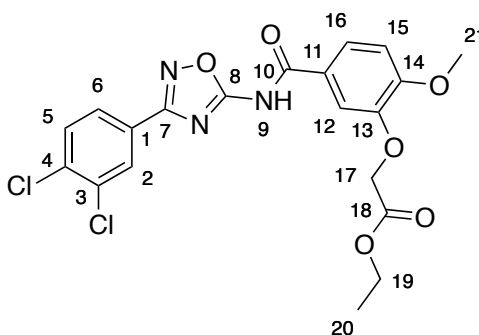
4-Methoxy-3-(2-methoxy-2-oxoethoxy)benzoic acid **304**



10% Pd/C (200 mg, 0.19 mmol) was added to a solution of benzyl ester **303** (2.06 g, 6.2 mmol) in methanol (30 mL). The mixture was stirred under a hydrogen atmosphere for 48 h. The mixture was filtered through a pad of celite. The celite was washed with methanol (2 × 30 mL). The filtrate and the washings were combined and the solvent was removed under reduced pressure. The product was purified by column chromatography on silica (5% methanol/DCM) to give the product **304** as a colourless solid (1.07 g, 71%): m.p 147-150 °C; $\nu_{\text{max}}/\text{cm}^{-1}$ (nujol) 1770, 1752, 1724, 1690, 1602, 1587, 1521, 1216, 763; δ_{H} (300 MHz, CDCl_3) 7.86 (1H, dd, J = 8.5, 2.0 Hz, 6-H), 7.56 (1H, d, J = 2.0 Hz, 2-H), 6.99 (1H, d, J = 8.5 Hz,

5-H), 4.80 (2H, s, 8-H), 4.00 (3H, s, 11-H), 3.86 (3H, s, 10-H); δ_{C} (75 MHz, CDCl_3) 171.5 (C-7), 168.9 (C-9), 154.2 (C-4), 146.8 (C-3), 125.9 (C-6), 121.6 (C-1), 114.7 (C-2), 111.1 (C-5), 66.0 (C-8), 56.2 (C-11), 52.4 (C-10); HRMS m/z (ES^+) 263.0522 ($[\text{M}+\text{Na}]^+$, 100%) $\text{C}_{11}\text{H}_{12}\text{O}_6\text{Na}$ requires 263.0532.

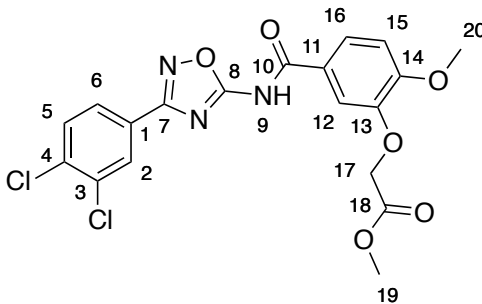
Ethyl 2-(5-((3-(3,4-dichlorophenyl)-1,2,4-oxadiazol-5-yl)carbamoyl)-2-methoxyphenoxy)acetate **284**



Benzoic acid **301** (398 mg, 1.5 mmol) and DMAP (478 mg, 3.9 mmol) were added to a solution of 5-amino-1,2,4-oxadiazole **224h** (300 mg, 1.3 mmol) in DCM (20 mL). EDCI (375 mg, 1.95 mmol) was added to the mixture, which was stirred for 16 h. Water (30 mL) and DCM (30 mL) were added to the yellow solution and the layers were separated. The aqueous layer was washed with DCM (2 × 30 mL). The combined organic layers were washed with HCl solution (2N, 30 mL) and brine solution. The organic layer was dried with magnesium sulfate and the solvent was removed under reduced pressure. The product was purified by recrystallisation from ethanol to give **284** as a colourless solid (459 mg, 75%): m.p 189-192 °C; $\nu_{\text{max}}/\text{cm}^{-1}$ (nujol mull) 3481, 3318, 1735, 1705, 1602, 1565, 1506, 1203, 1181; δ_{H} (300 MHz, $\text{D}_6\text{-DMSO}$) 12.53 (1H, s, 9-NH), 8.13 (1H, d, J = 1.9 Hz, 2-H), 7.96 (1H, dd, J = 8.4, 1.9 Hz, 6-H), 7.88 (1H, d, J = 8.4 Hz, 5-H), 7.77 (1H, dd, J = 8.6, 2.1 Hz, 16-H), 7.59 (1H, d, J = 2.1 Hz, 12-H), 7.18 (1H, d, J = 8.6 Hz, 15-H), 4.88 (2H, s, 17-H), 4.20 (2H, q, J = 7.1 Hz, 19-H), 3.89 (3H, s, 21-H), 1.23 (3H, t, J = 7.1 Hz, 20-H); δ_{C} (125 MHz, $\text{D}_6\text{-DMSO}$) 168.9 (C-18), 168.5 (C-8), 166.1 (C-7), 163.7 (C-10), 153.5 (C-14), 147.1 (C-13), 134.7 (C-1), 132.6 (C-3), 132.2 (C-5), 128.9 (C-2), 127.5 (C-4), 127.4 (C-6), 124.1 (C-11), 124.0 (C-16), 113.3 (C-12), 112.1 (C-15),

65.7 (C-17), 61.2 (C-19), 56.4 (C-21), 14.5 (C-20); HRMS m/z (ES^-) 464.0422 ($[M-H]^-$, 100%) $C_{20}H_{16}O_6N_3Cl_2$ requires 464.0422.

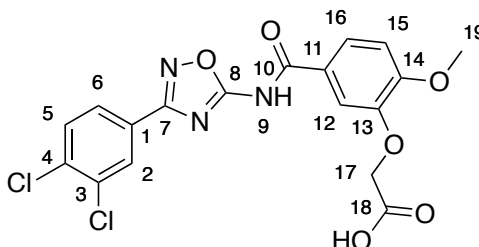
Methyl 2-(5-((3-(3,4-dichlorophenyl)-1,2,4-oxadiazol-5-yl)carbamoyl)-2-methoxyphenoxy)acetate **283**



Benzoic acid **304** (376 mg, 1.6 mmol) and DMAP (478 mg, 3.9 mmol) were added to a solution of 5-amino-1,2,4-oxadiazole **224h** (300 mg, 1.3 mmol) in DCM (20 mL). EDCI (375 mg, 1.96 mmol) was added to the mixture, which was then stirred for 16 h. Water (30 mL) and DCM (30 mL) were added to the yellow solution and the layers were separated. The aqueous layer was washed with DCM (2 × 30 mL). The combined organic layers were washed with HCl solution (2N, 30 mL) and brine solution. The organic layer was dried with magnesium sulfate and the solvent was removed under reduced pressure. The product was purified by column chromatography on silica (30% ethyl acetate/petroleum ether to 50% ethyl acetate/petroleum ether to 10% diethyl ether/ DCM) to give the product **283** as a white solid (435 mg, 74%): m.p 212-216 °C; ν_{max}/cm^{-1} (nujol) 3333, 1727, 1711, 1609, 1529, 754, 745; δ_H (400 MHz, D_6 -DMSO) 12.51 (1H, s, 9-NH), 8.11 (1H, d, J = 1.9 Hz, 2-H), 7.94 (1H, dd, J = 8.5, 1.9 Hz, 6-H), 7.85 (1H, d, J = 8.5 Hz, 5-H), 7.75 (1H, dd, J = 8.6, 2.1 Hz, 16-H), 7.58 (1H, d, J = 2.1 Hz, 12-H), 7.16 (1H, d, J = 8.6 Hz, 15-H), 4.89 (2H, s, 17-H), 3.87 (3H, s, 20-H), 3.71 (3H, s, 19-H); δ_C (75 MHz, D_6 -DMSO) 169.8 (C-18), 168.8 (C-8), 166.5 (C-7), 164.0 (C-10), 153.9 (C-14), 147.4 (C-13), 135.1 (C-1), 132.9 (C-3), 132.6 (C-5), 129.3 (C-2), 127.8 (C-4), 127.8 (C-6), 124.5 (C-11), 124.4 (C-16), 113.6 (C-12), 112.5 (C-15), 66.0 (C-17),

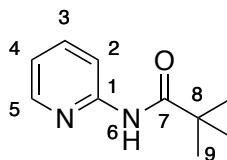
56.8 (C-20), 52.8 (C-19); HRMS m/z (ES^-) 450.0263 ($[M-H]^-$, 100%) $C_{19}H_{14}O_6N_3Cl_2$ requires 450.0265.

2-(5-((3-(3,4-Dichlorophenyl)-1,2,4-oxadiazol-5-yl)carbamoyl)-2-methoxyphenoxy)acetic acid **282**



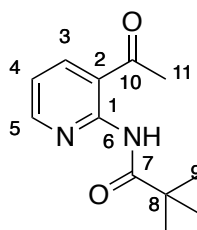
Methyl ester **283** (100 mg, 0.22 mmol) was added to a sodium hydroxide solution (1M, 2 mL) and the mixture was stirred for 30 min. THF (2 mL) was added and the mixture was stirred for a further 30 min after which TLC analysis showed complete consumption of the starting material. The solvent was removed under reduced pressure. Water (5 mL) was added and the solution was acidified with HCl solution (2M) to give a precipitate. The precipitate was collected and dried to give the product **282** as a white solid (59 mg, 61%): m.p. decomposition 258-262 °C; ν_{max}/cm^{-1} (nujol) 3326, 3188, 1741, 1716, 1615, 1377, 1080, 761; δ_H (300 MHz, D_6 -DMSO) 12.58 (1H, s, 9-NH), 8.11 (1H, d, $J=1.9$ Hz, 2-H), 7.94 (1H, dd, $J=8.4, 1.9$ Hz, 6-H), 7.85 (1H, d, $J=8.4$ Hz, 5-H), 7.74 (1H, dd, $J=8.6, 2.1$ Hz, 16-H), 7.56 (1H, d, $J=2.1$ Hz, 12-H), 7.15 (1H, d, $J=8.6$ Hz, 15-H), 4.78 (2H, s, 17-H), 3.87 (3H, s, 19-H); δ_C (75 MHz, D_6 -DMSO) 170.8 (C-18), 168.8 (C-8), 166.4 (C-7), 164.1 (C-10), 153.8 (C-14), 147.6 (C-13), 135.1 (C-1), 132.9 (C-3), 132.6 (C-5), 129.3 (C-2), 127.8 (C-6), 127.8 (C-4), 124.4 (C-11), 124.1 (C-6), 113.3 (C-12), 112.4 (C-15), 65.8 (C-17), 56.7 (C-19); HRMS m/z (ES^-) 436.0105 ($[M-H]^-$, 100%) $C_{18}H_{12}O_6N_3Cl_2$ requires 436.0103.

N-(Pyridin-2-yl)pivalamide **343**¹⁹⁰



2-Aminopyridine (15 g, 159 mmol) was added to a solution of DMAP (29 g, 239 mmol) in DCM (125 mL). The solution was cooled to 0 °C and trimethylacetyl chloride (23.5 mL, 191 mmol) was added dropwise. Once the addition was complete the solution was warmed to room temperature and stirred for 16 h. When TLC analysis indicated that all of the starting material had been consumed, a saturated solution of sodium bicarbonate (50 mL) was added. The layers were separated and the aqueous layer was re-extracted with DCM (2 × 50 mL). The combined organic layers were dried with magnesium sulfate and the solvent was removed under reduced pressure. The product was purified by column chromatography on silica (20% ethyl acetate/petroleum ether) to give the product **343** as a colourless solid (25.9 g, 91%): m.p 44-49 °C (Lit.¹⁹⁰ 71-73 °C); $\nu_{\max}/\text{cm}^{-1}$ (nujol) 3440, 3303, 1698, 1685, 1578, 1149; δ_{H} (300 MHz, CDCl₃) 8.31-8.25 (3H, m, 4,5,7-H), 7.73 (1H, dddd, J = 8.4, 7.4, 1.9, 0.5 Hz, 3-H), 7.06 (1H, ddd, J = 7.4, 5.0, 1.1 Hz, 5-H), 1.35 (9H, s, 9-H); δ_{C} (75 MHz, CDCl₃) 177.6 (C-7), 151.9 (C-1), 147.5 (C-5), 139.2 (C-2), 120.1 (C-4), 114.6 (C-3), 40.3 (C-8), 27.9 (C-9); HRMS m/z (Cl⁺) 179.1181 ([M+H]⁺, 100%) C₁₀H₁₅N₂O requires 179.1184

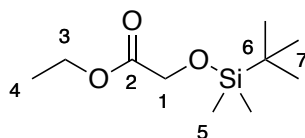
N-(3-Acetylpyridin-2-yl)pivalamide **344**²²⁷



Pyridyl amide **343** (2 g, 11.2 mmol) was dissolved in THF (50 mL). The solution was cooled to -50 °C. *N*-Butyl lithium (1.6 N solution in hexane, 17.6 mL, 28.0

mmol) was added dropwise keeping the temperature of the solution below -40 °C. The solution turned yellow after addition of all of the *n*-butyl lithium. When all of the *n*-butyl lithium had been added the solution was warmed to 0 °C for 1.5 h, during which time a yellow precipitate formed. The mixture was cooled to -40 °C and a solution of 4-acetylmorpholine (2.2 g, 1.97 mL) in THF (10 mL) was added dropwise. The mixture was stirred for 30 min at -40 °C during which time the precipitate disappeared. The reaction was quenched by the addition of saturated ammonium chloride solution (40 mL). DCM (40 mL) was added and the layers were separated. The aqueous layer was re-extracted with DCM (2 × 40 mL). The combined organic layers were washed with water (30 mL) and brine solution (30 mL). The organic layer was dried with magnesium sulfate and the solvent was removed under reduced pressure. The product was purified by column chromatography on silica (50% ethyl acetate/petroleum ether to 100% ethyl acetate) to give the product **344** as a white solid (1.55 g, 63%): m.p 32-34 °C (Lit.²²⁷ 67-68 °C); $\nu_{\text{max}}/\text{cm}^{-1}$ (nujol) 3444 1708, 1698, 1661, 1601, 1578; δ_{H} (300 MHz, CDCl₃) 11.55 (1H, s, 6-NH), 8.65 (1H, dd, *J* = 4.8, 1.9 Hz, 4-H), 8.21 (1H, dd, *J* = 7.9, 1.9 Hz, 3-H), 7.11 (1H, dd, *J* = 7.9, 4.8 Hz, 5-H), 2.66 (3H, s, 11-H), 1.35 (9H, s, 9-H); δ_{C} (75 MHz, CDCl₃) 201.3 (C-10), 177.3 (C-7), 153.7 (C-4), 152.4 (C-1), 140.6 (C-3), 118.4 (C-2, C-5), 41.1 (C-8), 28.4 (C-11), 27.8 (C-9); HRMS *m/z* (ES⁺) 243.1113 ([M+Na]⁺, 58%) C₁₂H₁₆N₂O₂Na requires 243.1109; 221.1295 ([M+H]⁺, 100) C₁₂H₁₇N₂O₂ requires 221.1290.

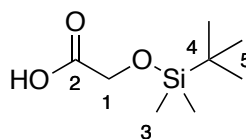
Ethyl 2-((*tert*-butyldimethylsilyl)oxy)acetate **350**¹⁹⁴



Imidazole (18.6 g, 288 mmol) and TBSCl (31.8 g, 212 mmol) were added portionwise to a solution of ethyl glycolate (20 g, 182 mmol) was dissolved in DCM (150 mL) that was cooled to 0 °C. The mixture was stirred for 16 h. Water (50 mL) was added and the layers were separated. The aqueous layer was re-extracted

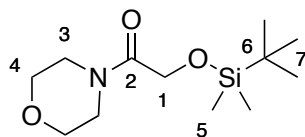
with DCM (2 × 50 mL). The combined organic layers were washed with water (50 mL) and brine solution (50 mL). The organic layer was dried with magnesium sulfate and the solvent was removed under reduced pressure. The product was purified by column chromatography on silica (5% ethyl acetate/petroleum ether) to give the product **350** as a colourless oil (37.4 g, 89%): $\nu_{\text{max}}/\text{cm}^{-1}$ (thin film) 2955, 2931, 2858, 1762, 1736, 1475, 1445.62, 1256, 1148; δ_{H} (300 MHz, CDCl_3) 4.13 (2H, s, 1-H), 4.09 (2H, q, $J = 7.2$ Hz, 3-H), 1.17 (3H, t, $J = 7.2$ Hz, 4-H), 0.81 (9H, s, 7-H), 0.00 (6H, s, 5-H); δ_{C} (75 MHz, CDCl_3) 172.1 (C-2), 62.2 (C-1), 61.1 (C-3), 26.1 (C-7), 18.8 (C-6), 14.6 (C-4), -5.7 (C-5); HRMS m/z (ES^+) 241.1240 ($[\text{M}+\text{Na}]^+$, 100%) $\text{C}_{10}\text{H}_{22}\text{O}_3\text{SiNa}$ requires 241.1236.

2-((*tert*-Butyldimethylsilyl)oxy)acetic acid **351**²²⁸



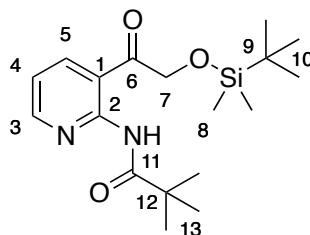
A solution of potassium hydroxide (2.68 g, 47.8 mmol) in ethanol (50 mL) was added to a solution of ethyl ester **350** (7.85 g, 35.9 mmol) in ethanol (240 mL). The mixture was stirred for 16 h. The solvent was removed under reduced pressure. DCM (200 mL) was added and the organic layer was washed with saturated ammonium chloride solution (100 mL). The organic layer was dried with magnesium sulfate and the solvent was removed under reduced pressure to give the product **351** as a colourless solid (4.70 g, 67%); m.p 74-76°C (Lit.²²⁸ 48-49 °C); $\nu_{\text{max}}/\text{cm}^{-1}$ (nujol) 3364, 1731; δ_{H} (500 MHz, CDCl_3) 4.19 (2H, s, 1-H), 0.91 (9H, s, 5-H), 0.1 (6H, s, 3-H); δ_{C} (125 MHz, CDCl_3) 172.0 (C-2), 62.4 (C-1), 25.6 (C-5), 18.5 (C-4), -5.4 (C-3); HRMS m/z (ES^-) 189.0949 ($[\text{M}-\text{H}]^-$, 100%) $\text{C}_8\text{H}_{17}\text{O}_3\text{Si}$ requires 189.0947.

2-((*tert*-Butyldimethylsilyl)oxy)-1-morpholinoethanone **352**



Morpholine (4.14 mL, 47.9 mmol) and DMAP (585 mg, 4.8 mmol) were added to a solution of carboxylic acid **351** (7.02 g, 36.8 mmol) in DCM (50 mL). DCC (9.89 g, 47.9 mmol) was added to the solution and a precipitate formed. The mixture was stirred for 16 h. The precipitate was filtered off and water (50 mL) was added to the filtrate and the layers were separated. The aqueous layer was re-extracted with DCM (2 × 50 mL). The combined organic layers were washed with brine solution (30 mL). The organic layer was dried with magnesium sulfate and the solvent was removed under reduced pressure. The product was purified by column chromatography on silica to give the product **352** as a colourless oil (3.68 g, 38%): $\nu_{\text{max}}/\text{cm}^{-1}$ (thin film) 3490, 2956, 2929, 2857, 1654; δ_{H} (300 MHz, CDCl_3) 4.18 (2H, s, 1-H), 3.59-3.56 (4H, m, H), 3.51-3.47 (4H, m, H), 0.8 (9H, s, 7-H), 0.00 (6H, s, 5-H); δ_{C} (125 MHz, CDCl_3) 169.3 (C-2), 66.8 (C-4), 66.8 (C-4), 64.0 (C-1), 45.8 (C-3), 42.2 (C-3), 25.7 (C-7), 18.2 (C-6), -5.5 (C-5); HRMS m/z (ES^+) 282.1512 ($[\text{M}+\text{Na}]^+$, 100%) $\text{C}_{12}\text{H}_{25}\text{NO}_3\text{SiNa}$ requires 282.1501.

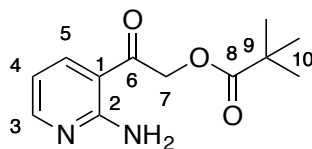
N-(3-(2-((*tert*-butyldimethylsilyl)oxy)acetyl)pyridin-2-yl)pivalamide **353**



Pyridyl amide **343** (4 g, 22.4 mmol) was dissolved in THF (50 mL). The solution was cooled to -50 °C. *N*-Butyl lithium (1.6 N solution in hexane, 35.2 mL, 56.0 mmol) was added dropwise keeping the temperature of the solution below -40 °C. The solution turned yellow after addition of all of the *n*-butyl lithium. After the

addition of *n*-butyl lithium was complete the solution was warmed to 0 °C for 1.5 h, during which time a yellow precipitate formed. The mixture was cooled to -40 °C and ethyl ester **350** (7.34 g, 33.6 mmol) was added dropwise. The mixture was stirred for 30 min at -40 °C during which time the precipitate disappeared. The reaction was quenched by the addition of saturated ammonium chloride solution (40 mL). DCM (40 mL) was added and the layers were separated. The aqueous layer was re-extracted with DCM (2 × 40 mL). The combined organic layers were washed with water (30 mL) and brine solution (30 mL). The organic layer was dried with magnesium sulfate and the solvent was removed under reduced pressure. The product was purified by column chromatography on silica (20% ethyl acetate/ petroleum ether to 30% ethyl acetate/ petroleum ether) to give the product **353** as a yellow oil (4.77 g, 61%): $\nu_{\text{max}}/\text{cm}^{-1}$ (thin film) 3288, 2955, 2858, 1711, 1579, 1507, 971; δ_{H} (300 MHz, CDCl_3) 11.06 (1H, s, NH), 8.53 (1H, dd, J = 4.8, 1.9 Hz, 4-H), 8.05 (1H, dd, J = 7.9, 1.9 Hz, 5-H), 6.96 (1H, dd, J = 7.9, 4.8 Hz, 3-H), 4.73 (2H, s, 7-H), 1.24 (9H, s, 13-H), 0.80 (9H, s, 10-H), 0.00 (6H, s, 8-H); δ_{C} (75 MHz, CDCl_3) 200.5 (C-6), 177.1 (C-11), 153.9 (C-4), 152.3 (C-2), 139.1 (C-5), 118.3 (C-3), 116.9 (C-1), 68.3 (C-7), 41.0 (C-12), 27.9 (C-13), 26.2 (C-10), 18.8 (C-9), -4.9 (C-8); HRMS m/z (ES^+) 373.1931 ($[\text{M}+\text{Na}]^+$, 100%) $\text{C}_{18}\text{H}_{30}\text{N}_2\text{O}_3\text{SiNa}$ requires 373.1923.

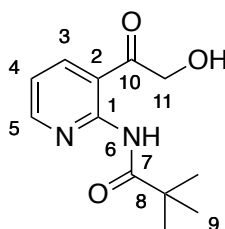
2-(2-Aminopyridin-3-yl)-2-oxoethyl pivalate **354**



TBAF (1N solution in THF, 2.7 mL, 2.7 mmol) was added dropwise to a solution of ketone **353** (872 mg, 2.5 mmol) in THF (10 mL). The solution turned black and stirring was continued for 2 h. Ethyl acetate (30 mL) and water (30 mL) were added and the layers were separated. The aqueous layer was re-extracted with ethyl acetate (3 × 40 mL). The combined organic layers were washed with brine solution (30 mL). The organic layer was dried with magnesium sulfate and the solvent was

removed under reduced pressure. The product was purified by column chromatography on silica (30% ethyl acetate/petroleum ether to 40% ethyl acetate/petroleum ether) to give the product **354** as a colourless solid (186 mg, 32%): m.p 115-119 °C; $\nu_{\max}/\text{cm}^{-1}$ (nujol) 3400, 1741, 1670, 1624, 1563, 1142, 967, 764, 722; δ_{H} (500 MHz, CDCl_3) 8.27 (1H, dd, J = 4.7, 1.7 Hz, 4-H), 7.89 (1H, dd, J = 7.9, 1.7 Hz, 5-H), 6.65 (1H, dd, J = 7.9, 4.7 Hz, 3-H), 5.26 (2H, s, 7-H), 1.31 (9H, s, 10-H); δ_{C} (125 MHz, CDCl_3) 192.4 (C-6), 177.9 (C-8), 158.4 (C-2), 154.7 (C-4), 138.0 (C-5), 112.0 (C-3), 110.3 (C-1), 65.1 (C-7), 38.9 (C-9), 27.0 (C-10); m/z (ES+) 259.23 ($[\text{M}+\text{Na}]^+$, 100%), 237.25 ($[\text{M}+\text{H}]^+$, 48); HRMS m/z (ES+) 237.1240 ($[\text{M}+\text{H}]^+$, 100%) $\text{C}_{12}\text{H}_{17}\text{N}_2\text{O}_3$ requires 237.1239.

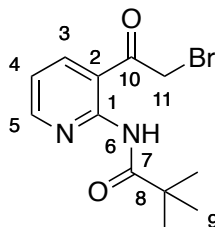
N-(3-(2-Hydroxyacetyl)pyridin-2-yl)pivalamide **357**



Acetyl chloride (883 μL , 12.4 mmol) was added to a solution of ketone **353** (3.96 g, 11.3 mmol) in methanol (20 mL). The solution was stirred for 3 h. When TLC indicated consumption of all the starting material, water (30 mL) and DCM (40 mL) were added and the layers were separated. The aqueous layer was re-extracted with DCM (3 \times 30 mL). The combined organic layers were washed with brine solution. The organic layer was dried with magnesium sulfate and the solvent was removed under reduced pressure. The product was purified by column chromatography on silica (1% methanol/DCM to 2% methanol/DCM to 5% methanol/DCM) to give the product **357** as brown solid (1.53 g, 57%): m.p 104-106 °C; $\nu_{\max}/\text{cm}^{-1}$ (nujol mull) 3350, 3079, 1714, 1650, 1601, 1579, 1259, 1157, 1051; δ_{H} (400 MHz, CDCl_3) 11.1 (1H, s, NH), 8.54 (1H, dd, J = 4.8, 1.9 Hz, 5-H), 8.01 (1H, dd, J = 7.9, 1.9 Hz, 3-H), 7.06 (1H, dd, J = 7.9, 4.8 Hz, 4-H), 4.83 (2H, s, 11-H), 1.28 (9H, s, 9-H); δ_{C} (75 MHz, CDCl_3) 200.5 (C-10), 176.8 (C-7), 154.2 (C-5), 151.5 (C-

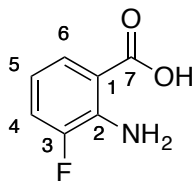
1), 137.7 (C-3), 118.3 (C-4), 115.7 (C-2), 65.8 (C-11), 40.6 (C-8), 27.4 (C-9); HRMS m/z (ES^+) 259.1058 ($[M+Na]^+$, 100%) $C_{12}H_{16}N_2O_3Na$ requires 259.1059.

N-(3-(2-Bromoacetyl)pyridin-2-yl)pivalamide **345**



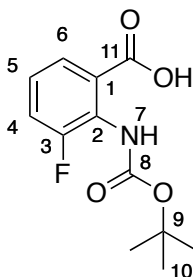
Triphenylphosphine (113 mg, 0.43 mmol) and carbontetrabromide (144 mg, 0.43 mmol) were added to a solution of alcohol **357** (93 mg, 0.4 mmol) in DCM (5 mL). The solution was stirred in the dark for 8 h. The solvent was removed under reduced pressure and the oil was dry loaded onto magnesium sulfate. The product was purified by column chromatography on silica (30% ethyl acetate/petroleum ether to 40% ethyl acetate/petroleum ether) to give the product as a yellow oil (38 mg, 32%): δ_H (300 MHz, $CDCl_3$) 10.72 (1H, s, NH), 8.65 (1H, dd, J = 4.8, 1.8 Hz, 5-H), 8.18 (1H, dd, J = 7.9, 1.8 Hz, 3-H), 7.15 (1H, dd, J = 7.9, 4.8 Hz, 4-H), 4.43 (2H, s, 11-H), 1.36 (9H, s, 9-H); δ_C (75 MHz, $CDCl_3$) 193.5 (C-10), 176.9 (C-7), 153.7 (C-5), 151.6 (C-1), 139.6 (C-3), 118.4 (C-4), 117.1 (C-2), 40.5 (C-8), 31.2 (C-11), 27.4 (C-9); m/z (ES^+) 330.86 ($[M^{79}Br+Na]^+$, 100%), 322.86 ($[M^{81}Br+Na]^+$, 82), HRMS m/z (ES^+) 299.0392 ($[M+H]^+$, 14%) $C_{12}H_{16}O_2N_2Br$ requires 299.0395

2-Amino-3-fluorobenzoic acid **364**¹⁹⁶



7-Fluoroisatin (10 g, 60.6 mmol) was added to a solution of sodium hydroxide (8.34 g, 208 mmol) in water (300 mL). Hydrogen peroxide (30% w/w, 40 mL) was added dropwise. A gas was evolved. The solution was warmed to 50 °C for 30 min. The solution was allowed to cool before HCl (2N solution) was added dropwise until a pH of 4 was reached. A precipitate formed which was filtered and the precipitate was recrystallised from ethanol/water to give the product **364** as a brown solid (5.14 g, 55%): m.p 179-183 °C (Lit.¹⁹⁶ 183-184 °C); δ_{H} (300 MHz, CDCl_3) 7.72 (1H, ddd, $J = 8.1, 1.5, 1.2$ Hz, 6-H), 7.16 (1H, ddd, $J = 11.3, 7.9, 1.5$ Hz, 4-H), 6.60 (1H, ddd, $J = 8.1, 7.9, 5.0$ Hz, 5-H), 5.81 (2H, s, NH_2); δ_{C} (75 MHz, CDCl_3) 172.6 (C-7), 151.5 (d, $J = 239.7$ Hz, C-3), 140.5 (d, $J = 14$ Hz, C-2), 127.2 (d, $J = 3.5$ Hz, C-6), 119.4 (d, $J = 18.2$ Hz, C-4), 114.9 (d, $J = 7.2$ Hz, C-5), 111.3 (d, $J = 4.2$ Hz, C-1); δ_{F} (282 MHz, CDCl_3) -136.59 (1F, ddd, $J = 11.3, 5, 1.2$ Hz); m/z (Cl^+) 156.05 ($[\text{M}+\text{H}]^+$, 22%), 155.04 ($[\text{M}]^+$, 28), 138.03 ($[\text{M}-\text{OH}]^+$, 100), HRMS m/z (Cl^+) 156.0458 ($[\text{M}+\text{H}]^+$, 22%) $\text{C}_7\text{H}_7\text{NO}_2\text{F}$ requires 156.0461.

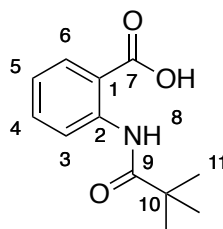
2-((*tert*-Butoxycarbonyl)amino)-3-fluorobenzoic acid **361**²²⁹



Benzoic acid **364** (900 mg, 5.8 mmol) was added to a solution of THF/Water (20:20 mL). Sodium hydroxide (580 mg, 14.5 mmol) was added to the solution. Di-*tert*-

butyl dicarbonate (1.52 g, 6.9 mmol) was added and the solution was stirred for 16 h. The volatile solvent was removed under reduced pressure the pH was adjusted to 6 and ethyl acetate (40 mL) was added. The aqueous layer was re-extracted with ethyl acetate (2 × 40 mL). The combined organic layers were dried with magnesium sulfate and the solvent was removed under reduced pressure. The product was purified by column chromatography on silica (20% ethyl acetate/petroleum ether to 30% ethyl acetate/petroleum ether) to give the product **361** as a brown solid (961 mg, 65%): m.p 180-182 °C; $\nu_{\text{max}}/\text{cm}^{-1}$ (nujol) 3518, 3393, 1717, 1667; δ_{H} (300 MHz, CDCl_3) 7.55 (1H, ddd, J = 8.1, 1.3, 1.3 Hz, 6-H), 7.23 (1H, ddd, J = 11.7, 7.9, 1.5 Hz, 4-H), 6.52 (1H, ddd, J = 8.1, 7.9, 5.0 Hz, 5-H), 1.46 (9H, s, 10-H); δ_{C} (75 MHz, CDCl_3) 168.9 (d, J = 3.5 Hz, C-11), 150.9 (d, J = 238.2 Hz, C-3), 146.2 (C-8), 140.0 (d, J = 14.3 Hz, C-2), 126.6 (d, J = 3.1 Hz, C-6), 118.3 (d, J = 18.0 Hz, C-4), 113.6 (d, J = 7.2 Hz, C-5), 112.3 (d, J = 4.6 Hz, C-1), 85.6 (C-9), 26.8 (C-10); δ_{F} (282 MHz, CDCl_3) -135.14 (1F, dd, J = 11.7, 5 Hz).

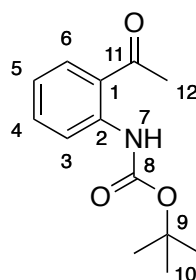
2-((*tert*-Butoxycarbonyl)amino)benzoic acid **368**¹⁹⁸



Anthranilic acid (5 g, 36.4 mmol) was added to a solution of water and 1,4-dioxan (1:1, 200 mL). Sodium hydroxide (4.38 g, 109 mmol) was added to the solution. Di-*tert*-butyl dicarbonate (9.55 g, 43.7 mmol) was added to the solution, which was stirred for 16 h. The solvent was removed under reduced pressure. Water (100 mL) was added and the product was precipitated by the addition of 1 N HCl until pH 4 was reached. The product was purified by recrystallisation from ethanol and water to give the product **368** as a brown solid (4.44 g, 51%): m.p 150-154 °C (Lit.¹⁹⁸ 150-152 °C); $\nu_{\text{max}}/\text{cm}^{-1}$ (nujol) 3308, 1728, 1670, 1587, 1534, 1523, 1268, 1151, 759; δ_{H} (300 MHz, D_6 -DMSO) 10.66 (1H, s, NH), 8.27 (1H, dd, J =8.5, 0.9 Hz, 3-H), 7.96

(1H, dd, J = 7.9, 1.6 Hz, 6-H), 7.55 (1H, ddd, J = 8.5, 7.2, 1.6 Hz, 5-H), 7.06 (1H, ddd, J = 7.9, 7.2, 1.1 Hz, 4-H), 1.45 (9H, s, 11-H); δ_{C} (75 MHz, D_6 -DMSO) 170.5 (C-7), 152.8 (C-9), 142.4 (C-1), 135.1 (C-5), 132.1 (C-6), 122.3 (C-4), 118.8 (C-3), 115.9 (C-2), 81.0 (C-10), 28.8 (C-11); m/z (ES^-) 236.0924 ($[\text{M}-\text{H}]^-$, 95%), 162.0190 ($[\text{M}-\text{C}_4\text{H}_{10}\text{O}]^-$, 100), (ES^+) 260.0888 ($[\text{M}+\text{Na}]^+$, 62), 138.0546 ($[\text{M}-\text{C}_5\text{H}_9\text{O}_2]^+$, 100), HRMS m/z (ES^-) 236.0924 ($[\text{M}-\text{H}]^-$, 95%) $\text{C}_{12}\text{H}_{14}\text{NO}_4$ requires 236.0928.

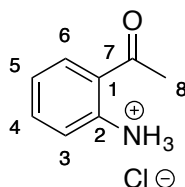
tert-Butyl (3-acetylphenyl)carbamate **369**²³⁰



Methylmagnesium bromide (3 M solution in Et_2O , 5 mL, 15 mmol) was added dropwise, under argon, to a solution of benzoic acid **368** (711 mg, 3 mmol) in THF (10 mL) at 0 °C. The solution was allowed to warm to room temperature and the mixture was stirred for 16 h. The mixture was poured onto ice and the pH was adjusted to 4 and ethyl acetate (50 mL) was added. The layers were separated and the aqueous layer was re-extracted with ethyl acetate (2 × 20 mL). The combined organic layers were dried with magnesium sulfate and the solvent was removed under reduced pressure the product was purified by column chromatography on silica (10% ethyl acetate/petroleum ether) to give the product **369** as a colourless solid (343 mg, 49%): m.p 52- 55 °C; $\nu_{\text{max}}/\text{cm}^{-1}$ (nujol) 3518, 3393, 3254, 3229, 1735, 1712, 1657, 1587, 1531, 1249, 1157, 1054, 1028, 956, 837, 741; δ_{H} (400 MHz, CDCl_3) 10.94 (1H, s, NH), 8.47 (1H, dd, J = 8.6, 0.8 Hz, H), 7.85 (1H, dd, J = 8.0, 1.5, H), 7.53-7.49 (1H, m, H), 7.02 (1H, ddd, J = 8, 7.3, 1.2 Hz, H), 2.64 (3H, s, Me), 1.52 (9H, s, $(\text{CH}_3)_3$); δ_{C} (75 MHz, CDCl_3) 202.2 (C-11), 153.1 (C-7), 141.8 (C-1), 134.9 (C-5), 131.6 (C-3), 121.4 (C-2), 120.9 (C-4), 119.2 (C-6), 80.5 (C-9), 28.6

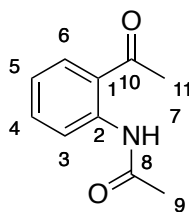
(C-12), 28.3 (C-10); HRMS m/z (ES^+) 258.1101 ($[M+Na]^+$, 100%) $C_{13}H_{17}NO_3Na$ requires 258.1106.

2-Acetylbenzenaminium chloride **370** ¹⁹⁹



HCl (4N in 1,4-dioxan, 2.5 mL, 10.1 mmol) was added to a solution of ketone **369** (795 mg, 3.4 mmol) in diethyl ether (2.5 mL). The mixture was stirred for 1 h. The precipitate was filtered which gave the product **370** as a yellow solid (305 mg, 53%): m.p 136-140 °C; δ_H (300 MHz, D_6DMSO) 8.72 (3H, s, NH_3), 7.77 (1H, dd, J = 8.1, 1.5 Hz, 6-H), 7.29 (1H, ddd, J = 8.4, 7, 1.5 Hz, 5-H), 6.87 (1H, dd, J = 8.4, 1.2 Hz, 3-H), 6.67 (1H, ddd, J = 8.1, 7.0, 1.2 Hz, 4-H), 2.50 (3H, s, Me); δ_C (75 MHz, D_6DMSO) 200.5 (C-7), 148.4 (C-1), 134.5 (C-5), 132.5 (C-6), 119.2 (C-2), 118.4 (C-3), 116.8 (C-4), 28.3 (C-8); m/z (ES^+) 158.06 ($[M+Na]^+$, 85%), 136.09 ($[M+H]^+$, 100), HRMS m/z (ES^+) 136.0766 ($[M+H]^+$, 85%) $C_8H_{10}NO$ requires 136.0762.

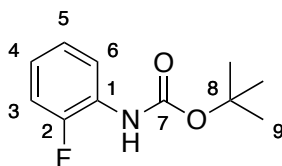
N-(2-Acetylphenyl)acetamide **371** ²⁰⁰



Acetic anhydride (205 μ l, 2.1 mmol) was added to a solution of amine **370** (250 mg, 1.5 mmol) in pyridine (10 mL). The mixture was stirred for 16 h. The reaction was quenched by the addition of saturated sodium bicarbonate solution (20 mL). DCM (20 mL) was added and the layers were separated. The aqueous layer was re-extracted with DCM (2 \times 20 mL). The combined organic layers were washed with water (30 mL) and brine solution (30 mL). The organic layer was dried with

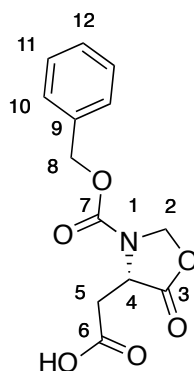
magnesium sulfate and the solvent was removed under reduced pressure. The product was purified by column chromatography on silica (20% ethyl acetate/petroleum ether) to give the product **371** as a colourless solid 209 mg, 73%): m.p 68-70 °C (Lit.²⁰⁰ 70-75 °C); $\nu_{\max}/\text{cm}^{-1}$ (nujol) 3222, 1688, 1652, 1605, 1584, 1528, 1249, 1240, 1169, 1010, 963, 765, 754; δ_{H} (300 MHz, CDCl_3) 11.63 (1H, s, 7-NH), 8.67 (1H, dd, J = 8.5, 1.1 Hz, 6-H), 7.82 (1H, dd, J = 8.0, 1.5 Hz, 3-H), 7.51-7.45 (1H, m, 4-H), 7.04 (1H, ddd, J = 8, 7.3, 1.2 Hz, 5-H), 2.60 (3H, s, 9-H), 2.16 (3H, s, 11-H); δ_{C} (75 MHz, CDCl_3) 202.9 (C-10), 169.5 (C-8), 141.1 (C-2), 135.2 (C-4), 131.6 (C-3), 122.3 (C-5), 121.7 (C-1), 120.8 (C-6), 28.7 (C-11), 25.6 (C-9); HRMS m/z (ES^+) 200.0688 ($[\text{M}+\text{Na}]^+$, 100%) $\text{C}_{10}\text{H}_{11}\text{NO}_2\text{Na}$ requires 200.0687.

tert-Butyl (2-fluorophenyl)carbamate **374**²³¹



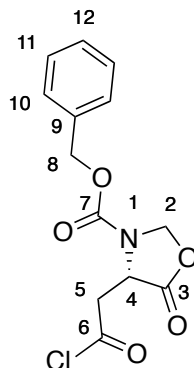
2-Fluoroaniline (10 mL, 11.51 g, 104 mmol) was added to di-*tert*-butyl dicarbonate (16.68 g, 71.85 mmol) and the mixture was heated at 80 °C for 2 h. The solution was allowed to cool. The product was purified by column chromatography on silica (10% ethyl acetate/ petroleum ether) to give the product **374** as a white solid (9.12 g, 56%): m.p 44-46 °C (Lit.²³¹ 48-49 °C); $\nu_{\max}/\text{cm}^{-1}$ (nujol) 3452, 3292, 1742, 1621, 1595, 1531, 1233, 1158, 1050, 749; δ_{H} (300 MHz, CDCl_3) 8.12 (1H, dd, J = 8 Hz, 4-H), 7.16-7.05 (2H, m, 3,5-H), 6.99 (1H, dddd, J = 8.3, 7.1, 5.3, 1.7 Hz, 6-H), 6.76 (1H, s, NH), 1.57 (9H, s, 9-H); δ_{C} (75 MHz, CDCl_3) 152.4 (C-7), 152.1 (d, J = 242.1 Hz, C-2), 126.9 (d, J = 10 Hz, C-1), 124.5 (d, J = 3.7 Hz, C-5), 122.9 (d, J = 7.5 Hz, C-6), 120.1 (C-4), 114.7 (d, J = 19 Hz, C-3), 81.0 (C-8), 28.3 (C-9); $\delta_{\text{F}\{\text{H}\}}$ (282 MHz, CDCl_3) 132.77 (s); HRMS m/z (ES^+) 234.0895 ($[\text{M}+\text{Na}]^+$, 100%) $\text{C}_{11}\text{H}_{14}\text{NO}_2\text{FNa}$ requires 234.0906.

(2S)-2-(3-((Benzyloxy)carbonyl)-5-oxooxazolidin-4-yl)acetic acid **376** ²⁰²



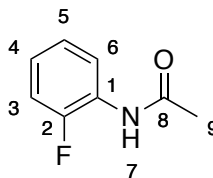
Paraformaldehyde (1.8 g, 59.8 mmol) and *p*-toluenesulfonic acid (342 mg, 1.8 mmol) were added to a solution of (2-*S*)-(((benzyloxy)carbonyl)amino)succinic acid (8 g, 30 mmol) in toluene (200 mL). The mixture was heated to reflux and the water was removed using dean-stark apparatus. After 5 h when no more water was produced the mixture was allowed to cool. The solvent was removed under reduced pressure. The product was purified by column chromatography (30 % ethyl acetate/ petroleum ether) to give the product **376** as a colourless oil which solidified with scratching (7.41 g, 87%): m.p 78-82 °C (Lit.²⁰² 82-84 °C); $[\alpha]_D^{20} +131.1$ (c 1.06 in CHCl₃) (Lit +124 c 3.53 in CHCl₃ ²⁰²); $\nu_{\max}/\text{cm}^{-1}$ (nujol) 3594, 3113, 1823, 1798, 1668; δ_{H} (300 MHz, CDCl₃) 8.71 (1H, s, H), 7.42-7.36 (5H, m, 10,11,12-H), 5.52 (1H, s, 2-H), 5.34 (1H, d, $J = 3.1$ Hz, 2-H), 5.28-5.11 (2H, m, 8-H), 4.38 (1H, s, 4-H), 3.39-3.05 (2H, m, 5-H); δ_{C} (75 MHz, CDCl₃) 175.7 (3), 172.0 (6), 153.3 (7), 135.5 (Ar), 129.2 (Ar-H), 129.1 (Ar-H), 128.8 (Ar-H), 78.7 (2), 68.7 (8), 51.8 (4), 34.4 (5); HRMS m/z (ES⁻) 278.0658 ([M-H]⁻, 100%) C₁₃H₁₂NO₆ requires 278.0665.

(2S)-Benzyl 4-(2-chloro-2-oxoethyl)-5-oxooxazolidine-3-carboxylate **318**^{184, 204}



Carboxylic acid **376** (7 g, 25 mmol) was dissolved in toluene (50 mL). A few drops of DMF were added followed by oxalyl chloride (10 mL, 117 mmol). The solution was refluxed for 3 h. The solution was allowed to cool and the solvent was removed under reduced pressure to give the product as a dark oil which was used without further purification (5.32 g, 71%): δ_{H} (300 MHz, CDCl_3) 7.47- 7.37 (5H, m, 10,11,12-H), 5.52 (1H, s, 2-H), 5.36 (1H, d, J = 3.3 Hz, 2-H), 5.26 (1H, d, J = 12.1 Hz, 8-H), 5.21 (1H, d, J = 12.1 Hz, 8-H), 4.38-4.36 (1H, m, 4-H), 3.89-3.56 (2H, m, 5-H), δ_{C} (75 MHz, CDCl_3) 172.1 (C-6), 170.3 (C-3), 152.6 (C-7), 135.0 (Ar), 128.9 (Ar-H), 128.8 (Ar-H), 128.5 (Ar-H), 78.4 (C-2), 68.4 (C-8), 51.6 (C-4), 46.4 (C-5).

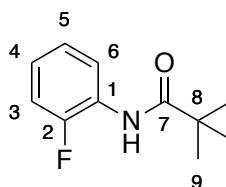
N-(2-Fluorophenyl)acetamide **379**²³²



Acetic anhydride (850 μL , 9 mmol) was added a solution of 2-fluoroaniline (1g, 9 mmol) and triethylamine (1.4 mL, 9.9 mmol) in DCM (20 mL). The mixture was stirred for 16 h. Aqueous saturated sodium bicarbonate (20 mL) was added. The product was extracted with DCM (2 \times 20 mL) and the combined organic layer was washed with brine solution (20 mL). The organic layer was dried with magnesium sulfate and the solvent was removed under reduced pressure. The product was

purified by recrystallisation from ethanol/ water to give the product **379** as a colourless solid (742mg, 54%): m.p 74-78 °C (Lit.²³² 78-80 °C); $\nu_{\max}/\text{cm}^{-1}$ (nujol) 3246, 3132, 1663, 1615, 1547; δ_{H} (500 MHz, CDCl_3) 8.31 (1H, t, J = 7.8 Hz, 4-H), 7.50 (1H, s, NH), 7.16-7.06 (3H, m, 3,5,6-H), 2.25 (3H, s, 9-H); δ_{C} (125 MHz, CDCl_3) 168.4 (C-8), 152.4 (d, J = 243.2 Hz, C-2), 126.3 (d, J = 10.3 Hz, C-1), 124.6 (d, J = 3.5 Hz, C-5), 124.3 (d, J = 7.6 Hz, C-6), 121.9 (C-4), 114.8 (d, J = 18.8 Hz, C-3), 24.7 (C-9); δ_{F} (470 MHz, CDCl_3) -131.35 (1F,); HRMS m/z (ES^+) 176.0482 ($[\text{M}+\text{Na}]^+$, 100%) $\text{C}_8\text{H}_8\text{NOFNa}$ requires 176.0488.

N-(2-Fluorophenyl)pivalamide **380**²³³



Triethylamine (12.5 mL, 90 mmol) was added to a solution of 2-fluoroaniline (5 g, 45 mmol) in DCM (100 mL) and the solution was cooled to 0 °C. Trimethylacetyl chloride (6.6 mL, 54 mmol) was added dropwise to the solution. The solution was warmed to room temperature once the addition was complete and the solution was stirred for 16 h. A saturated solution of sodium bicarbonate was added (100 mL) and the layers were separated. The aqueous layer was extracted with DCM (2 × 100 mL). The combined organic layers were dried with magnesium sulfate and the solvent was removed under reduced pressure. To give the product **380** as a white solid (9.8 g, quant.) which was dried under high vacuum for 6 h and then used without any further purification: m.p 61-64 °C (Lit.²³³ 68 °C); $\nu_{\max}/\text{cm}^{-1}$ (nujol) 3347, 1661, 1256; δ_{H} (300 MHz, CDCl_3) 8.37-8.31 (1H, m, 4-H), 7.63 (1H, s, NH), 7.16-6.19 (3H, m, 3,5,6-H), 1.33 (9H, s, H^9); δ_{C} (75 MHz, CDCl_3) 176.7 (C-7), 152.6 (d, J = 242.2 Hz, C-2), 126.7 (d, J = 9.8 Hz, C-1), 124.6 (d, J = 3.7 Hz, C-5), 124.1 (d, J = 7.8 Hz, C-6), 121.7 (C-4), 114.6 (d, J = 19.3 Hz, C-3), 40.0 (C-8), 27.6 (C-9); $\delta_{\text{F}\{\text{H}\}}$

(282 MHz, CDCl₃) -132.1 (s); HRMS *m/z* (ES⁺) 196.1127 ([M+H]⁺, 100%)
C₁₁H₁₅NOF requires 196.1138.

References

1. G. W. Beadle, H. K. Mitchell and J. F. Nyc, *Proc. Natl. Acad. Sci. U.S.A.*, 1947, **33**, 155-158.
2. N. P. Botting, *Chem. Soc. Rev.*, 1995, **24**, 401-412.
3. T. W. Stone and M. N. Perkins, *Eur. J. Pharmacol.*, 1981, **72**, 411-412.
4. T. W. Stone, C. M. Forrest and L. G. Darlington, *FEBS J.*, 2012, **279**, 1386-1397.
5. M. N. Perkins and T. W. Stone, *Brain Res.*, 1982, **247**, 184-187.
6. T. W. Stone and L. G. Darlington, *Nat. Rev. Drug Discov.*, 2002, **1**, 609-620.
7. H. Baran and R. Schwarcz, *J. Neurochem.*, 1990, **55**, 738-744.
8. K. L. Colabroy and T. P. Begley, *J. Am. Chem. Soc.*, 2004, **127**, 840-841.
9. W. A. Koontz and R. Shiman, *J. Biol. Chem.*, 1976, **251**, 368-377.
10. M. Salter, R. G. Knowles and C. I. Pogson, *Biochem. J.*, 1986, **234**, 635-647.
11. T. J. Connor, N. Starr, J. B. O'Sullivan and A. Harkin, *Neurosci. Lett.*, 2008, **441**, 29-34.
12. L. Kolodziej, E. Paleolog and R. Williams, *Amino Acids*, 2011, **41**, 1173-1183.
13. A. Macchiarulo, E. Camaioni, R. Nuti and R. Pellicciari, *Amino Acids*, 2009, **37**, 219-229.
14. S. A. Rafice, N. Chauhan, I. Efimov, J. Basran and E. L. Raven, *Biochem. Soc. Trans.*, 2009, **37**, 408-412.
15. F. Forouhar, J. L. R. Anderson, C. G. Mowat, S. M. Vorobiev, A. Hussain, M. Abashidze, C. Bruckmann, S. J. Thackray, J. Seetharaman, T. Tucker, R. Xiao, L.-C. Ma, L. Zhao, T. B. Acton, G. T. Montelione, S. K. Chapman and L. Tong, *Proc. Natl. Acad. Sci. U.S.A.*, 2007, **104**, 473-478.

16. J. Basran, S. A. Rafice, N. Chauhan, I. Efimov, M. R. Cheesman, L. Ghamsari and E. L. Raven, *Biochemistry*, 2008, **47**, 4752-4760.
17. M. W. Taylor and G. S. Feng, *FASEB J.*, 1991, **5**, 2516-2522.
18. D. Batabyal and S.-R. Yeh, *J. Am. Chem. Soc.*, 2007, **129**, 15690-15701.
19. M. Sono, *Biochemistry*, 1989, **28**, 5400-5407.
20. N. J. C. King and S. R. Thomas, *Int. J. Biochem. Cell. Biol.*, 2007, **39**, 2167-2172.
21. S. Adams, N. Braid, A. Bessesde, B. J. Brew, R. Grant, C. Teo and G. J. Guillemin, *Cancer Res.*, 2012, **72**, 5649-5657.
22. B. J. Samelson-Jones and S.-R. Yeh, *Biochemistry*, 2006, **45**, 8527-8538.
23. H. Sugimoto, S.-i. Oda, T. Otsuki, T. Hino, T. Yoshida and Y. Shiro, *Proc. Natl. Acad. Sci. U.S.A.*, 2006, **103**, 2611-2616.
24. S. J. Thackray, C. Bruckmann, J. L. R. Anderson, L. P. Campbell, R. Xiao, L. Zhao, C. G. Mowat, F. Forouhar, L. Tong and S. K. Chapman, *Biochemistry*, 2008, **47**, 10677-10684.
25. S. G. Cady and M. Sono, *Arch. Biochem. Biophys.*, 1991, **291**, 326-333.
26. N. Chauhan, S. J. Thackray, S. A. Rafice, G. Eaton, M. Lee, I. Efimov, J. Basran, P. R. Jenkins, C. G. Mowat, S. K. Chapman and E. L. Raven, *J. Am. Chem. Soc.*, 2009, **131**, 4186-4187.
27. G. A. Hamilton, in *Advances in Enzymology and Related Areas of Molecular Biology*, John Wiley & Sons, Inc., 1969, pp. 55-96.
28. O. Hayaishi, S. Rothberg, A. H. Mehler and Y. Saito, *J. Biol. Chem.*, 1957, **229**, 889-896.
29. E. G. Kovaleva, M. B. Neibergall, S. Chakrabarty and J. D. Lipscomb, *Acc. Chem. Res.*, 2007, **40**, 475-483.
30. L. W. Chung, X. Li, H. Sugimoto, Y. Shiro and K. Morokuma, *J. Am. Chem. Soc.*, 2010, **132**, 11993-12005.
31. I. Efimov, J. Basran, S. J. Thackray, S. Handa, C. G. Mowat and E. L. Raven, *Biochemistry*, 2011, **50**, 2717-2724.

32. D. H. Munn, M. Zhou, J. T. Attwood, I. Bondarev, S. J. Conway, B. Marshall, C. Brown and A. L. Mellor, *Science*, 1998, **281**, 1191-1193.
33. S. V. Novitskiy and H. L. Moses, *Cancer Discovery*, 2012, **2**, 673-675.
34. D. Nagarathnam and M. Cushman, *J. Org. Chem.*, 1991, **56**, 4884-4887.
35. D.-Y. Hou, A. J. Muller, M. D. Sharma, J. DuHadaway, T. Banerjee, M. Johnson, A. L. Mellor, G. C. Prendergast and D. H. Munn, *Cancer Res.*, 2007, **67**, 792-801.
36. N. Eguchi, Y. Watanabe, K. Kawanishi, Y. Hashimoto and O. Hayaishi, *Arch. Biochem. Biophys.*, 1984, **232**, 602-609.
37. M. Sono and S. G. Cady, *Biochemistry*, 1989, **28**, 5392-5399.
38. P. Gaspari, T. Banerjee, W. P. Malachowski, A. J. Muller, G. C. Prendergast, J. DuHadaway, S. Bennett and A. M. Donovan, *J. Med. Chem.*, 2005, **49**, 684-692.
39. A. Pereira, E. Vottero, M. Roberge, A. G. Mauk and R. J. Andersen, *J. Nat. Prod.*, 2006, **69**, 1496-1499.
40. H. C. Brastianos, E. Vottero, B. O. Patrick, R. Van Soest, T. Maitinaho, A. G. Mauk and R. J. Andersen, *J. Am. Chem. Soc.*, 2006, **128**, 16046-16047.
41. G. Carr, M. K. W. Chung, A. G. Mauk and R. J. Andersen, *J. Med. Chem.*, 2008, **51**, 2634-2637.
42. G. J. Hooper, M. T. Davies-Coleman, M. Kelly-Borges and P. S. Coetzee, *Tetrahedron Lett.*, 1996, **37**, 7135-7138.
43. A. Rives, T. Delaine, L. Legentil and E. Delfourne, *Tetrahedron Lett.*, 2009, **50**, 1128-1130.
44. E. Dolušić, P. Larrieu, C. Meinguet, D. Colette, A. Rives, S. Blanc, T. Ferain, L. Pilotte, V. Stroobant, J. Wouters, B. Van den Eynde, B. Masereel, E. Delfourne and R. Frédérick, *Biorg. Med. Chem. Lett.*, 2013, **23**, 47-54.
45. S. Kumar, D. Jaller, B. Patel, J. M. LaLonde, J. B. DuHadaway, W. P. Malachowski, G. C. Prendergast and A. J. Muller, *J. Med. Chem.*, 2008, **51**, 4968-4977.

46. E. W. Yue, B. Douty, B. Wayland, M. Bower, X. Liu, L. Leffet, Q. Wang, K. J. Bowman, M. J. Hansbury, C. Liu, M. Wei, Y. Li, R. Wynn, T. C. Burn, H. K. Koblish, J. S. Fridman, B. Metcalf, P. A. Scherle and A. P. Combs, *J. Med. Chem.*, 2009, **52**, 7364-7367.
47. A. C. Terentis, M. Freewan, T. S. Sempértegui Plaza, M. J. Raftery, R. Stocker and S. R. Thomas, *Biochemistry*, 2009, **49**, 591-600.
48. Q. Han, T. Cai, D. Tagle and J. Li, *Cell. Mol. Life Sci.*, 2010, **67**, 353-368.
49. F. Rossi, R. Schwarcz and M. Rizzi, *Curr. Opin. Struct. Biol.*, 2008, **18**, 748-755.
50. P. Guidetti, L. Amori, M. T. Sapko, E. Okuno and R. Schwarcz, *J. Neurochem.*, 2007, **102**, 103-111.
51. P. Yu, N. A. Di Prospero, M. T. Sapko, T. Cai, A. Chen, M. Melendez-Ferro, F. Du, W. O. Whetsell, P. Guidetti, R. Schwarcz and D. A. Tagle, *Mol. Cell. Biol.*, 2004, **24**, 6919-6930.
52. P. Yu, Z. Li, L. Zhang, D. A. Tagle and T. Cai, *Gene*, 2006, **365**, 111-118.
53. Q. Han, J. Fang and J. Li, *Biochem. J.*, 2001, **360**, 617-623.
54. F. Rossi, Q. Han, J. Li, J. Li and M. Rizzi, *J. Biol. Chem.*, 2004, **279**, 50214-50220.
55. F. Rossi, S. Garavaglia, V. Montalbano, M. A. Walsh and M. Rizzi, *J. Biol. Chem.*, 2008, **283**, 3559-3566.
56. Q. Han, H. Robinson and J. Li, *J. Biol. Chem.*, 2008, **283**, 3567-3573.
57. Q. Han, H. Robinson, T. Cai, D. A. Tagle and J. Li, *Mol. Cell. Biol.*, 2009, **29**, 784-793.
58. Q. Han, H. Robinson, T. Cai, D. A. Tagle and J. Li, *Biosci. Rep.*, 2011, **31**, 323-332.
59. D. Bellocchi, A. Macchiarulo, A. Carotti and R. Pellicciari, *Biochim. Biophys. Acta*, 2009, **1794**, 1802-1812.
60. S. Erhardt, K. Blennow, C. Nordin, E. Skogh, L. H. Lindström and G. Engberg, *Neurosci. Lett.*, 2001, **313**, 96-98.

61. L. K. Nilsson, K. R. Linderholm, G. Engberg, L. Paulson, K. Blennow, L. H. Lindström, C. Nordin, A. Karanti, P. Persson and S. Erhardt, *Schizophr. Res.*, 2005, **80**, 315-322.
62. S. K. Olsson, M. Samuelsson, P. Saetre, L. H. Lindström, E. G. Jönsson, C. Nordin, G. Engberg, S. Erhardt and M. Landén, *J. Psychiatry Neurosci.*, 2010, **35**, 196-199.
63. M. Varasi, A. Della Torre, F. Heidempergher, P. Pevarello, C. Speciale, P. Guidetti, D. R. Wells and R. Schwarcz, *Eur. J. Med. Chem.*, 1996, **31**, 11-21.
64. A. B. Dounay, M. Anderson, B. M. Bechle, B. M. Campbell, M. M. Claffey, A. Evdokimov, E. Evrard, K. R. Fonseca, X. Gan, S. Ghosh, M. M. Hayward, W. Horner, J.-Y. Kim, L. A. McAllister, J. Pandit, V. Paradis, V. D. Parikh, M. R. Reese, S. Rong, M. A. Salafia, K. Schuyten, C. A. Strick, J. B. Tuttle, J. Valentine, H. Wang, L. E. Zawadzke and P. R. Verhoest, *ACS Med. Chem. Lett.*, 2012, **3**, 187-192.
65. J. B. Tuttle, M. Anderson, B. M. Bechle, B. M. Campbell, C. Chang, A. B. Dounay, E. Evrard, K. R. Fonseca, X. Gan, S. Ghosh, W. Horner, L. C. James, J.-Y. Kim, L. A. McAllister, J. Pandit, V. D. Parikh, B. J. Rago, M. A. Salafia, C. A. Strick, L. E. Zawadzke and P. R. Verhoest, *ACS Med. Chem. Lett.*, 2012, **4**, 37-40.
66. J. L. Henderson, A. Sawant-Basak, J. B. Tuttle, A. B. Dounay, L. A. McAllister, J. Pandit, S. Rong, X. Hou, B. M. Bechle, J.-Y. Kim, V. Parikh, S. Ghosh, E. Evrard, L. E. Zawadzke, M. A. Salafia, B. Rago, R. S. Obach, A. Clark, K. R. Fonseca, C. Chang and P. R. Verhoest, *MedChemComm*, 2013, **4**, 125-129.
67. S. Röver, A. M. Cesura, P. Huguenin, R. Kettler and A. Szente, *J. Med. Chem.*, 1997, **40**, 4378-4385.
68. J. Qi, K. Kizjakina, R. Robinson, K. Tolani and P. Sobrado, *Anal. Biochem.*, 2012, **425**, 80-87.
69. Y. Nishimoto, F. Takeuchi and Y. Shibata, *J. Chromatogr. A*, 1979, **169**, 357-364.
70. T. Uemura and K. Hirai, *J. Biochem.*, 1998, **123**, 253-262.

71. K. Hirai, H. Kuroyanagi, Y. Tatebayashi, Y. Hayashi, K. Hirabayashi-Takahashi, K. Saito, S. Haga, T. Uemura and S. Izumi, *J. Biochem.*, 2010, **148**, 639-650.
72. J. Breton, N. Avanzi, S. Magagnin, N. Covini, G. Magistrelli, L. Cozzi and A. Isacchi, *Eur. J. Biochem.*, 2000, **267**, 1092-1099.
73. D. Alberati-Giani, A. M. Cesura, C. Broger, W. D. Warren, S. Röver and P. Malherbe, *FEBS Lett.*, 1997, **410**, 407-412.
74. K. R. Crozier and G. R. Moran, *Protein Expression Purif.*, 2007, **51**, 324-333.
75. M. Amaral, C. Levy, D. J. Heyes, P. Lafite, T. F. Outeiro, F. Giorgini, D. Leys and N. S. Scrutton, *Nature*, 2013, **496**, 382-385.
76. C. Mowat and M. Wilkinson, *Unpublished work*, Edinburgh University
77. R. Pellicciari, B. Natalini, G. Costantino, M. R. Mahmoud, L. Mattoli, B. M. Sadeghpour, F. Moroni, A. Chiarugi and R. Carpenedo, *J. Med. Chem.*, 1994, **37**, 647-655.
78. K. R. Crozier-Reabe, R. S. Phillips and G. R. Moran, *Biochemistry*, 2008, **47**, 12420-12433.
79. *WIPO Pat.*, 199928316, 1999.
80. *WIPO Pat.*, 199928306, 1999.
81. *WIPO Pat.*, 2008022286, 2008.
82. *WIPO Pat.*, 2004060369, 2004.
83. *WIPO Pat.*, 199902506, 1999.
84. *European Pat.*, 1475088, 2004.
85. *WIPO Pat.*, 199803469, 1998.
86. *WIPO Pat.*, 199717316, 1997.
87. *WIPO Pat.*, 199715550, 1997.
88. *WIPO Pat.*, 199503271, 1995.
89. *WIPO Pat.*, 2004048361, 2004.

90. *WIPO Pat.*, 199916771, 1999.
91. *WIPO Pat.*, 199916753, 1999.
92. *WIPO Pat.*, 199906375, 1999.
93. *WIPO Pat.*, 199906374, 1999.
94. *WIPO Pat.*, 199805660, 1998.
95. A. Giordani, L. Corti, M. Cini, R. Bormetti, M. Marconi, O. Veneroni, C. Speciale and M. Varasi, *Adv. Exp. Med. Biol.*, 1996, **398**, 531-534.
96. A. Giordani, L. Corti, M. Cini, M. Marconi, A. Pillan, R. Ferrario, R. Schwarcz, P. Guidetti and C. Speciale, *Adv. Exp. Med. Biol.*, 1996, **398**, 499-505.
97. A. Giordani, P. Pevarello, M. Cini, R. Bormetti, F. Greco, S. Toma, C. Speciale and M. Varasi, *Biorg. Med. Chem. Lett.*, 1998, **8**, 2907-2912.
98. M. J. Drysdale, S. L. Hind, M. Jansen and J. F. Reinhard, *J. Med. Chem.*, 1999, **43**, 123-127.
99. Y. Feng, B. F. Bowden and V. Kapoor, *Biorg. Med. Chem. Lett.*, 2012, **22**, 3398-3401.
100. O. Kurnasov, V. Goral, K. Colabroy, S. Gerdes, S. Anantha, A. Osterman and T. P. Begley, *Chem. Biol.*, 2003, **10**, 1195-1204.
101. P. Malherbe, C. Köhler, M. Da Prada, G. Lang, V. Kiefer, R. Schwarcz, H. W. Lahm and A. M. Cesura, *J. Biol. Chem.*, 1994, **269**, 13792-13797.
102. V. Calderone, M. Trabucco, V. Menin, A. Negro and G. Zanotti, *Biochim. Biophys. Acta*, 2002, **1596**, 283-292.
103. Y. Zhang, K. L. Colabroy, T. P. Begley and S. E. Ealick, *Biochemistry*, 2005, **44**, 7632-7643.
104. I. Đilović, F. Gliubich, G. Malpeli, G. Zanotti and D. Matković-Čalogović, *Biopolymers*, 2009, **91**, 1189-1195.
105. K. L. Colabroy, H. Zhai, T. Li, Y. Ge, Y. Zhang, A. Liu, S. E. Ealick, F. W. McLafferty and T. P. Begley, *Biochemistry*, 2005, **44**, 7623-7631.
106. L. D. Keys and G. A. Hamilton, *J. Am. Chem. Soc.*, 1987, **109**, 2156-2163.

107. M. Linderberg, S. Hellberg, S. Björk, B. Gotthammar, T. Högberg, K. Persson, R. Schwarcz, J. Luthman and R. Johansson, *Eur. J. Med. Chem.*, 1999, **34**, 729-744.
108. P. M. Packman and W. B. Jakoby, *J. Biol. Chem.*, 1965, **240**, 4107-4108.
109. K. T. Hughes, A. Dessen, J. P. Gray and C. Grubmeyer, *J. Bacteriol.*, 1993, **175**, 479-486.
110. S. Sinclair, K. Murphy, C. Birch and J. Hamill, *Plant Mol. Biol.*, 2000, **44**, 603-617.
111. E. Okuno, R. J. White and R. Schwarcz, *J. Biochem.*, 1988, **103**, 1054-1059.
112. H. Liu, K. Woznica, G. Catton, A. Crawford, N. Botting and J. H. Naismith, *J. Mol. Biol.*, 2007, **373**, 755-763.
113. R. Bhatia and K. C. Calvo, *Arch. Biochem. Biophys.*, 1996, **325**, 270-278.
114. H. Cao, B. L. Pietrak and C. Grubmeyer, *Biochemistry*, 2002, **41**, 3520-3528.
115. J. C. Eads, D. Ozturk, T. B. Wexler, C. Grubmeyer and J. C. Sacchettini, *Structure*, 1997, **5**, 47-58.
116. V. Sharma, C. Grubmeyer and J. C. Sacchettini, *Structure*, 1998, **6**, 1587-1599.
117. R. Schwarzenbacher, L. Jaroszewski, F. von Delft, P. Abdubek, E. Ambing, T. Biorac, L. S. Brinen, J. M. Canaves, J. Cambell, H.-J. Chiu, X. Dai, A. M. Deacon, M. DiDonato, M.-A. Elsliger, S. Eshagi, R. Floyd, A. Godzik, C. Grittini, S. K. Grzechnik, E. Hampton, C. Karlak, H. E. Klock, E. Koesema, J. S. Kovarik, A. Kreusch, P. Kuhn, S. A. Lesley, I. Levin, D. McMullan, T. M. McPhillips, M. D. Miller, A. Morse, K. Moy, J. Ouyang, R. Page, K. Quijano, A. Robb, G. Spraggon, R. C. Stevens, H. van den Bedem, J. Velasquez, J. Vincent, X. Wang, B. West, G. Wolf, Q. Xu, K. O. Hodgson, J. Wooley and I. A. Wilson, *Proteins: Struct. Funct. Bioinform.*, 2004, **55**, 768-771.
118. M.-k. Kim, Y. J. Im, J. H. Lee and S. H. Eom, *Proteins: Struct. Funct. Bioinform.*, 2006, **63**, 252-255.

119. G. B. Kang, M.-K. Kim, H.-S. Youn, J. Y. An, J.-G. Lee, K. R. Park, S. H. Lee, Y. Kim, S.-I. Fukuoka and S. H. Eom, *Acta Crystallogr., Sect. F: Struct. Biol. Cryst. Commun.*, 2011, **67**, 38-40.
120. E. di Luccio and D. K. Wilson, *Biochemistry*, 2008, **47**, 4039-4050.
121. A. Rozenberg and J. K. Lee, *J. Org. Chem.*, 2008, **73**, 9314-9319.
122. W. Tao, C. Grubmeyer and J. S. Blanchard, *Biochemistry*, 1996, **35**, 14-21.
123. L. Sherwood, *Human physiology : From cells to systems*, 3rd Edition edn., Wadsworth, Belmont, CA, 1997.
124. J. P. Neoptolemos, M. Raraty, M. Finch and R. Sutton, *Gut*, 1998, **42**, 886-891.
125. K. Mergener and J. Baillie, *BMJ*, 1998, **316**, 44-48.
126. J.-L. Frossard, M. A. Matthay and C. M. Pastor, *Chest*, 2003, vol. 124, p. 2341-2351.
127. C. J. McKay, S. Evans, M. Sinclair, C. R. Carter and C. W. Imrie, *BJS*, 1999, **86**, 1302-1305.
128. D. J. Mole, N. V. McFerran, G. Collett, C. O'Neill, T. Diamond, O. J. Garden, L. Kylanpaa, H. Repo and E. A. Deitch, *BJS*, 2008, **95**, 855-867.
129. D. J. Mole, *Unpublished work*, Edinburgh University
130. M. Hynninen, M. Valtonen, H. Markkanen, M. Vaara, P. Kuusela, I. Jousela, A. Piilonen and O. Takkunen, *Shock*, 2000, **13**, 79-82.
131. L. Grégoire, A. Rassoulpour, P. Guidetti, P. Samadi, P. J. Bédard, E. Izzo, R. Schwarcz and T. Di Paolo, *Behav. Brain Res.*, 2008, **186**, 161-167.
132. A. Richter and M. Hamann, *Eur. J. Pharmacol.*, 2003, **478**, 47-52.
133. G. A. Patani and E. J. LaVoie, *Chem. Rev.*, 1996, **96**, 3147-3176.
134. J. Boström, A. Hogner, A. Llinàs, E. Wellner and A. T. Plowright, *J. Med. Chem.*, 2011, **55**, 1817-1830.
135. K. E. Andersen, A. S. Jørgensen and C. Bræstrup, *Eur. J. Med. Chem.*, 1994, **29**, 393-399.

136. F. I. Carroll, J. L. Gray, P. Abraham, M. A. Kuzemko, A. H. Lewin, J. W. Boja and M. J. Kuhar, *J. Med. Chem.*, 1993, **36**, 2886-2890.
137. A. R. Gangloff, J. Litvak, E. J. Shelton, D. Sperandio, V. R. Wang and K. D. Rice, *Tetrahedron Lett.*, 2001, **42**, 1441-1443.
138. A. Pace and P. Pierro, *Org. Biomol. Chem.*, 2009, **7**, 4337-4348.
139. N. S. Ooi and D. A. Wilson, *J. Chem. Soc. Perk. Trans. 2*, 1980, 1792-1799.
140. K. Venkataraman and D. R. Wagle, *Tetrahedron Lett.*, 1979, **20**, 3037-3040.
141. M. Weitman, K. Lerman, A. Nudelman, D. T. Major, A. Hizi and A. Herschhorn, *Eur. J. Med. Chem.*, 2011, **46**, 447-467.
142. M. F. A. Adamo and M. Nagabelli, *Tetrahedron Lett.*, 2007, **48**, 4703-4706.
143. H. Ishibashi, T. S. So, K. Okochi, T. Sato, N. Nakamura, H. Nakatani and M. Ikeda, *J. Org. Chem.*, 1991, **56**, 95-102.
144. A. Kamal, K. V. Ramana, H. B. Ankati and A. V. Ramana, *Tetrahedron Lett.*, 2002, **43**, 6861-6863.
145. B. C. Ranu, A. Sarkar and R. Chakraborty, *J. Org. Chem.*, 1994, **59**, 4114-4116.
146. I. Rodriguez and R. Voges, *J. Labelled Compd. Radiopharm.*, 2000, **43**, 169-176.
147. E. B. Rowland, G. B. Rowland, E. Rivera-Otero and J. C. Antilla, *J. Am. Chem. Soc.*, 2007, **129**, 12084-12085.
148. K. S. Feldman, D. B. Vidulova and A. G. Karatjas, *J. Org. Chem.*, 2005, **70**, 6429-6440.
149. L. Chen, M. Hainrichson, D. Bourdetsky, A. Mor, S. Yaron and T. Baasov, *Biorg. Med. Chem.*, 2008, **16**, 8940-8951.
150. W. R. Roush, M. R. Michaelides, D. F. Tai, B. M. Lesur, W. K. M. Chong and D. J. Harris, *J. Am. Chem. Soc.*, 1989, **111**, 2984-2995.
151. S. Raghavan and K. A. Tony, *Tetrahedron Lett.*, 2004, **45**, 2639-2641.
152. E. J. Correy, D.-H. Lee and S. Choi, *Tetrahedron Lett.*, 1992, **33**, 6735-6738.

153. B. Beier, K. Schurrle, O. Werbitzky and W. Piepersberg, *J. Chem. Soc., Perkin Trans. 1*, 1990, **0**, 2255-2262.
154. M. Pohl, M. Thieme, P. G. Jones and J. Liebscher, *Liebigs Ann.*, 1995, **1995**, 1539-1545.
155. R. A. Kenley, C. D. Bedford, O. D. Dailey, R. A. Howd and A. Miller, *J. Med. Chem.*, 1984, **27**, 1201-1211.
156. A. Corsaro, U. Chiacchio, A. Compagnini and G. Purrello, *J. Chem. Soc., Perkin Trans. 1*, 1980, 1635-1640.
157. Y. Yamaguchi, I. Katsuyama, K. Funabiki, M. Matsui and K. Shibata, *J. Heterocycl. Chem.*, 1998, **35**, 805-810.
158. D. N. Ridge, J. W. Hanifin, L. A. Harten, B. D. Johnson, J. Menschik, G. Nicolau, A. E. Sloboda and D. E. Watts, *J. Med. Chem.*, 1979, **22**, 1385-1389.
159. T. Sasaki, T. Yoshioka and Y. Suzuki, *Bull. Chem. Soc. Jpn.*, 1969, **42**, 3335-3338.
160. F. Eloy and R. Lenaers, *Helv. Chim. Acta*, 1966, **49**, 1430-1432.
161. B. T. Burlingham and T. S. Widlanski, *J. Chem. Educ.*, 2003, **80**, 214.
162. M. Dixon, *Biochem. J.*, 1972, **129**, 197-202.
163. S. Webster, K. McGuire and D. J. Mole, *Unpublished work*, Edinburgh University
164. M. Stiborová, E. Frei, M. Wiessler and H. H. Schmeiser, *Chem. Res. Toxicol.*, 2001, **14**, 1128-1137.
165. J. Kazius, R. McGuire and R. Bursi, *J. Med. Chem.*, 2004, **48**, 312-320.
166. T. Orsière, M. De Méo, P. Rathelot, J. Pompili, M. Galas, M. Castegnaro, P. Vanelle and G. Duménil, *Food Chem. Toxicol.*, 2003, **41**, 275-290.
167. Schrodinger, LLC, *The PyMOL Molecular Graphics System, Version 1.3r1*, (2010).
168. J. P. Gallivan and D. A. Dougherty, *Proc. Natl. Acad. Sci. U.S.A.*, 1999, **96**, 9459-9464.

169. Y. Kita, M. Arisawa, M. Gyoten, M. Nakajima, R. Hamada, H. Tohma and T. Takada, *J. Org. Chem.*, 1998, **63**, 6625-6633.
170. D. A. Casteel and S. P. Peri, *Synthesis*, 1991, **1991**, 691-693.
171. Q. Zhang, K. S. Raheem, N. P. Botting, A. M. Z. Slawin, C. D. Kay and D. O'Hagan, *Tetrahedron*, 2012, **68**, 4194-4201.
172. T. Ikawa, H. Sajiki and K. Hirota, *Tetrahedron*, 2004, **60**, 6189-6195.
173. J. Matulic-Adamic, P. Haeberli and N. Usman, *J. Org. Chem.*, 1995, **60**, 2563-2569.
174. L. Azéma, C. Lherbet, C. Baudoin and C. Blonski, *Biorg. Med. Chem. Lett.*, 2006, **16**, 3440-3443.
175. G. M. Blackburn and D. Ingleson, *J. Chem. Soc., Perkin Trans. 1*, 1980, 1150-1153.
176. T. S. Elliott, A. Slowey, Y. Ye and S. J. Conway, *MedChemComm*, 2012, **3**, 735-751.
177. L. D. Lavis, *ACS Chem. Biol.*, 2008, **3**, 203-206.
178. R. Appel and G. Berger, *Chem. Ber.*, 1958, **91**, 1339-1341.
179. M. Okada, S. Iwashita and N. Koizumi, *Tetrahedron Lett.*, 2000, **41**, 7047-7051.
180. C. B. de Koning, J. P. Michael and A. L. Rousseau, *J. Chem. Soc., Perkin Trans. 1*, 2000, 787-797.
181. P. H. J. Carlsen, T. Katsuki, V. S. Martin and K. B. Sharpless, *J. Org. Chem.*, 1981, **46**, 3936-3938.
182. A. Shah, J. L. Font, M. J. Miller, J. E. Ream, M. C. Walker and J. A. Sikorski, *Biorg. Med. Chem.*, 1997, **5**, 323-334.
183. F. C. Ross, N. P. Botting and P. D. Leeson, *Tetrahedron*, 1997, **53**, 15761-15770.
184. K. M. Muirhead and N. P. Botting, *ARKIVOC*, 2002, **2002**, 37-45.
185. R. Pellicciari, M. A. Gallo-Mezo, B. Natalini and A. M. Amer, *Tetrahedron Lett.*, 1992, **33**, 3003-3004.

186. D. H. Fitzgerald, K. M. Muirhead and N. P. Botting, *Biorg. Med. Chem.*, 2001, **9**, 983-989.
187. K. C. O'Shea and N. P. Botting, *BMC Biochem.*, 2003, **4**, 13.
188. A. Giordani, L. Corti, M. Cini, M. Marconi, A. Pillan, R. Ferrario, R. Schwarcz, P. Guidetti, C. Speciale and M. Varasi, in *Recent Advances in Tryptophan Research*, eds. G. Filippini, C. L. Costa and A. Bertazzo, Springer US, 1996, vol. 398, pp. 499-505.
189. N. Hasegawa, V. Charra, S. Inoue, Y. Fukumoto and N. Chatani, *J. Am. Chem. Soc.*, 2011, **133**, 8070-8073.
190. J. A. Turner, *J. Org. Chem.*, 1983, **48**, 3401-3408.
191. T. J. Murray, S. C. Zimmerman and S. V. Kolotuchin, *Tetrahedron*, 1995, **51**, 635-648.
192. L. C. King and G. K. Ostrum, *J. Org. Chem.*, 1964, **29**, 3459-3461.
193. B. M. Trost, J. Xu and M. Reichle, *J. Am. Chem. Soc.*, 2006, **129**, 282-283.
194. C.-V. T. Vo, T. A. Mitchell and J. W. Bode, *J. Am. Chem. Soc.*, 2011, **133**, 14082-14089.
195. P. Zhang, E. A. Terefenko and J. Slavin, *Tetrahedron Lett.*, 2001, **42**, 2097-2099.
196. M. L. Carmellino, G. Pagani, M. Pregnotato, M. Terreni and F. Pastoni, *Eur. J. Med. Chem.*, 1994, **29**, 743-751.
197. T. Vilaivan, *Tetrahedron Lett.*, 2006, **47**, 6739-6742.
198. K. Bromfield, J. Cianci and P. Duggan, *Molecules*, 2004, **9**, 427-439.
199. K. G. Thakur, D. Ganapathy and G. Sekar, *Chem. Commun.*, 2011, **47**, 5076-5078.
200. P. Astolfi, L. Greci, C. Rizzoli, P. Sgarabotto and G. Marrosu, *J. Chem. Soc. Perk. Trans. 2*, 2001, **0**, 1634-1640.
201. F. Kolundzic, M. N. Noshi, M. Tjandra, M. Movassaghi and S. J. Miller, *J. Am. Chem. Soc.*, 2011, **133**, 9104-9111.

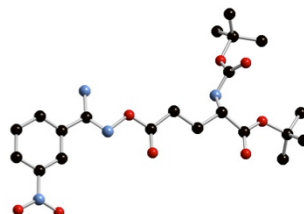
202. S. P. Singh, A. Michaelides, A. R. Merrill and A. L. Schwan, *J. Org. Chem.*, 2011, **76**, 6825-6831.
203. J. E. Baldwin and E. Lee, *Tetrahedron*, 1986, **42**, 6551-6554.
204. A. D. Abell, M. D. Oldham and J. M. Taylor, *J. Org. Chem.*, 1995, **60**, 1214-1220.
205. C. La Motta, S. Sartini, S. Salerno, F. Simorini, S. Taliani, A. M. Marini, F. Da Settimo, L. Marinelli, V. Limongelli and E. Novellino, *J. Med. Chem.*, 2008, **51**, 3182-3193.
206. Y. Kobayashi, H. Onuki and K. Tachibana, *Biorg. Med. Chem.*, 1999, **7**, 2073-2081.
207. J. A. Durden and D. L. Heywood, *J. Org. Chem.*, 1971, **36**, 1306-1307.
208. R. S. Ramón, J. Bosson, S. Díez-González, N. Marion and S. P. Nolan, *J. Org. Chem.*, 2010, **75**, 1197-1202.
209. R. H. Wiley and B. J. Wakefield, *J. Org. Chem.*, 1960, **25**, 546-551.
210. A. Ridley and W. Taylor, *Aust. J. Chem.*, 1987, **40**, 631-634.
211. Z. Fang, Y. Song, T. Sarkar, E. Hamel, W. E. Fogler, G. E. Agoston, P. E. Fanwick and M. Cushman, *J. Org. Chem.*, 2008, **73**, 4241-4244.
212. F. Eloy and A. Deryckere, *Bull. Soc. Chim. Belg.*, 1969, **78**, 41-46.
213. M. Mroczkiewicz and R. Ostaszewski, *Tetrahedron*, 2009, **65**, 4025-4034.
214. L. Crombie and B. S. Roughley, *Tetrahedron*, 1986, **42**, 3147-3156.
215. S. R. Neufeldt and M. S. Sanford, *Org. Lett.*, 2009, **12**, 532-535.
216. C. F. Barfknecht and T. R. Westby, *J. Med. Chem.*, 1967, **10**, 1192-1193.
217. A. O. Jones, G. M. Green, J. B. Shoesmith, C. E. Sosson, R. H. Slater, G. G. Henderson and A. Robertson, *J. Chem. Soc.*, 1926, **129**, 2760-2762.
218. K.-C. Liu, B. R. Shelton and R. K. Howe, *J. Org. Chem.*, 1980, **45**, 3916-3918.
219. A. K. Yatsimirski, K. Martinek and I. V. Berezin, *Tetrahedron*, 1971, **27**, 2855-2868.

220. G. D. Vilela, R. R. da Rosa, P. H. Schneider, I. H. Bechtold, J. Eccher and A. A. Merlo, *Tetrahedron Lett.*, 2011, **52**, 6569-6572.
221. J.-J. Xia and G.-W. Wang, *Molecules*, 2007, **12**, 231-236.
222. L. Di Nunno, P. Vitale and A. Scilimati, *Tetrahedron*, 2008, **64**, 11198-11204.
223. K. R. Huffman and F. C. Schaefer, *J. Org. Chem.*, 1963, **28**, 1816-1821.
224. F. Carta, D. Vullo, A. Maresca, A. Scozzafava and C. T. Supuran, *Biorg. Med. Chem.*, 2013, **21**, 1564-1569.
225. G. R. Pettit, B. Toki, D. L. Herald, P. Verdier-Pinard, M. R. Boyd, E. Hamel and R. K. Pettit, *J. Med. Chem.*, 1998, **41**, 1688-1695.
226. W. Yang, J. Liu and H. Zhang, *Tetrahedron Lett.*, 2010, **51**, 4874-4876.
227. Y.-Q. Fang, J. Yuen and M. Lautens, *J. Org. Chem.*, 2007, **72**, 5152-5160.
228. Z. Yao, J. Bhaumik, S. Dhanalekshmi, M. Ptaszek, P. A. Rodriguez and J. S. Lindsey, *Tetrahedron*, 2007, **63**, 10657-10670.
229. *WIPO Pat.*, 2005056550, 2005.
230. L. Piovan, M. D. Pasquini and L. H. Andrade, *Molecules*, 2011, **16**, 8098-8109.
231. T. Jensen, H. Pedersen, B. Bang-Andersen, R. Madsen and M. Jørgensen, *Angew. Chem. Int. Ed.*, 2008, **47**, 888-890.
232. A. Ramanathan and L. S. Jimenez, *Synthesis*, 2010, **2010**, 217-220.
233. O. Lerman, Y. Tor, D. Hebel and S. Rozen, *J. Org. Chem.*, 1984, **49**, 806-813.

Appendix

Single crystal X-ray diffraction data

Crystallographic information for **146**



A. Crystal Data

Empirical Formula	C ₂₁ H ₃₆ N ₄ O ₈
Formula Weight	472.54
Crystal Color, Habit	colorless, platelet
Crystal Dimensions	0.280 X 0.030 X 0.010 mm
Crystal System	monoclinic
Lattice Type	Primitive
Lattice Parameters	a = 5.463(2) Å b = 23.038(7) Å c = 19.067(6) Å β = 97.464(8) ° V = 2379.5(12) Å ³
Space Group	P2 ₁ (#4)
Z value	4
D _{calc}	1.319 g/cm ³
F ₀₀₀	1016.00
μ(CuKα)	8.487 cm ⁻¹

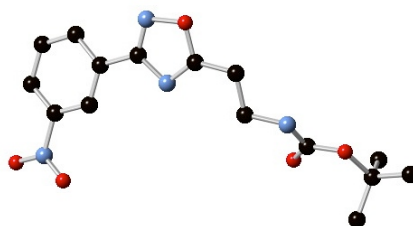
B. Intensity Measurements

Radiation	CuKα (λ = 1.54187 Å)
Voltage, Current	40kV, 20mA
Temperature	-100.0 °C
Detector	0 x 0 mm
Aperture	
2θ _{max}	136.6°
No. of Reflections Measured	Total: 29215
Corrections	Unique: 8099 (R _{int} = 0.0458) Friedel pairs: 3731 Lorentz-polarization Absorption trans. factors: 0.839 - 0.992)

C. Structure Solution and Refinement

Structure Solution	Direct Methods
Refinement	Full-matrix least-squares on F^2
Function Minimized	$\sum w (F_o^2 - F_c^2)^2$
Least Squares Weights	$w = 1 / [\sigma^2(F_o^2) + (0.2000 \cdot P)^2 + 0.0000 \cdot P]$ where $P = (\text{Max}(F_o^2, 0) + 2F_c^2)/3$
2 θ_{max} cutoff	136.6 $^\circ$
Anomalous Dispersion	All non-hydrogen atoms
No. Observations (All reflections)	8099
No. Variables	266
Reflection/Parameter Ratio	30.45
Residuals: R1 ($I > 2.00\sigma(I)$)	0.1140
Residuals: R (All reflections)	0.1213
Residuals: wR2 (All reflections)	0.3463
Goodness of Fit Indicator	1.460
Flack Parameter (Friedel pairs = 3731)	-0.1(4)
Max Shift/Error in Final Cycle	0.072
Maximum peak in Final Diff. Map	0.97 e $^-/\text{\AA}^3$
Minimum peak in Final Diff. Map	-0.79 e $^-/\text{\AA}^3$

Crystallographic information for **152**



A. Crystal Data

Empirical Formula	C ₁₈ H ₁₈ N ₄ O ₇ S
Formula Weight	434.42
Crystal Color, Habit	colorless, needle
Crystal Dimensions	0.240 X 0.020 X 0.010 mm
Crystal System	monoclinic
Lattice Type	C-centered
Lattice Parameters	a = 23.300(7) Å b = 5.1253(13) Å c = 14.015(4) Å β = 107.583(10) °
Space Group	V = 1595.4(8) Å ³ C2 (#5)
Z value	3
D _{calc}	1.356 g/cm ³
F ₀₀₀	678.00
μ(MoKα)	1.984 cm ⁻¹

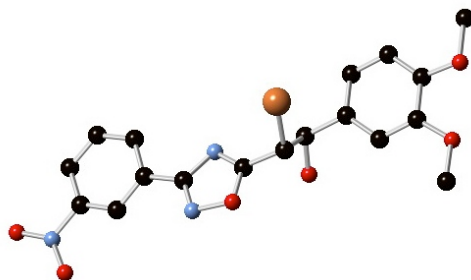
B. Intensity Measurements

Diffractometer	Saturn70
Radiation	MoKα (λ = 0.71075 Å)
Voltage, Current	50kV, 16mA
Temperature	-180.0 °C
Detector Aperture	70 x 70 mm
ω oscillation Range	1.0 - 0.0°
Pixel Size	0.034 mm
2θ _{max}	53.6°
No. of Reflections Measured	Total: 4542 Unique: 2460 (R _{int} = 0.1104) Friedel pairs: 974
Corrections	Lorentz-polarization

C. Structure Solution and Refinement

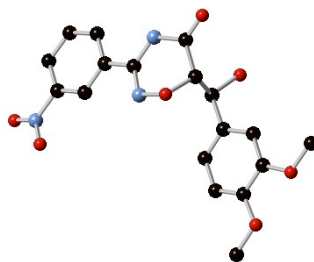
Structure Solution	Direct Methods	Residuals: R (All reflections)	0.1769
Refinement	Full-matrix least-squares on F ²	Residuals: wR2 (All reflections)	0.3646
Function Minimized	Σ w (F _o ² - F _c ²) ²	Goodness of Fit Indicator	1.204
Least Squares Weights	w = 1/ [σ ² (F _o ²) + (0.0738 · P) ² + 29.6061 · P] where P = (Max(F _o ² , 0) + 2F _c ²)/3	Flack Parameter (Friedel pairs = 974) Max Shift/Error in Final Cycle	5(6) 0.062
2θ _{max} cutoff	53.6°	Maximum peak in Final Diff. Map	0.59 e ⁻ /Å ³
Anomalous Dispersion	All non-hydrogen atoms	Minimum peak in Final Diff. Map	-0.45 e ⁻ /Å ³
No. Observations (All reflections)	2460	Residuals: R1 (I > 2.00σ(I))	0.1606
No. Variables	97		
Reflection/Parameter Ratio	25.36		

Crystallographic information for 165



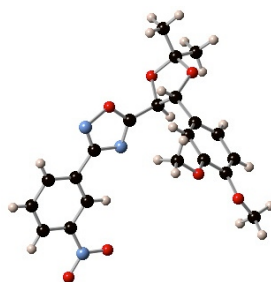
A. Crystal Data		B. Intensity Measurements	
Empirical Formula	C ₁₈ H ₁₆ BrN ₃ O ₆	Diffractometer	Mercury70
Formula Weight	450.24	Radiation	MoK α (λ = 0.71075 Å)
Crystal Color, Habit	colorless, prism	Voltage, Current	50kV, 16mA
Crystal Dimensions	0.120 X 0.120 X 0.100 mm	Temperature	-180.0 °C
Crystal System	monoclinic	Detector Aperture	70 x 70 mm
Lattice Type	Primitive	ω oscillation Range	1.0 - 0.0°
Lattice Parameters	a = 15.182(4) Å	Pixel Size	0.068 mm
	b = 14.698(3) Å	2 θ _{max}	50.7°
	c = 8.280(2) Å	No. of Reflections Measured	Total: 11619
	β = 93.572(7) °	Corrections	Unique: 3353 (R_{int} = 0.0365)
	V = 1844.0(8) Å ³		Lorentz-polarization
Space Group	P2 ₁ /c (#14)		Absorption
Z value	4		(trans. factors: 0.664 - 0.796)
D _{calc}	1.622 g/cm ³	C. Structure Solution and Refinement	
F ₀₀₀	912.00		
μ (MoK α)	22.777 cm ⁻¹		
Structure Solution	Direct Methods		
Refinement	Full-matrix least-squares on F ²		
Function Minimized	$\sum w (F_o^2 - F_c^2)^2$		
Least Squares Weights	$w = 1 / [\sigma^2(F_o^2) + (0.0597 \cdot P)^2 + 38.6462 \cdot P]$		
	where P = (Max(F_o^2 , 0) + 2F _c ²)/3		
2 θ _{max} cutoff	50.7°		
Anomalous Dispersion	All non-hydrogen atoms		
No. Observations (All reflections)	3353		
No. Variables	113		
Reflection/Parameter Ratio	29.67		
Residuals: R1 ($I > 2.00\sigma(I)$)	0.0603		
Residuals: R (All reflections)	0.0636		
Residuals: wR2 (All reflections)	0.1394		
Goodness of Fit Indicator	0.697		
Max Shift/Error in Final Cycle	12.832		
Maximum peak in Final Diff. Map	2.01 e ⁻ /Å ³		
Minimum peak in Final Diff. Map	-1.15 e ⁻ /Å ³		

Crystallographic information for **167**



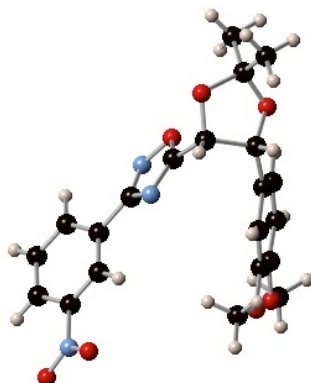
A. Crystal Data		B. Intensity Measurements	
Empirical Formula	C ₁₈ H ₁₉ N ₃ O ₈	Diffractometer	Mercury70
Formula Weight	405.36	Radiation	MoK α (λ = 0.71075 Å)
Crystal Color, Habit	colorless, prism	Voltage, Current	50kV, 16mA
Crystal Dimensions	0.100 X 0.100 X 0.100 mm	Temperature	-100.0 °C
Crystal System	triclinic	Detector Aperture	70 x 70 mm
Lattice Type	Primitive	Pixel Size	0.068 mm
Lattice Parameters	a = 7.158(2) Å b = 7.924(2) Å c = 17.511(6) Å α = 81.23(2) ° β = 89.94(3) ° γ = 68.73(2) ° V = 913.1(5) Å ³	2 θ max	50.7°
Space Group	P-1 (#2)	No. of Reflections Measured	Total: 5750
Z value	2	Corrections	Unique: 3218 (R_{int} = 0.0423) Lorentz-polarization Absorption (trans. factors: 0.539 - 0.988)
D _{calc}	1.474 g/cm ³		
F ₀₀₀	424.00		
μ (MoK α)	1.176 cm ⁻¹		
C. Structure Solution and Refinement			
Structure Solution	Direct Methods	Residuals: R1 ($I > 2.00\sigma(I)$)	0.1066
Refinement	Full-matrix least-squares on F ²	Residuals: R (All reflections)	0.1253
Function Minimized	$\sum w (F_o^2 - F_c^2)^2$	Residuals: wR2 (All reflections)	0.3619
Least Squares Weights	$w = 1 / [\sigma^2(F_o^2) + (0.2000 \cdot P)^2 + 0.0000 \cdot P]$ where $P = (Max(F_o^2, 0) + 2F_c^2) / 3$	Goodness of Fit Indicator	1.373
		Max Shift/Error in Final Cycle	0.247
		Maximum peak in Final Diff. Map	0.84 e ⁻ /Å ³
2 θ max cutoff	50.7°	Minimum peak in Final Diff. Map	-0.41 e ⁻ /Å ³
Anomalous Dispersion	All non-hydrogen atoms	Reflection/Parameter Ratio	12.28
No. Observations (All reflections)	3218		
No. Variables	262		

Crystallographic information for **173**



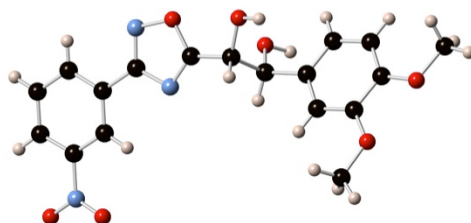
A. Crystal Data		B. Intensity Measurements	
Empirical Formula	C ₂₁ H ₂₁ N ₂ O ₇	Radiation	CuK α (λ = 1.54187 Å)
Formula Weight	413.41		multi-layer mirror monochromated
Crystal Color, Habit	colorless, prism	Take-off Angle	2.8°
Crystal Dimensions	0.150 X 0.030 X 0.030 mm	Detector Aperture	2.0 - 2.5 mm horizontal
Crystal System	monoclinic		2.0 mm vertical
Lattice Type	Primitive	Crystal to Detector Distance	21 mm
No. of Reflections Used for Unit		Voltage, Current	40kV, 20mA
Cell Determination (2 θ range)	1590 (82.2 - 138.6°)	Temperature	-100.0 °C
Lattice Parameters	a = 19.6141(10) Å b = 5.182(2) Å c = 22.043(11) Å β = 114.340(10) ° V = 2041.3(13) Å ³	Scan Type	ω -2 θ
		Scan Rate	0.0°/min (in ω) (up to 0 scans)
		Scan Width	(0.00 + 0.00 tan θ)°
		2 θ max	137.0°
		No. of Reflections Measured	Total: 20103
Space Group	P2 ₁ /c (#14)		Unique: 3739 (R _{int} = 0.0671)
Z value	4	Corrections	Lorentz-polarization Absorption
D _{calc}	1.345 g/cm ³		(trans. factors: 0.769 - 0.975)
F ₀₀₀	868.00		
μ (CuK α)	8.597 cm ⁻¹		
C. Structure Solution and Refinement			
Structure Solution	Direct Methods (SHELX97)	Reflection/Parameter Ratio	13.35
Refinement	Full-matrix least- squares on F ²	Residuals: R1 (I>2.00 σ (I))	0.0503
Function Minimized	$\sum w (F_o^2 - F_c^2)^2$	Residuals: R (All reflections)	0.0570
Least Squares Weights	w = 1/[$\sigma^2(F_o^2)$ + (0.1820 · P) ² + 1.9876 · P] where P = 3	Residuals: wR2 (All reflections)	0.1724
		Goodness of Fit Indicator	0.652
		Max Shift/Error in Final Cycle	0.084
2 θ max cutoff	137.0°	Maximum peak in Final Diff. Map	0.50 e ⁻ /Å ³
Anomalous Dispersion	All non- hydrogen atoms	Minimum peak in Final Diff. Map	-0.26 e ⁻ /Å ³
No. Observations (All reflections)	3739	No. Variables	280

Crystallographic information for **174**



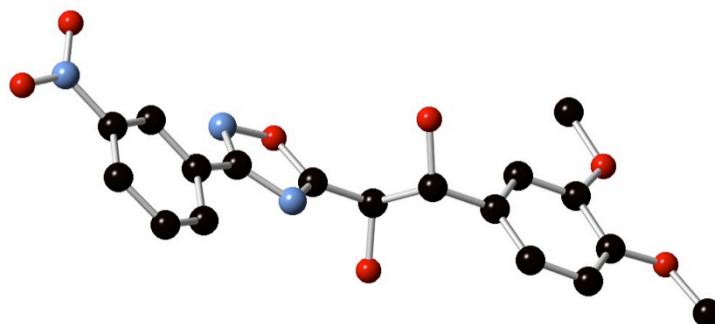
A. Crystal Data		B. Intensity Measurements	
Empirical Formula	C ₂₁ H ₂₁ N ₃ O ₇	Diffractometer	Saturn70
Formula Weight	427.41	Radiation	CuK α (λ = 1.54187 Å)
Crystal Color, Habit	colorless, prism	Voltage, Current	40kV, 20mA
Crystal Dimensions	0.200 X 0.010 X 0.010 mm	Temperature	-100.0 °C
Crystal System	monoclinic	Detector Aperture	70 x 70 mm
Lattice Type	Primitive	Pixel Size	0.034 mm
Lattice Parameters	a = 6.420(5) Å	2 θ _{max}	136.2°
	b = 27.13(2) Å	No. of Reflections Measured	Total: 56813
	c = 23.82(2) Å		Unique: 7445 (R _{int} = 0.3694)
	β = 95.84(2) °	Corrections	Lorentz-polarization
	V = 4127(5) Å ³		Absorption
Space Group	P2 ₁ /n (#14)		(trans. factors: 0.508 - 0.991)
Z value	8		
D _{calc}	1.376 g/cm ³		
F ₀₀₀	1792.00		
μ (CuK α)	8.839 cm ⁻¹		
C. Structure Solution and Refinement			
Structure Solution	Direct Methods (SHELX97)	No. Variables	559
Refinement	Full-matrix least-squares on F ²	Reflection/Parameter Ratio	13.32
Function Minimized	$\sum w (F_o^2 - F_c^2)^2$	Residuals: R1 ($I > 2.00\sigma(I)$)	0.1658
Least Squares Weights	$w = 1 / [\sigma^2(F_o^2) + (0.1000 \cdot P)^2 + 0.0000 \cdot P]$	Residuals: R (All reflections)	0.2755
	where P = (Max(F_o^2 , 0) + 2 F_c^2)/3	Residuals: wR2 (All reflections)	0.3519
2 θ _{max} cutoff	136.2°	Goodness of Fit Indicator	1.342
Anomalous Dispersion	All non-hydrogen atoms	Max Shift/Error in Final Cycle	0.389
No. Observations (All reflections)	7445	Maximum peak in Final Diff. Map	0.26 e ⁻ /Å ³
		Minimum peak in Final Diff. Map	-0.37 e ⁻ /Å ³

Crystallographic information for 175



Empirical formula	C ₁₈ H ₁₇ N ₃ O ₇	
Formula weight	387.35	
Temperature	93(2) K	
Wavelength	0.71073 Å	
Crystal system	Triclinic	
Space group	P-1	
Unit cell dimensions	a = 4.7534(16) Å	α = 87.096(16)°.
	b = 12.188(4) Å	β = 85.011(14)°.
	c = 16.651(5) Å	γ = 89.637(15)°.
Volume	959.8(5) Å ³	
Z	2	
Density (calculated)	1.340 Mg/m ³	
Absorption coefficient	0.105 mm ⁻¹	
F(000)	404	
Crystal size	0.12 x 0.05 x 0.03 mm ³	
Theta range for data collection	2.46 to 25.34°.	
Index ranges	-5 ≤ h ≤ 5, -14 ≤ k ≤ 12, -16 ≤ l ≤ 19	
Reflections collected	6015	
Independent reflections	3369 [R(int) = 0.0352]	
Completeness to theta = 25.00°	96.4 %	
Absorption correction	Multiscan	
Max. and min. transmission	1.000 and 0.550	
Refinement method	Full-matrix least-squares on F ²	
Data / restraints / parameters	3369 / 0 / 274	
Goodness-of-fit on F ²	1.505	
Final R indices [I > 2σ(I)]	R ₁ = 0.0990, wR ₂ = 0.3413	
R indices (all data)	R ₁ = 0.1103, wR ₂ = 0.3677	
Extinction coefficient	0.07(3)	
Largest diff. peak and hole	1.165 and -0.396 e.Å ⁻³	

Crystallographic information for 176



A. Crystal Data

Empirical Formula	C ₁₈ H ₇ N ₃ O ₇
Formula Weight	377.27
Crystal Color, Habit	colorless, prism
Crystal Dimensions	0.120 X 0.120 X 0.030 mm
Crystal System	triclinic
Lattice Type	Primitive
Lattice Parameters	a = 7.368(5) Å b = 8.445(6) Å c = 14.827(8) Å α = 92.813(7) ° β = 94.34(2) ° γ = 107.44(3) ° V = 875.1(10) Å ³
Space Group	P-1 (#2)
Z value	2
D _{calc}	1.432 g/cm ³
F ₀₀₀	384.00
μ (CuK α)	9.784 cm ⁻¹

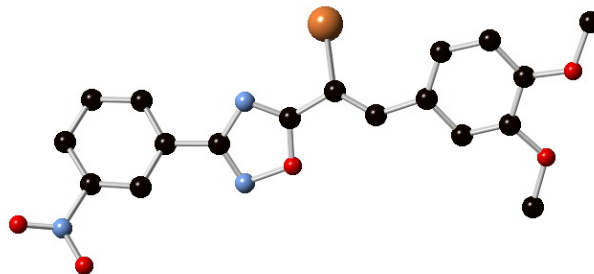
B. Intensity Measurements

Diffractometer	Saturn70
Radiation	CuK α (λ = 1.54187 Å)
Voltage, Current	40kV, 20mA
Temperature	-100.0 °C
Detector Aperture	70 x 70 mm
Pixel Size	0.034 mm
2 θ _{max}	136.0°
No. of Reflections Measured	Total: 2987 Unique: 2987 (R _{int} = 0.0000)
Corrections	Lorentz-polarization Absorption (trans. factors: 0.788 - 0.971)

C. Structure Solution and Refinement

Structure Solution	Direct Methods	Reflection/Parameter Ratio	11.81
Refinement	Full-matrix least-squares on F ²	Residuals: R1 (I>2.00 σ (I))	0.0951
Function Minimized	$\sum w (F_o^2 - F_c^2)^2$	Residuals: R (All reflections)	0.0993
Least Squares Weights	$w = 1 / [\sigma^2(F_o^2) + (0.2000 \cdot P)^2 + 0.0000 \cdot P]$ where P = (Max(F _o ² , 0) + 2F _c ²)/3	Residuals: wR2 (All reflections)	0.3553
		Goodness of Fit Indicator	1.614
		Max Shift/Error in Final Cycle	1.004
2 θ _{max} cutoff	136.0°	Maximum peak in Final Diff. Map	0.78 e ⁻ /Å ³
Anomalous Dispersion	All non-hydrogen atoms	Minimum peak in Final Diff. Map	-0.39 e ⁻ /Å ³
No. Observations (All reflections)	2987	Maximum peak in Final Diff. Map	0.78 e ⁻ /Å ³
No. Variables	253	Minimum peak in Final Diff. Map	-0.39 e ⁻ /Å ³

Crystallographic information for **189**



A. Crystal Data

B. Intensity Measurements

Empirical Formula	C ₁₈ H ₁₄ BrN ₃ O ₅
Formula Weight	432.23
Crystal Color, Habit	colorless, prism
Crystal Dimensions	0.120 X 0.030 X 0.030 mm
Crystal System	triclinic
Lattice Type	Primitive
Lattice Parameters	a = 7.272(3) Å b = 10.669(3) Å c = 12.039(3) Å α = 66.43(2) ° β = 85.54(3) ° γ = 80.06(3) ° V = 843.3(5) Å ³
Space Group	P-1 (#2)
Z value	2
D _{calc}	1.702 g/cm ³
F ₀₀₀	436.00
μ (MoK α)	24.822 cm ⁻¹
Diffractometer	Mercury70
Radiation	MoK α (λ = 0.71075 Å)
Voltage, Current	50kV, 16mA
Temperature	-180.0 °C
Detector Aperture	70 x 70 mm
Pixel Size	0.068 mm
2 θ _{max}	50.7°
No. of Reflections Measured	Total: 5404
	Unique: 2970 (R _{int} = 0.0426)
Corrections	Lorentz-polarization Absorption (trans. factors: 0.737 - 0.928)

C. Structure Solution and Refinement

Structure Solution	Direct Methods	No. Variables	244
Refinement	Full-matrix least-	Reflection/Parameter Ratio	12.17

Function Minimized	squares on F^2	Residuals: R1 ($I > 2.00\sigma(I)$)	0.0594
Least Squares	$\sum w (F_o^2 - F_c^2)^2$	Residuals: R (All reflections)	0.0732
Weights	$w = 1 / [\sigma^2(F_o^2) + (0.1122 \cdot P)^2 + 4.5702 \cdot P]$	Residuals: wR2 (All reflections)	0.1692
	where $P = (\text{Max}(F_o^2, 0) + 2F_c^2)/3$	Goodness of Fit Indicator	0.804
2 θ_{max} cutoff	50.7 $^\circ$	Max Shift/Error in Final Cycle	0.014
Anomalous Dispersion	All non-hydrogen atoms	Maximum peak in Final Diff. Map	0.94 e $^-/\text{\AA}^3$
No. Observations (All reflections)	2970	Minimum peak in Final Diff. Map	-0.68 e $^-/\text{\AA}^3$